RUSSIAN ACADEMY OF SCIENCES

# GEOMORPHOLOGY

Vol. 53 No. 5 2022

FOUNDED 1970 QUARTERLY



*Founders*: Russian Academy of Sciences, Institute of Geography Russian Academy of Sciences
*The Editorial Staff*:
E.A. Karaseva – head of Editorial office (manager editor)
*The Editorial Board Adress*: Staromonetniy lane, 29,
Institute of Geography Russian Academy of Sciences, 119017 Moscow, Russia
*Phone*: 8 (499) 238-03-60
*E-mail*: geomorfologiya@mail.ru

The subscription index in Rospechat catalogue 70215
ISSN 0435-4281 (Print)
ISSN 2658-4530 (Online)

# СОДЕРЖАНИЕ

**Том 53, номер 5, 2022**

## СПЕЦИАЛЬНЫЙ ВЫПУСК
## ПУТИ ЭВОЛЮЦИОННОЙ ГЕОГРАФИИ 2.
## ЧАСТЬ 2. ПРОБЛЕМЫ ПАЛЕОПОЧВОВЕДЕНИЯ, ГЕОАРХЕОЛОГИИ, ФЛЮВИАЛЬНОЙ ГЕОМОРФОЛОГИИ

От редколлегии 5

## ПРОБЛЕМЫ ПАЛЕОПОЧВОВЕДЕНИЯ И ГЕОАРХЕОЛОГИИ

Динамика древесной растительности и антропогенная активность по данным анализа древесных углей из городищ раннего железного века и раннего средневековья на верхней Волге

*М. В. Бобровский, Д. А. Куприянов, А. Л. Смирнов, Л. Г. Ханина, М. В. Добровольская* 7

Детальная палеоэкологическая летопись Валдайского криохрона (МИС 4–2) из почвенно-осадочной серии среднепалеолитического памятника Хотылёво I

*М. А. Коркка, Т. В. Романис, Л. А. Савельева, С. Н. Седов, А. К. Очередной* 25

Реконструкция палеоландшафтов средних веков на основе изучения погребенных почв Гочевского археологического комплекса (Курская область)

*Ф. Г. Курбанова, Т. А. Пузанова, Е. Н. Асеева, П. Г. Куст, О. В. Руденко* 32

Влияние состава и свойств Хвалынских отложений на эволюцию почв Волго-Уральского междуречья (по результатам минералогических и микроморфологических исследований)

*М. П. Лебедева, О. О. Плотникова, Н. А. Чурилин, Т. В. Романис, В. А. Шишков* 48

О времени появления человека современного вида на северо-востоке Восточно-Европейской равнины и на Урале (по данным изучения палеолитической стоянки Заозерье)

*П. Ю. Павлов* 60

Отражение вековых и тысячелетних изменений природной среды в палеопочвах верхнепалеолитических стоянок Восточно-Европейской равнины в МИС 3 и МИС 2

*С. Н. Седов, А. А. Синицын, А. А. Бессуднов, С. Ю. Лев, А. Н. Бессуднов, С. А. Сычёва, Т. В. Романис, В. С. Шейнкман, М. А. Коркка* 69

Локальная стратиграфия и палеоэкология стоянки поздней поры верхнего палеолита Дивногорье 1 в бассейне среднего Дона

*С. А. Сычёва, А. А. Бессуднов, А. Н. Бессуднов, С. Н. Тимирева, Ю. М. Кононов, А. Н. Симакова, Е. Ю. Захарова, К. Г. Филиппова* 78

Строение и условия формирования палеопочв раннего плейстоцена в лёссово-почвенной серии разреза Алчак-Седловина (Республика Крым)

*М. В. Хмелева, П. Г. Панин, А. Л. Чепалыга, Н. В. Карпухина, О. Д. Найдина, А. В. Бухонов* 89

Палеочерноземы времени развития срубной культуры и тренды позднеголоценовой эволюции почв лесостепи Восточно-Европейской равнины

*Ю. Г. Чендев, Т. А. Пузанова, Ф. Г. Курбанова* 103

## ПРОБЛЕМЫ ФЛЮВИАЛЬНОЙ ГЕОМОРФОЛОГИИ

Влияние газогидротермальной деятельности на формирование рельефа речных долин геотермальных зон

*Е. В. Лебедева* 116

Строение поймы реки Мокши как ключ к позднеплейстоценовой истории развития долины

*Е. Ю. Матлахова, В. Ю. Украинцев* 127

Палеореконструкция долины Нижней Лены в голоцене и позднем неоплейстоцене: новые данные, противоречия и проблемы

*С. А. Правкин, Д. Ю. Большиянов* 134

Пойменный аллювий бассейна р. Селенги: строение, возраст, этапы формирования

*Ю. В. Рыжов, В. А. Голубцов, М. В. Смирнов* 144

Некоторые особенности применения радиоцезиевого метода изучения потерь почвы вследствие эрозии в перигляциальной области бассейна верхней Оки

*Л. Н. Трофимец, Е. А. Паниди, А. А. Лаврусевич* 154

Строение и история формирования долин прорыва верхней Волги

*А. О. Уткина, А. В. Панин* 162

СОДЕРЖАНИЕ Том 53, Номер 1–5, 2022 173

# CONTENTS

**Vol. 53, No. 5, 2022**

## SPECIAL ISSUE
## PATHWAYS OF EVOLUTIONARY GEOGRAPHY 2.
## PART 2. PROBLEMS OF PALAEOPEDOLOGY, GEOARCHAEOLOGY, FLUVIAL GEOMORPHOLOGY

Editorial

*E. Yu. Novenko* 5

## PROBLEMS OF PALAEOPEDOLOGY AND GEOARCHAEOLOGY

Woodland dynamics and human activity based on charcoal analysis from hillforts of the iron age and early middle ages in the Upper Volga River

*M. V. Bobrovsky, D. A. Kupriyanov, A. L. Smirnov, L. G. Khanina, and M. V. Dobrovolskaya* 7

Detailed paleoenvironmental record for the Valday Cryochron (MIS 4–2) from the soil-sedimentary sequence of the Middle Palaeolithic site Khotylevo I

*M. A. Korkka, T. V. Romanis, L. A. Savelieva, S. N. Sedov, and A. K. Otcherednoy* 25

Reconstruction of medieval paleolandscapes based on the study of paleosols of Gochevsky archaeological complex (Kursk region, Russia)

*F. G. Kurbanova, T. A. Puzanova, E. N. Aseyeva, P. G. Kust, and O. V. Rudenko* 32

Influence of the composition and properties of Khvalynian deposits on the evolution of soils of the Volga-Ural interfluve (based on the results of mineralogical and micromorphological studies)

*M. P. Lebedeva, O. O. Plotnikova, N. A. Churilin, T. V. Romanis, and V. A. Shishkov* 48

On the time of appearance of anatomically modern humans in the northeast of East European Plain and in the Urals (based on data from the Zaozer'e site)

*P. Yu. Pavlov* 60

Paleosols of the Upper Palaeolithic sites in the East European Plain reflect the environmental fluctuations of centennial to millennial scale during MIS 3 and MIS 2

*S. N. Sedov, A. A. Sinitsyn, A. A. Bessudnov, S. Yu. Lev, A. N. Bessudnov, S. A. Sycheva, T. V. Romanis, V. S. Sheinkman, and M. A. Korkka* 69

Local stratigraphy and palaeoecology of the late Upper Palaeolithic site Divnogorie 1 in the basin of the Middle Don

*S. A. Sycheva, A. A. Bessudnov, A. N. Bessudnov, S. N. Timireva, Yu. M. Kononov, A. N. Simakova, E. Yu. Zakharova, and K. G. Filippova* 78

The structure and formation conditions of the early Pleistocene paleosols in the loess-paleosol sequence of the Alchak-Sedlovina section (Republic of Crimea)

*M. V. Khmeleva, P. G. Panin, A. L. Chepalyga, N. V. Karpukhina, O. D. Naidina, and A. V. Bukhonov* 89

Paleochernozems of the Srubnaya culture period and trends of Late Holocene evolution of soils in the East European Plain forest-steppe

*Yu. G. Chendev, T. A. Puzanova, and F. G. Kurbanova* 103

## PROBLEMS OF FLUVIAL GEOMORPHOLOGY

Gas-hydrothermal activities impact on the relief formation of geothermal zones' river valleys

*E. V. Lebedeva* 116

The structure of the Moksha River floodplain as a key to the Late Pleistocene history of the valley development

*E. Yu. Matlakhova and V. Yu. Ukraintsev* 127

Holocene and Late Neopleistocene paleoreconstructions for the lower Lena River valley: new data, contradictions and problems

*S. A. Pravkin and D. Yu. Bolshiyanov* 134

Floodplain alluvium in the Selenga River basin: structure, age, formation stages

*Yu. V. Ryzhov, V. A. Golubtsov, and M. V. Smirnov* 144

Some features of the radiocaesium method applied to study of soil losses due to erosion on the periglacial area of the Upper Oka basin

*L. N. Trofimetz, E. A. Panidi, and A. A. Lavrusevich* 154

Upper Volga's incision valleys: geomorphological aspects and development history

*A. O. Utkina and A. V. Panin* 162

Contents Vol. 53, Numbers 1–5, 2022 173

**EDN:** TATHHZ
*ГЕОМОРФОЛОГИЯ, 2022, том 53, № 5, с. 5–6*

# СПЕЦИАЛЬНЫЙ ВЫПУСК ПУТИ ЭВОЛЮЦИОННОЙ ГЕОГРАФИИ 2. ЧАСТЬ 2. ПРОБЛЕМЫ ПАЛЕОПОЧВОВЕДЕНИЯ, ГЕОАРХЕОЛОГИИ, ФЛЮВИАЛЬНОЙ ГЕОМОРФОЛОГИИ

## ОТ РЕДКОЛЛЕГИИ

**DOI:** 10.31857/S043542812205011X

## SPECIAL ISSUE PATHWAYS OF EVOLUTIONARY GEOGRAPHY 2. PART 2. PROBLEMS OF PALAEOPEDOLOGY, GEOARCHAEOLOGY, FLUVIAL GEOMORPHOLOGY

### EDITORIAL

This special issue of the journal "Geomorfologiya" is the second volume of selected papers followed the 2nd International Conference "Pathways of Evolutionary Geography" (November 2021, Moscow) dedicated to the 90th anniversary of professor A.A. Velichko, the famous Russian geographer, who made a great contribution into the Quaternary science, geomorphology, soil science and studies of human-environment interaction in the past.

The special issue includes 15 papers grouped into two thematic chapters – problems of palaeopedology and geoarchaeology (put together as in most papers ancient soils were studied at archaeological sites), and problems of fluvial geomorphology. The papers highlight the main directions of evolutionary geography developed by A.A. Velichko and present the results of recent studies conducted in various regions of Eastern Europe, Western and Eastern Siberia.

The special issue begins with the paper by M.V. Bobrovsky and his co-authors who presented the detail reconstruction of the tree species composition in the Upper Volga River basin (Peno District, Tver Region) during the Early Iron Age (the Dyakovo culture) the Early Middle Ages inferred from soil charcoal and archaeological excavations. Authors demonstrated that the soil charcoal was the robust evidence of tree species occurrence in the study area in different periods and gave them a possibility for detail studies of vegetation history and human impact on forests.

The studies of M.A. Korkka and her co-authors were devoted to reconstruction of the Late Pleistocene paleoenvironment conditions (MIS 5-MIS 1) in vicinity of the Middle Paleolithic Khotylevo I sites, one of the largest Middle Paleolithic archaeological findings in Eastern Europe, located in the central part of the East European Plain (Bryansk region). Based on precise description of paleosol morphology and properties authors revealed short-term climatic fluctuations during the MIS 3. Authors determined a period of extracontinental semi-arid climate followed by more humid conditions appeared as paleosol sequences from Cambic Cryosol to Gleysol. The paper of F.G. Kurbanova with co-authors is also focused on paleosol studies at the archaeological complex in the centre of European Russia (Kursk region). The multyproxy research included the detailed morphological description of the buried soils in the Gochevsky burial ground of Medieval age, grain size analysis, elemental composition and iron fraction measurements, micromorphological studies, pollen analysis and non-pollen palynomorphs identification. The obtained data showed the complex temporal dynamics of forest-steppe landscape in the region in X–XI centuries with short-term humid and wet phases, possibly, influenced on human migration in Eurasian steppe.

The intensive paleopedological studies of the last decades clearly demonstrate the importance of sedimentological approaches in paleogeography. M.P. Lebedeva with co-authors obtained the new data on the composition and properties of Khvalynian deposits and the evolution of soils in the Volga-Ural interfluve using mineralogical and micromorphological analysis. The paper of M.V. Khmeleva and co-authors presented the preliminary results of studies of the loess-paleosol sequence of the Alchak-Sedlovina section (Crimea Penunsula).

Archaeological research and studies of human-environment interactions are the important issues in paleogeography that was denoted by A.A. Velichko, who devoted a lot attention to Paleolithic archaeological sites and environment conditions of human occupation. The time of appearance of anatomically modern humans (*Homo sapiens sapiens*) in the northeast of East European Plain and on the Urals was discussed by P.Yu. Pavlov. Based on archaeological materials from the Palaeolithic site Zaozer'e (35–31 $^{14}$C kyr BP) located in the North-East of East European plain in Upper Kama River basin, he revealed that modern humans probably reached the sub-arctic zone ca. 3–4 thousand years after their first appearance in the centre of the East European Plain.

The studies of environmental changes during the Palaeolithic are continued by articles of Sedov et al. and Sycheva et al. S.N. Sedov and his co-authors proved that the paleosol-sedimentary sequences encountered at the Upper Palaeolithic archaeological sites within the central part of the East European Plain indicated the short-term climatic fluctuations, similar ones revealed from Greenland ice core proxy. Detailed research and dating of paleosols at the archaeological sites of Kostenki and Divnogorie gave rise to the compound correlation scheme which covers the second half of MIS 3 and MIS 2. The study of S.A. Sycheva with co-authors was focused on the local stratigraphy and palaeoecology of the Upper Palaeolithic site Divnogorie-1. Using paleopedological approach authors traced a shift from the Late Glacial paleoenvironments to the Holocene.

The Late Holocene of soil evolution in the forest-steppe and steppe zones of the East European Plain were described in the paper of Chendev et al. They realized a comparative analysis of chernozems buried under the mounds of the Srubnaya culture (Late Bronze age) and their earlier and later analogues. Authors demonstrated biochemical transformations of the soil profiles and compared them with Holocene climatic changes. The interesting results of paleosol studies at the Eneolithic – Late Bronze Age archaeological site Yamgort in West Siberia (Yamalo-Nenets Autonomous Area) are presented in the paper by L.N. Plekhanova and co-authors.

The second chapter of this special issue devoted to the problems of fluvial geomorphology is prefaced by the paper of E.V. Lebedeva about the gas-hydrothermal activities and their impact on river valleys in geothermal zones. She argued that solfataric gases outputs, mud volcanic manifestations and mineralized thermal waters contribute to the formation of various specific landforms on slopes and bottoms of river valleys in the areas of modern volcanism.

The structure of the floodplain in Moksha River valley (middle Oka River basin) as a key to the understanding of the evolution of river valleys during the Late Pleistocene was discussed in the paper of E.Yu. Matlakhova and V.Yu. Ukraintsev. Authors using geomorphological and lithological analysis, and radiocarbon AMS-dating reconstructed the main stages of the Moksha River valley development during the Late Pleistocene and Pleistocene/Holocene transition.

The new data of the Late Pleistocene and Holocene sedimentation and development of the Lower Lena River valley were presented in the paper of S.A. Pravkin and D.Yu. Bolshiyanov. Based on field observations, sedimentological descriptions, radiocarbon and IR-OSL dating of alluvial deposits, they proved that the floodplain and first terraces in the Lower Lena River valley was caused by sea level fluctuations at the end of Late Pleistocene and in the Holocene. Authors showed that the glaciations of Verkhoyansk Ridge could not influence to configuration of the Lena River valley as mountain glaciers had not rich the Lena River since the end of the Middle Pleistocene. The novel materials of floodplain formation in the Selenga River basin were presented in the paper of Yu.V. Ryzhov and co-authors. Authors focused on the structure and age of floodplain alluvium of the main levels of floodplain, morphology of the Selenga River valley, dynamics of water discharge, structural and tectonic conditions of the river basin during the Holocene. Authors determined the event of a sharp change in the lithological composition of deposits as high floods at 3.8–3.4 kyr BP.

An advantage of the radiocaesium method for investigation of soil losses due to erosion in the periglacial area of the Upper Oka River basin were presented in the paper of L.N. Trofimetz and her co-authors. They discussed the influence of paleocryogenic polygonal-block microrelief of the study area to caesium-137 distribution in soil cover.

The evolution of the upstream part of the Volga River was discussed in the paper of A.O. Utkina and A.V. Panin. Authors suggested the new mechanism of formation and age of the Plyos and Tutayev incision valleys during MIS 2 and tested it using geomorphological observation, luminescence dating and modelling approach.

The papers presented in the special issue cover a broad range of scientific problems, methodological approaches and study regions with a focus on evolutionary geography, geomorphology, palaeopedology and geoarchaeology. The guest Editor expresses deep gratitude to all the many authors, who submitted their novel interesting results and valuable discussions to the current volume, thus helping in closing some gaps in knowledge and indicating directions for future work.

*E. Yu. Novenko, guest editor*

**EDN:** DPLUND
*ГЕОМОРФОЛОГИЯ, 2022, том 53, № 5, с. 7–24*

## ПРОБЛЕМЫ ПАЛЕОПОЧВОВЕДЕНИЯ И ГЕОАРХЕОЛОГИИ

*УДК 551.89:574:902/904 (470.331)*

# ДИНАМИКА ДРЕВЕСНОЙ РАСТИТЕЛЬНОСТИ И АНТРОПОГЕННАЯ АКТИВНОСТЬ ПО ДАННЫМ АНАЛИЗА ДРЕВЕСНЫХ УГЛЕЙ ИЗ ГОРОДИЩ РАННЕГО ЖЕЛЕЗНОГО ВЕКА И РАННЕГО СРЕДНЕВЕКОВЬЯ НА ВЕРХНЕЙ ВОЛГЕ

**© 2022 г. М. В. Бобровский[1,*], Д. А. Куприянов[2,3,**], А. Л. Смирнов[3,***], Л. Г. Ханина[4,****], М. В. Добровольская[3,*****]**

[1]*Институт физико-химических и биологических проблем почвоведения РАН – обособленное подразделение ФИЦ "Пущинский научный центр биологических исследований РАН", Пущино, Россия*

[2]*Московский государственный университета имени М.В. Ломоносова, географический факультет, Москва, Россия*

[3]*Институт археологии РАН, Москва, Россия*

[4]*Институт математических проблем биологии РАН, филиал Института имени Келдыша РАН, Пущино, Россия*

**E-mail: maxim.bobrovsky@gmail.com*

***E-mail: dmitriykupriyanov1994@yandex.ru*

****E-mail: ari1828@bk.ru*

*****E-mail: khanina.larisa@gmail.com*

******E-mail: mk_pa@mail.ru*

Поступила в редакцию 14.06.2022 г.
После доработки 27.06.2022 г.
Принята к публикации 15.07.2022 г.

Были исследованы угли в культурных слоях трех городищ, расположенных в верховьях р. Волги (Пеновский район Тверской области). Угли изучали в кернах и археологических шурфах. Характеристика культурных слоев городищ позволяет отнести их к палеоурбаноземам, "Archaeological Dark Earth" мощностью от 50 до 80 см. Возраст углей и археологические находки показали, что культурные слои городищ Заборовка-Лихуши и Ворошилово относятся к раннему железному веку (Дьяковская культура), а городища Руна-Заборовка – к раннему средневековью. Определены концентрация и таксономический состав углей в образцах, отобранных с разных глубин. Всего было определено 629 углей, относящихся к 13 родам древесных растений. На основе анализа углей из 12 датированных образцов дана оценка изменения таксономического состава деревьев во времени. Во все периоды доминировали древесные угли *Pinus*, за ними по числу следовала *Picea*; доли этих таксонов увеличивались от раннего железного века к позднему средневековью. Наибольшее число таксонов (9 родов) отмечено для раннего железного века, в том числе встречены *Quercus*, *Ulmus* и *Acer*. Информация, полученная в результате изучения древесного угля в почве, является ценным свидетельством присутствия таксонов деревьев на конкретной территории в определенные отрезки времени; позволяет воссоздать историю взаимодействия человека и древесной растительности в верховьях Волги.

*Ключевые слова:* педоантракология, палеоурбаноземы, Дьяковская культура, дровяная древесина, радиоуглеродное датирование

**DOI:** 10.31857/S0435428122050030

## 1. INTRODUCTION

The Early Iron Age and subsequent centuries in the forest region of Eastern Europe is a crucial time of structural change in human–nature interactions. Therefore it is highly important to study the sites of the Dyakovo and neighboring cultures in terms of settlement, reconstruction of economy types, land use features, and anthropogenic impact on landscapes. In this regard, one of the most well-studied regions for the Early Iron Age is the Moskva River basin (Syrovatko, 2009; Krenke, 2011; Ershova et al., 2014, 2016; Syrovatko et al., 2016; Uspensky, Chaukin, 2016; Veksler, Gusakov, 2017; Islanova, 2017; Krenke, 2019; Lopatina, 2019). The monuments of the Dyakovo culture in the Upper Volga River and Valdai have been studied comparatively little (Islanova, 2012, 2013, 2014 a, b). This territory remains a "white spot" in the Early Iron Age, a poorly populated area in the middle to second half of the 1st millennium AD (Islanova, 2020). In terms of settlement and archaeological finds, the subsequent period (second half of the 1st millennium AD) in neighboring areas, such as Novgorod region (Eremeev, Dzyuba, 2016), ancient Smolensk and its surroundings, including the Gnezdovo archaeological complex (Ershova et al., 2020; Krenke et al., 2021), is much better studied.

The target of our study is the sites of fortifications (hillforts) in the upper Volga and the Western Dvina rivers, located in the contact zone of the Dyakovo and the Dnieper-Dvina cultures (northern part of the Peno district of the Tver region). Research of archival materials and reconnaissance in recent years allowed to judge the existence of hillforts of different size in the study area (Smirnov et al., 2021). Archaeological settlements mostly belong to the Early Iron Age, although some of them according to the few ceramic finds, could have appeared in the Early Middle Ages. The sparse networks of small hillforts identified in recent years raise questions about how the Early Iron Age people may have influenced the dynamics of ecosystems and how their lives were influenced by natural conditions.

In the last decade, pedoanthrocological studies have been actively developed to reconstruct the history of specific sites based on the analysis of charcoals in soil and sediments and their dating (Carcaillet, Talon, 1996; Carcaillet, Thinon, 1996; Talon et al., 2005; Nelle et al., 2013; Ohlson et al., 2017; Saulnier et al., 2019). These methods are widely used in the study of archaeological sites (Figueiral, 1996; O'Donnell, 2017; Masi et al., 2018; Moskal-del Hoyo et al., 2021; Novák et al., 2021; Ruiz-Giralt, 2021). They are often used together with other methods of paleoecological studies, primarily the study of different proxies in bog or lake sediments that provide information about the broader geographic and paleohistorical context. Applied to the region under the study, such work has been done for the Krivetsky Mokh bog (Mazei et al., 2020).

We focused on an anthracological study of areas of three hillforts of the Iron Age and the Early Middle Ages with the aim to identify the peculiarities of the interaction between humans and woody vegetation. The objectives of the research were to: (1) determine the thickness of the cultural layer and analyze the stratigraphy and concentration of charcoals in the hillfort; (2) analyze the taxonomic composition of charcoals with regard to their stratigraphy; and (3) determine the age of charcoals from different locations in the cultural layer and reconstruct changes in the taxonomic composition of charcoals in the hillfort areas during different historical periods.

## 2. STUDY AREA

Study area is located in the north of the Valdai Upland located in the central part of the East European Plain, in the Peno district of the Tver region (fig. 1).

The area is located in the hemiboreal forest region (European Russian Forests, 2017), in the southern subzone of the taiga forest. Landscapes are represented by a hilly plain (150–250 m a.s.l. with a maximum elevation of 275 m) moderately dissected by gullies, valleys of small streams and depressions. Quaternary deposits are formed by moraine materials and fluvioglacial sands. Moraine ridges and hills are mainly oriented from northwest to southeast, have a height of 6 to 20 and a length of 100 to 1500 m. The area is characterized by a large number of lakes and mires developed in depressions between moraine hills.

The climate is temperate and moderate continental with relatively cold winters (mean January temperature is –5.9°C) and warm summers (mean July temperature is 18.3°C) (the Toropets weather station, 80 km southwest from the study area, 1988–2019; http://www.meteo.ru). The mean annual temperature is +5.6°C. The mean annual precipitation is about 761 mm.

Forests are usually dominated by *Pinus sylvestris* (Scots pine) and *Picea abies* (European spruce) with the participation of *Betula* spp. (birch) and *Populus tremula* (common aspen). In the understorey, *Sorbus aucuparia* and *Frangula alnus* often occur. *Vaccinium myrtillus*, *V. vitis-idaea*, and green mosses prevail in the forest floor. Boreal and nemoral herbaceous species, such as *Hepatica nobilis, Calamagrostis arundinacea, Dryopteris filix-mas, Oxalis acetosella, Convallaria majalis, Galeobdolon luteum, Asarum europaeum,* and *Stellaria holostea* are common. *Anemone nemorosa* can often be found in spring. Broadleaf trees rarely occur in the vegetation. *Quesrcus robur* (pedunculate oak) is common in the understory of *Pinus sylvestris* forests while it rarely occurs in the overstory.

Small adult individuals of *Tilia cordata* (small-leaved lime) usually occurs in lowlands, near streams. *Acer platanoides* (Norway maple), *Ulmus glabra* (Scots elm), and *Fraxinus excelsior* (common ash) can be found in the north of the region where moraine hills prevail. We did not meet elm and ash in the study area; Norway maple was occasionally found. In wet depressions, often close to swamps, there are forests dominated by *Alnus incana* (grey alder); they also occur on moraine hills.

Sandy soils Albic and Entic Podzols prevail on watersheds and slopes; Stagnic Podzols and Histosols are common in depressions on the border with bogs (IUSS Working Group, 2015).

## 3. MATERIALS AND METHODS

We have studied soil charcoal in the area of three hillforts discovered in 2018–2019 (fig. 1, tabl. 1) (Smirnov et al., 2021), on which there were no large-scale archaeological excavations. The each hillfort is located on the edge of a moraine ridge (an oz ridge). Zaborovka-Likhusha and Runa-Zaborovka hillforts are located inside the forest tracts. Voroshilovo hillfort is located on a wooded hill surrounded by modern and

(a)

(b)

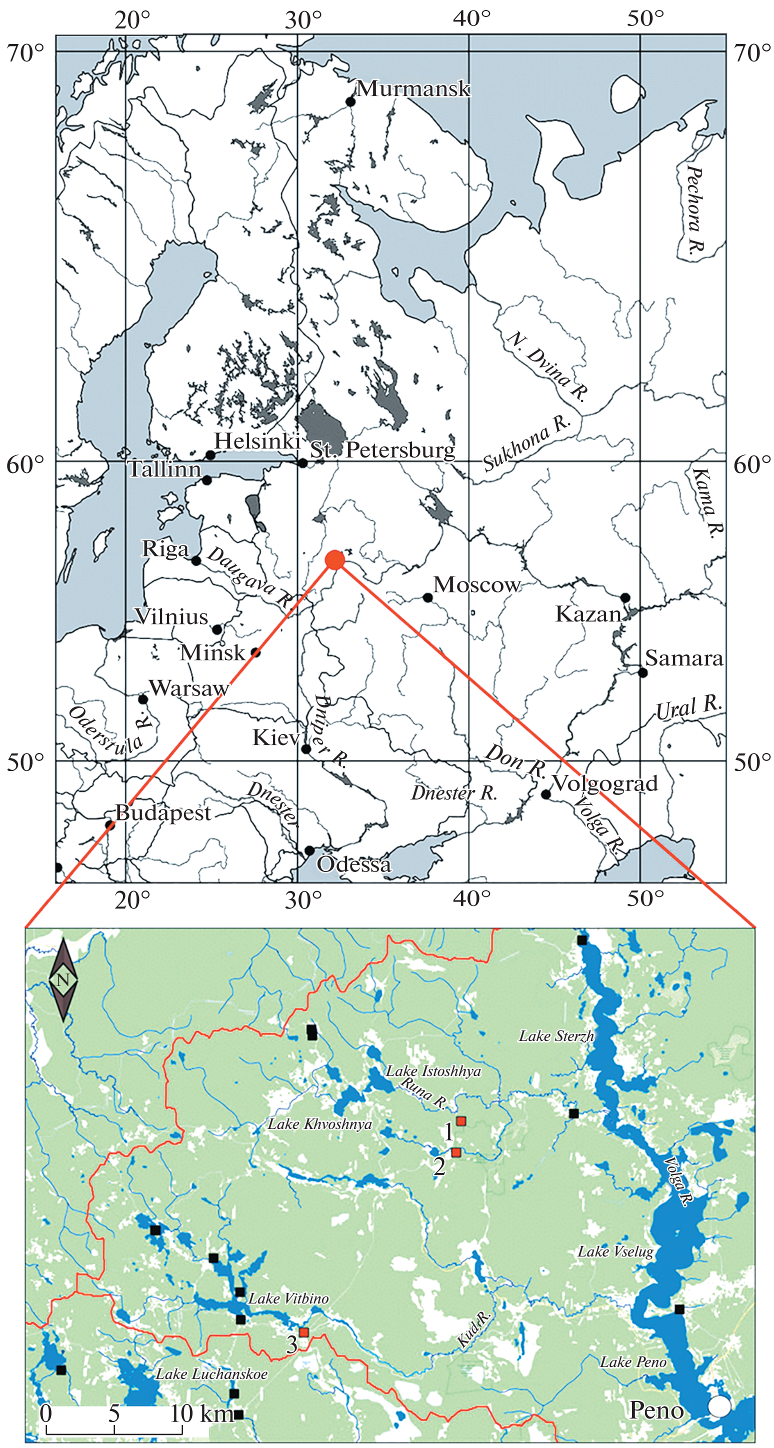


**Fig. 1.** Location (a) and map (b) of the study region with the hillforts (squares): 1 – Runa-Zaborovka, 2 – Zaborovka-Likhusha, 3 – Voroshilovo.

**Рис. 1.** Местонахождение (а) и карта (b) исследуемого района с городищами (квадраты): 1 – Руна-Заборовка, 2 – Заборовка-Лихуша, 3 – Ворошилово.

abandoned arable lands. *Pinus sylvestris* and *Picea abies* dominate in the forest canopy in all hillforts. According to the tree cores, *Pinus sylvestris* ranged from 80 to 110 years old in 2019. The brash *Lonicera xylosteum* and *Daphne mezereum* were common in the understory. Forest floor vegetation in the hillforts differed from the surrounding forests by low participation of boreal dwarf-shrubs and green mosses. Nemoral

**Table 1.** Points of soil sampling to define the concentration and taxonomic composition of charcoal
**Таблица 1.** Точки отбора проб почвы для определения концентрации и таксономического состава древесного угля

| Hillfort | ID | Description | Number of samples used for charcoal concentration / taxonomical composition |
|---|---|---|---|
| Zaborovka-Likhusha | ZL-1 | Soil core 1 in the inner site | 8/8 |
| | ZL-2 | Soil core 2 in the inner site | 8/8 |
| | ZL-3 | Soil core 3 in the inner site | 8/8 |
| | ZL-4 | Soil core 4 in the inner site | 3/3 |
| | ZL-5 | Archaeological excavation, depth 30–45 cm | 0/1 |
| | ZL-6 | Archaeological excavation, depth 45–60 cm | 0/1 |
| | ZL-7 | Archaeological excavation, depth 45–60 cm | 0/1 |
| | ZL-8 | Archaeological excavation, depth 15–30 cm | 0/1 |
| | ZL-9 | Ancient moat | 0/3 |
| Voroshilovo | V-1 | Soil core 1 in the inner site | 8/8 |
| | V-2 | Soil core 2 in the inner site | 8/8 |
| | V-3 | Soil core 3 in the inner site | 5/5 |
| | V-4 | Hillock of treefall with uprooting | 0/1 |
| | V-5 | Archaeological excavation, depth 45–60 cm | 0/1 |
| | V-6 | Archaeological excavation, depth 45–60 cm | 0/1 |
| Runa-Zaborovka | RZ-1 | Soil core 1 in the inner site | 6/6 |
| | RZ-2 | Soil core 2 in the inner site | 6/6 |
| | RZ-3 | Soil core 3 in the inner site | 6/6 |
| | RZ-4 | Archaeological excavation, depth 15–30 cm | 0/1 |

herbs, such as *Galeobdolon luteum, Asarum europaeum, Stellaria holostea, Pulmonaria obscura, Aegopodium podagraria*, etc. were common together with *Hepatica nobilis* and *Urtica dioica*.

Hillforts are elevations surrounded by fortification structures. Zabarovka-Likhusha hillfort (fig. 2) is ringed by a creek to west and north and a bog to east. Size of the inner platform (inner site) is 35×21 m; height above the creek is 14 m. The fortification structure includes the rampart of the settlement itself, a moat in the south, and an additional cape rampart and moat in the north. Voroshilovo hillfort (fig. 3) has an oval inner area of 47×18 m; height of the site from the bottom is 5.5 m; traces of ramparts and moats can be seen from southwest and northeast. Runa-Zaborovka hillfort (fig. 4) has a rounded inner area with a diameter of 25 m; height of the site is 3.5 m.

Soil samples were taken at the inner site of each hillfort with a soil auger with a depth step of 15 cm to determine the concentration and taxonomic composition of charcoal. The diameter of soil auger was 5 cm; the volume of soil samples was about 235 cm$^3$. Soil samples were also taken from two archaeological excavations (1×1 m) both for the concentration /composition of charcoal and for radiocarbon dating with a soil sample volume of about 600 cm$^3$.

In Zaborovka-Likhusha hillfort, the following sampling was performed. Four soil cores were taken to a depth of 120 cm. Charcoals were also taken from an archaeological excavation: from a burnt wooden structure in a depth of 55 cm and from the depth of 35 cm (both for radiocarbon dating) and four samples at different depths for charcoal concentration and taxonomical composition (tabl. 1). Three soil samples were also taken from a pit dug on the western slope at the bottom of the hillfort, where an ancient moat was uncovered.

In Voroshilovo hillfort, the following sampling was done. Three soil cores to a depth of 120 cm were taken. Two charcoal samples were taken from an archaeological excavation located at the edge of the inner platform. Soil was also sampled from a hillock formed by a recent treefall with uprooting that was located in the inner platform and where a Dyakovo type spindle whorl was found.

In Runa-Zaborovka hillfort, three soil cores to a depth of 90 cm were selected and one soil sample was taken from a small archaeological excavation on the inner hillfort platform.

Fragments of textile ceramics, typical for the Dyakovo culture of the early Iron Age, were found at the Zaborovka-Likhusha and Voroshilovo hillforts. At Runa-Zaborovka hillfort, only stucco ceramics satu-

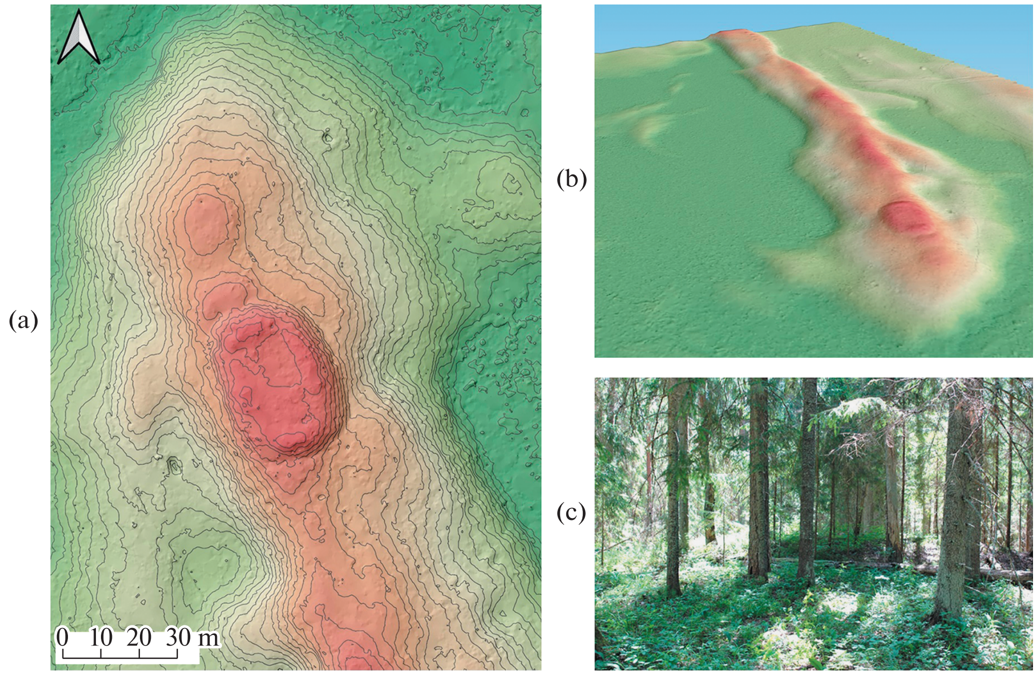


**Fig. 2.** Zaborovka-Likhusha hillfort: (a) – map of the hillfort with the LiDAR-derived local relief model; (b) – LiDAR-derived local relief model of the hillfort on the moraine ridge; (c) – forest vegetation in the area of the hillfort.

**Рис. 2.** Городище Заборовка-Лихуша: (a) – цифровая модель рельефа городища по данным лидарной съемки; (b) – цифровая модель рельефа моренной гряды с городищем по данным лидарной съемки; (c) – лесная растительность в районе городища.

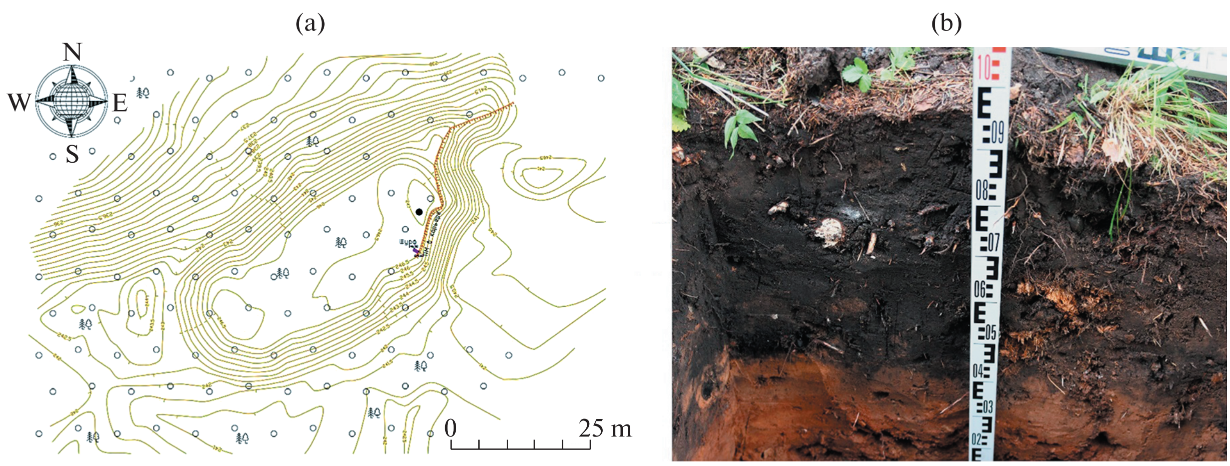


**Fig. 3.** Voroshilovo hillfort: (a) – map of the hillfort; (b) – soil (cultural layer) profile in an archaeological excavation.

**Рис. 3.** Городище Ворошилово: (a) – схема городища с горизонталями; (b) – профиль почвы (культурного слоя) в археологическом шурфе.

rated with gruss has been found so far. The latter is typical both for the early Iron Age and for the early Middle Ages, so small fragments of this pottery cannot be used as chronological indicators.

Soil samples were dried on air and gently sieved dry through 2 mm mesh size (Carcaillet, Talon, 1996). Charcoal fragments were extracted by hand from the sieved samples and then weighed to calculate charcoal concentration (or anthracomass, g of charcoal per kg of dry soil).

Taxonomic identification of charcoals was performed using a reflected light microscope (40–400×) using wood anatomy atlas (Benkova, Schweingruber, 2004). The transverse, radial and tangential anatomic planes of each charcoal were observed to identify charcoals at the genus taxonomic level. When calculating

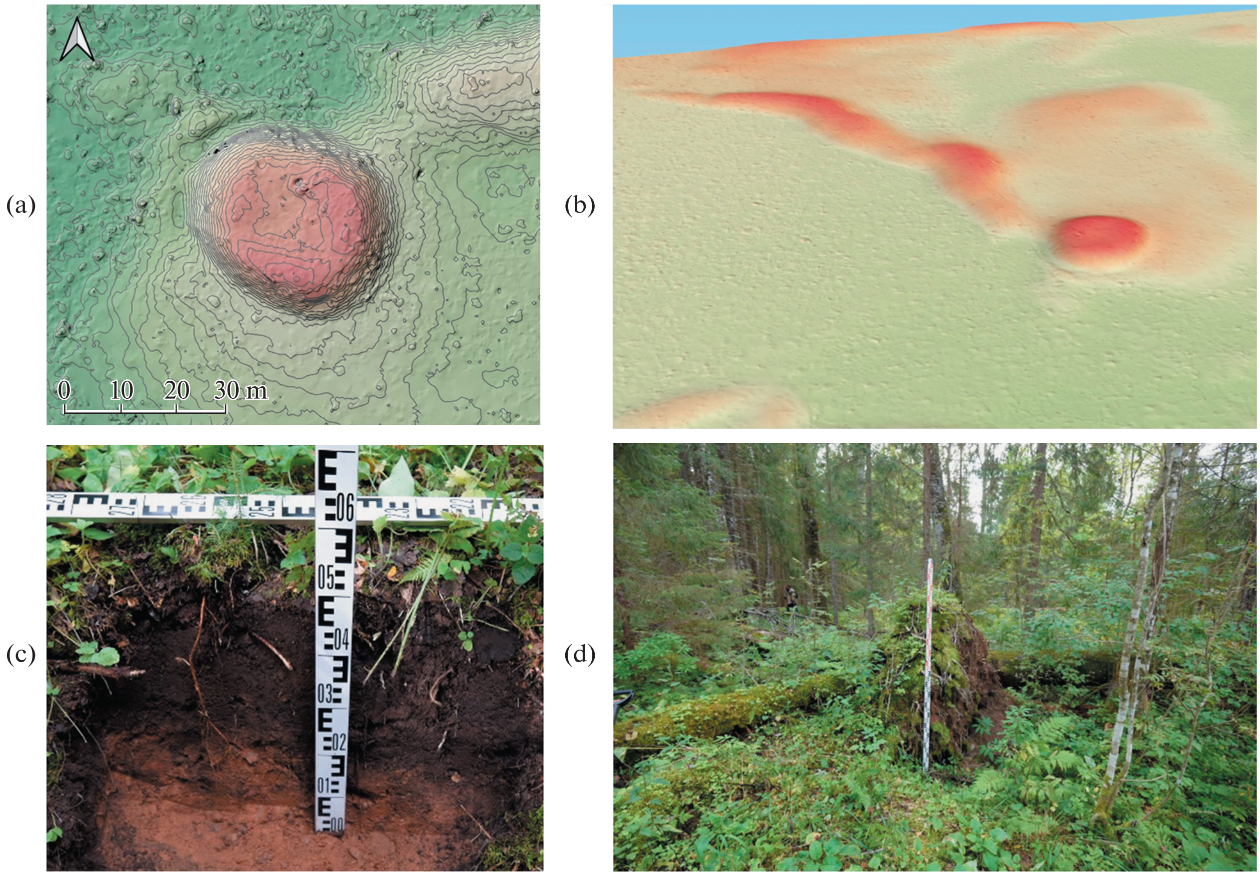


**Fig. 4.** Runa-Zaborovka hillfort: (a) – map of the hillfort with the LiDAR-derived local relief model; (b) – LiDAR-derived local relief model of the hillfort on the moraine ridge; (c) – soil (cultural layer) profile in an archaeological excavation; (d) – forest vegetation in the area of the hillfort.

**Рис. 4.** Городище Руна-Заборовка: (a) – цифровая модель рельефа городища по данным лидарной съемки; (b) – цифровая модель рельефа моренной гряды с городищем по данным лидарной съемки; (c) – профиль почвы (культурного слоя) в археологическом шурфе; (d) – лесная растительность в районе городища.

the percentage composition of taxa, all identified charcoals larger than 2 mm were counted.

Fourteen charcoal samples were radiocarbon dated by accelerator mass spectrometer – AMS in the Laboratory of Radiocarbon Dating and Electron Microscopy in the Institute of Geography of the Russian Academy of Sciences (IG RAS). The radiocarbon dates were calibrated with the IntCal20 (Reimer et al., 2013) using OxCal (Ramsey, 2009). For the reconstruction of historical dynamics of woody taxa in the area of hillforts studied, we assumed that the degree of mixing of the cultural layer material is not very high and the age of the dated charcoal corresponds to the age of the remaining charcoals in the sample. Thus, data on 12 radiocarbon samples were extrapolated to 209 charcoals.

For each hillfort, taxa diversity was estimated by taxa richness calculated as (i) the total number of taxa in all samples studied within the hillfort, (ii) taxa density estimated as the mean number of taxa per a sample, and (iii) Shannon's and Simpson's diversity indices calculated by standard formulas and accounting for the taxa abundance (Magurran, 2004).

## 4. RESULTS

*Cultural layer, soil charcoal stratigraphy and concentration.* The cultural layer (topsoil) of all the studied hillforts had a dark coloring due to the abundance of fine charcoal. In some places, cultural layer had inclusions of stones destroyed by incideration. The thickness of the cultural layer varied from 50 to 75 cm and from 50 to 80 cm in Zaborovka-Likhusha and Voroshilovo hillforts, respectively, and it was about 50 cm in Runa-Zaborovka. In archaeological excavations, the cultural layer looked relatively homogeneous in structure and color to a depth of 50 cm in Zaborovka-Likhusha and Voroshilovo inner sites, and to 30–40 cm in Runa-Zaborovka. Deeper, lighter and darker spots and interlayers alternated, and traces of pedoturbations were visible.

**Table 2.** Mean charcoal concentrations in the soil cores in the study sites, g × $kg^{-1}$ of dry soil
**Таблица 2.** Средние концентрации древесного угля в образцах почвы на исследуемых участках, г × $кг^{-1}$ сухой почвы

| Depth, cm | Zaborovka-Likhusha | | Voroshilovo | | Runa-Zaborovka | |
|---|---|---|---|---|---|---|
| | Mean | SE | Mean | SE | Mean | SE |
| 0–15 | 3.59 | 2.19 | 0.34 | 0.21 | 0.42 | 0.27 |
| 15–30 | 0.95 | 0.21 | 0.59 | 0.05 | 0.51 | 0.29 |
| 30–45 | 0.37 | 0.13 | 0.43 | 0.10 | 0.36 | 0.19 |
| 45–60 | 0.90 | 0.76 | 0.30 | 0.22 | 0.29 | 0.18 |
| 60–75 | 0.02 | 0.02 | 0.70 | 0.58 | 0.21 | 0.18 |
| 75–90 | 0.03 | 0.01 | 0.16 | 0.16 | 0.00 | 0.00 |
| 90–105 | 0.02 | 0.01 | 0.22 | 0.22 | NA | |
| 105–120 | 0.06 | 0.04 | 0.23 | 0.23 | NA | |

The highest values of both maximum (10 g $kg^{-1}$ of dry soil) and average (1.24 ± 0.55 g $kg^{-1}$) concentrations of charcoals in the cultural layer were observed in Zaborovka-Likhusha hillfort. These values were 1.84 and 0.47 ± 0.12 g $kg^{-1}$ in Voroshilovo and 1.06 and 0.40 ± 0.10 g $kg^{-1}$ in Runa-Zaborovka hillforts.

In all sites, charcoal concentration strong varied both spatially and by depth (fig. 5, tabl. 2). In Zaborovka-Likhusha, it varied in different columns at depth up to 60 cm and then decreased sharply. In Voroshilovo, in two columns (V-1 and V-3) charcoal occurred only within the cultural layer; in the third column (V2), the maximum concentration of charcoal was in the lower part of the cultural layer, but even deeper, up to 120 cm, charcoals were found in abundance. In Runa-Zaborovka, charcoal concentrations varied between columns to the greatest extent among all hillforts, but charcoal was not found deeper than 75 cm.

The soil pit at the bottom of Zaborovka-Likhusha hillfort (across the ancient moat) comprised three layers of sediments with boundaries at a depth of 16, 35, and 49 cm. The layers contained charcoals and consisted of brown sand, lighter in color than the material of the cultural layer.

*Soil charcoal taxonomy: distribution and diversity.* We extracted 932 charcoal fragments from 64 soil samples; 5 soil samples were without charcoal. A total of 629 charcoal fragments belonging to 13 woody genera were taxonomically identified: 304 in Zaborovka-Likhusha, 173 in Voroshilovo, and 119 in Runa-Zaborovka hillforts.

In taxa composition of charcoals (fig. 6), *Pinus* dominated (66 and 40%, respectively) in Zaborovka-Likhusha and Voroshilovo hillforts, followed by *Picea* (16 and 20%). Charcoals of four hardwood trees were also found in these sites: *Quercus*, *Ulmus*, *Acer*, and *Tilia* (11% from all charcoals) were identified in Zaborovka-Likhusha and *Quercus*, *Ulmus*, *Acer*, and *Corylus* (16%) in Voroshilovo. Runa-Zaborovka hillfort differed notably in the composition of charcoals from the other two sites. *Picea* charcoals prevailed (50%) and only few *Pinus* charcoals occurred (6%). *Quercus* charcoals were second in number (26%), but this was the contribution of one soil sample from the archaeological excavation; charcoals of *Ulmus, Acer,* and *Tilia* were absent, while the proportion of *Alnus* (6%) was greater than in the other sites.

In the inner site of Zaborovka-Likhusha hillfort (ZL-1 – ZL-8), *Pinus* charcoals were found throughout the depths; charcoals of *Picea* prevailed in the upper part while *Populus, Betula*, and *Alnus* dominated in the bottom part of the cultural layer (fig. 7). Charcoals of hardwoods, such as *Ulmus, Acer,* and *Tilia,* occurred at depth from 15 to 60 cm; it means they were neither in the upper part, nor under the cultural layer. In soil pit across the ancient moat (ZL-9), only *Pinus* charcoals were found throughout the depths, whereas *Picea* and *Betula* occurred only in the upper sediment layer.

In Voroshilovo hillfort, charcoals of the hardwood species *Quercus, Ulmus*, and *Acer* were found within the cultural layer, except for the upper 15 cm (fig. 8). Charcoals of *Corylus,* on the contrary, was found only to a depth of 15 cm. The taxonomic composition was richest in the lower part of the cultural layer at the level of 45–60 cm (up to 5 taxa in the sample). Thus, in the sample V-6 from the archaeological excavation we found charcoals of *Picea, Populus, Ulmus, Acer,* and *Salix;* in the sample from treefall hillock (V-4) charcoals of *Pinus, Picea,* and *Alnus* were found together with the Dyakovo spindle whorl.

In Runa-Zaborovka hillfort, almost all charcoals were found within the cultural layer, except for a few in the column RZ-2 (fig. 9). *Picea* charcoals dominated in most samples. *Pinus* and *Alnus* were found at different depths. Charcoals of *Quercus* occurred mainly at a depth of 15–30 cm; *Corylus* and *Salix* only in the upper 15 cm.

All taxa diversity indices were highest in Voroshilovo (tabl. 3). They were followed by Runa-Zaborovka

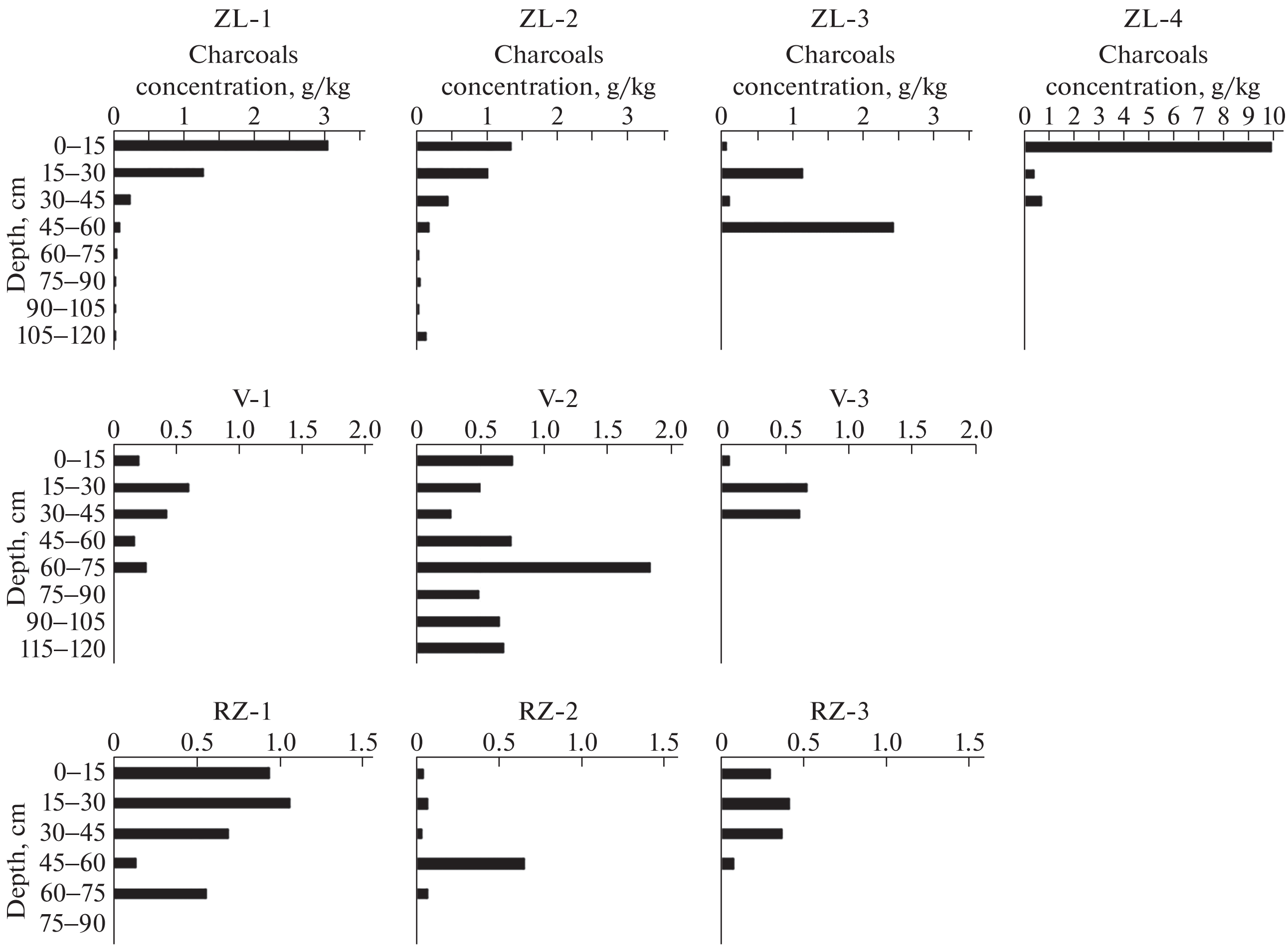


**Fig. 5.** Charcoal concentration in the soil cores taken in the inner sites of hillforts.
**Рис. 5.** Концентрация древесного угля в образцах, взятых на внутренних площадках городищ (обозначения в тексте).

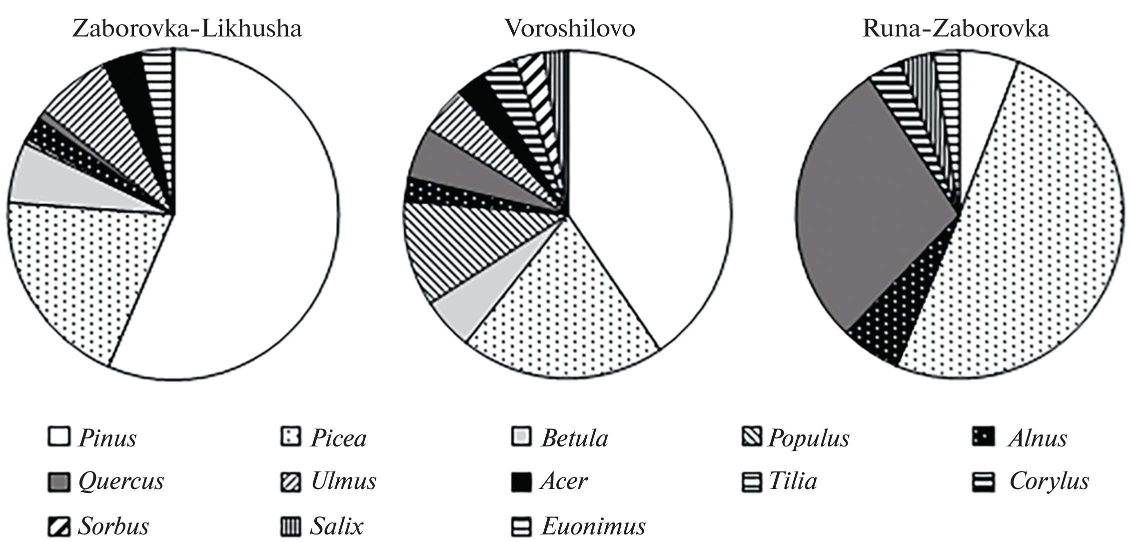


**Fig. 6.** Taxonomical composition of soil charcoals from the hillforts.
**Рис. 6.** Таксономический состав углей из культурного слоя городищ.

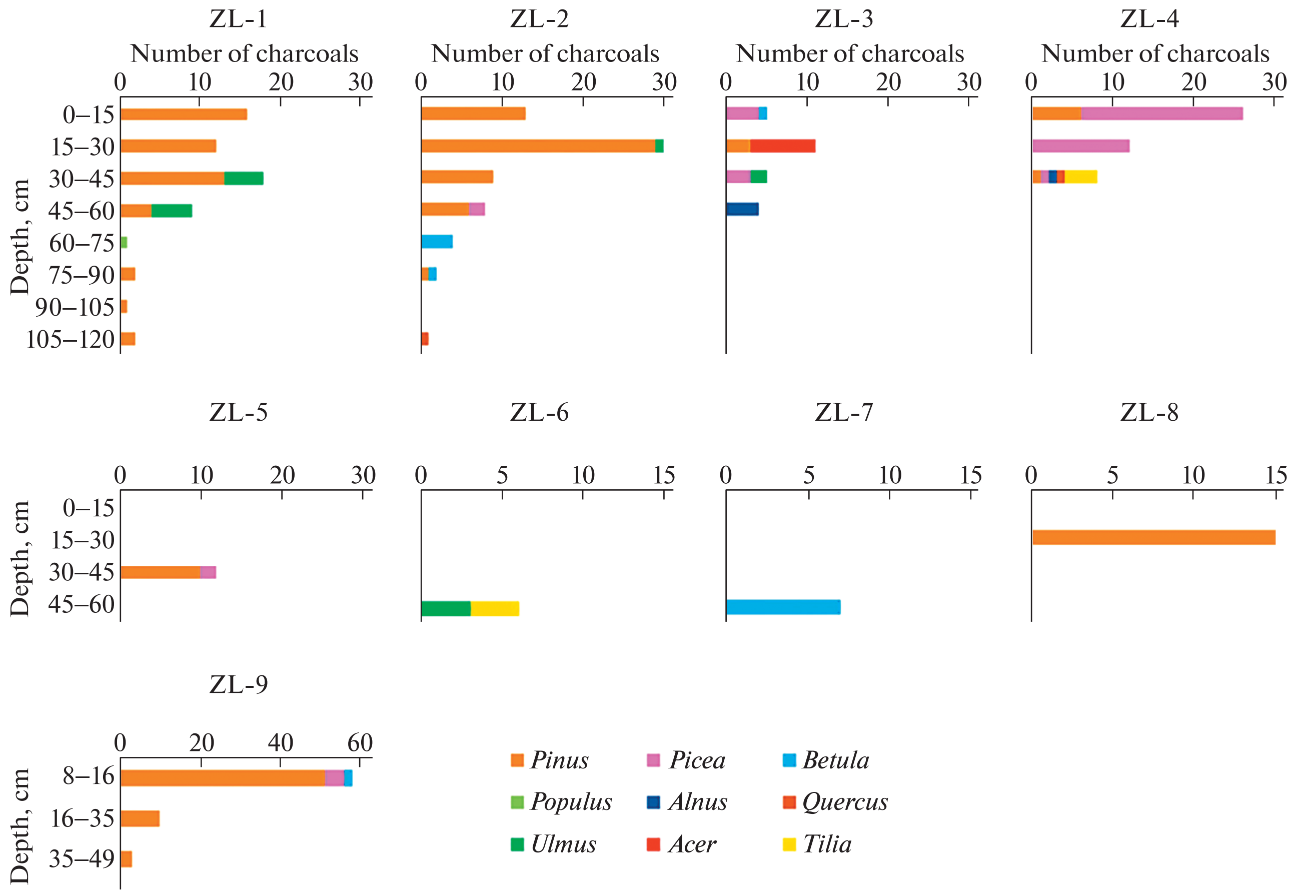


**Fig. 7.** The number of charcoals of different taxa in Zaborovka-Likhusha hillfort.
**Рис. 7.** Число углей разных таксонов в культурном слое городища Заборовка-Лихуша.

indices with the exception of the taxa richness, which was lower in Runa-Zaborovka (7 taxa) than in Zaborovka-Likhusha (9 taxa), probably due to twice as many samples in the latter. Simpson's index shows that dominance was the highest in Zaborovka-Likhusha.

*Radiocarbon dating of soil charcoal samples.* In Zaborovka-Likhusha hillfort the oldest date was obtained for charcoal from the burnt wooden structure from the lower part of the cultural layer (from a depth of 55 cm), about 296 cal. BC (IGANAMS-7118, tabl. 4, fig. 10). A relatively close date was obtained from the sediment at the bottom of the moat (IGANAMS-7297). The third date belonging to the Early Iron Age was obtained for charcoal from the soil core from the depth of 15–30 cm (IGANAMS-8075). Thus, for Zaborovka-Likhusha hillfort, the dates within the Early Iron Age were in the interval from 3rd c. BC to 1st c. AD. Three more dates fell on the early Middle Ages, 7th–8th cc. AD. There were two samples from the cultural layer: charcoal from the archaeological excavation from 35 cm depth (IGANAMS-7119) and from the soil core at 45–60 cm depth (IGANAMS-8075). Also charcoal from the second (16–35 cm) sediment layer in the moat under the hillfort (IGANAMS-7298) belong to this period. The calibrated age of charcoal from the

**Table 3.** Taxa diversity of charcoals from the cultural layers of hillforts
**Таблица 3.** Таксономическое разнообразие древесных углей из культурных слоев городищ

| Hillfort | Taxa richness | Taxa density | Shannon's diversity index | Simpson's diversity index | Number of samples with charcoals |
|---|---|---|---|---|---|
| Zaborovka-Likhusha | 9 | 1.6 | 0.27 | 0.83 | 29 |
| Voroshilovo | 11 | 2.9 | 0.84 | 0.51 | 17 |
| Runa-Zaborovka | 7 | 2.1 | 0.44 | 0.75 | 13 |

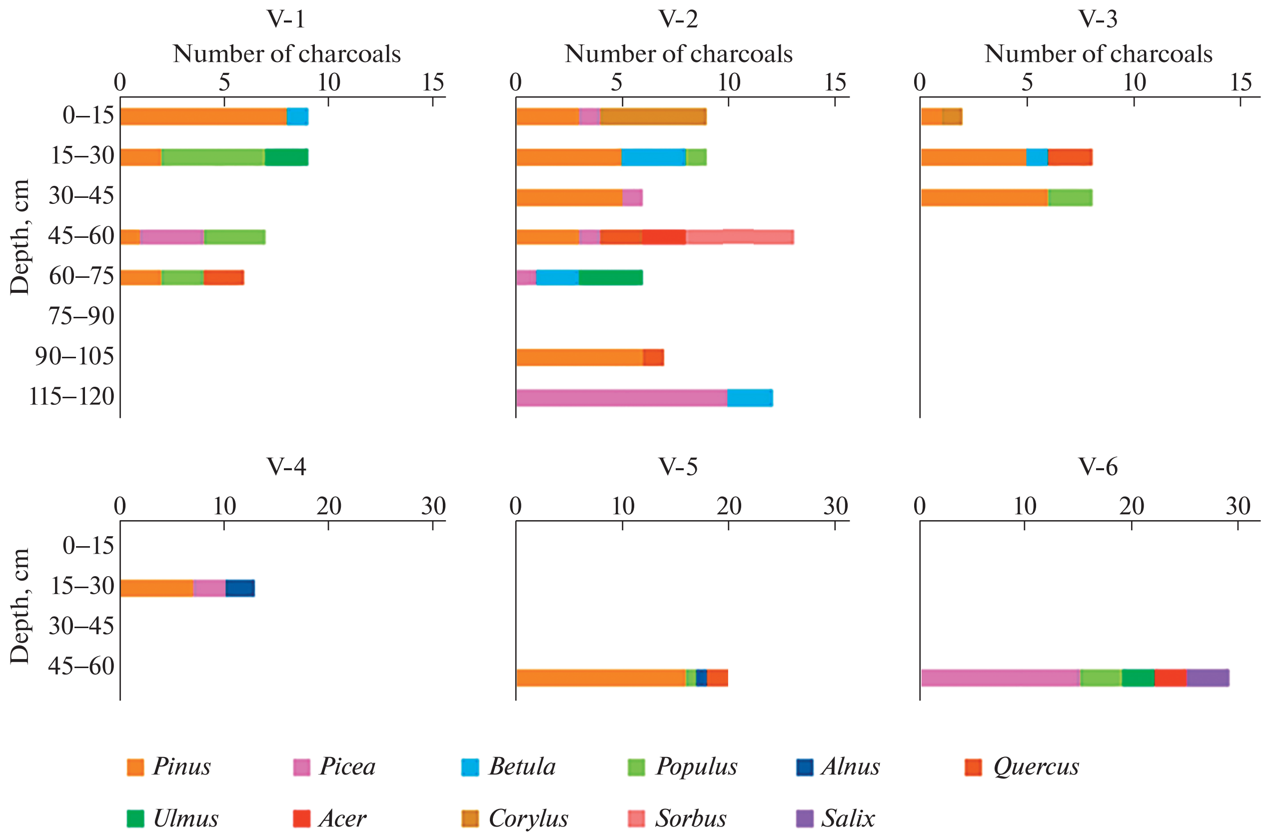


**Fig. 8.** The number of charcoals of different taxa in Voroshilovo hillfort.
**Рис. 8.** Число углей разных таксонов в культурном слое городища Ворошилово.

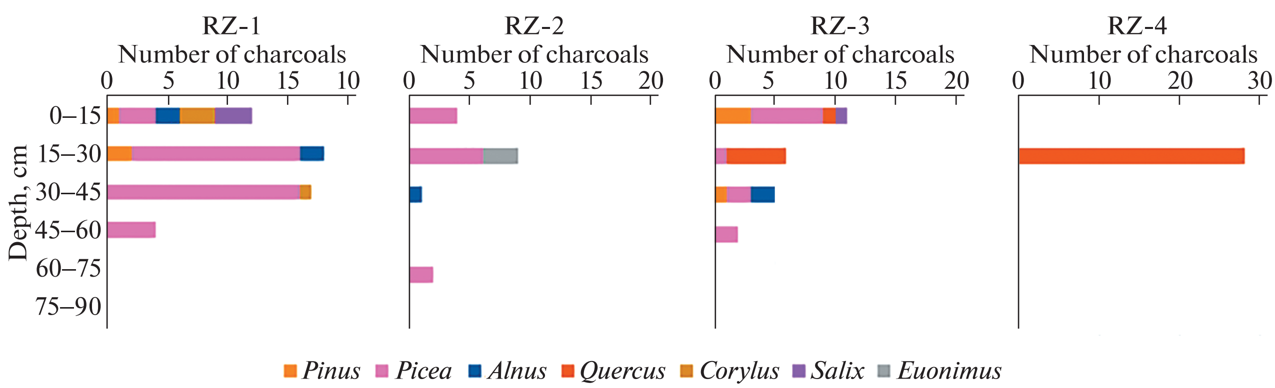


**Fig. 9.** The number of charcoals of different taxa in Runa-Zaborovka hillfort.
**Рис. 9.** Число углей разных таксонов в культурном слое городища Руна-Заборовка.

upper sediment layer in the moat (IGANAMS-7299) corresponded to 16th–17th cc. AD.

For Voroshilovo hillfort, all 4 radiocarbon dates fell within the interval of the Early Iron Age (tabl. 4, fig. 10). The oldest date for all samples was obtained from charcoal from a soil core at the depth of 105–120 cm (IGANAMS-8084) and corresponded to ca. 4th–3rd cc. BC. Since the charcoals were located deeper than the cultural layer, it is unknown whether their origin is related to the existence of the hillfort. Charcoals from the lower part of the cultural layer dated from 1st c. BC up to 1st c. AD: charcoals were from the archaeological excavation at 45–60 cm depth (IGANAMS-7293) and from the soil core at 70–75 cm depth (IGANAMS-8083). The earliest date of charcoal from the core at 15–30 cm depth (IGANAMS-8082) corresponded to ca. 4th c. AD.

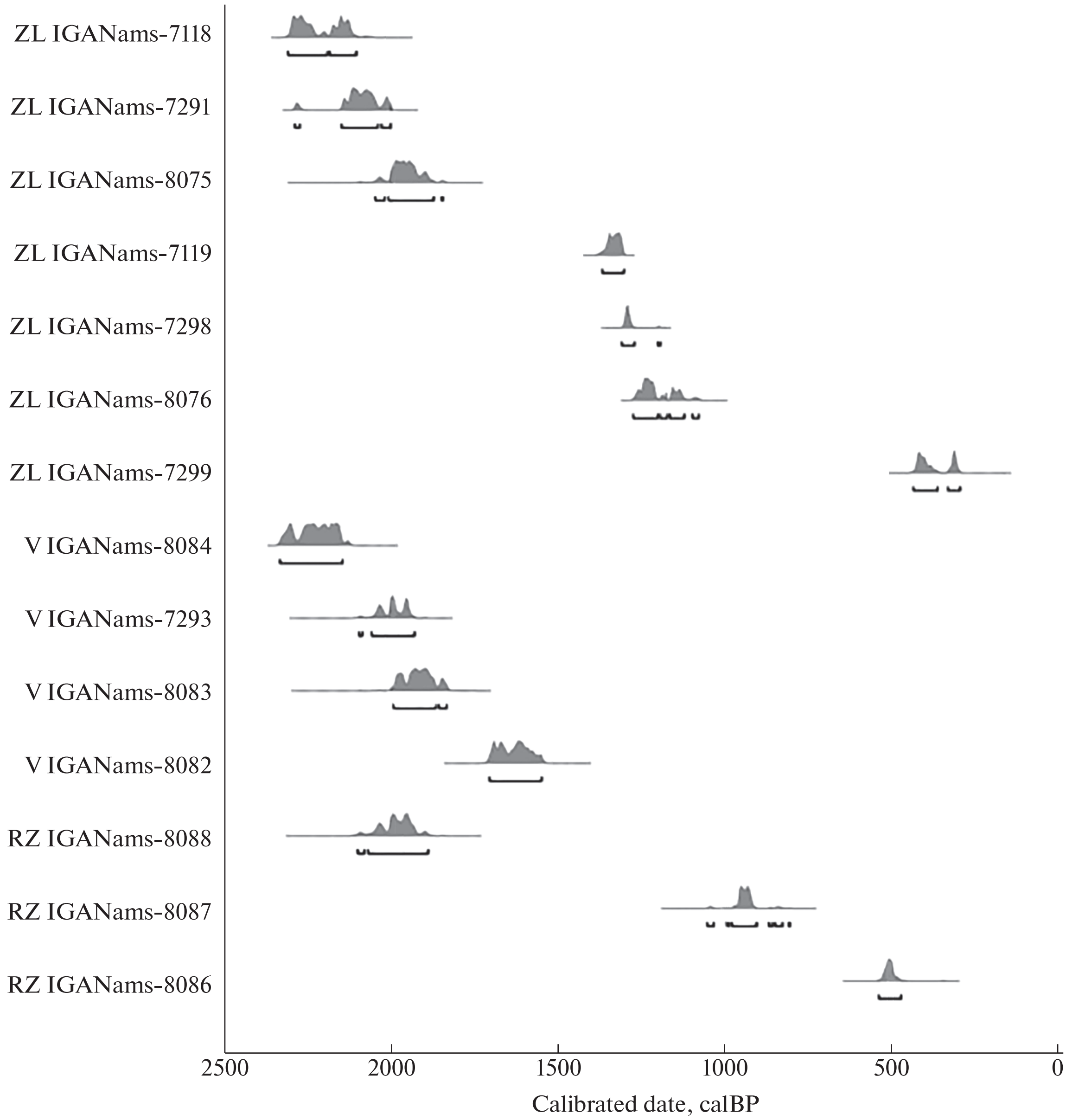


**Fig. 10.** Probability curves of calibrated radiocarbon dates for soil charcoals from the hillforts: ZL – Zaborovka-Likhusha, V – Voroshilovo, RZ – Runa-Zaborovka.

**Рис. 10.** Вероятностные кривые калиброванных радиоуглеродных дат для углей из культурного слоя городищ: ZL – Заборовка-Лихуша, V – Ворошилово, RZ – Руна-Заборовка.

For Runa-Zaborovka hillfort, all dated charcoals were taken from soil cores (tabl. 4, fig. 10). The sample from 60–75 cm depth (IGANAMS-8088) was located below the cultural layer and contained a significant number of charcoal fragments. Its calibrated age corresponded to the interval from 1st c. BC up to 1st c. AD. The calibrated dates of charcoals from the cultural layer from a depth of 15–30 cm corresponded to ca. 11th c. AD, from a depth of 0–15 cm to 15th–16th cc. AD.

On the whole, the burning activities in the studied sites can be represented as three main clusters: about 2000, 1300, and 500 cal. BP (fig. 11).

Due to a small number of dated charcoal samples, we can perform only a preliminary reconstruction of historical dynamics of woody taxa in the area of hillforts studied (fig. 12). Based on 12 radiocarbon samples of 209 charcoals belonging to 11 taxa, it can be concluded that *Pinus* charcoal dominated all the time, followed by *Picea* which increased from Early Iron Age to High-Late Middle Ages. For the Early Iron Age, there was the greatest number of taxa: 9 woody species including *Quercus, Ulmus*, and *Acer*. For Early Middle Ages, four taxa, including *Ulmus*, were registered. For

**Table 4.** Radiocarbon dates for charcoals from the hillforts calibrated according (to Reimer et al., 2013)
**Таблица 4.** Радиоуглеродные даты древесных углей из городищ, калиброванные (по Reimer et al., 2013)

| Identi-ficator | Sampling | Horizon | Depth, cm | Material | Lab. Code | Lab. radiocarbon age (BP) | Cal. radiocarbon age (BP) |
|---|---|---|---|---|---|---|---|
| Zaborovka-Likhusha hillfort | | | | | | | |
| ZL-1 | Auger sampling | Axp | 45–60 | Charcoal | $IGAN_{AMS}$-8076 | 1250 ± 20 | 2310–2104 |
| ZL-2 | Auger sampling | Axp | 15–30 | Charcoal | $IGAN_{AMS}$-8075 | 2020 ± 30 | 2289–2002 |
| | Archaeological excava-tion | Axp | 55 | Charcoal (burnt con-struction) | $IGAN_{AMS}$-7118 | 2180 ± 25 | 2047–1844 |
| | Archaeological excava-tion | Axp | 35 | Charcoal | $IGAN_{AMS}$-7119 | 1450 ± 20 | 1367–1302 |
| ZL-9 | Soil pit | M1(AxpB) | 8–16 | Charcoal | $IGAN_{AMS}$-7299 | 290 ± 20 | 1308–1192 |
| ZL-9 | Soil pit | M2(AxpB) | 16–35 | Charcoal | $IGAN_{AMS}$-7298 | 1360 ± 20 | 1274–1078 |
| ZL-9 | Soil pit | M3(AxpB) | 35–49 | Charcoal | $IGAN_{AMS}$-7297 | 2125 ± 20 | 433–294 |
| Voroshilovo hillfort | | | | | | | |
| V-1 | Auger sampling | Axp | 15–30 | Charcoal | $IGAN_{AMS}$-8082 | 1740 ± 30 | 2334–2146 |
| V-2 | Auger sampling | Axp | 60–75 | Charcoal | $IGAN_{AMS}$-8083 | 1985 ± 30 | 2097–1930 |
| V-2 | Auger sampling | BC | 105–120 | Charcoal | $IGAN_{AMS}$-8084 | 2220 ± 30 | 1993–1833 |
| V-5 | Archaeological excava-tion | Axp | 45–60 | Charcoal | $IGAN_{AMS}$-7293 | 2050 ± 20 | 1705–1549 |
| Runa-Zaborovka hillfort | | | | | | | |
| RZ-1 | Auger sampling | Axp | 0–15 | Charcoal | $IGAN_{AMS}$-8086 | 450 ± 30 | 2100–1889 |
| RZ-2 | Auger sampling | Axp | 15–30 | Charcoal | $IGAN_{AMS}$-8087 | 1030 ± 30 | 1051–804 |
| RZ-2 | Auger sampling | BC | 60–75 | Charcoal | $IGAN_{AMS}$-8088 | 2040 ± 30 | 537–470 |

High and Late Middle Ages, there were 6 taxa: apart from *Pinus* and *Picea* these were *Betula, Alnus, Corylus*, and *Salix*.

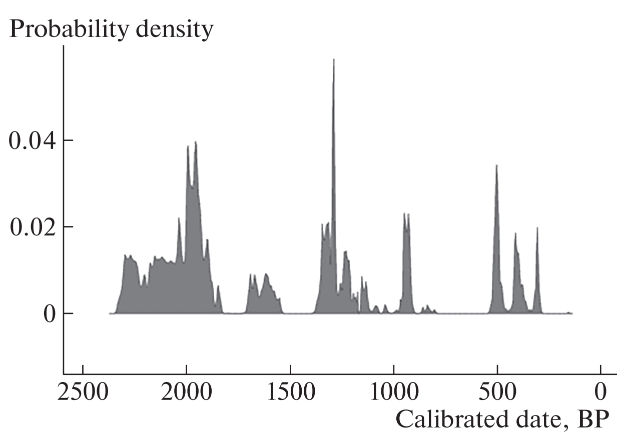


**Fig. 11.** Cumulative probability curve of calibrated radiocarbon dates for soil charcoal from the hillforts.

**Рис. 11.** Кумулятивная кривая вероятности калиброванных радиоуглеродных дат для углей из культурных слоев исследованных городищ.

## 5. DISCUSSION

There are several common features of the studied hillforts. The geomorphological basis for the fortified settlements was a cape of moraine hill, at the foot of which there was at least one water stream. The shape of the hillfort when viewed from above was closest to an oval. The cultural layer was from 50 to 80 cm thick, dark-colored and filled with fine charcoal particles. Quality characteristics of the cultural layers of the hillforts allow us to refer them to the category of archaeological Dark Earths (Anthropogenic Dark Earths, ADE), which are poorly stratified dark-colored soils, usually rich in charcoal and other anthropogenic inclusions.

As at many sites of the Dyakovo culture (Krenke, 2011) and at later archaeological sites with similar soils (Sedov et al., 1999; Ershova et al., 2020), the Early Iron Age layer is often overlapped by later cultural layers. The thickness of the cultural layer varies greatly. For example, in Gnezdovo the thickness of ADE soil ranges from 20 to 150 cm (Sedov et al., 1999; Trofimov et al., 2004).

In recent years, ADEs have been investigated across Europe (Devos et al., 2009, 2019; Ackcel et al.,

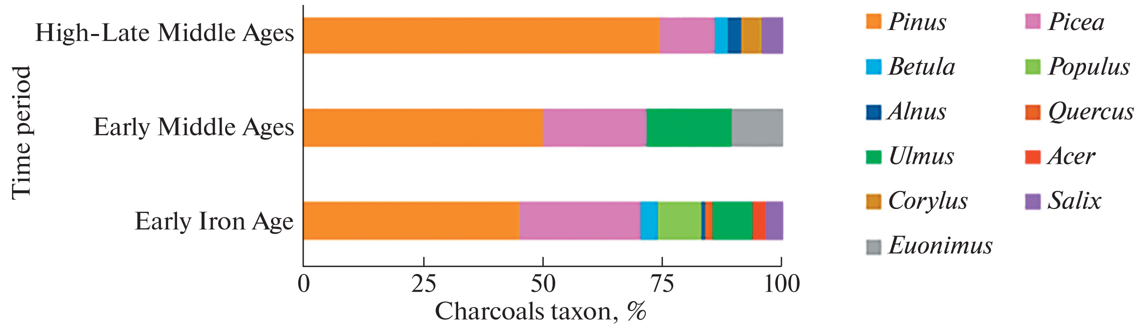


**Fig. 12.** Proportions of charcoals of different taxa from the studied hillforts by the historical periods: Early Iron Age from 5th c. BC to 5th c. AD, Early Middle Ages from 6th to 10th cc. AD, and High and Late Middle Ages from 11th to 16th cc. AD.

**Рис. 12.** Соотношение углей разных таксонов из исследованных городищ по историческим периодам: ранний железный век (5 в. до н. э. – 5 в. н. э.), раннее средневековье (6–10 вв. н. э.), высокое и позднее средневековье (11–16 вв. н. э.).

2017; Dotterweich, Schreg, 2019; Negassa et al., 2019; Asare et al., 2021). Dark Earths are common in settlement areas throughout much of Europe, but predominate in northern Europe, where they are sometimes referred to as “Baltic black earths”. The formation of these soils began between 3800 and 2000 BC (Acksel et al., 2017), but the formation of most Dark Earths is attributed to the Viking and Northern Slavic economy in the 1st millennium CE (Wiedner et al., 2015). The properties of these soils have been attributed to the long-term application of organic waste, charcoal, and fecal matter (Acksel et al., 2016). The existence of Dark Earths demonstrates the ability of sandy soils in the European climate to retain a high content of organic matter for hundreds of years when economic use is discontinued. Although the origin of Dark Earths is closely related to settlements, there is speculation that it was used for plant cultivation (gardening) (Wiedner et al., 2015). In this case, such soils may have been an important component of the economy.

The peculiarities of ADE in the investigated sites are their location on the modern surface, absence of obvious signs of late anthropogenic influences, and the existence of forest at the sites for at least the last centuries. Both the age of charcoals in the cultural layer and the archaeological findings (primarily textile pottery) show that the main thickness of the ADE at the hillforts of Zaborovka-Likhusha and Voroshilovo was formed in the Early Iron Age.

For Zaborovka-Likhusha hillfort, the interval of ADE formation was ca. 300 cal. BC – 10 cal. AD, corresponding to Early Iron Age (500 BC – 500 AD). However, in Zaborovka hillfort, we can also assume human activity in the Early Middle Ages, accompanied by possible reconstruction of the hillfort and its use. This is indicated both by an episode of erosion of material with charcoals (sediment in the moat) around 610 cal. AD, and charcoals in the cultural layer around 730 cal. AD. The sediment in the moat with charcoals of about 1580 cal. AD may be related both to the fire and more likely to local human activity on the hillfort (no archaeological findings later than Early Iron Age were found). The cultural layer of Zaborovka-Likhusha had the most obvious (among all three sites) signs of soil mixing, which can include reversion of dates (occurrence of charcoals of the same period at different depths and younger charcoals deeper than the older ones) and variability of the charcoal concentration by depth.

For Voroshilovo hillfort, the time of ADE formation can be attributed to 70 cal. BC – 320 cal. AD. Charcoal of about 300 cal. BC were also encountered at the Voroshilovo site, for which no connection with the cultural layer was established. There were no significant visible signs of soil mixing within the main ADE thickness.

For Runa-Zaborovka hillfort, it is most difficult to attribute the time of ADE formation. The charcoals of about 30 cal. BC were located deeper than the cultural layer. The findings of smooth-walled (Smirnov et al., 2021) date the time of the formation of the hillfort to the Early Medieval period, and the date of about 1010 cal. AD from the middle of the depth of the cultural layer refers to the end of this period. The charcoals on the surface date to about 1440 cal. AD, it is difficult to associate them with a specific activity because no archaeological findings from this time have been found.

Thick Anthropogenic Dark Earths are the result of complex interactions of anthropogenic and natural factors lasting at least several centuries. It is impossible to identify these factors without detailed archaeological excavations, which are so far the task of future research.

The diversity of tree taxa described at the hillforts seems to be high for the southern taiga region, in the area of modern pine forest dominance with a relatively poor species composition. According to the stratigraphy of charcoals and the taxonomic composition of dated samples, the greatest species richness was peculiar to the Early Iron Age. The greatest diversity of hardwood tree species was also detected for this time.

Often for Europe, a decrease in species diversity or even a complete change of species complexes is noted based on the results of studies of charcoals in soils and archaeological sites (Bobek et al., 2019). This is especially the case in mountainous areas (Benatti et al., 2019; Saulnier et al., 2020; Tolksdorf et al., 2020).

For the loess areas of southern Poland, a comparison was made of charcoal complexes from archaeological sites between the Neolithic period, the Early and Middle Bronze Age (Moskal-del Hoyo, 2021). There was no change in species, only a change in their participation, but there was probably a change in plant communities. The species composition depended to a greater extent on the landscape: important regional differences between, on one hand, the loessic uplands and the forelands, and, on the other, the foothills were shown. A large-scale study was carried out by Novák et al. (2021) for lowlands in the Czech Republic, analyzing charcoal records from 474 localities. A significant differentiation in the dynamics of taxa between different landscapes there was shown. The smallest changes were noted for landscapes with the predominance of *Quercus* and high abundance of *Pinus*. The Late Holocene woodland transformation was related to the migration trends of *Carpinus, Fagus,* and *Abies*; the activity of changes decreases from west to east.

There were no changes in the species composition and migration of woody species in the Late Holocene in our study area, either from charcoal records or from pollen data (Mazei et al., 2020). All our charcoal findings of species are within their current distribution areas, but as noted in the study area section, some tree species are rare in the region (*Acer* and *Ulmus*), especially as mature trees. At the same time, almost all genera of trees whose ranges cover the study area, except for ash (*Fraxinus*), were found as charcoal.

The reasons for the presence of certain species in the form of charcoal in the cultural layer are always the result of several factors, such as the availability of the tree species, its economic function, and the features of wood burning and charcoal preservation (Novenko et al., 2009).

The principle of least effort, assuming that charcoal frequency direct reflects the prevalence of woody taxa, has usually been used to interpret the results of charcoal findings. However, as Rubiales et al. (2011) noted, charred remains are the final result of diverse human activities; consequently, archaeological charcoals are not haphazardly distributed by the sole effect of climatic and environmental conditions. In our study, it is likely that most of the charcoals are firewood; some (probably small) portion may belong to burnt buildings. As far as can be judged from the soil cores and archaeological excavations, there were no obvious areas of confined charcoal concentration, although the thickness of the cultural layer and charcoal concentrations varied. The charcoals were found in the cultural layer throughout the studied area. It is probably the result of long-term burning of wood, horizontal movement of charcoals, and vertical pedoturbations. In general, these are the mechanisms of the formation of all ADEs, but the elucidation of specific factors requires detailed study.

We can talk about a significant and likely dominant participation of *Pinus* in the area of the studied hillforts. In the areas of Zaborovka-Likhusha and Voroshilovo, the occurrence of *Pinus* and its probably significant participation in the stands was recorded already at the time of the first burning in the sites in 3rd–1st cc. BC. The presence of a prominent proportion of hardwood charcoals probably indicates their availability and common presence in the vegetation near the hillforts. For *Tilia,* we can assume rather an occasional presence in the composition of firewood. *Quercus* had a very diverse and wide range of uses, including as firewood. However, the use of *Acer* and *Ulmus*, especially the latter, as firewood is not straightforward or cost-effective. The intended use of wood of these species (on a par with *Quercus*) is not excluded when it is necessary to obtain high flame temperatures, for example, in smelting of metals. The significant predominance of *Picea* charcoals in different layers of Runa-Zaborovka hillfort, including in the Early Iron Age, may be evidence of its predominance in the surrounding forests with little participation of other tree species. The use of spruce wood can hardly be considered intentional, as it is not the optimal species for firewood.

The results correlated well with the palynological data obtained from the study of the nearby Krivetsky Mokh bog (Mazei et al., 2020). Hardwood trees have dominated the region since about 9000 cal. BP. Around 4300 cal. BP, the relative abundance of *Picea* and *Pinus* increased. The most notable changes in vegetation occurred at the turn of the Early Iron Age, ca. 2600 cal. BP. From that time, the proportion of *Betula* and *Alnus* increased, while most other deciduous trees (*Tilia, Quercus*, and *Ulmus*) decreased in abundance. *Quercus* further increasing participation, the decrease of *Tilia* and *Ulmus* was irreversible. There is insufficient data to judge the participation and dynamics of *Acer* and *Fraxinus* in the vegetation. The abundance of *Picea* and *Pinus* varied greatly. This time was marked by an increased proportion of *Artemisia* and *Plantago,* as well as other grasses (*Poaceae, Chenopodiaceae*). During this period there was a slight (not strong) increase in charcoal input, but also an increase in the frequency of local fires, which became more regular (about one episode per 250 years) after a large period of their rarity (more than one episode per 1000 years).

The results of a study of another complex of bogs located on Valday Upland to southeast of the region we studied (Central Forest Nature Reserve) showed that significant changes in the vegetation composition occurred there somewhat later, ca. 2000 cal. BP. At this time, the content of *Picea* pollen decreased, the content of pollen of hardwood trees noticeably decreased, and the proportion of *Betula* pollen increased (Novenko et al., 2009).

The information we obtained from the soil charcoal composition is a valuable evidence of the presence of a tree taxon at a particular site at a particular point in time, detailing the reconstruction of the vegetation history in the upper reaches of the Volga River.

## 6. CONCLUSION

Cultural layer of all studied hillforts was presented by Archaeological Dark Earth saturated with charcoal and 50 to 80 cm thick. At Zaborovka-Likhusha hillfort on the basis of charcoal dating, three periods of human activity were identified: (i) from 3rd to 1st c. BC, (ii) from 7th to 8th c. AD, and (iii) 16th c. AD. At Voroshilovo hillfort, two periods were marked: (i) from 3rd c. BC to 1st c. AD and (ii) 4th c. AD. At Runa-Zaborovka hillfort, human activities were in 11th and 15th c. AD while charcoal of 1st c. BC also occurred. Thus the duration of the cultural layer formation was probably hundreds of years; Zaborovka-Likhusha and Voroshilovo hillforts belong to the Early Iron Age (the Dyakovo culture) whereas Runa-Zaborovka hillfort belongs to the Early Middle Ages.

A significant number of woody species taxa (13 genera) were identified in the cultural layer of the hillforts. There were no drastic changes in the composition of the regional species pool, such as the species disappearance. Among the three periods: Early Iron Age (from 5th c. BC to 5th c. AD), Early Middle Ages (from 6th to 10th cc. AD), and High and Late Middle Ages (from 11th to 16th cc. AD), the greatest diversity of woody species genera was recorded for Early Iron Age, where charcoals of *Quercus*, *Ulmus*, *Acer*, and *Populus* were found. Runa-Zaborovka hillfort noticeably differed in the taxonomic composition of charcoals, and there were no archaeological Early Dyakovo finds here.

The sparse network of small hillforts identified in recent years in the Valdai Upland in the northern part of the Peno District of the Tver Region raises questions about how Early Iron Age peoples may have influenced the dynamics of ecosystems and how their life depended on natural conditions. The study of charcoal in other hillforts and in the surrounding soils in the region will make it possible both to estimate the activity of the population in the areas of hillforts and to reveal the peculiarities of the anthropogenic transformation of the adjacent areas.

# WOODLAND DYNAMICS AND HUMAN ACTIVITY BASED ON CHARCOAL ANALYSIS FROM HILLFORTS OF THE IRON AGE AND EARLY MIDDLE AGES IN THE UPPER VOLGA RIVER

**M. V. Bobrovsky**[a,#], **D. A. Kupriyanov**[b,c,##], **A. L. Smirnov**[c,###], **L. G. Khanina**[d,####], **and M. V. Dobrovolskaya**[c,#####]

[a] *Institute of Physicochemical and Biological Problems in Soil Science of RAS, Pushchino Scientific Center for Biological Research of RAS, Pushchino, Russia*

[b] *Lomonosov Moscow State University, Faculty of Geography, Moscow, Russia*

[c] *Institute of Archaeology RAS, Moscow, Russia*

[d] *Institute of Mathematical Problems of Biology RAS, Branch of the Keldysh Institute of Applied Mathematics of RAS, Pushchino, Russia*

[#] *E-mail: maxim.bobrovsky@gmail.com*
[##] *E-mail: dmitriykupriyanov1994@yandex.ru*
[###] *E-mail: ari1828@bk.ru*
[####] *E-mail: khanina.larisa@gmail.com*
[#####] *E-mail: mk_pa@mail.ru*

Soil charcoals in cultural layers of three hillforts located in the upper Volga River (Peno District, Tver Region) were studied in soil cores and archaeological excavations. The characteristics of the cultural layers of the hillforts allow us to refer it to the category of Archaeological Dark Earth with a thickness from 50 to 80 cm. The age of charcoals and archaeological findings showed that the cultural layers of Zaborovka-Likhusha and Voroshilovo hillforts belong to the Early Iron Age (the Dyakovo culture) and Runa-Zaborovka hillfort belongs to the Early Middle Ages. A total of 629 charcoal fragments belonging to 13 woody genera were taxonomically identified. The charcoals of the 12 dated samples were evaluated for changes in the taxonomic composition over time. In all periods, *Pinus* charcoals dominated, followed by *Picea*; their proportions increased from the Early Iron Age to the High-Late Middle Ages. For the Early Iron Age, the largest number of taxa, 9 woody species, including *Quercus, Ulmus,* and *Acer,* was observed. The information obtained from the soil charcoal composition is a valuable evidence of the presence of tree taxa in a particular area at a particular time; it details the reconstruction of the history of vegetation in the upper Volga River.

*Keywords:* pedoanthracology, Archaeological Dark Earth, Dyakovo culture, firewood, radiocarbon dating

ACKNOWLEDGMENTS

The authors are sincerely grateful to Mr. G. A. Lekarev: without his comprehensive assistance, consultations and hospitality the fieldworks could never be implemented. The work was supported by Russian Science Foundation, project No. 22-28-01761.

## REFERENCES

Acksel A., Amelung W., Kühn P., Gehrt E., Regier T., and Leinweber P. Soil organic matter characteristics as indicator of Chernozem genesis in the Baltic Sea region. *Geoderma Regional*. 2016. Vol. 7. No. 2. P. 187–200. https://doi.org/10.1016/j.geodrs.2016.04.001

Acksel A., Kappenberg A., Kühn P., and Leinweber P. Human activity formed deep, dark topsoils around the Baltic Sea. *Geoderma Regional*. 2017. Vol. 10. P. 93–101. https://doi.org/10.1016/j.geodrs.2017.05.005

Asare M.O., Horák J., Šmejda L., Janovský M., and Hejcman M. A medieval hillfort as an island of extraordinary fertile Archaeological Dark Earth soil in the Czech Republic. *European Journal of Soil Science*. 2021. Vol. 72. No. 1. P. 98–113. https://doi.org/10.1111/ejss.12965

Benatti A., Bal M., Allée P., Bosi G., and Mercuri A.M. Plant landscape reconstruction above the current timberline at the Monte Cimone and Corno alle Scale mountain areas (Northern Apennines, Italy) during the Late Holocene: The evidence from soil charcoal. *Holocene*. 2019. Vol. 29. No. 11. P. 1767–1781. https://doi.org/10.1177/0959683619862033

Benkova V.E. and Schweingruber F.H. Anatomy of Russian Woods. An Atlas for the Identification of Trees, Shrubs, dwarf Shrubs and Woody Lianas from Russia. Bern: Etc. Haupt Verlag, 2004. 456 p.

Bobek P., Svobodová-Svitavská H., Pokorný P., Šamonil P., Kune P., Kozáková R., Abraham V., Klinerová T., Švarcová M.G., Jamrichová E., Krauseová E., and Wild J. Divergent fire history trajectories in Central European temperate forests revealed a pronounced influence of broadleaved trees on fire dynamics. *Quaternary Science Reviews*. 2019. Vol. 222. P. 105865. https://doi.org/10.1016/j.quascirev.2019.105865

Carcaillet C. and Talon B. A view of the wood charcoal stratigraphy and dating in soil: a case study of some soils from the French. *Géographie physique et Quaternaire*. 1996. Vol. 50. No. 2. P. 233–244.

Carcaillet C. and Thinon M. Pedoanthracological contribution to the study of the evolution of the upper treeline in the Maurienne Valley (North French Alps): methodology and preliminary data. *Review of Palaeobotany and Palynology*. 1996. Vol. 91. No. 1–4. P. 399–416. https://doi.org/10.1016/0034-6667(95)00060-7

Devos Y., De Groote K., Moens J., and Vrydaghs L. Facing complexity: An interdisciplinary study of an early medieval Dark Earth witnessing pasture and crop cultivation fromthe centre of Aalst (Belgium) Soils as records of past and Present. From soil surveys to archaeological sites: research strategies for interpreting soil characteristics. *Raakvlak*. 2019. P. 159–171. http://doi.org/10.5281/zenodo.3420729

Devos Y., Vrydaghs L., Degraeve A., and Fechner K. An archaeopedological and phytolitarian study of the "Dark Earth" on the site of Rue de Dinant (Brussels, Belgium). *Catena*. 2009. Vol. 78. No. 3. P. 270–284. https://doi.org/10.1016/j.catena.2009.02.013

Dotterweich M. and Schreg R. Archaeonics-(Geo) archaeological studies in Anthropogenic Dark Earths (ADE) as an example for future-oriented studies of the past. *Quaternary International*. 2019. Vol. 502. P. 309–318. https://doi.org/10.1016/j.quaint.2018.09.026

Eremeev I.I. and Dzyuba O.F. *Ocherki istoricheskoi geografii lesnoi chasti. Puti iz varyag v greki. Arkheologicheskie i paleogeograficheskie issledovaniya mezhdu Zapadnoi Dvinoi i ozerom Il'men'* (Essays on the historical geography of the forest part of the Way from the Varangians to the Greeks. Archaeological and paleogeographic research between the Western Dvina and Lake Ilmen). St. Petersburg: Nestor-Istoriya (Publ.), 2010. 670 p. (in Russ.)

Ershova E.G., Alexandrovskiy A.L., and Krenke N.A. Evolution of landscapes of the Moskva River floodplain in the Atlantic and Subboreal: Pedological and palynological records. *Catena*. 2016. Vol. 137. P. 611–621. https://doi.org/10.1016/j.catena.2014.12.034

Ershova E.G., Alexandrovskiy A.L., and Krenke N.A. Paleosols, paleovegetation and Neolithic occupation of the Moskva River floodplain, Central Russia. *Quaternary International*. 2014. Vol. 324. P. 134–145. https://doi.org/10.1016/j.quaint.2014.01.031

Ershova E.G., Krenke N.A., Kittel P., and Lavrenov N.G. Archaeological sites in the Katynka river basin (Smolensk Region). *IOP Conference Series: Earth and Environmental Science*. 2020. Vol. 438. No. 1. P. 012007. https://doi.org/10.1088/1755-1315/438/1/012007

Figueiral I. Wood resources in north-west Portugal: their availability and use from the late Bronze Age to the Roman period. *Vegetation History and Archaeobotany*. 1996. Vol. 5. No. 1. P. 121–129. https://doi.org/10.1007/BF00189442

Islanova I.V. *Drevnosti v verkhov'yakh Volgi (rannii zheleznyi vek i rannee srednevekov'e)* (Antiquities in the Upper Volga (Early Iron Age and Early Middle Ages). Moscow: IA RAN (Publ.), 2012. 219 p. (in Russ.).

Islanova I.V. *Kul'turno-istoricheskie protsessy vo II–VIII vv. n. e. v basseinakh Verkhnei Volgi i Verkhnei Msty* (Cultural and historical processes in the II–VIII centuries AD in the Upper Volga and Upper Msta basins). *PhD thesis*. Moscow: IA RAN (Publ.), 2020. 51 p. (in Russ.)

Islanova I.V. *Poseleniya rannego zheleznogo veka na Verkhnei Volge (istochnikovaya baza)* (Settlements of the early Iron Age on the Upper Volga (source base)). *Kratkie soobshcheniya Instituta arkheologii*. 2014a. Vol. 233. P. 46–54. (in Russ.).

Islanova I.V. *Pozdned'yakovskie pamyatniki tipa Varvarina Gora* (Late Dyakovo monuments of the Varvarin Gora type). *Rossiiskaya arkheologiya*. 2017. Vol. 2. P. 115–129. (in Russ.)

Islanova I.V. *Problemy izucheniya drevnostei I tys. n. e. Verkhnego Povolzh'ya i Valdaya* (Problems of studying antiquities of the 1st millennium AD. Upper Volga and Valdai). *Voprosy medievistiki*. 2013. Vol. 51. P. 54–61. (in Russ.)

Islanova I.V. *Voprosy izucheniya d'yakovskikh drevnostei Verkhnevolzh'ya i Valdaya* (Questions of studying the Dyakovo antiquities of the Upper Volga and Valdai). *Rossiiskaya arkheologiya*. 2014b. Vol. 1. P. 14–19. (in Russ.)

IUSS Working Group. World reference base for soil resources 2014 (update 2015), international soil classification system for naming soils and creating legends for soil maps. *World Soil Resources Reports*. 2015. Vol. 106.

Krenke N.A. *Drevnosti basseina Moskvy-reki ot neolita do srednevekov'ya: etapy kul'turnogo razvitiya, formirovanie proizvodyashchei ekonomiki i antropogennogo landshafta* (Antiquities of the Moskva River basin from the Neolithic to the Middle Ages: stages of cultural development, the formation of a productive economy and an anthropogenic landscape). Smolensk: Svitok (Publ.), 2019. 392 p. (in Russ.)

Krenke N.A. *D'yakovo gorodishche: kul'tura naseleniya basseina Moskvy-reki v I tys. do n. e. – I tys. n. e.* (Dyakovo settlement: culture of the population of the Moskva River basin in the 1st millennium BC. – I millennium AD). Moscow: IA RAN (Publ.), 2011. 546 p. (in Russ.)

Krenke N.A., Kazansky M., Lopatin N.V., Ganichev K., Ershov I.N., Ershova E., Modestov F.E., and Raeva V.A. *Gorodishcha Demidovka i Vyazoven'ki na Smolenshchine: ob ierarkhii, khronologii i kul'turnoi atributsii* (Settlements of Demidovka and Vyazovenki in the Smolensk region: about hierarchy, chronology and cultural attribution). *Rossiiskaya arkheologiya*. 2021. Vol. 1. P. 140–159. (in Russ.).
https://doi.org/10.31857/S086960630013711-1

Lopatina O.A. *Keramika moskvoretskikh i okskikh pamyatnikov d'yakovskoi kul'tury kak istoricheskii istochnik* (Ceramics of the Moskvoretsky and Oka monuments of the Dyakovo culture as a historical source). *PhD thesis*. Moscow: IA RAN (Publ.), 2019. 31 p. (in Russ.)

Magurran A.E. Measuring biological diversity. *Blackwell Science Ltd*. 2004. 272 p.

Masi A., Balossi Restelli F., Sabato D., Vignola C., and Sadori L. Timber exploitation during the 5th–3rd millennia BCE at Arslantepe (Malatya, Turkey): environmental constraints and cultural choices. *Archaeological and Anthropological Sciences*. 2018. Vol. 10. No. 2. P. 465–483. https://doi.org/10.1007/s12520-017-0499-0

Mazei Yu., Tsyganov A., Bobrovsky M., Mazei N., Kupriyanov D., Gałka M., Rostanets D., Khazanova K., Stoiko T., Pastukhova Yu., Fatynina Yu., Komarov A., Babeshko K., Makarova A., Saldaev D., Zazovskaya E., Dobrovolskaya M., and Tiunov A. Peatland development, vegetation history, climate change and human activity in Valdai Uplands (Central European Russia) during the Holocene: A multi-proxy palaeoecological study. *Diversity*. 2020. Vol. 12. No 12. P. 462.
https://doi.org/10.3390/d12120462

Moskal-del Hoyo M. Open canopy forests of the loess regions of southern Poland: A review based on wood charcoal assemblages from Neolithic and Bronze Age archaeological sites. *Quaternary International*. 2021. Vol. 593. P. 204–223.
https://doi.org/10.1016/j.quaint.2020.11.013

Negassa W., Acksel A., Eckhardt K.U., Regier T., and Leinweber P. Soil organic matter characteristics in drained and rewetted peatlands of northern Germany: Chemical and spectroscopic analyses. *Geoderma*. 2019. Vol. 353. P. 468–481.
https://doi.org/10.1016/j.geoderma.2019.07.002

Nelle O., Robin V., and Talon B. Pedoanthracology: analysing soil charcoal to study Holocene palaeoenvironments. *Quaternary International*. 2013. Vol. 289. P. 1–4.
https://doi.org/10.1016/j.quaint.2012.11.024

Novák J., Kočárová R., Kočár P., and Abraham V. Long-term history of woodland under human impact, archaeoanthracological synthesis for lowlands in Czech Republic. *Quaternary International*. 2021. Vol. 593. P. 195–203.
https://doi.org/10.1016/j.quaint.2020.10.054

Novenko E.Y., Volkova E.M., Nosova M.B., and Zuganova I.S. Late Glacial and Holocene landscape dynamics in the southern taiga zone of East European Plain according to pollen and macrofossil records from the Central Forest State Reserve (Valdai Hills, Russia). *Quaternary International*. 2009. Vol. 207. No. 1–2. P. 93–103.
https://doi.org/10.1016/j.quaint.2008.12.006

O'Donnell L. Woodland dynamics and use during the Bronze Age: New evidence from Irish archaeological charcoal. *Holocene*. 2017. Vol. 27. No. 8. P. 1078–1091.
https://doi.org/10.1177/0959683616683252

Ohlson M., Ellingsen V.M., del Olmo M.V., Lie M.H., Nybakken L., and Asplund J. Late-Holocene fire history as revealed by size, age and composition of the soil charcoal pool in neighbouring beech and spruce forest landscapes in SE Norway. *Holocene*. 2017. Vol. 27. No. 3. P. 397–403.
https://doi.org/10.1177/0959683616660174

Ramsey C.B. Bayesian analysis of radiocarbon dates. *Radiocarbon*. 2009. Vol. 51. No. 1. P. 337–360.
https://doi.org/10.1017/S0033822200033865

Reimer P.J., Bard E., Bayliss A., Beck J.W., Blackwell P.G., Bronk Ramsey C., Buck C.E., Cheng H., Edwards R.L., Friedrich M., Grootes P.M., Guilderson T.P., Haflidason H., Hajdas I., Hatté C., Heaton T.J., Hoffmann D.L., Hogg A.G., Hughen K.A., Kaiser K.F., Kromer B., Manning S.W., Niu M., Reimer W., Richards D.A., Scott E.M., Southon J.R., Staff R.A., Turney C.S.M., and van der Plicht J. IntCal13 and Marine13 radiocarbon age calibration curves, 0–50,000 Years cal BP. *Radiocarbon*. 2013. Vol. 55. P. 1869–1887.
https://doi.org/10.2458/azu_js_rc.55.16947

Rubiales J.M., Hernández L., Romero F., and Sanz C. The use of forest resources in central Iberia during the Late Iron Age. Insights from the wood charcoal analysis of Pintia, a Vaccaean oppidum. *Journal of Archaeological Science*. 2011. Vol. 38. No. 1. P. 1–10.
https://doi.org/10.1016/j.jas.2010.07.004

Ruiz-Giralt A., Bouchaud C., Salavert A., Lancelotti C., and D'andrea A.C. Human-woodland interactions during the Pre-Aksumite and Aksumite periods in northeastern Tigray, Ethiopia: insights from the wood charcoal analyses from Mezber and Ona Adi. *Veg. Hist. Archaeobot*. 2021. Vol. 30. No. 6. P. 713–728.
https://doi.org/10.1007/s00334-021-00825-2

Saulnier M., Cunill Artigas R., Foumou L.F., Buscaino S., Métailié J.P., Galop D., and Py-Saragaglia V. A study of late Holocene local vegetation dynamics and responses to land use changes in an ancient charcoal making woodland in the central Pyrenees (Ariège, France), using pedoanthracology. *Vegetation History and Archaeobotany*. 2020. Vol. 29. No. 2. P. 241–258. https://doi.org/10.1007/s00334-019-00740-7

Sedov S.N., Zazovskaya E.P., Bronnikova M.A., Kazdim A.A., and Rosov S.Y. Late Holocene man-induced environmental change in central Russian plain: paleopedological evidences from early-medieval archaeological site. *Chinese Science Bulletin*. 1999. Vol. 44. P. 159.

Smirnov A.L., Menshikov M.Yu., Bobrovsky M.V., Kupriyanov D.A., Kleshchenko E.A., Svirkina N.G., Tiunov A.V., and Dobrovolskaya M.V. *Rasselenie i istoricheskie landshafty na zapade Valdaya v rannem zheleznom veke i srednevekov'e* (Settlement and historical landscapes in the west of Valdai in the early Iron Age and the Middle Ages). *Rossiiskaya arkheologiya*. 2021. Vol. 3. P. 80–96. (in Russ.). https://doi.org/10.31857/S086960630013168-3

Smirnova O.V., Bobrovsky M.V., and Khanina L.G. (Eds.) European Russian Forests. Their Current State and Features of Their History. S*pringer Netherlands,* 2017. 566 p.

Syrovatko A.S. *Yugo-vostochnoe Podmoskov'e v zheleznom veke: k kharakteristike lokal'nykh variantov d'yakovskoi kul'tury* (South-Eastern Moscow Region in the Iron Age: to the Characteristics of Local Variants of the Dyakovo Culture). Moscow: CheBuk (Publ.), 2009. P. 28–35. (in Russ.)

Syrovatko A.S., Panin A.V., Troshina A.A., and Semenyak N.S. *Rol' paleotopografii i landshaftno-klimaticheskikh izmenenii v formirovanii Shchurovskogo arkheologicheskogo kompleksa* (The role of paleotopography and landscape-climatic changes in the formation of the Shchurovsky archaeological complex). *Arkheologiya Podmoskovya*. 2016. Vol. 12. P. 53–63. (in Russ.)

Talon B., Payette S., Filion L., and Delwaide A. Reconstruction of the long-term fire history of an old-growth deciduous forest in Southern Québec, Canada, from charred wood in mineral soils. *Quaternary Research*. 2005. Vol. 64. P. 36–43. https://doi.org/10.1016/j.yqres.2005.03.003

Théry-Parisot I., Chabal L., and Chrzavzez J. Anthracology and taphonomy, from wood gathering to charcoal analysis. A review of the taphonomic processes modifying charcoal assemblages, in archaeological contexts. *Palaeogeography, Palaeoclimatology, Palaeoecology*. 2010. Vol. 291. No. 1–2. P. 142–153. https://doi.org/10.1016/j.palaeo.2009.09.016

Tolksdorf J.F., Kaiser K., Petr L., Herbig C., Kočár P., Heinrich S., Wilke F.D.H., Theuerkauf M., Fülling A., Schubert M., Schröder F., Křivánek R., Schulz L., Bonhage A., and Hemker C. Past human impact in a mountain forest: geoarchaeology of a medieval glass production and charcoal hearth site in the Erzgebirge, Germany. *Regional Environmental Change*. 2020. Vol. 20. No. 3. P. 1–20. https://doi.org/10.1007/s10113-020-01638-1

Trofimov S.Y., Yakimenko O.S., Sedov S.N., Dorofeeva E.I., Gorshkova E.I., Zazovskaya E.P., Dorofeeva E.I., Oleinik S.A., Gorshkova E.I., and Demin V.V. Composition and properties of organic matter in the soils of ancient Slavic settlements in the forest zone. *Eurasian Soil Science*. 2004. Vol. 37. No. 9. P. 927–936.

Uspensky P.S. and Chaukin S.N. *Areal gorodishch d'yakova tipa* (The area of hillforts of the Dyakov type). *Kratkie soobshcheniya Instituta arkheologii*. 2016. Vol. 242. P. 71–80. (in Russ.)

Veksler A.G. and Gusakov M.G. *K voprosu pozdnei stadii D'yakovskoi kul'tury* (To the question of the late stage of the Dyakovo culture). *Arkheologiya Evraziiskikh stepei*. 2017. Vol. 4. P. 257–286 (in Russ.).

Wiedner K., Schneeweiß J., Dippold M.A., and Glaser B. Anthropogenic dark earth in northern Germany – The nordic analogue to terra preta de indio in Amazonia. *Catena*. 2015. Vol. 132. P. 114–125. https://doi.org/10.1016/j.catena.2014.10.024

**EDN:** XLFYRM
*ГЕОМОРФОЛОГИЯ, 2022, том 53, № 5, с. 25–31*

## ПРОБЛЕМЫ ПАЛЕОПОЧВОВЕДЕНИЯ И ГЕОАРХЕОЛОГИИ

*551.89:574→631.42:902/904 (470.333)*

# ДЕТАЛЬНАЯ ПАЛЕОЭКОЛОГИЧЕСКАЯ ЛЕТОПИСЬ ВАЛДАЙСКОГО КРИОХРОНА (МИС 4–2) ИЗ ПОЧВЕННО-ОСАДОЧНОЙ СЕРИИ СРЕДНЕПАЛЕОЛИТИЧЕСКОГО ПАМЯТНИКА ХОТЫЛЁВО I

**© 2022 г. М. А. Коркка[1,2,*], Т. В. Романис[3,4], Л. А. Савельева[1], С. Н. Седов[5,6,7], А. К. Очередной[8]**

[1]*Санкт-Петербургский государственный университет, Институт наук о Земле, Санкт-Петербург, Россия*
[2]*Институт географии РАН, Москва, Россия*
[3]*Почвенный институт имени В.В. Докучаева, Москва, Россия*
[4]*Институт мерзлотоведения имени П.И. Мельникова СО РАН, Якутск, Россия*
[5]*Институт геологии, Национальный автономный университет Мексики, Дель. Койоакан, Мехико, Мексика*
[6]*Институт криосферы, ФИЦ "Тюменский Научный центр" СО РАН, Тюмень, Россия*
[7]*Тюменский государственный университет, Тюмень, Россия*
[8]*Институт истории материальной культуры РАН, Санкт-Петербург, Россия*
**E-mail: maria.a.korkka@gmail.com*

Поступила в редакцию 14.06.2022 г.
После доработки 27.06.2022 г.
Принята к публикации 15.07.2022 г.

Группа разновременных среднепалеолитических памятников Хотылёво I расположена в Брянской области, в 400 км к юго-западу от Москвы в верхнем течении р. Десны. В 2021 г. в рамках работ на разрезе № 3 Хотылёво I была уточнена стратиграфия почвенно-осадочной серии последней ледниковой эпохи. В разрезах представлены почвы последнего макро-цикла МИС 5а–с – МИС 3 (датирование OSL, AMS). Почвы МИС 5 расположены в нижней части разреза, слабо дифференцированы и включают артефакты разного возраста, различающиеся по степени сохранности культурных отложений, их культурной принадлежности и интенсивности обитания человека. Почвы МИС 3 представлены в виде нескольких уровней почвообразования. Одна из почв (почва IV возраст 34.1–32.7 тыс. лет $^{14}$C) имеет полный набор генетических горизонтов, не нарушенных криогенезом (похожие почвы описаны в Германии и Австрии), AO-E-Bw-Bk-BCk, современным аналогом которой являются палевые почвы (Cambic Cryosol) Якутии. Формироваться эта почва должна была в экстраконтинентальном семиаридном климате под таежными лесами. Тем не менее в разрезах Хотылёво I палеопочва IV отражает и последующий этап гумидизации климата, что выражено во вторичном оглеении горизонтов профиля и находит отражение в результатах спорапыльцевого анализа. В целом разрез 3 Хотылёво I сохраняет подробную палеопочвенную запись, отражающую даже кратковременные климатические колебания.

*Ключевые слова:* средний палеолит, Хотылёво I, Микок/KMG, палеопочвы, средний Валдай, палевая почва, МИС 3

**DOI:** 10.31857/S0435428122050066

## 1. INTRODUCTION

An important objective in the research of the paleoenvironment of the last cryochron on the territory of the East European Plain continues to be the detailed study of the paleosols of that period. The longest and most favorable interval for vegetation and soil formation during the last half-cycle correlates with marine isotope stage 3 (MIS 3). Undoubtedly, under the conditions of a cryochron, pedogenesis was restricted by rather harsh climate, but, nonetheless, various sections demonstrate soil-sedimentary sequences with several levels of MIS 3 soils, some of which have rhythmic structure. In general, such sections are described in gully deposits, where accumulating colluvium regularly interrupted pedogenesis. These soils are thin, poorly developed and their structure is disturbed by cryogenic processes (Sycheva, Khokhlova, 2015; Korkka et al., 2017a; Korkka et al., 2017b). Sometimes these multiple events of soil development can be correlated with the Greenland interstadials (Haesaerts et al., 2010).

Only one MIS 3 soil level is usually preserved in sections at flat upland landsurfaces. In Russian literature this soil is called the Bryansk paleosol. This pa-


**Fig. 1.** The scheme of Khotylevo I site locations.
**Рис. 1.** Схема расположения разрезов на памятнике Хотылёво I.

leosol has a well-formed soil profile disturbed by cryogenic deformations. It is described in detail in the works of A. Velichko and colleagues and included as a marker of the MIS 3 level in his East European loess stratigraphy (Velichko, 1990). A similar situation is observed in most European Late Pleistocene upland loessic sequences: MIS 3/Middle Pleniglacial is represented mostly by one or two well-developed paleosols (Stillfried B in Austria, PK1 in Czech Republic, Lohne in Germany, etc.) (Kadereit et al, 2013; Terhorst et al., 2015). The relation of these paleosols to the multiple contrasting climatic fluctuations during MIS 3 is still under discussion. In particular, the hypothesis of their polygenetic nature was formulated (Sedov et al., 2013). S.A. Sycheva and O.S. Khokhlova supposed that pedogenesis of the Bryansk paleosol occurred not only during MIS 3, but also extended into early MIS 2, during which cryogenic features were acquired (Sycheva, Khokhlova, 2015). We described a loess-soil sequence of the last cryochron in the sections of the Khotylevo I site in which a full-profile MIS 3 soil is diagnosed. The horizons of this soil have polypedogenetic features and are not deformed by pseudomorphs along ice wedges from the Vladimir cryogenic horizon (LGM). Soil profile preservation of the Khotylevo I site is comparable to the soils of Western Europe located on watersheds and is a distinguishing difference from the MIS 3 paleosols of the loess-soil sequences described on the territory of Russia.

## 2. OBJECTIVES AND METHODS

The Khotylevo I archaeological site is located at the northern boundary of the Khotylevo Village in Bryansk Oblast’, approximately 20 km west of Bryansk city center and 400 km southwest of Moscow (fig. 1).

The site includes a complex of Middle Paleolithic cultural horizons and cultural layers of different ages varying in the extent of preservation of deposits, their cultural appurtenance, and human habitation intensity within each identified cultural horizon. According to preliminary data, most of the cultural horizons could have Micoquian/KMG (*Keilmessergruppe*) assemblages. The overall length of the site along the right bank of the Desna River is up to 1 km, making it one of the largest Middle Paleolithic sites in Eastern Europe (Otcherednoy, Voskresenskaya, 2009; Korkka et al., 2017a).

The objects of study are loess-soil sequences Section 3 and Section Kryuchka. They are located in the middle of the northern slope, at an elevation of about 150 m a.s.l. The pedogenetic levels of these sections are morphologically similar. These paleosols and sediments are described and sampled. We collected bulk samples for physical and chemical laboratory analyses, and undisturbed soil samples were taken from the genetic horizons for thin sections. However, in this article we describe morphology in detail as the most important basis for subsequent paleogeographic interpretation of the data. Most of the data presented herein are for Section 3. We used morphological data from Section Kryuchka to confirm the distribution of the described pedogenic levels over a significant area of Middle Paleolithic Khotylevo I sites. Soils and horizons were identified using the World Reference Base for Soil Resources 2014, update 2015.

The comparative geographic and soil stratigraphic methods were used in this work. For absolute dating the AMS dating method was applied (humified lenses from soils III and IV were dated).

Preliminary results of a pollen analysis were obtained from soil IV. Nine samples were collected from horizons AO-E-Bw and one from the thickness overlapping the soil. Samples were taken with 1.5–4.0 cm intervals and prepared applying standard chemical treatment with 10% HCl and NaOH and heavy liquid separation (Grichuk, Zaklinskaya, 1948). To estimate pollen concentrations, two tablets containing a known concentration of *Lycopodium* spores were added to each sample prior to preparation (Stockmarr, 1971). Non-pollen palynomorphs were identified, when possible, on the pollen slides. The mass of each sample ranged from 10 to 20 g.

## 3. RESULTS

*Stratigraphy.* In 2021, within the scope of the work at one of the areas of the Khotylevo I site (Section 3), the stratigraphy of a soil-sedimentary sequence of the last ice age was clarified, including MIS5a-5c and MIS3 soils (fig. 2, (a, b)). The section is positioned in the middle of the northern slope of a promontory which points at the Desna (fig. 2, (c)). The high bedrock coast of the river is composed of Late Cretaceous rock: Cenomanian quartz-glauconite sands with phosphorite inclusions overlapped by Turonian marly chalky rock with concretions of grayish black flint. The thickness of the profile is approximately 20 meters.

The section can be nominally divided into three blocks (from top to bottom).

1. Late Valday loams (fig. 2, (a), depth 0.0–5.2 m) slightly more than 5 m thick. Poorly layered, homogenous, light greenish gray. A modern Holocene Luvisol is formed within, and a cultural layer of a settlement dating to the XIII – XVII centuries is documented.

2. A Middle Valday soil-sedimentary sequence (fig. 2, (a), soil I–IV), 4.5 m thick, consisting of four unrelated soil levels. A detailed description of this unit is provided below:

– 5.2 m. Poorly developed soil I, with horizons AB-Bk-BG, well-pronounced in all section walls. The soil inherits the properties of underlying loess-like loams, is gleyed (light olive horizon, ferruginization in root channels). All horizons are pierced by worm burrows, the maximum of which is seen in horizon AB. Horizon Bk is lightened with powder carbonates. Horizon BG is dense, extensively gleyed. The soil is underlaid by poorly gleyed loess-like loams.

– 5.5 (5.8) m. Another poorly developed soil (soil II) consisting of two soil formation rhythms divided by Middle Valday loess-like loams. Soils with horizons AB-Bk which are similar in color and density inherit a hummock relief (the diameter of a “mound” is about 20 cm). The thickness of each rhythm is approximately 30 cm. The transition from the below soil layer to underlying loams is gradual, the boundary is very wavy. The soils are underlaid by loess-like loams with weak signs of gleiing.

– 6.1 (6.6) m. Soil III (AMS date 27.8–26.7 $^{14}$C kyr BP) as a dark gray, humified thickness 40–60 cm thick. Disturbed in the upper part by several generations of small wedges (up to 20 cm) from overlying loess-like loams. In the central part abundant humified, very dark gray lenses untouched by cryogenesis are preserved. Overwetting is noted in Fe-Mn concretions, ferruginous and olive brown spots. In the bottom part the soil level includes lenses of yellow underlying sand. No genetic relation between the organic and underlying horizons has been determined. Supposedly, the humified horizon slid from higher hypsometric levels in more humid periods.

– 6.6 (7.7) m. A redeposited loamy sand material from the underlying soil presenting as humified, peated lenses integrated into the remains of horizon Bw.

– 7.7 (8.2) m. Soil IV – Middle Valday polygenetic paleosol AO-E-Bw-Bk-BCk (fig. 2, (b)). Horizons AO-E present as thin redeposited lenses 20–30 cm thick. Horizon AO is black, peated, with inclusions of charcoal.

Horizon E is light gray, sandified. Dessication cracks tinted by humified material protrude from AO-E lenses into lower horizons Bw and Bk.

Horizon Bw (25–30 cm thick) is dark yellowish brown, slightly loamy.

Horizon Bk (50–60 cm thick) is moderately loamy, dense, with powder carbonates. Insignificantly disturbed by a network of cracks. Uniformly present in all section walls. Gleyed. Bioturbated (krotovinas). Heterogeneous in color (from light brownish gray to light yellowish brown). The transition to the horizon below presents as lenses and krotovinas, the boundary is straight.

Horizon BCk (20–30 cm thick) is a thin-layered, yellowish brown loamy sand. Gleyed zones and carbonate coating are seen in root channels. The thickness of soil IV is 120 cm.

– 8.9 m. Very pale brown sandy layered unit 2.5 m thick.

3. Early Valday deposits corresponding to OSL dating results (Hein et al., 2020) and interstadial soils formed within them. In the upper part the unit of loess-like loams (approximately 2.5 m thick) is a light olive gray color. Underneath them is a unit of layered (interlayers of loam and loamy sand) crumpled loamy sands (approximately 2.5 m thick) overlapping paleohorizons. The unit is underlaid by marly chalky colluvium with inclusions of sandy lenses and layers (the thickness is approximately 1.5 m). Further down, Cenomanian sand begins.

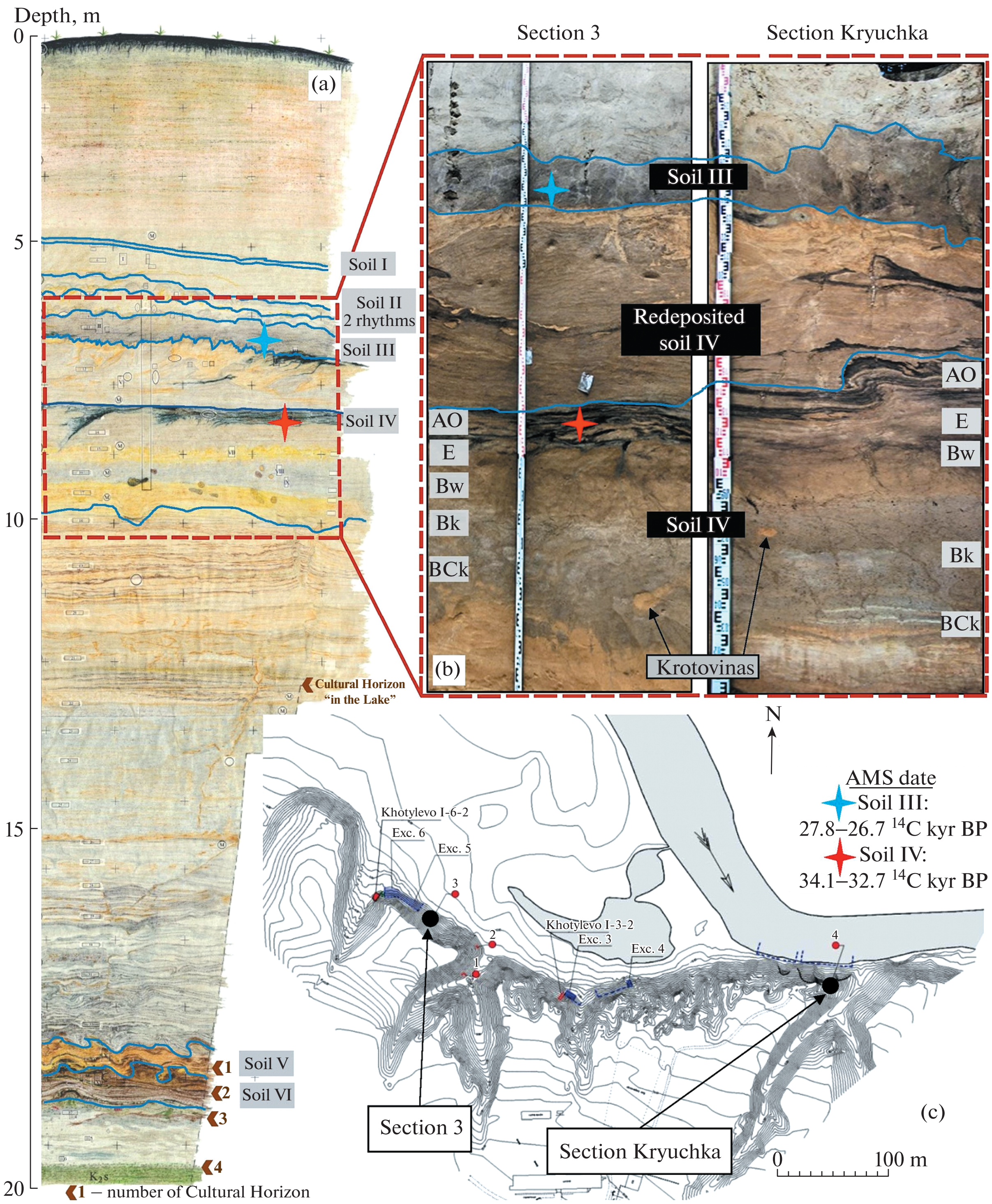


**Fig. 2.** Position of the Middle Valday polygenic paleosol: on the principal scheme of Section 3 ((a) – based on the results of work from 2019, 2021) and the photos of sections 3 and Kryuchka (b) with the indication of their position on the relief (c).

**Рис. 2.** Положение средневалдайской палеопочвы: на принципиальной схеме разреза 3 ((a) – по результатам работ 2019, 2021 годов) и фотографиях разреза № 3 и разреза Крючка (b) с указанием их расположения на рельефе (c).

The paleosols of this block are presented by two levels of soil formation separated by an interlayer of olive gray sand. Loamy sandy soil V, 30–50 cm thick, presents as very dark gray, dark gray, reddish brown and dark yellowish brown layers. The soil is pushed in the direction of the river channel by 60–90 cm.

Soil VI, 20–30 cm thick, light brownish gray, with abundant inclusions of marl, chalk and flint debris, is underlaid by heavy chalky loams. The soil is extensively crumpled by underlying rock.

Data on the stratigraphy of Section 3 which were obtained in 2021 can be compared to Section Kryuchka, which was established in 2013 in the exposure of the promontory (more than 300 m down the course of the Desna River from Section 3) (fig. 2, (c)). There is no preserved record of the paleoecological environment during the Early Valday time in Section Kryuchka, but there are two main levels of Middle Valday paleosols which match in morphology those described by us in Section 3 (fig. 2, (b)). A brief description of this section is provided below, seeing as the material has not been published previously:

1. Late Valday loams approximately 2 m thick, in which a modern highly eroded Holocene Luvisol is described.

2. 1.9 (2.1) m. Middle Valday loess-like loams. In the upper part of the unit (on the boundary with Early Valday deposits) there are signs of residual soil formation (stands out in color, leftover soil structure, light gleiing).

– 2.4 (2.5) m. Paleosol (analogous to soil III of Section 3) presenting as a grayish brown humified thickness which is heterogeneous in color (zones of very dark gray or grayish brown material), up to 50 cm thick, saturated with Fe-Mn mottles, nodules and soft concretions, ferruginous spots. Like in soil III of Section 3, the upper part of the thickness is disturbed by small cryogenic wedges filled with material from the loess unit above. It is underlaid by a layered loamy sand horizon (interlayers of fine and coarse sand) of a yellow color.

– 3.4 (3.8) m. Paleosol with horizons AO-E-Bw-Bk-BCk, which match the horizons of soil IV from Section 3: horizons AO and E present as lenses (the result of sliding) from 2 to 30 cm thick. The color is very dark gray (AO) and light yellowish brown (E). Charcoal is present in the lenses. Horizon E was fragmentally preserved under the lenses. Heterogeneous, very pale brown, 10–15 cm thick. The transition to horizon Bw is noticeable. The thickness of Bw is approximately 30 cm. It is pierced by dessication cracks from the overlapping horizon. Dark yellowish brown. There are many Fe-Mn soft concretions and mottles, nodules. Bw is well-pronounced stratigraphically. The transition is abrupt, the boundary is straight. Horizon Bk, approximately 70 cm thick, consists of two subhorizons: an upper light greenish gray one and a lower light brownish gray one. In the lower part the material is lighter, sometimes layered (interlayers from horizon BCk below). Pierced by Fe-Mn soft concretions and mottles, nodules. Pale olive gleyification spots and carbonate veins and filaments are present. Many krotovinas are present. The horizon is disturbed by a network of cracks. The transition is gradual, the boundary is straight. The BCk horizon is layered, loamy sandy, grayish brown. Fe-Mn mineral concentrations occur in soft segregation.

– 5.1 (5.3) m. A unit of layered very pale brown sands.

– 7.2 (7.5) m. Cenomanian sand.

*Archaeological context.* Comprehensive study of the paleogeographic conditions of the Khotylevo I archaeological site allows us to clarify the structure of the lower alluvial thickness containing a series of human habitation levels, the extent of its preservation, confirm the location of some of the Middle Paleolithic cultural horizons (CH) in situ. In the bottom part of Section 3 four CH of varying extents of preservation, with Middle Paleolithic tools and debitage, were documented:

CH 1 presents primarily as cores and different-sized flakes, as well as infrequent findings of bones. All tools in CH 1 are situated in accordance with the angles of the slope of displaced soil V tongues;

CH 2 is composed of small areas of concentration of debitage, with individual cores and their fragments, areas of concentration seen in CH 2 are situated subhorizontally on the surface and within soil VI;

CH 3 was documented on exposed areas in a displaced condition in lenses and interlayers of carbonate loams and loamy sands which are part of the composition of marly chalky colluvium which underlies soil VI, among the findings it is necessary to highlight expressive tool shapes, which indicates that the given cultural horizon belongs to the Micoquian/KMG;

CH 4 is the most structurally complex in the cultural horizon series of Section 3. The tool set and specific debitage from this cultural horizon also indicate that it belongs to the Micoquian/KMG of Eastern and Central Europe.

In Section Kryuchka, the Khotylevo I site is presented only by the cultural horizon situated in alluvial deposits which overlap the thickness of Cenomanian sand. The characteristics of the cultural layer match CH 4 both in terms of location conditions and assemblage composition.

*Palynology (Soil IV).* Pollen and spores were absent or presented by single grains of *Betula nana*, *Salix*, Poaceae pollen and *Botrychium* sp. spores in loamy sand samples. In peaty (organic-rich) samples from horizon AO pollen and spores were presented in insignificant amounts, from 15 to 80 grains per slide, and their total concentration varied from 172 to 2800 grains $g^{-1}$. Such extremely low grain concentration is observed in sediments of different genesis which formed during cold conditions in the past. For example, between 200 and 5000 pollen grains $g^{-1}$ were registered in bottom deposits of Lake Ladoga, which were sedimented during the Younger Dryas stadial (Savelieva et al., 2019). The poorly preserved pollen (mineralized, flattened, crumpled) dominated in all analyzed samples.

Herb pollen presented mainly by Poaceae and poorly preserved tricolpate pollen, which could not be identified more specifically, dominated in the pollen spectra of peaty samples. *Artemisia*, Asteraceae, Brassicaceae, Cyperaceae pollens are also presented in the spectra, as well as shrub pollen of *Betula nana* and *Salix*. Single grains of *Botrychium* sp. and *Huperzia* sp. are noted among spores.

## 4. DISCUSSION

The obtained composition of pollen spectra, poor preservation of pollen grains and the presence of aquatic non-pollen palynomorphs allow us to suppose that the formation of the top soil horizons occurred in floodplain conditions. The pollen results possibly indicate cold conditions and open landscapes with a dominance of grasses and meadow herbs within the studied area, as well as the dwarf birch and willow. The pollen results may also indicate vegetation of the latest stage of the development of the paleosol and the beginning of significant cooling.

In Section Kryuchka and in the top part of Section 3 the most preserved soils have a common morphological structure, similar secondary properties and matching sedimentary layers. The main feature of the sections is the presence of a well-preserved Middle Valday paleosol with a complete set of genetic horizons, the closest modern equivalent of which are the palevye (pale) soils, or Cambic Cryosols (according to WRB (IUSS Working Group WRB, 2015)), of Yakutia. These soils form under conditions of extracontinental semi-arid climate on the territory of the middle taiga zone. Cambic Cryosols have weak cryoturbation (or no cryoturbation at all) and a carbonate Bk and dark yellowish brown Bw horizons. Based on the same indicators (middle horizons, minimal cryoturbation), we can attribute our soil (AO-E-Bw-Bk-BCk) to the Cambic Cryosol of Yakutia. At the same time, this soil's profile is polygenetic and inherits the change in climate: from a Cambic Cryosol, which forms under cryo-arid conditions underneath taiga vegetation, with powder carbonates and krotovinas, to a Gleysol (IUSS Working Group WRB, 2015), with a peated humus horizon and secondary gleiing of the profile. Similar Cambic Cryosols of the middle of the last cryochron which are undisturbed by cryogenic deformations are described in Germany and Austria. These soils correlate with the Cambic Cryosol we describe in the sections of the Khotylevo I archaeological site.

The Middle Valday soils of the East European Plain which have been described by numerous authors are disturbed by cryogenic deformations of the LGM (for example, the Middle Valday soils of the Alexandrovskiy quarry). Usually, these soils are located close to the modern surface, and in some cases are even part of contemporary pedogenesis. The Bryansk paleosols in Khotylevo I sections differ in the absence of signs of secondary cryogenesis in the soil profile. Our hypothesis is that this may be related to the magnitude of the thickness of the overlapping deposits, which have preserved the Middle Valday soils and kept their full genetic profile intact, spatially dividing the stages of pedo- and cryogenesis. The obtained results serve as evidence that, owing to high deposition rates and the development of weak sliding slope processes, a detailed paleosol record reflecting short-term climatic fluctuations has survived in Khotylevo I sections.

# DETAILED PALEOENVIRONMENTAL RECORD FOR THE VALDAY CRYOCHRON (MIS 4-2) FROM THE SOIL-SEDIMENTARY SEQUENCE OF THE MIDDLE PALAEOLITHIC SITE KHOTYLEVO I

**M. A. Korkka[a,b,#], T. V. Romanis[c,d], L. A. Savelieva[a], S. N. Sedov[e,f,g], and A. K. Otcherednoy[h]**

[a] *Saint Petersburg State University, Institute of Earth Sciences, Saint Petersburg, Russia*

[b] *Institute of Geography RAS, Moscow, Russia*

[c] *Dokuchaev Soil Science Institute, Moscow, Russia*

[d] *Melnikov Permafrost Institute, Yakutsk, Russia*

[e] *Instituto de Geología, Universidad Nacional Autónoma de México, Del. Coyoacán, Mexico*

[f] *Earth Cryosphere Institute, Tyumen Scientific Centre SB RAS, Tyumen, Russia*

[g] *Tyumen State University, Tyumen, Russia*

[h] *Institute for the History of Material Culture RAS, Saint Petersburg, Russia*

[#] *E-mail: maria.a.korkka@gmail.com*

Khotylevo I, one of the largest Middle Paleolithic sites in Eastern Europe, is located in Bryansk Oblast', 400 km southwest of Moscow, in the upper course of the Desna River. The site's sections are presented by soil-sedimentary deposits of the last macro-cycle MIS 5-MIS 1 (OSL, AMS dating). Paleosols of varying degrees of preservation have matching pedofeatures and stratigraphic patterns throughout the area.

In the bottom part of the sections, soils MIS 5 a-c contain a group of areas of different ages varying in the extent of preservation of cultural deposits, their cultural appurtenance and human habitation intensity. The MIS 3 soil presents as several levels of soil formation. One of the soils (soil IV, AMS date 34.1–32.7 $^{14}$C kyr BP) has a full set of genetic horizons undisturbed by cryogenesis (similar paleosols are described in Germany and Austria), AO-E-Bw-Bk-BCk, the contemporary analogue of which is Yakutia's Cambic Cryosol. The formation of these soils occurs in extracontinental semi-arid climate conditions on the territory of the middle taiga zone. In Khotylevo I sections the paleosol inherits the change in climate: from Cambic Cryosol to Gleysol. Owing to high deposition rates and the development of weak earthslide slope processes, a detailed paleosol chronicle reflecting short-term climatic fluctuations has survived in these soils' profiles.

*Keywords:* Middle Paleolithic, Khotylevo I, Micoquian/KMG, paleosol, MIS 3, Cambic Cryosol, Middle Valday

## ACKNOWLEDGMENTS

The study was funded by RFRB research projects No. 19-29-05267 mk and RFBR No. 20-09-00233, within the framework of the Program of Fundamental Scientific Research of the State Academies of Sciences, State Assignment No. FMZF-2022-0012.

## REFERENCES

Faegri K. and Iversen J. Textbook of Pollen Analysis. Chichester: Wiley (Publ.), 1989. P. 237.

Grichuk V.P. and Zaklinskaya E.D. *Analiz iskopaemykh pyl'tsy i spor i ego primenenie v paleogeografii* (Analysis of fossil pollen and spores and its application in paleogeography) Moscow: OGIZ (Publ.), 1948. P. 224. (in Russ.).

Haesaerts P., Borziac I., Chekha V.P., Chirica C., Drozdov N.I., Koulakovska L., Orlova L.A., van der Plicht J., and Damblon F. Charcoal and wood remains for radiocarbon dating Upper Pleistocene loess sequences in Eastern Europe and Central Siberia. *Palaeogeography, Palaeoclimatology, Palaeoecology.* 2010. Vol. 291. P. 106–27. https://doi.org/10.1016/j.palaeo.2010.03.034

Hein M., Weiss M., Otcherednoy A., and Lauer T. Luminescence chronology of the key-Middle Paleolithic site Khotylevo I (Western Russia) – Implications for the timing of occupation, site formation and landscape evolution. *Quaternary Science Advances.* 2020. Vol. 2. P. 1–18. https://doi.org/10.1016/j.qsa.2020.100008

IUSS Working Group WRB. World Reference Base for Soil Resources 2014, update 2015. International soil classification system for naming soils and creating legends for soil maps. *World Soil Resources Reports.* 2015. Vol. 106. FAO. Rome.
https://www.fao.org/3/i3794en/I3794en.pdf

Kadereit A., Kind C.J., and Wagner G.A. The chronological position of the lohne soil in the Nussloch Loess Section – re-evaluation for a European loess-marker horizon. *Quaternary Science Reviews.* 2013 Vol. 59. P. 67–86. https://doi.org/10.1016/j.quascirev.2012.10.026

Korkka M.A., Rusakov A.V., Bagrova S.M., and Rybin G.V. Morphology and pedostratigraphy of Holocene and Late Pleistocene soils of the Yamskaya steppe section (Belgorod oblast). *Mat-ly III Vserossiiskoi nauchnoi konferentsii s mezhdunarodnym uchastiem.* Moscow: KMK (Publ.), 2017a. P. 306–10.

Korkka M.A., Sedov S.N., Sinitsyn A.A., Otcherednoy A.K., and Kühn P. Paleosols in the sections of Kostenki 14 and Khotylevo I: Chronicle of the natural conditions and archaeological complexes OIS 3. *International Theoretical and Practical Conference Multidisciplinary methods in the study and preservation of sites in the Kostenki-Borshchevo archaeological area.* Voronezh: Voronezh State University (Publ.), 2017b. P. 27–47. (in Russ.)

Otcherednoy A.K. and Voskresenskaya E.V. Stratigraphic data on middle paleolithic sites in the upper Desna basin. *Archaeology, Ethnology & Anthropology of Eurasia.* 2009. Vol. 37. P. 28–36.
https://doi.org/10.1016/j.aeae.2009.08.013

Savelieva L.A., Andreev A.A., Gromig R., Subetto D.A., Fedorov G.B., Wennrich V., Wagner B., and Melles M. Vegetation and climate changes in northwestern Russia during the Lateglacial and Holocene inferred from the Lake Ladoga pollen record. *Boreas.* 2019. Vol. 48. P. 349–360. https://doi.org/10.1111/bor.12376

Sedov S., Terhorst B., and Rusakov A.V. Polygenesis of MIS 3 paleosols in Central and Eastern Europe: identification of phases and utilization for pedogenetic interpretation. *Materials of the XIIth Int. Symp. and Field Workshop on Paleopedology (ISFWP).* Kursk: Institute of Geography RAS (Publ.), 2013. P. 11.

Stockmarr J. Tablets with spores used in absolute pollen analysis. *Pollen et Spores.* 1971. Vol. 13 P. 615–21.

Sycheva S.A. and Khokhlova O.S. Genesis, $^{14}$C age, and duration of development of the Bryansk paleosol on the Central Russian Upland based on dating of different materials. *Quaternary International.* 2015. Vol. 399. P. 111–121.
http://dx.doi.org/10.1016/j.quaint.2015.08.055

Terhorst B., Sedov S., Sprafke T., Peticzka R., Meyer-Heintze S., Kühn P., and Rebolledo E.S. Austrian MIS 3/2 loess-palaeosol records-Key sites along a west-east transect. *Palaeogeography, Palaeoclimatology, Palaeoecology.* 2015. Vol. 418. P. 43–56.
https://doi.org/10.1016/j.palaeo.2014.10.020

Velichko A.A. Loess-paleosol formation on the Russian Plain. *Quaternary International.* 1990. Vol. 7. P. 103–14.
https://doi.org/10.1016/1040-6182(90)90044-5

**EDN:** WZKHKY
*ГЕОМОРФОЛОГИЯ, 2022, том 53, № 5, с. 32–47*

## ПРОБЛЕМЫ ПАЛЕОПОЧВОВЕДЕНИЯ И ГЕОАРХЕОЛОГИИ

*УДК 551.89:574→631.42:902/904 (470.323)*

# РЕКОНСТРУКЦИЯ ПАЛЕОЛАНДШАФТОВ СРЕДНИХ ВЕКОВ НА ОСНОВЕ ИЗУЧЕНИЯ ПОГРЕБЕННЫХ ПОЧВ ГОЧЕВСКОГО АРХЕОЛОГИЧЕСКОГО КОМПЛЕКСА (КУРСКАЯ ОБЛАСТЬ)


**Ф. Г. Курбанова[1,*], Т. А. Пузанова[2], Е. Н. Асеева[2], П. Г. Куст[3], О. В. Руденко[4]**
*[1]Институт географии РАН, Москва, Россия*
*[2]Московский государственный университет имени М.В. Ломоносова, географический факультет, Москва, Россия*
*[3]Почвенный институт имени В.В. Докучаева, Москва, Россия*
*[4]Орловский государственный университет имени И.С. Тургенева, Орел, Россия*
**E-mail: fatima.kurbanova@igras.ru*
Поступила в редакцию 14.06.2022 г.
После доработки 20.06.2022 г.
Принята к публикации 15.07.2022 г.

Благодаря изолированности от внешней среды, почвы, погребенные под курганными могильниками, являются ценными архивами, которые содержат информацию о природных условиях прошлых эпох. Приведены результаты изучения почв, погребенных под курганами в средневековье с небольшим временным интервалом – 25–50 лет. В исследования входили подробное полевое морфологическое описание почв, гранулометрический анализ, изучение элементного состава, фракционного железа и некоторых других физико-химических параметров. Помимо этого, был выполнен анализ спор, пыльцевых и непыльцевых палиноморф. Для сравнения была исследована фоновая почва в непосредственной близости от курганов. Полученные данные позволили определить динамику лесостепных ландшафтов в X–XI вв. Произошедшие в этот временной отрезок средневековое потепление и последующее увлажнение климата за короткий период могли существенно повлиять на природные условия и миграцию населения степей Евразии.

*Ключевые слова:* палеопочвы, споро-пыльцевой анализ, палеоклимат, голоцен, средневековый климатический оптимум

**DOI:** 10.31857/S0435428122050078

## 1. INTRODUCTION

Soils buried under burial mounds are one of the natural archives that can store information on the natural conditions of the past. Due to isolation from the external environment, “conservation” occurs. As a result, the profile of the buried soil can preserve some signs that retain information about the features of the natural environment at the time of its burial.

A comparative analysis of the properties of soils buried under archaeological sites of different ages allows a detailed study of the changes in the natural environment and its components over time. In addition, soils can store a whole range of additional features of non-pedogenic origin, which can be used for a more detailed reconstruction of the natural environment. Thus, spores and pollen of plants, phytoliths, faunal remains, etc., are preserved in the soil profile. Therefore, the soil profile can be considered a kind of data archive containing unique information about the features of past natural settings.

Currently, the climatic changes during the Medieval Climate Optimum and the Little Ice Age within the forest-steppe of Central Russia have been poorly understood. According to accepted chronology, a Medieval Climate Anomaly corresponds to the 8th–13th centuries AD (Klimenko et al., 2001; Goosse et al., 2012). This period was characterised by sharp warming of the climate for most of the northern hemisphere. The warming peak was noted for the chrono-interval of the 10th–11th centuries AD. The analysis of Russian chronicles indicated that the climate of the European part of Russia changed significantly during this time (Borisenkov et al., 1983). In some periods, during extreme natural phenomena such as droughts, climate change led not only to the famine of population but also to social upheaval. According to the chronicles, the climate of ancient Russia during the period of the Medieval Climate Optimum in the 9th and 11th centuries was characterised by frequent droughts. From the 12th century, Russian chronicles indicate an increase in intra-seasonal and extreme climate variability and a shift to long cold winters, rainy weather in the

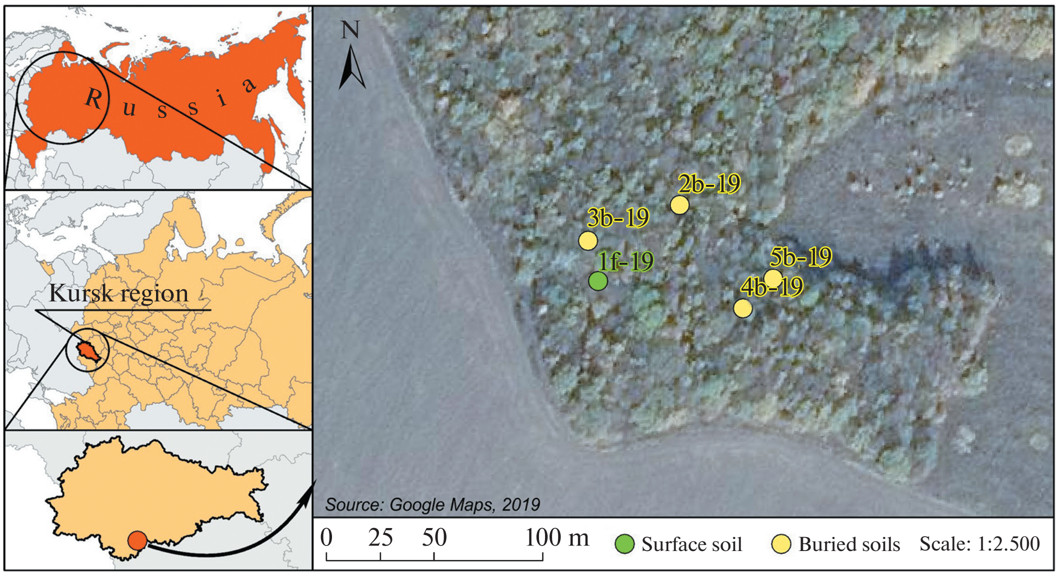


**Fig. 1.** Location of the study area (Kurbanova et al., 2020).
**Рис. 1.** Местоположение территории исследования (Kurbanova et al., 2020).

summer seasons, early frost in late summer and early fall. All these weather phenomena were the precursors of the Little Ice Age. The first third of the 12th century is considered the transition to the Little Ice Age. At this time, the number of floods and summer early frosts increased, which led to the death of crops and was the cause of hunger, epidemics and population fall (Borisenkov et al., 1983).

However, during medieval climate warming and cooling periods, there were significant decadal and secular temperature fluctuations. So, on the territory of the Russian Plain, the warmest over the past 2000 years was the 10th century, after which there was a clear trend towards a cooling of the climate. The Medieval Climate Optimum, which began about 1100 years ago, was characterised by the average annual temperature and by higher humidity. Precipitation during this period was ~25–50 mm more than nowadays (Kupriyanova et al., 1972).

We studied the surface soils and the soils buried under four mounds of the Gochevsky archaeological complex, located in the Kursk region, Russia. All mounds were constructed during the 11th century, with time intervals ranging from 25 to 50 years, enabling one to provide a detailed reconstruction of paleolandscapes for the 11th century. Our study aimed to evaluate the transformation of various properties of the soils in the forest-steppe zone over 25–50 years based on the study of a short-time soil series formed under similar lithological and topographic conditions using a single set of soil and biomorphic methods. This approach has already been used in several studies. In particular, O.S. Khokhlova (2016) compared soils under mounds with a difference in burial time of 25–50 years in the steppe zone.

## 2. STUDY AREA

The Gochevsky archaeological complex is located on the right bank of the river Psel near settlement Gochevo in Belovsky district (Kursk region, Russian Federation) within the Central Russian forest-steppe province of the East European Plain (fig. 1). The Gochevsky burial ground is one of the largest identified and survived monuments in modern Eastern Europe. The entire burial ground consisted of three thousand burial mounds; however, after intensive ploughing, only sites under the forest survived. In total, about 800 mounds were preserved in a small area currently occupied by deciduous forests. Gochevsky burial ground contains funeral rites of the old Russian population of the southeast of Russia at the end of the 10–12 centuries AD. All soil pits are located in the watershed area.

The climate of the study area is temperate continental, with moderately cold winters and warm summers. The average annual air temperature is about +7°C. Mean annual precipitation ranges from 475 to 640 mm. The warm period (April-October) accounts for 65–70% of the annual precipitation. Permanent snow cover is established in the second ten days of December; in early March, snowmelt begins, lasting about 20 days. The height of the snow cover ranges from 15 to 30 cm (maximum 50 cm) and persists on average for 2–2.5 months.

The natural steppe vegetation, typical of the forest-steppe zone, is preserved in the Central Chernozem Nature Reserve. It occurs only on slopes of gullies in the study area since the entire area has been almost completely ploughed. The forest vegetation covers less than 10% of the study area. It is represented mainly by oak forests and also by forest shelterbelts.

Quaternary loess deposits serve as parent material for soil formation. At depth, loess is underlain by Paleogene and Neogene sands and argillaceous deposits. The dominant soil type in the study area is chernozem (75%); dark grey forest soils occur under broad-leaved forests. Due to ploughing, the soils are highly eroded.

## 3. MATERIAL AND METHODS

*Research objects.* Soils buried under four mounds with a thickness of 40–60 cm were examined. The soils were formed in the same topographic position, in the interfluve area covered by forest vegetation and in the similar parent material. Their soil profiles were considered as a data archive containing information on the past environments. The soils 3b, 4b, 5b were buried over the period from the second quarter to the middle of the 11th century, while the soil 2b was buried later, in the second half of the 11th century. Burial mounds were dated by archaeological method (Puzanova et al., 2018). To compare the conditions of the past to the modern ones, the surface soil (1f) formed in the was also studied. All buried and surface soils were located under one forest patch at a distance of 25–100 meters from each other.

Sampling and laboratory analyses. Samples were collected from the buried soils below the burial mound from every 10 cm down to 1 m (and every 20 cm below 1 m) but with the preservation of the soil horizon intact. Samples of soils for pollen analysis were taken from the upper 0–5 cm of the buried and the surface soils. The soils were described according to the FAO Guidelines for Soil Description (2006). Soil colour was determined in the field using the Munsell Soil Color Charts (2014).

Two methods to determine particle size distribution in soil horizons were used: pipette method, in which soil was dispersed by treating with a solution of sodium pyrophosphate ($Na_4P_6O_{18}$) and laser granulometry method using FRITSCH laser particle sizer Analysette 22. Laser Klasse 1 (Germany). The boundaries between particle size classes were defined by the Russian conventional fraction groups: the coarse and medium sand fraction (1–0.25 mm); the fine sand fraction (0.25–0.05 mm); the coarse (0.05–0.01 mm), the medium (0.005–0.001 mm), the fine silt (0.005–0.001 mm) and the clay fraction (<0.001 mm). Textural classes were approximated according to the FAO Guidelines for soil description (2006).

Dithionite and oxalate extractable fractions of iron were determined according to Mehra and Jackson (1960) using Cary 60 Spectrophotometer (Agilent Technologies, Santa Clara, CA, USA). The elemental analysis was performed by X-ray fluorescence spectrometry method after a loss on ignition determination (1000°C) using the Philips PW2400 Sequential WXRF Spectrometer (Malvern Panalytical, Almelo, The Netherlands). In sample preparation for the XRF analysis, ~1 g of sample was dried in the oven at 105°C. Samples were powdered, mixed with a lithium tetraborate flux and then melted to produce a glass disc.

The elemental data treatment included the calculation of the ratios of immobile elements – Ti, Al, Nb and Zr – which were used to evaluate the parent material uniformity (Sheldon et al., 2009). The amount of loss and gain in soil horizons relative to the parent material was quantitatively assessed using the eluvial/illuvial coefficient, or EIC [$EIC(\%) = ((Xh/Ih)/(Xr/Ir) - 1) \times 100\%$ (1), where $Xh$ and $Xr$ are the contents of element X, while $Ih$ and $Ir$ are the contents of an immobile element (Al) in soil horizons and parent rocks, respectively. Positive *EIC* values mean that the element has been enriched in the soil horizon and a negative value indicates the loss of the element. Eluvial-illuvial coefficients were estimated for relatively mobile elements, such as Ca, Sr, and also for Fe.

Micromorphological features of the thin sections made from undisturbed oriented samples were studied in plain (PPL) and polarized (XPL) light under 40 to 200 times magnification using an Olympus BX51 polarizing microscope. Olympus StreamBasic software was used for image capturing. In total 36 thin sections were described based on the terminology of Stoops (2003), with special attention on the variability of humus content, carbonate and clay pedofeatures. The work was carried out using the equipment of the Collective Centre “Functions and properties of soils and soil cover” of the V.V. Dokuchaev Soil Science Institute RAS.

For the extraction of microfossils, centrifugal separation in potassium-cadmium ($KJ + CdJ_2$) heavy liquid with a density of 2.3 g/cm$^3$ was used. Prior to this, samples were processed with cold 10-% solution of HCl and 10-% solution of KOH to dissolve carbonates and then decanted with distilled water to remove clay particles. Samples were stored in glycerin and examined under 400× magnification. Pollen identification and taxonomy follows Beug (2004), Kupriyanova and Aleshina (1972) and electronic databases of photos (http://www.europeanpollendatabase.net/index.php; https://www.paldat.org/) as well. Organic residues of aquatic microorganisms, spores of coprophilous and parasitic fungi on decaying plants and roots, indefinable spores of fungi were grouped as non-pollen palynomorphs (NPP), counted in addition and identified following NPP database (Shumilovskikh et al., 2021). In each sample, the number of micro-charcoal particles, which are among the effective eco-indicators, was also counted. Both pollen and NPP diagrams were constructed using Tilia 2.0.2 and TGView software

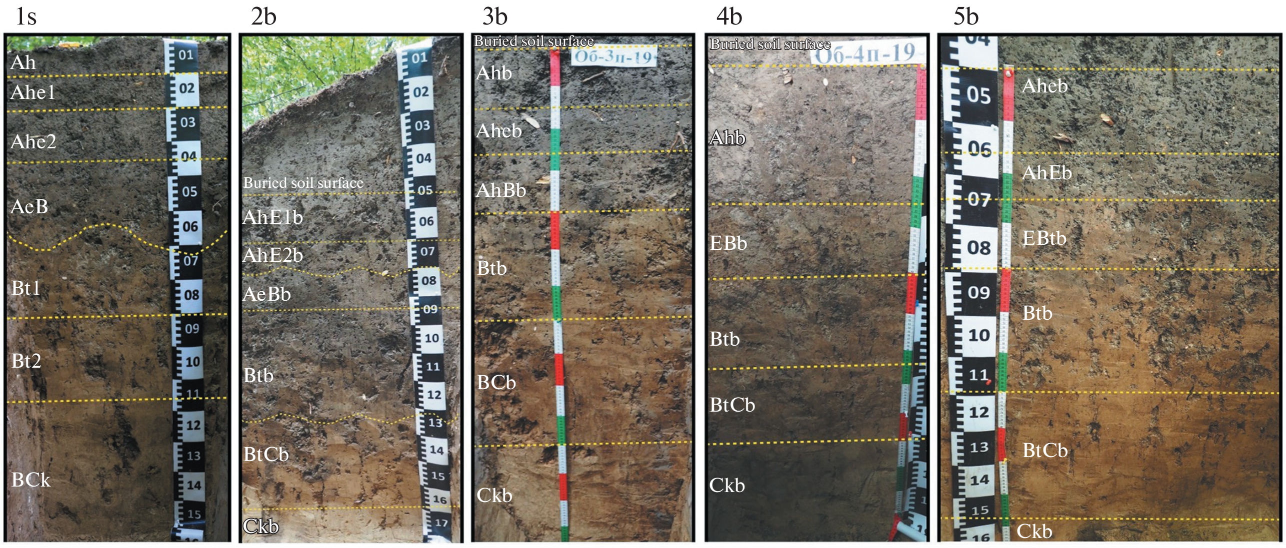


**Fig. 2.** Profiles of buried and surface soils.
**Рис. 2.** Профили погребенных и фоновой почв.

(Grimm, 1991). Calculation of pollen percentages was based on the terrestrial pollen sum – arboreal pollen (AP) plus non-arboreal pollen (NAP) without aquatic plants, spores and NPP. Their percentages were calculated based on AP+NAP sum.

## 4. RESULTS AND DISCUSSION

*4.1. Soil morphology.* All soils were formed in loess sediments and were classified as Greyzemic Luvic Phaeozem Cutanic. Uncoated silt and sand grains on the ped faces in the lower part of a humic horizon (AhE) indicate Greyzemic features (IUSS WRB Working group, 2015). The argic horizon is characterised by angular blocky/prismatic structure and clay cutans on the ped surfaces. Soils differed by the colour of humus horizon, amount and forms of carbonates, and intensity of greyzemic features.

The surface soil (1s) is represented by the following horizons: Ah-Ahe1-Ahe2-AeB-Bt1-Bt2- BCk (fig. 2-1s). The Ah horizon is characterised by granular structure and brownish-grey colour (7.5 YR 4–5/1). The next two horizons have subangular blocky and platy structures and contain uncoated quartz and feldspar grains on ped surfaces. Transitional AeB horizon, as well as Bt horizon, have an angular blocky structure with grey siltans (7.5 YR 7/1) and dark brownish-black cutans (5 YR 3/2). Bt2 horizon is characterised by prismatic structure and darker colour of cutans covering all transhorizontal cracks. The lowermost horizon BCk is distinguished by dull yellowish-orange colour (10 YR 6/4) and the presence of carbonates occurring as soft nodules and tiny tubules.

The thickness of the mound under buried soil 2b is 55 cm. The mound consists of dark grey material with abundant siltanes on angular blocky peds. The surface of the buried soil is determined by the darker colour of the humus horizon. The soil consists of the following horizons: AhE1b- AhE2b- AeBb- Btb- BtCb-Ckb (fig. 2–2b). The AhE1b horizon is grey/dark grey (10 YR 5–4/1) with abundant siltans. The second horizon has a darker colour (10 YR 3/1 very dark grey) and also contains uncoated sand and silt grains on the peds surfaces. In the AeBb the siltans are less distinct, and thin rare clay cutans appear. The structure in the Btb horizon is angular blocky, and prismatic; siltans are still present, but less common. At a depth of 110 cm, the Ckb horizon begins. It has a weak structure and contains carbonates presented as plasma and small dull yellowish-orange (10 YR 6/4) tubules.

The paleosoil 3b consists of the following horizons: Ahb- Aheb- AhBb- Btb- BCb-Ckb. The distinctive feature of this soil is the dark colour of the Aheb horizon (10YR 2/1). Greyzemic features are less intensive in this soil compared to other buried and surface soils (fig. 2–3b). The subsoil contains a high amount of dark cutans and is characterised by moderate angular blocky and prismatic structure. The deepest Ckb horizon has rounded ooids with brownish colour and carbonates in the form of small tubules that also occur in other soils from the archaeological complex.

The buried soils 4b and 5b (fig. 2–4b, 5b) have similar morphological characteristics. The following horizons represent the soil profiles: Ahb-EBb-Btb-BCb-Ckb (4b), and Aheb-AhEb-EBtb-BtCb-Ckb (5b). The upper horizons in both soils are characterised by dark grey colour (10 YR 3/1) and have a subangular blocky structure. Uncoated quartz and feldspar grains are frequent in the EBb (4b soil) and EBtb (5b soil) horizons. The Bt horizons have a prismatic structure and contain clay-humus cutans. The transitional BCb horizons are not homogeneous in colour: they have a yellowish-brown colour of the soil matrix and a dark yellowish-brown (10 YR 4/4) colour of the coatings. The Ckb horizons were distinguished by weak structure and very pale brown colour with rounded brown ooids.

Although all soils were formed in loess deposits and were classified as *Folic Greyzemic Luvic Phaeozem Cutanic*, they differed in the colour of humus horizons and the deepness of the uncoated sand and silt grains occurrence. The soil 3b had a darker colour of the humus horizon (10YR 2/1) than other soils of the archaeological complex (10YR 3/1). The depth where uncoated sand and silt grains still occurred was also different; in the surface soil, they reached the depth of 90 cm; in the soil 2b, they could be traced up to 80 cm; in other soils uncoated sand and silt grains penetrated not deeper than 70 cm. In all the studied soils, the cutan complex was equally well expressed; however, humus cutans across transhorizontal cracks were found only in the surface soil.

*4.2. Particle size distribution.* All studied soils are characterised by silty loam texture. The dominant particle size fraction in the soil material in all five soil profiles is the coarse silt (fig. 3) because the soils are developed in loess deposits that formed during the Late Pleistocene cold periods. The amount of this particle size fraction varies between 40 and 61%. The surface soil 1f and the buried soils 2b and 3b contain nearly equal average amounts of the coarse silt particles (52–53%). However, its share in the buried soils 4b and 5b is slightly higher (55–56%). The sand is dominated by the fine sand fraction (0.25–0.05 mm). All soils don't differ significantly according to their average amount (4–5%) except the buried soil 2b containing a lower proportion of the sand-sized material. The vertical distribution of the sand particles follows different patterns in the studied soils. Distinct accumulation of the fine sand was recorded in the surface soil in its upper horizons, but in soil 2b the middle horizons contain more sand than other horizons, and in the soil profiles 4b and 5b the sand tends to accumulate in the BC or C horizons. The enrichment of the uppermost horizons with sand particles might be due to losses of finer material with infiltrating water, while the accumulation in the lower strata can be due to the effect of underlying sandy lithology. The vertical distribution of the clay in different soil profiles does not imply strong textural contrast between their upper and middle (Bt) horizons. In the surface soil, the clay fraction displays depletion in the topsoil and a relative increase in the lowermost parent material, where the clay content reaches its maximum (14%). No notable enrichment in the clay-sized material is registered in the Bt horizon. In the buried soils 2b, 3b and 4b, the changes are very smooth: the ratio of the clay contents in the AhEb and Bt horizons does not exceed 1.1 and the clay size particles tend to enrich subsoil.

In contrast to these soils, soil profile 5b shows a maximum clay content in the middle horizons. The estimated ratio for the AhEb and BtC horizons varies between 1.2–1.4. Thus, the clay fraction distribution in most soil profiles is rather uniform except for the surface soil and the buried soil 5b.

*4.3. Soil micromorphology.* At the microscale, a differentiation of humus horizons by colour is visible. Buried soils 2b, 4b, 5b show microzonality with low contrast between the light and dark microzones characterised by different amounts of humus (fig. 4, (c-f)). This contrast increases in the soil 1s mostly because of the darker humus microzones than in the soils 2b, 4b, 5b (fig. 4, (g, h)). In soil 3b, the humus horizon is homogeneous and has a darker colour compared to the other studied profiles (fig. 4, (a, b)).

The described features point out: 1) the stability of humus material at the moment of the soil 3b; 2) weak degradation of humus at the moment of soils 2b, 4b, 5b burial and a relatively higher degree of humus material degradation at present. The latter can be caused by a higher amount of precipitation described for the modern environment (Makeev et al., 2020).

Weak signs of humus horizon degradation in soil 3b correspond to the weakly developed complex of coatings in this profile (fig. 5, (a, b)). In the other buried soils, the degradation of the humus horizon is accompanied by the expression of clay coatings (fig. 5, (c–e)) and coatings of clear silt grains. In soils, 4b, 5b, abundant silty coatings are represented by lighter elongated zones around the aggregates (fig. 4, (c, d)). In the 2b soil profile, abundant well-defined silty coatings correlate with the better developed two-layered complex coatings. Such coatings consist of a clay layer (typical for all profiles) and a layer of dark clay-humus coatings (fig. 5, (e, f)) which are described only in 2b and surface soils. Abundant clay coatings increase in soils as follows: 3b – 4b, 5b – 2b – 1s (fig. 6, (a–d)).

Clay coatings are well expressed in all studied soils up to the depth of 100–120 cm. In the lower horizons, they are superimposed and overlap carbonate pedofeatures which are typical in lower horizons in all soils and especially in soil 3b (fig. 6, (e)). The carbonate pedofeatures are represented by micritic coatings. However, in the 3b profile, sparite nodules, which are typical for a more arid environment (National Soil Atlas..., 2011), were also detected (fig. 6, (f)). Carbonate and clay coatings interlayer suggests that the carbonate coatings have been formed first, and clay coatings started to form after them, but before the burial of 3b soil. Later, clay coatings were only slightly transformed, increasing their thickness at the further stages of evolution (2b – 1s), reflecting the changes in the paleoenvironment.

All studied soils save features of the previous stages of soil formation with palimpsests type of soil memory (Soil memory, 2008). Thus, earlier arid features are a) carbonate material in the lower layer of complex coat-

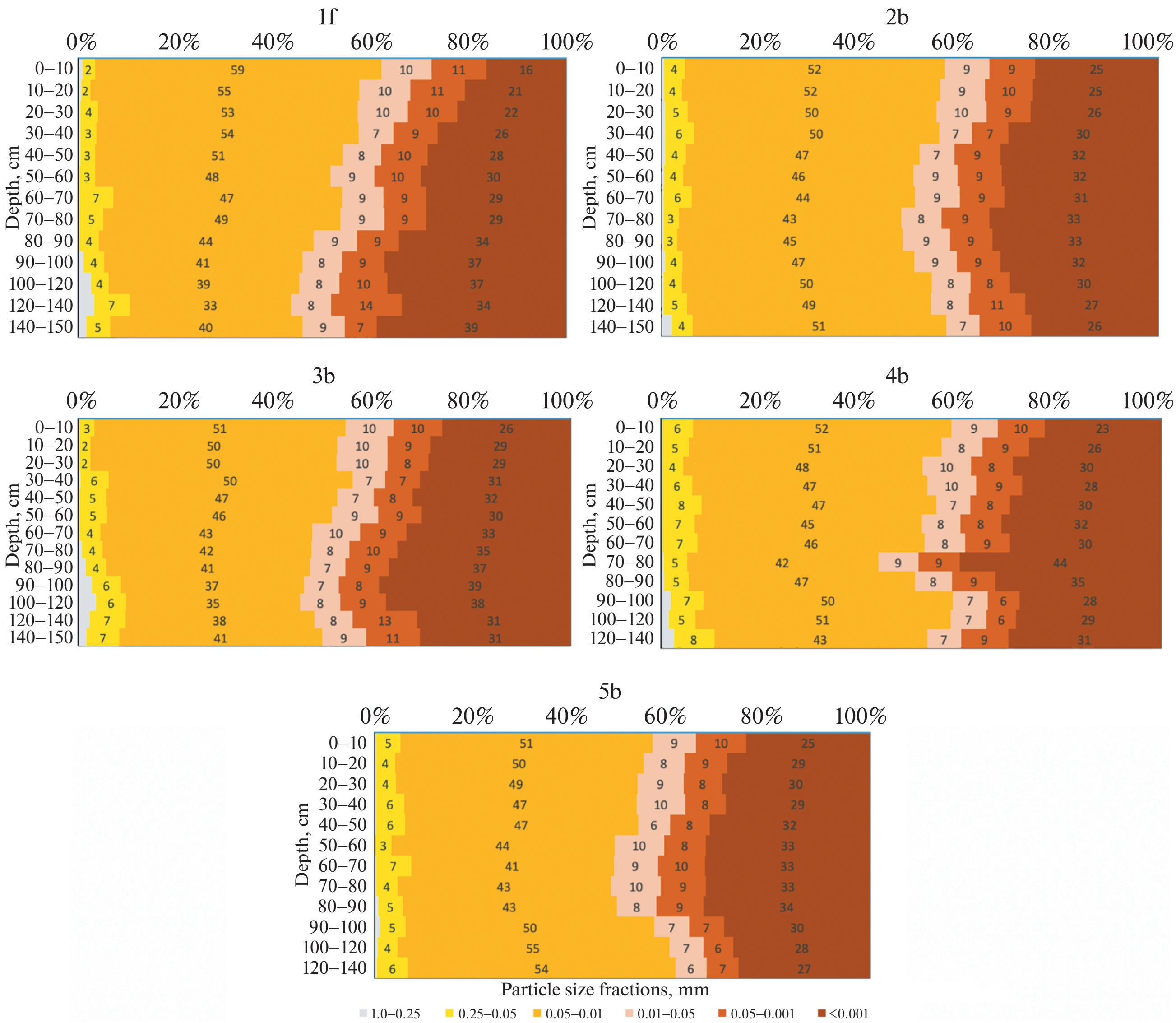


**Fig. 3.** Particle size distribution, with depth, in the surface soil 1s and the buried soils 2b, 3b, 4b and 5b.
**Рис. 3.** Гранулометрический состав почв в фоновой почве 1s и погребенных почвах 2b, 3b, 4b, 5b.

ings, b) dark humus horizons or microzones; later humid features are: a) silty coatings in the humus horizons, b) upper clay layers in complex coatings.

Fe-Mn pedofeatures were also described at the microscale in the studied soils. However, we can use them only as an additional indicator of soil-forming conditions since they are very alterable in time. Nevertheless, they are almost absent in the 3b profile (fig. 4, (a, b)), higher amounts – in the 4b and 5b profiles (fig. 4, (c, d)), the maximum amount was described in soils 2b, 1s (fig. 4, (e, f)).

*4.4. Elemental analysis.* The elements Ti, Zr and Nb are presumably not lost due to weathering and translocation (Sheldon et al, 2009, Muir et al., 1982, Schaetzl et al., 2005), and Al which is also inert under semi-humid climatic conditions, were chosen for the detection of lithogenic discontinuities. The ratios of these elements calculated for the soils' parent materials are nearly equal (tabl. 1), indicating that the sediments had been very likely derived from the same source. Additionally, the values calculated for soil horizons in each soil profile display very low variations (in most cases less than 10%), which means that lithogenic discontinuities are not present and the soil strata at each site are relatively homogeneous in terms of parent material origin and its mineralogical composition (Marsan et al., 1988). Taking into account these facts, it is possible to relate the pedogenic differences between the buried and surface soils to environmental changes that occurred after the burial.

In all five studied soils, the eluvial-illuvial coefficients calculated for Ca and Sr had negative values in

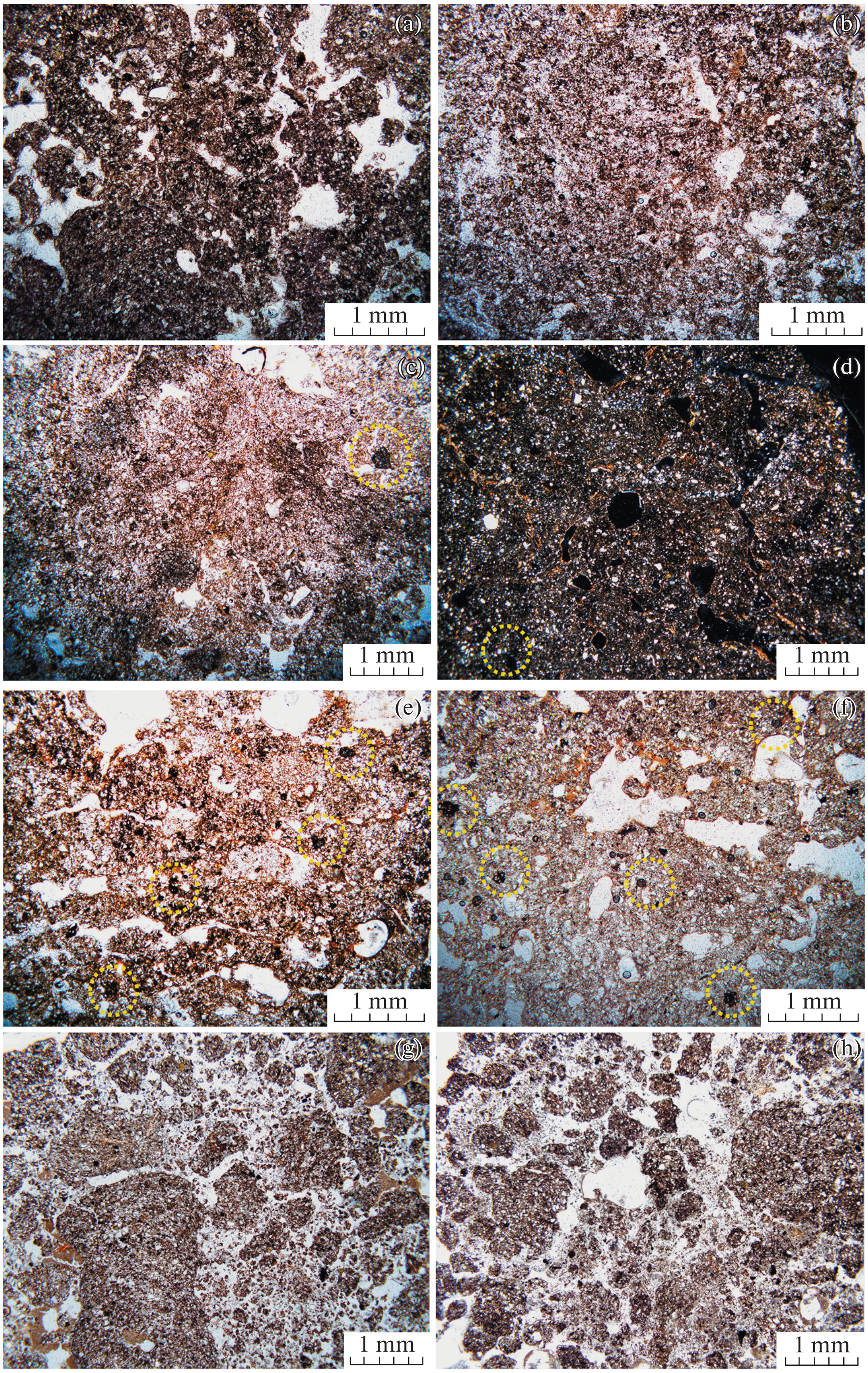


**Fig. 4.** Micromorphology of upper horizons. (a) – Soil 3b, 2–7 cm. Dark brown material. NII, (b) – Soil 3b, 16–24 cm. Dark brown material with rare slightly bleached microzones. NII, (c) – Soil 4b, 5–10 cm. Dark brown and brown microzones incorporation. NII, (d) – Soil 5b, 22–28 cm. Thick silty coatings within the pore space. Note abundant thin clay coatings. NX, (e) – Soil 2b, 0–10 cm. Dark brown and brown microzones incorporation. NII. Note abundant brown microzones. NII, (f) – Soil 2b, 16–24 cm. Bleached brown material with numerous clay coatings. NII, (g) – Soil 1s, 5–10 cm. Brown material. NII, (h) – Soil 1s, 22–30 cm. Thick silty coatings between brown aggregates.

On (a) and (b) note the absence of Fe-Mn pedofeatures, on (c) and (d) note few Fe-Mn micronodules (marked by yellow dashed line ellipse), on (e) and (f) note abundant Fe-Mn micronodules (marked by yellow dashed line ellipses).

**Table 1.** Ratios of immobile elements in the buried and the surface soils
**Таблица 1.** Соотношение неподвижных элементов в погребенных и фоновой почвах

| Ratio | Ratio value in parent material | | | | | Arithmetic mean for soil profiles / (variation coefficients, %) | | | | |
|---|---|---|---|---|---|---|---|---|---|---|
| | 1s* | 2b | 3b | 4b | BS5 | 1s | 2b | 3b | 4b | 5b |
| | 100–150** | 100–140 | 100–150 | 100–140 | 100–120 | $n$*** = 9 | $n$ = 10 | $n$ = 9 | $n$ = 8 | $n$ = 8 |
| Ti/Zr | 9 | 7 | 8 | 7 | 6 | 7/(20) | 7/(3) | 7/(7) | 7/(8) | 7/(5) |
| Ti/Nb | 276 | 277 | 268 | 280 | 277 | 274 (3) | 276/(4) | 273/(4) | 280/(4) | 285/(4) |
| Ti/Al | 0.10 | 0.11 | 0.11 | 0.11 | 0.11 | 0.10 (10) | 0.10/(7) | 0.10/(3) | 0.10/(6) | 0.10/(4) |

* – soil profile index; ** – depth of the sampled parent strata in cm; *** – $n$ – number of samples in a soil profile.

the upper and middle horizons, indicating intense leaching of these elements. However, in the surface and buried soils 2b and 4b, the absolute values of EIC in the middle horizons for Ca and Sr are higher than in buried soils 3b and 5b (fig. 7), which may indicate less humid climatic conditions that existed before the burial of the latter.

The analysis of the $SiO_2/Al_2O_3$ ratio showed that the studied soils have different levels of this parameter both in their upper horizons and in the parent material (fig. 8). The surface soil 1s and the buried soil 2b are remarkable for the high $SiO_2/Al_2O_3$ ratio in their topsoil material (fig. 8), which might be associated with losses of fine particles with infiltrating water and/or relative accumulation of quarts. The maximum value of this ratio in the subsoil is typical of the buried soil 4b, 5b and 2b (fig. 8) which more likely is associated with a lithological factor. The buried soil 3b is characterised by a low $SiO_2/Al_2O_3$ ratio and very smooth changes of this parameter across soil horizons, which makes it different from other soils. The enrichment of the uppermost horizons with Si in the surface soil is in agreement with sand enrichments to losses of finer material with infiltrating water while the accumulation in the lower strata can be due to the effect of underlying sandy lithology.

The study of *iron*, the element with medium mobility dependent on redox condition, helps to detect its participation in pedogenic processes. The depth functions of total iron (Fetotal) content normalised to immobile element Al revealed the absence of distinct patterns in total iron distribution throughout the soil profiles. The divergence in $Fe_2O_3/Al_2O_3$ values from parent material (fig. 9, (a)) does exceed 10–15% in most of the buried soils (2b, 3b and 4b). In the surface soil and the buried soil 5b the divergence is slightly higher (30%) (fig. 9, (a)). The EIC values in the surface soil are negative, indicating that Fe has been depleted in the soil strata, especially in upper horizons, while in the buried soil 5 the EIC values are positive, indicating the slight enrichment of the solum with this element, especially in the upper part of the horizons BtC. The study of iron fractions revealed that the share of pedogenic, or free, iron (Fed) of the total iron concentrations (Fetotal) is rather low, and the silicate iron compounds prevail over others (fig. 9, (b)). The proportion of pedogenic iron in total iron content indicating weathering intensity (Vodyanitsky, 2008) varies across different soils and soil horizons within a relatively narrow range from 26 to 36%. The highest share of Fed is found in the upper horizons of soil 5b (fig. 9, (b)). However, the free iron that occurs in this soil is represented mainly by non-active crystalline forms (85–95%, fig. 9, (c)). The contribution of the crystalline compounds to pedogenic iron is also high in soils 3b and 4b compared to the surface soil 1s and the buried soil 2b, where the relative proportion of crystalline iron is distinctly lower (fig. 9, (c)), and the contribution of the oxalate extractable (non-crystalline, Feo) iron to the pedogenic iron is higher. In the upper horizons of these two soils, pedogenic iron has the highest values of 26–18%, compared to similar horizons of soils 3, 4 and 5 with a very low iron activity index (Feo/Fed).

←

**Рис. 4.** Микроморфология верхних горизонтов. (a) – почва 3b, 2–7 см. Темно-коричневый материал. NII, (b) – почва 3b, 16–24 см. Темно-коричневый материал с немного осветленной частью. NII, (c) – почва 4b, 5–10 см. Темно-коричневый материал с коричневыми микрозонами. NII, (d) – почва 5b, 22–28 см. Мощные пылеватые кутаны в поре. Отмечены обильные тонкие глинистые кутаны. NX, (e) – почва 2b, 0–10 см. Темно-коричневый материал с коричневыми микрозонами NII, (f) – почва 2b, 16–24 см. Осветленный коричневый материал с глинистыми кутанами. NII, (g) – почва 1s, 5–10 см. Коричневый материал. NII, (h) – почва 1s, 22–30 см. Мощные пылеватые кутаны между коричневыми агрегатами.

На рисунках (a) и (b) обратите внимание на отсутствие Fe-Mn конкреций, на (c) и (d) обратите внимание на несколько Fe-Mn микроконкреций (отмечены желтым пунктирным эллипсом), на (e) и (f) обратите внимание на обильные Fe-Mn конкреции (обозначены желтыми пунктирными эллипсами).

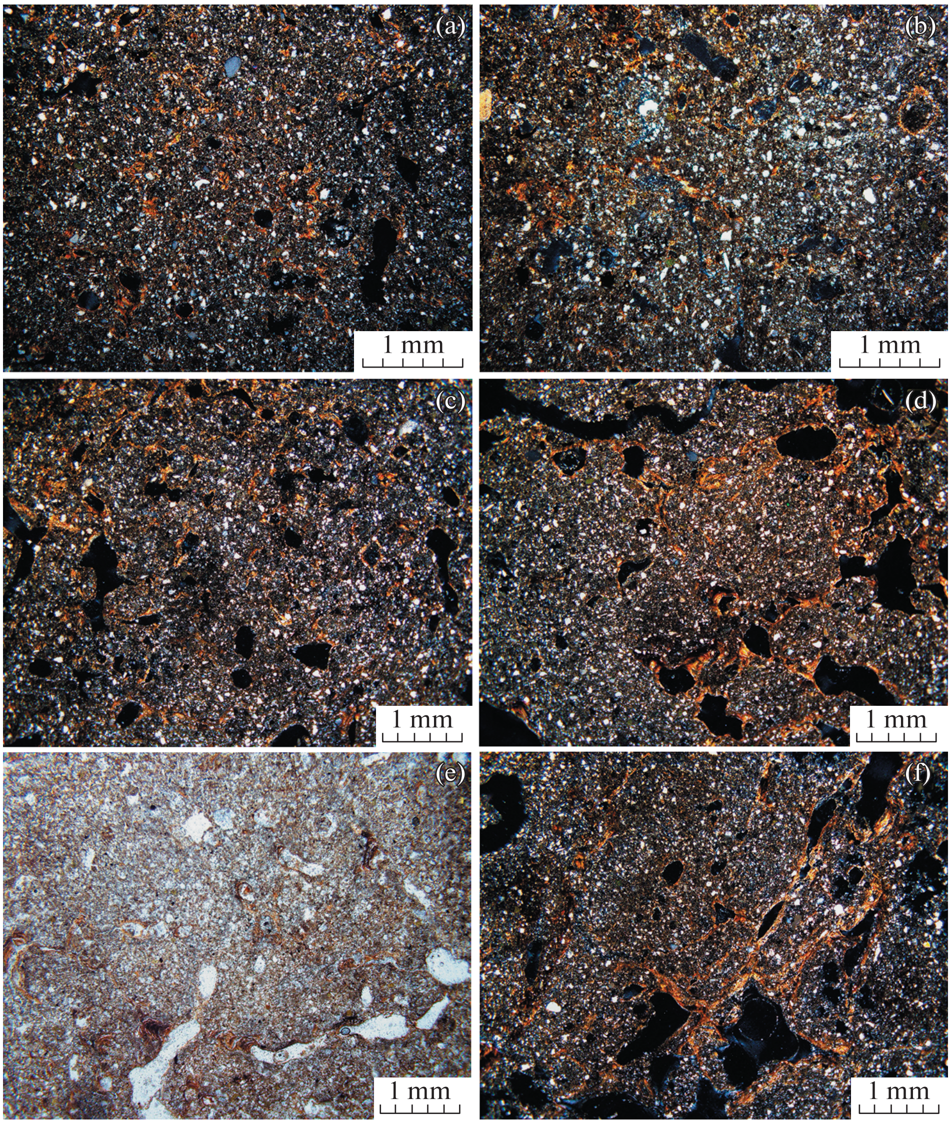


**Fig. 5.** Micromorphology of middle horizons. (a) – Soil 3b, 27–32 cm. Rare thin clay coatings cover about 30% of pores. NX, (b) – Soil 3b, 50–58 cm. Clay coatings cover about 60% of pores. NX, (c) – Soil 5b, 30–36 cm. Abundant clay coatings, covering 80–90% of pores. NX, (d) – Soil 4b, 50–60 cm. Thick clay coatings within the pore space cover up to 90% of pores. NX, (e) – Soil 2b, 24–30 cm. Compound clay coatings with dark brown and brown layers. NII, (f) – Soil 1s, 60–67 cm. Compound clay coatings covering 80–90% of pores. NX.

**Рис. 5.** Микроморфология средних горизонтов. (a) – почва 3b, 27–32 см. Тонкие глинистые кутаны покрывают ~30% пор. NX, (b) – почва 3b, 50–58 см. Глинистые кутаны покрывают 60% пор. NX, (c) – почва 5b, 30–36 см. Обильные глинистые кутаны покрывают 80–90% пор. NX, (d) – почва 4b, 50–60 см. Мощные глинистые кутаны покрывают 90% пор. NX, (e) – почва 2b, 24–30 см. Составные глинистые кутаны с темно-коричневыми и коричневыми слоями. NII, (f) – почва 1s, 60–67 см. Составные глинистые кутаны покрывают 80–90% пор. NX.

In summary, the study of the chemical composition of the five soils, one surface soil and four buried ones, implies that the surface soil 1f has many similar features with the buried soil 2b, while other soils have only partial similarity (the soil 4b and to a lesser extent soil 5b) or little similarities (soil 3b). The latter soil, in contrast to soils 1f and 2b, displays many features which might indicate drier conditions of its formation that existed before its burial (limited losses of Ca and Sr from the upper and middle soil horizons, higher share of crystalline forms in the pedogenic iron, lower values of $SiO_2/Al_2O_3$ ratio and their very smooth vertical changes in the profile). The soil 5b is similar to soil 3b, while the buried soil 4b occupies an intermediate position between the soils 1f and 2b, and "drier" soils 5b and especially 3b.

*4.5. Pollen analysis.* The sample from the surface soil (1s) turned out to be the most representative quantitatively and taxonomically diverse. The pollen spectrum more or less adequately reflects the modern veg-

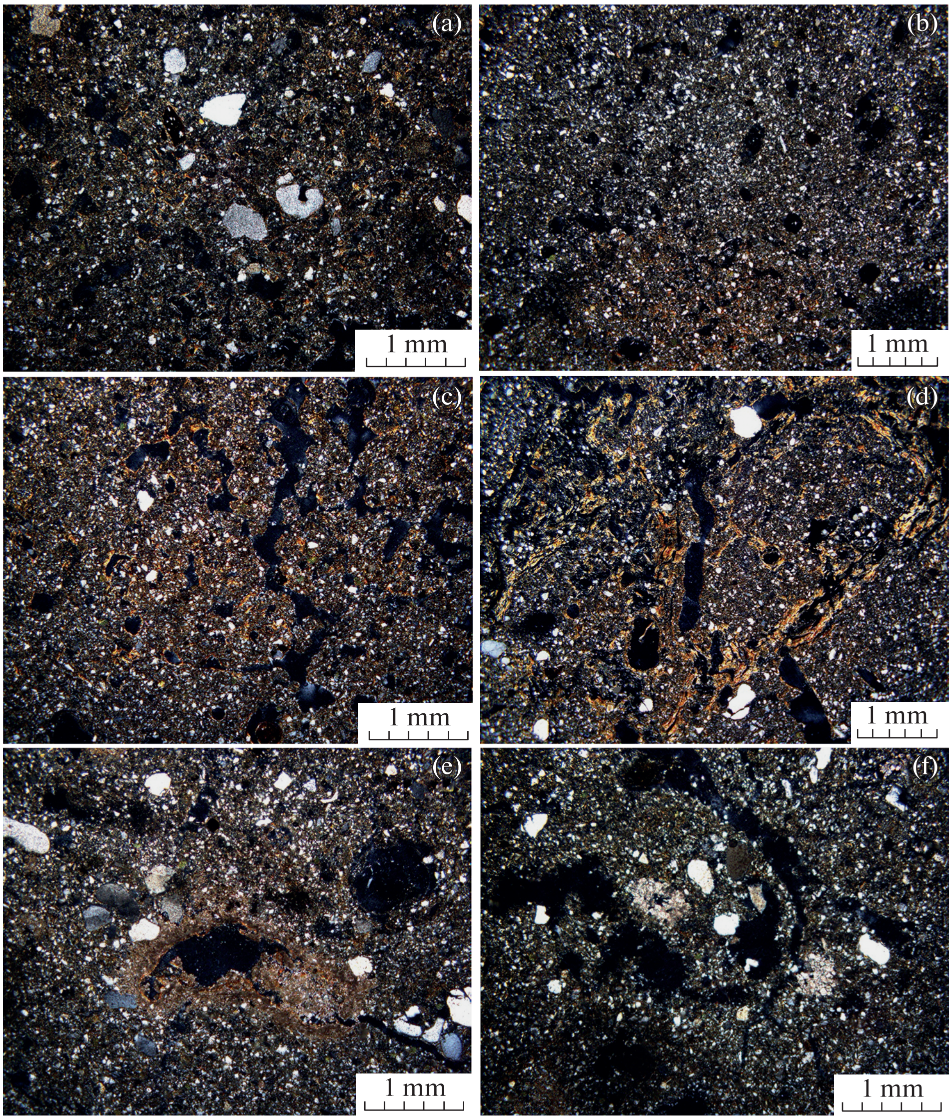


**Fig. 6.** Micromorphology of lower horizons. (a) – Soil 3b, 80–90 cm. Single thin clay coatings cover about 5–10% of pores. NX, (b) – Soil 4b, 90–100 cm. Rare thin clay coatings cover about 10–15% of pores. NX, (c) – Soil 2b, 84–94 cm. Clay coatings, covering 40–50% of pores. NX, (d) – Soil 1s, 90–100 cm. Thick clay coatings within the pore space cover up to 70–80% of pores. NX, (e) – Soil 3b, 115–123 cm. Complex clay-carbonate coatings with upper dark-brown clay coatings and micritic lower layer. NX, (f) – Soil 3b, 115–123 cm. Sparite nodules. NX.

Note the increasing amount of coatings from A to C.

**Рис. 6.** Микроморфология нижних горизонтов. (a) – почва 3b, 80–90 см. Единичные тонкие глинистые кутаны покрывают 5–10% пор. NX, (b) – почва 4b, 90–100 см. Редкие тонкие глинистые кутаны покрывают 10–15% пор. NX, (c) – почва 2b, 84–94 см. Глинистые кутаны, покрывающие 40–50% пор. NX, (d) – почва 1s, 90–100 см. Мощные кутаны в поровом пространстве, которые покрывают 70–80% пор. NX, (e) – почва 3b, 115–123 см. Комплексные глинисто-карбонатные кутаны с темно-коричневыми глинистыми кутанами сверху и микритовыми кутанами снизу. NX, (f) – почва 3b, 115–123 см. Нодули спарита. NX.

Отмечено увеличение количества и мощности кутан от горизонта А к горизонту С.

etation of the territory – a broadleaf forest (*Quercus robur*, *Tilia cordata*) with an undergrowth of *Corylus* and *Euonymus verrucosus*. At the same time, *Pinus silvestris* dominates AP group (fig. 10), accounting for up to 57% of 75.9% of AP total percentage. This feature is very characteristic of the palynospectra of the northern forest-steppe (Novenko et al. 2016) and occurs from the high pollen productivity of pine and the good adaptability of its pollen to air transport.

The group of non-arboreal pollen (24.1% in total) is dominated by pollen of Asteraceae, Chenopodiaceae, Poaceae and Cyperaceae, which is quite consistent with the geobotanical description of the territory (*Chenopodium album, Carex pilosa*) and a photo show-

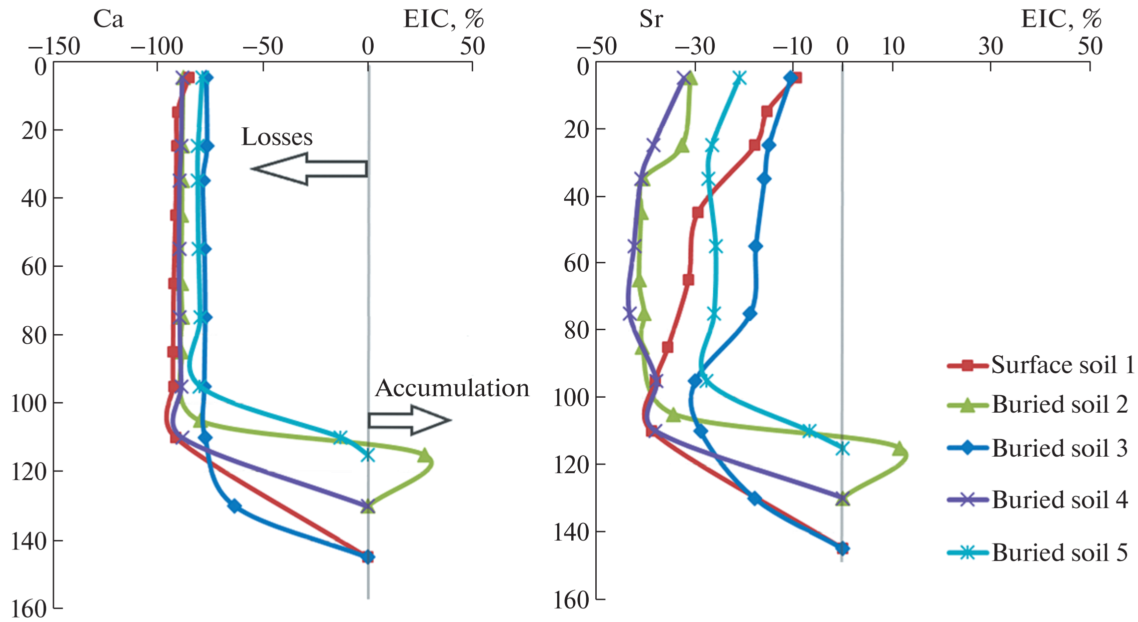


**Fig. 7.** Depth functions of eluvial – illuvial coefficients (EIC) calculated for CaO and Sr.

**Рис. 7.** Распределение элювиально-иллювиальных коэффициентов (ЭИК) по профилю, рассчитанные для CaO и Sr.

ing that arable land is adjacent to the forest. The group of synanthropic plants is represented by pollen of Urticaceae, *Plantago* sp., *Artemisia*, *Chicorium, Centaurea cyanus* and some others (see pollen diagram). In general, the composition of NAP group reflects the

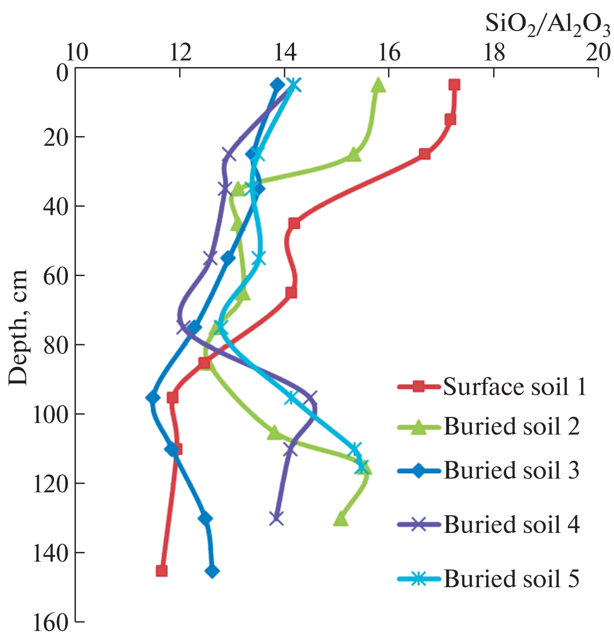


**Fig. 8.** Depth function of $SiO_2/Al_2O_3$ ratio for the surface soil 1s and the buried soils 2b, 3b, 4b, 5b.

**Рис. 8.** Распределение отношения $SiO_2/Al_2O_3$ по профилю для фоновой почвы 1s и погребенных почв 2b, 3b, 4b, 5b.

xerophytic appearance of herbaceous vegetation. *Sphagnum* mosses and *Lycopodium annotinum* dominate the spores group.

Pollen spectra from paleosols have quite significant differences both from the surface soil and from each other. An extremely small amount of Scots pine pollen in all samples from buried soils may indicate a higher productivity of plants of local biocenoses. Our data show that the common difference between the spectra from buried and surface soils is a significantly smaller proportion of arboreal pollen (from 26.1 to 49.4% versus 75.9%, respectively). The dominant in the spectra from buried soils is birch pollen, a pioneer plant of secondary forests inhabiting areas of clear cuts and conflagrations. It actively replaces pine and broadleaf plants as a much more competitive plant (Kuznetsova et al., 2019).

A large number of charcoal microparticles as well as single findings of *Gelasinospora,* an indicator of fires (van Geel, 1986) were recorded in all samples from buried soils. In the herbaceous part of the spectra, pollen from plants of arid steppes and field weeds is most abundant, which, along with the presence of pollen of *Ephedra*, Euphorbiaceae, Cannabaceae indicates a significant agro-load on landscapes and a greater heat supply and dryness of the climate. In general, the composition of the spectra is characteristic of the forest-steppe with sections of birch forests, meadow communities, and a significant proportion of ploughed territories.

Among pollen assemblage from the soil buried under the mound No. 86 and dating back to the second half of the 11th century (the 2b soil), birch pollen

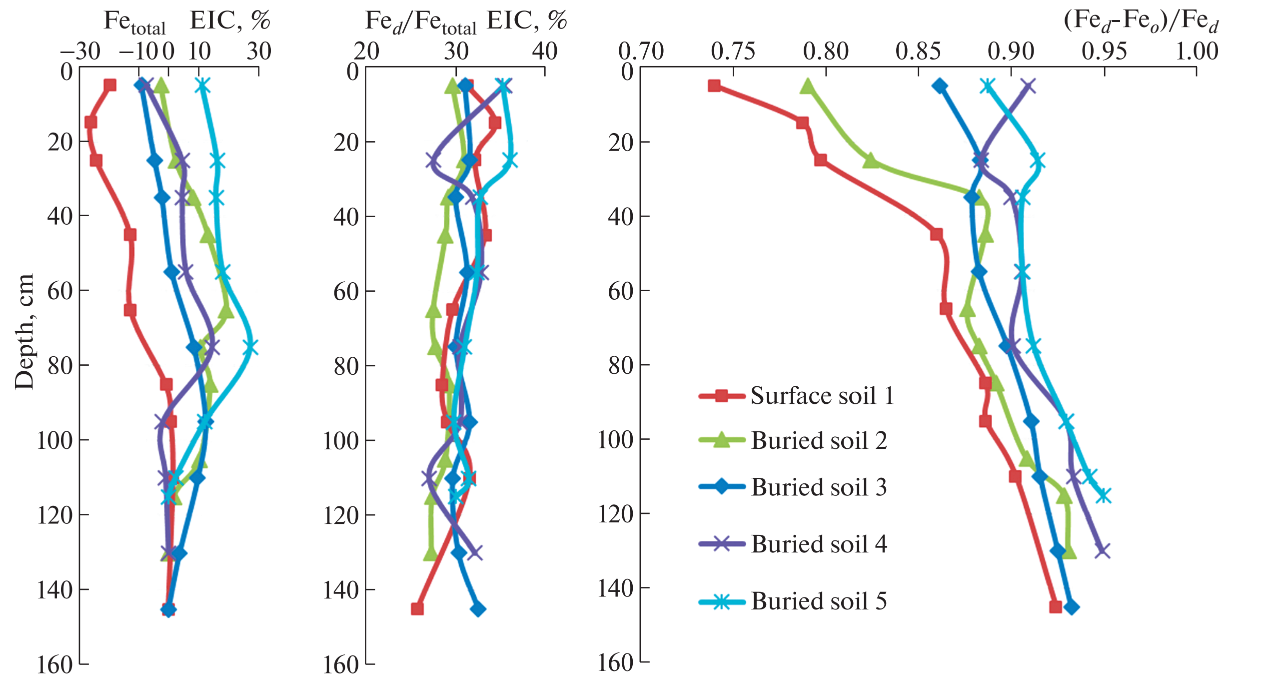


**Fig. 9.** Depth functions of eluvial – illuvial coefficients (EIC) calculated for total Fe (a) and weathering indexes (b, c) in the surface and the buried soils.

**Рис. 9.** Распределение элювиально-иллювиальных коэффициентов (ЭИК) по профилю, рассчитанных для общего железа (a) и индексов выветривания (b, c) в фоновой и погребенных почвах.

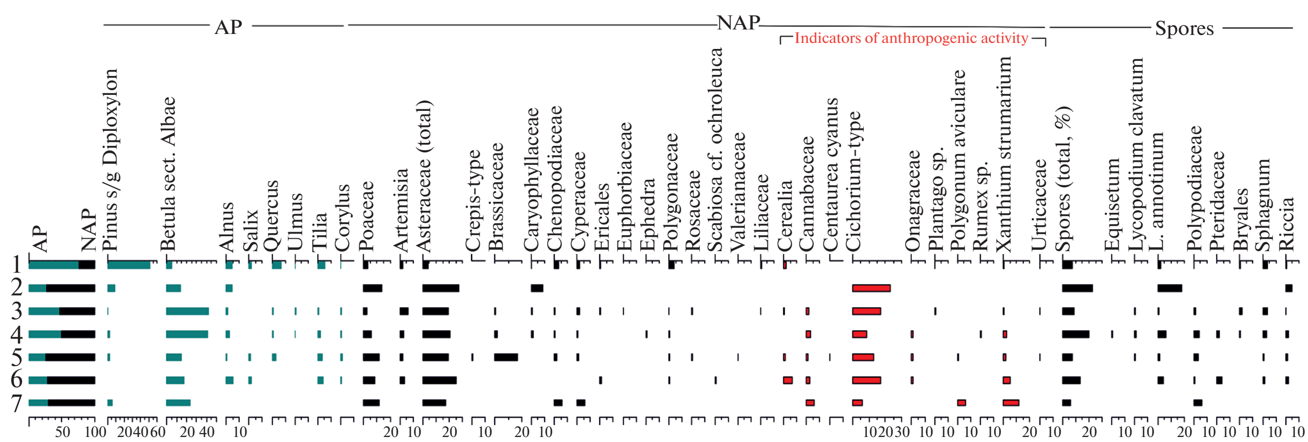


**Fig. 10.** Pollen diagram of the Gochevsky site: *1* – surface soil 1s, *2* – buried soil 3b, *3* – buried soil 2b (1), *4* – buried soil 2b (2), *5* – buried soil 4b, *6* – buried soil 5b (1), *7* – buried soil 5b (2).

**Рис. 10.** Пыльцевая диаграмма Гочевского участка: *1* – фоновая почва 1s, *2* – погребенная почва 3b, *3* – погребенная почва 2b (1), *4* – погребенная почва 2b (2), *5* – погребенная почва 4b, *6* – погребенная почва 5b (1), *7* – погребенная почва 5b (2).

dominates (more than 40%), which may indicate the presence of a birch-oak forest at the time of the burial. In the pollen spectrum from the 3b soil, the pollen of herbaceous plants accounts for more than 72%, of which almost 50% is pollen of Asteraceae and Cichorioideae. Taking into account the almost complete absence of pollen from plants typical of meadow-steppe communities, this, apparently, may reflect the wide distribution of open steppe spaces or arable land around the site of the burial mound. However, the unsatisfactory preservation of pollen indicates that a certain part of it, including pollen of herbaceous plants, has completely decomposed, and in this case any paleogeographic conclusions will be very arbitrary.

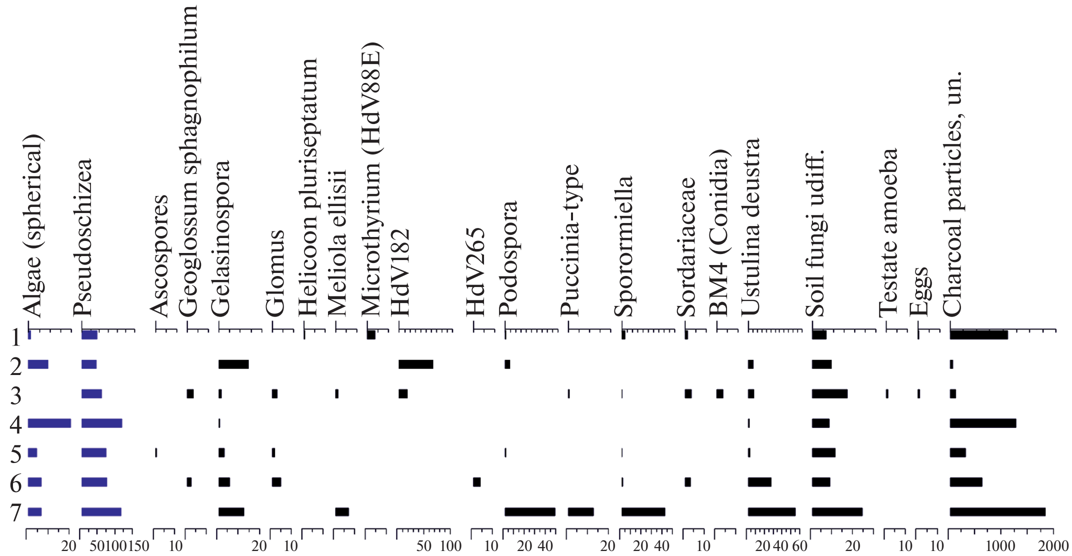


**Fig. 11.** NPP diagram of the Gochevsky site: *1* – surface soil 1s, *2* – buried soil 3b, *3* – buried soil 2b (1), *4* – buried soil 2b (2), *5* – buried soil 4b, *6* – buried soil 5b (1), *7* – buried soil 5b (2).

**Рис. 11.** Диаграмма непыльцевых палиноморф Гочевского комплекса: *1* – фоновая почва 1s, *2* – погребенная почва 3b, *3* – погребенная почва 2b (1), *4* – погребенная почва 2b (2), *5* – погребенная почва 4b, *6* – погребенная почва 5b (1), *7* – погребенная почва 5b (2).

In the 5b soil, the maximum content of Cannabaceae pollen was documented, which can be interpreted as a signal of hemp cultivation in the region, which is consistent with the pollen evidence from the Sudzha oxbow lake in the Kursk region (Shumilovskikh et al., 2019).

The NPP group is poorly diverse (fig. 11). Only soil algae *Pseudoschizea* are abundant, as well as spores of the coprophilous fungi *Sporormiella* and *Sordaria*, which may indicate the proximity of the pasture zone. The abundance of algae *Pseudoschizea* is not entirely clear and, in general, is hardly characteristic of xerophytic environments. However, soil algae are able to exist even under extremely unfavorable environmental conditions, which explains their wide distribution and the speed of their growth even with the short-term appearance of favorable factors, in the case of xerophytic conditions – during the rainfall season.

All the soils were formed in loess sediments and were classified as *Folic Greyzemic Luvic Phaeozem Cutanic*. Uncoated silt and sand grains on the ped faces in the lower part of a humic horizon (AhE) indicate greyzemic features. The argic horizon clay cutans on the ped surfaces indicate that all studied soils passed through the forest pedogenesis.

Despite the similarities, the detailed analysis of the morphological and chemical features made it possible to identify the difference between the studied soils and to relate them to climatic changes that took part in the 11th century and set a transition from a dryer period to subsequent humidification of the climate.

Our results showed that soil 3b, which was buried approximately at the beginning of the 11 century, displays many signs of drier conditions such as the darker colour of the humus horizon, less accumulation of Fe–Mn concretions and presence of sparite nodules. The results of analysis of elemental limited losses of Ca and Sr from the upper and middle soil horizons, a higher share of crystalline forms in the pedogenic iron, lower values of $SiO_2/Al_2O_3$ ratio and their very smooth vertical changes in the profile composition also points to drier conditions before the burial of the 3b soil. In addition, according to pollen records, the spectra of this soil are dominated by pollen of herbaceous plants, mainly Asteraceae and Cichorioideae, accounting for 72%, which reflects the existence of open spaces around the mound, most likely arable land.

The shift to a more humid environment coincided with the burial of soil 5b and 4b. Humidification of the climate increased up to the recent levels over a short period towards the burial of the soil 2b, which took place in the second half of the 11 century (fig. 12). Buried soil 2b has many properties similar to the surface soil, such as expression of greyzemic features, both soils showed a high $SiO_2/Al_2O_3$ ratio in their topsoil material, which also indicates wetter conditions. Pollen data from this soil indicate the presence of a birch-oak forest around the mound site.

## 5. CONCLUSIONS

The soils studied at the Gochevsky burial ground (including the surface soil and five buried soils under mounds) have developed over different periods but

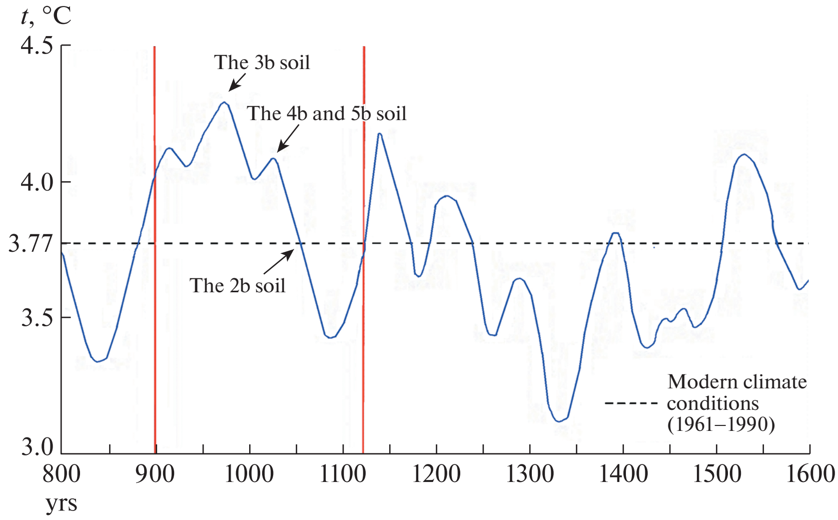


**Fig. 12.** Average annual air temperature in the central part of the Russian Plain in the 9th–16th centuries. The graph shows the suggested burial time of the studied soils (after Klimenko et al., 2001).

**Рис. 12.** Среднегодовая температура воздуха в центральной части Русской равнины в IX–XVI вв. На графике показаны предполагаемые даты погребения исследованных почв (по Клименко и др., 2001).

show relatively small differences in other soil-forming factors and, therefore can be used as a soil chronosequence to identify the differences between the present environment and the environments that existed at the time of the soil burial in the middle and the second half of the 11th century.

According to a set of soil properties, the soil can be arranged chronologically: soil 3b – 4b and 5b – soil 2b (fig. 12). Soil, which was buried approximately at the beginning of the 11 century (3b), displays signs of drier conditions. According to pollen records, the spectra of the above mentioned soils are dominated by pollen of herbaceous plants, mainly Asteraceae and Cichorioideae, accounting for 72%, which reflects the existence of open spaces around the mound.

Humidification of the climate increased to the present level in a short period towards to the soil 2b burial, which occurred in the second half of the 11th century. The transition to a more humid environment coincided with the burial of soils 5b and 4b. Pollen data from these soils indicate the presence of a birch-oak forest around the mound site.

## RECONSTRUCTION OF MEDIEVAL PALEOLANDSCAPES BASED ON THE STUDY OF PALEOSOLS OF GOCHEVSKY ARCHAEOLOGICAL COMPLEX (KURSK REGION, RUSSIA)

**F. G. Kurbanova[a,#], T. A. Puzanova[b], E. N. Aseyeva[b], P. G. Kust[c], and O. V. Rudenko[d]**

[a] *Institute of Geography RAS, Moscow, Russia*

[b] *Lomonosov Moscow State University, Faculty of Geography, Moscow, Russia*

[c] *Dokuchaev Soil Science Institute, Moscow, Russia*

[d] *Turgenev Orel State University, Orel, Russia*

[#] *E-mail: fatima.kurbanova@igras.ru*

Due to isolation from the external environment, the soils buried under the mounds of burial complexes are valuable natural archives that provide information on the past environments. Soils buried under mounds in the Middle Ages with a short time interval – 25–50 years were studied in present paper. The research included the detailed field morphological description of the buried soils, particle size analysis and the study of elemental composition, iron fraction, some other chemical parameters and spores, pollen and non-pollen palynomorphs. Surface soil in the immediate vicinities of the mounds was studied for comparison. The data obtained allowed the forest-steppe landscape dynamics in the 11th century. Medieval warming and subsequent humidification of the climate over a short period could significantly impact natural conditions and the migration of the population of the steppes of Eurasia.

*Keywords:* paleosols, pollen, paleoclimate, Holocene, Medieval Climatic Optimum

ACKNOWLEDGEMENTS

The authors are grateful to Olga Khokhlova for assistance in field studies. Spore-pollen and soil analysis, micromorphological investigations and field research was financially supported by the Russian Science Foundation (project No. 19-18-00327). Analysis of iron fractions were performed in the framework of the State Task of the Institute of Geography, Russian Academy of Sciences No. AAAA-A19-119021990092-1 (FMWS-2019-0008).

REFERENCES

Beug H.J. Leitfaden der Pollenbestimmung für Mitteleuropa und angrenzende Gebiete (Guide to the Pollen Analysis for Central Europe and the Adjacent Areas). Verlag Dr. Friedrich Pfeil, München, 2004. 542 p.

Borisenkov E.P. and Pasecki V.M. Extreme natural phenomena in Russian chronicles of the XI–XVII centuries. Leningrad: Hydrometeoizdat (Publ.), 1983. 241 p. (in Russ.) Database for Palynological Data (PalDat) [Electronic data]. URL: https://www.paldat.org/

European Pollen Database [Electronic data]. URL: http://www.europeanpollendatabase.net/index.php

FAO Guidelines for soil description. Fourth edition. Rome: Food and Agriculture Organization of The United Nations, 2006. 109 p.

Goosse H., Guiot J., Mann M.E., Dubinkina S., and Sallaz-Damaz Y. The medieval climate anomaly in Europe: Comparison of the summer and annual mean signals in two reconstructions and simulations with data assimilation Global and Planetary Change. 2012. No. 84–85. P. 35–47.

Grimm E.C. TILIAGRAPH vl.25 (computer software). Illinois State Museum, Research and Collections Center, Springfield, IL, USA. 1991.

IUSS Working Group WRB. World Reference Base for Soil Resources 2014, update 2015. An international soil classification system for naming soils and creating legends for soil maps. World Soil Resources Reports 106. Rome: FAO, 2015. 203 p.

Khokhlova O.S. Short-term variability of properties of paleosols buried under Earth mounds (kurgans) and temporal scale of the derived paleoclimatic reconstructions. *Materialy Vserossiiskoi nauchnoi konferentsii, posvyashchennoi pamyati professora A.A. Velichko (Moskva, 23–25 noyabrya 2016 g.)*. Moscow, 2016. P. 591–596. (in Russ.)

Klimenko V.V., Klimanov V.A., Sirin A.A., and Sleptsov A.M. Climate changes in Western European Russia in the late Holocene. *Doklady Earth Sciences*. 2001. Vol. 377 (2). P. 190–194.

Kupriyanova L.A. and Aleshina L.A. Pollen and spores of plants of the USSR flora. Vol. 1. Leningrad: Nauka (Publ.), 1972. 171 p. (in Russ.)

Kurbanova F.G., Puzanova T.A., Rudenko O.V., and Starodubtsev G.V. Dataset on the soils of Medieval archaeological monuments in the forest-steppe zone of the East European Plain. Data in Brief. 2020. No. 30. P. 1–24.

Kuznetsova N. and Sautkina M. Forest State and Dynamics of their Species Composition in the Central Federal Distric. *Lesovedenie i lesovodstvo*. 2019. No. 2. P. 25–45. (in Russ.)

Makeev A.O., Rusakov A.V., Kurbanova F.G., Khokhlova O.S., Kust P., Lebedeva M.P., Milanovskiy E.Yu., Egli M., Denisova E., Aseyeva E.N., Rusakova E., and Mihailov E.A. Soils at archaeological monuments of the bronze age – a key to the Holocene landscape dynamics in the broadleaf forest area of the Russian Plain. *Quaternary International*. 2020. Vol. 590. P. 1–22. https://doi.org/10.1016/j.quaint.2020.09.015

Marsan F.A., Bain D.C., and Duthie D.M.L. Parent material uniformity and degree of weathering in a soil chronosequence, northwestern Italy. *Catena*. 1988. Vol. 15. No. 6. P. 507–517. https://doi.org/10.1016/0341-8162(88)90002-1

Mehra O.P. and Jackson M.L. Iron oxide removal from soils and clays by a dithionite-citrate system buffered with sodium bicarbonate. *Clays and Clay Minerals*. 1960. No. 7. P. 317–327. https://doi.org/10.1346/CCMN.1958.0070122

Muir J.W. and Logan J. Eluvial/illuvial coefficients of major elements and the corresponding losses and gains in three soil profiles. *European Journal of Soil Science*. 1982. Vol. 33. No. 2. P. 295–308. https://doi.org/10.1111/j.1365-2389.1982.tb01767.x

Munsell Soil Color Charts. Grand Rapids: Munsell Color, 2014.

Novenko E.Y., Tsyganov A.N., Rudenko O.V., Volkova E.V., Zuyganova I.S., Babeshko K.V., Olchev A.V., Losbenev N.I., Payne R.J., and Y.A. Mazei. Mid- and late-Holocene vegetation history, climate and human impact in the forest-steppe ecotone of European Russia: new data and a regional synthesis. *Biodiversity and Conservation*. 2016. Vol. 25. No. 12. P. 2453–2472. https://doi.org/10.1007/s10531-016-1051-8

Puzanova T.A., Aseeva E.N., Lebedeva M.P., Kurbanova F.G., and Chernov T.I. The methods of re-search of buried soils under archaeological sites. Proceedings of 18 international multidisciplinary scientific geoconference SGEM 2018, Soils, Forest ecosystems, Marine and Ocean Ecosystems, Sofia, Bulgaria. 2018. Vol. 16. P. 611–619. http://dx.doi.org/10.5593/sgem2018/3.2

Schaetzl R.J. and Anderson S. Soils: Genesis and Geomorphology. New York: Cambridge University Press, 2005. 833 p.

Sheldon N.D. and Tabor N.J. Quantitative paleoenvironmental and paleoclimatic reconstruction using paleosols'. *Earth-Science Reviews*. 2009. Vol. 95. No. 1–2. P. 1–52. https://doi.org/10.1016/j.earscirev.2009.03.004

Shoba S.A. (Ed.) *Natsional'nyi atlas pochv Rossiiskoi Federatsii* (National Soil Atlas of Russian Federation). Moscow: Astrel (Publ.), 2011. 632 p. (in Russ.)

Shumilovskikh L.S., Rodinkova V.Ye., Rodionova A., Troshina A., Ershova E., Novenko E., Zazovskaya E., Sycheva S.A., Kiselev D.I., Schlütz F., and Schneeweiß J. Insights into the late Holocene vegetation history of the East European forest-steppe: case study Sudzha (Kursk region, Russia). *Vegetation History and Archaeobotany*. 2019. No. 28. P. 513–528. https://doi.org/10.1007/s00334-018-00711-4

Shumilovskikh L.S., Shumilovskikh E.S., Schlütz F., and van Geel B. NPP-ID: Non-Pollen Palynomorph Image Database as a research and educational platform. Vegetation History and Archaeobotany. 2021. Published online. https://doi.org/10.1007/s00334-021-00849-8

Stoops G. Guidelines for Analysis and Description of Soil and Regolith Thin Sections. Madison: Soil Science Society of America, 2003. 256 p.

Targulian V.O. and Goryachkin S.V. (Eds.) Soil Memory: Soil as a Memory of Biosphere-Geosphere-Anthroposphere Interaction. Moscow: URSS (Publ.), 2008. 692 p. (in Russ.)

van Geel B. Application of fungal and algal remains and other microfossils in palynological analysis. *Handbook of Holocene Palaeoecology and Palaeohydrology*. Wiley, Chichester, 1986. P. 497–505.

Vodyanitsky Y.N. Heavy metals and metalloids in soils. Moscow: Dokuchaev Soil Science Institute (Publ.), 2008. 86 p. (in Russ.)

**EDN:** JEXXXB
*ГЕОМОРФОЛОГИЯ, 2022, том 53, № 5, с. 48–59*

## ПРОБЛЕМЫ ПАЛЕОПОЧВОВЕДЕНИЯ И ГЕОАРХЕОЛОГИИ

*УДК 551.89:574→631.42:902/904(470.45)*

# ВЛИЯНИЕ СОСТАВА И СВОЙСТВ ХВАЛЫНСКИХ ОТЛОЖЕНИЙ НА ЭВОЛЮЦИЮ ПОЧВ ВОЛГО-УРАЛЬСКОГО МЕЖДУРЕЧЬЯ (ПО РЕЗУЛЬТАТАМ МИНЕРАЛОГИЧЕСКИХ И МИКРОМОРФОЛОГИЧЕСКИХ ИССЛЕДОВАНИЙ)


**М. П. Лебедева[1,*], О. О. Плотникова[1], Н. А. Чурилин[1], Т. В. Романис[1], В. А. Шишков[2]**

*[1]Почвенный институт имени В.В. Докучаева, Москва, Россия*
*[2]Институт географии РАН, Москва, Россия*
**E-mail: m_verba@mail.ru*

Поступила в редакцию 14.06.2022 г.
После доработки 26.06.2022 г.
Принята к публикации 15.07.2022 г.

В северо-западной части Прикаспийской равнины для двух разных типов почв, подстилаемых слоистыми отложениями, проведено сравнение макро-, микроморфологических, гранулометрических, физико-химических показателей и минералогического кварц-полевошпатового коэффициента криогенной контрастности (ККК). Значения ККК для подстилающих почвы отложений ≥1 свидетельствуют о криогенных преобразованиях осадка. Скачкообразное распределение коэффициента ККК в зависимости от текстурного класса слоев (ККК <1 для суглинистых, ККК ≥1 для глинистых) слоистых шоколадных глин у оз. Эльтон в обнажении Лисья балка (+12 м над у. м.) указывает на сезонный привнос и отложение материала верхней части нижнехвалынских морских отложений в водоемы со слабой проточностью на границе голоцен-плейстоцена. Для территории с высотой +26 м над у. м. (Джаныбекский стационар) тоже выявлены лессовидные слои с ККК ≥1, в которых отмечены включения фрагментов шоколадных глин, похожих на глины у озера Эльтон. Это свидетельство того, что отложения слоистых шоколадных глин близ оз. Эльтон являются одним из источников нижних лессовидных слоев отложений на территории Джаныбекского стационара. В сравниваемых почвах на одной и той же глубине (около 100 см) отмечены признаки синлитогенного криоаридного педогенеза: гранулярная структура и гипсовые аккумуляции с признаками растворения и перекристаллизации. В поверхностных “теплых” слоях отложений сформированы разные типы почв, что связано с разными факторами почвообразования в современных и палеоклиматических условиях голоцена. Предполагаем, что после этапа повышенного атмосферного увлажнения в хроноинтервале 3500–3000 л. н. развитие поверхностных почв происходило по-разному. На недренированной территории стационара при неглубоком залегании грунтовых соленых вод сформировался характерный трехчленный солонцовый комплекс с микрорельефом, включающий изученный разрез солонца на микроповышении. На дренированной плоской поверхности у оз. Эльтон промытость почвы от легкорастворимых солей до глубины 70 см маркирует этап повышенного атмосферного увлажнения. Карбонатность лессовидных “теплых” отложений, низкий уровень грунтовых вод и современный аридный педогенез не позволили на этой территории проявиться солонцовому процессу. В результате на этой поверхности сформирована бурая аридная гипсоносная почва. С 2000-х гг. на Джаныбекской равнине происходит увеличение аридности климата, сопровождающееся небольшим увеличением количества осадков зимнего периода, что вызывает более глубокое весеннее промачивание почвы. В результате в верхних 50 (70) см изученных почв отмечены повышенная биогенная активность и усиление гумусонакопления, вынос легкорастворимых солей и перераспределение карбоната кальция. Микрорельеф обусловливает относительную выраженность этих процессов.

*Ключевые слова:* Solonetz, Calcisol, эволюция почв, изменение климата
**DOI:** 10.31857/S0435428122050091

## 1. INTRODUCTION

The Volga-Ural interfluve occupies a major part of the Caspian lowland, which covers the northern coast of the Caspian Sea in a semicircle. The deposits of the Volga-Ural Interfluve are closely related to changes in the boundaries of the Caspian Sea as a result of transgressions and regressions leading to a change in the lithological composition of surface sediments. These processes are reflected in the features of the composition and structure of the soil-forming rocks. The coastal boundary of the maximum transgression of the Caspian Sea in the Khvalynian period was located at an altitude of +48...50 m, reaching in the north to the foot of the Common Syrt and the slopes of the Syrt Zavolzhye. The question of the stages of the Khvalynian regression of the Caspian Sea and the stages of its delay at different hypsometric levels remains debatable. Retreating at the end of the Upper Quaternary, the Caspian Sea exposed a flat, south-sloping seabed, which already had irregularities due to the activity of sea waters and salt tectonics. As the sea receded, the formation of peculiar landscapes characteristic of the modern semi-desert zone of the south-east of the Russian Plain gradually began on the drained surface.

The entire surface of the Caspian lowland is covered with marine sediments of different ages, which are mainly represented in the north by yellow-brown heavy and medium loams, in the south they are replaced by light and desalinated loams and sands. The most specific for the soil formation of the Lower Volga region are Lower Khvalynian Chocolate clays. They are confined to the second terraces of the Volga and Ural rivers and are not characteristic of the Volga-Ural interfluve (Svitoch et al., 2017). The age of Lower Khvalynian Chocolate sediments according to the latest available dates lies in the range of 25–12.6 thousand years ago (Yanina et al., 2017; Kurbanov et al., 2021). Chocolate clays have a complex polyfacial layering and characteristic crystallooptical properties (Lebedeva et al., 2018). The most frequent occurrence of Chocolate clays in the Volga-Ural Interfluve was noted in a series of depressions located parallel to the Volga valley. This was described earlier by M.P. Britsyna (1954) and confirmed by our field studies and analysis of soil literature (fig. 1). For many Holocene soils, it was noted that the Khvalynian layered (or covertly layered) sediments with the inclusion of seashells are covered by a layer of younger terrestrial formations, which is loess.

Since the late 1970s, an increase in climate humidity has been observed in the Northern Caspian region. At first glance, the changes are insignificant: total annual temperature increased by 1.3°C, precipitation increased by 50 mm, evaporation during the warm period decreased by 70 mm. However, it is known that arid and semiarid landscapes are very sensitive to such changes. Since the territory is drainless, the change in climate humidity leads to a synchronous increase in the groundwater level. These changes have already been reflected in the vegetation of the north of the Caspian lowland. Thus, an increase in the participation of mesophytic vegetation species and an increase in the projective coverage on all elements of the microrelief were registered (Novikova et al., 2004; Sizemskaya, Sapanov, 2010).

The aim of study is to identify the features of microstructure, mineralogical and physico-chemical properties of soils associated with the composition and structure of soil-forming rocks, with modern and relict processes of soil formation in a changing climate.

## 2. MATERIALS AND METHODS

The first study site is located on micro-elevation between 3d and 4th State Forest Belts of the Janybek Experimental Station (Institute of Forestry, RAS) (+26 m altitude, 49°23′54.2″ N 46°47′46.6″ E). Living soil cover consists of *Bassia prostrata* (L.) A.J. Scott, *Salsola laricifolia, Lepidium perfoliatum* L., *Agropyron desertorum* (Fisch. ex Link) Schult., *Festuca valesiaca* Schleich. ex Gaudin, *Tortula desertorum* Broth. The soil (pit 2–15, 49°23′14.0″ N 46°47′25.0″ E) on this site is attributed to Gypsic Solonetz (Albic Clayic Cutanic Differentic Magnesic Hypernatric Raptic). This soil section belongs to one of the chronographs of the combined study of changes in soil properties and climatic conditions on the subject of the Russian Science Foundation project No. 21-74-20121. Water table is 5.35 m. The second study site is located on the 8 m high exposure at the Fox Dry Valley near Elton Lake (+12 m altitude), so the groundwater has not been opened. The soil (pit 6–19, 49°16′39.5″ N 46°40′32.0″ E) on this site is attributed to Haplic Calcisol (Loamic, Raptic) with close bedding by Lower Khvalynian Chocolate clays. The age of the deposits was determined from the shells of a marine mollusk (*Didacna ebersini*) in the lower layers of Chocolate clays on the depth of 4 m. Living soil cover is represented by *Artemísia vulgáris* (L.).

Field description was performed according to FAO Guidelines for Soil Description (2006). Soil types were determined using the World Reference Base for Soil Resources (2015). Micromorphological analysis was conducted using international terminology (Stoops, 2021) with equipment of the Center for Collective Use “Functions and properties of soils and soil cover” of the FRC V.V. Dokuchaev Soil Science Institute. The grain size analyses for fine earth material (<1 mm) was performed by the conventional pipette method (Kachinskiy, 1965). Textural classes were scaled to international standards (Guidelines for Soil Description, 2006) using the construction of cumulative curves (Shein, 2005). Soil salinization was assessed according to the criteria given in the monograph “Salt-affected soils of Russia” (Pankova et al., 2006). The organic carbon was determined by the modified Tyurin method (GOST 26213-91, 1992). Clay fraction (<0.001 mm) was extracted according to Gorbunov (1963). To characterize the degree of participation of the cryogenic weathering process in the formation of deposits and soils the coefficient of cryogenic contrast was used:

$$CCC = Q1/F1 : Q2/F2,$$

(a)

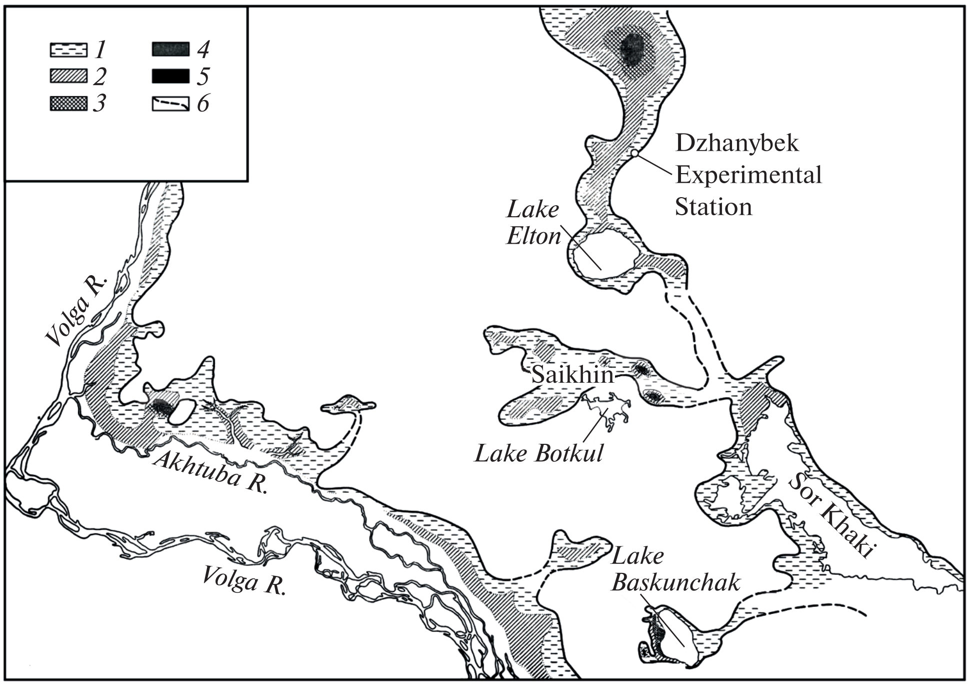


(b)

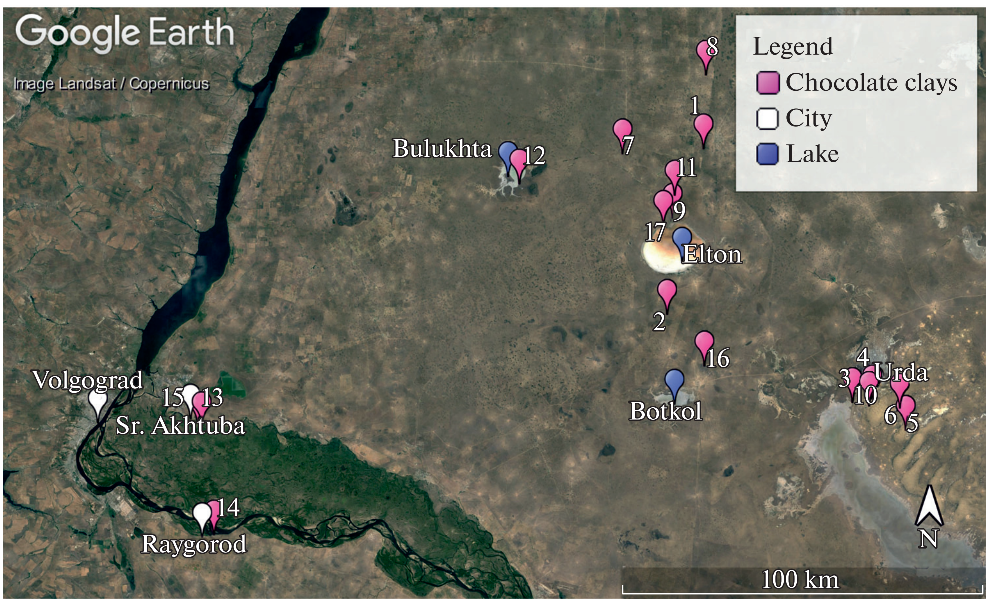


**Fig. 1.** (a) – spatial distribution of Chocolate clays in the Northern Caspian and Volga regions (Britsyna, 1954): 1–5 – horizons of Chocolate clays with a thickness of 0–2, 2–5, 5–8, 8–13 and over 13 m, respectively; 6 – the assumed boundary of the distribution of Chocolate clays before their destruction by denudation processes. (b) – distribution of Chocolate clays according to literature data and personal findings: 1 – Rode and Polsky (1961); 2–4 – Kovda (1950); 5–6 – Yakubov (1938); 7 – Plotnikova et al. (2019); 8 – Demkin and Ivanov (1978); 9–12, 17 – personal finds of M.P. Lebedeva; 13 – Lebedeva et al. (2018); 14–15 – Makshaev and Svitoch (2016); 16 – Britsyna (1954).

**Рис. 1.** (a) – схема распространения шоколадных глин в Северном Прикаспии и Поволжье (Britsyna, 1954): 1–5 – горизонты шоколадных глин толщиной 0–2, 2–5, 5–8, 8–13 и более 13 м соответственно; 6 – предполагаемая граница распространения шоколадных глин до начала их разрушения и денудации. (b) – распространение шоколадных глин согласно литературным данным и личным находкам ученых: 1 – Роде, Польский (Rode, Polsky, 1961); 2–4 – Ковда (Kovda, 1950); 5–6 – Якубов (Yakubov, 1938); 7 – Плотникова и соавт. (Plotnikova et al., 2019); 8 – Демкин, Иванов (Demkin, Ivanov, 1978); 9–12, 17 – личные находки М.П. Лебедевой; 13 – Лебедева и соавт. (Lebedeva et al., 2018); 14–15 – Макшаев, Свиточ (Makshaev, Svitoch, 2016); 16 – Брицына (Britsyna, 1954).

where Q1 and F1 are the content of quartz and feldspar, respectively, in the fraction 0.05–0.01 mm; Q2 and F2 are the content of quartz and feldspar, respectively, in the fraction 0.1–0.05 mm (Rogov, 2009).

Fractions 0.05–0.01 and 0.1–0.05 mm for the calculation of CCC were obtained by sieving from the total residue of particles ≥0.01 mm after clay extraction. The quartz and feldspar content were determined using a SEM microanalyzer JEOL JSM-6610LV (Center for Collective Use "Laboratory of Radiocarbon Dating and Electron Microscopy", Institute of Geography RAS).

## 3. RESULTS AND DISCUSSION

*3.1. Field morphology.* According to the obtained data, the smoothing of the hummock-hollow microrelief described for the Janybek station caused by the lowering of the surface of micro-elevations has now been noted (Konyushkova, Abaturov, 2016). This is most clearly appeared near the depression or near the burrows of soil animals. Moistening of salic lower horizons as a result of rise in groundwater levels (from 7 to 4–5 m over the last 30–40 years) and the transition of sodium sulfate (thenardite) into solution, causing repacking and compaction of subsolonetzic pseudo-sandy material, is considered as a mechanism leading to lowering of modern microrelief (Lebedeva, Konyushkova, 2016). Suffusion subsidence is characteristic of loess and is described as one of the mechanisms of formation of microhollows for territories with meadow-steppe solonetzic complexes. With close bedding of soils with Chocolate clays, the subsidence of the surface is not characteristic (Britsyna, 1954).

*Gypsic Solonetz (soil pit 2.15).* The main type of structure in the E horizon is tiled, but in some zones there is clearly visible differentiation by type of porosity. The upper part of the horizon is dense, below there is a microhorizon (0.5 cm thick) with well-developed vesicular pores, which is gradually turning into a microhorizon with a platy structure (0.5–2 cm) below. The coffee-brown solonetzic horizon with characteristic prismatic (columnar) structure lies under E horizon. Salt pedofeatures of various forms (fading, streaks) appear from 20 cm. Soil effervescence from 10% HCl is recorded from the same depth. Small gypsum veins and yellowish saline mineral concentrations are marked from a depth of 30 cm, large gypsum intergrowths are confined to clay layers from a depth of 70 cm. There are many small roots in the upper horizons, there are few roots in the lower horizons, but they are larger.

On the depth of 70–100 cm litogenic layered structure was described, in the lower horizon (100–120) signs of layered structure are presented. An oval mole passage with chocolate-colored clay material is marked in this layer (fig. 2, (a)).

*Haplic Calcisol (soil pit 6.19).* There are a lot of burrowing animal emissions on the surface. The soil material is silty loam and silty clay. The soil profile has a well-defined reddish-fawn color with a large number of ochre spots (presumably with an increased iron content). Soil effervescence from 10% HCl is recorded from the surface.

From a depth of 50 cm, small fragments of Chocolate clay appear (fig. 2, (b)). From a depth of 70 cm, thin layers of Chocolate clay and loess deposits alternate. In the 70–102 cm layer, Chocolate clay layers lie horizontally parallel to each other, ochre spots and soft ochre layers are confined to the contacts of Chocolate clays and loess. Chocolate clays with a gray hue lie in a layer of 102–138 cm. From a depth of 120 cm, the color of the profile changes – there are brown interlayers on the pale yellow silty material. In a layer of 138–160 cm, there is a layer of loose gray clays with ochre spots and gypsum veins and large crystals. In a layer of 160–200 cm thick units of gray-dove-coloured clays alternate with layers of loess. A *Monodacna caspia* shell was found at a depth of 130 cm. Small fragments of unidentifiable shells were found at a depth of 160–170 cm. From a depth of 200 cm there are vitreous gypsum intergrowths.

Therefore, at the macro level, the morphological properties of the compared soils are different, which determined their different classification position.

*3.2. Soil micromorphology.* In the upper horizons of both soils, low humus content and zoogenic aggregation of silt material was noted. In Calcisol, fragments of Chocolate clays are often found already at a depth of 0–7 cm (fig. 3, (b)), in contrast to the similar horizon of the Solonetz, which is characterized by a thin lenticular structure (fig. 3, (a)).

Below is solonetzic horizon (6–20 cm), which has a characteristic angular-blocky microstructure and striated b-fabric. The features are a relatively small number of thin clay coatings, the presence of humus-clay and clay-ferruginous coatings, including around the microbiota passages. Excrements of soil microfauna, strongly decomposed plant residues and Fe-Mn nodules were also noted. The pedofeatures noted in the solonetzic horizon indicate the current stage of an increase in average annual temperatures with an increase in precipitation and the development of mesophytic vegetation (Novikova et al., 2004). This led to a decrease in the mobility of fine matter, the appearance of ferruginous-manganese nodules in the solonetzic horizon of the Solonetz. Also this led to an increase in the amount of plant residues and an increase in the degree of their humification both in the Solonetz and Calcisol (fig. 4, (a)).

In Calcisol, at a depth of 20–35 cm, various transformations of Chocolate clays fragments were noted with their inclusion in the intrapedal material with micrite impregnation. Micrite nodules with diffuse boundaries are noted in the groundmass near large

(a) (b)

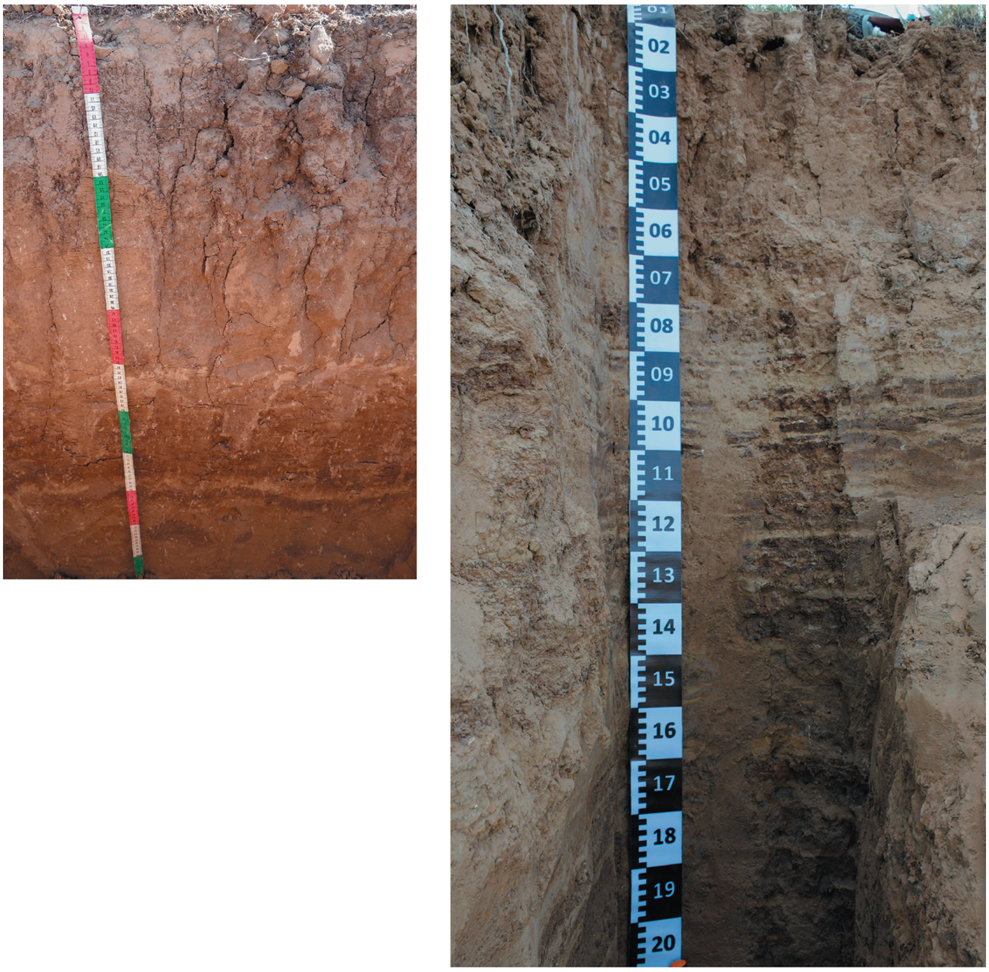

**Fig. 2.** Study sites: (a) Gypsic Solonetz; (b) Haplic Calcisol.
**Рис. 2.** Изученные почвенные профили: (a) Gypsic Solonetz; (b) Haplic Calcisol.

voids. Clay fragments have angular and rounded shapes, small fragments predominate (140–300 μm), there are larger ones (800 μm, occasionally 1250 μm), which consist of a fine silt clay material (fig. 3, (d)). There were no pedofeatures of mobility of clay micromass.

In Solonetz at a depth of 30–50 cm, clays fragments are so strongly assimilated that they greatly increase the content of fine micromass among the silt particles, creating a compacted silty-clay groundmass (fig. 3, (c)). Below (50–100 cm), a loose packing of semi-rounded clay fragments of silt and fine sand dimensions among silicate grains is noted, forming a pseudo-sandy horizon, which is characteristic for the Solonetzes of the Janybek station (Rode, Polsky, 1961). Below 100 cm, the horizon ABkzb was diagnosed with micro features of relict soil formation (fig. 4, (b)): high aggregation of clay-humus-carbonate material (biogenic, cryogenic ooid), a small number of gypsum infillings. This makes it possible to consider this horizon as a buried slightly humic horizon formed in cold arid conditions. We assume that the Fe-Mn dendritic nodules noted here are the result of the current high groundwater level.

In Calcisol in mono-clay layers at a depth of 55–63 cm, fracturing and fragmentation Chocolate clays into platy units were noted (fig. 3, (f)), and at a depth of 70–77 cm there were also micro features of different generations of gypsum infillings (fig. 5, (d)). In Solonetz at a depth of 50–70 cm, the material of Chocolate clays with the same composition does not have a platy structure. It is aggregated (fig. 3, (e)) and forms hypocoatings. Gypsum infillings in Solonetz (fig. 5, (c)) are most likely formed as a result of the capillary ascension of saline groundwater and crystallization in the pores in the capillary-moisture zone. We assume that in Calcisol, smaller gypsum crystals were formed as a result of the dissolution of larger old gypsum crystals and redeposition from solution, since we see crystals of different shape, size and fracturing next to each other

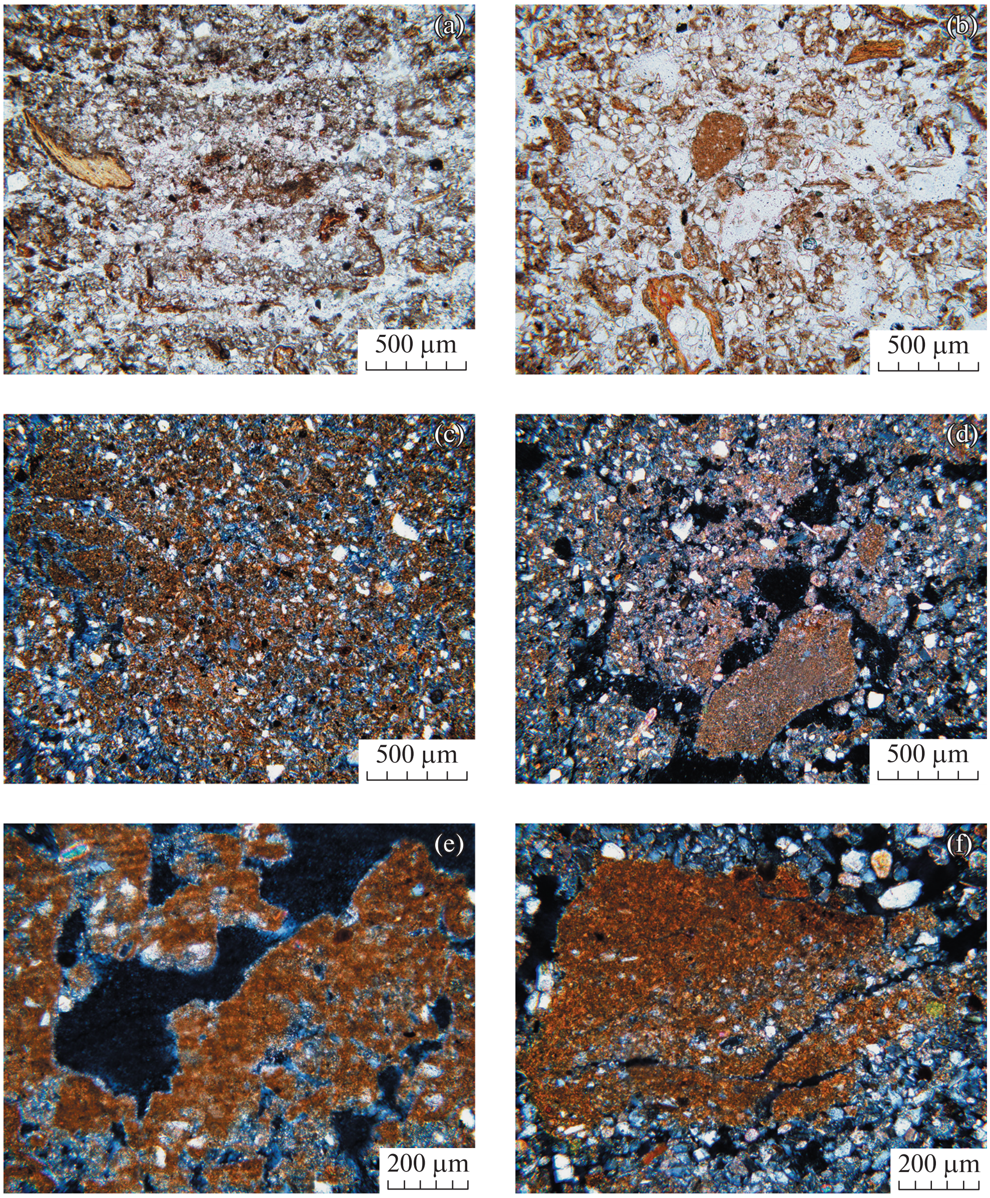


**Fig. 3.** The microstructure of Solonetz (a, c, e) and Calcisol (b, d, f) with close bedding by Lower Khvalynian Chocolate clays: (a) – lenticular microstructure (0–6 cm, PPL); (b) – fragments of Chocolate clays in Ek horizon (0–7 cm, PPL); (c) – assimilated fragments of Chocolate-like clay material (30–50 cm, XPL); (d) – fragments of Chocolate-like material assimilated to varying degrees (20–35 cm, XPL); (e) – fragments of Chocolate clays transformed by pedogenesis (50–70 cm, XPL); (f) – having a larger size than in Solonetz, disintegrating fragment of Chocolate clay (55–63 cm, XPL).

**Рис. 3.** Микроструктура солонца (a, c, e) и бурой аридной почвы (b, d, f) с близким подстиланием Нижнехвалынскими шоколадными глинами: (a) – линзовидная микроструктура (0–6 см, PPL); (b) – фрагменты шоколадных глин в горизонте Ek (0–7 см, PPL); (c) – ассимилированные фрагменты материала, по составу сходного с шоколадными глинами (30–50 см, XPL); (d) – в разной степени ассимилированные фрагменты материала, по составу сходного с шоколадными глинами (20–35 см, XPL); (e) – трансформированные почвообразованием фрагменты материала, по составу сходного с шоколадными глинами (50–70 см, XPL); (f) – крупный разрушающийся фрагмент шоколадной глины (55–63 см, XPL).

(fig. 5, (d)). In Solonetz at a depth of 80–90 cm, clay is microaggregated and included in the silty material (fig. 5, (a)). In Calcisol at a depth of 70–77 cm, Chocolate clay aggregates have the same composition and shape in separate microlayers (fig. 5, (b)), which are combined with layers of silty material. This allows us to assume the same genesis of these layers in the studied soils that are distant from each other.

The modern Calcisol in the Fox Dry Valley is formed on a polyfacial layered thickness of Chocolate clays (fig. 5, (e, f)). The similarity of the composition and structure of Chocolate clays in the profiles of So-

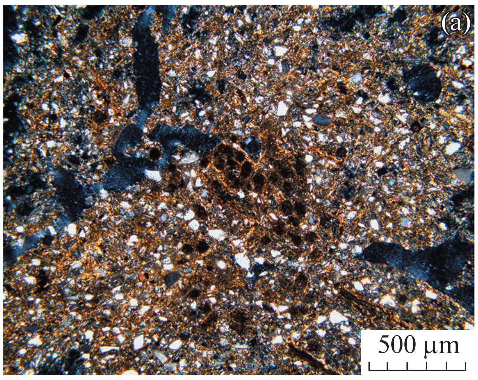


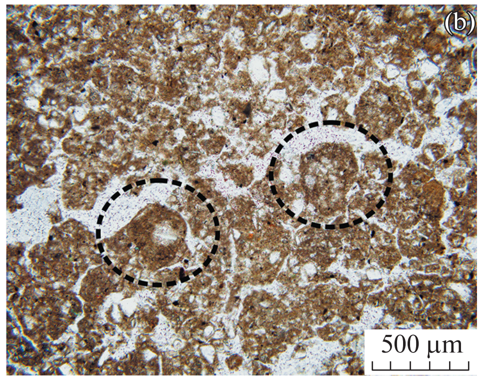


**Fig. 4.** Microstructure of Solonetz, Caspian Lowland: (a) subangular blocky microstructure, striated b-fabric, organic residues and excrements in Btnz horizon (6–20 cm, XPL); (b) rounded biogenic aggregates (black outline) with fine organic material in the groundmass in BCkzb horizon (100–120 cm, PPL).

**Рис. 4.** Микроструктура солонца, Каспийская низменность: (a) округло-блоковая микроструктура, струйчатая ориентация тонкодисперсного глинистого вещества, органические остатки и экскременты в горизонте Btnz (6–20 см, XPL); (b) округлые биогенные агрегаты (черный контур) с органическим веществом в составе тонкодисперсной массы в горизонте BCkzb (100–120 см, PPL).

lonetz and Calcisol shows that the source of clay fragments in the Solonetz of the Janybek station are deposits of the Lower Khvalynian Chocolate clays from dry valleys near the lake Elton, including from the Fox Dry Valley located 20 km from the station.

*3.3. Analytical features.* The studied soils differ from each other in the degree of biogenic processing of the upper thickness (0–50 cm) – Calcisol contains more organic carbon than Solonetz. The compared soils differ greatly in the thickness of the upper horizons washed from salts. The upper 50 cm of Calcisol are not saline, and below the salinity appears, but remains weak to a depth of 120 cm. Solonetz is a highly salinized soil over the entire thickness of the profile, except for the unsaline horizon E. In Solonetz, Cl-$SO_4$ with gypsum and Na type of salinization prevails. In Calcisol, $SO_4$ with Na type of salinization prevails. Toxic salts predominate in the composition of the salts of all saline horizons (tabl. 1).

The profile distribution of calcium carbonate of the studied soils is very notably different. The upper 20 cm of Solonetz is washed from calcium carbonate, while Calcisol effervesce from 10% HCl from the surface. In Solonetz the calcium carbonate content increases with depth and reaches a maximum at a depth of 100–120 cm, and then decreases again. In Calcisol the calcium carbonate content also increases with depth, but reaches a maximum at a depth of 50–70 cm. The maximum content of calcium carbonate in Calcisol is only 1% lower than in Solonetz, but the values of calcium carbonate content in the lower layers of both soils (170–200 cm) are very close (tabl. 1).

The clay content in the upper horizon (0–6 cm) of the Solonetz is 2 times less than in the underlying one. This is an attribute of the eluvio-illuvial differentiation of the clay content in the soil profile, which is characteristic of the Solonetz. In the other horizons of the Solonetz the clay content varies slightly with depth. However, it should be noted that the upper 50 cm are characterized by an increased content of the fraction with a size of 0.002–0.063 mm. Deeper than 50 cm its content decrease (tabl. 2).

On the contrary, in Calcisol, the clay content varies significantly from horizon to horizon, which is related to the number of assimilated Chocolate clays fragments and reflecting lithological heterogeneity. The granulometric composition of Solonetz change little with depth (silty clay, silty clay loam), only horizon E (0–6 cm) has a silt loam texture class. At the same time, the granulometric composition of Calcisol is heterogeneous, silt loam, silty clay loam и silty clay layers alternate (tabl. 2). The heterogeneity of the granulometric composition of the Calcisole profile reflects the lithogenetic heterogeneity of this soil.

The CCC value close to 1 in the E horizon of the Solonetz is a sign of seasonal freezing, which is additionally diagnosed by the separation of fine-silty material in lenticular aggregates (fig. 3, (a)). The value of CCC ≥1 in the Solonetz was noted from a depth of 50 cm and below (tabl. 2), which indicates that the material of these horizons has experienced a period of permafrost (Rogov, 2009). We assume that the presence of rounded Chocolate clay aggregates in the silty material is due to these harsh conditions (fig. 3, (c, e), fig. 5, (a)).

In Calcisol, similar microstructure features and the highest CCC values (≥1.2) were noted for layers of Chocolate clays with a higher content of clay fraction (70–77 and 87–120 cm), which indicates their identical genesis and comparable freezing conditions with

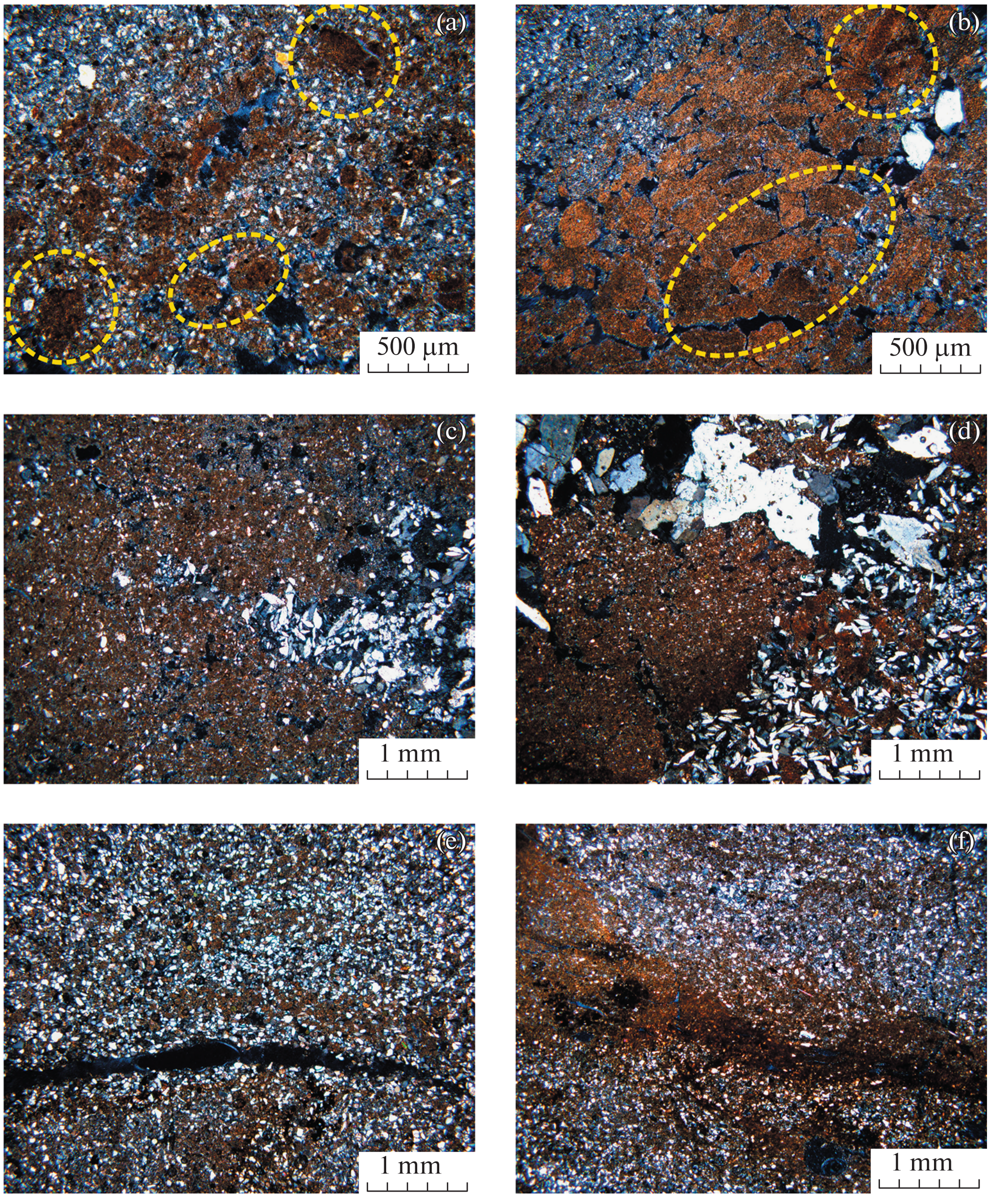


**Fig. 5.** The microstructure of Solonetz (a, c,) and Calcisol (b, d–f) with close bedding by Lower Khvalynian Chocolate clays (XPL): (a, b) – aggregated silty clay material showed by yellow outline (82–86 and 70–77 cm respectively); (c, d) – gypsiym cristals of different age and origin (100–120 and 70–77 cm respectively); (e, f) – intermittent layers of clay and fine sand materials (146-160 and 160–200 cm respectively).

**Рис. 5.** Микроструктура солонца (a, c,) и бурой аридной почвы (b, d–f) с близким подстиланием Нижнехвалынскими шоколадными глинами (XPL): (a, b) – агрегированный пылевато-глинистый материал, показанный желтым контуром (82–86 и 70–77 см соответственно); (c, d) – гипсовые кристаллы разного возраста и происхождения (100–120 и 70–77 см соответственно); (e, f) – перемежающиеся слои глины и тонкого песка (146–160 и 160–200 см соответственно).

clay layers in the studied Solonetz (tabl. 2). For most of the silty layers in Calcisol, CCC< 1, which suggests that they formed under warmer conditions. Such a distribution of CCC in layers with different granulometric composition allows us to assume the seasonality of their deposition dynamics. The possibility of such a genesis of layered Chocolate clays was described earlier (Arkhipov, 1958; Moskvitin, 1962), but this requires further research.

## 4. CONCLUSION

The comparison of microfeatures, grain size distribution and coefficient of the cryogenic contrast

**Table 1.** Selected chemical features of the soils of Caspian Lowland
**Таблица 1.** Некоторые химические показатели почв Каспийской низменности

| Horizon | Lower boundary, cm | Corg, % | $CaCO_3$, % | Total sum of dissolved ions (%) | Sum of toxic salts, % | Degree and type of soil salinization |
|---|---|---|---|---|---|---|
| Soil pit 2.15 | | | | | | |
| E | 6 | 0.74 | NA | 0.1 | 0.1 | non existent |
| Btnz1 | 20 | 0.47 | non existent | 0.1 | 0.1 | slight, $SO_4$-Cl with participation of soda and Na |
| Btnz2 | 30 | 0.29 | 1.85 | 1.1 | 1.0 | strong, $SO_4$ Na |
| Bknyz | 50 | 0.14 | 4.58 | 2.4 | 1.9 | very strong, Cl-$SO_4$ with gypsum and Mg-Na |
| Bkyz1 | 70 | NA | 6.95 | 2.3 | 2.1 | very strong, Cl-$SO_4$ and Mg-Na |
| Bkyz2 | 100 | NA | 6.07 | 2.6 | 2.3 | very strong, Cl-$SO_4$-Na |
| ABkzb | 120 | NA | 8.18 | 2.2 | 2.0 | very strong, Cl-$SO_4$-Na |
| Ckyz1 | 150 | NA | 6.34 | 2.3 | 1.9 | very strong, Cl-$SO_4$ with gypsum and Na |
| Ckyz2 | 170 | NA | 5.54 | 2.4 | 2.0 | very strong, Cl-$SO_4$ with gypsum and Na |
| Ckyz3 | 200 | NA | 4.75 | 2.0 | 1.7 | very strong, Cl-$SO_4$ with gypsum and Na |
| Soil pit 6.19 | | | | | | |
| Ek | 7 | 1.08 | 2.80 | 0.2 | 0.1 | non existent |
| Bk1 | 20 | 0.46 | 4.41 | 0.1 | 0.1 | non existent |
| Bk2 | 35 | 0.44 | 6.21 | 0.1 | 0.1 | non existent |
| Bk3 | 50 | 0.50 | 7.21 | 0.1 | 0.1 | non existent |
| Bkyz | 70 | NA | 4.21 | 0.7 | 0.2 | slight, $SO_4$ with gypsum and Na |
| 2Cdky | 77 | NA | 4.41 | 0.6 | 0.3 | slight, $SO_4$-Mg |
| 3Cdky | 87 | NA | 4.80 | 0.4 | 0.3 | slight, $SO_4$-Mg-Na |
| 4Cdky | 120 | NA | 4.59 | 0.4 | 0.3 | slight, $SO_4$-Mg-Na |
| 5Cdz | 150 | NA | | 1.1 | 1.0 | strong, $SO_4$ Na |
| 6Cdz | 170 | NA | | 0.6 | 0.6 | medium, $SO_4$ Na |
| 6Cdz | 200 | NA | | 0.9 | 0.8 | strong, $SO_4$ Na |

(CCC) of two soils was carried out: Calcisol on an outcrop in the Fox Dry Valley near Lake Elton (+13 m altitude) and Solonetz on micro-elevation on the territory of the Janybek station (+26 m altitude). General and specific features due to paleoclimatic and lithogenic factors of soil formation have been identified. In different soils at a distance of approximately 15 km from each other, the same pattern was noted: the change of CCC at a depth of 50 (70) cm from "warm" to "cold" deposits. The upper loess-like material with CCC <1 can be called "warm", and the lower material because of CCC ≥1 is "cold". The apparent morphological and granulometric layering of the Lower Khvalynian chocolate clays in the Fox Dry Valley outcrop, underlying the Calcisol, is accompanied by a discontinuous distribution of CCC, which suggests their deposition in conditions of seasonal freezing. There was no discontinuous distribution in the values of CCC for the Solonetz, possibly due to the fact that samples were not taken from very thin dusty lenses and interlayers noted in the description in the field. We assume that the layers in the compared soils with the same cryogenic contrast coefficient were formed under the same paleoecological conditions – strongly freezing. The presence of sharp-angled small fragments of chocolate clays mainly in the "cold" lower loess layer and destroyed fragments of clays in the "warm" upper layer of Solonetz, located at a greater

**Table 2.** Grain size distribution, textural classes and the coefficient of cryogenic contrast in the selected horizons of the studied soils, Caspian Lowland

**Таблица 2.** Гранулометрический состав, текстурные классы и коэффициент криогенной контрастности изученных почв Каспийской низменности

| Horizon | Lower boundary, cm | Grain size distribution | | | Textural classes | CCC |
|---|---|---|---|---|---|---|
| | | Clay (<0.002 mm), % | Silt (0.002–0.063 mm), % | Sand (0.063–2 mm), % | | |
| Soil pit 2.15 | | | | | | |
| E | 6 | 17.8 | 66.5 | 15.7 | silt loam | 0.92 |
| Btnz1 | 20 | 37.5 | 52.4 | 10.1 | silty clay loam | 0.64 |
| Btnz2 | 30 | 41.1 | 50.2 | 8.7 | silty clay | 0.87 |
| Bknyz | 50 | 36.9 | 52 | 11.1 | silty clay loam | 0.49 |
| Bkyz1 | 70 | 45.2 | 44.1 | 10.7 | silty clay | 1.13 |
| Bkyz2 | 100 | 43.3 | 47.3 | 9.4 | silty clay | 1.00 |
| ABkzb | 120 | 41.3 | 47.4 | 11.3 | silty clay | 1.00 |
| Ckyz1 | 150 | 37.7 | 46.3 | 16 | silty clay loam | 0.92 |
| Ckyz2 | 170 | 37.6 | 48.4 | 14 | silty clay loam | NA |
| Ckyz3 | 200 | 37.9 | 50.7 | 11.4 | silty clay loam | NA |
| Soil pit 6.19 | | | | | | |
| Ek | 7 | 12.6 | 58.3 | 29.1 | silt loam | 0.85 |
| Bk1 | 20 | 21.1 | 56 | 22.9 | silt loam | 0.72 |
| Bk2 | 35 | 30.2 | 55.9 | 13.9 | silty clay loam | 0.65 |
| Bk3 | 50 | 34.3 | 52.9 | 12.8 | silty clay loam | 0.4 |
| Bkyz | 70 | 22.5 | 55 | 22.5 | silt loam | 0.56 |
| 2Cdky | 77 | 48.5 | 44.6 | 6.9 | silty clay | 1.27 |
| 3Cdky | 87 | 18.2 | 70.2 | 11.6 | silt loam | 0.64 |
| 4Cdky | 120 | 49.7 | 44.5 | 5.8 | silty clay | 1.22 |
| 5Cdz | 150 | 31.9 | 53.2 | 14.9 | silty clay loam | 0.99 |
| 6Cdz | 170 | 17.8 | 59.3 | 22.9 | silt loam | 0.85 |
| 6Cdz | 200 | 22.5 | 56.4 | 21.1 | silt loam | 1.43 |

altitude than the Calcisol, allows us to consider it as a product of aeolian denudation of the dusty-clay layers of the Lower Khvalynian marine sediments near Lake Elton.

In layered sediments with the same value of the cryogenic contrast coefficient for both pits, signs of paleopedogenesis were noted. In Calcisol, granular aggregation of clay material in plane voids between chocolate clay tiles was noted, in Solonetz, characteristic cryoarid aggregation was noted in loess material at a depth of more than 1 m. Large irregular-shaped gypsum accretions marking layers near the saline water level during the retreat of the Khvalynian Sea (Rode, Polsky, 1961) are relict for both soil pits, since their genesis is associated with zones of complete saturation with sulfate waters (Lebedeva, Konyushkova, 2016). The modern recrystallization of gypsum with the formation of small rhomboidal crystals indicating a weak modern washing regime of soils in modern arid conditions is noted. The washing of the upper part of the Calcisol from soluble salts indicates the presence of a stage of increased atmospheric moisture in its evolutionary development. On the one hand, the suffosion microrelief characteristic of loess has not been formed here due to the layering of sediments and the high drainage of the territory. On the other hand, due to the rapid discharge of water down a gentle slope into the lake, a Solonetz profile has not formed here either. For the undrained Janybek plain, soil salinization due to periodic capillary ascension of saline groundwater from a depth of 4–8 m is occurred. The period of increased atmospheric humidification was noted for the chronointerval 3500–3000 years ago (Borisov et al., 2006). Exactly at this time the three-component solonetz complexes characteristic of the modern soil cover of the Janybek plain were formed. The degree of chocolate clay fragments integrity in the upper "warm" loess layer depends on the intensity of modern soil formation processes: biogenic activity, humus accumulation, eluvial-illuvial migration of the humus and clay components, surface hydromorphism. Currently, these processes are conducting with increased intensity due to climate change (Romanis et al., 2022).

# INFLUENCE OF THE COMPOSITION AND PROPERTIES OF KHVALYNIAN DEPOSITS ON THE EVOLUTION OF SOILS OF THE VOLGA-URAL INTERFLUVE (BASED ON THE RESULTS OF MINERALOGICAL AND MICROMORPHOLOGICAL STUDIES)

**M. P. Lebedeva[a,#], O. O. Plotnikova[a], N. A. Churilin[a], T. V. Romanis[a], and V. A. Shishkov[b]**

[a] *Dokuchaev Soil Science Institute, Moscow, Russia*

[b] *Institute of Geography RAS, Moscow, Russia*

[#] *E-mail: m_verba@mail.ru*

In the northwestern part of the Caspian Plain, a comparison of macro-, micromorphological, granulometric, physico-chemical parameters and mineralogical quartz-feldspar cryogenic contrast coefficient (CCC) was carried out for two different types of soils underlain by layered sediments. The values of the CCC for the underlying sediments are ≥1, which indicates cryogenic transformations of the sediment. The abrupt distribution of the CCC depending on the texture class of layers (CCC <1 for loamy material, CCC≥1 for clay) of layered chocolate clays near Lake Elton in the Fox Dry Valley outcrop (+12 m altitude) indicates the seasonal introduction and deposition of material from the upper part of the Lower Khvalynian marine sediments into reservoirs with weak flow at the boundary of the Holocene-Pleistocene. For the territory with of +26 m altitude (Janybek station), loess-like layers with CCC≥1 were also identified, in which inclusions of fragments of chocolate clays are similar to clays near Lake Elton. This is evidence that the deposits of layered chocolate clays from Fox Dry Valley are one of the sources of the lower loess-like layers of sediments on the territory of Janybek station. In the compared soils at the same depth (about 100 cm), signs of synlithogenic cryoarid pedogenesis were noted: granular structure and gypsum accumulations with signs of dissolution and recrystallization. Different types of soils were formed in the surface "warm" layers of sediments (CCC<1), which is associated with different factors of soil formation in modern and paleoclimatic conditions of the Holocene. We assume that after the stage of increased atmospheric humidification in the chronointerval 3500–3000 years ago, the development of surface soils occurred in different ways. On the undrained territory of the station, with a shallow occurrence of saline water-table, a characteristic three-component solonetz complex with a microrelief was formed, including the studied soil pit of the Gypsic Solonetz on a micro-elevation. On a drained flat surface near Lake Elton, the washing of the soil from easily soluble salts to a depth of 70 cm marks the stage of increased atmospheric moisture. The carbonate content of loess-like "warm" sediments, deep water-table and modern arid pedogenesis did not allow the solonetzic pedogenesis to manifest in this area. As a result, Haplic Calcisol was formed on this surface.

Since the 2000s, there has been an increase in climate aridity on the Janybek plain, accompanied by a slight increase in winter precipitation, which causes deeper spring soil wetting. As a result, in the upper 50(70) cm of the studied soils, increased biogenic activity and increased humus accumulation, removal of soluble salts and redistribution of calcium carbonate were noted. The microrelief determines the relative severity of these processes.

*Keywords:* solonetz, brown arid soil, soil evolution, climate change

## ACKNOWLEDGEMENTS

The study of the Gypsic Solonetz was carried out using the funds of the Russian Science Foundation project No. 21-74-20121.

## REFERENCES

Arkhipov S.A. On the lithological and facies characteristics of Khvalynian chocolate clays and the conditions of their formation. *Byulleten' komissii po izucheniyu chet-*

*vertichnogo perioda*. Vol. 22. Moscow: USSR Academy of Sciences (Publ.), 1958. P. 19–25. (in Russ.)

Borisov A.V., Demkin V.A., and Demkina T.S. *Paleopochvy i klimat Ergenei v epokhu bronzy, IV–II tysyacheletie do n. e.* (Paleosoils and climate of Ergeni in the Bronze Age, IV–II millennium BC). Moscow: Nauka (Publ.), 2006. 210 p. (in Russ.)

Britsyna M.P. Distribution of Khvalynian Chocolate clays and some issues of paleogeography of the Northern Caspian. *Trudy Instituta geografii AN SSSR*. 1954. Vol. 62. P. 5–27. (in Russ.)

Bujanovskij M.S., Doskach A.G., and Fridland V.M. *Priroda i sel'skoe khozyaistvo Volgo-Ural'skogo mezhdurech'ya* (Nature and agriculture of the Volga-Ural interfluve). Moscow: USSR Academy of Sciences (Publ.), 1956. 231 p. (in Russ.)

Demkin V.A. and Ivanov I.V. The age of the microrelief and the complexity of the soil cover in the conditions of the semi-desert of the Northern Caspian. *Struktura pochvennogo pokrova i ispol'zovanie pochvennykh resursov*. Moscow: Nauka (Publ.), 1978. P. 171–178. (in Russ.)

Gorbunov N.I. *Vysokodispersnye mineraly i metody ih izucheniya* (Highly dispersed minerals and methods of their study). Moscow: USSR Academy of Sciences (Publ.), 1963. 302 p.

GOST 26213-91 Soils. Methods of determination of organic matter. Moscow: Publishing House of standards, 1992. 8 p. (in Russ.)

Guidelines for Soil Description (4th ed). Food and Agriculture Organization of the United Nations. Rome (Publ.), 2006.

IUSS Working Group WRB 2015 World Reference Base for Soil Resources 2014, update 2015 International soil classification system for naming soils and creating legends for soil maps. *World Soil Resources Reports*. 2015. Vol. 106.

Kachinskiy N.A. *Fizika pochv* (Soil Physics). Moscow: Vysshaya shkola (Publ.), 1965. 320 p. (in Russ.)

Konyushkova M.V. and Abaturov B.D. The specificities and properties of soils of solonetzic complex on the latest stages of development in the area of Caspian sea region. *Dokuchaev Soil Bulletin*. 2016. Vol. 83. P. 53–76. (in Russ.)

Kovda V.A. *Pochvy Prikaspiiskoi nizmennosti (severo-zapadnoi chasti)* (Soils of the Caspian lowland (north-western part)). Moscow: USSR Academy of Sciences (Publ.), 1950. 256 p. (in Russ.)

Kurbanov R., Murray A., Thompson W., Svistunov M., Taratunina N., and Yanina T. First reliable chronology for the early Khvalynian Caspian Sea transgression in the Lower Volga River valley. *Boreas*. 2021. Vol. 50. No. 1. P. 134–146.
https://doi.org/10.1111/bor.12478

Lebedeva M., Makeev A., Rusakov A., Romanis T., Yanina T., Kurbanov R., Kust P., and Varlamov E. Landscape dynamics in the Caspian Lowlands since the last deglaciation reconstructed from the pedosedimentary sequence of Srednaya Akhtuba, Southern Russia. *Geosciences*. 2018. Vol. 8 (12). No. 492. P. 1–21.
https://doi.org/10.3390/geosciences8120492

Lebedeva M.P. and Konyushkova M.V. Solonetzic soilscapes in the northern Caspian Lowland: local and spatial heterogeneity of pedofeatures and their changes in time. *Dokuchaev Soil Bulletin*. 2016. Vol. 86. P. 77–95. (in Russ.)

Makshaev R.R. and Svitoch A.A. Chocolate clays of the Northern Caspian Sea Region: Distribution, structure, and origin. *Quaternary International*. 2016. Vol. 409. P. 44–49.
https://doi.org/10.1016/j.quaint.2015.07.018

Moskvitin A.I. Pleistocene of the Lower Volga region. *Trudy geologicheskogo instituta AN SSSR*. 1962. Vol. 64. 264 p. (in Russ.)

Novikova N.M., Volkova N.A., and Khitrov N.B. Vegetation of the solonetz complexes within rezerved steppe patch at North Pricaspyi. *Arid ecosystems*. 2004. Vol. 10. No. 22–23. P. 9–18. (in Russ.)

Pankova E.I., Vorobyova L.A., Gadzhiyev I.M., Gorokhova I.N., Elizarova T.N., Korolyuk T.V., Lopatovskaya O.G., Novikova A.F., Reshetov G.G., Skripnikova M.I., Slavnyi Yu.A., Chernousenko G.I., and Yamnova I.A. *Zasolennye pochvy Rossii* (Salt-Affected Soils of Russia). Moscow: Akademkniga (Publ.), 2006. 854 p. (in Russ.)

Plotnikova O., Lebedeva M., Varlamov E.B., Nukhimovskaya Yu.D., and Shuyskaya E.V. Micromorphological features of soils of semidesertic solonetzic complexes under different herbaceous communities with the participation of fodder plant Kochia prostrata (Caspian lowland). *Dokuchaev Soil Bulletin*. 2019. Vol. 100. P. 83–116. (in Russ.)

Rode A.A. and Polsky M.N. Soils of the Janybek station, their morphological structure, mechanical and chemical composition and physical properties. *Trudy pochvennogo instituta imeni V.V. Dokuchaeva AN SSSR*. 1961. Vol. 56. P. 3–214. (in Russ.)

Rogov V.V. *Osnovy kriogeneza* (Fundamentals of cryogenesis). Novosibirsk: Academic publishing house "GEO" (Publ.), 2009. 203 p. (in Russ.)

Romanis T., Lebedeva M., Kolesnikov A., Sapanov M., and Sizemskaya M. A dataset of soil microstructure features and the weather conditions affecting them from 2005 to 2021 in the Caspian Depression. *Data in Brief*. 2022. Vol. 41.
https://doi.org/10.1016/j.dib.2022.107957

Shein E.V. *Kurs fiziki pochv* (Course of soil physics). Moscow: MSU Publishing House (Publ.), 2005. 432 p. (in Russ.)

Sizemskaya M.L. and Sapanov M.K. The modern condition of ecosystems and strategy of adaptive nature management in Northern Pricaspian semi-desert. *Arid ecosystems*. 2010. Vol. 16. No. 5 (45). P. 15–24. (in Russ.)

Stoops G. Guidelines for analysis and description of soil and regolith thin sections. *John Wiley & Sons* (Publ.), 2021. 240 p.

Svitoch A.A., Makshaev R.R., Rostovtseva Yu.V., Klyuvitkina T.S., Berezner O.S., Tregub T.F., and Khomchenko D.S. *Shokoladnye gliny Severnogo Prikaspiya* (Chocolate clays of the Northern Caspian). Krasnogorsk: Geographical Faculty of Moscow State University Krasnogorsk Printing House (Publ.), 2017. 140 p. (in Russ.)

Yakubov T.F. Sands of the Naryn semi-desert of the Lower Volga region. Works of the sector of sands and deserts. *Trudy pochvennogo instituta imeni V.V. Dokuchaeva AN SSSR*. 1938. Vol. 17. P. 7–118. (in Russ.)

Yanina T.A., Svitoch A.A., Kurbanov R.N., Murray A.S., Tkach N.T., and Sychev N.V. *Opyt datirovaniya pleistotsenovykh otlozhenii nizhnego Povolzh'ya metodom opticheski stimulirovannoi lyuminestsentsii* (Paleogeographic analysis of the results of optically stimulated luminescence dating of pleistocene deposits of the lower Volga area). *Vestnik Moskovskogo universiteta. Seriya 5. Geografiya*. 2017. Vol. 1. P. 20–28. (in Russ.)

**EDN:** SMOECJ
*ГЕОМОРФОЛОГИЯ, 2022, том 53, № 5, с. 60–68*

## ПРОБЛЕМЫ ПАЛЕОПОЧВОВЕДЕНИЯ И ГЕОАРХЕОЛОГИИ

*УДК 551.89→569.9:902/904(470.53)*

# О ВРЕМЕНИ ПОЯВЛЕНИЯ ЧЕЛОВЕКА СОВРЕМЕННОГО ВИДА НА СЕВЕРО-ВОСТОКЕ ВОСТОЧНО-ЕВРОПЕЙСКОЙ РАВНИНЫ И НА УРАЛЕ (ПО ДАННЫМ ИЗУЧЕНИЯ ПАЛЕОЛИТИЧЕСКОЙ СТОЯНКИ ЗАОЗЕРЬЕ)

**© 2022 г. П. Ю. Павлов[1,*]**
[1]*Институт языка, литературы и истории ФИЦ Коми научный центр УрО РАН, Сыктывкар, Россия*
**E-mail: ppavlov120@gmail.com*

Поступила в редакцию 14.06.2022 г.
После доработки 27.06.2022 г.
Принята к публикации 15.07.2022 г.

Палеолитическая стоянка Заозерье (40–34 тыс. л. н.) расположена в бассейне верхней Камы. Возраст, особенности каменного и костяного инвентаря и украшения, найденные в культурном слое памятника, позволяют уверенно отнести стоянку к началу верхнего палеолита. Комплекс инвентаря стоянки Заозерье имеет определенные черты сходства с инвентарем практически синхронных стоянок костенковской группы памятников начала верхнего палеолита (Костенки XIV, слой IVb и Костенки XVII, II слой). Памятник, вероятно, относится к одному из инициальных рейдов человека современного вида в Восточную Европу. Материалы стоянки Заозерье показывают, что человек современного вида впервые проник в субарктические широты Европы в обстановке интерстадиального потепления климата около 40 тыс. л. н., практически одновременно с его появлением в центре Восточно-Европейской равнины.

*Ключевые слова:* начало верхнего палеолита, северо-восток Европы, инициальное расселение в Субарктике

**DOI:** 10.31857/S0435428122050121

## 1. INTRODUCTION

The history of occupation of the anatomically modern human and spreading of Upper Palaeolithic culture in Eastern Europe – one of the important topics of researches in Eurasian archaeology of the last decade (Hoffecker, 2009; Hublin, 2015; Hublin et al., 2020). Essential aspect of this fundamental problem is determination of the time of human occupation of the regions with extreme climatic conditions, including Arctic and Subarctic (Pavlov et al., 2004; Pitulko et al., 2004; Pavlov, 2015, 2021). The data obtained in the northeast of Europe – one of the few regions of Northern Eurasia where sites of the beginning of the Upper Palaeolithic are known – important for this research (Kanivets, 1976; Pavlov, 2008).

In the northeast of the East European plain, in the basins of Pechora and Upper Kama, and in the western foothills of Middle and Subpolar Urals four sites of the beginning of the Upper Palaeolithic are known (Pavlov, 2015). They are subdivided into two chronological groups. The sites existing in the region at the end of the Leningrad interstadial of Middle Valdai (GI9–H4) comprise the first group (43–34.5 kyr BP). These are sites Mamontova Kurya (Pechora River basin) and the Zaozer'e (Upper Kama River basin). Sites of the second chronological group (33–30 kyr BP), belong to the end of the Middle-beginning of the Late Valdai (GI5–H3) (Byzovaya, Pechora River basin and Garchi I, Upper Kama River basin) (Svendsen et al., 2010).

So even though it's impossible to make an unambiguous correlation one could suspect that at least some of the early phases of human occupation took place during "interstadials" rather than "stadials". It is noteworthy that the timing of the early human visits to the north seems to correspond with a long-lasting period when the Barents-Kara Ice Sheet was small or absent (Svendsen et al., 2010). According to Yu.N. Gribchenko (Gribchenko, 2017) judging from geomorphic and stratigraphic position of the Late Paleolithic sites in the Upper Kama stream, it may be supposed that the most favorable conditions for the migrations of the prehistoric communities into the region developed there by the second half of the Middle Valday interstadial (Gribchenko, 2006).

It is clear enough that the northward migration routes of the early communities depended heavily on physiographic characteristics of the region and specif-

(a)


(b)


**Fig. 1.** Location map.

(a) – Location of the initial Upper Paleolithic (IUP) sites, mentioned in the text: *1* – Zaozer'e, *2* – Kostenki, *3* – Altai IUP sites. (b) – Zaozer'e topographical situation (Google Earth image).

**Рис. 1.** Расположение археологических памятников.

(a) – местоположение памятников начального верхнего палеолита, упоминаемых в тексте: *1* – Заозерье, *2* – Костенки, *3* – алтайские памятники. (b) – космоснимок расположения стоянки Заозерье (по Google Earth).

ic features of the relief-forming processes. Thin cover of snow during the winter seasons and a productive steppe with a dry and firm substrate were important factors that favored large animals and their predators. Rich herbivore diversity was probably a premise for human colonization at this high latitude. These environmental conditions also facilitated the mobility of humans (Svendsen et al., 2010).

## 2. ZAOZER'E SITE

Among the sites of the first chronological group the site Zaozer'e represents significant interest determined by geographical position, comparatively early age, and unique features of the site's assemblage (Pavlov, 2009) The site Zaozer'e (58°09′15″ N; 56°56′32″ E, 118 m a.s.l.) is situated on the south bank of the Kama Reservoir (former river Chusovaya), some 40 km to the east of Perm city (fig. 1). The age of the site according to radiocarbon and OSL dating 35–31 $^{14}$C kyr BP (41–34.5 cal kyr BP) (for details see: [Svendsen et al., 2010; SOM]). The site is located on a ledge in the river valley, on the promontory of third river terrace.

The site location is bounded on two sides by large gullies with steep slopes. The surface of the site itself rises gradually from 15 m above the reservoir to 18–22 m. The loess loam overlying the cultural layer forms a mantle varying in thickness from 4.5 to 3.0 m.

Site's stratigraphy was studied by Yu.N. Gribchenko (2006, 2017). According to his observations the cultural finds were mostly recovered from a humified horizon with distinguishable fragments of multiple-aged soil formation. Stone implements and animal bones are often confined to gleied lenses indicative of excessive moistening periods at the time of human habitation (Gribchenko, 2006). Such formations may be related to buried seasonal-thawing layer dated to the middle Valday interstadial. After period of human occupation an active eolian and eolian-diluvial accumulation of loess started that was interrupted at least twice by short periods of the surface stability; those episodes were recorded by two levels of ephemeral soil formation and the development of large fault systems. The occurrence of the soil complex in the site sections displays signs of weak downslope movements. There are lenses of darker organic-rich material related genetically to an earlier soil formation (presumably dated to the Early Valday interstadial). The underlying horizon displays morphotypical characteristics of horizon B of the interglacial (Mikulino) fossil soil (Gribchenko, 2017). Three OSL-dates that were obtained from just below this zone gave ages in the range 104–92 ka BP, supporting the assumption that this basal part of the aeolian loess accumulated during MIS 5 (Svendsen et al., 2010).

Site's faunal remains include horse (*Equus sf. latipes*), woolly rhinoceros (*Coelodonta antiquitatis*), reindeer (*Rangifer tarandus*), hare (*Lepus timidus*), and mammoth (*Mammuthus primignius*) (ident. by P.A. Kosintsev, IPAE, Ekaterinsburg). Main object of hunting for the site's visitors was a horse. Dense elements of low food value are under-represented in inventory of skeletal parts, which apparently reflects selective retrieval of parts from the kill location. This assumption believes that the place of hunting was in the nearest vicinity of the site.

Along with the horse, the permanent object of hunting was such small animal as a hare. Bones of this animal is found in the close to fireplaces within the living floors. Most likely, hares were hunted for the sake of fur, which was used for making warm clothes.

According to the palaeogeographical reconstruction the site the Zaozer'e was surrounded by open landscapes: the transition from the grassy forest to the steppe (Pavlov, 2009; Silaev et al., 2019).

Palynologist V.V. Pisareva concluded that, during the formation of a cultural layer near the site, probably in the valley of the river, was developed boreal and northern boreal vegetation. Local vegetation consisted of swamp, water and ruderal groups, characteristic for the forming terraces of river valleys and river floodplains. The vicinity of the site was swampy (Pavlov, 2009).

The site Zaozer'e in general, probably, represents remnants of several small temporary hunting camps visited for one or several seasons and situated on place, convenient for hunting. Despite the relatively small excavated area the site's (ca. 200 sq. m) overall layout can be set quite definitely. At least three find concentrations were recognized within the excavated area, and it appears as if each find category (e.g., bones, specific types of tools, and burnt materials) has a unique and restricted spatial distribution, suggesting some organized use of space during the period of human presence The studied objects have, as a rule, one sharp boundary that probably demonstrates existence of an artificial barrier – a wind shield (?) (Svendsen et al., 2010).

The assemblage of the site contains more than 2 thousand artifacts. Besides stone implements the assemblage consist of bone and antler implements, and personal ornaments.

The main type of raw materials on the site (more than 50%) – gray-brown and dark gray concretion and tabular flint from outcrops in Upper Perm limestones. Pebbles from alluvial deposits, mainly dark gray and black Carboniferous siliceous slate, rhinestone and other siliceous rocks was also used (more than 30%). It should be notated that many fragments of siliceous slate found in several congestions near the fireplaces were probably subjected to thermal treatment (?).

Technology of primary knapping is characterized by prevalence of volumetric splitting. Preforms of edge-facetted (?) cores (fig. 2, *1*), longitudinal chips from prismatic cores (fig. 2, *2*) and crested blade (fig. 2, *4*) are found. But radial core (fig. 2, *5*) also presents in the site's assemblage. Among chips of systematic splitting large and middle blades dominate (fig. 3, *1–3*, *9–13*, *22–23*).

End scrapers on flakes prevail in the assemblage's toolset. Large tools with ventral trimming dominate (fig. 2, *7*, *9*, *10*), including high form end-scrapers with a straight edge (fig. 2, *6*, *7*), but majority of the scrapers has a convex edge with planar retouch (fig. 2, *11–13*). Small scrapers made on rock crystal flakes with retouch on one of the longitudinal edges also present (fig. 2, *14*). End scrapers on blades practically absent: only single tool on distal part of large, massive blade (?) represented in the assemblage (fig. 2, *8*).

The artefact assemblage can be categorized in two different classes according to the applied stone technology. The Upper Palaeolithic group represented by implements on blades. It consists of points (fig. 3, *28–31*), burins on truncation and break (fig. 3, *4*, *21*), blades with marginal scalar and steep (in some cases abrupt) retouch (fig. 3, *14–20*), segments ("lunates") (fig. 3, *24*, *25*) and "arch-backed tools" (fig. 3, *26*). It is possible that some implements with a burin spall in fact are cores for producing "Protoaurignacien" straight narrow bladelets (fig. 3, *27*, *32*). Fragments of such bladelets without secondary processing are available in assemblage (fig. 3, *5–8*). Also, small curved lamellar chips without secondary processing which are, most likely, chips of fashion of edges of high form scrapers are found (bladelets *Dufour*?). Fragmentation of lamellar blanks also noted.

The second technical and morphological group of stone assemblage consisted of ovoid unifaces (fig. 4, *6*, *8–11*) and bifaces (fig. 4, *3*, *7*), the backed Kielmesser-type knife (fig. 4, *4*) and partially bifacial straight side-scrapers (fig. 4, *1–2*, *5*). Practically all bifaces have plano-convex retouch which is the leading technological feature of the Middle Palaeolithic Kielmessergruppen industries (KMG) of Eastern Europe (Chabay, 2004).

Particularly noteworthy is the intensive reduction of many tools, and repeated rejuvenation of their working edges.

Implements made of antler and bone presented by blank of projectile (?) (fig. 5, *1*), fragile awl (fig. 5, *3*). and reindeer antlers cropped from one or two sides (fig. 5, *2*). Retouchers on the fragments of large tubular bones also present in the assemblage. Abrasives of fine-grained sandstone for processing organic materials were found in the cultural layer (fig. 5, *12*).

Personal ornaments are represented by the pendants of an oval form made of shell of freshwater Unio mollusks (fig. 5, *4–5*) and beads from fossil crinoids (fig. 5, *7–8*). One pendant has two one side drilled holes located near the center of the pendant. The second pendant is represented by a large fragment with a partly preserved hole. In the assemblage there are also a blank of such a pendant. Also blanks of polished ivory beads (?) and the ivory bladelets (fig. 5, *11*) were found (fig. 5, *10*). In the assemblage there is also a fragment of a roundish thin bone with two cut-through holes (fig. 5, *6*) and the fragment of horse (?) rib dyed by ochre (fig. 5, *13*).

Thus, the complex of the basic characteristics of the site, including spatial organization and the main features of the site's assemblage, completely fit within the AMH behavioral "package" (Benazzi et al., 2020) and unambiguously allow to relate Zaozer'e to the beginning of the Upper Palaeolithic.


**Fig. 2.** Zaozer'e. Stone assemblage.
**Рис. 2.** Заозерье. Каменный инвентарь.

## 3. DISCUSSION

The geographical location of the site the Zaozer'e, practically on border between Europe and Asia (fig. 1), causes the necessity to carry out its comparison with sites of two main neighbouring areas where the sites of beginning of the Upper Palaeolithic are known – East European and North Asian.

In the centre of the East European plain to sites of the initial stages of the Upper Palaeolithic (36–34 $^{14}$C kyr BP) belong sites of ancient chronological group of the Kostenki region in the centre of East European plain (Dinnis et al., 2019) (fig. 1). These are resembling "Protoaurignacien" and early Aurignacien complexes of Kostenki XVII, layer II and Kostenki XIV (layers of IVb-IVw and LVA), Kostenki I (layer III) and also local Streletskian assemblages – Kostenki I, layer V, Kostenki VI, Kostenki XII, layer Ia and III (Dinnis et al., 2019).

The site Zaozer'e has a certain similarity on structure of assemblage and some technical and typological characteristics of stone implements with the sites of


**Fig. 3.** Zaozer'e. Stone assemblage.
**Рис. 3**. Заозерье. Каменный инвентарь.

"Aurignacoid" group of Kostenki sites and especially with assemblages of IVb layer of Kostenki XIV (36.5–35.5 $^{14}$C kyr BP). For stone assemblage of this site, somewhat earlier than the Zaozer'e, blade technology of primary splitting is also characteristic. Assemblage characterized by combination of scrapers, dihedral burins, pieces esquilles and bifacial oval and subtriangular implements. Noteworthy presence of bone tools and personal ornaments in the assemblage. Some traits of similarity could be traced with assemblage of the second layer of the Kostenki XVII. Last assemblage is completely deprived of any archaic features and the basic technical-morphological and technological characteristics refers to Proto-Aurignacien

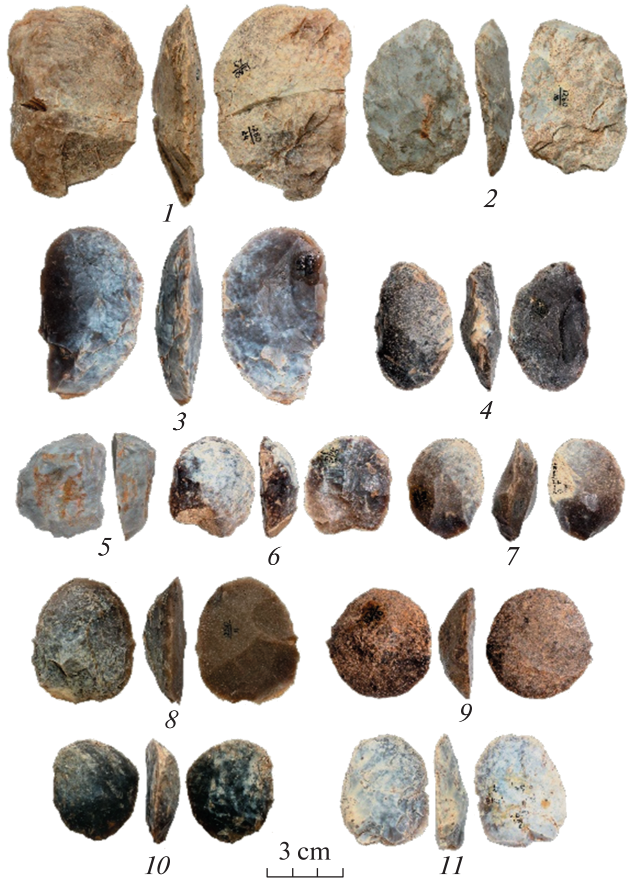


**Fig. 4.** Zaozer'e. Stone assemblage.
**Рис. 4**. Заозерье. Каменный инвентарь.

technocomplex (Dinnis et al., 2019). Some essential elements of this technocomplex, first, the volumetric knapping, and manufacturing of large blades, also characteristic for Zaozer'e assemblage.

Another common and important feature – the presence of personal ornaments in the assemblages of these sites. Personal ornaments of Zaozer'e and sites of the beginning of the Upper Palaeolithic of the Kostenki area also have undoubted lines of similarity. However, unlike stone assemblage, Zaozer'e kit of personal ornaments has significant similarity with ornaments from the second layer of Kostenki XVII. The pendants with drilled hole made of belemnite, the flattened pebbles, fossil corals and canines of polar fox are found in this layer (Stepanova et al., 2020). In addition, it should be noted that personal ornaments of the site Zaozer'e according to classification by M. Vanhaeren and F. D'Erriko (2006), refer to the southern group of European Early Upper Palaeolithic ornaments to which use of shells of sea molluscs and fossils is characteristic.

Sites of the early stages of the Upper Palaeolithic also known in neighbouring Asian region – in Altai: These are such Initial Upper Palaeolithic (IUP) sites as Denisova cave (43–31 kyr BP), Kara-Bom (41–31 kyr BP), Ust-Karakol (35–30 kyr BP) (Belousova, 2018; Derevianko et al., 2020) (fig. 1). The stone inventory of these sites significantly retains characteristic of the local Middle Palaeolithic sites which preceded them. In the industry of the Initial Upper Palaeolithic (50–40 kyr BP), in the Denisova cave subprismatic and edge-facetted cores are often intended for producing large blades. Methods of radial and Levallois splitting also were used. Among tools side-scrapers of Middle Palaeolithic forms prevail. Upper

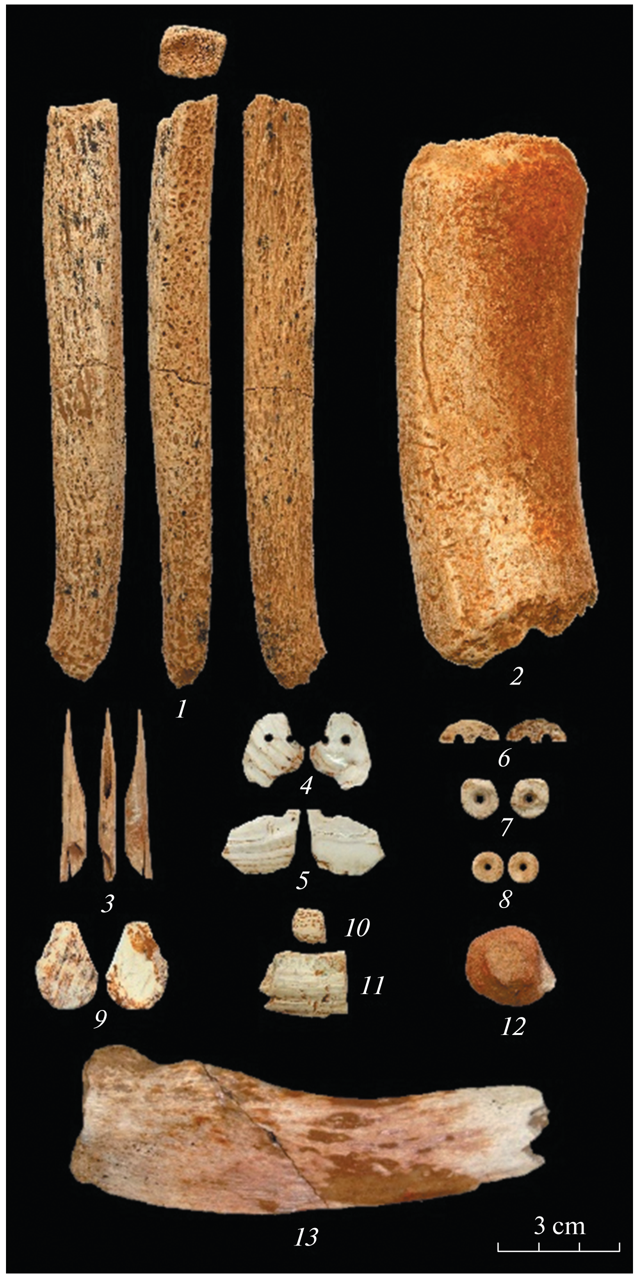


**Fig. 5.** Zaozer'e. Bone implements and ornaments.
**Рис. 5.** Заозерье. Костяные изделия и украшения.

Palaeolithic categories are presented by the elongated points, end scrapers and burins, awls, *pieces esquilles*, retouched prismatic blades (Derevianko et al., 2020).

In the primary knapping of early Kara-Bom assemblages (46–43 kyr BP) the technology of bipolar splitting absolutely prevails. As characteristic tools of this tradition retouched points on blades with a ventral trimming of the base, the simple retouched points on blades and microblades, truncated-facetted implements and, perhaps, the *pieces esquilles* on blades could be mentioned (Belousova, 2018).

Obvious similarity to the Altai sites could be traced in personal ornaments. In layers of the beginning of the Upper Palaeolithic in the Denisova cave, the representative assemblage of a beads and pendants made of bone, stone and fossil shells are collected (Derevianko et al., 2020).

Thus, Zaozer'e has with Altai IUP stone industries some similarity in technology of primary splitting: use of subprismatic, edge-facetted and radial cores and the leading type of blank – a large blade. At the same time the typological features of the industries are significantly different. The industries of the beginning of the Upper Palaeolithic in Eastern Europe and Siberia also differentiated by Middle Palaeolithic substrate. Middle Palaeolithic component in East European's assemblages represented, as usual, by plano-convex bifaces which are *fossil directeur* of the European Middle Palaeolithic *Kielmessergruppen* (KMG) industries (Chabay, 2004), in contemporaneous Siberian assemblages Middle Palaeolithic component represented by Levallois forms typical for local Middle Palaeolithic (Derevianko et al., 2020). In general, Zaozer'e considerably differs on structure and technical-morphological features of the assemblages from significantly older Initial Upper Palaeolithic Altai sites.

Particularly noteworthy is the presence of crescent-shaped and arch-backed tools in Zaozer'e assemblage. These categories are one of the most distinctive typological features of the units of the beginning of the Upper Palaeolithic or Transitional industries such as Chatelperonian in Central and Southern France and Northern Spain, and Uluzzian in Italy and Greece (Hublin, 2015; Moroni et al., 2018; Stefanski, 2018). A few assemblages with arch-backed points have been reported from Central and Eastern Europe. Chronologically, these units are sandwiched between Mousterian and Aurignacian in Western and Southern Europe (Stefanski, 2018). Zaozer'e crescent-shaped tools resembles Uluzzian lunates (Villa et al., 2018), arch-backed points like those of Kraków Zwierzyniec 1 (Stefanski, 2018).

These sites belong to one of initial waves of the AMH occupation of European continent which began ca. 46 kyr BP (Hoffecker, 2011; Hublin et al., 2020). Data of the analysis of DNA of the first migrants show that wide spreading of the anatomically modern human in Europe was followed by continuous contacts with the native Neanderthal population (Fu et al., 2016; Hajdinjak et al., 2021). This fact could serve as plausible explanation of presence of Middle Palaeolithic component in some regional East European industries of the first half of the Upper Palaeolithic, including Zaozer'e.

## 4. CONCLUSIONS

The main features of Zaozer'e assemblages and spatial organization of the site itself evidently could be interpreted as requisites of a modern cultural model. Zaozer'e probably belongs to the first pioneer wave of modern humans moving into Eastern Europe, expanding from the south of the European continent. It is possible to assume that the Zaozer'e, along with sites like layer IVb-w Kostenki XIV, consist of group of sites of beginning of the Upper Palaeolithic which represent the distinct East European industrial tradition having common features with complexes of the beginning of the Upper Palaeolithic of Southern and Southwest Europe. The Zaozer'e materials demonstrate that modern humans reached the Northeast of the East European plain and the Urals (i.e., Subarctic zone of the Eastern Europe) ca. 40 cal. kyr.

# ON THE TIME OF APPEARANCE OF ANATOMICALLY MODERN HUMANS IN THE NORTHEAST OF EAST EUROPEAN PLAIN AND IN THE URALS (BASED ON DATA FROM THE ZAOZER'E PALAEOLITHIC SITE)

**P. Yu. Pavlov**[a,#]

[a]*Institute of Language, Literature and History, Federal Research Centre Komi Science Centre Urals Division RAS, Syktyvkar, Russia*

[#]*E-mail: ppavlov120@gmail.com*

The article discusses the materials of the Palaeolithic site Zaozer'e (35–31 $^{14}$C kyr BP) situated on the North-East of East European plain in Upper Kama River basin. The age, distinctive features of stone and bone assemblage and the types of personal ornaments unambiguously allow to relate Zaozer'e to the beginning of the Upper Palaeolithic. The site's features incorporate most of the traits which have been interpreted as requisites of cultural model of the anatomically modern human (AMH). The assemblage of Zaozer'e site has certain similarity to assemblages of the contemporaneous sites of the Kostenki group (Kostenki XVII, layer II and Kostenki XIV, layers IVb), but also yielded some implements resembling elements of the Uluzzian and Protoaurignacien assemblages of Southern and Southwestern Europe. The site's materials show that modern humans reached the sub-arctic zone of Eastern Europe during the relatively warm interstadial climate epoch ca. 40 cal. kyr practically concurrently with their first appearance in the central part of the East European Plain.

*Keywords:* beginning of the Upper Palaeolithic, North-eastern Europe, initial inhabitation of the Subarctic zone

## ACKNOWLEDGEMENTS

The author acknowledges state assignment No. 122040800168-4 “Features of formation of the population of the North of the European part of Russia during Stone, Early Metal and the Middle Ages according to archeological data”.

Field works on Zaozer'e site were financially supported by the grant of The Wenner Gren Foundation (ICRG41) (2002–2006) and RFHR and Maison de l'Homme (France) project No. 08-01-94952a (2008–2010).

## REFERENCES

Belousova N.E. *Kamennye industrii nachala verkhnego paleolita Gornogo Altaya* (Stone assemblages of the beginning of the Upper Palaeolithic in Altai mountains). PhD thesis. Novosibirsk: IAEA (Publ.), 2018. 28 p. (in Russ.)

Benazzi S., Arrighi S., Badino F., Bortolini E., Figus C., Lugli F., Marciani G., Oxilia G., Romandini M., Silvestrini S., Boscato P., Cipriani A., Moroni A., Negrino F., Peresani M., Pini R., Ravazzi C., Ronchitelli A., and Spinapolice E. Peopling dynamics in the Mediterranean area between 45 and 39 ky ago: State of art and new data. *Quaternary International*. 2020. Vol. 551. P. 1–6.
https://doi.org/10.1016/j.quaint.2020.06.029

Chabay V.P. *Srednii paleolit Kryma*. (The Middle Palaeolithic of Crimea). Simferopol: Shliakh (Publ.), 2004. 304 p. (in Russ.)

Derevianko A.P., Shunkov M.V., and Kozlikin M.B. Who were Denisovian? *Archaeology Ethnology and Anthropology of Eurasia*. 2020. Vol. 48. No. 3. P. 3–32. (in Russ.)

Dinnis R., Bessudnov A., Reynolds N., Deviese T., Pate A., Sablin M., Sinitsyn A., and Higham T. New data for the Early Upper Palaeolithic of Kostenki (Russia). *Journal of Human Evolution*. 2019. Vol. 127. P. 21–40. https://doi.org/10.1016/j.jhevol.2018.11.012

Fu Q., Posth C., Hajdinjak M., Petr M., Mallick S., Fernandes D., Furtwängler A., Haak W., Meyer M., Mittnik A., Nickel B., Peltzer F., Rohland R., Slon V., Talamo S., Lazaridis I., Lipson M., Mathieson I., Schiffels S., Skoglund P., Derevianko A., Drozdov N., Slavinsky V., Tsybankov A., Cremonesi R-G., Mallegni F., Gély B., Vacca E., González Morales M., Straus L-G., Neugebauer-Maresch C., Teschler-Nicola M., Constantin S., Moldovan O-T, Benazzi S., Peresani M., Coppola D., Lari M., Ricci S., Ronchitelli A., Valentin F., Thevenet C., Wehrberger K., Grigorescu D., Rougier H., Crevecoeur I., Flas D., Semal P., Mannino M.A., Cupillard C., Bocherens H., Conard N., Harvati R., Moiseyev V., Drucker D.G., Svoboda J., Richards M.P., Caramelli D., Pinhasi R., Kelso J., Patterson N., Krause J., Pääbo S., and Reich D. The genetic history of Ice Age Europe. *Nature*. 2016. Vol. 534 (7606). P. 200–205.
https://doi.org/10.1038/nature17993

Gribchenko Yu.N. Environments of the Northeastern East European Plain at the time of the initial human colonization. Human Colonizationof the Arctic: The Interaction Between Early Migration and the Paleoenvironment. Moscow: Academic Press (Publ.), 2017. P. 105–136. (in Russ.)

Gribchenko Yu.N. Lithology and Stratigraphy of loess-soil series and cultural layers of Late Palaeolithic campsites in Eastern Europe. *Quaternary International*. 2006. Vol. 152–153. P. 153–163.
https://doi.org/10.1016/j.quaint.2005.12.006

Hajdinjak M., Mafessoni F., Skov L., Vernot B., Hübner A., Fu Q., Esse E., Nagel S., Nickel B., Richter J., Moldovan O-T., Constantin S., Endarova E., Zahariev N., Spasov R., Welker F., Smith G.M., Sinet-Mathiot V., Paskulin L., Fewlass H., Talamo S., Rezek Z., Sirakova S., Sirakov N., McPherron Sh., Tsanova T., Hublin J.-J., Peter B., Meyer M., Skoglund P., Kelso J., and Pääbo S. Initial Upper Palaeolithic humans in Europe had recent Neanderthal ancestry. *Nature*. 2021. Vol. 592. P. 253–257.
https://doi.org/10.1038/s41586-021-03335-3

Hoffecker J. The early Upper Paleolithic of Eastern Europe reconsidered. *Evolutionary Anthropology*. 2011. Vol. 20. P. 24–39.
https://doi.org/10.1002/evan.20284

Hoffecker J. The spread of modern humans in Europe. *Proceedings of the National Academy of Sciences (PNAS)*. 2009. Vol. 106. No. 38. P. 16040–16045.
https://doi.org/10.1073/pnas.090344610

Hublin J.-J. The modern human colonization of western Eurasia: when and where? *Quaternary Science Review*. 2015. Vol. 118. No. 1. P. 194–210.
https://doi.org/10.1016/j.quascirev.2014.08.011

Hublin J., Sirakov N., Aldeias V., Bailey S., Bard E., Delvigne V., Endarova E., Fagault Y., Fewlass H., Hajdinjak M., Kromer B., Krumov I., Marreiros J., Martisius N.L., Paskulin L., Sinet-Mathiot V., Meyer M., Pääbo S., Popov V., Rezek Z., Sirakova S., Skinner M.M., Smith G.M., Spasov R., Talamo S., Tuna T., Wacker L., Welker F., Wilcke A., Zahariev N., McPherron S.P., and Tsenka Tsanova T. Initial Upper Palaeolithic Homo sapiens from Bacho Kiro Cave, Bulgaria. *Nature*. 2020. Vol. 581. P. 299–302.
https://doi.org/10.1038/s41586-020-2259-z

Kanivets V.I. *Paleolit krainego severo-vostoka Evropy* (The Palaeolithic of North-Eastern Europe). Moscow: Nauka (Publ.), 1976. 98 p. (in Russ.)

Moroni A., Ronchitelli A., Arrighi S., Aureli D., Bailey S., Boscato P., Boschin F., Capecchi G., Crezzini J., Douka K., Marciani G., Panetta D., Ranaldo F., Ricci S., Scaramucci S., Spagnolo V., and Benazzi S. The Uluzzian in the mirror. *Journal of Anthropological Sciences*. 2018. Vol. 96. P. 125–160.

Pavlov P. On the human occupation of the northeast of East European plain and the Urals at the beginning of Upper Palaeolithic (MIS 3). *Academia Letters*. 2021. Article 2077. https://doi.org/10.20935/AL2077.

Pavlov P.Yu. On Initial inhabitation of the Northern Urals. *Urals Historical Journal*. 2015. Vol. 47. No. 2 P. 50–60. (in Russ.).

Pavlov P.Yu. The Palaeolithic of Nort-Eastern Europe: new data. *Archaeology Ethnology and Anthropology of Eurasia*. 2008. Vol. 33. No. 1. P. 33–45. https://doi.org/10.1016/j.aeae.2008.04.014

Pavlov P.Yu. Zaozer'e: an early Upper Paleolithic site in the European Northeast. *Rossiiskaya arkheologia (Russian Archaeology)*. 2009. No. 1. P. 5–17. (in Russ.)

Pavlov P., Roebroeks W., and Svendsen J-I. The Pleistocene Colonization of Northeastern Europe: A Report on Recent Research. *Journal of Human Evolution*. 2004. Vol. 47. No. 1–2. P. 3–17. https://doi.org/10.1016/j.jhevol.2004.05.002

Pitulko V.V., Nikolsky P.A., Girya E.Yu., Basilyan A.E., Tumskoy V.E., Koulakov S.A., Astakhov S.N., Pavlova E.Yu., and Anisimov M.A. The Yana RHS Site: Humans in the Arctic Before the Last Glacial Maximum. *Science*. 2004. No. 303. P. 52–56. https://doi.org/10.1126/science.108521

Silaev V.I., Shanina S.N., Smoleva I.V., Kiseliova D.V., Cheredinchenko N.V., Khazov A.F., Tumanova E.A., and Pavlov P.Yu. *Opyt ispol'zovania mineralogo-geokhimicheskikh svoistv kostnykh ostatkov dlya rekonstruktsii sredy obitaniya na paleoliticheskoi stoyanke Zaozer'e (Srednii Ural)*. (Testing the use of mineralogical and geochemical characteristics of fossil bone remains as a tool for reconstructing palaeolandscapes at the Paleolithic site of Zaozer'e (Middle Urals). *Pervobytnaya arkheoogia. Journal mezhdistsiplinarnykh issledovanii (Prehistoric Archaeology. Journal of Inerdisciplinary Research)*. 2019. No. 2. P. 35–77. (in Russ.)

Stefanski D. The Early Upper Palaeolithic assemblage of arch-backed points from Kraków-Zwierzyniec site 1. Multas per gentes et multa per saecula. Amici magistro et collegae suo Ioanni Christopho Kozłowski dedicant (Krakow: Jagellonian Univ. Press). 2018. P. 63–70.

Stepanova K., Maliutina A.A., Girya E.Yu., and Bessudnov A.A. Personal ornaments of the Initial Upper Palaeolithic sites in Kostenki: raw material selection and technology of processing. *Proc. of VI (XXII) Russian Archaeological Congress in Samara*. Vol . I. Samara. 2020. P. 88–90. (in Russ.)

Svendsen J-I., Heggen H.P., Hufthammer A-K., Mangerud J., Pavlov P., and W. Roebroeks. Geo-archaeological investigations of Palaeolithic sites along the Ural Mountains – On the northern presence of humans during the last Ice Age. *Quaternary Science Reviews*. 2010. Vol. 29. No. 23–24. P. 3138–3156. https://doi.org/10.1016/j.quascirev.2010.06.043

Vanhaeren M. and D'Errico F. Aurignacian ethno-linguistic geography of Europe revealed by personal ornaments. *Journal of Archaeological Science*. 2006. Vol. 33. No. 8. P. 1105–1128. https://doi.org/10.1016/j.jas.2005.11.017

Villa P., Pollarolo L., Conforti J., Marra F., Biagioni C., Degano I., Lucejko J.J., Tozzi C., Pennacchioni M., Zanchetta G., Nicosia C., Martini M., Sibilia E., and Panzeri L. From Neandertals to modern humans: new data on the Uluzzian. *PLoS ONE*. 2018. Vol. 13. No. 5. https://doi.org/10.1371/journal.pone.0196786

**EDN:** RUIMYL
*ГЕОМОРФОЛОГИЯ, 2022, том 53, № 5, с. 69–77*

## ПРОБЛЕМЫ ПАЛЕОПОЧВОВЕДЕНИЯ И ГЕОАРХЕОЛОГИИ

*УДК 551.89:574→569.9:902/904(470.3)*

# ОТРАЖЕНИЕ ВЕКОВЫХ И ТЫСЯЧЕЛЕТНИХ ИЗМЕНЕНИЙ ПРИРОДНОЙ СРЕДЫ В ПАЛЕОПОЧВАХ ВЕРХНЕПАЛЕОЛИТИЧЕСКИХ СТОЯНОК ВОСТОЧНО-ЕВРОПЕЙСКОЙ РАВНИНЫ В МИС 3 И МИС 2



**С. Н. Седов[1,2,3,*], А. А. Синицын[4], А. А. Бессуднов[4], С. Ю. Лев[5], А. Н. Бессуднов[6], С. А. Сычёва[7], Т. В. Романис[8,9], В. С. Шейнкман[2,3], М. А. Коркка[10]**

*[1]Институт геологии, Национальный Автономный Университет Мексики, Университетский городок, Дель. Койоакан, Мехико, Мексика*

*[2]Федеральный исследовательский центр "Тюменский научный центр" СО РАН, Институт криосферы, Тюмень, Россия*

*[3]Тюменский государственный университет, Тюмень, Россия*

*[4]Институт истории материальной культуры РАН, Санкт-Петербург, Россия*

*[5]Институт археологии РАН, Москва, Россия*

*[6]Липецкий государственный педагогический университет имени П.П. Семенова-Тян-Шанского, Липецк, Россия*

*[7]Институт географии РАН, Москва, Россия*

*[8]Почвенный институт имени В.В. Докучаева, Москва, Россия*

*[9]Институт мерзлотоведения имени П.И. Мельникова СО РАН, Якутск, Россия*

*[10]Санкт-Петербургский государственный университет, Институт наук о Земле, Санкт-Петербург, Россия*

**E-mail: serg_sedov@yahoo.com*

Поступила в редакцию 14.06.2022 г.
После доработки 20.06.2022 г.
Принята к публикации 15.07.2022 г.

В Восточной Европе мало исследований континентальных геологических летописей, содержащих информацию о кратковременных контрастных климатических флуктуациях во время последней ледниковой эпохи, которые задокументированы в характеристиках Гренландских ледяных кернов. Мы считаем, что восполнить этот пробел могут почвенно-осадочные серии, вскрытые на верхнепалеолитических стоянках в пределах центральной части Русской равнины. Детальное исследование и датирование палеопочв, описанных в разрезах археологических раскопов на стоянках Костёнки и Дивногорье, позволили построить сводную корреляционную схему, охватывающую вторую половину МИС 3 и МИС 2. Эта схема включает эмбриональные палеопочвы, формировавшиеся преимущественно во время потеплений и, соответствующие 8 последним Гренландским интерстадиалам. С другой стороны, формирование палеопочвы, обнаруженной на Зарайской стоянке, приходится на холодный интервал – Гренландский стадиал 2 – и соответствует потеплению в интервале 18–21 тыс. л. н. в пределах этого стадиала. Полученные результаты показывают, что палеопочвы в почвенно-осадочных толщах палеолитических стоянок могут служить весьма чувствительными индикаторами климатических флуктуаций длительностью от нескольких столетий до 1–2 тысячелетий. Несмотря на кратковременное развитие, педогенетические характеристики этих палеопочв содержат ценную информацию о локальной истории природной среды, важную для геоархеологических исследований.

*Ключевые слова:* Восточно-Европейская равнина, почвенно-осадочные архивы, палеопочвы, верхний палеолит, Гренландская климатическая летопись

**DOI:** 10.31857/S0435428122050157

## 1. INTRODUCTION: ANTECEDENTS AND APPROACH

Reconstruction of the regional paleoenvironmental changes during the Middle and Late Valday (Weichselian) epoque has major importance for understanding of the social-ecological interactions during the initial dispersal of Homo Sapiens and posterior development of the Upper Palaeolithic cultures in Eastern Europe. General longeval tendencies of these changes deciphered from various proxies as well as their influence on the cultural development are presented in the works on A.A. Velichko and his collaborators (2012). However more recently the detailed records from the Greenland ice cores and deep-sea sediments of Northern Atlantic have shown that the short term (centennial to 1–2 millennia) but pronounced and contracting fluctuations of climate had major importance during this period (Rasmussen et al., 2014). The search for detailed terrestrial geological archives which could reflect the landscape response to these global fluctuations in the occupation region of particular Palaeolithic cultures comprises an important challenge for the current geoarchaeological research.

Soil-sedimentary sequences could provide such archives. The study of detailed loess-paleosol sections in Western and Central Europe as well as Southern Siberia provided with extensive sets of instrumental dates have shown that their development was controlled by the short-term climatic cycles: incipient soil formation took place during the warmer intervals, correlative to the Greenland Interstadials (GI) whereas sedimentary strata and cryogenic features (cryoturbations, involutions, ice wedge casts) correspond to the cold phases – Greenland Stadials (GS) (Haesaerts et al., 2010).

Within the East European plain, the terrestrial records reflecting this short-term cyclicity are very poorly documented. We speculate that paleosols encountered at the Palaeolithic sites and associated with the cultural layers could bear signals about the climate fluctuations analogous to those recorded by the Greenland ice cores and thus could be used for interregional and even global correlations. A major advantage for paleopedological research at the world-famous archaeological localities with a long research history consists in the available datasets of instrumental dates as well as various palaeoecological results. The detailed information about ancient cultures provides additional tools for developing the chronological scale, correlations as well as independent palaeoecological reconstructions.

However only in very few cases it is possible to detect reliably the levels corresponding to the individual events of the Greenland record directly basing on the instrumental age determinations, because very often the confidence intervals of the obtained dates are comparable with the duration of these events. The design of the proposed correlation scheme relies on the basic principle that attributes formation of paleosols to the periods of milder climatic conditions whereas geomorphic processes (erosion/sedimentation) and cryogenesis were more active during the phases of colder paleoclimate. In fact, this principle is a derivate from the classic scheme of landscape development by Rohdenburg (2010) who postulated the alternation of morphodinamic activity and stability phases throughout the Pleistocene; it is applied for a number of continental soil-sedimentary successions at different time scales (most consistently and successfully – to the loess sequences). Below we present our attempt to find the equivalents of the short-term climatic fluctuations of the Greenland ice core record in the paleosol-sedimentary stratigraphies of the 3 famous Upper Palaeolithic sites of Central East European Plain: Kostenki and Divnogorie in the Upper Don Basin and Zaraysk in the Middle Oka Basin (fig. 1).

## 2. RESULTS AND DISCUSSION

The sections of the Upper Palaeolithic sites of the Kostenki-Borshchevo archaeological district provide detailed paleosol-sedimentary sequences with multiple layers of buried soils. These soils although thin and incipient could be clearly traced and in many cases are associated with the cultural layers or levels of findings. In particular, the section Kostenki-14 (K14) contains 8 major cultural layers developed within the interval 42–27 cal ka BP and at the same time comprises in total about 16 individual paleosols grouped into 5 paleopedological units, labelled as K14/I – K14/V (Sedov et al., 2010). The section is supplied with extensive sets of radiocarbon and luminescence dates and also contains an important independent chronological marker – the layer of volcanic ash, attributed to Campanian Ignimbrite. This tephra layer known in a number of terrestrial and marine geological profiles is reliably dated to ~40 cal ka BP.

Already the attempts have been made to relate the sections in Kostenki with the Greenland ice core record. Levkovskaya et al. (2015) carried out detailed palynological investigation of the profile K12 and identified in its lowest most ancient part the paleosol levels, corresponding to GI 14, 12 and (with certain doubt) 11. It is very interesting that in the upper part of K12 above the layer of Campanian Ignimbrite these authors could not carry out similar detailed correlation. In this part of the profile they identified only one palynological megastage D and stated that “Several interstadials and stadials alternated within this long coniferous megastage (~42–12 ka BP), but their specific features are not clear”. Sinitsyn (2015) demonstrated the correspondence of the main cultural layers of K14 and other key sites of Kostenki with the Greenland curve. The detailed correlation of the soil-sedimentary stratigraphic scheme of K14 with the events of the GRISP and also with the detailed terrestrial records from Carpathian region and Southern Siberia were presented by Haesaerts et al. in their talk at the conference “Multidisciplinary methods in the study and preservation of sites in the Kostenki-Borshchevo archaeological area (Voronezh, September 15–17, 2016). This correlation followed the main principle formulated above: paleosol levels were associated with the warm phases of the Greenland record (Greenland Interstadials). In many aspects the scheme which we propose in this paper agrees with that developed by Haesaerts et al.

We argue that at the current stage of research, the reliable correlation of the K14 section with the Greenland record is possible for the middle and upper parts comprised by the paleopedological units K14-I and K14-II, located above the marker horizons of Campa-


**Fig. 1.** Geographical location of the studied sections.
**Рис. 1.** Географическое положение исследованных разрезов.

nian ignimbrite. In particular, the dark-colored paleosols of the K14-II unit, known as the Upper Humus Bed forms the key block for the proposed correlation. This unit contains Cultural layers II and III with a number of radiocarbon dates from charcoal and bone, which establish its chronological interval between 31.5–36.6 cal ka BP. Within the Upper Humus Bed, the number of individual dark paleosols vary from two in the southern wall of the K14 main excavation (Velichko et al., 2009; Sedov et al., 2010), three in the profile K17, to four in the profile K14 – west (Korkka et al., 2017). We conclude that four paleosols of this most detailed variant of the Upper Humus Bed sequence could be correlated with the Greenland Interstadials (GI) 5, 6, 7 and 8 (fig. 2).

The overlying two brown paleosols of the unit K14-I described in the southern wall of the main excavation (the upper one of them is related to the Cultural layer I dated 27.0–27.9 cal ka BP) (Velichko et al., 2009; Sedov et al., 2010) could be correlated with the Greenland Interstadials 4 and 3. During the excavations of 2008 a paleodepression cut into the Upper Humus Bed was exposed; within the fill of this paleodepression additional brown paleosol levels were encountered above the Cultural layer 1 (Korkka et al., 2017), (fig. 2, 3). We suppose that these uppermost paleosols located directly below the Holocene Chernozem could be correlated with the complex Greenland Interstadial 2. If this correlation is right, we could conclude that the paleosol units K14-I and K14-II correspond to seven Greenland Interstadials from GI8 to GI2, covering the second half of MIS 3 and beginning of MIS 2.

Despite small thickness and short formation period of the paleosols their features, being produced by the fast soil forming processes, permit pedogenetic and paleoenvironmental interpretation, although sometimes ambiguous. In the sections K14 and K17 in the brown paleosols of the superior K14-I paleopedological unit we observed decrease of redoximorphic features and less organic materials and increase of aggregation (both biogenic and cryogenic) as well as carbonate neoformation due to short-range migration processes (Sedov et al., 2010). We associate these features with the cooling and aridization of paleoclimate at the end of MIS 3 – transition to MIS 2 that resulted in decrease of bioproductivity and supply of organic residues as well as soil moisture deficit which allowed only intra-horizontal carbonate recrystallization. This agrees well with the palynological data from K14

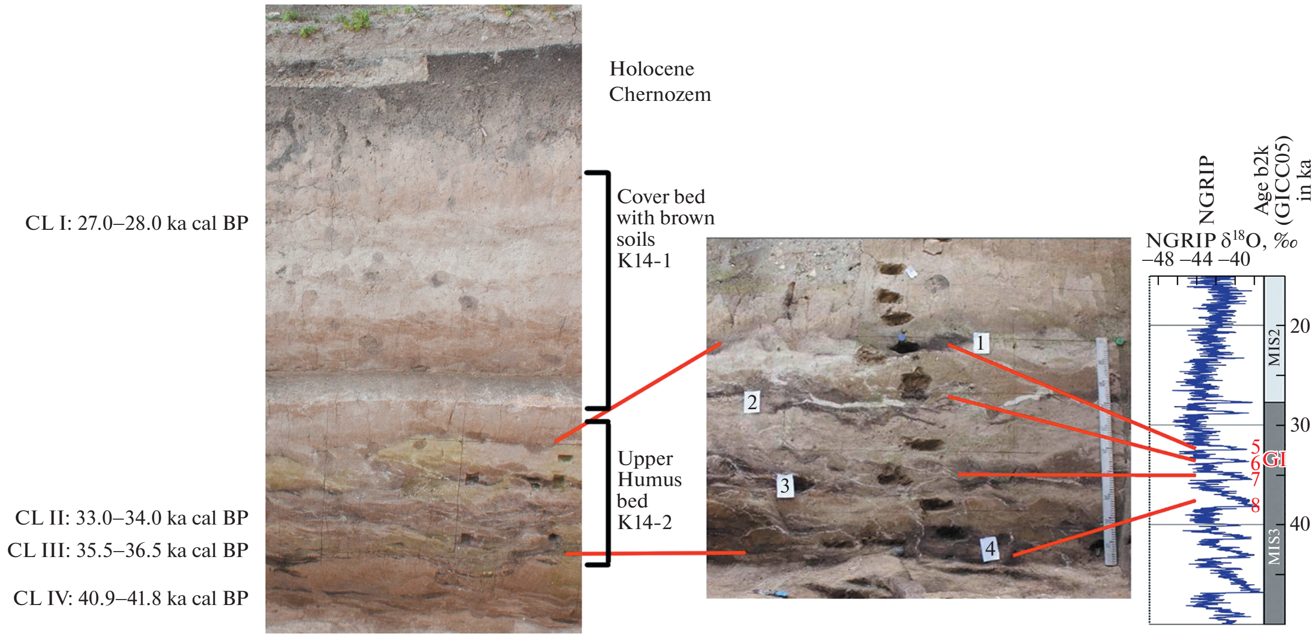


**Fig. 2.** Paleosols of the Upper Humus Bed in the section Kostenki14-west and their correlation with the Greenland Interstadials (GI). CL – cultural layer.

**Рис. 2.** Палеопочвы Верхней Гумусовой Толщи в разрезе Костёнки 14-западный раскоп и их корреляция с Гренландскими интерстадиалами (GI). CL – культурный слой.

(Velichko et al., 2009) which shows sharp decrease of tree pollen and increase of xerophytic herbs in the uppermost paleosols, as well as with the continental paleoenvironmental tendencies reflected by numerous records (loessic, lacustrine, etc.).

Detailed study of more developed dark paleosols of the K14-II Unit/Upper Humus Bed generated multiple scenarios of their pedogenesis. The first hypothesis supposed accumulation of dark organic matter in the waterlogged position affected by the groundwater discharge (Holliday et al., 2007). However further laboratory results strongly challenged the hydromorphic hypothesis. The dark horizons of the Upper Humus Bed showed strong maxima of magnetic susceptibility, typical for well drained topsoil but usually not observed in the reduced waterlogged soil environment. Micromorphological observations revealed evidence of mesofauna activity as well as presence of fungi – aerobic organisms which could not tolerate anoxic water saturated conditions. Basing on these data the alternative hypothesis of cold steppe cryo-arid soil development was put forward (Sedov et al., 2010). One more explanation is development of a Rendzina type soil under local forest stand – this version agrees best with the palynological data which show maximum of arboreal pollen (in particular spruce) in the Upper Humus Bed (Velichko et al., 2009). Characteristics of parent material – colluvial deposits are quite suitable for development of Rendzina: they contain abundant primary carbonates derived from their source materials – loessic deposits and underlying Cretaceous chalky limestone. From the other hand the hypothesis of human induced soil formation – Palaeolithic Technosol development – is justified by numerous microartifacts observed in thin sections. Within this hypothesis maxima of magnetic susceptibility in the dark horizons of the Upper Humus Bed could be explained not by pedogenic enhancement but as an effect of burning. Further laboratory research is needed to justify the latter three versions which at the present state of our knowledge could be considered as equally possible.

We further speculate that after the warmer stage corresponding to GI marked by humic paleosol development, the subsequent cold stage – GS is characterized by higher activity of the sedimentary (colluvial, eolian) and cryogenic processes, which bury and deform the paleosol developed earlier. Cryogenic features could provide certain information about paleoecological conditions of the cold stages. The most notorious are the signs of displacement and fragmentation of the thin humus horizons which are related with the slow downslope movement of the water-saturated thixotropic material – this process is known as solifluction and develops within the active layer above permafrost in the period of seasonal thawing. The winter freezing was also rather intensive as far as the solifluction structures are combined with the cryoturbation features which develop in the beginning of cold season between two freezing fronts (seasonal freezing and permafrost). Some small pockets or oval bodies of dark humus material (involutions) could be interpreted as small frost heave hummocks; such structures develop in presence of permafrost with the temperature

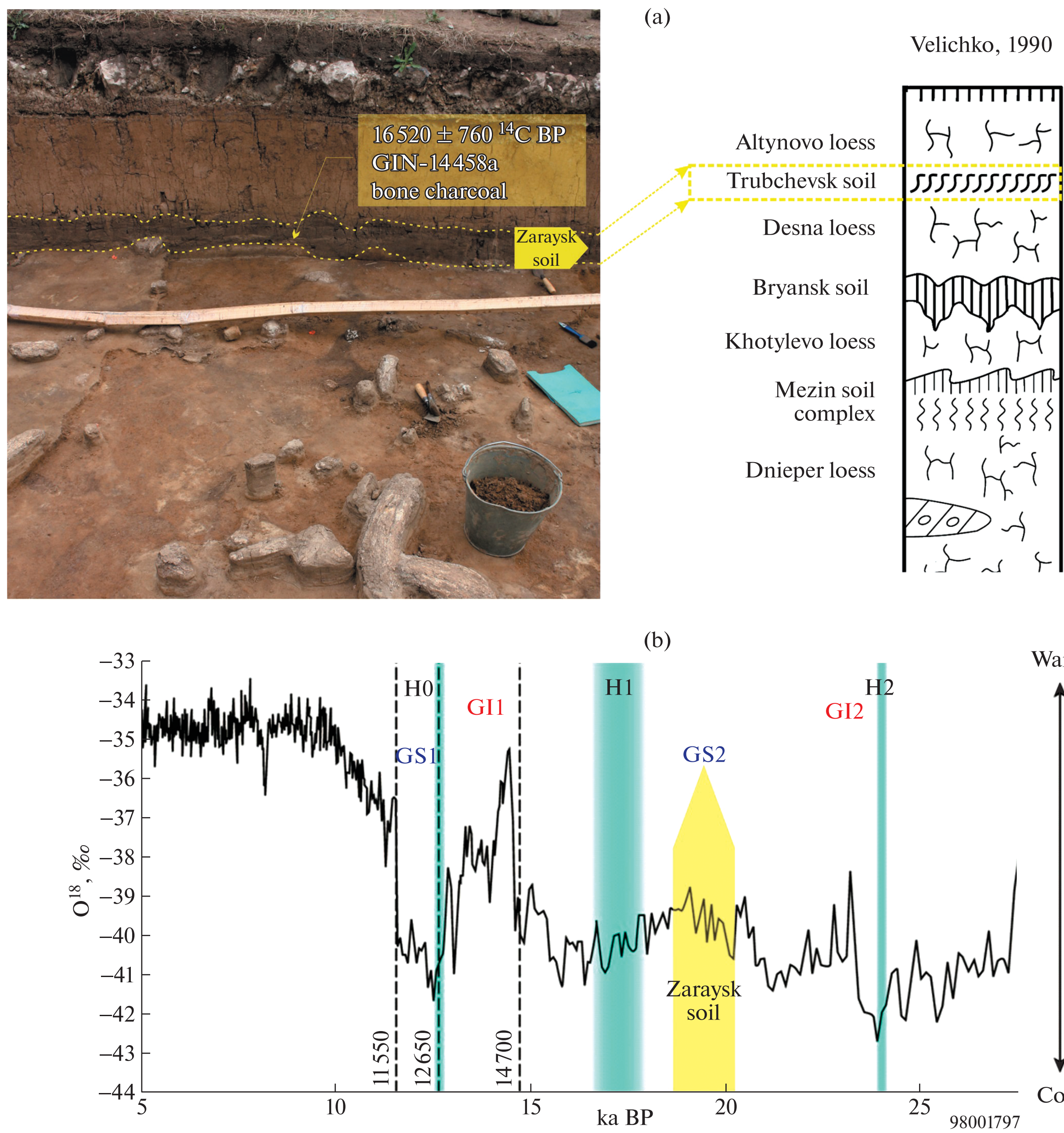


**Fig. 3.** Paleosol of the Zaraysk site (a) and its correlation with the East European loess stratigraphy and with the Greenland ice-core record (b).

**Рис. 3.** Палеопочва Зарайской стоянки (a) и ее корреляция Восточноевропейской стратиграфической схемой лёссовой формации и с Гренландской ледниковой летописью (b).

below −0.5°C. However, we suppose that the permafrost temperature was not too low – most probably above −2°C – because no ice wedge casts were observed in the studied sequence. Redoximorphic features in the layers overlying the dark humus horizons present an additional indirect evidence of permafrost. In the well-drained positions of the K14 and K17 profiles water saturation conditions, necessary for development of redoximorphic processes, could develop due to waterlogging above impermeable permafrost table.

Some specific paleoecological and correlative problems arose when studying the paleosol encountered in the Zaraysk Eastern Gravettian site; this paleosol contains the upper cultural layer, whereas the lower cultural layers of the same Kostenki-Avdeevo archaeological culture are incorporated into the underlying sandy loamy sediments (fig. 3). The interval of paleosol formation established according to the radiocarbon dates of charred bone fragments encountered in the upper cultural layer lies between 15 and 17 C14 ka BP (18–21 cal ka BP). Recently radiocarbon ages of paleosol humus were obtained in the samples from the section excavated at the location Zaraysk B in 2019; these ages fit well into the same interval. This chronological attribution allows to correlate the Zaraysk paleosol with the Trubchevsk paleopedological level of the stratigraphic scheme of the loess formation of the East European Plain by A.A. Velichko (1990); also, in the neighboring regions of the Central and Eastern Europe synchronous paleosol units have been encountered (Romanis et al., 2021). Unexpectedly the Greenland paleoclimatic record (Rasmussen et al., 2014) does not indicate within the formation interval of Zaraysk soil any warming that could correspond to a Greenland Interstadial. On the contrary this interval is part of a longeval cold phase Greenland Stadial (GS) 2 and corresponds to its medium part GS2b when the climate was only a little bit milder. We conclude that in this case, the East European continental paleosol-sedimentary records registered more pronounced fluctuation of environmental conditions than that reflected in the Greenland ice core record.

Pedogenetic features of the Zaraysk paleosol witness however its formation under rather severe paleoclimatic conditions (Romanis et al., 2021). Besides moderate accumulation of dark humus the signs of gleization – iron-manganese nodules – were observed. Taking into account that pedogenesis developed at this site in a very well drained geomorphic position (a promontory of the high right bank of Osetr river) this gleization most probably was conditioned by the impermeable permafrost horizon. Direct signs of cryogenic processes: wedges with the humus fillings at the lower boundary of the paleosol, cryoturbations and grainsize sorting of soil matrix in its the upper, confirm the conclusion about strong frost effects in the Zaraysk paleosol.

Paleosol with the Eastern Gravettian archaeological materials is overlain by a silty loamy sediment which provided parent material for development of the Holocene Grey Forest soil (Eutric Luvisol), which in turn served as a base for the Medieval cultural layer. Composition, stratigraphic and geomorphological position of this silty layer leaves no doubt in its eolian origin (Romanis et al., 2021), we further speculate that it could be correlated with the Altynovo loess horizon (Loess III) of the stratigraphic scheme by Velichko (Velichko, 1990). We relate this phase of eolian sedimentation with one of the short but strong cooling events of the Late Valday (late MIS 2) period: Oldest and/or Younger Dryas. Wedges with pale loamy infillings which penetrate from the silty layer into the dark paleosol confirm cold paleoclimatic conditions of the time of the silt deposition. Conspicuously this event of eolian sedimentation was strongest at the Zaraysk site during the last glacial period. No silty eolian deposits of comparable thickness below the Zaraysk paleosol (which would have corresponded to Desna loess, or Loess II of Velichko's scheme (Velichko, 1990) accumulated during the first half of MIS 2) were found at the site.

The cold episodes of the late Glacial alternated with the warm phases: Bølling (peaked around 14.5 cal ka BP) and Allerød (13 cal ka BP), joined together in the Bølling–Allerød warming which in the Greenland ice core record correspond to the GI 1. During these warm phases, as in the earlier GIs, stabilization of land surfaces and incipient soil development took place in the accumulative geomorphic positions. Buried Divnogorie pedocomplex presents a detailed record of the last warming of the Terminal Pleistocene, preceding the Holocene (fig. 4).

This pedocomplex was exposed in the fill of ancient ravine where also the fireplace and the evidence of an ephemeral Palaeolithic campsite were encountered at the site Divnogorie 9 in the Voronezh region, some 50 km to the south of Kostenki (Sycheva et al., 2016). Divnogorie pedocomplex consists of two, sometimes three individual paleosol levels, separated by slope deposits which form the upper colluvial unit of the ravine fill. The colluvium rests upon the thick laminated alluvial stratum with abundant bones of Pleistocene fauna, predominantly of horses. Within the upper colluvial unit two lenses of charcoal were encountered with the radiocarbon dates about 12 $^{14}$C ka BP (13.7–14.2 cal ka BP). Down the ravine slope the charcoal lenses merge into poorly developed humic paleosols. Above one more brown paleosol is encountered, coloured with the ferruginous pigment. Thus, Divnogorie pedocomplex consists of two main paleosols: the upper called Divnogorie I corresponding to Allerød and the lower Divnogorie II formed in Bølling. In the smaller gullies of the ravine slope the lower Divnogorie II paleosol splits in two soils, both of Rendzic Leptosol type. The upper Divnogorie I paleosol was classified as Cambisol – incipient brown soil. All paleosols of pedocomplex are thin, poorly differentiated and contain primary carbonates due to incomplete leaching that is explained by a short period of their formation (several hundreds of years). Palynological results show that these soils could be developed under forest vegetation. In the beginning of Bølling the climate amelioration resulted in the spread of pine-spruce forests predominantly in the valley. Further warming during Allerød promoted development of forest-steppe ecosystems with forest patches consisting of pine and birch, with minor contribution of the broad leaf species.

At the fig. 5 we present the compound scheme of correlation of paleosols from all considered sections with the Greenland ice core record. This is just the first step towards understanding of how "soil memory" recorded the short-term cyclic climate changes

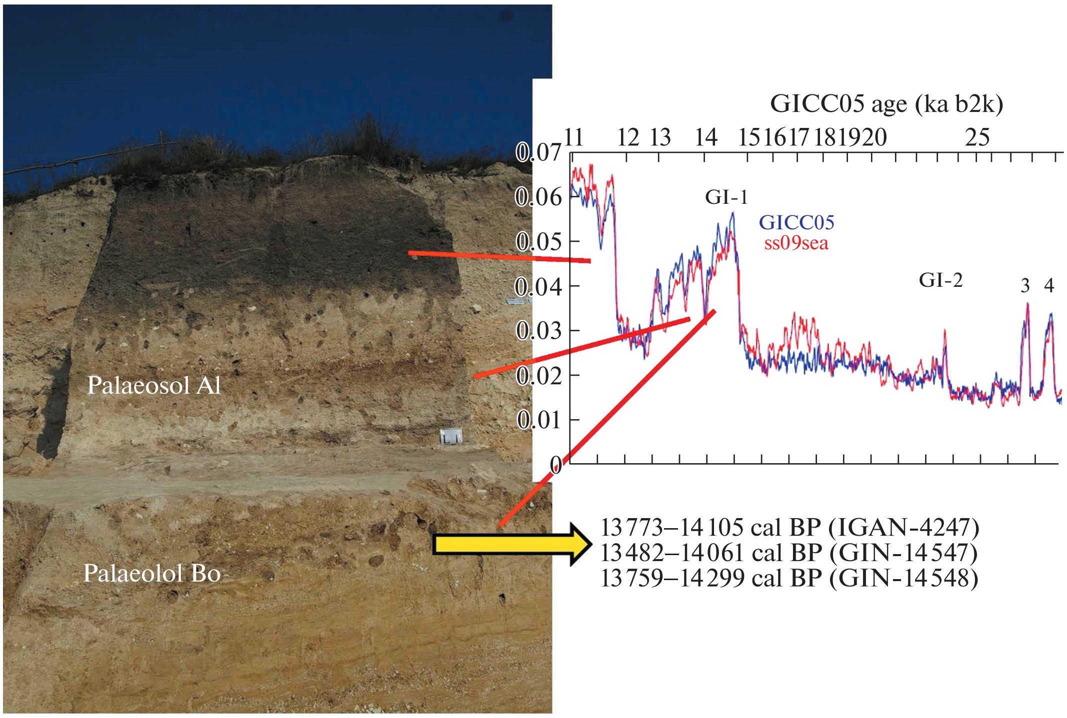


**Fig. 4.** Paleosols of the Divnogorie 9 site and their correlation with the Greenland Interstadial 1.
**Рис. 4.** Палеопочвы стоянки Дивногорье 9 и их корреляция с Гренландским интерстадиалом 1.

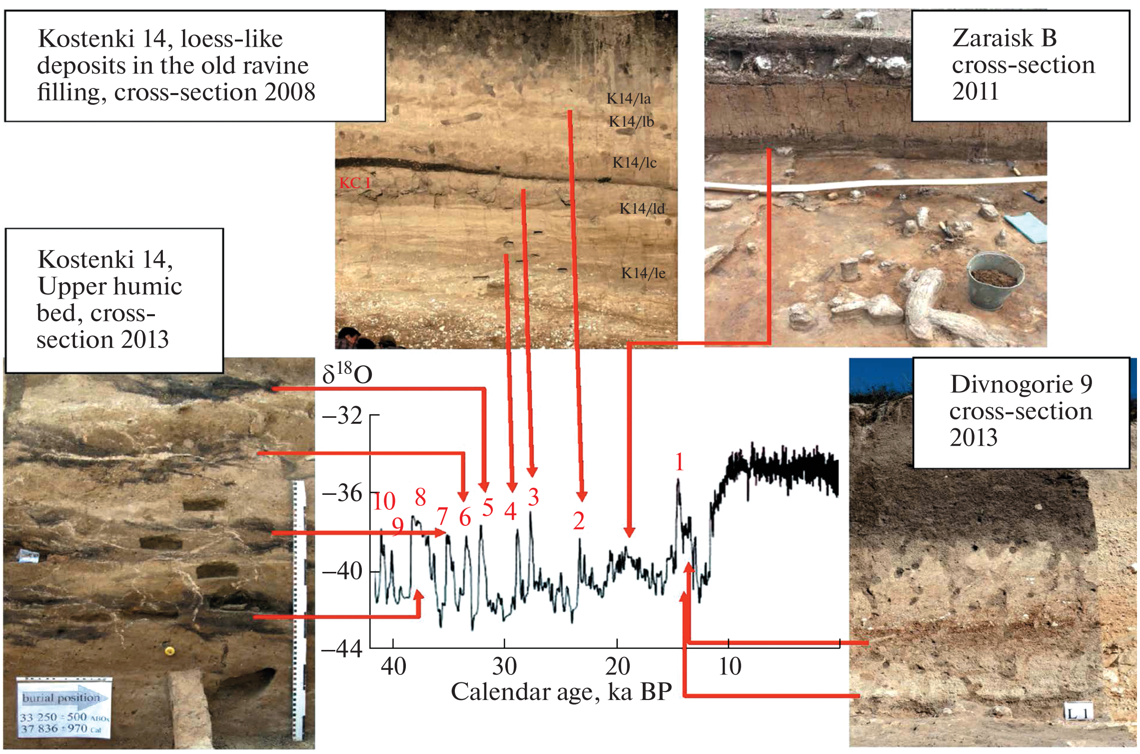


**Fig. 5.** Compound correlation scheme of paleosols at the Upper Palaeolithic sites of central Russian plain and the Greenland ice-core record.
**Рис. 5.** Сводная схема корреляции палеопочв верхнепалеолитических стоянок центра Русской равнины и Гренландской ледниковой летописи.

during the Late Pleistocene in the Eastern Europe. Further perspectives of this research include the widening of the chronological framework and incorporation into the correlation analysis of a number of new sections both from the archaeological sites and from natural soil-sedimentary bodies.

# PALEOSOLS OF THE UPPER PALAEOLITHIC SITES IN THE EAST EUROPEAN PLAIN REFLECT THE ENVIRONMENTAL FLUCTUATIONS OF CENTENNIAL TO MILLENNIAL SCALE DURING MIS 3 AND MIS 2

**S. N. Sedov**[a,b,c,#], **A. A. Sinitsyn**[d], **A. A. Bessudnov**[d], **S. Yu. Lev**[e], **A. N. Bessudnov**[f], **S. A. Sycheva**[g], **T. V. Romanis**[h,i], **V. S. Sheinkman**[b,c], **and M. A. Korkka**[j]

[a]*Instituto de Geología, Universidad Nacional Autónoma de México, Del. Coyoacán, Mexico*
[b]*Federal Research Center "Tyumen Scientific Centre", SB RAS, Earth Cryosphere Institute, Tyumen, Russia*
[c]*Tyumen State University, Tyumen, Russia*
[d]*Institute for the History of Material Culture RAS, Saint Petersburg, Russia*
[e]*Institute of Archaeology RAS, Moscow, Russia*
[f]*Semenov-Tyan-Shansky Lipetsk State Pedagogical University, Lipetsk, Russia*
[g]*Institute of Geography RAS, Moscow, Russia*
[h]*Dokuchaev Soil Science Institute, Moscow, Russia*
[i]*Melnikov Permafrost Institute, Yakutsk, Russia*
[j]*Saint Petersburg State University, Institute of Earth Sciences, Saint Petersburg, Russia*
[#]*E-mail: serg_sedov@yahoo.com*

In the Eastern Europe there are very few studies of the terrestrial records which registered the contrasting short-term climate fluctuations during the last glacial period demonstrated by the Greenland ice core proxy. We argue that the paleosol-sedimentary sequences encountered at the Upper Palaeolithic archaeological sites within the central Russian Plain reflect such climatic fluctuations, the incipient paleosols being formed predominantly during the warm episodes corresponding to the Greenland Interstadials. Detailed research and dating of paleosols described in the sections of the archaeological sites of Kostenki and Divnogorie gave rise to the compound correlation scheme which covers the second half of MIS 3 and MIS 2. This scheme contains the levels of incipient paleosols correlative to the last 8 Greenland Interstadials. In case of the Zaraysk site the formation of the paleosol found there took place during the Greenland Stadial 2 and marks a warmer phase 18–21 cal ka BP within this cold interval. The obtained results show that the paleosols of the soil-sedimentary sequences of the Palaeolithic sites could provide a sensitive record of the climatic fluctuations of centennial to 1–2 millennia scale. Despite their incipient development the pedogenetic features of these paleosols provide valuable information about local paleoenvironments important for geoarchaeological research.

*Keywords:* East European Plain, soil-sedimentary archives, paleosols, Upper Palaeolithic, Greenland climate record

## ACKNOWLEDGEMENTS

The reported study was funded by RFBR research projects No. 19-29-05267, No. 19-29-05024mk, No. 20-09-00233, RSF No. 20-78-10151. Part of the research was carried out within the framework of the state assignments No. FMZF-2022-0012, No. 121042000078-9, No. 122011200271-7 and No. 121041600042-7.

## REFERENCES

Haesaerts P., Borziac I., Chekha V.P., Chirica V., Drozdov N.I., Koulakovska L., Orlova L.A., van der Plicht J., and Damblon F. Charcoal and wood remains for radiocarbon dating Upper Pleistocene loess sequences in Eastern Europe and Central Siberia. *Palaeogeography, Palaeoclimatology, Palaeoecology*. 2010. Vol. 291. P. 106–127. https://doi.org/10.1016/j.palaeo.2010.03.034

Holliday V.T., Hoffecker J.F., Goldberg P., Macphail R.I., Forman S.L., Anikovich M., and Sinitsyn A. Geoarchaeology of the Kostenki–Borshchevo sites, Don River Valley, Russia. *Geoarchaeology*. 2007. Vol. 22. P. 181–228. https://doi.org/10.1002/gea.20163

Korkka M.A., Sedov S.N., Sinitsyn A.A., Otcherednoy A.K., and Kühn P. Paleosols in the section of Kostenki 14 and Khotylevo I: chronicle of the natural conditions and archaeological complexes. Multidisciplinary methods in the study and preservation of sites in the Kostenki-Borshchevo archaeological area. Voronezh: VSU (Publ.), 2017. P. 27–46. (in Russ.)

Levkovskaya G.M., Shumilovskikh L.S., Anikovich M.V., Platonova N.I., Hoffecker J.F., Lisitsyn S.N., Pospelo-

va G.A., Kuzmina I.E., and Sanko A.F. Supra-regional correlations of the most ancient paleosols and Paleolithic layers of Kostenki-Borschevo region (Russian Plain). *Quaternary International*. 2015. Vol. 365. P. 114–134.
https://doi.org/10.1016/j.quaint.2014.11.043

Rasmussen S.O., Bigler M., Blockley S.P., Blunier T., Buchardt S.L., Clausen H.B., Cvijanovic I., Dahl-Jensen D., Johnsen S.J., Fischer H., Gkinis V., Guillevic M., Hoek W.Z., Lowe J.J., Pedro J.B., Popp T., Seierstad I.K., Steffensen J.P., Svensson A.M., Vallelonga P., Vinther B.M., Walker M.J.C., Wheatley J.J., and Winstrup M.A. Stratigraphic framework for abrupt climatic changes during the Last Glacial period based on three synchronized Greenland ice-core records: refining and extending the INTIMATE event stratigraphy. *Quaternary Science Reviews*. 2014. Vol. 106. P. 14–28.
https://doi.org/10.1016/j.quascirev.2014.09.007

Rohdenburg H. Morphodynamische Aktivitäts- und Stabilitätszeiten statt Pluvial- und Interpluvialzeiten. *E&G Quaternary Science Journal*. 1970. Vol. 21. P. 81–96. https://doi.org/10.3285/eg.21.1.07, 1970.

Romanis T., Sedov S., Lev S., Lebedeva M., Kondratev K., Yudina A., Abrosimov K., Golyeva A., and Volkov D. Landscape change and occupation history in the Central Russian Upland from Upper Palaeolithic to medieval: Paleopedological record from Zaraysk Kremlin. 2021. *Catena*. Vol. 196. 104873.
https://doi.org/10.1016/j.catena.2020.104873

Sedov S.N., Khokhlov, O.S., Sinitsyn A.A., Korkka M.A., Rusakov A.V., Ortega B., Solleiro E., Rozanova M.S., Kuznetsova A.M., and Kazdym A.A. Paleosol sequences as an instrument for the local paleogeographic reconstruction of the Kostenki 14 key section (Voronezh oblast) as an example. *Euras. Soil Sci*. 2010. Vol. 43. No. 8. P. 876–892.

Sinitsyn A.A. Kostenki 14 (Markina gora) – a key-section of cultural and geological sequences for the East European Upper Palaeolithic in the chronological framework of 27–42 ka (GS-11–GI-3) In: *Ancient Cultures of Eastern Europe: Key Sites and Reference Complexes in the Context of Modern Archaeological Research (Zamyatninskii sbornik Vol. 4)*. Saint Petersburg: MAE RAS (Publ.), 2015. P. 40–59. (in Russ.)

Sycheva S.A., Bessudnov A.N., Chepalyga A.L., Sadchikova T.A., Sedov S.N., Simakova A.N. and Bessudnov A.A. Divnogorie pedolithocomplex of the Russian Plain: Latest Pleistocene deposits and environments based on study of the Divnogorie 9 geoarchaeological site (middle reaches of the Don River). *Quaternary International*. 2016. Vol. 418. P. 49–60.
https://doi.org/10.1016/j.quaint.2015.11.006

Velichko A.A. *Evolutsionnaya geografiya: problemy i resheniya* (Evolutionary geography: problems and solutions). Moscow: GEOS (Publ.), 2012. 563 p.

Velichko A.A. Loess-paleosol formation on the Russian Plain. *Quaternary International*. 1990. Vol. 7–8. P. 103–114.
https://doi.org/10.1016/1040-6182(90)90044-5

Velichko A.A., Pisareva V.V., Sedov S.N., Sinitsyn A.A. and Timireva S.N. Paleogeography of Kostenki-14 (Markina Gora). *Archaeology, Ethnology and Anthropology of Eurasia*. 2009. Vol. 37. No. 4. P. 35–50.
https://doi.org/10.1016/j.aeae.2010.02.002

**EDN:** BSTVAG
*ГЕОМОРФОЛОГИЯ, 2022, том 53, № 5, с. 78–88*

## ПРОБЛЕМЫ ПАЛЕОПОЧВОВЕДЕНИЯ И ГЕОАРХЕОЛОГИИ

*УДК 551.89:574→902/904(470.324)*

# ЛОКАЛЬНАЯ СТРАТИГРАФИЯ И ПАЛЕОЭКОЛОГИЯ СТОЯНКИ ПОЗДНЕЙ ПОРЫ ВЕРХНЕГО ПАЛЕОЛИТА ДИВНОГОРЬЕ 1 В БАССЕЙНЕ СРЕДНЕГО ДОНА

**© 2022 г. С. А. Сычёва[1,*], А. А. Бессуднов[2,**], А. Н. Бессуднов[3,***], С. Н. Тимирева[1,****], Ю. М. Кононов[1], А. Н. Симакова[4,*****], Е. Ю. Захарова[5,******], К. Г. Филиппова[1]**

[1]*Институт географии РАН, Москва, Россия*
[2]*Институт истории материальной культуры РАН, Санкт-Петербург, Россия*
[3]*Липецкий государственный педагогический университет имени П.П. Семенова-Тян-Шанского, Липецк, Россия*
[4]*Геологический институт РАН, Москва, Россия*
[5]*Воронежский государственный университет, Воронеж, Россия*
**E-mail: sychevasa@mail.ru*
***E-mail: bessudnov_a22@mail.ru*
****E-mail: bessudnov_an@mail.ru*
*****E-mail: stimireva@mail.ru*
******E-mail: simak2001@mail.ru*
*******E-mail: ez@hist.vsu.ru*

Поступила в редакцию 16.06.2022 г.
После доработки 28.06.2022 г.
Принята к публикации 15.07.2022 г.

Верхнепалеолитическая стоянка Дивногорье 1 расположена на низкой террасе реки Тихая Сосна, сложенной перигляциальным аллювием, который перекрыт пролювиально-делювиальными отложениями. В позднеледниковой толще фиксируются два уровня слабого педогенеза, два уровня мерзлотных и эрозионных нарушений, а также культурный слой стоянки с радиоуглеродным возрастом 13 800–13 300 л. н. Проведенные междисциплинарные геоархеологические исследования показали смену перигляциальной флювиальной обстановки субаэральной – вначале перигляциальной (в позднеледниковье), а затем межледниковой – лесостепной и периодически степной (в голоцене). Очень динамичный характер климата и ландшафтов был характерен для начала голоцена и особенно ярко выражен для позднего ледникового периода.

*Ключевые слова:* позднеледниковье, стоянка верхнего палеолита, терраса, конус выноса оврага, перигляциальная растительность, педо-, крио-, биоиндикаторы

**DOI:** 10.31857/S0435428122050169

## 1. INTRODUCTION

The final stage of the last – Valdai – glaciation (15.000–11.700 years ago) was a time when the glacier over north-western Europe was retreating and there was an improvement in the climate after the maximum cryochron (Karpuz, Jensen, 1992; Peltier, Fairbanks, 2006; Lavrushin, 2007; Velichko et al., 2017). This process did not proceed smoothly, but with sharp fluctuations. Short periods of warming (between phases) would give way to periods of cooling (Broecker et al., 1985; Dynamics ..., 2002; Borisova, 2011). During the warming in subaerial conditions, soils would begin to form (Sycheva, 2006 a, b). During the periods of cooling destruction of soils would begin or they would be buried beneath new deposits, mainly wind-borne sediments or slope deposits. Abrupt and frequent changes in climate are conducive to destabilisation of surfaces. The degradation of permafrost and increasing sediment loads in the transitional periods between cooling and warming would lead to the creation of new erosion forms in the mesorelief and the partial filling of these in the next “warming – cooling” sequence (Panin et al., 2011; Sidorchuk, 2015). At that time major changes were taking place in the landscapes of the area being investigated – landscapes ranging from extraglacial steppe to forest-steppe (Spiridonova, 1991). Pleistocene animals were dying out on a mass scale. The feed base for humans also underwent change. The ancient population led an active way of life and people were used to adapting to unstable conditions: they used to settle near bodies of water on the newly formed surfaces of slopes, flood-plains and terraces.

Sedimentation archives preserving data about the rapid and often changing natural situation in the Late Glacial period are not often available. As a rule, they are patchy and incomplete. This is why each new find of a site like this is of major scientific interest. Sites which provide information not just about changes in climate and landscapes, but also about traces of habitation of ancient humans living in such unstable environmental conditions, are particularly significant.

The sites Divnogorie 1 and Divnogorie 9 in the basin of the middle reaches of the River Don are just such features (Bessudnov et al., 2012, 2020; Sycheva et al., 2016). The importance of studies of how the landscapes and climate in the environs of Divnogorie developed is bound up not only with the discovery of new Late Upper Palaeolithic sites at the beginning of the 21st century but also with the unique nature of their position within the relief. The Divnogorie 1 and Divnogorie 9 sites were located on different geomorphological surfaces formed at the end of the Valdai glaciation. It has been established that the geoarchaeological site Divnogorie 9, which is an extensive accumulation of bones – mainly those of horses – and also a place which ancient hunters used to inhabit on a temporary camp, is located at the bottom of the half-filled ravine (Bessudnov, Bessudnov, 2010; Burova et al., 2019). It is not possible to give such a categorical definition of the position of the Divnogorie1 site. In the opinion of A.N. Bessudnov and A.A. Bessudnov (2010) the site is located on the low fluvial terrace above the floodplain. Yu.A. Lavrushin and A.V. Berezhnoy (pers. com.), however, believed that the cape-shaped hill was a fragment of a deluvial-proluvial tail, since no specifically alluvial deposits were found in the trenches.

Although both sites date from the Late Glacial period (OIS 2.1), their different geomorphological positions would indicate differences in the stratigraphy of their sections. Scope for compiling stratigraphic diagrams of such features through study of basic geological sections is limited. Diagrams of that kind give an idea of the general, regional structure of the Quaternary deposits and do not reflect local characteristics of the stratigraphy of Palaeolithic sites. Research into features of this kind requires the compilation of a local stratigraphy of sediments containing ancient cultural layers (Sycheva, 2006b).

## 2. SITE AND METHODS OF THE RESEARCH

A geological test-pit was sunk at the Divnogorie 1 site, in an area of the low terrace on the east bank of the Tikhaya Sosna River within the confines of the Divnogorie Farmstead in the Liski District of the Voronezh Region. The test-pit and the site were on a low elevation (Coordinates: N50°56′57.774″ E39°16′46.746″), at a height of approximately 3–5 metres above the floodplain of the Tikhaya Sosna (fig. 1). The area on which the site was located was approximately 50 m wide and along the edge of the road it was adjacent to the valley slope of a chalk plateau reaching a height of 55–60 m above the river valley (fig. 2).

The site was discovered by A.A. Bessudnov in 2008 and was investigated in the years that followed. In 2018, after the investigation of the Palaeolithic cultural layer in the southern part of the trench, a stratigraphic test-pit was sunk down to a depth of around 5 m. Subsequently the section of that test-pit was the object of detailed palaeo-geographical research.

Multidisciplinary field research into the test-pit involved detailed morphological description and was followed by careful selection of samples for later lithological, palaeo-pedological and palaeo-botanical investigations.

*Colors of the sediments and soils* were determined in accordance with the "Munsell Soil Color Charts". The *particle size analysis* was made using the laser diffractometer Malvern Mastersizer 3000. Only silicate constituent of the sediment, which is most resistant to diagenesis, was analyzed, while both organic matter and carbonates had been removed in the process of samples preparation. The latter included a sequential treatment of the sample with 20% solution of hydrogen dioxide (to remove organic matter), then with 10% solution of hydrochloric acid (to remove carbonates), and finally with 4% solution of sodium pyrophosphate (to disperse the clay aggregates). After the treatment with chemical agents, the material was transferred by pipette to a liquid tray in the material dispersion unit where it was subjected to ultrasonic at a power of 40 W for 100 seconds and intensely stirred at 2400 rounds per minute. After the ultrasonic having been shut down, the measurements were repeated ten times, and the results were averaged using a Mastersizer v.3.62 application. The particle size distribution by fraction was calculated using the Fraunhofer approximation model.

*The loss on ignition (LOI)* was determined with the aim of estimating the content of organic matter and carbonates in the sample, which is important in the paleosol diagnostics. The LOI values obtained at 550°C show the organic matter content, while the difference between LOI values obtained at 950°C and those at 550°C (LOI 950°C – LOI 550°C) indicates the loss of carbonate $CO_2$. The samples, each of 10 ml in volume, were dried up for 12 h at 105°C for water (including hygroscopic) removal. Then they were incinerated in a muffle furnace at two temperature regimes (4 hours at 550°C and 2 hours at 950°C). The loss on ignition was found as the difference in weight before and after ignition using the electronic balance with the accuracy of 0.01 g. The resulting values formulas are:

$$LOI550 = \frac{DW105 - DW550}{DW105} \times 100;$$

$$LOI950 - 550 = \frac{DW550 - DW950}{DW105} \times 100,$$


**Fig. 1.** Location of Divnogorie on the map of Europe (a) and location of Divnogorie 1 and Divnogorie 9 Palaeolithic sites on the topographic map of the area where the Tikhaya Sosna River flows into the River Don. Liski District, Voronezh Region (b).
**Рис. 1.** Расположение Дивногорья на карте Европы (a) и палеолитические стоянки Дивногорье 1 и Дивногорье 9 на топографической карте района, где р. Тихая Сосна впадает в р. Дон. Лискинский район, Воронежская область (b).

where DW is dry weight. *Magnetic susceptibility (MS)* measurements were performed using the magnetic susceptibility meter ZH Instruments SM-30.

The maceration of pollen samples was performed by the method adopted in the Geological Institute of the RAS, which is a modification of the separation method, namely, the samples were additionally treated by sodium pyrophosphate and hydrofluoric acid. The study of palynological preparations was carried out on an optical microscope Motic BA 400 with a camera Moticam 2300, at working magnification ×400. Pollen diagrams were constructed in Tilia 2.0.41 program, which allows to calculate the general spectrum (arborescent pollen + nonarborescent pollen + + spores = 100%) and individual components as a portion of the total amount of pollen grains.

## 3. MATERIALS AND RESULTS OF THE RESEARCH

*3.1. Archaeology.* At the present time the total area of the Divnogorie1 site, which has been investigated using trenches and test-pits, amounts to 85 m$^2$. In the Upper Palaeolithic cultural layer in most of the cleared sections, the finds have included bones, lithics, chips of stone plaques and occasional pieces of red ochre. The absence of any habitation structures reflects the fact that Palaeolithic humans spent only relatively short periods here. The lithic assemblage includes over 2.500 pieces and among these the most common tools are end-scrapers, burins on truncations, backed implements, oblique points and truncated blades. The appearance of the collection is typical for the Eastern Epigravettian sites (Bessudnov et al., 2012).

A trench was sunk in 2018 in order to investigate a peripheral section of the site, in which the density of finds within the cultural layer was significantly less than in the central section. The Palaeolithic cultural layer was represented by a thin level of finds, which had been seriously damaged by burrowing animals at a depth of between 1.75 and 1.85 m from the surface and which consisted of intact and fragmentary animal bones, flint and quartzite items and fragments of stone plaques. The total number of lithics from the 2018 trench came to just over 100. Items with secondary modification were tool types traditional for the site.

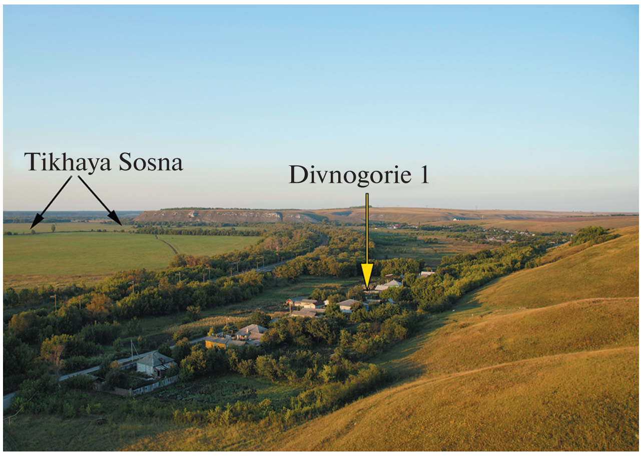


**Fig. 2.** View over the valley of the Tikhaya Sosna River and the Divnogorie 1 site. Photograph taken from the chalk plateau.

**Рис. 2.** Вид на долину р. Тихая Сосна и стоянку Дивногорье 1. Фото сделано с мелового плато.

In the osteological collection from Divnogorie 1, obtained in 2018, in total 98 bone fragments were identified from Pleistocene and modern species of large mammals. Among the Pleistocene fauna, bones of a wild horse (Equus ferus Boddaert, 1785), reindeer (Rangifer tarandus Linnaeus, 1758) and, for the first time at this site, those of a musk ox (Ovibos moschatus Zimmermann, 1780) were found (Bessudnov et al., 2020; Burova et al., 2019).

On two of the bones found in the cultural layer – the calcaneus of the musk ox and a long bone of the horse – cut-marks made with stone tools were identified. On certain diaphysis fragments, and also on proximal and distal bone parts, flake scars resulting from targeted blows were recorded (Burova et al., 2019).

In the stratum containing Holocene levels, traces of humans from various archaeological cultures were identified (Repin, Late Abashevo, Srubnaya and Saltovo-Mayatskaya cultures), which did not occupy clearly defined positions in the stratigraphy. In general, the collection was represented by ceramic and osteological material (Bessudnov et al., 2020).

*3.2. Structure of the section.* Nine main layers have been singled out in the structure of the section at the Divnogorie 1 site: a redeposited layer (surface level of mixed soil) containing a newly created undeveloped soil (Layer 1), a modern cultural layer (2a), a Holocene layer consisting of thick chernozem, which has been anthropogenically reconstituted (2b, 2c), a Late Glacial proluvial stratum (3–6) and a Late Valdai periglacial alluvium (7–9) (fig. 3, tabl. 1). The Late Glacial sequence of deposits is the most complex: it consists of four layers of loam and loamy sand – two of them with permafrost features (top of Layer 4 and Layer 6) and another two with fossil-soil features (bottom of Layer 4 and Layer 7) covered by loess-like loams (Layer 3) and separated by a layered loess-like stratum (Layer 5).

*3.3. Lithological Investigation.* The highest levels of magnetic susceptibility (MS) are to be found, as a rule, in buried soils (Babanin et al., 1995). In the Divnogorie 1 section, the maximum values for MS coincide with the modern cultural layer (Layer 2a) for which the average MS values are 0.7605–0.632 × $10^{-3}$ SI. In Layer 3 immediately beneath the soil consisting of loess loams, the MS values drop sharply to 0.05 × × $10^{-3}$ SI while in Layer 4 a substantial increase in MS is to be observed, up to 0.25 × $10^{-3}$ SI, which is most probably linked to processes in initial soil formation. Lower down (Layers 5-9) MS values are fairly consistent.

As regards granulometric composition, the share of sand is represented by thin, shallow and medium fraction sand fluctuates significantly between 9 and 48%. The higher values for sand are found in the upper part of the section (Layer 1). There are also peaks to be observed in Layer 4, in the lower part of Layer 5 and in the upper part of Layer 9. In certain layers, sands with a large and coarse fraction are noted: the highest level of that sand content is ~10%, which was recorded in the upper part of the section, in Layer 1. The share of aleuritein the section fluctuates between 30 and 75%. The highest values coincide with the lower part of the section starting from Layer 6, while the content of the clay fraction varies from 10 to 22% (in the lower part of Layer 2b).

The loss on ignition (LOI) values at 550°C reflecting the content of organic matter, change over the section within the range 1.41 to 9.64%. The maximum values are to be found in the upper part of the section, in Layer 2, the humus-rich Chernozem levels. Starting from Layer 3, fluctuations are very small: between 1.41 and 4.41%. A slight increase – up to ~ 3.5% –was to be observed in Layers 4 and 6, connected with low humus formation.

The LOI values at 950°–350°, reflecting the carbonate content, change through the section from 1.12 to 20.15%. The maximum values coincide with Layers 1 (anthropogenic), 3 (Bk horizon of Chernozem) and 4. An increase in that indicator has also been observed at the base of the section at a depth of 4.75 m.

*3.4. Spores and pollen analysis.* The abundance of palynomorphs in the samples is not the same throughout the section. The largest concentrations of pollen and spores are to be found in the top 1.6 m. On the basis of changes in the composition of the spore-pollen spectra, the diagram was divided up into 8 palynozones (from now on PZ; fig. 4).

PZ I (4.35–4.75 m) distinguishes Layer 9. Isolated grains of *Picea*, *Pinus*, Asteraceae, Chenopodiaceae are found there. Pollen grains of *Picea* and *Pinus sibirica* are present.

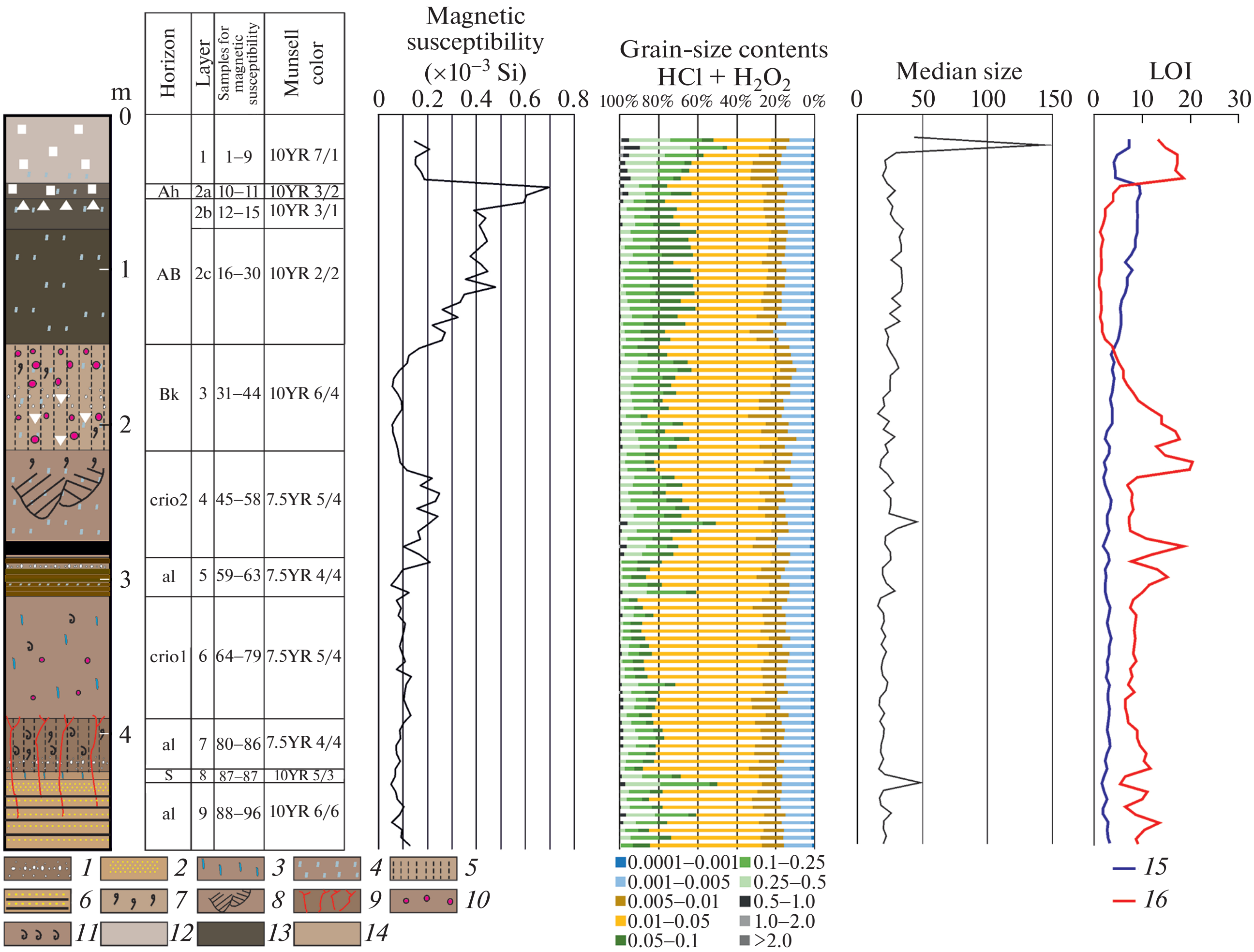


**Fig. 3.** Lithological research data. The numbers correspond to the layer numbers in the text.
*1* – crushed stone, *2* – sand, *3* – carbonate tubules and other carbonate concretions, *4* – chalk crumbs, *5* – loess-like loam, *6* – interbedding of sands and loams, *7* – cutans, *8* – scours with layered filling, *9* – cracks, *10* – molehills, *11* – mollusc shells, *12* – modern cultural layers, *13* – Bronze Age cultural layers, *14* – Upper Paleolithic cultural layers, *15* – LOI 550°, *16* – LOI 950°.

**Рис. 3.** Данные литологических исследований. Цифры соответствуют номерам слоев в тексте.
*1* – щебень, *2* – песок, *3* – карбонатные трубочки и др. карбонатные конкреции, *4* – меловая крошка, *5* – лёссовидный суглинок, *6* – переслаивание песков и суглинков, *7* – кутаны, *8* – промоины со слоистым заполнением, *9* – трещины, *10* – кротовины, *11* – раковины молюсков, *12* – современные культурные слои, *13* – эпохи бронзы, *14* – верхнего палеолита, *15* – ППП 550°, *16* – ППП 950°.

PZ II spectra are found in Layers 5–8 (at depths between 2.9 and 4.35 m) and they contain insignificant amounts of pollen grains. In all these Layers, however, grass pollens predominate (accounting for 70–85%), mainly Asteraceae, Chenopodiaceae, *Artemisia* and Brassicaceae. At a depth of 3.45 m green algae, *Botryococcus braunii,* were found and at a depth of 3.15 m re-deposited grains of *Podocarpus.* In the lower part of Layer 5 (at a depth of 3.05 m) a conspicuous inclusion of plant residues and fungi were noted, including *Glomus.*

PZ III reflects the vegetation in the lower part of Layer 4 (2.6–2.9 m). In the relevant spectra there is an increase in pollen of trees to be observed (up to 50%) – *Pinus sylvestris*, *Betula* sect. *Albae*, *Alnus*. Isolated algae *Botryococcus braunii*, soil fungi and soil mites are found.

In the spectra of PZ IV (1.85–2.6 m) palynomorphs are virtually absent.

PZ V (1.75–1.85 m) corresponds to the upper part of Layer 3. The samples taken there contain isolated pollen grains of *Artemisia*, Asteraceae, and Cichorioideae. Plant residues and charcoal particles are present and also fungi (*Glomus* sp. (NN-126), Quamar, Stivrins, 2021). Re-deposited grains of *Gleichenia* and *Carya* have also been noted.

In palyzones VI-VIII the concentration of palynomorphs increases, as does the variety of fungi remains. Grains of *Pseudoschizaea* sp. ((NN-61); Christopher,

**Table 1.** Morphological Description of the section at the Divnogorie1 site
**Таблица 1.** Морфологическое описание разреза стоянки Дивногорье 1

| Layer, Level | Depth, cm | Description |
|---|---|---|
| 1 | 0–38 | Modern Cultural Layer. Dark-grey medium loam. Top 20 cm include numerous anthropogenic remains: brick, glass, nut shells and fruit trees pits. Transition gradual. |
| 2, a+b+c | 38–145 | Chernozem from Holocene period.<br>Ah. Dark-grey medium loam, of lumpy-granular structure. Molehills and roots of fruit trees are noted. At a depth of 50–60 cm is found a large number of pottery fragments (Bronze Age CL). Abrupt change in colour, edge along the tunnels of burrowing animals.<br>AB. Non-homogenous grey-pale loam, with a fine-porous structure and containing ancient pale-grey and modern black coprolites, chalk crumbs and pebbles; already badly broken up by burrowing animals; thin clay coatings are observed and candidiasis along the pores. |
| 3 | 145–215 | Bk. Light, pale-yellow loam, loess-like and porous; pores are covered with carbonate films. Loam contains a large quantity of small chalk inclusions; prone to rapid boiling from hydrochloric acid; broken up by frequently used tunnels of burrowing animals. Dense carbonate greyish-white colours are observed. At a depth of 175–185 cm, finds from the Upper Palaeolithic from 13300–13800 uncal BP. |
| 4 | 215–285 | Layer badly damaged by cryogenic and erosion deformation. It consists of a series of small rills with finely layered in-fill. The transverse profiles of the rills are cone-shaped, 60–70 cm wide, and between 40–50 and 70 cm deep. The layered nature of the rills can be observed most clearly in their in-fill. In the rills there are secondary erosion potholes also with layered in-fill. Cores of the in-fill of the rills are more homogenous and consist mainly of bright-brown heavy loam with clay coatings. Between the rills and above them lies material consisting mainly of rock debris. An inter-layer containing large pieces of chalk has been crushed by permafrost: it is sometimes embedded underneath the rills or higher up between them. |
| 5 | 285–310 | Layered loamy sequence, consisting of inter-layers (from the bottom up): brown or reddish-brown loam (2 cm); chalk debris (2–3 cm); reddish-brown heavy loam (5 cm); pale-yellow/reddish-brown heavy loam (3 cm); reddish-brown loam (2 cm); pale-yellow /reddish brown loam containing small chalk crumbs (4 cm); reddish-brown medium loam, slightly ferruginous (5 cm); brownish/reddish-brown light loam (5 cm). |
| 6 | 310–390 | Light, reddish-brown loam consisting of three sub-layers and with small pores. In the lower part of the layer, at a depth of 340 cm, sub-vertical veins of pale-yellow heavy loam are visible. Rare molehills used once or frequently are encountered, chalk inclusions, carbonate tubes and concretions greyish-white in colour. Pieces of mollusc shells are found. Sub-vertical cracks at lower limit measuring 8–20 cm penetrating to a depth of 450 cm, sometimes deeper. |
| 7 | 390–425 | Layered mainly loamy, non-homogenous stratum consisting of inter-layers; patches of pale-yellow/grey loam with slight humus content (390–403 cm), with an inclusion of dot-like chalk crumbs and small mollusc shells; heavy pale-yellow/reddish-brown loam (405–414 cm) with reddish-brown coatings; pale-yellow loam containing crushed stone (414–420 cm). In the bottom pale-yellow inter-layer there are carbonate concretions. An inter-layer of chalk crumbs 2–3 mm in size is embedded beneath the horizon containing white spots of lime. Rounded pebbles are also encountered. |
| 8 | 425–430 | Light loam, grey/reddish-brown in colour, non-homogenous, containing grey patches and porous: carbonate tubes along the pores, rapid boiling from hydrochloric acid; contains films of rust. Possibly the initial soil. |
| 9 | 430–476 | Thinly layered sequence of loams, loamy sands and sands. Loams are pale-yellow or very pale yellow, the sands are pale-yellow or yellow. In the middle part of the layer is an inter-layer of chalk crumbs measuring 5–15 cm. Sandy loams and loams boil from hydrochloric acid; the sandy inter-layers do not. In the upper part of the sequence (433–439 cm) there is an inter-layer of pale-yellow sand containing manganese ortsteins. Sand and sandy loam are also layered (thickness 0.1–0.5 mm). On one of the walls of the test-pit a displacement of those layers has been noted, which is associated with the permafrost crack from layer 6, which has broken through this layer as well. |

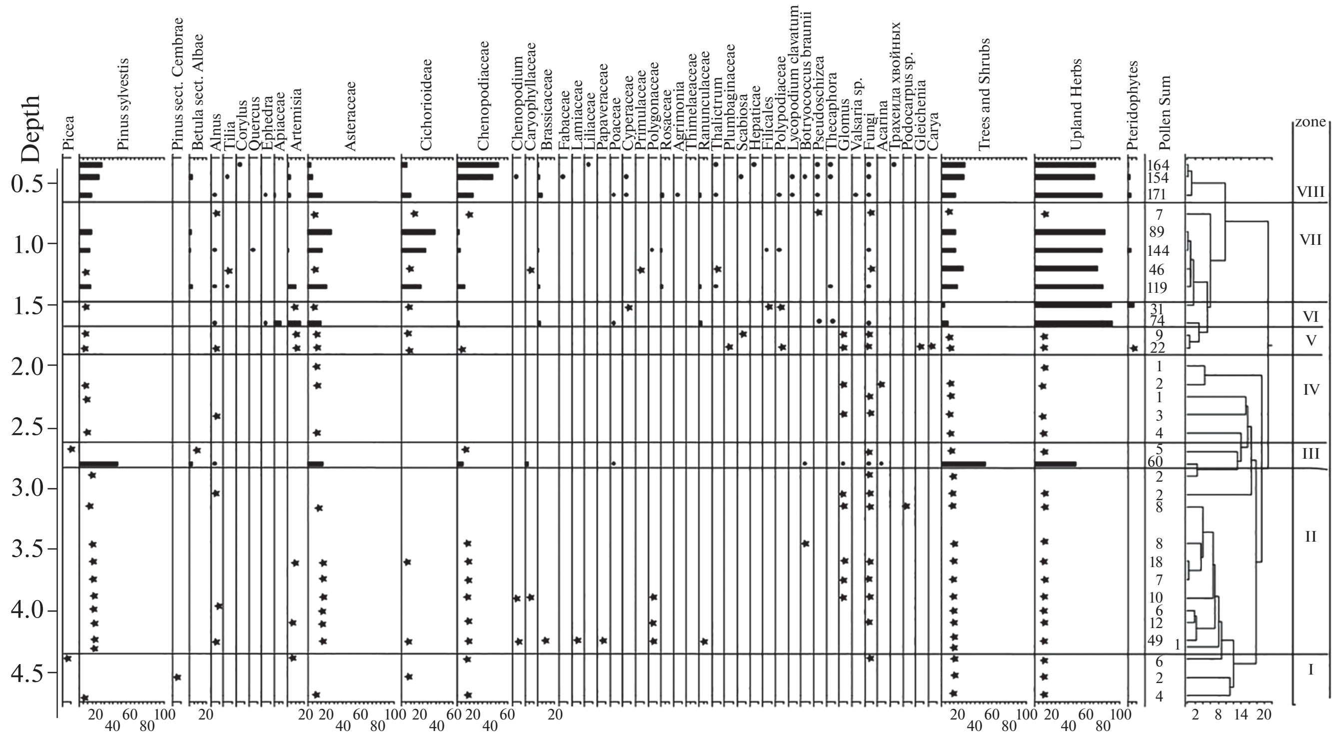


**Fig. 4.** Results of the spores and pollen analysis. Star – single grains; dot – content in the spectrum less than 3%.
**Рис. 4.** Результаты споро-пыльцевого анализа. Звездочка – единичные зерна; точка – содержание в спектре менее 3%.

1976), which could belong to algae (Gadens-Marcon, 2014; Mudie et al., 2010).

PZ VI distinguishes Layer 3 (1.5–1.75 m). Pollens of grasses and bushes predominate (up to 95%): in particular pollen of *Artemisia* and Asteraceae. Pollen grains of *Ephedra*, Chenopodiaceae, Brassicaceae and Plumbaginaceae are also present. The spectra indicate the predominance of open steppe and semi-steppe landscapes. Various fungi remains are found in this layer as well: *Thecaphora*, *Alternaria* ((BFA-6), Halbwachs et al., 2021), cf. *Delitschia* sp. ((NN-138); Quamar, Stivrins, 2021) and grains of *Pseudoschizaea* sp.

Pollen spectra from PZ VII (75 cm–1.50 m) were obtained from Layer 2. In these the quantity of tree pollens increased to 30%. Pollen of birch, lime and oak appear and the quantity of Cichorioideae pollen increases up to 40%: also present are Caryophyllaceae, Cyperaceae, Brassicaceae, Polygonaceae, Rosaceae and isolated Polypodiaceae spores. In the samples a large quantity of plant residues and charcoal particles was noted and soil fungi were identified. Forest-steppe landscapes predominated (a combination of meadow-steppe vegetation with some areas of mixed forest).

PZ VIII (35–75 cm) stands out on account of the spectra present: the amount of Asteraceae in them decreases and that of Chenopodiaceae gradually increases (up to 50%). In the tree group the pollens of *Pinus*, *Betula*, *Alnus*, *Tilia* and *Corylus* are present. Grains of *Ephedra*, Brassicaceae, Poaceae, *Agrimonia*, *Thalictrum* and *Scabiosa* were found and spores of *Riccia* and *Lycopodium clavatum*. The samples contain plant residues (including coniferous tracheids), charcoal particles, soil fungi and fresh-water algae. Steppe landscapes predominated, including some areas of mixed forest in conditions of a warm-climate situation.

## 4. DISCUSSION

In the base of the section alluvium was found which includes a flood-plain-oxbow facies (Layer 7) and a river-bank facies in the low flood-plain terrace of the Tikhaya Sosna River, which are difficult to distinguish from each other. The horizontal layered nature of some sequences, including those of hair – like fineness bear witness to the periodic freezing of the alluvial stratum (Layer 8) (Konischev, Rogov, 1994). A similar structure of deposits indicates that there has been accumulation of periglacial alluvium at the base of the section (Selli, 1981; Handbook ..., 1982). Conditions of this kind are also borne out by the presence of *Pinus sibirica* grains.

Heterogeneous deposits higher up the section (Layers 6–3) are distinguished by their cyclical structure: alternating inter-layers filled with dense chalk crumbs, crushed chalk and chalk pebbles; layered loamy sands; loess loams with features of soil-formation and cryogenesis. The nature of these sediments testifies to their having accumulated in the peripheral zone of alluvial cones in ravines which cut through the nearby valley slopes (Botvinkina, 1965; Guide ..., 1987).

The key role of proluvial processes can be clearly traced from a depth of 3.45–3.15 m (Layer 6) not only on the basis of lithological features, but also on the basis of palynological data, which indicate a water component in the formation of the deposits and the presence of redeposited microfossils, which are represented by *Podocarpus*, *Carya* and *Gleichenia* coinciding in date with the upper parts of Layers 6 and 3. Palaeomorphsare represented in insignificant quantities in Layers 5–7, which also testifies to fine earth having repeatedly been redeposited.

Reddish-brown loess-like loams embedded in the lower part of Layer 4 and in the in-fill of gullies, are probably pedosediments – deposits formed from destroyed soil levels (consisting of illuvial clay) and redeposited a small distance away. It is possible that the gullies had initially been permafrost wedge-shaped cracks, later modified through erosion processes and then filled with layered heavy loams and clays. Smaller gullies often turned into ravines in which crushed stone was deposited.

The results of the lithological research confirmed in the main the sequence of layers which had been identified during field-work. Levels from the final horizons of the Pleistocene era with features of soil formation (Layers 4 and 6) stand out fairly clearly and, for these, growth in the values of magnetic susceptibility was recorded and some increase in the median size of the component particles.

Levels in which humus accumulates and transitional levels of Chernozem stand out clearly, on account of the increase in the LOI 550° values and also the carbonate horizon on account of the increasing difference between LOI 950° and LOI 550°. A small increase in organic matter emerges for Layer 4, the top of Layer 5, the top and bottom of Layer 6, in relation to which initial fossil soils or pedosediments have been described.

The significant quantity of plant residues, the increase in pollen from tree species, the diversity in fungi remains (*Glomus*, *Valsaria* ((Hdv-1008); Van Geel et al., 2011), *Thecaphora*, *Tetraploa* ((Hdv-89); van Geel, 1978), *Alternaria*) and the occasional presence of *Acarina* soil mites indicate that soil processes played a part in the formation of the bottom part of Layer 4 and to some extent Layer 5 as well. It is likely that during the time when those sediments were taking shape, there had been some increase in humidification. In the upper part of Layer 4 where cryogenic and erosion processes used to show up particularly clearly, there are virtually no palaeomorphs to be seen.

Loess-like loams, resulting from deluvium accumulation or aeolian processes (Layer 3) indicate that accelerated ravine erosion processes leading to the formation of removal cones, their merging and the formation of a plume at the foot of a valley slope were far less frequent than before.

The surfaces of ravines had dried out and become more stable and more convenient for temporary habitation. The Upper Palaeolithic cultural layer (assigned an age of 13.300–13.800 uncal BP on the base of radiocarbon dating) is thought to coincide with the top level of loess loams: a characteristic feature of that time period was an increase in plant and charcoal residues and the appearance of hazel trees.

A predominance of limb bones (mainly feet), i.e. “non-fleshy” parts, a specific lithic assemblage and the thin cultural layer at the Divnogorie 1 site would indicate that the site is an accumulation of remains from a short (possibly, seasonal) camp, where the inhabitants specialised in butchering horse carcasses (Bessudnov et al., 2013; Burova et al., 2019). The question of belonging to the surface on which the camp of Divnogorie 1 was located was whether it was a low river terrace above the floodplain of the Tikhaya Sosna River or a proluvial plume? This question had already been resolved during the investigation in the field of the geological-lithological structure of the section and the answer to it subsequently confirmed on the basis of data obtained through laboratory research. It is the surface of a low fluvial terrace above the flood-plain – a terrace which has been covered over by deluvium and proluvial deposits, incorporating initial soils, their pedosediments and layers with cryogenic deformations.

The presence of *Pseudoschizaea* and absence of *Glomus* spores in the spectra within the upper 1.60 m of the test-pit could indicate the substitution of ravine-alluvium deposits by an accumulation of humus in conditions with a stable surface in the Holocene period. *Pseudoschizaea* is often present in the spectra of archaeological sites from the Bronze Age onwards (Environment ..., 2019).

On the loess-like loams (Layer 3) covering the proluvial-alluvial stratum, a typical Chernozem formed, containing accumulations of humus, transitional and carbonate levels. The presence of artefacts from various archaeological cultures in the humus profile of the Chernozem shows that from time to time it took shape under the influence of the anthropogenic factor. The Bronze-Age finds were encountered mainly at a depth of 50–60 cm. It is at that level that pollen of ruderal species and garden plants appears.

The upper part of the section consists of modern cultural layers: a redeposited layer (Layer 1) and a layer formed in that position (Layer 2a). Palynological research has revealed that the highest concentrations of pollen and spores coincide in date with the top 1.60 metres – with the profile for Holocene Chernozem. Soil processes are reflected to the greatest degree in Layers 3, 2 and 1. Those layers often contain insignificant amounts of pollen grains, which is a feature characteristic of humus-rich soils in which a high degree of microbiological activity is to be found.

## 5. CONCLUSION

The site of Divnogorie1 is located on the Late Glacial low fluvial terrace above the flood-plain, which is covered by a proluvial plume. By the time short-term settlement of the area had begun, active relief-forming processes had slowed down considerably. The periglacial type of landscape was confirmed by the results of the palynological research.

The cones of the ravine outflow as a result of the merger turned into a single deluvial-proluvial plume, which covers a low over-floodplain terrace. Initial soils and pedosediments are described in the sediments of the gullies removal cones, which is confirmed by the results of lithological and spore-and-pollen analyses. They formed during short intervals when there was a reduction in relief-forming processes.

Palaeolithic cultural layer of the site was seen to coincide with the upper part of the aeolian and deluvian loams – the parent basis of the Chernozem – which had turned into the carbonate horizon as a result of soil formation. In the cultural layer an increase was noted in plant and charcoal residues. Over the period when the camp was functioning, open-steppe landscapes and even semi-desert ones predominated, which later gave way to forest-steppe landscapes (combinations of meadow vegetation with areas of mixed forest).

Palynological research has made it possible to establish changes in the nature of vegetation and climatic conditions during the time when the deposits in the section were taking shape. In the Holocene there were a number of changes giving rise to either wetter or drier conditions. Steppe landscapes (Layer 3) gradually gave way to forest-steppe ones – to a combination of meadow-steppe vegetation and small areas of coniferous/broad-leaved forest in conditions of a warm climate situation. The drier climate at the end of the Final Pleistocene and during the first half of the Holocene was followed by a moister climate in the second half of the Holocene era.

The multi-disciplinary research carried out has shown consistent change from a periglacial fluvial situation to a subaerial one – initially periglacial and then interglacial – of a wooded-steppe and sometimes a steppe situation of a moderate zone. In the Late Glacial stratum two levels have been recorded for the appearance of features of slight pedogenesis and also two levels of permafrost deformations. A highly dynamic sequence of landscapes was identified both in the Late Glacial period (due to sharp fluctuations in temperature gradients, less humidification) and also in the Holocene (change of aridity and humidity).

# LOCAL STRATIGRAPHY AND PALAEOECOLOGY OF THE LATE UPPER PALAEOLITHIC SITE DIVNOGORIE 1 IN THE BASIN OF THE MIDDLE DON

**S. A. Sycheva[a,#], A. A. Bessudnov[b,##], A. N. Bessudnov[c,###], S. N. Timireva[a,####], Yu. M. Kononov[a], A. N. Simakova[d,#####], E. Yu. Zakharova[e,######], and K. G. Filippova[a]**

[a] *Institute of Geography RAS, Moscow, Russia*

[b] *Institute for the History of Material Culture RAS, Saint Petersburg, Russia*

[c] *Semenov-Tyan-Shanskii Lipetsk State Pedagogical University, Lipetsk, Russia*

[d] *Institute of Geology RAS, Moscow, Russia*

[e] *Voronezh State University, Voronezh, Russia*

[#] *E-mail: sychevasa@mail.ru*

[##] *E-mail: bessudnov_a22@mail.ru*

[###] *E-mail: bessudnov_an@mail.ru*

[####] *E-mail: stimireva@mail.ru*

[#####] *E-mail: simak2001@mail.ru*

[######] *E-mail: ez@hist.vsu.ru*

The Upper Palaeolithic site Divnogorie1 situated on a low terrace of the Tikhaya Sosna River, consists of periglacial alluvium, covered with proluvial and deluvial deposits. In the Late Glacial layer two levels of initial pedogenesis have been identified, two levels of permafrost and erosional disturbances and also a Palaeolithic cultural layer with a radiocarbon age of 13.800–13.300 years ago. The multi-disciplinary geo-archaeological research carried out so far has revealed a shift from a periglacial fluvial situation to a subaerial one – initially a periglacial one and then an interglacial one – in a forest-steppe and occasionally steppe setting. The highly dynamic nature of the climate and the landscapes was characteristic of the Holocene period and particularly pronounced for the Late Glacial period.

*Keywords:* Late Glacial period, Upper Palaeolithic site, terrace, ravine removal cone, periglacial vegetation, pedo-, cryo-, bioindicators

## ACKNOWLEDGEMENTS

This work was undertaken within the framework of RFBR No. 19-29-05024mk, RNF No. 20-78-10151, State assignments of the Institute of Geography RAS (State Task No. 0148-2019-0005) and the Geological Institute RAS.

## REFERENCES

Babanin V.Ph., Trukhin V.I., Karpachevskii L.O., Ivanov A.V., and Morozov V.V. *Magnetizm pochv* (Soil magnetism). Moscow–Yaroslavl: Yaroslavl State Technical University (Publ.), 1995. 233 p. (in Russ.)

Bessudnov A.A. and Bessudnov A.N. *Novye verkhnepaleoliticheskie pamyatniki u khutora Divnogor'e na Srednem Donu* (New Upper Palaeolithic sites near Divnogor'ye village on the Middle Don). *Russian Archaeology*. 2010. No. 2. P. 136–145. (in Russ.)

Bessudnov A.N., Bessudnov A.A., Burova N.D., Lavrushin Yu.A., and Spiridonova E.A. *Nekotorye rezul'taty issledovanii paleoliticheskikh pamyatnikov u khutora Divnogor'e na Srednem Donu* (Some results of investigations of Palaeolithic sites near Divnogorie farmstead on the Middle Don (seasons 2007–2011)). *Brief Comm. Inst. Archaeology RAS*. 2012. No. 227. P. 144–154. (in Russ.)

Bessudnov A.N., Zakharova E.Yu., Bessudnov A.A., Rodionov A.M., Vladimirov S.I., Sycheva S.A., Girya E.Yu., and Burova N.D. Research of Divnogor'ye archaeological expedition 2018–2019. *Arkheologicheskie issledovaniya v Tsentral'nom Chernozem'e 2019,* Lipetsk–Voronezh: Novyi vzglyad (Publ.). 2020. P. 52–56. (in Russ.)

Borisova O.K. *Korotkoperiodnye landshaftno-klimaticheskie izmeneniya pozdnelednikov'ya: osnovnye etapy, rezul'taty i perspektivy issledovanii* (Short-term Landscape-Climatic Changes of the Late Glacial: Main Stages, Results and Perspectives of Research). *Materialy VI Vserossiiskogo soveshchaniya po izucheniyu chetvertichnogo perioda*. Apatity: Institute of Geology KSC RAS (Publ.), 2011. P. 92–94. (in Russ.)

Botvinkina L.N. *Metodicheskoe rukovodstvo po izucheniyu sloistosti* (Methodological guide to the study of layering). *Trudy GIN AN SSSR*. 1965. Vol. 119. 260 p. (in Russ.)

Broecker W.S., Peteet D.M., and Rind D. Does the ocean-atmosphere system have more than one stable mode of operation? *Nature*. 1985. Vol. 315. P. 21–25. https://doi.org/10.1038/315021a0

Burova N.D., Bessudnov A.A., and Bessudnov A.N. *Zooarkheologicheskii analiz kostnykh ostatkov krupnykh mlekopitayushchikh verkhnepaleoliticheskoi stoyanki Divnogor'e 1 (Voronezhskaya oblast')* (Zooarchaeological analysis of large mammals bone remains from the Late Upper Palaeolithic site of Divnogor'ye 1 (Voronezh region)). *Camera Praehistorica*. 2019. No. 2 (3). P. 40–65. (in Russ.) https://doi.org/10.31250/2658-3828-2019-2-40-65

Gadens-Marcon G., Guerra-Sommer M., Mendonça-Filho J., Mendonça J., Carvalho M., and Hartmann L. Holocene Environmental Climatic Changes Based on Palynofacies and Organic Geochemical Analyses from an Inland Pond at Altitude in Southern Brazil. *American Journal of Climate Change*. 2014. No. 3. P. 95–117. https://doi.org/10.4236/ajcc.2014.31009

Izdebski A. and Mulryan M. (Eds.). Environment and Society in the Long Late Antiquity brings together scientific, archaeological and historical evidence on the interplay of social change and environmental phenomena at the end of Antiquity and the dawn of the Middle Ages, ca. 300-800 AD. Leiden: Koninklijke Brill NV. 2019. 408 p.

Karpuz N.R. and Jensen E. A high-resolution Diatom Record of the Last Deglaciation from the SE Norwegian Sea: Documentation of Rapid Climatic Changes. *Paleoceanography and Paleoclimatology*. 1992. Vol. 7. No. 4. P. 160–161. https://doi.org/10.1029/92PA01651

Konischev V.N. and Rogov V.V. *Metody kriolitologicheskikh issledovanii* (Methods of Cryolithological Research). Moscow: Moscow State University (Publ.), 1994. 136 p. (in Russ.).

Lavrushin Yu.A. *Ekstremal'nye prirodnye sobytiya v basseine Severnogo Ledovitogo okeana v poslednie 60 tys. let* (Extreme Natural Events in the Arctic Ocean Basin in the Last 60 Thousand Years). *Byulleten' komissii po izucheniyu chetvertichnogo perioda*. 2007. No. 67. P. 20–35. (in Russ.)

Mudie P.J., Marret F., Rochon A., and Aksu A.E. Non-pollen palynomorphs in the Black Sea corridor. *Vegetation History and Archaeobotany*. 2010. Vol. 19. P. 531–544. https://doi.org/10.1007/s00334-010-0268-9

Panin A.V., Matlakhova E.Yu., Belyaev Yu.R., Buylaert J.P., Dubis L.F., Murray A.S., Pakhomova O.M., Selezneva E.V., and Filippov V.V. *Osadkonakoplenie i formirovanie terras v rechnykh dolinakh tsentra Russkoi ravniny vo vtoroi polovine pozdnego pleistotsena* (Sedimentation and formation of terraces in the river valleys of the center of the Russian Plain in the second half of the Late Pleistocene). *Byulleten' komissii po izucheniyu chetvertichnogo perioda*. 2011. No. 71. P. 47–74. (in Russ.)

Peltier W.R. and Fairbanks R.G. Global glacial ice volume and Last Glacial Maximum duration from an extended Barbados sea level record. *Quaternary Science Reviews*. 2006. Vol. 25. No. 23–24. P. 3322–3337. https://doi.org/10.1016/j.quascirev.2006.04.010

*Rukovodstvo po izucheniyu noveishikh otlozhenii* (Guide to the study of recent deposits). Moscow: Moscow State University (Publ.), 1987. 238 p. (in Russ.)

Selli R.K. *Vvedenie v sedimentologiyu* (Introduction to Sedimentology). Moscow: Nedra (Publ.), 1981. 370 p. (in Russ.)

Sidorchuk A. Gully erosion in the cold environment: Risks and hazards. Advances in Environmental Research. Hauppauge NY: Nova Science Publ., 2015. No. 44. P. 92–139.

Spiridonova E.A. *Evolyutsiya rastitel'nogo pokrova v verkhnem pleistotsene – golotsene* (Evolution of the Vegetation Cover of the Don Basin in the Upper Pleistocene – Holocene). Moscow: Nauka (Publ.), 1991. 227 p. (in Russ.)

Sycheva S.A. *Pedologicheskie materialy* (Pedologycal materials). *Paleoekologiya ravninnogo paleolita (na primere kompleksa verkhnepaleoliticheskikh stoyanok Kamennaya Balka v Severnom Priazov'e)*. Moscow: Novyi mir (Publ.), 2006a. P. 85–100. (in Russ.)

Sycheva S.A. Pioneer soils, cultural layers and host deposits of the Late Paleolithic site Kamennaya Balka II. *Kul'turnye sloi arkheologicheskikh pamyatnikov. Teoriya, metody i praktika issledovanii. Materialy nauchnoi konferentsii*. Moscow: IG RAS, IA RAS, NIA-Priroda (Publ.), 2006b. P. 180–186. (in Russ.)

Sycheva S.A., Bessudnov A.N., Chepalyga A.L., Sadchikova T.A., Sedov S.N., Simakova A.N., and Bessudnov A.A. Divnogorie pedolitocomplex of Russian plain: the final Pleistocene deposits and environments based on the Divnogorie 9 geoarchaeological site (middle reaches of the Don river). *Quaternary International*. 2016. No. 418. P. 49–60.
http://dx.doi.org/10.1016/j.quaint.2015.11.006

Vassoevich N.B. (Ed.). *Spravochnik po litologii* (Handbook of Lithology). Moscow: Nedra (Publ.), 1983. 509 p. (in Russ.)

Velichko A.A. (Ed.). *Dinamika landshaftnykh komponentov i vnutrennikh morskikh basseinov Severnoi Evrazii za poslednie 130000 let* (Dynamics of Landscape Components and Inland Marine Basins of Northern Eurasia over the Last 130000 years). Moscow: GEOS (Publ.), 2002. 231 p. (in Russ.)

Velichko A.A., Faustova M.A., Pisareva V.V., and Karpukhina N.V. History of the Scandinavian ice sheet and surrounding landscapes during Valday ice age and the Holocene. *Ice and Snow*. 2017. Vol. 57 (3). P. 391–416. (in Russ.).
https://doi.org/10.15356/2076-6734-2017-3-391-416

**EDN:** JYCQSZ
*ГЕОМОРФОЛОГИЯ, 2022, том 53, № 5, с. 89–102*

## ПРОБЛЕМЫ ПАЛЕОПОЧВОВЕДЕНИЯ И ГЕОАРХЕОЛОГИИ

*УДК 551.89: 574→569.9:902/904 (470.75)*

# СТРОЕНИЕ И УСЛОВИЯ ФОРМИРОВАНИЯ ПАЛЕОПОЧВ РАННЕГО ПЛЕЙСТОЦЕНА В ЛЁССОВО-ПОЧВЕННОЙ СЕРИИ РАЗРЕЗА АЛЧАК-СЕДЛОВИНА (РЕСПУБЛИКА КРЫМ)

**© 2022 г. М. В. Хмелева[1,*], П. Г. Панин[1], А. Л. Чепалыга[1], Н. В. Карпухина[1], О. Д. Найдина[2], А. В. Бухонов[3]**

[1]*Институт географии РАН, Москва, Россия*

[2]*Геологический институт РАН, Москва, Россия*

[3]*Институт физико-химических и биологических проблем почвоведения РАН, Пущино, Россия*

**E-mail: khmeleva@igras.ru*

Поступила в редакцию 16.06.2022 г.
После доработки 29.06.2022 г.
Принята к публикации 15.07.2022 г.

Палеопочвы являются одним из основных палеоэкологических индикаторов, фиксирующих изменения окружающей среды в лёссово-почвенных сериях. Понимание особенностей строения палеопочв и природных процессов, которые их вызвали, позволяет реконструировать ландшафтно-климатические условия на искомых территориях. В статье представлены новые исследования лёссово-почвенной серии разреза Алчак-Седловина, расположенного в горной местности южной части полуострова Крым. В разрезе вскрыты две автоморфные палеопочвы (PS1-AS и PS3-AS) и одна гидроморфная (PS2-AS), которые мы сопоставляем с палеопочвами воронского педокомплекса (МИС 13/15). Это предположение базируется на данных, полученных по результатам комплексного анализа, включающего морфологическое обследование палеопочв и их физико-химические показатели. Установлено, что лёссово-почвенная серия исследуемого разреза Алчак-Седловина формировалась на отложениях V Перчемской террасы, которая соответствует интервалу МИС17. Палеопочвы PS2-AS и PS3-AS развивались по типу Cambisols в условиях теплых степей или лесостепей с периодическим увлажнением и нередко локальным застоем влаги; в холодное время года наблюдалось незначительное промерзание поверхности. Профиль палеопочвы PS1-AS также соответствует типу Cambisols, но он формировался в более сухом климате под степной растительностью, схожей с современной. В районе исследования в периоды аккумуляции лёссового материала и почвообразования сопровождались постоянными эрозионными процессами. В результате чего в лёссово-почвенной серии разреза Алчак-Седловина фиксируются слои крупнообломочного материала, а поверхностные горизонты палеопочв эродированы. Полученный материал позволил по-новому взглянуть на развитие палеопочвенного покрова в горной местности Крымского полуострова. Выявленные характеристики палеопочв разреза Алчак-Седловина, в дальнейшем, можно сопоставить с другими палеопочвами п-ова Крым для интерпретации их возраста и условий формирований.

*Ключевые слова:* морфология почв, морская терраса, морфоскопия кварцевых зерен, плейстоцен, мучкапское межледниковье

**DOI:** 10.31857/S0435428122050054

## 1. INTRODUCTION

Loess covers about 10% of the Earth's surface (Pye, 1987; Haase et al., 2007; Lu et al., 2020; a.o.). Their deposits preserve ancient soils, representing the climatic conditions in which they were formed (Velichko, Morozova, 2015; Panin et al., 2018; 2019a; a.o.). The sequence of such paleosols in the loess is called the loess-paleosol sequences (LPS), which is used to reconstruct the climatic conditions of past epochs. Thus, the loess cover is one of the main archives reflecting landscape and climatic changes in the Quaternary. This paper proposes a study of the loess-paleosol section Alchak-Sedlovina, located on the Crimean Peninsula. In this area, mainly paleosol studies were carried out only in the western part of the peninsula, where coastal cliffs are composed of thick loess deposits with red-colored paleosols (Veklich, 1968; Veklich, Sirenko, 1976; Pevzner et al., 2004; Panin et al., 2018; a.o.). The uniqueness of the Alchak-Sedlovina section is that it is located in the mountainous part of the Crimea, where detailed studies of paleosols have practically not been carried out.

The LPS of the section is represented by three paleosols, the profiles of which are superimposed on

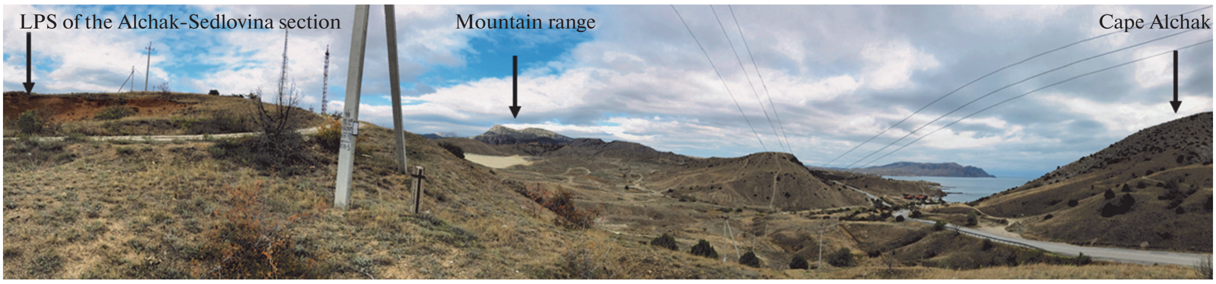


**Fig. 1.** General view of the Alchak-Sedlovina section and landscape.
**Рис. 1.** Панорамный вид разреза Алчак-Седловина и ландшафта.

each other, they are crowned by the modern Calcic Cambisol. Their study will expand knowledge about the structure and development of the paleosols of the Crimean Mountains (Veklich, Sirenko, 1976). Multi-proxy analysis with detailed sampling will make it possible to classify the paleosols type and compare them with modern soil analogues. Based on this, we will be able to reconstruct the landscape and climatic conditions that prevailed in this area in the Early Pleistocene.

## 2. REGIONAL SETTINGS AND METHODS

The study area belongs to the southern coast of the Crimean Peninsula. The landscape is characterized by a hilly-ravine relief; landslide processes and erosional landforms are widely developed here (Muratov, 1960). In the study area, near the town of Sudak, limestone cliffs and mountain ranges (Alchak, Mandjil, Perchem, Sokol, etc.) stand out (Muratov, 1960). The LPS of the Alchak-Sedlovina section (44°50′18″ N; 34°59′44″ E, 54 m asl) (fig. 1, 2) was uncovered on a foothill elevation in a saddle near the northern slope of Mount Alchak, between Mount Alchak and Mount Ay-Georgiy on the paleo-terrace. The loess formation of the studied section based on loams underlain by the V Perchem marine terrace (Chepalyga, 2015; 2017). The study area belongs to the South Coast climatic region, zone IB (Cherenkova, 1959), with a dry subtropical climate of the Mediterranean type (Sudnicin, 2014). According to the climate classification of Köppen-Geiger (Kottek et al., 2006), the territory of the southern coastal zone of Crimea belongs to the Mediterranean type Csa, but the Sudak coast is compared with the more arid zone – Submediterranean subtype. The annual precipitation does not exceed 325 mm (Cherenkova, 1959). The average air temperature in July is 24°C, in January 3...–4°C (Ved', 2000).

*2.1. Black sea marine terraces age.* To determine the age of the LPS of the Alchak-Sedlovina, section it was necessary the age of the terraces of the town of Sudak and, first of all, the V Perchem Terrace. The first generalization on the terraces of the town of Sudak was carried out by the famous Russian geologist Andrusov (1889), who substantiated up to 4–5 cyclic terraces. At the same time, the author believed that in addition to these terrace levels, there are several more intermediate terraces in the town of Sudak area.

At the beginning of the XXI century, on the basis of detailed interdisciplinary research, it was possible to significantly supplement the Sudak system of terraces in the altitude range of 0–200 m asl up to 12 terrace levels, reveal their structure and age based on paleomagnetic and paleofaunal data (Arkhangelskij, Strakhov, 1938; Arslanov et al., 1983; Chepalyga, 2017). A cyclicity in the structure of the deposits and the height of the surface, as well as in the age of the corresponding terraces, was found to be close to the cyclicity of the Marine Isotope Stage (MIS). As a result, the local system of terraces was based the Sudak Typical Terrace Profile. Based on the height of the top of the marine facies of the terraces, it was possible to establish that the rate of uplift of the southern coast of Crimea in the Sudak region averaged 0.1 mm/year over the past 2 Ma (Chepalyga, 2017).

Eastern vicinities of the town Sudak (from the Eastern Highway to the Frantzuzhenka Cape), terraces are clearly morphologically and geologically expressed from sea level to a height of 75 m asl Some of them are of interest for this work.

II Karangat terrace up to 10–15 m high, in the Sudak terrace system, Cape Frantzuzhenka, Cape Meganom, etc. are exposed in sections and contain the leading species of mollusks *Acanthocardia tuberculata*, *Paphia senescens*, *Mactra corallina*, etc., also characteristic of the Tyrrhenian deposits of the Mediterranean Sea. Therefore, the preliminary name of this terrace according to Andrusov (1889; 1912) is Tyrrhenian. Later, this name was changed to the local Black Sea one along Cape Karangat, where the stratotype of the Karangat deposits was established (Arkhangelskij, Strakhov, 1938). From the deposits of the Karangat stratotype, as well as the parastratotype Eltigen and Tuzla sections, optically stimulated luminescence series of datings were obtained in the interval of 70–140 ka (Kurbanov et al., 2019; 2020). This age of the Karangatian terrace, as well as the parastratotype, was confirmed by the data of paleomagnetic analysis, in connection with the discovery in the lower Karangat

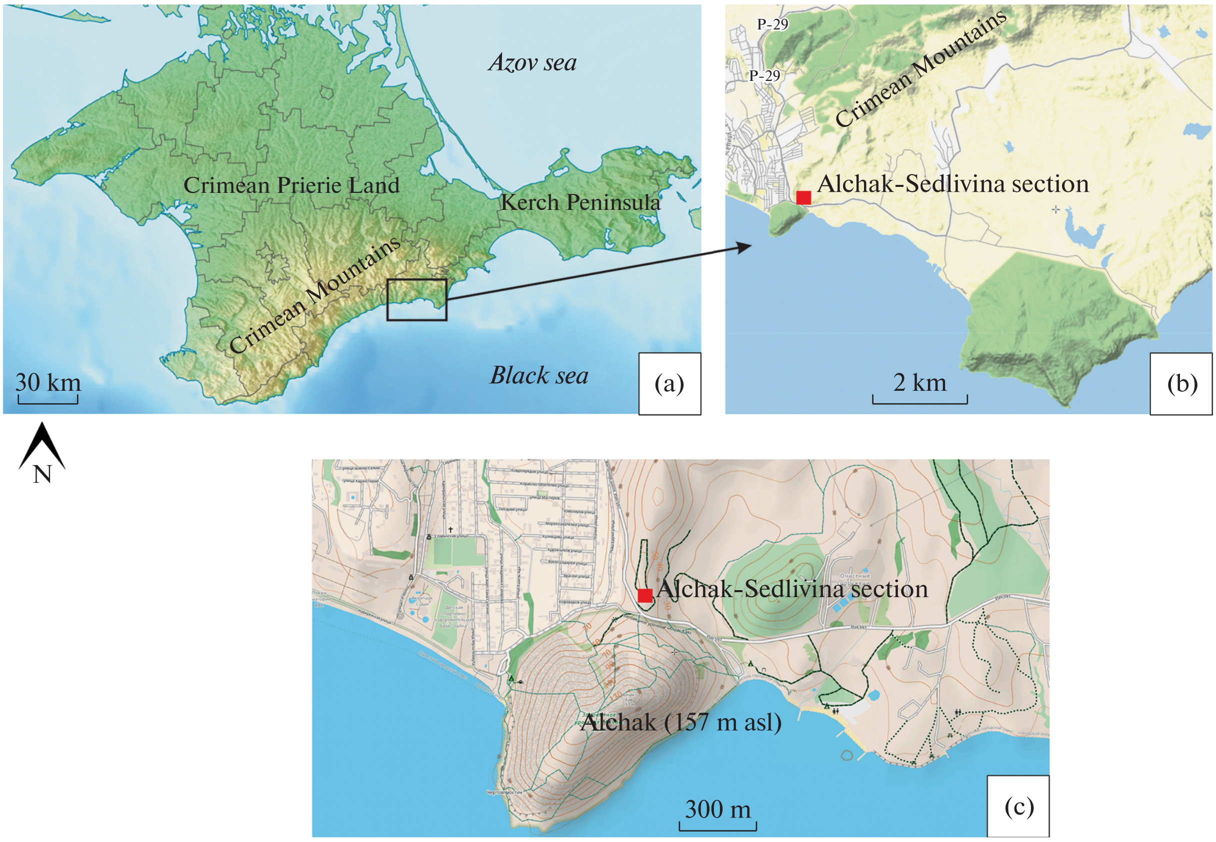


**Fig. 2.** Geographical position of the Alchak-Sedlovina section (a, b), topography plan (c).
**Рис. 2.** Географическое положение разреза Алчак-Седловина (a, b), топографический план (c).

of the reverse polarity of the Blake event (~100–121 ka) (Pilipenko, Trubikhin, 2012). All these data indicate the age of the Karangat terrace during the Mikulino interglacial (MIS 5).

The V Perchem terrace has a surface height of about 50 m, a basement of 45 m asl, distinguished by Andrusov (1889) in the town of Sudak. The stratotype of this terrace was established in the Alchak-Sedlovina section, where later a section of subaerial deposits with paleosols was found (Chepalyga, 2015; Chepalyga et al., 2019). The terrace sequence is represented by marine basal pebbles up to 1 m thick and overlain by silts and sands of marine facies 5–6 m thick. The terrace V is analogous to the deposits of the Chauda basin of the Black Sea at Cape Chauda, where the stratotype of the Chauda stage and deposits of the Upper Chauda with rich endemic fauna of the Caspian type are located: *Tschaudia tschaudae*, *Submonodacna pleistopleura*, *Didacna pseudocrassa*, etc. (Andrusov, 1912). In the upper part of these deposits, for the first time in the Black Sea basin, Mediterranean species and planktonic foraminifers appear, which marks the first penetration of sea water into the Black Sea from the Mediterranean at the beginning of the Middle Pleistocene. These sediments with marine species were identified as a new phase of the Chauda basin, called Karadeniz (Chepalyga, 1997) and Epichauda (Fedorov, 1978). The age of the terrace V is determined by MIS 17.

The VI Sugdey terrace 62–64 m high, basement 50–56 m asl is older than the V Perchem terrace. It was identified for the first time and named after the ancient name of the town of Sudak with a stratotype near the Alchak-Sedlovina section (Chepalyga, 2015; Chepalyga et al., 2019). The marine sequence of this terrace corresponds to the deposits of the Lower Chauda at Cape Chauda with the fauna of molluscs of the Caspian type *Didacna baericrassa*, but without representatives of the endemic genus *Tschaudia*. In the stratotype of the Lower Chauda, the normal magnetization of the Brunhes epoch younger than 781 ka was revealed. Age correlates with MIS 19 stage.

*2.2. Field survey and samples.* The Alchak-Sedlovina section is morphologically described according to the FAO (2006). The color of the deposits was determined using the Munsell color system (2000) on a fresh section wall. Sampling for laboratory analysis was performed continuously with a step of 4 cm. Magnetic susceptibility (MS) in field was measured with a PIMV kappameter with same measuring interval. A total of 51 bulk samples were taken for physical and chemical analyses. Also, 10 bulk samples were taken from each paleosol horizon for morphoscopy of sandy quartz grains. Soils were described according to IUSS Working Group WRB 2014 (2015).

*2.3. Laboratory analyses.* The particle size distribution of the samples was analyzed using a laser diffractometer Malvern Mastersizer 3000 with liquid sample dispersion unit Hydro EV. The distribution of particles over size fractions was calculated on the basis of the Fraunhofer approximation (Blott, Pye, 2001). Preparation of a bulk sample included the following steps: filling with 10% HCl solution of acid for 24 hours; treatment with 30% hydrogen peroxide solution $H_2O_2$ until the completed reaction; treatment of the material with a 4% solution of $Na_4P_2O_7$, followed by dispersion of the material using ultrasound. Mastersizer v.3.62 software was used to calculate grain size statistics. When describing soil characteristics, the system 2000–63–2 μm was used (FAO–ISRIC, 1990).

The quartz grain shape and surface were studied following the procedure developed in the Institute of Geography, RAS (Velichko, Timireva, 1995). The modern soil was characterized by 1 sample, followed by 3 samples from each paleosol horizon (fig. 3, 5(a)). Quartz grains with a diameter of 0.5–1 mm were isolated using wet sieving and treated with 10% HCl. The sample of 50 quartz grains from each soil sample were examined under a stereomicroscope at ×40-×50 magnifications. During the analysis, the degree of roundness, relief features, and the type of quartz grain surface was recorded. The roundness class was assessed according to the Khabakov visual scale (Khabakov, 1946) using the Rukhin template (Rukhin, 1969), which includes 5 classes: from 0 to IV, where IV is the perfectly rounded, 0 – angular at all. Next, the roundness coefficient (Q) and the degree of matting (Cm) were calculated (Velichko, Timireva, 1995). For a more detailed characterization of the surface, individual quartz grains were additionally studied using a JEOL JSM-6610LV scanning electron microscope, maximum magnification ×950, all images are made in secondary electrons. The description of surfaces was performed in accordance with Krinsley and Doornkamp (Krinsley, Doornkamp, 1973).

Eight samples taken from paleosol profiles were analyzed for pollen content. Laboratory processing of samples was carried out by the separation method (Grichuk, Zaklinskaya, 1948). To remove carbonates, the samples were heated in a 10% HCl solution, followed by bringing the solution to a neutral pH. Next, the resulting material was treated with 10% $Na_4P_2O_7$ $10H_2O$. The resulting precipitate was separated in a heavy liquid with a density of 2.25 g/cm$^3$.

## 3. RESULTS

*3.1. Soil morphology.* The LPS of the Alchak-Sedlovina section is shown in figs. 4 and 5. Here, the profile of modern soil is represented by two horizons:

ABk (0.4 m) – dark brown (10 YR 5/6) fine-porosity, loam. The structure is granular. Carbonate pseudomycelia stands out along the roots, small carbonate concretions;

BCk (0.9 m) – light brown (10 YR 6/6), loam. The structure is blocky subangular, the horizon is denser. Small carbonate concretions and carbonate pseudomycelia stand out along the surfaces of the aggregates.

Below lies the PS1-AS paleosol, which consists of hor. Bk and BCk. The soil stands out in the LPS with a brownish-pale color, carbonate concretions, and an abundance of clay-humus coatings along the root courses.

Bk (1.88 m) – pale brown (7.5 YR 6/6) lighter in the upper part due to nearby loess, clay loam. Porosity, well structured, granular structure, thin clay coatings along the surfaces of the structure. Carbonate mycelium in pores.

BCk (0.25 m) – brown (7.5 YR 6/6) granular-blocky, clay loam. A molehill was found in the horizon. Carbonate concretions 1 cm in diameter. There are inclusions of unrounded gravel up to 2 cm in diameter.

The PS2-AS paleosol. Its profile is represented by three horizons: Ak, BCk and Ckg.

Ak (0.26 m) – brown (10 YR 6/5), loam. The structure is granular. There are rare inclusions of gravel. A lens 5 cm in diameter was found here, filled with an accumulation of *Helicella Striata* (Z.) snails. There is the crack coming from the layer.

BCk (0.20 m) – brown with a bluish tint (10 YR 6/4) very dense, loam, rarely porous, granular structure. Rare crystals of gypsum have been found. Clay coatings along the surfaces of the structure. Horizon with cracks and layers of fine gravel.

Ckg (0.28 m) – gray with a brown tint (10 YR 6/4), loam, granular structure. The upper part is represented by a layer of gravel, very dense, slightly porous. Carbonate material and formed carbonate concretions up to 2 cm in diameter throughout the layer. Clay coatings and bluish patches gleying along the surfaces of the aggregates.

The profile of the underlying paleosol PS3-AS is as follows: ABk, Bk, BCk.

ABk (0.20 m) – brown (10 YR 5/6) clay loam, lumpy-granular structure, fine-porosity, the layer is permeated with pores up to 0.5 cm in diameter, inclusions of large gravel up to 7 cm in diameter. Clay coatings along the faces of structural units, intense carbonated pseudomycelia and carbonated concretions.

Bk (0.32 m) – pale yellow with a brown tint (10 YR 6/4, 6/6) dry, granular structure, porosity, Fe-Mn coatings on the faces of peds and pores, coprolites, rare inclusions of gravel up to 1 cm in diameter, identical to the overlying layers. Rare concentrations of crystalline gypsum and small carbonated concretions. To the bottom of the horizon, the amount of gravel increases.

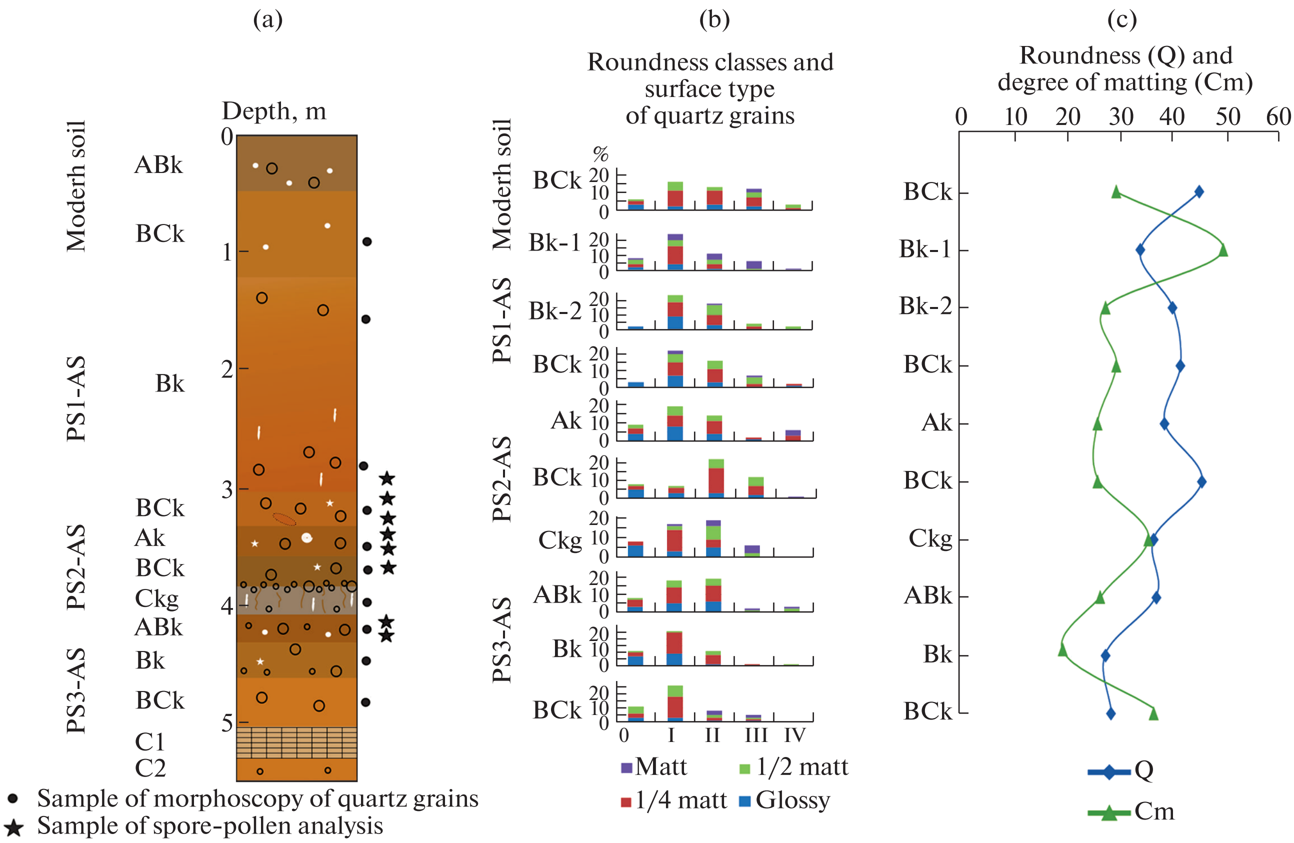


**Fig. 3.** The LPS of the Alchak-Sedlovina section: (a) – sampling point for spore-pollen analysis and morphoscopy of quartz grains. Morphoscopy of sand quartz grains: (b) – histograms of roundness classes and surface type of quartz grains. *Figure captions*: 0, I, II, III, IV – roundness classes; (c) – distribution charts of Q and Cm coefficient.

**Рис. 3.** ЛПС разреза Алчак-Седловина: (а) – места отбора проб на спорово-пыльцевой анализ и морфоскопию песчаных кварцевых зерен. Морфоскопия песчаных кварцевых зерен: (b) – гистограммы окатанности и типов поверхности кварцевых зерен. *Условные обозначения:* 0, I, II, III, IV – классы окатанности; (c) – графики распределения значений коэффициентов Q и Cm.

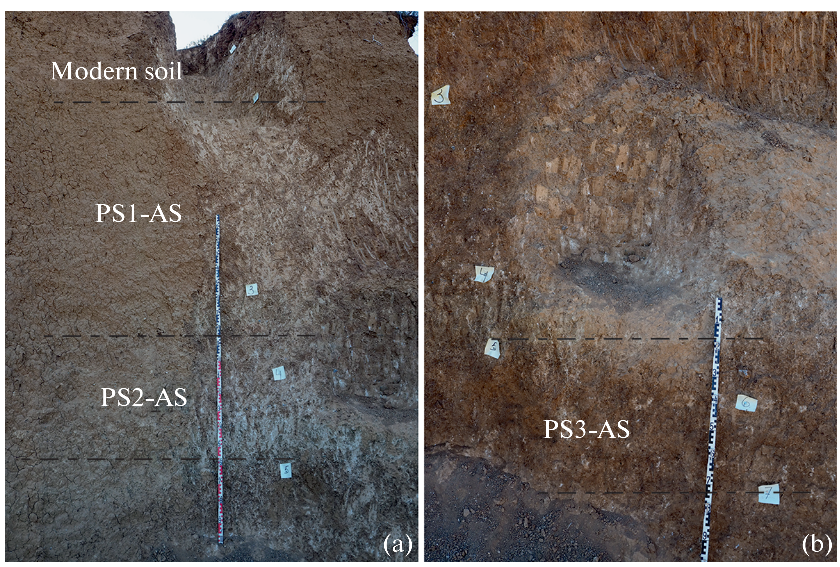


**Fig. 4.** The Alchak-Sedlovina section with paleosols: (a) – PS1-AS and PS2–AS; (b) – PS3-AS.

**Рис. 4.** Профили палеопочв в разрезе Алчак-Седловина: (a) – PS1-AS и PS2-AS; (b) – PS3-AS.

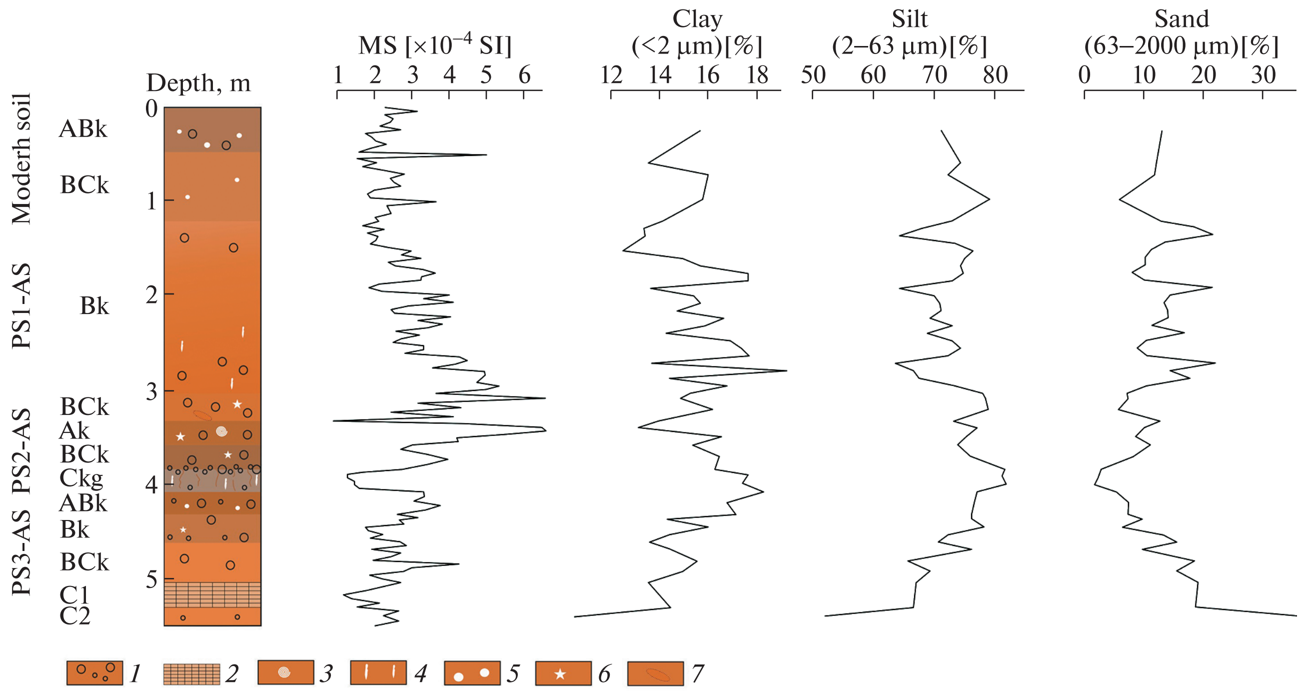


**Fig. 5.** The LPS of the Alchak-Sedlovina section, values of MS and particle size distribution.

*1* – gravel; *2* – gravel layer; *3* – shells of *Helicella Striata* (Z.) snails; *4* – oblong shape carbonate pedofeatures; *5* – carbonate nodules; *6* – crystalline gypsum; *7* – mole burrows.

**Рис. 5.** ЛПС разреза Алчак-Седловина, значения магнитной восприимчивости и гранулометрического состава.

*1* – гравий; *2* – гравелистый слой; *3* – ракушки улиток *Helicella Striata* (Z.); *4* – карбонатные новообразования продолговатой формы; *5* – карбонатные конкреции; *6* – кристаллический гипс; *7* – кротовина.

BCk (0.44 m) – pale yellow (10 YR 6/4, 7/6), dry. Granular structure, non-porous, small gravel inclusions up to 1 cm in diameter. Fe-Mn coatings along the surfaces of the structure and impregnated with carbonates.

The PS3-AS paleosol underlies layer C1, which is a mixture of loam, gravel, and pebbles.

*3.2. Particle size and magnetic susceptibility distribution.* The LPS of the Alchak-Sedlovina is composed mainly of silt fraction (fig. 5), from 50 to 80% of all fractions. The silt fraction is uniformly distributed over the section; the values decrease towards the bottom of the PS3-AS paleosol. The indicators of the clay fraction are also distributed evenly and do not exceed 20%. There is an insignificant accumulation of the clay fraction towards the bottom of horizons BCk (PS1-AS) and Ckg (PS2-AS). The distribution of clay and silt particles along the profile of the LPS is eluvial-illuvial. The high content of the sandy fraction is confined to the PS1-AS paleosol; individual peaks (up to 20%) are distinguished here. In Ak and BCk horizons of the PS2-AS paleosol, the sand content increases to 15%. Sand mainly accumulates in the lower part of the section, here the values gradually increase from PS3-AS to the C1 horizon.

MS indicates the levels of humus horizons. Low MS values are associated with modern soil ($1.7–3.2 \times 10^{-4}$ SI), individual peaks are visible. In the paleosol PS1-AS MS gradually increases downwards, to a maximum of $6.9 \times 10^{-4}$ SI at the bottom of the BCk horizon and fall in the transitional part of the BCk horizon to PS2-AS ($2.4 \times 10^{-4}$ SI). The PS2-AS profile shows two MS peaks: in the Ak ($6.9 \times 10^{-4}$ SI) and BCk ($4.2 \times 10^{-4}$ SI) horizons. In the Ckg horizon of this paleosol, the MS values drop sharply. In the PS3-AS paleosol, the average MS values are slightly lower than the overlying paleosols: horizon ABk ($3.4 \times 10^{-4}$ SI), horizon Bk ($2.38 \times 10^{-4}$ SI) and horizon BCk ($2.6 \times 10^{-4}$ SI).

*3.3. Morphoscopy of quartz grains.* Grains of the I roundness class predominate in the modern soil, as well as in PS1-AS and PS3-AS paleosols, while the I and II roundness classes predominate in PS2-AS (fig. 3, (b)). The coefficient of roundness (Q) across the LPS does not differ in variability and varies from 27.5–45.5% (fig. 3, (c)). The minimum roundness coefficients are found in the lower horizons of the PS3-AS paleosol and take values of 27–28%, the maximum in the BCk horizon of the PS2-AS. In all soils, grains with a quarter-matte and glossy surface predominate, and a small amount of half-matte grains is also present. The coefficient of matting (Cm) ranges from 29 to 45%.

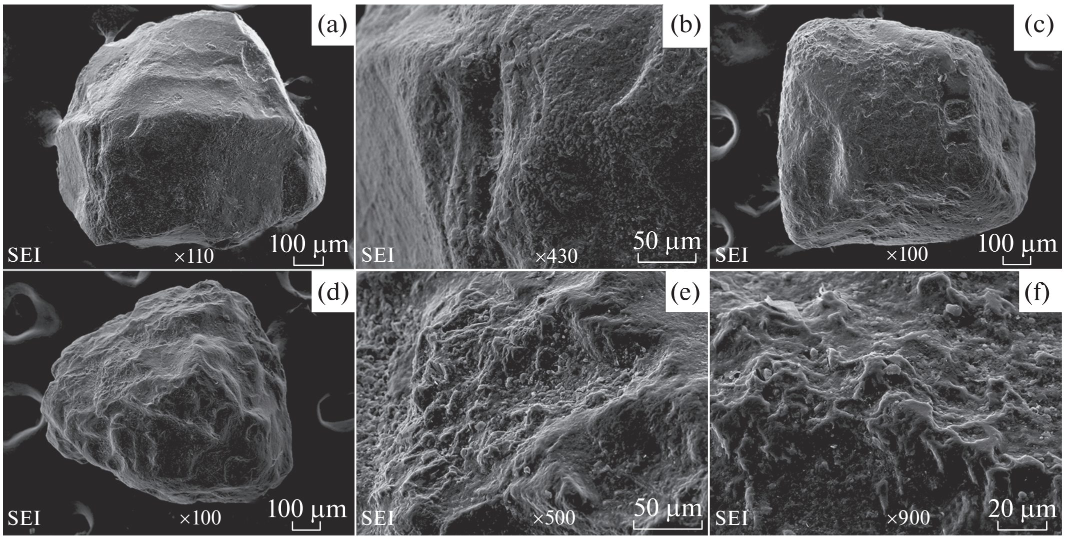


**Fig. 6.** Quartz grain morphoscopy in the modern soil: (a, b) – parallel grooves; (c, d) – grain with pitted surface; (e, f) – crescent pits.

**Рис. 6.** Морфоскопия кварцевых зерен из современной почвы: (a, b) – параллельные борозды; (c, d) – зерна с ямчатой поверхностью; (e, f) – серповидные ямки.

Modern soil is characterized by domination of grains I, II and III class of roundness. A large number of grains with a quarter-matt surface. Special interest are particles having two parallel grooves (fig. 6, (a, b)). There are also grains with a pitted surface (fig. 6, (c, d)) and grains with conchoidal fractures. Signs of diagenesis are reflected in crescent pits (fig. 6, (e, f)) and etched zones on quartz grains.

The dominant class of roundness in PS-1AS is I and II, glossy and quarter-matt grains. Quartz grains in the PS1-AS are characterized by a pitted surface (fig. 7, (a, b)) with silica films, large and small conchoidal fractures (fig. 7, (c, d)) and crescent pit (fig. 7, (b, e)). Split grains with etched zones (fig. 7, (f)) and "fresh" grains are not uncommon (fig. 7, (g)). In horizon Bk, compared to other horizons of paleosols, the maximum number of perfectly matt grains was found. These grains belong to the III class of roundness (fig. 7, (h)). The entire paleosol also has a high content of glossy grains.

The dominant class of roundness in PS2-AS is I and II, quite a lot of grains with quarter-matt and glossy surface. A significant number of grains with semi-matt surface. Quartz grains in PS2-AS are characterized by particles having two parallel grooves and conchoidal fractures. The number of roundness class 0 grains increases, glossy grains are noted with V-shaped pits (fig. 8, (a)), grains are often split in half (fig. 8, (b)), "fresh" grains are noted (fig. 8, (c)), grains with large conchoidal fractures (fig. 8, (e)). In the Ak horizon, the percentage of class IV grains increases. In a small amount, particles with aeolian characteristics are noted: with flat and crescent pits (fig. 8, (d)), grains with a micro-pitted surface (fig. 8, (f)).

In the PS3-AS paleosol the maximum number of grains of the 0, I roundness classes and completely angular grains are recorded in the entire profile. The humus horizon ABk of the PS3-AS is also characterized by a high content of grains of class II; grains of class III and IV are also recorded in a small amount. The grains in this soil are angular (fig. 9, (a)), with a pitted surface (fig. 9, (b, c)). Often there are grains with glossy potholes (fig. 9, (d, e)), parallel grooves (fig. 9, (f)) and single deep grooves filled with silica (fig. 9, (g)). Conchoidal fractures and flat pits are numerous. Grains with signs of chemical etching on the surface are registered (fig. 9, (h)).

The processes of diagenetic transformation of material in all paleosols are clearly identified: V-pits (fig. 10, (a)), dense silica precipitations (fig. 10, b, c), as well as filling of pits with silica (fig. 10, (d)), etching zones (fig. 10, (e)) are marked on the surface of the grains. Newly formed gypsum crystals (fig. 10, (f)) are also noted in paleosols PS2-AS and PS3-AS. Abundant carbonate coatings are recorded on grains not treated with acid.

*3.4. Spore-pollen analysis.* In the PS1-AS paleosol, 180 grains were found in the sample collected from Bk horizon. Tree and shrub pollen is absent, grass pollen predominates 67.4%: Cyperaceae 22.6%, Poaceae 5.5%, Artemisia 5.5%, Chenopodiaceae 4.4%, *Plantago* 7.7%, *Urtica* 6.0%, single *Ephedra,* Asteraceae, Rosaceae, Fabaceae and other representatives of forbs were identified. The number of spores is 32% of the total number of counted grains. Spore plants are represented by a variety of Polypodiaceae, club-mosses and non-vascular mosses. In the BCk horizon, the number of pollen grains and spores is 198 units. *Salix*, *Quercus*

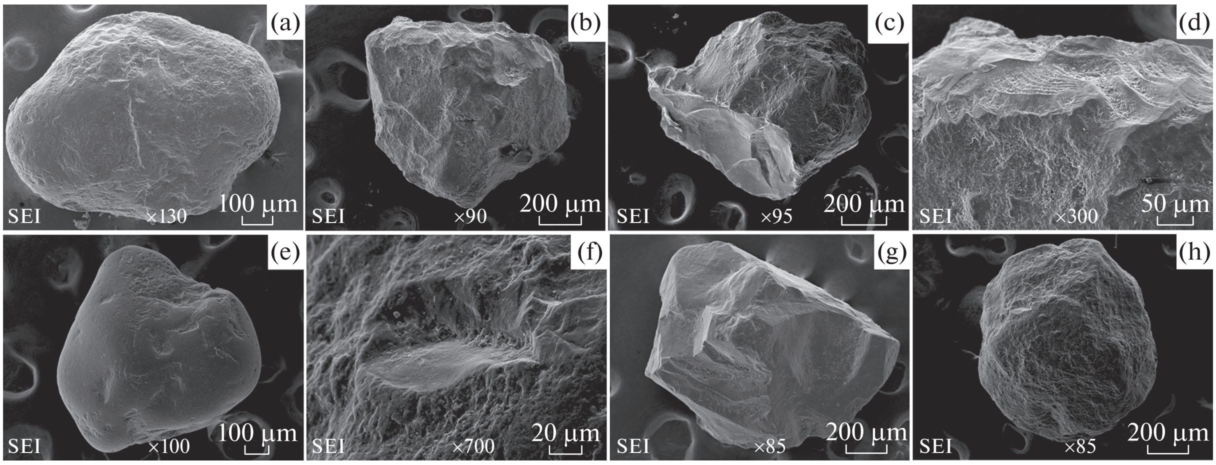


**Fig. 7.** Quartz grain morphoscopy in the PS1-AS paleosol: (a) – grain with pitted surface; (b) – pitted surface and conchoidal fractures; (c) – large conchoidal fractures (grain split in half); (d) – conchoidal fracture; (e) – crescent pit; (f) – etched zones and potholes; (g) – "fresh" grain; (h) – grain with pitted surface of III class of roundness.

**Рис. 7.** Морфоскопия кварцевых зерен палеопочвы PS1-AS: (a) – зерно с ямчатой поверхностью; (b) – ямчатая поверхность и раковистые изломы; (c) – крупный раковистый скол (зерно разбито пополам); (d) – раковистый скол; (e) – серповидные ямки; (f) – зона травления и выбоина; (g) – "свежее" зерно; (h) – зерно с мелкоямчатой поверхностью III класса окатанности.

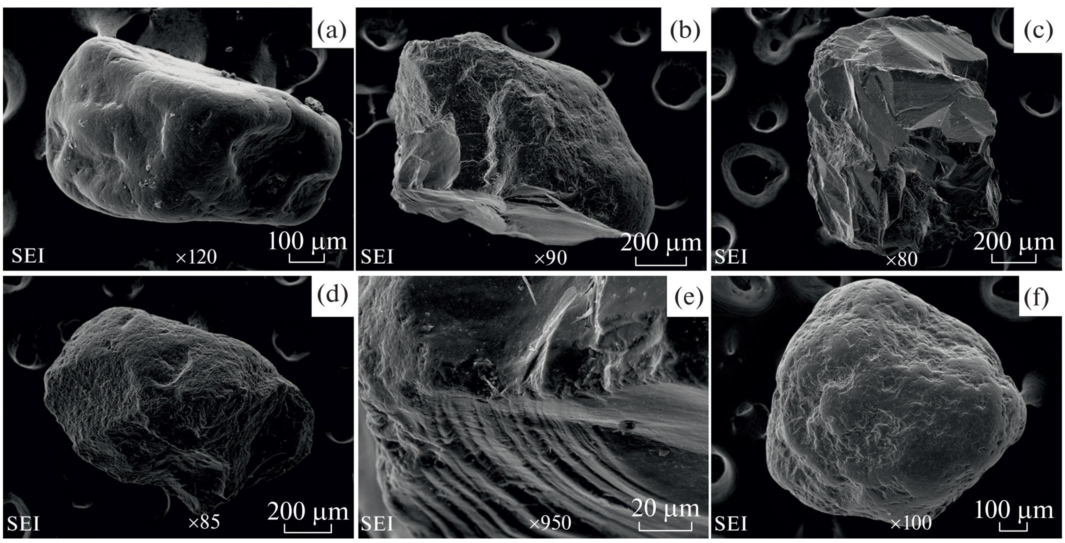


**Fig. 8.** Quartz grain morphoscopy in the PS2-AS paleosol: (a) – glossy grain with V-shaped pits; (b) – grain with conchoidal fractures (grain split in half); (c) – "fresh" grain; (d) – flat and crescent pits; (e) – conchoidal fracture; (f) – grain with micro-pitted surface.

**Рис. 8.** Морфоскопия кварцевых зерен палеопочвы PS2-AS: (a) – глянцевое зерно с V-ямками; (b) – зерно с раковистыми сколами (зерно разделено пополам); (c) – не окатанное "свежее" зерно; (d) – плоские и серповидные ямки; (e) – раковистый скол; (f) – зерно с микро-ямчатой поверхностью.

were noted among single woody 2.0%. Grass pollen prevails 73.7%, among which Poaceae 39.9%, Cyperaceae 24.7% and single pollen grains of *Plantago*, *Urtica*, Chenopodiaceae, Asteraceae, Polygonaceae, Rosaceae, Fabaceae. The number of spores reaches 24%, among which Polypodiaceae and *Lycopodium* are noted. In the lower part of the BCk horizon, 195 grains were counted. Among them, the pollen of *Salix* and *Ulmus* trees is single 1.5%. The amount of grass pollen 57.7% and spores 46.6% are approximately the same. Herbs are dominated by Poaceae 11.4%, Cyperaceae 7.6%, *Urtica* 8.7%, *Plantago* 6.1%, *Rumex* 5.6%. The largest number of spores was noted in the sample, among which spores of Polypodiaceae 15.3%, *Lycopodium* club-mosses 14.8% and non-vascular green mosses *Bryales* 13.3% predominate.

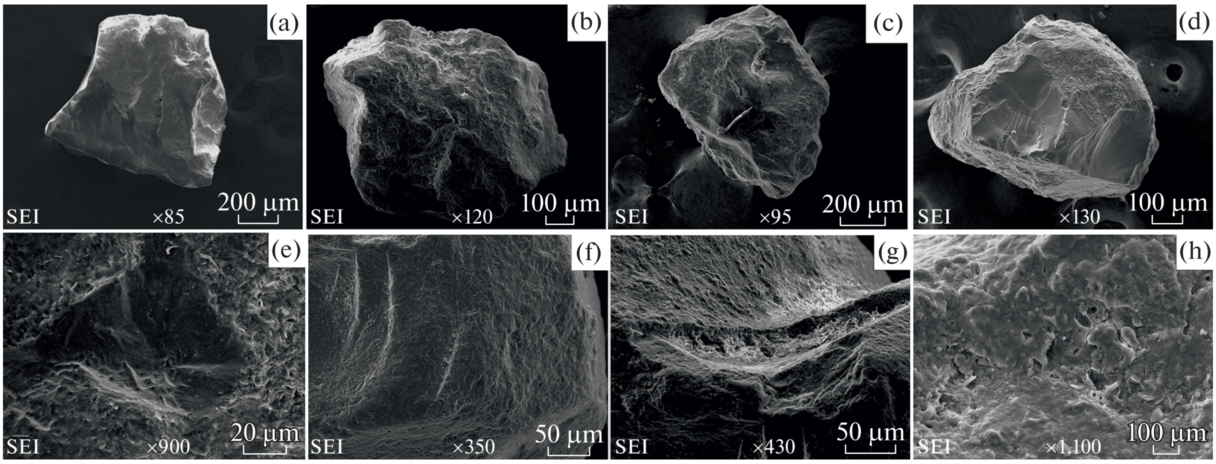


**Fig. 9.** Quartz grain morphoscopy in the PS3-AS paleosol: (a) – angular grain; (b, c) – pitted surface; (d, e) – glossy potholes; (f) – parallel grooves; (g) – deep grooves filled with silica; (h) – chemical etching on the surface.

**Рис. 9.** Морфоскопия кварцевых зерен палеопочвы PS3-AS: (a) – не окатанное зерно; (b, c) – зерна с ямчатой поверхностью; (d, e) – глянцевые выбоины на поверхности зерна; (f) – параллельные борозды; (g) – глубокая борозда, заполненная кремнеземом; (h) – зона травления.

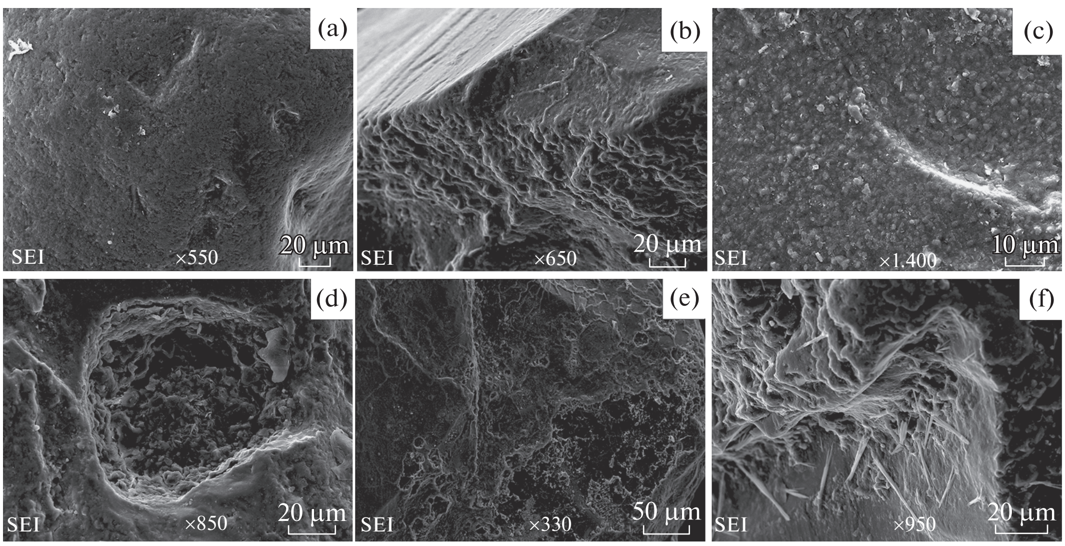


**Fig. 10.** Signs of diagenetic transformation of quartz grains surfaces: (a) – V-pits (horizon Ckg of the PS2-AS); (b) – silica precipitations (horizon Ckg of the PS2-AS); (c) – silica precipitations (horizon ABk of the PS3-AS); (d) – filling of pits with silica (horizon BCk of the modern soil); (e) – chemical etching on the surface (horizon BCk of the modern soil); (f) – gypsum crystals (horizon Ckg of the PS2-AS).

**Рис. 10.** Признаки диагенетического преобразования поверхности кварцевых зерен: (a) – V-ямки (горизонт Ckg палеопочвы PS2-AS); (b) – кремнеземистые пленки (горизонт Ckg палеопочвы PS2-AS); (c) – кремнеземистые пленки (горизонт ABk палеопочвы PS3-AS); (d) – ямки, заполненные кремнеземом (горизонт BCk современной почвы); (e) – зоны травления (горизонт BCk современной почвы); (f) – кристаллы гипса (горизонт Ckg палеопочвы PS2-AS).

In the PS-2AS paleosol, the sample from the upper part of the Ak horizon contains 184 grains, of which arboreal pollen contains 7.6% (*Salix*, *Ulmus*, *Quercus*), grass pollen 73.9%, among which Cyperaceae 12.5%, Poaceae 11.4%, *Urtica* 13.9%, *Rumex* 6.5%, *Plantago* 5.9%, Asteraceae 5.9%, Chenopodiaceae and other herbs. The number of spores reaches 18.4%, among which spores of Polypodiaceae predominate.

In the sample from the lower part of the same horizon, 220 grains were counted, woody – 5.4% (*Salix*, *Ulmus*, *Quercus*), herbaceous – 92.2%, dominated by Poaceae, Cyperaceae, *Rumex* 10.4%, *Urtica* 15.4%, single *Ephedra*, *Artemisia*, Chenopodiaceae. The amount of spores is small – 2.2%. The smallest amount of pollen and spores was found in the sample from the BCk horizon (104 grains). The pollen of woody plants is single 1.9%, contains grains of *Salix* and *Quercus*. Among herbs 76.9% dominated by Cyperaceae 19.2%, *Urtica* 14.4%, Polygonaceae 5.7%, *Plantago* 4.8%, *Rumex* 4.8%, Chenopodiaceae 4.8%, etc. The number of spores of *Bryales*, Polypodiaceae, *Lycopodium* reaches 21.1%.

The PS-3AS paleosol is characterized by the largest amount of pollen and spores. In the sample collected from upper part of the ABk horizon were found 272 grains. Here the pollen of woody plants is single 7.3%: *Ulmus* 5.5% and other (*Quercus, Carpinus*). Grass pollen prevails 89.3%, represented by a variety of *Varia*: *Ephedra*, Poaceae, Cyperaceae, Caryophyllaceae, Chenopodiaceae, Asteraceae (13.2%), *Rumex* 9.1%, *Plantago* 5.5%, *Urtica* 18.7%, *Potentila* 6.6%, etc. There are few spores – 3.3% of Polypodiaceae. In the lower part of horizon ABk, 232 grains were found. Among the pollen of woody plants, 10.7% were grains of *Betula*, *Salix*, *Carpinus*, *Ulmus*, *Quercus*. Grass pollen 77.5% is represented by Poaceae 4.3%, Cyperaceae 4.3%, *Rumex* 6.4%, *Plantago* 8.1%, *Urtica* 12.9%, Fabaceae 10.3%, Polygonaceae 4.3%, few pollen grains Asteraceae, Rosaceae and other herbaceous plants. Among the spore plants, 11.6% were spores of *Lycopodium* 5.1% and Polypodiaceae 4.3%.

## 4. DISCUSSION

*4.1. Genesis of paleosols.* The modern soil of the Alchak-Sedlovina section is carbonated, the humus horizon is well distinguished, however, the low values of magnetic susceptibility, even in the Ak horizon, are associated with a strong profile erosion. According to the results of the granulometric composition, the clay fraction is carried down the profile. Low-rounded quartz grains (I and II classes) with a parallel grooves, characterize the prevailing processes of water transport of particles. A small number of well-rounded grains (III class) with a micropitted surface indicates a slight aeolian transport of redeposited particles. The transport of particles by water was weak since the features weakly affect the surface of the grains, and there is no layering in the profile structure, which is typical for water erosion (Krinsley, Doornkamp, 1973). Signs of the soil-forming process, namely the action of soil solutions, are clearly visible on quartz grains; these are crescent pits and etching zones on quartz grains, confined mainly to fractures. The presence of carbonated concentrations, specific brown color and morphology allows us to attribute this soil to the Calcic Cambisol.

The PS1-AS paleosol is strongly carbonized in the lower part of the profile and eroded since the humus horizon is absent and the magnetic susceptibility increases towards the bottom; apparently, the BCk horizon was previously surfaced. It is possible that the absence of a humic horizon is associated with intense slope erosion of soils and the removal of surface horizons. According to the results of granulometric analysis and morphological description, lessivage processes were actively proceeding in this soil, which is recorded in clay coating. According to the results of morphoscopy, the largest number of grains of II and III classes of roundness is noted, among which there are a large number of particles with a glossy surface, which indicates an active introduction of fresh material by water (Krinsley, Doornkamp, 1973). Grains with a quarter-matt surface, on which micropits are fixed, indicate a weak aeolian winding of the material. A small amount of fresh grains (class 0) indicates the influence of slope processes. Grains with cracks of varying degrees about the secondary transformation of the soil under the influence of freezing (Krinsley, Doornkamp, 1973). Soil formation took place under different conditions: the lower horizons were formed under more humid warm conditions, then the conditions changed towards aridization and cooling, as evidenced by the data of spore-pollen analysis. Apparently, this paleosol developed according to the Calcic argic Cambisols type. The PS1-AS paleosol was formed under transitional vegetation from forest-steppes to cereals-sagebrush-motley.

In the PS2-AS paleosol, according to the MS results, humus ABk and transitional horizons BCk are clearly distinguished. The paleosol was formed with the participation of the processes of accumulation of clay and silty fractions, as well as stagnic conditions. The paleosol contains an abundance of new carbonate formations, which indicates an arid climate. The results of morphoscopy of quartz grains indicate the input of material with the participation of water flows (classes I and II) and the active input of unrounded material by slope processes: the number of grains of roundness class 0 increases, "fresh" and glossy grains are noted in the horizon, grains with V – shaped pits and conchoidal fractures. The aeolian transfer was insignificant: grains of III and IV classes with a quarter-matt and semi-matte surface are present in an insignificant amount. Often the grains are split in half, such signs are recorded after the deposition of material, which may be due to seasonal freezing (Krinsley, Doornkamp, 1973). Given the above, the PS2-AS paleosol was formed during waterlogging, possibly there was a stagnation of fluvial flows, as evidenced by the gray shade of the profile and gravel interlayers, which were introduced by water flows. Later, the climate became drier and warmer, the soil began to acquire signs of dry steppe soils. The PS2-AS paleosol can be attributed to the Gleyic Cambisols. The paleosol PS2-AS has a hydromorphic type of development and was formed under the transitional type of vegetation: from forest-steppes to cereals-grassland steppes in a temperate-warm climate.

Two MS peaks are in the PS3-AS paleosol: the first small peak in the humus horizon is associated with soil formation, and the second peak in the BCk horizon is associated with weak ferrugination. In this paleosol, in contrast to the overlying paleosols, the granulometric composition becomes lighter, the content of the sand fraction increases towards the BCk. Carbonate concretions in the paleosol are concentrated in a small amount in the upper horizons, thin Fe-Mn coatings are clearly traced to the bottom, such signs are associated with seasonal high soil moisture. The intensity of soil formation processes is recorded on the surfaces of quartz grains in the form of etching of fractures, silica powder, crescent pits (Krinsley, Doornkamp, 1973). Crystalline gypsum is recorded not only in the morphological description, but also on the fractures of quartz grains, similarly to the PS2-AS. Grains with signs of freezing are also noted. In the PS3-AS, according to the results of the morphological description of the section, the amount of gravelly material increases. This indicates an intensive supply of material. It is also confirmed by the morphoscopy of quartz grains, here the largest number of unrounded and slightly rounded glossy grains (0, I and II classes). Grains with parallel grooves, characteristic of water transport, and grains with a quarter-matt surface are recorded, which indicates a weak eolian processing. Large potholes on quartz grains also indicate high transfer and impact rates (Velichko, Timireva, 1995). Similar to the overlying the PS2-AS paleosol, grains could be processed and come with a fluvial flow. The PS3-AS paleosol was formed under conditions of dry warm steppes with periodic moistening, under mosaic-type vegetation: to cereals-grassland steppes, forests of the Mediterranean type and woodlands of birch. Given the above, it can be assumed that this soil belongs to the Cambisols type.

*4.2. The age correlation of paleosols.* On the territory of Crimea, paleosols of reddish hues are found mainly in Pliocene deposits (Veklich, Sirenko, 1976; Panin et al., 2019b). In the Alchak-Sedlovina section, the LPS is underlain by the V Perchem terrace, the age of which makes it possible to correlate the studied paleosols to the Pleistocene period, starting from MIS 17 and younger one. On the territory of the East European Plain, paleosols of this age with a reddish color are associated with the Vorona pedocomplex (MIS 13/15) (Veklich, Sirenko, 1976; Velichko et al., 2009a; 2009b; Panin et al., 2019a; 2019b). In the Platovo section of Rostov region, Lebedeva (1972) identified the V Platovo Chaudian terrace, which is covered by red-colored paleosols. Velichko et al. (2009a) compared these paleosols with the Vorona pedocomplex. Taking into account that the V Perchem terrace correlates with the V Platov marine terrace, it can be assumed that the paleosols of the Alchak-Sedlovina section can also belong to the Vorona pedocomplex. The data of spore-pollen analysis can serve as an indirect confirmation of the age of these paleosols. Where in paleosols, with a high degree of conditionality, the reconstructed vegetation is compared with the Lubny stage identified in Polesia and Carpathian foothills (Sirenko, 2017), which correlates with the Muchkap Interglacial. Sirenko and Turlo (1986) also distinguished the reddish-brown paleosols in the Lubny horizon of the Central Black Sea region.

The paleosols of the Vorona pedocomplex in the LPS of the Sea of Azov (Velichko et al., 2009b; Panin et al., 2019a) developed under more humid conditions than in the Crimea. Since in their profiles, in contrast to paleosols of the Alchak-Sedlovina section, there are plentiful Fe-Mn nodules and there are no gypsum crystals (Panin et al., 2019a), which are one of the main signs of an arid climate (Minashina, Shishov, 2002).

## 5. CONCLUSIONS

Based on the correlation of the age of the V marine terraces of the Black Sea and the Sea of Azov, the Alchak-Sedlovina LPS is presumably assigned to MIS 13/15. The soils of Alchak-Sedlovina belong to the Vorona pedocomplex, taking into account the age of the Perchem sea terrace and comparison of data obtained from the multi-proxy analysis of the Alchak-Sedlovina LPS, and the LPS of the Vorona pedocomplex of the Sea of Azov and the Lubny stage in the Steppe Crimea and the Black Sea region.

The investigation of the LPS of the Alchak-Sedlovina showed that in the mountainous part of the Crimea, the paleosol sequence is quite distinctly preserved, represented by paleosols of the Cambisols type, two automorphic soils and one hydromorphic soil. In the MIS 13/15 (Early Pleistocene), paleosols were formed under conditions of warm steppes or forest-steppes with periodic moistening and often local stagnation of moisture; in the cold season, there was slight freezing of the surface. During the formation of the lower part of the LPS profile (PS2-AS, PS3-AS), coarse clastic material was introduced. Later, the climate became drier and warmer, steppe, similar to the modern one; during the formation of the PS1-AS, such a climate dominated for a much longer time, but erosion processes were activated, which removed the humus horizon of the soil.

During soil formation, the stability of sedimentation was preserved. The main agent for the formation of the LPS was aeolian transport as a source of silty material, according to granulometric analysis data. According to the morphoscopy data of quartz grains, slope processes and temporary streams were the agents of sandy material. An insignificant number of grains with eolian signs and traces of eolian processing indicates the stabilization of eolian processes during the redeposition of the material. The predominant unrounded and slightly rounded grains of sandy material with glossy and quarter-matte surface types indicate that during the formation of the LPS, additional material was introduced from a nearby source, there is only one such source near the section – a mountain range.

# THE STRUCTURE AND FORMATION CONDITIONS OF THE EARLY PLEISTOCENE PALEOSOLS IN THE LOESS-PALEOSOL SEQUENCE OF THE ALCHAK-SEDLOVINA SECTION (REPUBLIC OF CRIMEA)

**M. V. Khmeleva[a,#], P. G. Panin[a], A. L. Chepalyga[a], N. V. Karpukhina[a], O. D. Naidina[b], and A. V. Bukhonov[c]**

[a]*Institute of Geography RAS, Moscow, Russia*
[b]*Geological Institute RAS, Moscow, Russia*
[c]*Institute of Physicochemical and Biological Problems in Soil Science RAS, Pushchino, Russia*
[#]*E-mail: khmeleva@igras.ru*

Paleosols are one of the main paleoecologic indicators that record changes in the environment in loess-paleosol sequence. Understanding the peculiarities of the structure of paleosols and the natural processes that caused them makes it possible to reconstruct the landscape and climatic conditions in the desired territories. The article presents new studies of the loess-paleosol sequence of the Alchak-Sedlovina section located in the mountainous area of the southern part of the Crimean Peninsula. The section exposed two automorphic paleosols (PS1-AS and PS3-AS) and one hydromorphic paleosol (PS2-AS), which we correlate with the paleosols of the Vorona pedocomplex (MIS13/15). This assumption is based on data obtained from the results of a comprehensive analysis, including a morphological description of paleosols and their physical-chemical parameters. It has been established that the loess-paleosol sequence of the Alchak-Sedlovina section under study was formed on deposits of V Perchem marine terrace, which corresponds to the MIS 17 interval. The paleosols PS2-AS and PS3-AS developed according to the Cambisols under conditions of warm steppes or forest-steppes with periodic moistening and often local moisture stagnation; during the cold season, a slight freezing of the surface was observed. The PS1-AS paleosol profile also corresponds to the Cambisols, but it was formed in a drier climate under steppe vegetation similar to the modern one. In the study area, during periods of accumulation of loess material and soil formation, they were accompanied by constant erosion processes. As a result, in the loess-paleosol sequence of the Alchak-Sedlovina section, layers of large rock fragments are fixed, and the surface horizons of paleosols are eroded. The obtained material allowed us to take a fresh look at the development of the paleosol cover in the mountains of Crimean Peninsula. The revealed characteristics of the paleosols of the Alchak-Sedlovina section can later be compared with other paleosols of the Crimean Peninsula to interpret their age and formation conditions.

*Keywords:* soil morphology, marine terrace, morphoscopy of quarts grains, Pleistocene, Muchkap interglacial

## ACKNOWLEDGMENTS

The investigation was performed within the framework of the state task of the Institute of Geography of the Russian Academy of Sciences AAAA-A19-119021990091-4 (FMGE-2019-0005) (the field survey and morphology) and AAAA-A19-119021990092-1 (FMWS-2019-0008) (the laboratory analyses). We are grateful to the Center of Collective Use of the Laboratory of Radiocarbon Dating and Electron Microscopy IGRAS staff for the opportunity to work on the JEOL JSM-6610LV scanning electron microscope. We are grateful to anonymous reviewers for the constructive comments and valuable suggestions that significantly improved the initial paper.

## REFERENCES

Andrusov N.I. *O verkhnepliotsenovykh otlozheniyakh mysa Chauda na Kerchenskom poluostrove* (On the Upper Pliocene deposits of Cape Chauda on the Kerch Peninsula). *Trudy S.-Peterb. obshchestva estestvoispytatelei*. 1889. Vol. 20. (in Russ.)

Andrusov N.I. *Terrasy okrestnostei Sudaka* (Terraces in the vicinities of Sudak). *Zapisky Kievskogo obshchestva estestvoispytatelei*. 1912. Vol. 22. No. 2. P. 1–88. (in Russ.)

Arslanov Kh.A., Balabanov I.P., and Gej N.A. *O vozraste i klimaticheskikh usloviyakh formirovaniya osadkov pozdne-pleistotsenovykh morskikh terras poberezh'ya Kerchenskogo proliva* (On the age and climatic conditions of sediments formation on the Late Pleistocene marine terraces of the Kerch Strait coast). *Vestnik LGU*. 1983. No. 12. P. 69–79. (in Russ.)

Arkhangelskij A.D. and Strakhov N.M. *Geologicheskoe stroenie i istoriya razvitiya Chernogo morya* (Geological structure and history of evolution of the Black Sea). Moscow-Leningrad: AN SSSR (Publ.), 1938. 226 p. (in Russ.)

Blott S.J. and Pye K. GRADISTAT: a grain size distribution and statistics package for the analysis of unconsolidated sediments. *Earth Surface Processes and Landforms*. 2001. Vol. 26. P. 1237–1248. https://doi.org/10.1002/esp.261

Cherenkova N.I. *Agroklimaticheskii spravochnik po Krymskoi oblasti* (Agroclimatic reference book on the Crimean region). Leningrad: Gidrometeoizdat (Publ.), 1959. 136 p. (in Russ.)

Chepalyga A.L. *Novaya kontseptsiya chernomorskikh terras Yugo-Vostochnogo Kryma* (New concept of the Black Sea marine terraces in south-eastern Crimea). *Bulletin of the Commission for Study of the Quaternary*. 2015. Vol. 74. P. 90–104. (in Russ.)

Chepalyga A.L. The unique system of the Black Sea terraces of the South Coast: the history of the Black Sea, the oldest Oldowan migrations and the primary settlement of Europe through the Crimea. *Materialy X Vserossiiskogo soveshchaniya po izucheniyu chetvertichnogo perioda "Fundamental'nye problemy kvartera: itogi izucheniya i osnovnye napravleniya dal'neishikh issledovanii"*. Moscow: GEOS (Publ.), 2017. P. 460–464. (in Russ.)

Chepalyga A.L., Sadchikova T.A., and Anisyutkin N.K. *Osobennosti stroeniya i formirovaniya eopleistotsenovoi Mandzhil'skoi terrasy raiona Sudaka v Krymu so sledami obitaniya drevnego cheloveka* (Features of the structure and formation of the Eopleistocene Manjil terrace of the Sudak region in the Crimea with traces of the habitation of an ancient man). *Byulleten' Komissii po izucheniyu chetvertichnogo perioda*. 2019. Vol. 77. P. 141–159. (in Russ.)

Chepalyga A.L. Detailed event stratigraphy of the Pleistocene of the Black Sea. *Chetvertichnaya geologiya i paleogeografiya Rossii*. Moscow: GEOS (Publ.), 1997. P. 196–201. (in Russ.)

FAO. Guidelines for Soil Description 4th edition. Rome: FAO. 2006. 97 p.

FAO–ISRIC. Guidelines for profile description 3rd edition. Rome: FAO. 1990.

Fedorov P.V. *Pleistotsen Ponto-Caspiya* (Pleistocene of the Ponto-Caspian). Moscow: Nauka (Publ.), 1978. 165 p. (in Russ.)

Grichuk V.P. and Zaklinskaya E.D. *Analiz iskopaemykh pyl'tsy i spor i ego primenenie v paleogeografii* (Analysis of fossil pollen and spores and its application in paleogeography). M: Geografizdat Press (Publ.), 1948. 224 p. (in Russ.)

Haase D., Fink J., Haase G., Ruske R., Pécsi M., Richter H., Altermann M., and Jäger K.-D. Loess in Europe – its spatial distribution based on a European Loess Map, scale 1:2.500.000. *Quaternary Science Reviews*. 2007. Vol. 26. No. 9–10. P. 1301–1312. https://doi.org/10.1016/j.quascirev.2007.02.003

IUSS Working Group WRB. World Reference Base for Soil Resources 2014, update 2015 International soil classification system for naming soils and creating legends for soil maps. Rome: FAO World Soil Resources Reports. 2015. Vol. 106. 181 p.

Kottek M., Grieser J., Beck C., Rudolf B., and Rubel F. World Map of the Köppen-Geiger climate classification updated. *Meteorologische Zeitschrift*. 2006. Vol. 15. No. 3. P. 259–263. https://doi.org/10.1127/0941-2948/2006/0130

Krinsley D.H. and Doornkamp J.C. Atlas of Quartz Sand Surface Textures. Cambridge: Cambridge University Press (Publ.), 1973. 91 p.

Kurbanov R.N., Yanina T.A., Murray E.S., Semikolennykh D.V., Svistunov M.I., and Shtyrkova E.I. *Vozrast Karangatskoi transgressii (pozdnii pleistotsen) Chernogo morya* (Age of the Karangat transgression (Late Pleistocene) of Black Sea). *Vestnik Moscovskogo Universiteta. Seriya 5. Geogrfia*. 2019. No. 6. P. 29–40. (in Russ.)

Kurbanov R.N., Semikolennykh D.V., Yanina T.A., Tyunin N.A., and Murray A.S. *Novye dannye o vozraste Karangatskoi transgressii Chernogo morya* (New data on the age of the Karangatian transgression of the Black Sea). *Vestnik Moskovskogo Universiteta. Seriya 5. Geogrfiya*. 2020. No. 6. P. 139–145. (in Russ.)

Khabakov A.V. *Ob indeksakh okatannosti galechnikov* (On roundness indexes of pebbles). *Sovetskaya Geologiya*. 1946. Vol. 10. P. 98–99. (in Russ.)

Lu H., Jia J., Yin Q., Xia D., Gao F., Liu H., Fan Y., Li Z., Wan X., Berger A., Oimuhammadzoda I., and Gadoev M. Atmospheric dynamics patterns in southern Central Asia since 800 ka revealed by loess-paleosol sequences in Tajikistan. *Geophysical Research Letters*. 2020. Vol. 47. No. 17. P. 1–10. https://doi.org/10.1029/2020GL088320

Lebedeva N.A. *Antropogen Priazov'ya* (Anthropogen of Priazovie). Moscow: Nauka (Publ.), 1972. 106 p. (in Russ.)

Minashina N.G. and Shishov L.L. Gypsum-containing soils: their distribution, genesis, and classification. *Eurasian Soil Science*. 2002. Vol. 35. No. 3. P. 240–247.

Munsell Color. Munsell Soil Color Charts. NY New Windsor: Gretag Macbeth (Publ.), 2000.

Muratov M.V. *Kratkii ocherk geologicheskogo stroeniya Krymskogo poluostrova* (A Short Essay on the Crimean Peninsula Geology). Moscow: Gosgeoltekhizdat (Publ.), 1960. 208 p. (in Russ.)

Panin P.G., Timireva S.N., Morozova T.D., Kononov Yu.M., and Velichko A.A. Morphology and micromorphology of the loess-paleosol sequences in the south of the East European plain (MIS 1 – MIS 17). *Catena*. 2018. Vol. 168. P. 79–101. https://doi.org/10.1016/j.catena.2018.01.032

Panin P.G., Timireva S.N., Konstantinov E.A., Kalinin P.I., Kononov Yu.M., Alekseev A.O., and Semenov V.V. Plio-pleistocene paleosols: Loess-paleosol sequence studied in the Beregovoye section, the Crimean Peninsula. *Catena*. 2019a. Vol. 172. P. 590–618. https://doi.org/10.1016/j.catena.2018.09.020

Panin P.G., Timireva S.N., Morozova T.D., and Velichko A.A. Micromorphology of the Late and Middle Pleistocene paleosols of the central East European Plain. *Geography, Environment, Sustainability*. 2019b. Vol. 12. No. 1. P. 34–62. https://doi.org/10.24057/2071-9388-2018-32

Panin P.G., Filippova K.G., Bukhonov A.V., Karpukhina N.V., Kalinin P.I., and Ruchkin M.V. High-resolution analysis of the Likhvin loess-paleosol sequence (the central part of the East European plain, Russia). *Catena*. 2021. Vol. 205. P. 105–445. https://doi.org/10.1016/j.catena.2021.105445

Pevzner M.A., Vangengeim E.A., Sadchikova T.A., Semenenko V.N., Kovalenko V.A., and Lyul'eva S.A. On the marine genesis and Pontian age of deposits from the Lyubimovka reference section in the Crimea. *Stratigraphy and Geological Correlation*. 2004. Vol. 12. No. 5. P. 523–533.

Pilipenko O.V. and Trubikhin V.M. *Geologicheskaya i paleomagnitnaya korrelyatsiya pleistotsenovykh razrezov yuga*

*Rossii, Ukrainy i Azerbaidzhana* (Geological and paleomagnetic correlation of Pleistocene sections of the southern Russia, Ukraine and Azerbaijan). *Byulleten' Komissii po izucheniyu chetvertichnogo perioda*. 2012. Vol. 72. P. 136–147. (in Russ.)

Pye K. Aeolian Dust and Dust Deposits. London: Academic Press. 1987. 334 p. https://doi.org/10.1016/0012-8252(88)90096-7

Rukhin L.B. *Osnovy litologii* (Basics of Lithology). Leningrad: Nedra (Publ.), 1969. 703 p. (in Russ.)

Sirenko N.A. and Turlo S.I. *Razvitie pochv i rastitel'nosti Ukrainy v pliotsene i pleistotsene* (Development of soils and vegetation of Ukraine in the Pliocene and Pleistocene). Kiev: Naukova Dumka (Publ.), 1986. 186 p. (in Russ.)

Sirenko E.A. *Palinostratigrafiya kontinental'nykh verkhnepliotsenovykh – nizhneneopleistotsenovykh otlozhenii yuzhnoi chasti Vostochno-Evropeiskoi platformy* (Palynostratigraphy of Continental Upper Pliocene – Lower Neopleistocene deposits of southern part of the East European Platform). Kiev: Naukova Dumka (Publ.), 2017. 165 p. (in Russ.)

Sudnicin I.I. *Gidrologicheskie svoistva i rezhimy pochv yuzhnogo berega Kryma* (Hydrological properties and regimes of soils of the Southern Coast of Crimea). *Moscow University Soil Science Bulletin*. 2014. Vol. 17. No. 4. P. 21–27. (in Russ.)

Ved' I.P. *Klimaticheskii atlas Kryma* (Climate Atlas of Crimea). Simferopol: Tavria-Plus (Publ.), 2000. 118 p. (in Russ.)

Veklich M.F. *Stratigrafiya lessovoi formatsii Ukrainy i sosednikh stran* (Stratigraphy of loess formation of Ukraine and adjacent countries). Kiev: Naukova Dumka (Publ.), 1968. 238 p. (in Russ.)

Veklich M.F. and Sirenko N.A. *Pliotsen i pleistotsen levoberezh'ya Nizhnego Dnepra i ravninnogo Kryma* (Pliocene and Pleistocene of the Left Side of the Dnieper left bank and the Crimean Peninsula). Kiev: Naukova Dumka (Publ.), 1976. 186 p. (in Russ.)

Velichko A.A. and Morozova T.D. The main features of soil formation in the Pleistocene on the East European Plain and its paleogeographic evolution of soil and soil cover. Evolution of soils and soil cover. Theory, diversity of natural evolution and anthropogenic soil transformations. Moscow: GEOS (Publ.), 2015. P. 321–337. (in Russ.)

Velichko A.A. and Timireva S.N. Morphoscopy and morphometry of quartz grains from loess and buried soil layers. *GeoJournal*. 1995. Vol. 36 (2/3). P. 143–149. https://doi.org/10.1007/BF00813159

Velichko A.A., Katto N.R., Tesakov A.S., Titov V.V., Morozova T.D., Semenov V.V., and Timireva S.N. Structural specificity of Pleistocene loess and soil formation of the Southern Russian Plain according to materials of Eastern Priazovie. *Doklady Earth Sciences*. 2009a. Vol. 428. No. 6. P. 815–819. https://doi.org/10.1134/S1028334X09080273

Velichko A.A., Katto N.R., Kononov Yu.M., Morozova T.D., Novenko E.Yu., Panin P.G., Ryskov Ya.G., Semenov V.V., Timireva S.N., Titov V.V., and Tesakov A.S. Progressively cooler, drier interglacials in southern Russia through the Quaternary: evidence from the sea of Azov region. *Quaternary International*. 2009b. Vol. 198. P. 204–219. https://doi.org/10.1016/j.quaint.2008.06.005

**EDN:** TYNKQA
*ГЕОМОРФОЛОГИЯ, 2022, том 53, № 5, с. 103–115*

## ПРОБЛЕМЫ ПАЛЕОПОЧВОВЕДЕНИЯ И ГЕОАРХЕОЛОГИИ

*УДК 551.89:574→569.9:902/904(470.3)*

# ПАЛЕОЧЕРНОЗЕМЫ ВРЕМЕНИ РАЗВИТИЯ СРУБНОЙ КУЛЬТУРЫ И ТРЕНДЫ ПОЗДНЕГОЛОЦЕНОВОЙ ЭВОЛЮЦИИ ПОЧВ ЛЕСОСТЕПИ ВОСТОЧНО-ЕВРОПЕЙСКОЙ РАВНИНЫ


**Ю. Г. Чендев[1,*], Т. А. Пузанова[2], Ф. Г. Курбанова[3]**

*[1]Белгородский государственный национальный исследовательский университет (BelSU), Белгород, Россия*
*[2]Московский государственный университет имени М.В. Ломоносова, географический факультет, Москва, Россия*
*[3]Институт географии РАН, Москва, Россия*
**E-mail: sciences@mail.ru*

Поступила в редакцию 16.06.2022 г.
После доработки 28.06.2022 г.
Принята к публикации 15.07.2022 г.

Выполнен сравнительный анализ признаков черноземов, погребенных под курганами периода срубной культурно-исторической общности (3600–3400 л. н.), их аналогов более ранних (4200–3700 л. н.) и более поздних (2500–2200 л. н.) периодов, а также современных компонентов почвенного покрова на территории центра Восточно-Европейской равнины. Черноземы периода срубной культуры формировались в обстановке заметных биоклиматических изменений, последовавших вслед за периодом среднесуббореальной аридизации климата. Установлено, что биохимическая перестройка профиля по содержанию почвенного органического вещества опережала морфологическую перестройку с формированием более мощной темноцветной части профиля черноземов. Автоморфные палеочерноземы срубного времени характеризовались большей однородностью морфологических свойств (на всех изученных участках – черноземы типичные) по сравнению с современными аналогами (возникли два ареала черноземов – выщелоченных и типичных). Черноземы выщелоченные возникли на участках с меньшими запасами карбонатов в почвообразующих породах по сравнению с чернозмами типичными. Общий тренд позднеголоценовой эволюции черноземов выщелоченных и типичных состоял в увеличении мощности гумусовых горизонтов (в среднем на 20 см) и почвенных профилей (в среднем на 20 см) при неизменности мощности переходной части профиля (A1B+BA1) и горизонтов B (Bк). Отличия состояли в разных глубинах выщелачивания почвенных профилей от карбонатов.

*Ключевые слова:* лесостепь, Восточная Европа, черноземы, эволюция почв, поздний голоцен, срубная культура

**DOI:** 10.31857/S0435428122050042

## 1. INTRODUCTION

In Russian paleopedology, a large amount of information about features of the soils buried under kurgans of different historical periods has been accumulated during the last decades (Zolotun, 1974; Aleksandrovskiy, 1984; Gennadiev, 1984; Ivanov, 1992; Demkin, 1997; Chendev et al., 2010; Khokhlova et al., 2010; Puzanova et al., 2017; Prikhodko, 2018; etc.).

Interest in the soils of the mounds is primarily dictated by the possibility of a comparative analysis of the properties of the soils buried under the mounds and their modern (surface) analogues. This comparison of the soils is frequently used to reveal the differences in the environmental conditions between the time of burial (the moment of the mound construction) and the present time.

The presence of a large number of mounds as objects of cultural and historical heritage and as archives of the paleoenvironmental information on the territory of the European and Asian parts of Russia determined the specifics of the development of the soil-evolutionary direction in Russian soil science. One of the advantages of studying the soils buried under the mounds is their good preservation under the thick earthen constructions, which protect the paleosols from the influence of modern soil-forming processes.

In other regions of the world, the soils of kurgan constructions are studied much less frequently and often in a rather specific way – either by studying only soil formation on kurgan embankments (Ruhe, Schotles, 1956; Parsons et al., 1962), or by drilling kurgans and buried soils with the extraction of columns of soil material and analysis of a limited set of properties (Kristiansen et al., 2003; Molnar et al., 2004), and much less often – through a full-profile study of the buried soils (Hejcman et al., 2013).

Most of the soil-archaeological research carried out is based on the study of paleosols associated with the cultural layers of settlements of different periods, while the thickness of the sediments of ancient settlements overlying the paleosols is not always large enough to protect buried soils from diagenetic changes (Holliday, 2004; Gerlach et al., 2006; Vislouzelova et al., 2015; Kamnueva-Wendt et al., 2020; etc.), which can introduce errors in the research results.

Earlier studies of buried and surface soils were often limited to a comparative analysis of their properties within local areas (Aleksandrovskiy, 1984; Gennadiev, 1984; Ivanov, 1992). However, as the space of soil-archaeological research expanded and the key sites increased, prerequisites for reconstructing of the soil properties and the conditions of soil formation in a wider geographical space began to arise (Chendev, Ivanov, 2007; Chendev et al., 2015).

In the proposed article, the primary attention is focused on studying the soils buried under the mounds of the Srubnaya Cultural-Historical Community. The frequency of occurrence of these objects in modern landscapes is relatively high due to the wide distribution of the area of this culture in the middle of the 1st millennium BC on a large territory of the forest-steppe and steppe zones of the East European Plain – from the Urals to the Dnieper basin (Gorbunov, 1994). The high density of the burial mounds of this era was reflected in a large number of archaeological excavations, in which soil scientists also participated.

The purpose of this research is a comparative study of the features of chernozems buried under the mounds of the Srubnaya Cultural-Historical Community and chernozems of an earlier and later period in the centre of Eastern Europe.

## 2. OBJECTS AND METHODS OF RESEARCH

The territory of our study is the forest-steppe and steppe of the East European Plain, which includes the southern part of the Central Russian Upland and the adjacent areas of the Poltava and Oka-Don Plains. All studied objects are located between 49 and 52 degrees north latitude and 35–41 degrees east longitude (fig. 1).

A large number of objects (11 out of 16), were studied by the authors of the presented article in different years. Some objects for this research were taken from other works (Margolina et al., 1988; Akhtyrtsev, Akhtyrtsev, 1990; Ivanov, 1992).

The burial mounds studied at each site were usually single objects (except the *Belgorodsky*, *Bogdanovka*, *Bobrovsky*, *Graivoronsky* and *Gubkinsky* key sites) and consisted from single-layer, i.e. constructed in one go. The mounds were dated by an archaeological method (using artefacts) with an accuracy of the century. For the study region the chronology of the Srubnaya culture is not developed well and in detail. Therefore, a more accurate radiocarbon dating method for bone, coal and wood (from the central burials of the mounds) was also used. The range of construction dates for all the studied mounds is from 3360 to 3620 yr. BP (3510–3960 cal. yr. BP). This is consistent with the opinion of one of the well-known specialists in the studied archaeological culture I.F. Kovaleva, according to which the spread of the Srubnaya culture in the basin of the upper reaches of the Seversky Donetsk river was limited mainly to the interval of the 15th-14th (not calibrated) centuries BC (Kovaleva, 1990). In addition to the mounds of the Srubnaya archaeological culture, one mound (the *Gorki* key site) was built by representatives of the late Catacomb culture about 3600 yr. BP (3950 cal. yr. BP). This mound was included in the list of studied objects due to the same period of the Srubnaya culture's existence for assessing and analyzing paleosols. In most cases, the thickness of the studied constructions of mounds exceeded 1 meter. This height and loamy composition of the embankments ensure good preservation of the original features of paleosols (according to Demkin, 1997). The height of some of the studied mounds was less than 1 meter – 0.6–0.9 meters due to ploughing. Their height exceeded 1 meter until the 1950s. The decrease in the surface of the mounds due to steam-row crops introduction and the heavy agricultural machinery use occurred relatively recently. It did not affect of the initial features of soils buried under the mounds.

The parent materials are presented by loess loams and clays, and only in one area (the *Gorki* site) moraine loams and clays of the Moscow glaciation period were identified. The parent materials from west to east are changed from lighter to heavier granulometric composition. All the studied mounds were located on well-drained watersheds with deep groundwater. Chernozems are widespread in all studied areas (according to field research and (Natsional'nyi..., 2011). On the *Bobrovsky* site, the current groundwater depth was four or more meters under the surface meadow-chernozemic soils, typical for the of the Oka-Don Plain's interfluves (Akhtyrtsev, Akhtyrtsev, 1990).

Most of the studied sites (14) are located in the forest-steppe area, and only two sites (*Bogdanovka* and *Starokriushinsky*) are located to the south, in the steppe zone (fig. 1).

All have studied buried soils had natural undisturbed surfaces, what was detected according to their flat or slightly wavy boundary with mound material; in most cases, on the surface of buried soils has been a visible thin pale yellow layer of parent material – ejection of loam from the grave pit of the central burials. By this layer border between the mound and buried soil was detected quite correctly.

The main approach of the study is the method of soil chrono-sequences, which is based on a comparative analysis of dated soils (buried and newly formed in mounds) and their surface full-Holocene analogues,

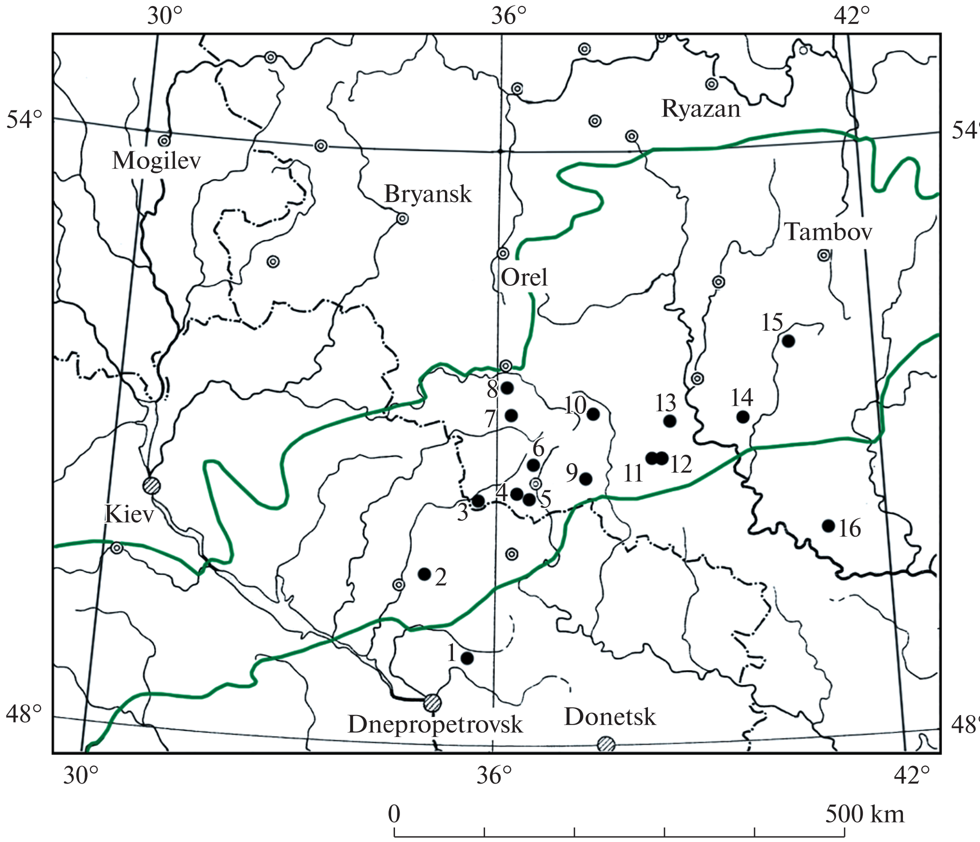


**Fig. 1.** Location of sites for soil-archaeological research of the Bronze Age burial mounds, created 3400–3600 years ago.

*Site names*: 1 – Bogdanovka (Ivanov, 1992); 2 – Storozhevoye (Chendev et al., 2011); 3 – Grayvoronsky (Chendev et al., 2015); 4 – Staraya Nelidovka (unpublished data); 5 – Belgorodsky (Chendev et al., 2015); 6 – Prokhorovsky (Chendev, 2008); 7 – Drozdy (Aleksandrovskiy, 1983; Margolina et al., 1988); 8 – Dubroshina (Aleksandrovskiy, 1983; Margolina et al., 1988); 9 – Gorozhenoe (unpublished data); 10 – Gubkinsky (Chendev, 2008); 11 – Novoe Ukolovo (unpublished data); 12 – Gorki (unpublished data); 13 – Boldyrevka (unpublished data); 14 – Bobrovsky (Akhtyrtsev, Akhtyrtsev, 1990); 15 – Chamlyk-Nikolsky (unpublished data); 16 – Starokriushinsky (Margolina et al., 1988). Green lines mark the northern and southern boundaries of the forest-steppe area.

**Рис. 1.** Схема местоположения участков почвенно-археологических исследований курганов бронзового века, созданных в интервале времени 3400–3600 лет назад.

*Названия участков*: 1 – Богдановка (Иванов, 1992); 2 – Сторожевое (Чендев и др., 2011); 3 – Грайворонский (Чендев и др., 2015); 4 – Старая Нелидовка (неопубликованные данные); 5 – Белгородский (Чендев и др., 2015); 6 – Прохоровский (Чендев, 2008); 7 – Дрозды (Александровский, 1983; Марголина и др., 1988); 8 – Дуброшина (Александровский, 1983; Марголина и др., 1985); 9 – Гороженое (неопубликованные данные); 10 – Губкинский (Чендев, 2008); 11 – Новое Уколово (неопубликованные данные); 12 – Горки (неопубликованные данные); 13 – Болдыревка (неопубликованные данные); 14 – Бобровский (Ахтырцев, Ахтырцев, 1990); 15 – Чамлык-Никольский (неопубликованные данные); 16 – Старокриушинский (Марголина и др., 1988). Зеленые линии – северная и южная границы лесостепи.

formed near archaeological sites in similar lithological and geomorphological positions (fig. 2).

Based on the differences between the buried and surface soils, conclusions were drawn about the changes in climatic conditions that took place.

In turn, the method of soil chrono-sequences includes a fundamental method of field soil research – the method of morphological description of the soil profile. The results of the morphological description of the studied soils have been presented in an abbreviated form in this article – the characteristics of the thickness of the soil horizons and the depth of effervescence for buried and surface soils are given in the text and tables.

For some key sites, laboratory analyses of soils, including characteristics such as bulk density (samples were taken using a cutting rings), particle size distribution (GOST (State Standard) 12536), pH aqueous GOST 26423–85), total organic carbon (according to Tyurin's (wet combustion) method (GOST 26213–91), the content of $CO_2$ carbonates by the acidimetric method were provided. These types of analysis of soil samples were carried out in the laboratories of the National Research University "Belgorod State University" and the Federal State Budgetary Institution "Center of Agrochemical Service "Belgorodsky"". Statistical calculations of the studied indicators (arithmetic mean, error of the mean, standard deviation, coefficient

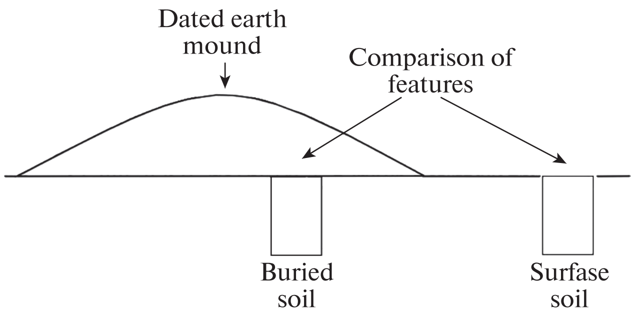


**Fig. 2.** Illustration of the method of soil chrono-sequences used in our soil-archaeological studies.

**Рис. 2.** Иллюстрация метода почвенных хронорядов в проведенных авторами почвенно-археологических исследованиях.

of variation) were performed using the STATISTICS program in Excel.

Two samples (bone from a mound at the *Staraya Nelidovka* site and a wood from a burial at the *Boldyrevka* site) were dated in the Isotope Research Laboratory of the Center for Collective Use "Geo-ecology" of the Russian State Pedagogical University A.I. Herzen.

The radiocarbon dating of the samples at *Gorozhenoe* site was carried out in the radiocarbon laboratory of the Institute of Environmental Geochemistry of the National Academy of Sciences of Ukraine (Kiev, Ukraine) using the liquid scintillate method (LSC) (Skripkin, Kovalyukh, 1998). The $^{14}C$ isotope content was measured on a Quantulys1220 T low-background spectrometer. The calibration of radiocarbon dates was carried out by A.V. Dolgikh (Institute of Geography RAS) using the OxCal v4.2.4 program (Bronk, Lee, 2017) based on the IntCal 13 calibration curve (Reimer et al., 2013).

## 3. RESULTS AND DISCUSSION

Srubnaya culture appeared in a wide geographic space between the Dnieper in the west and the Urals in the east. The standard burial ritual by representatives of this culture was burial in pits surrounded by wooden structures – log constructions, which were closed from above with wooden chopping blocks and covered with the ground until the formation of hills – mounds with different diameters and heights. According to Gorbunov (1994), the emergence of the Srubnaya culture in Eastern Europe is a unique phenomenon that marks the formation of the same type of rituals and similar infrastructure over a large territory. The reason for the spread of representatives of the Srubnaya cultural and historical community could be favourable climatic changes – the mid-Subboreal climatic optimum, which made it possible to widely develop landscapes and use cattle breeding by tribes of this culture in the forest-steppe and steppe of the East European Plain.

According to palynological data, the second half of the Subboreal period of Holocene (between 3970 and 3550 yr. BP) was marked by warming and humidification of the climate in the study area, which, in particular, led to an increase in the expansion of forests on the steppe areas (Spiridonova, 1991; Serebryannaya, 1992; Shumilovskikh et al., 2018). The found wood in the burials also testifies to the significant forest cover of the territory. Comparative analysis of the buried soils formed in different intervals of the second half of the Holocene in the typical chernozems modern area (forest-steppe zone), conveys a clearly defined regularity of the growth of the thickness of humus horizons and, in general, of the humified part of the profiles (A1 + A1B + BA1 horizons) of chernozems. Moreover, the process of leaching carbonates is also traced in studied buried soils (tabl. 1).

**Table 1.** Changes in the morphological features of typical chernozems in the centre of the forest-steppe zone of the East European Plain over the past 4200 years (uncalibrated)

**Таблица 1.** Изменение морфологических свойств черноземов типичных центра лесостепной зоны Восточно-Европейской равнины за последние 4200 лет (некалиброванных)

| Soil feature, % of modern features | Chronointervals (yr. BP) and the number of mounds studied ($n$) | | |
|---|---|---|---|
| | 4200–3700, $n$ = 5 | 3600–3400, $n$ = 9 | 2600–2200, $n$ = 16 |
| The thicknessof the A1 horizon | 57.0 ± 4.6 | 69.3 ± 6.2 | 95.6 ± 6.4 |
| The thickness of Ah + AhB + BAh horizons | 73.9 ± 2.3 | 80.0 ± 1.0 | 99.2 ± 4.0 |
| Depth of effervescence | 24.8 ± 13.2 | 57.1 ± 3.4 | 53.1 ± 4.5 |

*Note:* data for chronointervals are used: 4200–3700 yr. BP – unpublished data of the authors – two objects in the Poltava oblast, (Chendev, 2008) – one object in the Belgorod oblast, (Akhtyrtsev, Akhtyrtsev, 1994) – two objects in the Voronezh oblast; 3600–3400 yr. BP – unpublished data of the authors – three objects in Poltava, Belgorod and Voronezh oblasts, (Chendev, 2008) – four objects in the Belgorod oblast (Aleksandrovskiy, 1983; Margolina et al., 1988) – two objects in the Kursk oblast; 2600–2200 y. a. – unpublished data of the authors – one object in the Voronezh oblast, (Chendev, 2008) – 15 objects in the Belgorod and Voronezh oblasts.

*Примечание:* использованы данные для хроноинтервалов: 4200–3700 л. н. – неопубликованные данные авторов (два объекта в Полтавской области), Ю.Г. Чендева (2008) один объект в Белгородской области), Б.П. Ахтырцева, А.Б. Ахтырцева (1994) (два объекта в Воронежской области); 3600–3400 л. н. – неопубликованные данные авторов (три объекта в Полтавской, Белгородской и Воронежской областях), Ю.Г. Чендева (2008) (четыре объекта в Белгородской области), А.Л. Александровского (Александровский, 1983; Марголина и др., 1988) (два объекта в Курской области); 2600–2200 л. н. – неопубликованные данные авторов (один объект в Воронежской области), Ю.Г. Чендева (2008) (15 объектов в Белгородской и Воронежской областях).

The results of studying the morphometric characteristics of paleochernozems of the Srubnaya culture, their modern analogues in the forest-steppe part of the study area, and the differences revealed between them are reflected in tabl. 2. Table 2 is structured following the surface soils to different genetic groups: firstly, areas are indicated where the surface soils are leached chernozems, then areas with typical chernozems, and at the end, one area with meadow-chernozem soils is located.

According to the results of statistical calculations, in the studied paleosoil space within the automorphic positions of the relief (the *Bobrovsky* site was excluded), the thickness of the humified part of the soil profiles (A1 + A1B + BA1) as well as the total thickness of the soil profiles were characterized by minimal variability, and the maximum variability has been detected for the depth of effervescence (tabl. 3).

When comparing the average values of morphometric features of surface and paleochernozems, significant statistical differences are determined by such characteristics as the thickness of the humus horizons, the humified part of the profiles and the depth of effervescence. The high variability of all indicators (the coefficients of variation are in the range of 24–74%, tabl. 3) indicates the intraregional differences in the development of soil formation in the studied space, both in the past and at present. Table 3 shows an increase of the entire soil profiles up to 21 cm during the Late Holocene, which is comparable to an increase in the thickness of A1 horizons up to 20 cm.

At the same time, the thickness of the lower humus part of the profile (A1B + BA1, 23–27 cm), B (32 cm) and BC horizons (30–31 cm) remained unchanged.

Thus, over the past 3500 years, the leading role in the evolution of the profiles of chernozems on the territory of the forest-steppe zone in the centre of the East European Plain was played by the thickness of humus horizons and the depth of carbonates occurrence.

A comparative analysis of the temporal development of individual units of soil classification, – subtypes of leached chernozems ($n = 6$) and typical medium-thick chernozems ($n = 7$) is reflected in tabl. 4 (areas with thick and super-thick chernozems, in accordance with the traditional Russian soil classification (Classificatsiya..., 1977) (*Dubroshina* and *Drozdy* sites (Aleksandrovskiy, 1983; Margolina et al., 1988)) are excluded). Chernozems buried 3600–3400 yr. BP in the modern distribution areas of the two indicated subtypes of chernozems belongs to one unit of typical thin (close to medium thick) chernozems (tabl. 4). Throughout the studied area, they are characterised by the identity of the depths of the carbonate table (24–26 cm). However, in the area of distribution of modern typical chernozems, the development of more thick soil profiles took place in comparison with paleochernozems in the area of modern leached chernozems distribution (tabl. 4).

In the modern soil space, contrasting differences between the surface leached and typical chernozems are achieved only by significant differences in the depth of carbonate occurrence (in leached chernozems – on average 111 cm, and in typical chernozems – 56 cm) and weak insignificant differences in the thickness of all soil horizons and soil profiles in the whole. The considered surface subtypes of chernozems at the generic level belong to the category of medium-thick ones, with the thickness of the humified part of the profiles 73–76 cm (tabl. 4).

A comparative analysis of modern and buried soils revealed the formation of one typical chernozem area in the Srubny period within the two modern areas presented by leached and typical chernozems (tabl. 4). However, there were spatial differences within this area in the Srubny period – in place of modern leached chernozems soil profiles and horizons had less thickness comparatively with paleosoils within the modern typical chernozem area (tabl. 4). In particular, the less developed humified part of profiles ([A1+A1B+BA1]) in the paleospace of modern leached chernozems (tabl. 4) can be an indicator of less soil fertility in these places in the Srubny period.

We assume that one of the most probable reasons for the less or more degree of development chernozems within palaeosoil space could be the difference in the combination of soil-forming factors in the compared areas throughout a significant part of the Holocene. Among these differences, the most probable were intraregional differentiation of climatic conditions, as well as local differences in the lithological composition of parent materials. Leached chernozems tend to be form on more clayey and less calcareous soil-forming rocks in comparison with the rocks on which typical chernozems were formed. Previously, we have already expressed that the leached chernozems were formed in areas where loess loams were characterized by an initially smaller amount of carbonates (Chendev, 2008). Research carried out at new sites in our article confirms this assumption. As an example, we provided a comparison of the profile distribution of carbonates and their reserves in a 2-meter stratum of automorphic buried and surface leached chernozems in the *Staraya Nelidovka* site (Belgorod oblast), and buried and surface typical chernozems in *Boldyrevka* site (Voronezh oblast) (tabl. 5, fig. 3).

The general pattern of the two study areas is the leaching of carbonates from the upper one-meter layer of chernozems and their accumulation in the lower part of the profiles, in the 100–200 cm layer during the Late Holocene. The differences lie in the lower content and pools of carbonates in the buried and surface soils of the *Staraya Nelidovka* site concerning the buried and surface soils of the *Boldyrevka* site (tabl. 5, fig. 3).

**Table 2.** Morphometric features of the buried soils of the Srubnaya culture and their modern surface analogues on the territory of the forest-steppe centre of the East European Plain (compiled from unpublished data of the authors (sites *Boldyrevka*, *Gorozhenoe*, *Gorki*, *Novoye Ukolovo*, *Staraya Nelidovka*, *Storozhevoe*, *Chamlyk-Nikolsky*) and data from papers (Aleksandrovskiy, 1983; Margolina et al., 1988; Akhtyrtsev, Akhtyrtsev, 1990; Chendev, 2008)

**Таблица 2.** Морфометрические признаки подкурганных почв срубного времени и их фоновых аналогов на территории лесостепи центра Восточно-Европейской равнины (составлено по неопубликованным данным авторов (участки *Болдыревка, Гороженое, Горки, Новое Уколово, Старая Нелидовка, Сторожевое, Чамлык-Никольский*) и данным из работ (Aleksandrovskiy, 1983; Margolina et al., 1988; Akhtyrtsev, Akhtyrtsev, 1990; Chendev, 2008)

| No | Soil | Thickness (for effervescence – depth), numerator – cm, denominator –% of modern values | | | | | |
|---|---|---|---|---|---|---|---|
| | | A1 | A1B + BA1 | A1 + A1B + BA1 | B | Profile | Effervescence |
| | | *Staraya Nelidovka site, 3620 ± 45 yr. BP (radiocarbon date), surface soil – leached chernozem* | | | | | |
| 1 | buried | 18/42.9 | 13/59.1/ | 31/48.4 | 39/95.1 | 111/80.4 | 32/27.1 |
| | surface | 42/100 | 22/100 | 64/100 | 41/100 | 138/100 | 118/100 |
| | difference | +24/+51.1 | +9/+ 40.9 | + 33/+ 51.6 | +2/+4.9 | +27 /+18.6 | +86 /+72.9 |
| | | *Belgorodsky-1 site, 3500 yr. BP (arch. date), surface soil – leached chernozem* | | | | | |
| 2 | buried | 46/97.9 | 22/71 | 68 /87.2 | 21/84 | 113/78.5 | 24/16.7 |
| | surface | 47/100 | 31/100 | 78/100 | 25/100 | 144/100 | 144/100 |
| | difference | +1/+ 2.1 | +9/+29 | +10/+ 12.8 | +4/+16 | +31 /+21.5 | +120/+83.3 |
| | | *Prokhorovsky site, 3500 yr. BP (arch. date), surface soil – leached chernozem* | | | | | |
| 3 | buried | 35/56.5 | 22/122.2 | 57/71.3 | 21/95.5 | 103/81.7 | 35/37.2 |
| | surface | 62/100 | 18/100 | 80/100 | 22/100 | 126/100 | 94/100 |
| | difference | +27/+43.5 | –4/–22.2 | +23/+28.7 | +1/+4.5 | +23 /+18.3 | +59/+62.8 |
| | | *Gorozhenoe site, 3360 ± 25 yr. BP (radiocarbon date), surface soil – leached chernozem* | | | | | |
| 4 | buried | 17/41.5 | 15/65.2 | 32/50 | 20/80 | 114/100 | 17/23.6 |
| | surface | 41/100 | 23/100 | 64/100 | 25/100 | 114/100 | 72/100 |
| | difference | +24/+58.5 | +8/+34.8 | +32/+50.0 | +5/+20 | 0/0 | +55 /+76.4 |
| | | *Novoe Ukolovo site, 3500 yr. BP (arch. date), surface soil – leached chernozem* | | | | | |
| 5 | buried | 35/67.3 | 10/55.6 | 45/64.3 | 21/48.8 | 113/80.1 | 20/22.7 |
| | surface | 52/100 | 18/100 | 70/100 | 43/100 | 141/100 | 88/100 |
| | difference | +17/+32.7 | +8/+44.4 | +25/+35.7 | +22/+51.2 | +28 /+19.9 | +68/+77.3 |
| | | *Chamlyk-Nikolsky site, 3600-3550 yr. BP (arch. date), surface soil – leached chernozem* | | | | | |
| 6 | buried | 36/38.2 | 24/171.4 | 50/61 | 25 /69.4 | 98/71 | 14/9.3 |
| | surface | 68/100 | 14/100 | 82/100 | 36/100 | 138/100 | 150/100 |
| | difference | +42/+61.8 | –10/–71.4 | +32/+39 | +11/+30.6 | +40/+29 | +136/+90.7 |
| | | *Storozhevoye site, 3500 yr. BP (arch. date), surface soil – typical chernozem* | | | | | |
| 7 | buried | 17/48.6 | 38/115.2 | 55/80.9 | 47/97.9 | 144/90 | 17/25 |
| | surface | 35/100 | 33/100 | 68/100 | 48/100 | 160/100 | 68/100 |
| | difference | +18/51.4 | –5/–15.2 | +13/+19.1 | +1/+2.1 | +16 /+10 | +51/+75 |
| | | *Grayvoronsky site, 3500 yr. BP (arch. date), surface soil – typical chernozem* | | | | | |
| 8 | buried | 52/80 | 30/85.7 | 82/82 | 40/160 | 145/93.5 | 25 /59.5 |
| | surface | 65/100 | 35/100 | 100/100 | 25/100 | 155/100 | 42 /100 |
| | difference | +13/+20 | +5/+14.3 | +18/+18 | –15/–60 | +10/+6.5 | +17/+40.5 |
| | | *Belgorodsky -2 site, 3500 yr. BP (arch. date), surface soil – typical chernozem* | | | | | |
| 9 | buried | 50/74.6 | 16/76.2 | 66/75 | 19/73.1 | 107/79.3 | 25/55.6 |
| | surface | 67/100 | 21/100 | 88/100 | 26/100 | 135/100 | 45/100 |
| | difference | +17 /+25.4 | +5/+23.8 | +22 /+25 | +7/+26.9 | +28 /+20.7 | +20/+44.4 |

**Table 2.** Продолжение

| No | Soil | Thickness (for effervescence – depth), numerator – cm, denominator –% of modern values | | | | | |
|---|---|---|---|---|---|---|---|
| | | A1 | A1B + BA1 | A1 + A1B + BA1 | B | Profile | Effervescence |
| | | *Dubroshina site, 3500 yr. BP (arch. date), surface soil – typical chernozem* | | | | | |
| 10 | buried | 65/72.2 | 50/76.9 | 115/74.2 | 45/112.5 | 220/86.3 | 80/71.4 |
| | surface | 90/100 | 65/100 | 155/100 | 40/100 | 255/100 | 112/100 |
| | difference | +25/+27.8 | +15/+23.1 | +40/+25.8 | –5/–12.5 | +35 /+13.7 | +32/+28.6 |
| | | *Drozdy site, 3500 yr. BP (arch. date), surface soil – typical chernozem* | | | | | |
| 11 | buried | 55/78.6 | 45/75 | 100/76.9 | – | – | 100/80 |
| | surface | 70/100 | 60/100 | 130/100 | – | – | 125/100 |
| | difference | +15/+21.4 | +15/+25 | +30/+23.1 | – | – | +25/+20 |
| | | *Gubkinsky-1 site, 3500 yr. BP (arch. date), surface soil – typical chernozem* | | | | | |
| 12 | buried | 30/54.5 | 25/250 | 55/84.6 | 20/90.9 | 100/82 | 25/41.7 |
| | surface | 55/100 | 10/100 | 65/100 | 22/100 | 122/100 | 60/100 |
| | difference | +25/+45.5 | –15/–150 | +10/+15.4 | +2/+ 9.1 | +22/+18 | +35 /+58.3 |
| | | *Gubkinsky-2 site, 3500 yr. BP (arch. date), surface soil – typical chernozem* | | | | | |
| 13 | buried | 37/56.9 | 30/120 | 67/74.4 | 40/200 | 130/100 | 30/42.9 |
| | surface | 65/100 | 25/100 | 90/100 | 20/100 | 130/100 | 70/100 |
| | difference | +28/+43.1 | –5/–20 | +23/+25.6 | –20/–100 | 0/0 | +40/+57.1 |
| | | *Gorki site, 3600 yr. BP (arch. date), surface soil – typical chernozem* | | | | | |
| 14 | buried | 32/106.7 | 17/89.5 | 49/100 | 61/135.6 | – | 50/119 |
| | surface | 30/100 | 19/100 | 49/100 | 45/100 | – | 42/100 |
| | difference | –2/–6.7 | +2/+10.5 | 0/0 | –16/–35.6 | – | –8/–19 |
| | | *Boldyrevka site, 3383 ± 45 yr. BP (radiocarbon date), surface soil – typical chernozem* | | | | | |
| 15 | buried | 24/52.2 | 27/108 | 51/71.8 | 31/114.8 | 127/92.7 | 12/18.5 |
| | surface | 46/100 | 25/100 | 71/100 | 27/100 | 137/100 | 65/100 |
| | difference | +22/47.8 | –2/–8 | +20/+28.2 | –4/–14.8 | +10/+7.3 | +53/+71.5 |
| | | *Bobrovsky site, 3500 yr. BP (arch. date), surface soil – meadow-chernozem soil* | | | | | |
| 16 | buried | 36/75 | 36/73.5 | 72/74.2 | 60/– | 142/– | 0/0 |
| | surface | 48/100 | 49/100 | 97/100 | – | – | 54/100 |
| | difference | + 12/+25 | +13/+26.5 | +25/+25.8 | – | – | +54/+100 |

*Note:* in table "–" – no data.

*Примечание:* в таблице обозначение "–" – отсутствие данных.

In the two-meter soil layer of the compared sites, the carbonate stocks in the surface soils differ by 1.7 times and the buried soils by 2.9 times, towards higher values in the area of typical chernozems (tabl. 5). The given example shows the initial spatial differences in content and pools of carbonates of the parent materials, which influenced the Late Holocene evolution of the soils and soil cover. The natural spatial variability of carbonates distribution in the parent materials dictates the mosaic distribution of the areas of leached and typical chernozems.

A comparative analysis of the distribution of the Corg content through the profile in the buried and surface chernozems is of particular interest. As is known, after burial, diagenetic changes in some features occur in soils, including the content and stocks of organic matter (Ivanov, 1992; Demkin, 1997). The decrease in organic matter content is associated with the process of its mineralization by microorganisms, which occurs especially intensively in the uppermost layers of buried soils (Zolotun, 1974; Ivanov, 1992). That is why the carbon content of organic matter in buried chernozems is lower than in the surface soils in most cases. It is believed that over 250–300 years after the burial, about 50% of the original humus stocks are lost in the upper layers of chernozems. Further, the intensity of mineralization of organic matter weakens, but continues for many millennia. So, in the upper

**Table 3.** Average morphometric characteristics of chernozems buried 3600–3400 yr. BP, and their surface analogues in automorphic landscapes of the forest-steppe zone in the centre of the East European Plain
**Таблица 3.** Средние морфометрические признаки подкурганных черноземов, погребенных 3600–3400 л. н., и их фоновых аналогов в автоморфных ландшафтах лесостепи центра Восточно-Европейской равнины

| Statistical indicator | Thickness, cm | | | | | |
|---|---|---|---|---|---|---|
| | A1 | A1B+BA1 | A1+A1B+BA1 | B | profile | Depth of effervescence |
| *Buried chernozems, n = 15* | | | | | | |
| $X \pm \delta_X$ | 36 ± 3.8 | 26 ± 3.0 | 62 ± 5.9 | 32 ± 3.5 | 125 ± 9.0 | 34 ± 6.5 |
| δ | 14.88 | 11.57 | 23.04 | 13.25 | 32.38 | 25.00 |
| V, % | 41 | 44 | 37 | 41 | 26 | 74 |
| *Surface chernozems, n = 15* | | | | | | |
| $X \pm \delta_X$ | 56 ± 4.1 | 28 ± 4.0 | 84 ± 7.1 | 32 ± 2.6 | 146 ± 9.7 | 86 ± 9.3 |
| δ | 15.92 | 15.60 | 27.42 | 9.84 | 35.09 | 36.05 |
| V, % | 28 | 56 | 33 | 31 | 24 | 42 |

**Table 4.** Morphometric features of the buried chernozems 3600–3400 yr. BP and their surface analogues in the distribution areas of leached and typical automorphic chernozems on the territory of the forest-steppe centre of the East European Plain
**Таблица 4.** Морфометрические признаки подкурганных черноземов, погребенных 3600–3400 л. н., и их фоновых аналогов в ареалах распространения автоморфных черноземов выщелоченных и типичных на территории лесостепи центра Восточно-Европейской равнины

| Modern soil area | Statistical indicator | Thickness, cm | | | | | Depth of effervescence, cm |
|---|---|---|---|---|---|---|---|
| | | A1 | A1B+BA1 | A1+A1B+BA1 | B | profile | |
| | *Buried chernozems, n = 6* | | | | | | |
| Leached chernozems | $X \pm \delta_X$ | 30 ± 4.6 | 18 ± 2.3 | 48 ± 5.9 | 25 ± 3.0 | 109 ± 2.7 | 24 ± 3.4 |
| | δ | 11.26 | 5.75 | 14.39 | 7.31 | 6.59 | 8.36 |
| | V, % | 37 | 32 | 30 | 29 | 6 | 35 |
| | *Surface chernozems, n = 6* | | | | | | |
| | $X \pm \delta_X$ | 52 ± 4.5 | 21 ± 2.4 | 73 ± 3.3 | 32 ± 3.7 | 134 ± 4.6 | 111 ± 12.9 |
| | δ | 10.97 | 5.87 | 8.07 | 9.12 | 11.34 | 31.62 |
| | V, % | 21 | 28 | 11 | 29 | 8 | 28 |
| | *Buried chernozems, n = 7* | | | | | | |
| Typical chernozems | $X \pm \delta_X$ | 35 ± 4.9 | 26 ± 2.9 | 61 ± 4.4 | 37 ± 5.7 | 126 ± 7.6 | 26 ± 4.6 |
| | δ | 12.88 | 7.73 | 11.67 | 15.00 | 18.64 | 12.05 |
| | V, % | 37 | 30 | 19 | 41 | 15 | 46 |
| | *Surface chernozems, n = 7* | | | | | | |
| | $X \pm \delta_X$ | 52 ± 5.7 | 24 ± 3.2 | 76 ± 6.6 | 30 ± 4.3 | 140 ± 6.0 | 56 ± 4.8 |
| | δ | 15.17 | 8.50 | 17.58 | 11.27 | 14.72 | 12.58 |
| | V, % | 29 | 35 | 23 | 38 | 11 | 22 |

part of the buried chernozems of the Early Iron Age, about 40% of the original stocks of humus remain, and in the paleochernozems of the Bronze – Eneolithic Ages – about 30% of the original stocks (Zolotun, 1974; Ivanov, 1992; Demkin, 1997). Our calculations show that these are only general assumptions that require clarification.

Table 6 and fig. 4 show the data of the layered distribution of the organic matter content in the buried chernozems of the centre of the East European Plain within three different historical periods, expressed as a percentage relative to the values in identical layers of modern (surface) chernozems. In each chrono-sequence, averaged characteristics of paired compari-

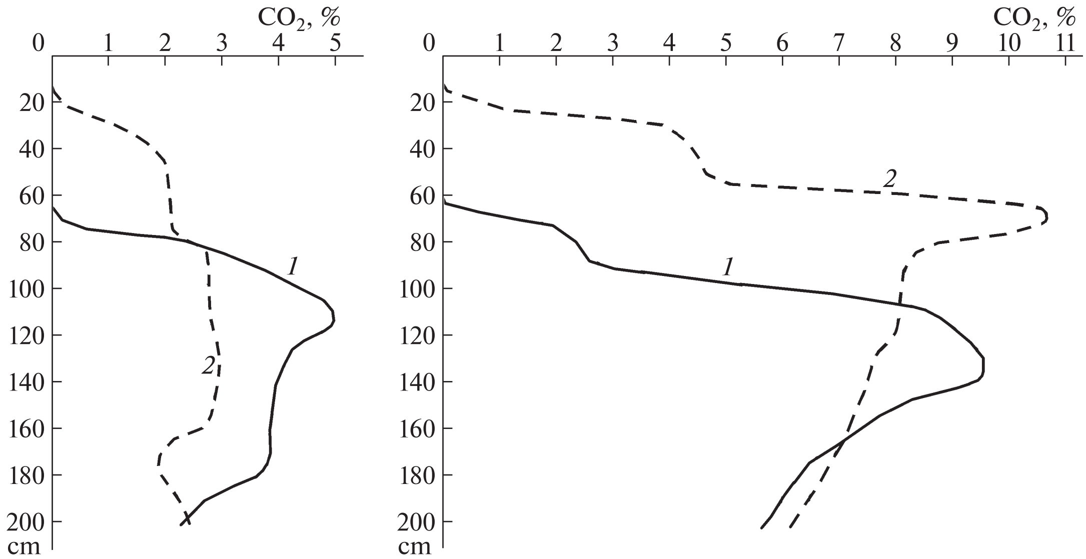


**Fig. 3.** Profile distributions of the carbonate $CO_2$ content in the soils of the Staraya Nelidovka ((a), surface soils – leached chernozems) and Boldyrevka sites ((b), surface soils – typical chernozems). *1* – the distribution of the carbonate $CO_2$ in the surface soils, *2* – the distribution of the carbonate $CO_2$ in the soils buried under the mounds of the Srubnaya culture period.

**Рис. 3.** Профильные распределения содержания $CO_2$ карбонатов в почвах участков Старая Нелидовка ((a), фоновые почвы – черноземы выщелоченные) и *Болдыревка* ((b), фоновые почвы – черноземы типичные). *1* – распределение показателя в фоновых почвах, *2* – распределение показателя в погребенных под курганами срубного времени почвах.

sons of buried and surface chernozems are presented by several sites (from 4 to 6).

As can be seen from the data in tabl. 6 and fig. 4, the paleochernozems of the Srubnaya culture (3600–3400 yr. BP) contain equal or greater content of organic matter in comparison with the paleochernozems buried about 1 thousand years later – in the Scythian period of the Early Iron Age.

We can conclude that during the period of the Srubny culture's existence, the climatic conditions in the forest-steppe area were very favorable for the formation of the humus-rich fertile chernozems. Probably, first of all, there was form hidden (bio-chemical, still without visual properties) enrichment of organic matter, and then (to the end of the Subboreal period, yet after the Srybny epoch), – its manifestation in morphological properties (thickness of A1 horizon and its dark color) (tabl. 1, fig. 4).

**Table 5.** Carbonates carbon stocks, t/ha in soil profiles of *Staraya Nelidovka* and *Boldyrevka* sites
**Таблица 5.** Запасы $С_{карб}$, т/га в профилях почв участков Старая Нелидовка и Болдыревка

| Soil | The layer, cm | | |
|---|---|---|---|
| | 0–100 | 100–200 | 0–200 |
| *Staraya Nelidovka site* | | | |
| Surface | 40.12 | 171.66 | 211.78 |
| Buried | 68.31 | 110.11 | 178.42 |
| Difference | –28.19 | +61.55 | +33.36 |
| *Boldyrevka site* | | | |
| Surface | 36.18 | 330.88 | 367.06 |
| Buried | 216.75 | 294.26 | 511.01 |
| Difference | –180.57 | +36.62 | –143.95 |

**Table 6.** Organic carbon content by layers in buried automorphic chernozems of different periods, % of modern values (forest-steppe centre of the East European Plain, modern typical chernozems area)
**Таблица 6.** Послойное содержание органического углерода в подкурганных автоморфных черноземах разных периодов, % от современных значений (Центральная лесостепь, фоновый компонент почвенного покрова – черноземы типичные)

| Layer, cm | Time of the burial, yr. BP, *n* – number of objects | | |
|---|---|---|---|
| | 4200–3700, *n* = 5 | 3600–3400, *n* = 6 | 2500–2200, *n* = 4 |
| 0–20 | 47 ± 3 | 70 ± 3 | 68 ± 5 |
| 20–40 | 45 ± 4 | 65 ± 4 | 71 ± 9 |
| 40–60 | 46 ± 7 | 80 ± 7 | 76 ± 12 |
| 60–80 | 43 ± 9 | 73 ± 17 | 86 ± 10 |
| 80–100 | 54 ± 12 | 91 ± 23 | 82 ± 11 |
| 100–120 | 65 ± 9 | 109 ± 21 | 80 ± 13 |
| 120–140 | 75 ± 9 | 95 ± 16 | 95 ± 8 |
| 140–160 | 89 ± 17 | 104 ± 21 | 93 ± 10 |

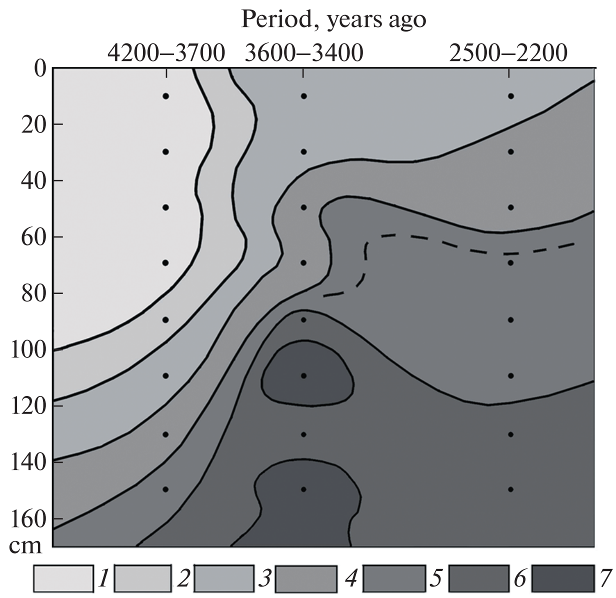


**Fig. 4.** Distribution of the organic carbon content in the profiles of buried chernozems of different periods (in % of modern values) within the modern typical chernozems area. *Organic carbon content from the current level, in %: 1* – less than 50, *2*–50–60, *3*–60–70, *4*–70–80, *5*–80–90, *6*–90–100, *7* – more than 100.

**Рис. 4.** Распределение содержания органического углерода в профилях подкурганных черноземов разных периодов (в % от современных значений) на территории распространения современных черноземов типичных. Содержание органического углерода от современного уровня, %: *1* – <50, *2*–50–60, *3*–60–70, *4*–70–80, *5*–80–90, *6*–90–100, *7* – >100.

In fig. 5 are represented distribution areas of the thicknesses of the humified part of the chernozems buried in the Srubny period (fig. 5, (a)), and also isohumus bands (fig. 5, (b)) are reflected the spatial differences of the buried chernozems of the Srubny period on soil organic matter content in the 0–20 cm layer.

According to the given schematic maps, the territory of the Central forest-steppe and adjacent steppe territories during the Srubny period was heterogeneous in terms of thickness of the humified part of soil profiles and organic matter content. Areas with the thickest humified part of the profiles of chernozems (fig. 5, (a)), are probably, related to optimal moisture regime (it was previously hypothetically associated with the close location of the Voeykov axis (Chendev et al., 2015). It was also noted that the organic matter content in the soils in the Srubny period increased eastward (fig. 5, (b)). This pattern for the surface soil cover of the East European chernozems at the end of the XIX century was established by Dokuchaev (Dokuchaev, 1883).

## 4. CONCLUSIONS

The conducted research allows us to draw a number of the following most important conclusions.

1. The Srubny period was marked by a change in natural conditions that followed the arid climate episode in the Middle Subboreal time on the East European Plain. The humus-rich part of the profile of the meadow-steppe chernozems of the forest-steppe zone

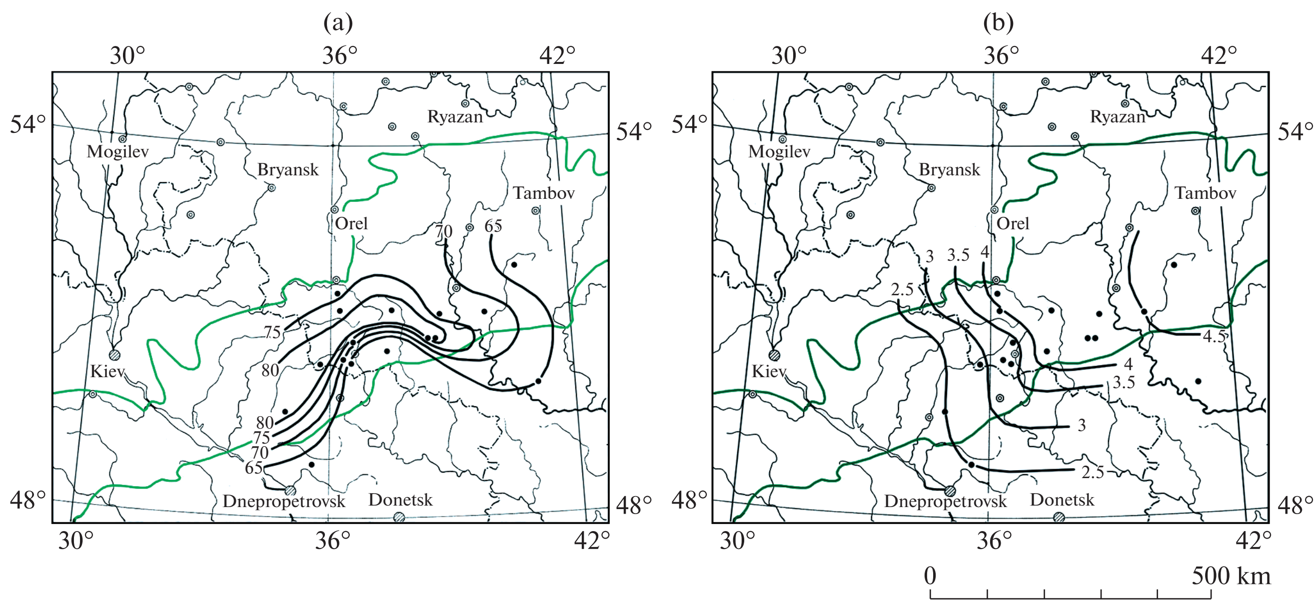


**Fig. 5.** The thickness of the humus-rich part of the profiles of the buried chernozems in the Srubny period (% of the current values) (a) and the humus content in the 0–20 cm layer of these soils, abs. % (b). Compiled on unpublished and literature data (noted in fig. 1).

**Рис. 5.** Мощность гумусированной части профилей подкурганных черноземов срубного времени (% от современных значений) (a) и содержание гумуса в слое 0–20 см этих почв, абс. % (b). Составлено по неопубликованным данным авторов статьи и литературным сведениям (указанным в подписи к рис. 1).

began to grow, and a less expressive tendency for leaching of carbonates was noted. “Hidden” (biochemical) enrichment of organic matter took place earlier than its manifestation in morphological properties of chernozems (growth of A1 horizon and its dark color formation). Buried chernozems of the Srubnaya culture in comparison with their later analogues of the Early Iron Age contain more organic matter despite the longer time of diagenesis.

2. On the territory of the forest-steppe centre of Eastern Europe, the automorphic paleochernozems of the Srubny period were characterised by a greater homogeneity of morphological properties (in all studied areas, they were identified as typical chernozems with high carbonate table) compared to their modern analogues (two areas of chernozems were formed – leached and typical). Leached chernozems are located in areas with lower carbonate content in the parent materials compared to the areas of typical chernozems.

3. The general trend of the Late Holocene evolution of leached and typical automorphic chernozems consisted of an increase in the thickness of humus horizons (by an average of 20 cm) and soil profiles (by an average of 20 cm). In contrast, the thickness of the transitional part of the profile (A1B + BA1) and horizons B (Bk) remained the same. Differences were connected with different depth of leaching from carbonates in the studied soils.

# PALEOCHERNOZEMS OF THE SRUBNAYA CULTURE PERIOD AND TRENDS OF LATE HOLOCENE EVOLUTION OF SOILS IN THE EAST-EUROPEAN PLAIN FOREST-STEPPE

**Yu. G. Chendev[a,#], T. A. Puzanova[b], and F. G. Kurbanova[c]**

[a]*Belgorod State National Research University (BelSU), Belgorod, Russia*

[b]*Lomonosov Moscow State University, Faculty of Geography, Moscow, Russia*

[c]*Institute of Geography RAS, Moscow, Russia*

[#]*E-mail: sciences@mail.ru*

A comparative analysis of the features of the chernozems buried under the mounds of the Srubnaya culture (3600–3400 years ago), earlier (4200–3700 years ago) and later analogues (2500–2200 years ago) have been carried out. Also, modern chernozems of the East European Plain central part were studied. The chernozems of the Srubnaya culture period were formed in an environment of noticeable bioclimatic transformations after the period of the Middle Subboreal climate aridization. It was found that the biochemical rearrangement of the profile in terms of the content of soil organic matter outplaced the morphological transformation with the formation of a thicker dark-colored part of the chernozem profile. The automorphic paleochernozems of the Srubny period were characterised by a greater homogeneity of morphological properties (in all studied areas, they were identified as typical chernozems with high carbonate table) compared to their modern analogues (two areas of chernozems were formed – leached and typical). Leached chernozems were formed in areas with lower carbonate content in the parent materials compared to the areas of typical chernozems. The general trend of the Late Holocene evolution of leached and typical automorphic chernozems consisted of an increase in the thickness of humus horizons (by an average of 20 cm) and soil profiles (by an average of 20 cm). In contrast, the thickness of the transitional part of the profile (A1B + BA1) and horizons B (Bk) remained the same. Differences were connected with different depth of leaching from carbonates in the studied soils.

*Keywords:* forest-steppe, Eastern Europe, chernozems, soil evolution, Late Holocene, Srubnaya culture

## ACKNOWLEDGEMENTS

This work was supported by grants from the Russian Science Foundation, project No. 19-18-00327) (analytical studies of the soils of the *Boldyrevka* and *Staraya Nelidovka* sites, systematization and generalization of literature data on the problem under study, graphic and cartographic interpretation of research results), as well as the Russian Foundation for Basic Research, project No. 19-29-05012 (field research at key sites *Boldyrevka* and *Staraya Nelidovka*, systematization of the results of field and laboratory studies carried out earlier at other key sites).

The author declares no conflict of interests. The present article performed in the framework the State Task No. AAAA-A19-119021990092-1 (FMWS-2019-0008), Institute of Geography, Russian Academy of Sciences.

## REFERENCES

Akhtyrtsev B.P. and Akhtyrtsev A.B. Meadow chernozem paleosols of the Bronze Age of the Oka–Don forest-steppe. *Pochvovedenie*. 1990. No. 7. P. 26–38. (in Russ.)

Akhtyrtsev B.P. and Akhtyrtsev A.B. Paleochernozems of the Central Russian forest-steppe in the Late Holocene. *Pochvovedenie*. 1994. No. 5. P. 14–24. (in Russ.)

Aleksandrovskiy A.L. *Evolyutsiya pochv Vostochno-Evropeiskoi ravniny v golotsene* (Evolution of the soils of the

East European Plain in the Holocene). Moscow: Nauka (Publ.), 1983. 150 p. (in Russ.)

Aleksandrovskiy A.L. The Holocene evolution of the chernozem occurring in the Middle Don basin. *Pochvovedenie*. 1984. No. 11. P. 5–13. (in Russ.)

Bronk Ramsey C. and Lee S. Recent and Planned Developments of the Program OxCal. *Radiocarbon*. 2013. Vol. 55. No. 2–3. P. 720–730. https://doi.org/10.2458/azu_js_rc.55.16215

Chendev Yu.G. *Evolyutsiya lesostepnykh pochv Srednerusskoi vozvyshennosti v golotsene* (Evolution of forest-steppe soils of the Central Russian Upland in the Holocene). Moscow: GEOS (Publ.), 2008. 212 p. (in Russ.)

Chendev Yu.G. and Ivanov I.V. Dynamics of soil cover in the south of Eastern Europe and in the Southern Trans-Urals in the subboreal period of the Holocene. *Pochvovedenie*. 2007. No. 11 P. 1298–1308. (in Russ.). https://doi.org/10.1134/S1064229307110026

Chendev Yu.G., Ivanov I.V., and Pesochina L.S. Trends of the natural evolution of chernozems on the East European Plain. *Pochvovedenie*. 2010. No. 7. P. 779–787. (in Russ.). https://doi.org/10.1134/S1064229310070021

Chendev Yu.G., Ivanov I.V., Kovalenko O.V., Lugovoy R.S., and Kuropata M.A. Comparative analysis of the Late Holocene chernozem evolution of the forest-steppe and steppe of the center of Eastern Europe. *Problemy regional'noi ecologii*. 2011. No. 2. P. 26–30. (in Russ.)

Chendev Yu.G., Lupo A.R., Lebedeva M.G., and Borbukova D.A. Regional specificity of the climatic evolution of soils in the southern part of eastern Europe in the second half of the Holocene. *Pochvovedenie*. 2015. No. 12. P. 1411–1423. (in Russ.). https://doi.org/10.1134/S1064229315120042

*Classificatsiya i diagnostika pochv SSSR* (Classification and diagnostics of soils in the USSR). Moscow: Kolos (Publ.), 1977. 223 p. (in Russ.)

Demkin V.A. *Paleopochvovedenie i arkheologiya: integratsiya v izuchenii prirody i obshchestva* (Paleopedology and archeology: integration in the study of nature and society). Pushchino: ONTI PNTS RAN (Publ.), 1997. 212 p. (in Russ.)

Dokuchaev V.V. *Russkii chernozem* (Russian Chernozem). SPb, 1883. 376 p. (in Russ.)

Gennadiev A.N. Time variability of the features of chernozems and the evolution of the natural environment (Stavropol Upland). *Vestnik Moskovskogo universiteta. Ser. 5 Geografiya*. 1984. No. 5. P. 10–16. (in Russ.)

Gerlach R., Baumewerd-Schmidt H., Borg K., Eckmeier E., and Schmidt M.W.I. Prehistoric alteration of soil in the Lower Rhine Basin, Northwest Germany – archaeological, $^{14}C$ and geochemical evidence. *Geoderma*. 2006. Vol. 136. No. 102. P. 38–50. https://doi.org/10.1016/j.geoderma.2006.01.011

Gorbunov V.S. On the assessment of the socio-economic and organizational structures of the Srubnaya Cultural-Historical Community. *Srubnaya culturno-istoricheskaya oblast': Materialy III Rykovskikh chtenii. Octyabr' 1994, Saratov*. Saratov: Izdatel'stvo Saratovskogo Universiteta (Publ.), 1994. P. 6–7. (in Russ.)

Hejcman M., Součková K., Krištuf P., and Peška J. What questions can be answered by chemical analysis of recent and paleosols from the Bell Beaker barrow (2500–2200 BC), Central Moravia, Czech Republic? *Quarternary International*. 2013. Vol. 316. No. 6. P. 179–189. https://doi.org/10.1016/j.quaint.2013.06.014

Holliday V.T. Soils in archaeological research. Oxford: Oxford university press, 2004. 448 p.

Ivanov I.V. *Evolutsiya pochv stepnoi zony v golotsene* (Evolution of steppe zone soils in the Holocene). Moscow: Nauka (Publ.), 1992. 143 p. (in Russ.)

Kamnueva-Wendt S., Mitusov A.V., Wendt J., and Bork H.R. Classification of buried soils, cultural, and colluvial deposits in the Viking town Hedeby. *Geoarchaeology*. 2020. Vol. 35. No. 3. P. 313–337. https://doi.org/10.1002/gea.21777

Khokhlova O.S., Zazovskaya E.P., Chichagova O.A., and Yablonsky L.T. Radiocarbon dating of different materials from kurgans of the early nomads of the southern Cis-Urals. *Izvestia Rossiiskoi Academii Nauk. Seriya geograficheskaya*. 2010. No. 3. P. 82–94. (in Russ.)

Kovaleva I.F. Srubnaya culture of the left-bank forested area of Ukraine. *Arkheologicheskie issledovaniya v Tsentral'nom Chernozem'e v dvenadtsatoi pyatiletke: Tezisy dokladov i soobshchenii II mezhvuzovskoi nauchnoi konferentsii, Belgorod, fevral' 1990*. Belgorod: Belgorod Pedagogical Institute (Publ.), 1990. P. 111–112. (in Russ.)

Kristiansen S.M., Dalsgaard K., Holst M.K., Aaby B., and Heinemeier J. Dating of prehistoric burial mounds by 14C analysis of soil organic matter fractions. *Radiocarbon*. 2003. Vol. 45. No. 1. P. 101–112. https://doi.org/10.1017/S0033822200032434

Margolina N.Ya., Aleksandrovsky A.L., Ilyichev B.A., Cherkinsky A.E., and Chichagova O.A. *Vozrast i evolutsiya chernozemov* (Age and evolution of chernozems). Moscow: Nauka (Publ.), 1988. 144 p. (in Russ.)

Molnar M., Joo K., Barczi A., Szanto Zs., Futo I., Palcsu L., and Rinyu L. Dating of total soil organic matter used in kurgan studies. *Radiocarbon*. 2004. Vol. 46. No. 1. P. 413–419. https://doi.org/10.1017/S0033822200039722

*Natsional'nyi atlas pochv Rossiiskoi Federatsii* (National atlas of soils of the Russian Federation). Moscow: Astrel (Publ.), 2011. 632 p. (in Russ.)

Parsons R.B., Schotles W.H., and Riecken F.F. Soil of Indian mounds in northern eastern Iowa as benchmarks for studies of Soil genesis. *Soil Science Society American Proceedings*. 1962. No. 26. P. 491–496.

Prikhodko V.E. Reconstruction of natural conditions and soils of the forest-steppe in the Holocene in the Central Chernozem Region and Western Siberia. *Pochvy v biosfere. Materialy Vserossiiskoi nauchnoi konferentsii s mezhdunarodnym uchastiem*. Novosibirsk-Tomsk: Izdatel'skii Dom Tomskogo gosudarstvennogo universiteta (Publ.), 2018. Is. 1. P. 86–94. (in Russ.)

Puzanova T.A., Makeev A.O., Khokhlova O.S., Aseeva E.N., and Kurbanova F.G. Holocene signals of climate dynamics in the profiles of soils buried under archaeological objects in the central part of the East European Plain. *Proceedings of 17 international multidisciplinary scientific geoconference SGEM 2017, Soils, Forest ecosystems*. Sofia, Bulgaria: Alexander Malinov (Publ.). 2017. No. 17. P. 273–281. http://dx.doi.org/10.5593/sgem2017/32/S13.036

Reimer P.J., Bard E., Bayliss A., Beck J.W., Blackwell P.G., Bronk Ramsey C., Grootes P.M., Guilderson T.P., Haflidason H., Hajdas I., Hatt C., Heaton T.J., Hoffmann D.L., Hogg A.G., Hughen K.A., Kaiser K.F., Kromer B., Manning S.W., Niu M., Reimer R.W., Richards D.A., Scott E.M., Southon J.R., Staff R.A., Turney C.S.M., and van der Plicht J. IntCal13 and Marine13 Radiocarbon Age Calibration Curves 0-50,000 Years cal BP. *Radiocarbon*. 2013. Vol. 55. No. 4. P. 1869–1887.
https://doi.org/10.2458/azu_js_rc.55.16947

Ruhe R.V., and Schotles W.N. Ages and development of soil landscapes in relation to climatic and vegetational changes in Iowa. *Soil Science Society of America Proceedings*. 1956. No. 20. P. 264–273.

Serebryannaya T.A. Dynamics of the boundaries of the Central forest-steppe in the Holocene. *Vekovaya dinamika biogeotsenozov. X Chteniya pamyati akademika V.N. Sukacheva*. Moscow: Nauka (Publ.), 1992. P. 54–71. (in Russ.)

Shumilovskikh L.S., Novenko E., and Giesecke T. Long-term dynamics of East-European forest-steppe ecotone. *Journal of Vegetation Science*. 2018. Vol. 29. No. 3. P. 416–426.
https://doi.org/10.1111/jvs.12585

Skripkin V. and Kovalyukh N. Recent developments in the procedures used at the SSCER laboratory for the preparation of Lithium Carbide. *Radiocarbon*. 1998. Vol. 40. No. 1. P. 211–214.
https://doi.org/10.1017/S0033822200018063

Spiridonova E.A. *Evolutsia rastitel'nogo pokrova basseina Dona v verkhnem pleistotsene – golotsene* (Evolution of the vegetation cover of the Don basin in the Upper Pleistocene – Holocene). Moscow: Nauka (Publ.), 1991. 221 p. (in Russ.)

Vyslouzilova B., Ertlen D., Sefrna L., Novak T., Viragh K., Rue M., Campaner A., Dreslerova D., and Schwartz D. Investigation of vegetation history of buried chernozem soils using near-infrared spectroscopy (NIRS). *Quaternary International*. 2015. No. 365. P. 203–211. https://doi.org/10.1016/j.quaint.2014.07.035

Zolotun V.P. *Razvitie pochv yuga Ukrainy za poslednie 45–50 vekov* (The development of soils in the south part of Ukraine for the last 45–50 centuries). *PhD thesis*. Kiev, 1974. 74 p. (in Russ.)

**EDN:** UGPZEX
*ГЕОМОРФОЛОГИЯ, 2022, том 53, № 5, с. 116–126*

## ПРОБЛЕМЫ ФЛЮВИАЛЬНОЙ ГЕОМОРФОЛОГИИ

*УДК 551.23:551.435.1*

# ВЛИЯНИЕ ГАЗОГИДРОТЕРМАЛЬНОЙ ДЕЯТЕЛЬНОСТИ НА ФОРМИРОВАНИЕ РЕЛЬЕФА РЕЧНЫХ ДОЛИН ГЕОТЕРМАЛЬНЫХ ЗОН

**© 2022 г. Е. В. Лебедева[1,]***
[1]*Институт географии РАН, Москва, Россия*
**E-mail: Ekaterina.lebedeva@gmail.com*
Поступила в редакцию 14.06.2022 г.
После доработки 27.06.2022 г.
Принята к публикации 15.07.2022 г.

Выходы сольфатарных газов, грязевулканические проявления, минерализованные термальные воды способствуют формированию разнообразных, иногда весьма специфических форм рельефа в днищах и на бортах речных долин территорий современного вулканизма. Проведена типизация денудационных и аккумулятивных форм преимущественно микро- и мезорельефа в речных долинах геотермальных зон в условиях проявлений газогидротермальной активности. Рассмотрены особенности влияния газогидротерм на характер геоморфологических процессов в пределах речных долин, проанализированы причины интенсификации склоновых процессов и эрозии. Основные выявленные закономерности типичны для большинства долин с газогидротермальными проявлениями, что подтверждают наблюдения в долинах рек, дренирующих склоны вулканов Тихоокеанского огненного кольца (в том числе Курильских островов, Камчатки, Новой Зеландии, Северной и Южной Америки), а также Исландии.

*Ключевые слова:* вулканизм, термальные воды, денудационные формы рельефа, аккумулятивные формы рельефа, склоновые процессы, выветривание, цементация

**DOI:** 10.31857/S043542812205008X

## 1. INTRODUCTION

Thermal waters and gases are formed in areas of increased heat flow. The source of water for hydrothermal springs is mainly atmospheric water but in the process of filtration, its composition largely changes compared to the initial one as a result of interaction with volcanic gases and rocks (Rychagov, 1993). Thermal springs solutions and steam-gas emissions from fumaroles intensively change both the host rocks and the geothermal zones landscapes.

Sites of active gas-hydrothermal manifestations are often found in the river valleys of modern and Late Pleistocene volcanism territories (fig. 1). This is due to the fact that the initiation of river valleys, as well as the location of thermal waters and gases outlets, is usually associated with fault and increased fracturing zones. But the influence of gas-hydrothermal manifestations on the fluvial relief formation is poorly understood: most studies are devoted to the analysis of the geological and hydrogeological structure of geothermal zones, the nature of hydrothermal manifestations, and the features of rock transformation under conditions of gas-hydrothermal impact (Belousov, Sugrobov, 1976; Hedenquist, Browne, 1989; Rychagov, 1993; Chudaev, 2003; Frolova et al., 2011; Bortnikova et al., 2013; Ladygin et al., 2014; Churchill et al., 2021).

The purpose of this research is to fill this gap and to analyze the effect of gas-hydrothermal activity on the nature of relief formation processes in the river valleys, as well as to classify the forms of denudation and accumulative relief the formation of which is directly or indirectly associated with the gas-hydrotherms activity.

## 2. MATERIALS AND METHODS

The research is based on the route studies carried out in the volcanic regions of North and South America, Iceland and New Zealand, as well as on the analysis of the largest geothermal zones of the world (Yellowstone, El Tatio, Taupo, Iceland, the Valley of Geysers) literary material and the satellite images study from these regions. Detailed geomorphological studies were carried out in the streams valleys on the slopes of Mendeleev and Baransky volcanoes (South Kuril Islands), Mutnovsky and Uzon-Geysernaya caldera (Kamchatka), where the key object was the Geysernaya River valley. The studies of river valleys and fluvial landforms morphology, the nature of the processes on their slopes and at the bottoms of the valleys, the

**Fig. 1.** River valleys with the different gas-hydrothermal manifestations: (a) – the Covunco River floodplain with geysers Los Tachos, alluvial and debrisflow deposits cemented by thermal solutions are visible nearby (Domuyo vlc., Argentine); (b) – hot waters of the Waimangu Stream upper reaches (Taupo Volcanic Zone, New Zealand); (c) – the sinter wall Vitrazh and (d) – geyser Bol'shoi edifice and sheet – both in the Geysernaya River valley (Uzon-Geysernaya caldera, Kamchatka, Russia); (e) – the boiling pool framed by sinter formations at the Fal'shivaya River right tributary floodplain (Mutnovskyi vlc., Kamchatka), (f) – geyser edifices in the Salado River upper reaches (El Tatio geyser field, Chile). Here and further photos of the author.

**Рис. 1.** Долины рек с различными газогидротермальными проявлениями: (a) – пойма р. Ковунко с гейзерами Лос-Тахос, рядом видны аллювиальные и селевые отложения, сцементированные термальными растворами (влк. Домуй, Аргентина); (b) – горячие воды в верхнем течении ручья Ваймангу (вулканическая зона Таупо, Новая Зеландия); (c) – натечная стенка Витраж и (d) – гейзеритовая постройка и плащ гейзера Большой – оба в долине р. Гейзерной (Узон-Гейзерная кальдера, Камчатка, Россия); (e) – кипящий котел, обрамленный натечными образованиями в пойме правого притока р. Фальшивая (влк. Мутновский, Камчатка), (f) – гейзерные постройки в верховьях р. Саладо (гейзерное поле Эль-Татио, Чили). Здесь и далее фото автора.

distribution of gas-hydrothermal manifestations areas and denudation and accumulation processes, the weathering features and secondary changes in channel sediments, the composition of neoformations composing accumulative landforms were carried out. The material composition results analysis of these territories' accumulative neoformations were published by us earlier (Lebedeva, Zharkov, 2022), and R.V. Zharkov (2014) also studied the thermal waters composition of the Kuril Islands. Therefore, in this work, we will not touch on these issues in order to focus on the river valleys relief features.

## 3. RESULTS. TYPIFICATION OF THE LANDFORMS ASSOCIATED WITH THE GAS-HYDROTHERMAL MANIFESTATIONS IN THE RIVER VALLEYS

For the first time, a typification of micro- and mesorelief forms resulting from the direct or indirect gas-hydrothermal activity impact in the geothermal zones' river valleys was carried out. The results are summarized in table 1. The influence of gas hydrotherms on the nature of the relief formation processes within the river valleys is considered. The russian geologists (Belousov, Sugrobov, 1976; Rychagov, 1993; Chudaev, 2003; Bortnikova et al., 2013) distinguish three main types of gas-hydrothermal manifestations: steam-gas emissions, mud volcanic manifestations, and thermal springs. As a rule, all of them are observed in solfatara fields – areas of the most active and high-temperature gas-hydrothermal manifestation. With more distance from the volcanic structures centers and the volcanic activity extinction, there are predominantly thermal springs of various physical and chemical properties, the temperature and mineralization of which also gradually decrease with the distance from the volcanic center.

*3.1. Denudation landforms*. The denudation processes are confined mainly to the valleys slopes – first of all to their upper part. Here, the *detachment cracks* are often formed. On the Geysernaya River valley slopes their width can reach 1–4 m, and the length – tens of meters. This would seem to be quite natural for the majority of deep valleys, but in our case the relationship between the cracks formation and hydrothermal activity is evidenced by soil vaporization areas within their range (Pinegina et al., 2008; Dvigalo, Melekestsev, 2009). The rocks weathering and moistening processes stimulate a wide range of *slope processes* (rockfalls, landslides, slumps, flow slides etc.) with the *landslides scarps* formation of various lengths and heights. In 2007 on the left side of the Geysernaya River valley, as a result of the hydrothermally altered deposits blocks collapse, a horseshoe-shaped collapse amphitheater was formed (about 150 m high and up to 800 m long, with almost a vertical wall), and in 2014 – a new wall (up to 200 m high and about 480 m long) was formed upstream.

The denudation is also observed on the *soaring sites* – the hot gas outputs areas, under the influence of which there is an active bedrock weathering. Here, the dissolved substance removal and the fine particles washing out during rains and snowmelt, underwashing, and fine-grained material deflation take place. A peculiar phenomenon on the sides of such valleys called *hydrothermal pediments* – which are slightly inclined (1–5°) platforms, the width of which is usually measured by a few meters, but they can reach even a several tens of meters. They are usually formed in the hydrothermal manifestations areas, where weathering is accompanied by increased moistening of the clayey rocks. Their formation occurs due to the gradual slope retreat, destruction material of which is carried out by seeping waters mainly during a planar washout (Lebedeva, 2019).

Unvegetated thermal areas with the pliable weathered rocks are actively eroded, and *badlands* can be formed on the valley slopes. Often the valleys themselves are deep V-shaped incisions. The Yellowstone River Grand Canyon, which depth reaches 270–340 m, and the Geysernaya River valley (depth up to 400–500 m), on the sides of which intensive hydrothermal rocks processing is clearly visible (fig. 2), are the most striking examples of this. *Erosion outliers* of various sizes are often found in the channels of actively downcutting streams, which are both fragments of denser bedrocks – lavas, dikes, extrusions of various compositions, or cemented pebble-boulder deposits. *Rapids and waterfalls* are usually associated with the such formations outlets in the channels.

*Denudation niches* of several square meters in size are formed on slopes and ledges above many thermal springs and geysers (in the steam and water emissions influence zone). They have different configuration – from a slightly concave ellipsoid to a reminiscent of small caves. In some cases, similar forms are also formed above mud volcano manifestations, but this is rarely observed.

The denudation forms in the valleys bottoms can be divided into the ground and underground. For *soaring sites* and solfataric fields, the subsurface cavities formation of various sizes (up to 0.5–1.0 $m^3$ and more) is typical due to the rocks dissolution when interacting with the steam saturated with aggressive gases, including sulfurous gases, and the material removal as a result of underwashing and chemical erosion. When the roofs of these cavities collapses, various *linear and isometric hollows* (small depressions) are formed on the surface. On the floodplain and terraces, and sometimes directly in the channels, so-called *pools (basins*) are observed – boiling, mud, which sometimes have a shape of *funnels*. From these small depressions filled with boiling water or mud, an active removal of dissolved and suspended matter occurs, especially intensifying during rains and floods periods (fig. 1, (e)).

**Table 1.** The landforms associated with the gas-hydrothermal manifestations in the river valleys
**Таблица 1.** Формы рельефа, обусловленные газогидротермальными проявлениями в долинах рек

<table>
<tr><th colspan="2" rowspan="2">Denudation landforms</th><th>Geomorphological position of gas-hydrothermal manifestations and their types</th><th colspan="5" rowspan="2">Accumulative landforms</th></tr>
<tr><th>A. Gas-hydrothermal manifestations in the valleys bottoms</th></tr>
<tr><td colspan="2">Soaring (steaming) sites</td><td rowspan="4">1. Steam-gas emissions</td><td colspan="5">Cone-shaped edifices around solfataras</td></tr>
<tr><td colspan="2" rowspan="2">Linear and isometric hollows</td><td colspan="5">Native sulfur crystal brushes</td></tr>
<tr><td colspan="5">Evaporation crusts</td></tr>
<tr><td colspan="2">Subsurface cavities</td><td colspan="5">Sulfur knolls</td></tr>
<tr><td colspan="2" rowspan="3">Mud pots</td><td rowspan="3">2. Mud volcanic manifestations</td><td colspan="2" rowspan="3">Mud</td><td colspan="3">tiny volcanoes</td></tr>
<tr><td colspan="3">tongues</td></tr>
<tr><td colspan="3">framing rings</td></tr>
<tr><td colspan="2" rowspan="2">Erosion outliers</td><td rowspan="11">3. Thermal springs<br>.......................................<br>including geysers</td><td colspan="4" rowspan="2">Terraces fragments composed of hydrothermally altered alluvial and debrisflow material</td><td>cemented</td></tr>
<tr><td>weathered to clay</td></tr>
<tr><td colspan="2">Rapids and waterfalls</td><td colspan="5">Floodplain fragments composed of pebble-boulder material cemented by thermal waters</td></tr>
<tr><td colspan="2" rowspan="5">Pools and funnels</td><td rowspan="4">Layered formations</td><td colspan="2" rowspan="3">In channels</td><td colspan="2">armored steps of waterfalls</td></tr>
<tr><td colspan="2">channel troughs</td></tr>
<tr><td colspan="2">festoons</td></tr>
<tr><td colspan="4">Crusts on the floodplain and terraces surfaces</td></tr>
<tr><td rowspan="4">Laminated sinter formations</td><td colspan="3" rowspan="2">Sinter</td><td>terraces</td></tr>
<tr><td colspan="2">Geyser basins</td><td>walls</td></tr>
<tr><td rowspan="2">Underground forms</td><td>conduites</td><td colspan="3" rowspan="2">Geysers’</td><td>cones-shaped or isometric edifices</td></tr>
<tr><td>cavities</td><td>sheets (shields)</td></tr>
<tr><td colspan="2">Detachement cracks</td><td rowspan="7">B. Different gas-hydrothermal manifestations on the valleys slopes</td><td colspan="5" rowspan="2">Landslide and block-slide terraces</td></tr>
<tr><td colspan="2">Landslides scarps</td></tr>
<tr><td colspan="2" rowspan="2">Hydrothermal pediments</td><td colspan="5">Landslide and debrisflow dams</td></tr>
<tr><td rowspan="2">Debris flow</td><td colspan="4">embankment</td></tr>
<tr><td colspan="2">Denudation niches</td><td colspan="4">terraces</td></tr>
<tr><td colspan="2">Ravines, deep valleys</td><td colspan="5" rowspan="2">Mudflow covers</td></tr>
<tr><td colspan="2">Badlands</td></tr>
</table>

The surface denudation forms are also *geysers basins*, which have different sizes (from tens of cm to more than 10 m). Sometimes they have a very bizarre configuration – more often when they are located on slopes, less often – when they are located on a subhorizontal surface – they are almost round. The underground forms, sometimes having a complex structure (Muñoz-Saez et al., 2015), include *tubes or conduits* (depends of their size) and *cavities* of geysers. Often, these tubes depth is measured in the first tens of meters: for example, at the Strokkur geyser (Iceland), it exceeds 20 m with a width of about 2 m (Walter et al., 2020). Thermal springs and mud pots have also their own underground supply *conduits* of a more modest size.

*3.2. Accumulative landforms.* In the bottoms of the valleys under consideration, as well as at the slopes foot, along with erosion, accumulation dominates in

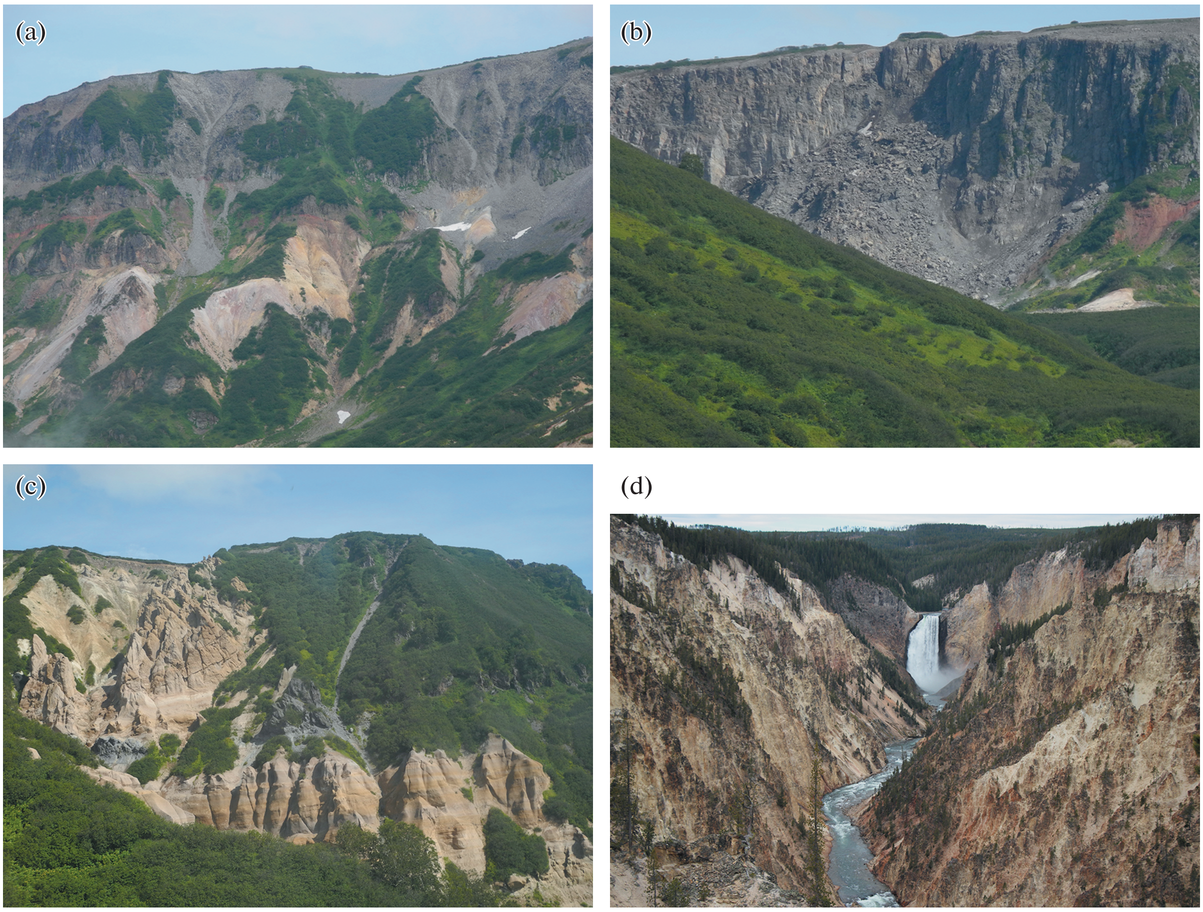


**Fig. 2.** Processes on river valleys slopes: (a) – landslides, (b) – rockfall, (c) – erosion and block landslides (Geysernaya River valley, Kamchatka, Russia) and (d) – erosion and rocks shedding (Yellowstone River Grand Canyon, Yellowstone, USA).

**Рис. 2.** Процессы на склонах речных долин: (a) – оползни, (b) – обвалы, (c) – эрозия и блоковые оползни (долина р. Гейзерной, Камчатка, Россия) и (d) – эрозия и осыпи (Большой Каньон р. Йеллоустон, кальдера Йеллоустон, США).

extended areas. Among the accumulative forms associated with the steam-gas vents, *brushes of sublimate crystals*[1] (each up to 1–2 cm height) along cracks in the *soaring sites* and the *solfataras cone-shaped edifices* up to 1–2 m high can be distinguished, also formed from the brushes of crystals, chemical composition of which is determined by the outgoing steam-gas jets composition, where sulfur usually dominates. Often there are *sulfur knolls* a few tens of cm high, also composed mainly of sulfur deposits, but not so well crystallized. The *soaring sites* are often covered with the brittle *evaporation crusts* (1–2 cm thick, sometimes wavy or intricately curved) that are formed on their surface as a result of the vapor–gas mixture interaction with the rocks. Often they mask the *subsurface cavities*. After the watercourse crosses the solfataras field downstream, there are usually observed traces of sulfur floods and sulfur interlayers of various thicknesses in the alluvium.

*The mud pots* – are the funnels and the small basins (as a rule, up to 3–7 m in diameter) filled with the liquid clay mass, which is a mixture of surface water with the steam and volcanic gases condensates and the clay particles of hydrothermally altered rocks – belong to the denudation forms. However, the accumulative *framing rings of clay material* a few tens of centimeters high are formed around them; sometimes the deposits of clay masses flows – the *mud tongues* – are traced with a length of a few meters, less often tens of meters. In some areas near the pots there are small groups of the *miniature mud volcanoes* tens cm of hight. Often these forms are located on the floodplain, respectively, during floods or during the rainy season, the removal of clay material by water flows can be observed there. In some cases, the mud volcanic forms are confined to the low terraces. For example, in the Geysernaya River valley they are located on a terrace-like sur-

[1] Sublimated crystal brushes and evaporation crusts can rather be attributed to relief nanoforms.

face with elevations of about 30 m above the river's level.

The accumulative landforms created with the thermal springs participation are the most widely represented. Three types of the *layered accumulative formations* are confined directly to the riverbeds: 1) the *channel troughs* – gutter-like channels sections a few meters long and up to 1.0 m wide, 2) the *festoons* – sites up to 0.5–1.0 m in size with a rounded edge stepwise located on the rapids-waterfall channel sections, 3) the *armored steps of waterfalls* covered with a layered crust, sometimes with the *eversion kettles* with a diameter of up to 0.5 m.

The next group is represented by the *laminated sinter formations* in the bottom of the valley and on the low terraces. These are the *sheets (aprons) or the shields* – horizontal or inclined covers up to 100–400 m$^2$ in area, framing the c*one-shaped or isometric edifices* of geysers and thermal springs (fig. 1, (d, f)). The dimensions of these structures are measured in the first meters: usually their heights do not exceed 3–8 m, and their diameter can reach 2–5 m or more (Karlstrom et al., 2013). They can have a variety of shapes – from a simple more or less pronounced cone to sometimes very complex structure in the form of the medieval castle ruins (the Castle Geyser, Yellowstone). The *sinter walls* are also distinguished – subvertical ledges of the terraces and sides of valleys below the thermal springs outlet, covered with the sinter crusts of various thicknesses, ranging from a few square meters to tens of meters. One of the most expressive is the Vitrazh wall in the Valley of Geysers (Kamchatka – fig. 1, (c)). The *sinter terraces* of various sizes and morphologies are often encountered, formation of which occurs in the marginal parts of the valleys due to the sinter deposits accumulation. As a rule, their area ranges from the few square meters to the tens, but in some cases – for example, in the Mammoth Springs area in the Gardner River valley (Yellowstone, USA), the size of such terraces reaches hundreds of square meters (fig. 3). The listed formations arise near the springs and the geysers as a result of outpouring or seepage of the mineralized thermal waters. All of them have a layered (or laminated) structure, which indicates the cyclical nature of their formation, which is usually seasonal.

In the valleys under consideration, fragments of the floodplain and the terraces are ubiquitous, covered with the layered crusts of newly formed minerals and/or composed of the alluvial and debrisflow deposits processed by the hydrothermal gas or water, and also their erosional outliers of various sizes in the channels. In this case, the formation of layered crusts is associated not only with the vapor-gas mixtures release but also with the water inflow from the thermal springs on the terraces surfaces. There are two types of the pebble-boulder (alluvial and debrisflow) material processing by the mineralized waters. Strong cementation of deposits, as a rule, by the ferruginous solutions is more often observed. The second type is the sediments weathering to the clays with the alluvium structure preservation. In the channel and on the floodplain, there are frequent different form outcrops of cemented units of pebble-boulder deposits – traces of the past accumulative processes, "fixed" by the thermal impact.

The hydrothermal clays distribution and the presence of the steam and thermal water outlets on the valleys slopes favor the numerous displacements, resulting in the formation of the local multi-level *landslide and block-slide terraces*. In some cases, several tiers of the similar terraces can be observed. In such areas, there is a significant widening of the valleys due to active slopes flattening. At the same time, in the bottoms, there is an accumulation of the slope material, displaced as a result of landslides and collapses with the periodic blocking of the valleys and the formation of the temporary *dams* and the dammed reservoirs, in which the river sediments accumulate. The dams length can reach 500–700 m. The further slope and alluvial material transportation and redeposition occur mainly due to the *debrisflows*, which are formed either directly during the gravity collapses, or during the dams destruction and the descent of temporarily dammed reservoirs. This is well confirmed by the observations carried out in the Geysernaya River valley (Pinegina et al., 2008; Dvigalo, Melekestsev, 2009; Lebedeva et al., 2020), where currently there are 2 similar dams – one (2007) is already cut by the river, and the other (2014) is in the early stages of erosion. The debrisflow deposits form the accumulative *terraces*; in the valleys of some watercourses, the *debrisflow embankments* with a length of a few hundred meters remain, which sometimes undergo cementation. During mudflow material splashes, the recorded heights of which can reach 40 m (Atlas..., 2015), *the mudflow material covers* with a thickness of 0.5–1.0 m to 3–5 m remain on the valley sides and its terraces. Similar debris and mudflow traces are typical of other watercourses of the high hydrothermal activity territories not only in the Kuril-Kamchatka region but also in most volcanic regions of the world (Lebedeva, 2018, 2019).

## 4. DISCUSSION. THE RELIEF FORMATION UNDER THE CONDITIONS OF GAS-HYDROTHERMAL MANIFESTATIONS

Endogenous energy is actively involved in the geothermal zones formation. Accordingly, in the gas-hydrothermal activity areas, the relief formation occurs under the thermal and the chemical processes impact. Due to the soil warming, the matter transformation occurs there all year round, even in temperate climates. The studies carried out have shown that the gas-hydrothermal manifestations can be confined both to the bottoms of river valleys (more often) and to


**Fig. 3.** The sinter terraces in the river valleys: *actively developing*: (a) – the Salado River upper reaches (El Tatio geyser field, Chile), (b) – the Sernaya River upper reaches basin (Baranskyi vlc., Iturup Is., Russia); *actively developing* (light) and *to varying degrees overgrown*: (c) – the Gardner River and (d) – the Firehole River valleys; *overgrown*: (e) – the Gibbon River valley; *disintegrating*: (f) – the Gardner River valley near Mammoth Springs (c–f – Yellowstone, USA).

**Рис. 3.** Натечные террасы в долинах рек: активно формирующиеся: (a) – верховья р. Саладо (гейзерное поле Эль-Татио, Чили), (b) – верховья бассейна р. Серной (влк. Баранского, о-в Итуруп, Россия); с активно формирующимися (светлыми) и в разной степени заросшими участками в долинах: (c) – р. Гарднер и (d) – р. Файрхоул; заросшие: (e) – долина р. Гиббон; разрушающиеся: (f) – долина р. Гарднер у Маммот-Спрингс (c–f – Йеллоустоун, США).

their slopes. The valleys themselves in the gas-hydrothermal activity areas have a peculiar structure with the specific forms of micro- and mesorelief.

Activation of the denudation processes in the geothermal zones river valleys occurs as a result of not only (1) *the flowing waters physical impact*, when the planar washout, linear erosion and the underwashing develop, and (2) the increased *slopes wetting* in the places where water and steam come out – where the landslide dominates, but also (3) the *chemical and thermal effects* of mineralized water and gas-rich steam, leading to the rocks dissolution and weathering. The most dynamically specific exogenous processes develop in the solfatara fields, where the lithogenic base is affected by the highest temperature gases and highly mineralized

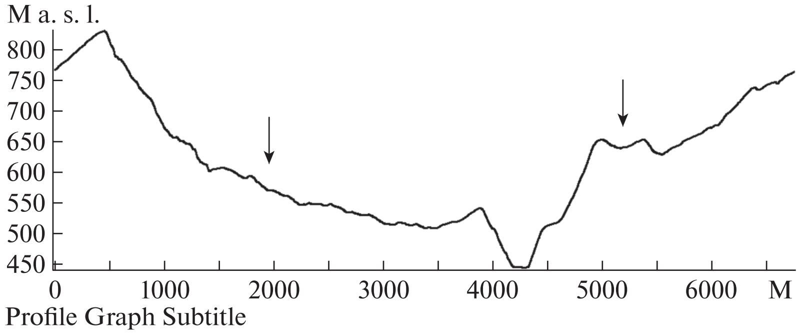


**Fig. 4.** Cross profile of the Geysernaya River valley (Uzon-Geysernaya caldera, Kamchatka, Russia) in its lower reaches. Arrows indicate areas of different types and ages landslides.

**Рис. 4.** Поперечный профиль долины р. Гейзерной (Узон-Гейзерная кальдера, Камчатка, Россия) в ее нижнем течении. Стрелками указаны участки оползней разного типа и возраста.

solutions, as well as on the valleys slopes, where the gas-hydrothermal action stimulates gravitational processes and erosion. Such territories are characterized by the successive catastrophic processes chains (Lebedeva, 2018; Lebedeva et al., 2020): the displacement of the slope material of significant volumes – the debrisflow – the formation of a dammed lake – the dam destruction – the repeated debrisflow.

The weathering in the regions under the consideration can proceed in the different ways. During the propylitization, rocks are compacted, their porosity is reduced, and their elastic and strength characteristics are increased. When the loose rocks strata is treated with the thermal solutions, especially those containing iron oxides and hydroxides, their *cementation* often occurs. However, the *rocks transformation into hydrothermal clays* is also widely observed, when their specific cohesion decreases by 1–2 orders of magnitude (Frolova et al., 2011), they acquire the plastic properties, but often retain their original color and structure. Moreover, this applies to both the bedrock volcanogenic rocks and the alluvial and the debrisflow deposits. The researchers (Scaringi, Loche, 2021), in turn, have established an increased clay rocks sensitivity to the temperature changes, which is associated with the physicochemical behavior of their microstructure, due to the presence of the absorbed water and the complex chemical bonds. Thus, as a result of the gas-hydrothermal impact, the composition and the properties of the loose sediments and bedrocks change, and, accordingly, the nature and the rate of relief formation processes. Moist clay substrate is easily eroded, the gravitational processes are activated on the slopes, all this leads to more intense denudation and the river valleys widening (fig. 4). On the contrary, rapids and waterfalls form in the riverbed at the outlets of cemented sediments, and the erosion slows down.

For the accumulative relief formation, the thermal springs waters composition and the geochemical barriers presence are of greatest importance, where the certain chemical compounds precipitate from the solution with the formation of the fluvial relief micro- and mesoforms. At the same time, as a rule, the microrelief forms, measured at a few meters, less often by tens of meters, are directly related to the gases and the thermal waters outlets (as and nanoforms), and the mesoforms, measured by tens – hundreds of meters, are due to the gravitational processes activation in the gas hydrotherms development areas on the slopes and subsequent processes of mudflow formation.

The layered formations in the channels (troughs, festoons, armored crusts) are formed mainly in the areas of rapids, where water is saturated with oxygen and the soluble compounds pass into an insoluble form and precipitate. The new formations in the form of layered crusts in the channel, alluvial deposits cementation can also be observed at the other geochemical barriers: at the watercourses confluences or their flow into water bodies with a different chemical composition of water. It is important to note that accumulative forms similar in morphology both directly in the channel and sinter formations on terraces and slopes can be formed with the different composition thermal waters participation and with the various compounds precipitation. For example, in the Kuril-Kamchatka region – from the siliceous tuffs to the jarosite (Lebedeva, Zharkov, 2022).

The field observations and the interpretation of multi-temporal images show that the gas-hydrothermal manifestations are generally characterized by the spatial migration: in some areas, thermal activity fades, in others it appears over time. In this case, transformation of the associated denudation and accumulative processes and, the forms of relief takes place accordingly. With attenuation of the gas-hydrothermal activity, the relief formation processes rates also fade or change their character, because the rocks temperature and their moisture change. The landslide bodies and the sinter forms gradually overgrow and morphologically look like the ordinary river terraces, which require special attention when studying such areas at the post-volcanic stage (fig. 3, (c–e)).

The rates of the sinter forms formation depend on the activity of the newly formed insoluble compounds precipitation process. In the Kuril-Kamchatka region, these processes have been studied very poorly: a single $^{14}C$ dating of a dwarf pine branch buried in geyserite indicates that the formation rate of the geyserite cover in the Geysernaya River valley (Troinoy geyser) was about 0.4 mm/year; modern processes observations show a rate of about 0.1 mm/yr (Sugrobov, Sugrobova, 1990; Sugrobov et al., 2009). Also in (Atlas..., 2015) the accumulation rate is estimated as 1–2 mm/year. Accordingly, large sinter structures in the Valley of Geysers are approximately 800–1000 years old. In the Yellowstone caldera, the age of the Castle geyser structure, about 5 m high with the base (shield) with an area of more than 400 m$^2$, was estimated by pollen (Churchill et al., 2021) as approximately 5500–11 000 years. Measurements taken near the borehole at the Hipaua-Waihi-Tokaanu geothermal field in Taupo Volcanic Zone (New Zealand) showed a silica sinter accumulation rate of about 10 mm/year, at a distance about 35m it decreases to 3.5 mm/year (Campbell et al., 2020). Experiments carried out (Lynn et al., 2019) showed that the silica sinter accumulation rate on small plates in thermal springs of the same Taupo zone varies within 3.9–7.6 mm/yr and depends on their orientation relative to the current, while the maximum accumulation rate observed not inside the water mass, but near its surface – during the water evaporation, and largely depends on its chemical composition.

The strength of new formations in the channels and on the slopes depends on their composition: the deposits saturated with the iron oxides and the hydroxides, as a rule, are more stable in time, and siliceous and carbonate compounds are rather quickly destroyed (fig. 3, (f)). In general, however, the accumulative forms described above for the most part (perhaps with the exception of sediments cemented by iron-manganese compounds) are poorly and rarely preserved after the end of the hydrothermal activity phase. However, the observations (Lynn, 2012) show that in case of repository, the amorphous silica in the form of opal transforms into the stable quartz over time. The findings of hydrothermal paleozones with the fossil geyserite formations are rather few, as well as their dates. In Russia, late Quaternary geyserites were found in Baikal rift zone on Olkhon Isl. (Sklyarov et al., 2004; Velokoslavinskii et al., 2017). Important steps towards the paleoforms study have been made by the specialists from New Zealand and the United States using mass spectrometry (Lynn, 2012; Campbell et al., 2018; Churchill et al., 2020). In some cases, the age of paleogeyserites was determined according to stratigraphy or using argon dating. The most ancient sinter forms fragments within the geothermal fields of these regions are up to 11–16 thousand years old and even 1 Ma (Lynn, 2012).

## 5. CONCLUSION

We have carried out the typification of the denudation and the accumulative relief forms, formation of which is associated with the gas hydrotherms within the volcanic regions river valleys. The main forms of micro- and mesorelief, directly or indirectly associated with the various gas-hydrothermal manifestations are identified; their characteristics are given, and the morphometric parameters are described.

These results allow us to conclude that in the geothermal zones stream valleys are formed under conditions of the numerous gas hydrotherms outputs of various compositions. As a result of complex interaction with them, the hydrothermal solutions rework the alluvial deposits and the bedrocks. This is why their properties change radically as well as the features of the denudation processes course. In the areas of rocks weathered to clays, their erosion intensifies, the deep erosion incisions and the badlands are formed. In case of sediments cementation, on the contrary, the erosion slows down, rapids and waterfalls are formed.

In such valleys, in the areas of weathered rocks and the gas-hydrothermal manifestations, slope processes activation is observed with the numerous, sometimes multi-tiered landslide terraces formation, which leads to a gradual river valleys widening, which eventually acquire a beads-like shape in plan. Such territories are characterized by a displacement of the significant volumes of material from the slopes, frequent debrisflows, and the dammed reservoirs formation.

Both in channels and on the river valleys slopes, due to the new mineral formations deposition, the specific forms of micro- and mesorelief arise, complicating and transforming the fluvial relief. The various chemical compounds fallout with formation of the characteristic landforms occur mainly on the geochemical barriers (in areas of rapids, waterfalls, in places where springs come out, etc.).

The main revealed patterns are typical for the most valleys with the gas-hydrothermal manifestations both in the Kuril-Kamchatka region and in the world, which is confirmed by observations on the geyser fields of Iceland, New Zealand (Taupo Volcanic Zone), America (including Yellowstone, El Tatio etc.).

# GAS-HYDROTHERMAL ACTIVITIES IMPACT ON THE RELIEF FORMATION OF GEOTHERMAL ZONES' RIVER VALLEYS

**E. V. Lebedeva**[a,#]

[a] *Institute of Geography RAS, Moscow, Russia*

[#] *E-mail: Ekaterina.lebedeva@gmail.com*

Solfataric gases outputs, mud volcanic manifestations and mineralized thermal waters contribute to the formation of various, sometimes very specific landforms on the slopes and the bottoms of river valleys in the modern volcanism territories. It has been carried out the typification of denudation and accumulative forms of predominantly micro- and mesorelief in river valleys of geothermal zones under the conditions of gas-hydrothermal activity manifestations. The features of gas hydrotherms influence on the nature of geomorphological processes within river valleys are considered, and analysed the reasons for intensification of the slope processes and erosion. The main patterns revealed are typical for the most valleys with gas-hydrothermal manifestations, which is confirmed by observations in the river valleys, draining the slopes of volcanoes of the Pacific Ring of Fire (including the Kuril Islands, Kamchatka, New Zealand, North and South America), as well as of Iceland.

*Keywords:* volcanism, thermal waters, denudation landforms, accumulative landforms, slope processes, weathering, cementation

## ACKNOWLEDGEMENTS

The author is grateful to the numerous colleagues who participated in the field research carried out as a part of the Institute of Geography of the Russian Academy of Sciences state assignment AAAA-A19-119021990091-4 (FMGE-2019-0005). The materials were summarized with the support of the Russian Science Foundation grant No. 21-17-00216.

## REFERENCES

Belousov V.I. and Sugrobov V.M. Geological and hydrogeological setting of geothermal regions and hydrothermal systems of Kamchatka. *Gidrotermal'nye sistemy i termal'nye polya Kamchatki*. Vladivostok: Dal'nauka (Publ.), 1976. P. 5–22. (in Russ.)

Bortnikova S.B., Bessonova E.P., Gora M.P., Shevko A.Ya., Panin G.L., Zharkov R.V., Eltsov I.N., Kotenko T.A., Bortnikova S.P., Manshtein Yu.A., Kotenko L.V., Kozlov D.N., Abrosimova N.A., Karin Yu.G., Pospeeva E.V., and Kazanskyi A.Yu. *Gazogidrotermy aktivnykh vulkanov Kamchatki i Kuril'skikh ostrovov: sostav, stroenie, genesis* (Gas hydrotherms of active volcanoes in Kamchatka and the Kuril Islands: composition, structure, genesis). Novosibirsk: INGiG SO RAS (Publ.), 2013. 282 p.

Campbell K.A., Guido D.M., John D.A., Vikre P.G., Rhys D., and Hamilton A. The Miocene Atastra Creek sinter (Bodie Hills volcanic field, California and Nevada): 4D evolution of a geomorphically intact siliceous hot spring deposit. *Journal of Volcanology and Geothermal Research*. 2018. Vol. 370. P. 65–81. https://doi.org/10.1016/j.jvolgeores.2018.12.006

Campbell K.A., Nicholson K., Lynn B.Y., and Browne P.R.L. 3D Anatomy of a 60-year-old siliceous hot spring deposit at Hipaua-Waihi-Tokaanu geothermal field, Taupo Volcanic Zone, New Zealand. *Sedimentary Geology*. 2020. Vol. 402. 105652. https://doi.org/10.1016/j.sedgeo.2020.105652

Chudaev O.V. *Sostav i usloviya obrazovaniya sovremennykh gidrotermal'nykh sistem Dal'nego Vostoka Rossii* (Composition and conditions of formation of modern hydrothermal systems in the Russian Far East). Vladivostok: Dalnauka (Publ.), 2003. 203 p.

Churchill D.M., Manga M., Hurwitz S., Peek S., Damby D.E., Conrey R., Wood J.R., Blaine McCleskey R., Keller W.E., Hosseini B., and Hungerford J.D.G. The structure and volume of large geysers in Yellowstone National Park, USA and the mineralogy and chemistry of their silica sinter deposits. *Journal of Volcanology and Geothermal Research*. 2021. Vol. 419. 107391. https://doi.org/10.1016/j.jvolgeores.2021.107391

Churchill D.M., Manga M., Hurwitz S., Peek S., Licciardi J., and Paces J.B. Dating silica sinter (geyserite): A cautionary tale. *Journal of Volcanology and Geothermal Research*. 2020. Vol. 402. 106991. https://doi.org/10.1016/j.jvolgeores.2020.106991

Dvigalo V.N. and Melekestsev I.V. Geological and geomorphological consequences of catastrophic rockfall and rockfall – landslides processes in the Kamchatka Valley of Geysers (according to aerial photogrammetry). *Volcanology and Seismology*. 2009. No. 5. P. 24–37. (in Russ.)

Frolova Yu.V., Ladygin V.M., and Rychagov S.N. Engineering-geological features of hydrothermal-metasomatic rocks of Kamchatka and the Kuril Islands. *Engineering geology*. 2011. No. 3. P. 40–54. (in Russ.)

Hedenquist J.W. and Browne P.R.L. The evolution of the Waiotapu geothermal system, New Zealand, based on the chemical and isotopic composition of its fluids, minerals and rocks. *Geochimica et Cosmochimica Acta*. 1989. No. 53. P. 2235–2257. https://doi.org/10.1016/0016-7037(89)90347-5

Karlstrom L., Hurwitz S., Sohn R., Vandemeulebrouck J., Murphy F., Rudolph M.L., Johnston M.J.S., Manga M., and Blaine McCleskey R. Eruptions at Lone Star Geyser, Yellowstone National Park, USA: 1. Energetics and eruption dynamics. *Journal of Geophysical Research:*

*Solid Earth*. 2013. Vol. 118. P. 4048–4062. https://doi.org/10.1002/jgrb.50251

Ladygin V.M., Frolova Yu.V., and Rychagov S.N. Transformation of effusive rocks under the influence of acid leaching by surface thermal waters (geothermal system of Baransky volcano, Iturup Is.). *Volcanology and Seismology*. 2014. No. 1. P. 20–37. (in Russ.)

Lebedeva E.V. Kinds of impacts of volcanic and post volcanic activity on fluvial relief. *Geomorfologiya*. 2019. No. 4. P. 49–66. (in Russ.). https://doi.org/10.31857/S0435-42812019449-66

Lebedeva E.V. Sequences of catastrophic geomorphic processes in the river valleys of volcanic regions. *Geomorfologiya*. 2018. No. 4. P. 38–55. (in Russ.). https://doi.org/10.7868/S0435428118040041

Lebedeva E.V. and Zharkov R.V. Accumulative landforms in valleys with gas-hydrothermal manifestations (the Kuril-Kamchatka region as an example). *Geomorfologiya*. 2022. Vol. 53. No. 1. P. 81–100. (in Russ.). https://doi.org/10.31857/S0435428122010096

Lebedeva E.V., Sugrobov V.M., Chizhova V.P., and Zavadskaya A.V. The valley of the river Geyzernaya (Kamchatka): hydrothermal activity and features of relief forming. *Geomorfologiya*. 2020. No. 2. P. 60–73. (in Russ.). https://doi.org/10.31857/S0435428120020066

Lynn B.Y. Mapping vent to distal-apron hot spring paleoflow pathways using siliceous sinter architecture. *Geothermics*. 2012. Vol. 43. P. 3–24. https://doi.org/10.1016/j.geothermics.2012.01.004

Lynn B.Y., Boudreau A., Smith I.J., and Smith G.J. Silica accumulation rates for siliceous sinter at Orakei Korako geothermal field, Taupo Volcanic Zone, New Zealand. *Geothermics*. 2019. Vol. 78. P. 50–61. https://doi.org/10.1016/j.geothermics.2018.11.007

Muñoz-Saez C., Manga M., Hurwitz S., Rudolph M.L., Namiki A., and Wang C.-Y. Dynamics within geyser conduits, and sensitivity to environmental perturbations: Insights from a periodic geyser in the El Tatio geyser field, Atacama Desert, Chile. *Journal of Volcanology and Geothermal Research*. 2015. Vol. 292. P. 41–55. https://doi.org/10.1016/j.jvolgeores.2015.01.002

Pinegina T.K., Delemen' I.F., Droznin V.A., Kalacheva E.G., Chirkov S.A., Melekestsev I.V., Dvigalo V.N., Leonov V.L., and Seliverstov N.I. Kamchatka Valley of Geysers after the catastrophe on 3 June. *Vestnik DVO RAN*. 2008. No. 1. P. 33–44. (in Russ.)

Rychagov S.N. Hydrothermal system of Baransky volcano (Iturup Island): model of geological structure. *Volcanology and Seismology*. 1993. No. 2. P. 59–75. (in Russ.)

Scaringi G. and Loche M. A thermo-hydro-mechanical approach to soil slope stability under climate change. *Geomorphology*. 2021. Vol. 401. 108108. https://doi.org/10.1016/j.geomorph.2022.108108

Sklyarov E.V., Fedorovskyi V.S., Kulagina N.V., Sklyarova O.A., and Skovitina T.M. Late Quaternary Valley of Geysers in the west of the Baikal Rift (Olkhon region). *Doklady Akademii nauk*. 2004. Vol. 395. No. 3. P. 1–5. (in Russ.)

Sugrobov V.M. and Sugrobova N.G. Pecularities of discharge of hightemperatured underground waters in the Valley of the Geysers. *Voprosy geografii Kamchatki*. 1990. Vol. 10. P. 81–89. (in Russ.)

Sugrobov V.M., Sugrobova N.G., Droznin V.A., Karpov G.A., and Leonov V.L. *Zhemchuzhina Kamchatki – Dolina Geyzerov. Nauchno-populyarnyi ocherk, putevoditel'* (The Pearl of Kamchatka is the Valley of Geysers). Petropavlovsk-Kamchatsky: Kamchatpress (Publ.), 2009. 108 p.

Velikoslavinskii S.D., Kotov A.B., Sklyarov E.V., Skovitina T.M., Tolmacheva E.V., Sklyarova O.A., and Prokopov N.S. Geochemical features and fluid regime of the formation of Late Quaternary geyserites in the Olkhon region and Olkhon Is. (Baikal rift zone). *Doklady Akademii nauk*. 2017. Vol. 474. No. 4. P. 465–470. (in Russ.)

Walter T.R., Jousset P., Allahbakhshi M., Witt T., Gudmundsson M.T., and Hersir P. Underwater and drone based photogrammetry reveals structural control at Geysir geothermal field in Iceland. *Journal of Volcanology and Geothermal Research*. 2020. Vol. 391. 106282. https://doi.org/10.1016/j.jvolgeores.2018.01.010

Zavadskaya A.V. (Eds.) *Atlas doliny reki Geizernoi v Kronotskom zapovednike* (Atlas of the Valley of the River Geysernaya in Kronotsky Reserve). Moscow: KRASAND (Publ.), 2015. 88 p.

Zharkov R.V. *Termal'nye istochniki Yuzhnykh Kuril'skikh ostrovov* (Termal springs of the South Kuril Islands). Vladivostok: Dalnauka (Publ.), 2014. 378 p.

**EDN:** WNIEBM
*ГЕОМОРФОЛОГИЯ, 2022, том 53, № 5, с. 127–133*

## ПРОБЛЕМЫ ФЛЮВИАЛЬНОЙ ГЕОМОРФОЛОГИИ

*УДК 551.435.122:551.89(470.313)*

# СТРОЕНИЕ ПОЙМЫ РЕКИ МОКШИ КАК КЛЮЧ К ПОЗДНЕПЛЕЙСТОЦЕНОВОЙ ИСТОРИИ РАЗВИТИЯ ДОЛИНЫ


**Е. Ю. Матлахова[1,*], В. Ю. Украинцев[2,3]**
*[1]Московский государственный университет имени М.В. Ломоносова, географический факультет, Москва, Россия*
*[2]Институт географии РАН, Москва, Россия*
*[3]Институт водных проблем РАН, Москва, Россия*
**E-mail: matlakhova_k@mail.ru*
Поступила в редакцию 14.06.2022 г.
После доработки 26.06.2022 г.
Принята к публикации 15.07.2022 г.

Геоморфологической особенностью изученного участка долины р. Мокши (бассейн средней Оки) является проявление в рельефе поймы многочисленных крупных палеорусел (макроизлучин), являющихся свидетельствами мощного речного стока во время их формирования. Для установления истории развития долины р. Мокши был изучен ключевой участок в ее нижнем течении от устья р. Цны до устья р. Мокши. Основываясь на результатах бурения, геоморфологического и литологического анализа, радиоуглеродного AMS-датирования отложений, были выделены следующие стадии развития долины р. Мокши в позднем плейстоцене. 1) Около 40–30 тыс. л. н. увеличение речного стока, обусловленное климатическими изменениями, привело к врезанию реки глубже современного уровня. 2) После этого сильное иссушение климата и снижение водности реки привели к заполнению долины (наиболее сильное иссушение климата и соответствовавшая ему аккумуляция относятся ко времени LGM, около 23–20 тыс. л. н.). 3) Новое увеличение водности реки 18.5–12 тыс. л. н. привело к образованию больших палеорусел (макроизлучин) и значительному расширению днища долины. 4) В голоцене речной сток снова уменьшился, а параметры русла стали близки к современным.

*Ключевые слова:* макроизлучины (большие палеорусла), история развития речных долин, палеогеография плейстоцена, флювиальная геоморфология
**DOI:** 10.31857/S0435428122050108

## 1. INTRODUCTION

Large paleochannels (macromeanders) are widespread on floodplains and low terraces in the river valleys of the East European Plain (Sidorchuk et al., 2000; Sidorchuk et al., 2011). The parameters of macromeanders are several times bigger than the characteristics of the modern rivers. As previous studies show such large paleochannels were formed over the periglacial zone of the Last Glaciation. These periglacial rivers were formed under conditions of high spring runoff. Formation of large paleochannels is usually associated with the Late Glacial (the end of MIS 2) (Panin et al., 2013).

The occurrence of macromeanders also characterizes the Moksha River valley in its lower part. Probably, the lower part of the Moksha river valley between the Tsna River confluence and the mouth of the Moksha River seems the best place to study macromeanders all over the Oka Basin. A great number of paleochannels are well preserved at the key site (fig. 1). Paleochannels of the Moksha River may be divided into two groups by their size: small paleochannels have the same parameters as the modern river channel, large paleochannels (macromeanders) are several times bigger.

We studied both large and small paleochannels to reconstruct palaeohydrology and history of the Moksha River valley development in the Late Pleistocene. Large paleochannels correspond to the time of high river runoff. The oldest ones of small paleochannels were studied to know the time of lowering of the river runoff.

The dating of the deposits from the paleochannels and the river valley bottom made it possible to reconstruct the Late Pleistocene history of the Moksha River valley development and to estimate changes in the river runoff during this period.

## 2. METHODS

In our study we used field and laboratory methods. Boreholes in large and small paleochannels were made during fieldwork in August-September 2019 and September 2020. Detailed lithological description was

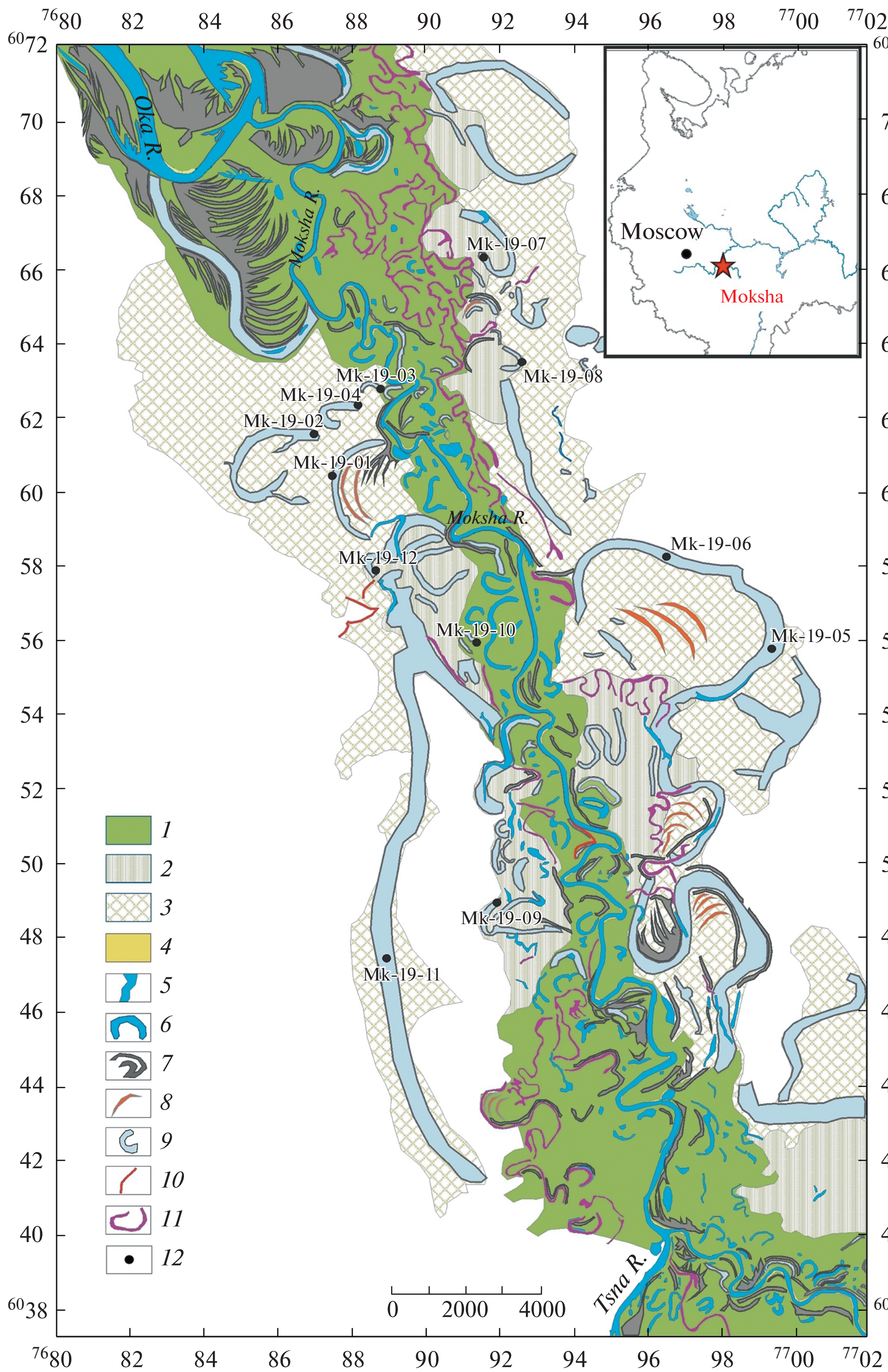


**Fig. 1.** Geomorphological map of the Moksha River floodplain.

*Floodplain: 1* – Late Holocene, *2* – Early Holocene, *3* – Late Pleistocene high; *4* – point bars; *5* – modern river channel; *6* – oxbow lakes; *7* – natural levees; *8* – scroll bars; *9* – palaeochannels; *10* – cut banks; *11* – floodplain channels; *12* – location of boreholes.

**Рис. 1.** Геоморфологическая карта ключевого участка поймы р. Мокши.

*Пойма: 1* – позднеголоценовая, *2* – раннеголоценовая, *3* – позднеплейстоценовая; *4* – прирусловые отмели; *5* – современное русло реки; *6* – старицы; *7* – прирусловые валы; *8* – гривы; *9* – палеорусла; *10* – эрозионные уступы; *11* – русла пойменных проток; *12* – положение скважин.

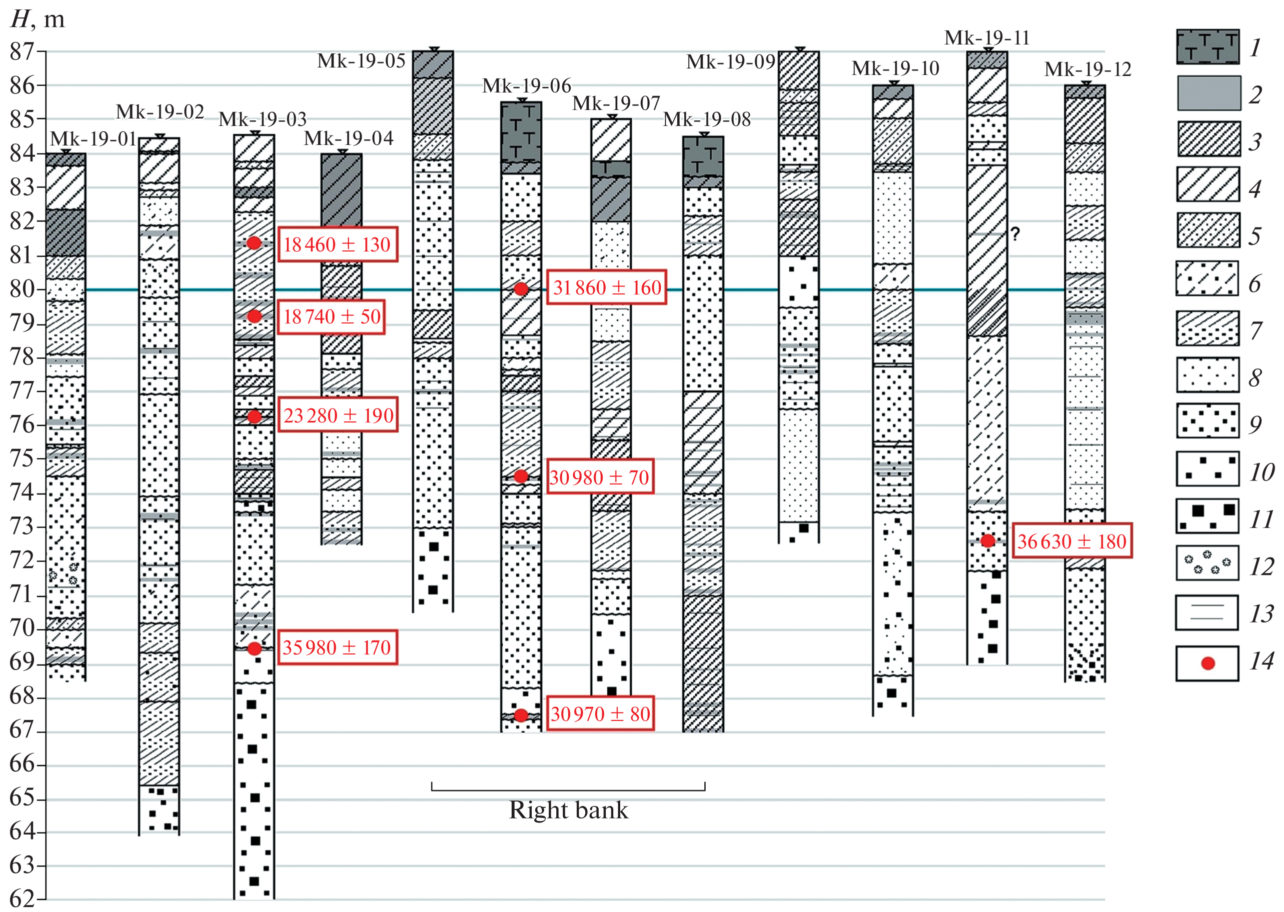


**Fig. 2.** Lithological structure of the boreholes in the Moksha River valley.

*1* – peat; *2* – peat content, organic interlayers; *loam: 3* – heavy, *4* – medium, light loam, *5* – sandy interlayers; *sand: 6* – silted, sandy loam, *7* – interlayering of sand and loam, *8* – fine, *9* – fine-medium, *10* – medium-coarse, *11* – coarse with inclusions of gravel; *12* – large carbonate concretions; *13* – interlayers of sand in loam, loam in sand; *14* – radiocarbon dates (calibrated). The blue line is the current low water level.

**Рис. 2.** Литологические колонки скважин в долине р. Мокши.

*1* – торф; *2* – оторфованность, прослои, богатые органикой; *суглинок: 3* – тяжелый, *4* – средний, легкий, *5* – опесчаненный; *песок: 6* – заиленный, супесь, *7* – переслаивание песка и суглинка, *8* – тонкозернистый, *9* – мелко-среднезернистый, *10* – средне-крупнозернистый, *11* – крупно-грубозернистый, с включениями гравия и гальки; *12* – крупные карбонатные конкреции; *13* – прослои песка в суглинке, суглинка в песке; *14* – радиоуглеродные даты (калиброванные). Голубой линией показан современный меженный урез воды в реке.

made for all boreholes in field. Organic material from alluvium of the river valley bottom was sampled to make radiocarbon (AMS) dating to find the time of river incision and aggradation, paleochannels' formation and infilling.

Radiocarbon (AMS) dating was done in the Laboratory of Radiocarbon Dating and Electronic Microscopy of the Institute of Geography (Russian Academy of Sciences, Moscow). Radiocarbon dates were calibrated (IntCal20) (Reimer et al., 2020) using the online version of OxCal 4.4 program (Bronk Ramsey, 2009).

## 3. RESULTS AND DISCUSSION

In our research we got data about morphology, geological structure and age of alluvial sediments from the infilling of the Moksha River valley bottom on the key site.

Summarizing the geomorphological data from the Moksha River valley the geomorphological map of the floodplain of the studied part of the valley was completed (fig. 1). Lithology of the studied boreholes can be found on the fig. 2.

*3.1. Morphology of the Moksha River valley on the key site.* Wide floodplain and two levels of terraces are present in the studied reach of the Moksha River valley. The height of the floodplain is from 1 to 6 m, of the first terrace – about 9–11 m, of the second terrace – 18–22 m. The width of the valley in the study area is about 14–16 km, but sometimes it can reach 20–22 km and more. The width of the floodplain is about 12–14 km.

**Table 1.** Dates of alluvium from the Moksha River valley infilling
**Таблица 1.** Даты по аллювию из заполнения долины р. Мокши

| Laboratory number | Borehole | Depth, m | $^{14}C$ Age*, years BP | Calibrated Age, years BP |
|---|---|---|---|---|
| IGAN-7719 | Mk-19-03 | 3.20–3.30 | 15075 ± 40 | 18460 ± 130 |
| IGAN-7720 | Mk-19-03 | 5.20–5.30 | 15410 ± 40 | 18740 ± 50 |
| IGAN-7723 | Mk-19-03 | 8.35–8.40 | 19320 ± 55 | 23280 ± 190 |
| IGAN-7728 | Mk-19-03 | 15.50–15.60 | 31630 ± 120 | 35980 ± 170 |
| IGAN-7721 | Mk-19-06 | 5.40–5.45 | 27950 ± 90 | 31860 ± 160 |
| IGAN-7724 | Mk-19-06 | 10.60–10.70 | 26690 ± 80 | 30980 ± 70 |
| IGAN-7729 | Mk-19-06 | 18.00–18.10 | 26660 ± 80 | 30970 ± 80 |
| IGAN-7727 | Mk-19-11 | 14.40–14.45 | 32320 ± 135 | 36630 ± 180 |

*Note:* * – all dates were made by total organic carbon (TOC).

Moksha has a meandering channel. At the studies site, the Moksha River has a wide floodplain with large and small paleochannels on its surface. Small paleochannels have the same parameters as the modern river channel: their width is about 100–150 m, wavelength is between 300–400 and 600–700 m. Large paleochannels' parameters are few times bigger: their width is about 250–300 m, wavelength is about 1500–2000 m (fig. 1).

*3.2. Geological structure of the paleochannels of the Moksha River valley on the key site.* The sediment infill of the Moksha River paleochannels is usually presented by the alternation of sands and loams, underlaid by medium and coarse sands (presumably, channel alluvium) (fig. 2). Usually under these channel alluvial sands one can find the continuing alternation of sands and loams, and only under this alternation – clear coarse channel sands. Apparently, all these sediments are different age generations of alluvial infilling of the valley (or infilling of paleochannels of different age). So, mostly it is unclear where the borders between different by age alluvial layers are situated.

Visual interpretation of the structure of the boreholes can also be difficult due to the sandy nature of the underlying pre-Quaternary deposits (Geologocheskaya..., 1998). Sometimes the contact with underlying marine sediments can be unclear.

Thereby, the following dating strategy was chosen. Instead of analyzing single samples in each borehole we decided to study in detail one borehole in a large paleochannel (Mk-19-06) and one borehole in a small paleochannel (Mk-19-03). We supposed that the results would make it possible to determine the borders between different alluvial units and the thickness of paleochannels' infilling. In addition we analyzed one more borehole in a big hollow between two fragments of the low terrace on the left bank of the Moksha River (Mk-19-11).

*3.3. Geochronology of the alluvial infilling of the Moksha River valley on the key site.* The borehole Mk-19-03 was situated in a small (modern-size) paleochannel (fig. 1). It seems that the infilling of this small paleochannel has thickness of less than 3 m and its age was not determined (because the upper part of this infilling did not contain the material suitable for dating). Up to the depth 2.3 m the infilling was represented mostly by loamy sediments, in the lower part – by interlayering of sand and loam. The deposits at the depth 3.2–3.3 m were dated 18460 ± 130 cal years BP, at the depth 5.2–5.3 m – 18740 ± 50 cal years BP (fig. 2, tabl. 1). These two dates correspond to the previous stage of the Moksha River valley development. Both dates were obtained from total organic carbon; dated layer (up to the depth of 5.9 m) is pure fine sand with interlayers of loam.

Below 5.9 m there were mostly medium sands with interlayers of loam and below 10.5 m the sands became coarse and the number of loam interlayers became much less. The alluvial sediments from the depth 8.4 and 15.5 m were dated to 23280 ± 190 and 35980 ± ± 170 cal years BP respectively.

The borehole Mk-19-06 was situated in a large paleochannel (macromeander) on the right bank of the Moksha River. The upper 1.7 m of the deposits were presented by peat, then up to the depth of 5.1 m the paleochannel's infilling was presented by medium and fine-medium sand with interlayers of loam. It seems that the infilling of this large paleochannel was not dated because there was no organic material in the upper 5 m (except for the peat layer in the top part of the paleochannel, but this peat is definitely much younger than the time of the paleochannel formation).

Below 5.1 m the next alluvial layer started. This layer was presented by loam with interlayers of sand or by sandy loam. Downwards the thickness of sandy interlayers increased and at the depth of 11 m sands started to prevail. Between 11 and 17 m sands from fine in the upper part of the strata become medium and then medium-coarse at the lower part (at depth about 17 m). These alluvial deposits were dated at the depths of 5.4, 10.6 and 18 m and showed very close ages:

31860 ± 160, 30980 ± 70 и 30970 ± 80 cal years BP respectively.

According to the topography and morphology of the valley at the key site the borehole Mk-19–11 was situated in a paleochannel of the Moksha River, or (more likely) in a paleo-valley of the Moksha tributary Tsna River. The second interpretation is supported by the large width of the hollow, much more than width of the large paleochannels of the Moksha River, and also by the rectilinear shape of the hollow, not typical for macromeanders of Moksha.

The structure of the borehole Mk-19-11 was the following. The upper 3.3 m were presented by interlayering of sandy loam, loam and fine sand. Then from 3.3 m to 8.3 m the thick layer of medium loam was described that changed to heavy loam in the lower part of the layer. From the depth of 8.3 m fine sand started, from 13.5 m it changed to medium sand and from 15.2 m – coarse sand with inclusions of gravel. The deposits on the depth 14.4 m were dated to 36630 ± ± 180 cal years BP. From the depth of 17 m another layer of loam with sand and gravel started; apparently this was bedrock underlying alluvial sediments.

## 4. DISCUSSION

*4.1. Interpretation of geomorphological, lithostratigraphical and geochronological data.* If we summarize all the data about structure and age of sediments of the valley infilling we can make the following interpretation. The results of dating may be divided into three groups: about 30–35 ka, about 23 ka and about 18–19 ka BP.

The alluvial sediments with the age 30–35 (40) ka BP (the end of MIS 3) were found at depths from 5.5 to 18 m in all three dated boreholes. That allows us to suggest that during this period the river was incised by more than 10–12 m relative to the modern river. This incision was probably driven by the increase of the river runoff associated with climatic changes as was established in the neighboring middle Dnieper basin (Panin et al., 2017). At the end of this epoch about 30 ka ago the infilling of the valley started, and continued in MIS 2 till the end of Late Glacial Maximum (20–23 ka ago).

The date from the borehole Mk-19-11 in the big hollow between two fragments of the low terrace shows that this hollow also was formed in that time. Presumably this hollow is the paleo-valley of Moksha's tributary Tsna that now flows into Moksha few km upstream.

The alluvial sediments dated to 23–23.5 ka BP from the depth of 8.4 m in the borehole Mk-19-03 correspond to the time of the valley infilling. Data from the other river valleys of the East European Plain show that the LGM time was characterized by intensive accumulation in the river valleys. In some valleys not only alluvial but also aeolian deposits were accumulated. These aeolian deposits formed aeolian covers and aprons on the river terraces (Matlakhova, Panin, 2015; et al.). However, such aeolian covers have not been found in the Moksha valley yet.

The next group of dates of about 18–18.5 ka BP from the borehole Mk-19-03 corresponds to the time of the macromeanders (large paleochannels) formation. Position of these dates compared to the others show that the incision of the river was not so deep as it was at the end of MIS 3. It's obvious that these dated sediments correspond to the time of the large paleochannels meandering, but the upper part of paleochannel's infilling was reworked by small (modern-size) paleochannels in the Holocene. This explains the presence of the small paleochannel on the surface of the floodplain here.

The ages of large paleochannels starting from about 18.5 ka BP were established in many river valleys of the East European Plain (Panin et al., 2001; Panin et al., 2011; Sidorchuk et al., 2011, Panin et al., 2013; Panin et al., 2017). For example our previous studies in Don River basin (in Upper Don, Khoper and Vorona river valleys) showed the ages of large paleochannels formation between 18.5 and 12 ka ago (Panin et al., 2013, Matlakhova et al., 2019; et al.).

The presence on macromeanders in the river valleys of the temperate climate zone of the Northern Hemisphere is an important paleohydrological phenomenon that was studied actively all over the world for the last few decades (Dury, 1964; Starkel, 1995; Vandenberghe, 2002; Sidorchuk et al., 2008; Panin et al., 2013; Vandenberghe, Sidorchuk, 2020; et al.). According to the existing ideas such macromeanders formed in the periglacial zone of the Last Glaciation under conditions of extremely high spring runoff. These macromeanders are several times larger than the modern river channels. This is explained by the specific hydrological regime of that time. It is considered that the river runoff was very uneven during the year. The predominance of winter precipitation led to high spring floods, and permafrost prevented filtration of the water that led to the increase of the surface runoff. The parameters of the large channels formed at this time were determined by the maximal spring runoff of that period (Sidorchuk et al., 2008).

Thus, big paleochannels of the Moksha River correspond to the period of high river runoff between 18.5 and 12 ka BP, which is typical for the East-European Plain (Panin et al., 2001; Panin et al., 2011). Small (modern-size) paleochannels formed in Holocene and changed the previous topography of the floodplain (also sometimes overlaying macromeanders). The lowest runoff and formation of smallest meanders in the rivers of central Russian Plain occurred in the Mid Holocene (Sidorchuk et al., 2012; Panin et al., 2014). Significant variations of river runoff were detected in the last Millennium (Golosov, Panin, 2006), but they are not exposed in the morphology of the Moksha valley.

*4.2. Late Pleistocene History of the Moksha River valley development.* Data analysis allowed us to make the following reconstructions.

In the interval between 40–30 ka ago, the river incised deeper than the present level. It is confirmed by dates of the alluvial sediments from the valley infilling. The tectonic situation in the region was stable during the analyzed period, so we can be sure that the incision of the river was connected with the increase of the river runoff associated with climatic changes.

Then the incision was replaced by the filling of the valley caused by the drying up of the climate and a lowering of the river runoff, which was more significant on the period of the Last Glacial Maximum (LGM, 23–20 ka ago). The previous studies in the river valleys of the central part of the East European Plain show that in some river valleys of the region aeolian covers and aprons on the river terraces' surfaces were formed.

Starting from 18.5 ka ago there was again a significant increase of the river runoff, which led to the formation of macromeanders and widening of the valley bottom. Modern wide high floodplain was formed at that time. Large paleochannels are well preserved in the topography of the floodplain on the key site of the Moksha River valley. Such macromeanders are widespread on the floodplains and low terraces in the river valleys of the East European Plain (Sidorchuk et al., 2000; Sidorchuk et al., 2011; Matlakhova, Panin, 2015; et al.) and are usually dated Late Glacial time (Panin et al., 2013; Matlakhova et al., 2019; et al.).

The Holocene was characterized by a decrease in runoff and channel parameters (width and wavelength) and narrowing of the meandering belt of the river. Despite this fact the Moksha River meanders actively nowadays, that is confirmed by the topography of the modern floodplain.

## 5. CONCLUSIONS

Summarizing all the data we can conclude the following.

The alternation of high and low river runoff was typical for the Moksha River valley in the end of the Late Pleistocene. This led to the alternation of river incision and aggradation in the valley.

High river runoff and incision of the river were characteristic features for periods 40–30 ka ago and 18.5–12 ka ago. At the second of these periods (18.5–12 ka ago) large paleochannels (macromeanders) were formed. These macromeanders prove the fact of a significant increase in the river runoff at this time.

Low river runoff and aggradation in river valleys were characteristic features for the period between ~30 and 18.5 ka ago. The most significant decrease in the river runoff was related to cryoarydic conditions of the LGM time (23–20 ka ago). The Holocene was also characterized by a decrease in runoff parameters in general. The river runoff in the Holocene was not constant too, but the fluctuations and the runoff in general were lower than in Late Pleistocene.

# THE STRUCTURE OF THE MOKSHA RIVER FLOODPLAIN AS A KEY TO THE LATE PLEISTOCENE HISTORY OF THE VALLEY DEVELOPMENT

**E. Yu. Matlakhova[a,#] and V. Yu. Ukraintsev[b,c]**

[a] *Lomonosov Moscow State University, Faculty of Geography, Moscow, Russia*

[b] *Institute of Geography RAS, Moscow, Russia*

[c] *Institute of Water Problems RAS, Moscow, Russia*

[#] *E-mail: matlakhova_k@mail.ru*

The noticeable geomorphic feature of the Moksha River valley (middle Oka River basin) is the occurrence of numerous large palaeomeanders that evidence a several fold rise of river discharges. To establish the history of valley development, the key study in the lower part of the Moksha River valley was organized between the mouth of the Tsna River and the mouth of the Moksha River. Based on the results of mechanical coring, geomorphological and lithological analysis, and radiocarbon AMS-dating we reconstructed the following main stages of the Moksha River valley development in the end of the Late Pleistocene. 1) About 40–30 ka ago the increase of the river runoff associated with climatic changes led to the river incision deeper than the present level. 2) After that the drying up of the climate and a lowering of the river runoff led to the filling of the valley (the strongest drying was in LGM time, about 23–20 ka ago). 3) Between 18.5–12 ka ago the river runoff increased and caused macromeanders formation and widening of the valley bottom. 4) In the Holocene runoff decreased again and the channel parameters became close to the modern ones.

*Keywords:* macromeanders (large paleochannels), the history of river valleys development, Pleistocene paleogeography, fluvial geomorphology

## ACKNOWLEDGMENTS

This study is supported by Russian Science Foundation (project No. 19-17-00215 "Research and modeling of possible scenarios for the formation of extreme paleohydrological phenomena in the Caspian basin after the Last Glacial Maximum"). Data processing was performed under the facilities of the Institute of Geography RAS, taskforce AAAA-A19-119021990091-4 (FMGE-2019-0005), and the Department of Geomorphology and Paleogeography of Moscow State University, taskforce 121040100323-5.


## REFERENCES


Dashevskij V.V. and Sychkin N.I. (Eds.) *Geologicheskaya karta dochetvertichnykh otlozhenii Ryazanskoi oblasti. Masshtab 1:500 000* (Geological map of pre-Quaternary deposits of the Ryazan region. Scale 1:500 000). Moscow: Ministerstvo prirodnykh resursov Rossiiskoi federacii (Publ.), 1998. 6 p. (in Russ.)

Dury G.H. General theory of meandering valleys. *U.S. Geological Survey professional paper*. 1964. Vol. 452-A. 67 p.

Golosov V. and Panin A. Century-scale stream network dynamics in the Russian Plain in response to climate and land use change. *Catena*. 2006. Vol 66 (1–2). P. 74–92. https://doi.org/10.1016/j.catena.2005.07.011

Matlahova E.Yu. and Panin A.V. The role of aeolian processes in the development of the river valleys in the central of the East European Plain in the Late Valdai. *Geomorfologicheskie resursy i geomorfologicheskaya bezopasnost': ot teorii k praktike. Sbornik materialov Vserossiiskoi konferentsii "VII Shchukinskie chteniya"*. Moscow: MAKS Press (Publ.), 2015. P. 459–462. (in Russ.)

Matlakhova E.Yu., Panin A.V., Belyaev V.R., and Borisova O.K. *Razvitie doliny Verkhnego Dona v kontse pozdnego pleistotsena* (The Upper Don River valley evolution in the end of the Late Pleistocene). *Vestnik Moskovskogo Universiteta. Seriya 5. Geografiya*. 2019. No. 3. P. 83–92. (in Russ.)

Panin A., Adamiec G., Buylaert J.-P., Matlakhova E., Moska P., and Novenko E. Two Late Pleistocene climate-driven incision/aggradation rhythms in the middle Dnieper River basin, west-central Russian Plain. *Quaternary Science Reviews*. 2017. Vol. 166. P. 266–288. https://doi.org/10.1016/j.quascirev.2016.12.002

Panin A.V., Adamiec G., Arslanov K.A., Bronnikova M.A., Filippov V.V., Sheremetskaya E.D., Zaretskaya N.E., and Zazovskaya E.P. Absolute chronology of fluvial events in the Upper Dnieper river system and its palaeogeographic implications. *Geochronometria*. 2014. No. 41 (3). P. 278–293. https://doi.org/10.2478/s13386-013-0154-1

Panin A.V., Sidorchuk A.Yu., and Chernov A.V. *Osnovnye etapy formirovaniya poim ravninnykh rek Severnoi Evrazii* (The Main Stages of the floodplains' formation in the plain river valleys of the Northern Eurasia). *Geomorfologiya*. 2011. No. 3. P. 20–31. (in Russ.). https://doi.org/10.15356/0435-4281-2011-3-20-31

Panin A.V., Sidorchuk A.Yu., and Vlasov M.V. *Moshchnyi pozdnevaldaiskii rechnoi stok v basseine Dona* (Great Late Glacial runoff in Don river basin). *Izvestiya RAN. Seriya geograficheskaya*. 2013. No. 1. P. 118–129. (in Russ.). https://doi.org/10.15356/0373-2444-2013-1-118-129

Panin A.V., Sidorchuk A.Yu., Baslerov S.V., Borisova O.K., Kovaliyuh N.N., and Sheremetskaya E.D. *Osnovnye etapy istorii rechnykh dolin tsentra Russkoi ravniny v pozdnem valdae i golocene: rezul'taty issledovanii v srednem techenii r. Seim* (Main events in the histroy of river valleys in the central Russian Plain in the Late Weichselian and Holocene: the middle Sejm River case study). *Geomorfologiya*. 2001. No. 2. P. 19–34 (in Russ.)

Ramsey C.B. Bayesian analysis of radiocarbon dates. *Radiocarbon*. 2009. No. 51 (1). P. 337–360. https://doi.org/10.1017/S0033822200033865

Reimer P.J., Austin W.E.N., Bard E., Bayliss A., Blackwell P.G., Ramsey C.B., Butzin M., Cheng H., Edwards R.L., Friedrich M., Grootes P.M., Guilderson T.P., Hajdas I., Heaton T.J., Hogg A.G., Hughen K.A., Kromer B., Manning S.W., Muscheler R., Palmer J.G., Pearson C., van der Plicht J., Reimer R.W., Richards D.A., Scott E.M., Southon J.R., Turney C.S.M., Wacker L., Adolphi F., Büntgen U., Capano M., Fahrni S.M., Fogtmann-Schulz A., Friedrich R., Köhler P., Kudsk S., Miyake F., Olsen J., Reinig F., Sakamoto M., Sookdeo A., and Talamo S. The IntCal20 Northern Hemisphere Radiocarbon Age Calibration Curve (0–55 cal kBP). *Radiocarbon*. 2020. No. 62 (4). P. 725–757. https://doi.org/10.1017/RDC.2020.41

Sidorchuk A., Panin A., and Borisova O. Surface runoff to the Black Sea from the East European Plain during Last Glacial Maximum–Late Glacial time. *Geological Society of America Special Paper*. 2011. Vol. 473. P. 1–25. https://doi.org/10.1130/2011.2473(01)

Sidorchuk A.Yu., Panin A.V., and Borisova O.K. Climate-induced changes in surface runoff on the North-Eurasian plains during the Late Glacial and Holocene. *Water Resources*. 2008. Vol. 35. No. 4. P. 386–396. https://doi.org/10.1134/S0097807808040027

Sidorchuk A.Yu., Borisova O.K., and Panin A.V. *Pozdnevaldaiskie paleorusla rek Russkoi ravniny* (Large palaeochannels of Late Weichselian age in the Russian Plain). *Izvestiya RAN. Seriya geograficheskaya*. 2000. No. 6. P. 73–78 (in Russ.).

Sidorchuk A.Yu., Panin A.V., and Borisova O.K. River Runoff Decrease in North Eurasian Plains during the Holocene Optimum. *Water Resources*. 2012. Vol. 39. No. 1. P. 69–81. https://doi.org/10.1134/S0097807812010113

Starkel L. The place of the Vistula river valley in the late Vistulian – early Holocene evolu-tion of the European valleys. *Palaeoclimate Research*. 1995. Vol. 14. P. 75–88.

Vandenberghe J. The relation between climate and river processes, landforms and deposits during the Quaternary. *Quaternary International*. Vol. 91. No. 1. 2002. P. 17–23. https://doi.org/10.1016/S1040-6182(01)00098-2

Vandenberghe J. and Sidorchuk A. Large Palaeomeanders in Europe: Distribution, Formation Process, Age, Environments and Significance. *Palaeohydrology. Geography of the Physical En-vironment*. Springer Cham. 2020. P. 169–186. https://doi.org/10.1007/978-3-030-23315-0_9

**EDN:** CGOUBF
*ГЕОМОРФОЛОГИЯ, 2022, том 53, № 5, с. 134–143*

## ПРОБЛЕМЫ ФЛЮВИАЛЬНОЙ ГЕОМОРФОЛОГИИ

*УДК 551.435.1:551.89 (571.56)*

# ПАЛЕОРЕКОНСТРУКЦИЯ ДОЛИНЫ НИЖНЕЙ ЛЕНЫ В ГОЛОЦЕНЕ И ПОЗДНЕМ НЕОПЛЕЙСТОЦЕНЕ: НОВЫЕ ДАННЫЕ, ПРОТИВОРЕЧИЯ И ПРОБЛЕМЫ

**© 2022 г. С. А. Правкин[1,*], Д. Ю. Большиянов[1]**
*[1]Арктический и антарктический научно-исследовательский институт, Санкт-Петербург, Россия*
**E-mail: s.pravkin@aari.ru*
Поступила в редакцию 16.06.2022 г.
После доработки 28.06.2022 г.
Принята к публикации 15.07.2022 г.

Река Лена вместе со своими притоками входит в число крупнейших речных систем мира. В течение трех полевых сезонов в долине Нижней Лены от устья Алдана до “Ленской трубы” было исследовано 18 обнажений террас различного уровня, сложенных аллювиальными отложениями. Высоты террас определялись по топографическим картам, при помощи метода нивелирования и GPS-съемки. Обнажения были описаны в полевых условиях с отбором образцов для датирования радиоуглеродным методом и методом инфракрасной стимулированной люминесценции (IR-OSL). Суммарно было получено 26 радиоуглеродных и IR-OSL значений возрастов отложений. Нижняя пойма наиболее детально была обследована на участке от устья Алдана до устья Вилюя, где ее высота составляет от 5–6 до 8–9 м. Отложения высокой поймы были изучены на отрезке между устьями Алдана и Вилюя, в районе устья Дянышки, а также на участке между селами Сиктях и Кюсюр. Ее высота варьирует от 6–10 до 15–16 м. Отложения первой террасы (7–15 м) и второй террасы (20–23 м) наиболее подробно исследованы в районе устья Дянышки. На ряде участков (нижнее течение Дянышки, вблизи устьев Менкере и Натары) были датированы отложения более высоких террас. Изучение и датирование отложений, слагающих пойму и первую террасу в долине Нижней Лены, подтверждают, что их формирование было обусловлено колебаниями уровня моря в голоцене и в конце позднего плейстоцена, так же, как и в дельте Лены. Результаты датирования аллювиальных отложений в обнажениях 40–60-метровых террас методом инфракрасной стимулированной люминесценции противоречат ранее принятым в 3-й четверти XX столетия представлениям о возрасте соответствующих террас. Оледенения Верхоянского хребта не могли повлиять на конфигурацию долины Лены, так как горные ледники не достигали Лены с конца среднего плейстоцена.

*Ключевые слова:* долина Нижней Лены, пойма, терраса, голоцен, поздний неоплейстоцен, датирование отложений
**DOI:** 10.31857/S0435428122050133

## 1. INTRODUCTION

The Lena River with its tributaries is one of the largest river systems in the world. The Lena River valley in the middle and lower reaches is completely located on the territory of the Yakutia (Russian Far East). The region has extremely difficult conditions for living and economic development due to the subarctic continental climate and the distribution of continuous permafrost. The Lena River is one of the most important transport arteries of Yakutia. Therefore, the study of the Lena River banks, its geological structure, morphology, history of its development is strategically important for the development of the region.

There is a relatively small number of published investigations dedicated to geomorphological structure and paleogeographic reconstruction of the Lower Lena Valley or to its separate parts, with the exception of the Lena River Delta. Most of them were published in the 3rd quarter of the 20th century, when ideas about the evolution of the Lena River Valley were based on the relative dating, spore and pollen analysis and paleofaunal reconstructions. Even then it was clear that the Lower Lena Valley has a vastly complex structure. Over time, it became clear that the existing ideas needed to be clarified on the base of new dating methods and new accumulated actual material.

From 1998 to the present, a Russian-German scientific expedition has been working in the Lena Delta. It has been organized by the Arctic and Antarctic Research Institute (St. Petersburg, Russia) and the Alfred Wegener Institute (Potsdam, Germany). Geomorphological and paleogeographic studies formed one of the central parts in the programs of this multidisciplinary expedition. Detailed results of geomor-

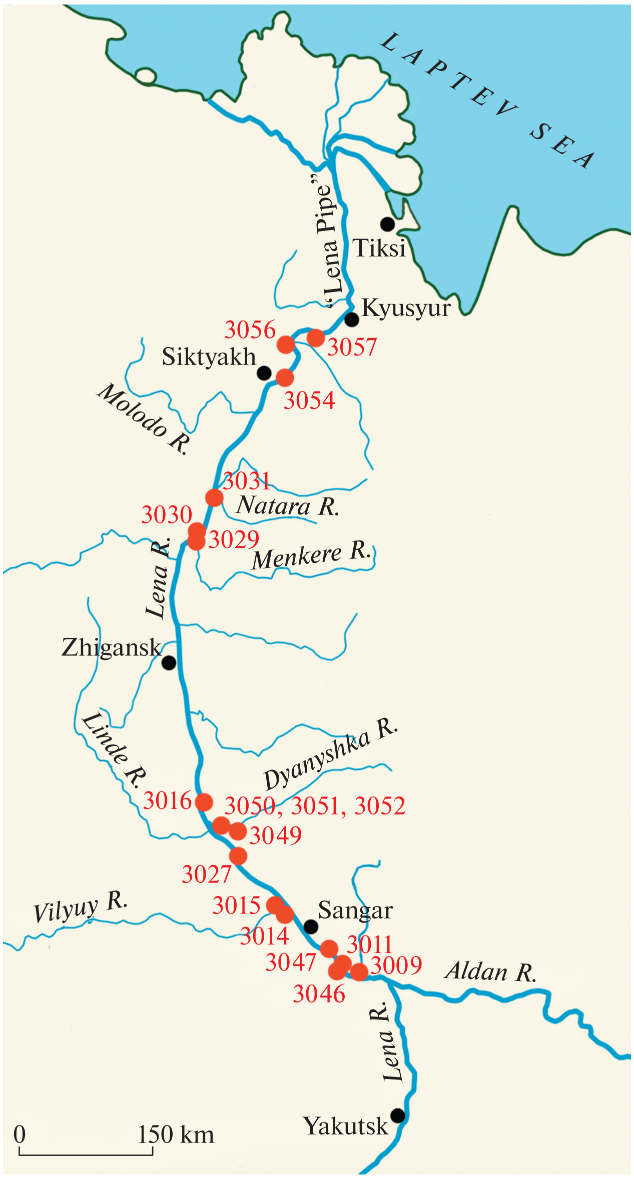


**Fig. 1.** Study area. Red dots and numbers are the studied outcrops and their IDs. Black dots are the settlements.

**Рис. 1.** Область исследования. Красными точками указаны изученные обнажения с их номерными обозначениями. Черные точки – населенные пункты.

phological studies of the Lena River Delta are presented in the article and in the monograph devoted to the origin and evolution of the delta (Bolshiyanov et al., 2013; Bolshiyanov et al., 2015). The marine factors of delta formation have been identified in sufficient detail. On the contrary, the role of riverine factors is not entirely clear. Therefore, in recent years, the idea of a comprehensive geomorphological study of the Lena River Valley has appeared. The main task of such a study became the paleogeomorphological reconstruction of the Lena River Valley from Yakutsk to the Delta as a single system during the Late Pleistocene-Holocene.

## 2. MATERIALS AND METHOD

To achieve the objective, three expeditions were organized in 2016, 2017 and 2019. During this period, 18 outcrops of alluvial deposits on terraces of different levels of the Lower Lena Valley were studied. The location of the outcrops is shown in fig. 1, and their coordinates are presented in tabl. 1. Terrace heights were determined using topographic maps, leveling and GPS survey. The outcrops were described in the field with sampling for radiocarbon dating and infrared stimulated luminescence (IR-OSL) method. These methods have been used to determine the depositional age of peat and fossil plant remains, as well as the depositional age of sands.

The easiest way to study the terraces is to explore them by moving along the river, but directly along the channels, the terraces can be traced locally and discontinuously. In vast valley, it is necessary to sail upstream along the tributaries of the Lena River to study terraces and deposits. In addition, satellite images and topographic maps should be deciphered, and the literature available on the problem should be analyzed.

Radiocarbon samples preparation and age determination were carried out in the Köppen laboratory of the Saint Petersburg State University (Russia). Lithium carbide was synthesized from a pre-cleaned sample by sintering with metallic lithium (Arslanov, 1987). Benzene was synthesized from lithium carbide via acetylene. The radiocarbon content in the benzene sample was determined on a liquid scintillation spectrometer "Quantululus-1220". The radiocarbon and calibrated age of the sample was calculated according to the results of measuring the activity of radiocarbon. The calibrated age values are based on the "OxCal 4.2" calibration program (Ramsey et al., 2010) and IntCal13 calibration curve (Reimer et al., 2013).

The IR-OSL age determination was carried out in the Research Laboratory for Quaternary Geochronology of the Tallinn University of Technology (Estonia). The samples were prepared for the luminescence analysis according to standard laboratory procedures (Molodkov, Bitinas, 2006).

A total of 26 radiocarbon and IR-OSL ages were obtained. The results are presented in tabl. 1.

## 3. RESULTS AND DISCUSSION

The floodplain in the Lower Lena Valley consists of low and high levels. The low floodplain has a predominantly fragmentary distribution. Generally, it occupies low river islands and areas near the mouths of the Lena tributaries. We have studied in more detail three outcrops of the low floodplain (3009, 3014 and 3015) in the section of the Lena River Valley between the mouths of the Aldan River and Vilyuy River, where it has a relative height from 5–6 to 8–9 m.

The outcrop 3009 is located at the mouth of the Belyanka River. It is a small right tributary of the

Lena River about 40 km downstream of the Aldan River. The outcrop is a vertical scarp with 4.3 m high. The lower part consists of a well-rounded, light gray and yellow gravel. The thickness of the layer is 0.8 m. The upper part of the outcrop consists of gray silty and sandy overbank deposits. The lower 0.5 m of this layer is rich in plant remains. The radiocarbon age of twigs near the contact with the active channel gravel is 470 ± 50 years BP (LU-8314).

The outcrops 3014 and 3015 are located at the mouth of the Vilyuy River: on the right bank and on the left bank. Both exposures are 9 m high. They are represented by horizontal bedding overbank sands containing plant remains. The radiocarbon age of buried wood from a height of 6.5 m on the outcrop 3014 is less than 200 years BP (LU-8660). The radiocarbon ages of small twigs from a height of 2.7 m and buried wood from a height of 3.0 m are 890 ± 70 years BP (LU-9020) and 340 ± 30 years BP (LU-8660) on the outcrop 3015.

Downstream from Zhigansk village, the height of the low floodplain increases to 9–12 m. We studied only two locations: Duoldanga-Aryta Island (the outcrop 3030) and Anna-Aryta Island (the outcrop 3054). Duoldanga-Aryta Island is a small river island located along the left bank of the Lena River approximately 150 km downstream from Zhigansk village. It has a height of 10 m. Radiocarbon dating of plant remains in the sediments of the island indicates that it continues to form in the present times. Anna-Aryta Island is one of the largest river islands located downstream from Siktyakh village to the "Lena Pipe". Central part of the island is a high floodplain with oxbow lakes, but its periphery should be attributed to the low floodplain not less than 7 m high. Radiocarbon age of plant remains collected from the edge of the outcrop is 230 ± ± 50 yr BP (LU-9402).

Compared to the low floodplain, the high floodplain is more widespread in the Lower Lena Valley. First of all, it occupies large massifs of river archipelagos, the islands in which are separated by numerous small branches of the Lena in areas along the left bank of the Lena River and locally along the right bank from the mouth of the Aldan River to the mouth of the Lungkha River, mainly along the left bank from the mouth of the Vilyuy River to the mouth of the Ulegir River, along the right bank from the mouth of the Oruchan River to the mouth of the Sobolokh-Mayan River and along the left bank from the mouth of the Khoruongka River to the Siktyakh village. The width of the high floodplain can reach about 30 km. In addition, we identified fragmentary narrow sections of a high floodplain along both banks of the Lena River between the villages of Siktyakh and Kyusyur. The height of the high floodplain from the mouth of the Aldan River to the "Lena pipe" increases from 6–10 to 15–16 m. Segmented-ridged and parallel-ridged floodplain relief is typical for the surface of high floodplain. In contrast to the low floodplain, the surface of the high floodplain is always covered by taiga and drift wood along the Lena main channel and its branches, which indicates the flooding of this surface in some years.

The high floodplain deposits have been studied in several key sections (fig. 2). The first section is located between the mouth of the Belyanka River and the Sangar village in a large river archipelago stretched along the right bank of the Lena River and separated from it by the Tab-Ary channel.

The outcrop 3011 is located on the Kurus Island, the left bank of the Tab-Ary channel. It has a height of 5 m above a sand river beach about 1 m high. The lower part of the outcrop (1–2.9 m above the river) is a talus. The middle part (2.9–4.3 m) is a horizontally layered silt strata with interlayers of sand and plant remains (small twigs and trunks). The upper part (4.3–6 m) is a horizontally layered oberbank sands and silts and cross-layered channel sands. A small trunk gave the radiocarbon age of 2460 ± 40 years BP (LU-8658) from a height of 3 m.

The outcrop 3046 is located on the left opposite bank of the Lena main channel. It had a height of 2.5 m at the time of observation at the end of the flooding processes. The edge of the outcrop has a height of approximately 6 m above the low-water level. The outcrop is composed by overbank deposits: horizontally layered sands, silt and plant remains. The plant remains gave the radiocarbon age of 2520 ± 70 years BP (LU-9396).

The Sya-Ary Island is located 20 km downstream from the mouth of the Tab-Ary channel near the right bank of the Lena (opposite the mouth of the Balamakan River). The outcrop 3047 was studied here. It has a similar height and similar structure to the outcrop 3046. The plant remains gave the radiocarbon age of 1530 ± 110 years BP (LU-9397).

In the section from the mouth of the Lyampushka River to the mouth of the Dyanyshka River, the Lena main channel expands sharply. The branching of river channels is the reason for the existence of a large river archipelago here. One of the largest islands here is the Ulakhan-Kistyakh. We attribute the level of its surface to a high floodplain. We studied the outcrop 3027 7 m high at the top of this island. It is composed of overbank deposits, less often channel deposits. There are horizontally bedded and cross-bedded fine-grained and medium-grained sands with interlayers and lenses of silt and a high content of plant remains in the scarp of the island. The plant remains gave the radiocarbon ages of 2810 ± 90 years BP (LU-2937) from a height of 2.1 m, 2620 ± 120 years (LU-8936) from a height of 2.6 m, and 1670 ± 90 years BP (LU-8935) from a height of 4.3 m.

In the section between the villages of Siktyakh and Kyusyur, we found that the upper part of the high floodplain is composed of layering organic and miner-

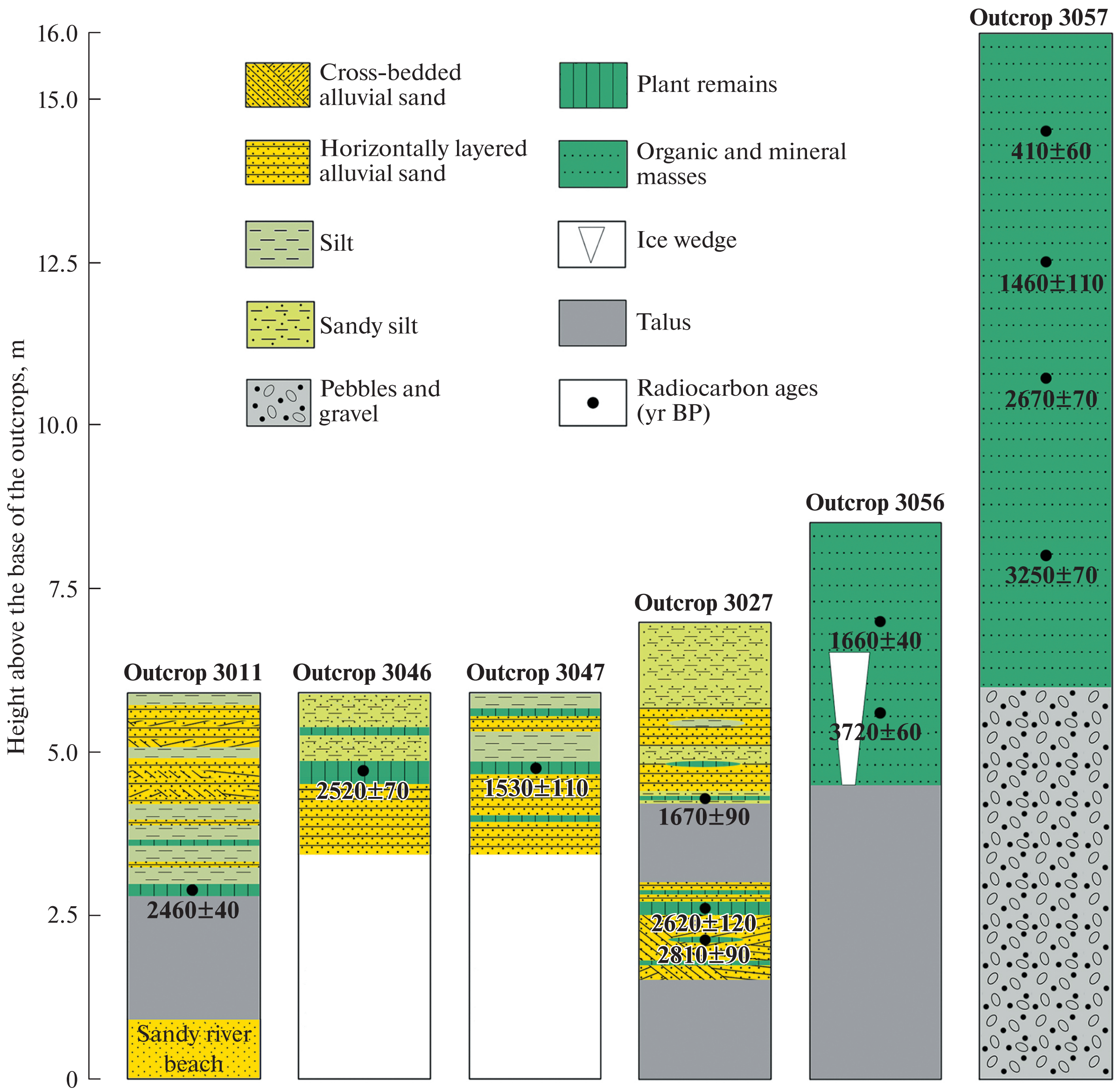


**Fig. 2.** Lithological logs of the high floodplain outcrops and radiocarbon ages of organic remains.
**Рис. 2.** Литологическое строение обнажений высокой поймы и радиоуглеродный возраст органических остатков.

al masses (strata of horizontally layered sands, silt and plant remains). Such kind of deposits is typical for the Lena River Delta complex (Bolshiyanov et al., 2013; Bolshiyanov et al., 2015). We studied two outcrops. The outcrop 3056 is located on the left bank of the Lena River near the Sutukilakh Island, 230 km upstream from the top of the Lena Delta. It has a height of 8–9 m. Layering organic and mineral deposits are 4 m thick and are penetrated by ice wedges. Radiocarbon ages of plant remains from a height of 5.6 m is 3720 ± ± 60 years (LU-9405) and from a height of 7.0 m is 1660 ± 40 years BP (LU-9404).

The outcrop 3057 was studied approximately 60 km downstream on the right bank of the Lena River. It has a height of 16 m. The bottom of the outcrop is the lower part of a high floodplain. The upper part, 10 m thick, is composed by organic and mineral masses. The radiocarbon ages of plant remains are 3250 ± 70 years BP (LU-9409) from a height of 2 m above the bench, 2670 ± 70 years BP (LU-9408) from a height of 4.8 m, 1460 ± 110 years BP (LU-9407) from a height of 6.5 m and 410 ± 60 years BP (LU-9406) from a height of 8.5 m.

The results of radiocarbon dating the organic and mineral masses composing the 1st terrace of the Lena River Delta (Bolshiyanov et al., 2013; Bolshiyanov et al., 2015) indicate that they accumulated in the same period when the deposits of the high floodplain were formed in the Lower Lena valley. During the Holocene, the Laptev Sea level repeatedly fluctuated up to

**Table 1.** Radiocarbon and IR-OSL dating results. The list is sorted in the order of location of the outcrops downstream of the Lena River
**Таблица 1.** Результаты радиоуглеродного и IR-OSL датирования по обнажениям, приведенным в списке сверху вниз по течению Лены

| Outcrop ID | Location | Coordinates | Lab No. | Sample type | $^{14}C$ ages | $^{14}C$ ages calibrated | IR-OSL ages |
|---|---|---|---|---|---|---|---|
| 3009 | Mouth of the Belyanka River | N 63°31′03.8″ E 128°49′36.3″ | LU-8314 | Twigs | 470 ± 50 | 510 ± 50 | – |
| 3011 | Kurus Island | N 63°39′37.6″ E 128°25′19.4″ | LU-8658 | Trunk | 2460 ± 40 | 2550 ± 100 | – |
| 3046 | Left bank of the Lena River, opposite the Tab-Ary channel | N 63°29′37.9″ E 128°18′22.1″ | LU-9396 | Plant remains | 2520 ± 70 | 2580 ± 100 | – |
| 3047 | Sya-Ary Island | N 63°53′03.3″ E 127°43′35.1″ | LU-9397 | Plant remains | 1530 ± 110 | 1450 ± 110 | – |
| 3014 | Mouth of the Vilyuy River, right bank | N 64°21′26.6″ E 126°25′48.5″ | LU-8660 | Wood | <200 | <200 | – |
| 3015 | Mouth of the Vilyuy River, left bank | N 64°22′30.6″ E 126°24′08.4″ | LU-9020 | Twigs | 890 ± 70 | 820 ± 70 | – |
| | | | LU-8661 | Wood | 340 ± 30 | 390 ± 50 | – |
| 3027 | Ulakhan-Kistyakh Island | N 64°47′31.1″ E 125°23′03.7″ | LU-8937 | Plant remains | 2810 ± 90 | 2950 ± 110 | – |
| | | | LU-8936 | Plant remains | 2620 ± 120 | 2690 ± 160 | – |
| | | | LU-8935 | Plant remains | 1670 ± 90 | 1580 ± 110 | – |
| 3049 | Lower reaches of the Dyanyshka River | N 65°00′45.2″ E 125°05′57.7″ | RLQG 2643–060 | Sand | – | – | 64500 ± 4500 |
| 3050 | Lower reaches of the Dyanyshka River | N 65°02′02.0″ E 125°03′22.9″ | RLQG 2644–060 | Sand | – | – | 6000 ± 400 |
| 3051 | Lower reaches of the Dyanyshka River | N 65°02′16.3″ E 125°02′42.0″ | LU-9399 | Twigs | 12030 ± 110 | 13900 ± 140 | – |

**Table 1.** Окончание

| Outcrop ID | Location | Coordinates | Lab No. | Sample type | $^{14}C$ ages | $^{14}C$ ages calibrated | IR-OSL ages |
|---|---|---|---|---|---|---|---|
| 3052 | Lower reaches of the Dyanyshka River | N 65°02′12.8″ E 125°01′55.4″ | LU-9400 | Peat | 9710 ± 60 | 11 090 ± 120 | – |
| | | | LU-9401 | Peat | 5740 ± 50 | 6540 ± 60 | – |
| 3016 | Right bank of the Lena River, 10 km downstream from the mouth of the Dyanyshka River | N 65°05′20.6″ E 124°47′42.8″ | RLQG 2466–067 | Sand | – | – | 6900 ± 600 |
| 3029 | ~3 km downstream from of the mouth of the Menkere River | N 68°01′58.0″ E 123°19′38.6″ | RLQG 2544–118 | Sand | – | – | 23 600 ± 1900 |
| 3030 | Duoldanga-Aryta Island | N 68°06′04.1″ E 123°19′43.4″ | LU-8938 | Plant remains | Recent | Recent | – |
| 3031 | Mouth of the Natara River | N 68°24′06.8″ E 123°55′27.9″ | RLQG 2552–118 | Sandy silt | – | – | 68 800 ± 5600 |
| 3054 | Anna-Aryta Island | N 69°58′04.1″ E 125°35′48.3″ | LU-9402 | Plant remains | 230 ± 50 | 230 ± 120 | – |
| 3056 | Left bank of the Lena River, between the villages of Siktyakh and Kyusyur | N 70°16′40.8″ E 125°58′09.8″ | LU-9405 | Plant remains | 3720 ± 60 | 4070 ± 90 | – |
| | | | LU-9404 | Plant remains | 1660 ± 40 | 1560 ± 60 | – |
| 3057 | Right bank of the Lena River, between the villages of Siktyakh and Kyusyur | N 70°29′47.6″ E 126°42′39.3″ | LU-9409 | Plant remains | 3250 ± 70 | 3480 ± 80 | – |
| | | | LU-9408 | Plant remains | 2670 ± 70 | 2800 ± 80 | – |
| | | | LU-9407 | Plant remains | 1460 ± 110 | 1380 ± 110 | – |
| | | | LU-9406 | Plant remains | 410 ± 60 | 430 ± 70 | – |

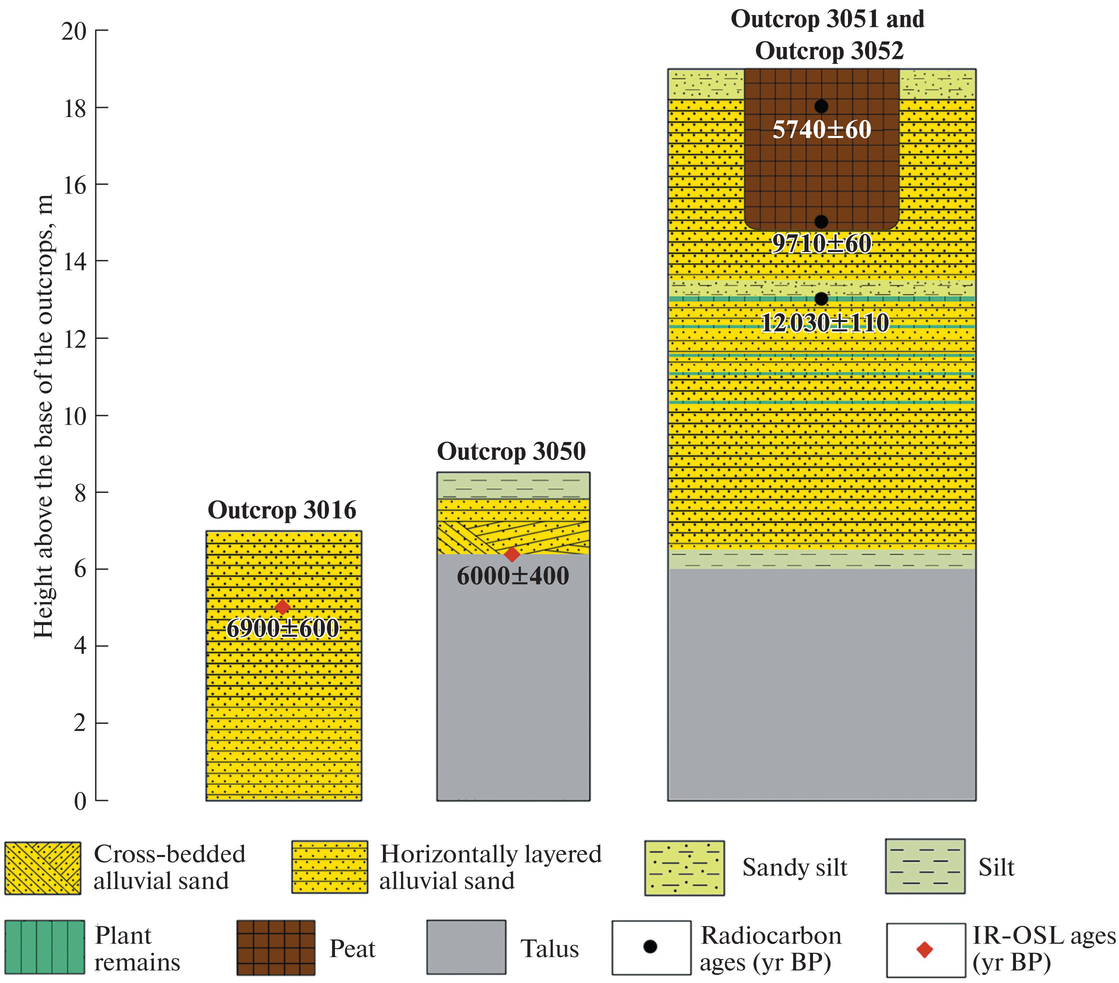


**Fig. 3.** Lithological logs of the 1st and 2nd terrace outcrops. Radiocarbon ages of organic remains and IR-OSL ages of alluvial sand deposits.

**Рис. 3.** Литологическое строение обнажений первой и второй террас. Радиоуглеродный возраст органических остатков и IR-OSL-возраст аллювиальных песков.

a height of 7–8 m above the present level (Bolshiyanov et al., 2013; Bolshiyanov et al., 2015). This is the reason for the accumulation of thick strata of specific ingressive organic and mineral deposits in the Lena River Delta.

Identification of terraces in the Lower Lena valley is a more difficult problem, because they are often separated from the river by large floodplain areas and are difficult to explore. M.N. Alekseev identified 7 terraces above the floodplain with a height of 15–16, 25–32, 40–45, 50–60, 65–80, 90–100 and 130–140 m (Alekseev et al., 1962). In his opinion, the first two are of Late Pleistocene age. In addition, in the Sobolokh-Mayan river basin, he noted fragments of a 200-meter terrace eroded by water flows and glaciers.

Two lowermost terrace levels are found everywhere throughout the Lower Lena River Valley, but we studied them in the most detail in the area of the mouth of the Dyanyshka River (fig. 3).

The first terrace has a scarp with 7–9 m high. It stretches along the Lena River from the mouth of the Dyanyshka River for about 25 km with a maximum width of about 7 km. The total height of the first terrace increases to 15 m at a distance from the Lena River. This terrace is composed by overbank horizontally layered, less often channel cross-layered, gray and yellow, fine-grained and medium-grained sands. Among sands there are also layers of silty sand, rarely thin layers of silt. Plant remains are very rare. This terrace was studied in two exposures. The outcrop 3016 is located on the right bank of the Lena River, 10 km from the mouth of the Dyanyshka River. Its height is 7 m. The IR-OSL age of sands from a depth of 2 m from the edge of the terrace scarp is 6.9 ± 0.6 ka (RLQG 2466–067). The outcrop 3050 is located on the right bank of the Dyanyshka River, 25 km from its mouth (about 6 km from the Lena River in a straight line). Its height is 8–9 m. The IR-OSL age of sands from a depth of 2.1 m from the edge of the terrace scarp is 6.0 ± 0.4 ka

(RLQG 2644–060). By analogy with the deposits of the high floodplain, the alluvium of the upper part of the first terrace is synchronized with the deposits accumulated in the Lena delta 6000–7000 BP, when the sea level was higher than present time.

Nearby at the Dyanyshka River there is the outcrop 3051 of the 2nd terrace of the Lena River. The exposure is a sandy-silty strata with separate layers of plant remains. Relative height of the terrace is 18–20 m (20–23 m above the Lena River). The results of radiocarbon dating indicated that it was formed in the end of the Late Pleistocene: the radiocarbon age of the twigs sampled at a depth of 6 m below the edge of the terrace is 12030 ± 110 BP (LU-9399). A peat bog was found 600 m downstream on the surface of this terrace. It occupies the upper part of the outcrop 3052, it has a thickness of 4.2 m, and it extends along the bank of the Dyanyshka River for 30 m (fig. 3). The results of radiocarbon dating indicated that the main part of its sequence was formed in the period from 9710 ± 60 BP (LU-9400, the sample from the peat bog bottom) to 5740 ± 50 BP (LU-9041, the sample from a depth of 1 m from the peat bog top). In general, this time interval corresponds to the time of the 1st terrace formation in the Lena River. It should be noted that according to other sources, the peat bog is a bit older – it began to form 12590 ± 300 BP (Siegert et al., 2007).

At the mouth of the Natara River, the outcrop 3031 of a strath terrace 45–50 m high was studied. Its upper part is composed of sandy silt overbank sediments. The IR-OSL age of a sample from a height of 35 m is 68.8 ± 5.6 ka (RLQG 2552–118). But according to M.N. Alekseev, these deposits should have been formed in the second half of the Middle Pleistocene, and the terrace is the 3rd highest in the Lower Lena valley (Alekseev et al., 1962). In addition, we obtained a similar result when dating the outcrop 3049 of the strath terrace 42 m high. It is located 30 km upstream from the mouth of the Dyanyshka River. The IR-OSL age of sand, sampled from a depth of 2 m from the surface, is 64.5 ± 4.5 ka (RLQG 2643–060).

In the lower reaches of the Molodo River (the left tributary of the Lena River), a group of Russian and German researchers drilled and studied the bottom sediments of the Kyutyunda Lake. The underlying alluvium near the contact with lake sediments has been dated to 38–32 thousand years (Biskaborn et al., 2016). The lake is located on the surface of a 40-meter terrace (50 m above the Lena River). This terrace has the same elevation as the terraces at the mouth of the Natara River and the lower reaches of the Dyanyshka River, but its alluvium has been formed much later. It is possible that all these terraces have been formed in the same long time interval, but additional dates are needed to verify this conclusion.

Approximately 3 km downstream from the mouth of the Menkere River on the right bank of the Lena River the outcrop 3029 is located. It is a part of the 4th 60-meter strath terrace, and its alluvium should be of Middle Pleistocene age (Alekseev et al., 1962). We assume that these deposits do not belong to the Lena River, but to its ancient tributary. Investigated well-sorted fine-grained and medium-grained sands with silt interlayers at a height of 33–34 m near the contact with bedrock have the IR-OSL age of 23.6 ± 1.9 ka (RLQG 2544–118). It means that these deposits began to form at the end of the Late Pleistocene.

Middle Pleistocene alluvial deposits of the 80-meter 5th terrace are traced to the northwest towards the lower reaches of the Olenek River in the area of the Siktyakh village and they are associated with the Ajakit-Kelimyar segment of the Lena paleovalley (Zhuravlev, 1960; Alekseev et al., 1962). The existence of a river paleovalley in this area is indirectly indicated by information obtained during the study of the El'gene-Kyuele Lake (Biskaborn et al., 2013). This lake is located presumably within its boundaries, and around the lake there is a specific composition of the ice complex sediments. There are no dates from alluvial deposits in this area.

The oldest known dated deposits formed by the Lena River in its lower reaches were studied in one of the outcrops of the Dyanyshka River valley. The IR-OSL age of the alluvium sample is 325 ka (Zech et al., 2011). The outcrop is confined by an uneven moraine surface (Alekseev et al., 1962) with absolute height of 100–160 m (55–115 m above the Lena River). The known coordinates of the outcrop (Zech et al., 2011), earlier information about the distribution of the Lena terraces in the Dyanyshka River valley, glacial and fluvioglacial deposits (Alekseev et al., 1962), suggest that the right side of the Lena River valley should be located further east than expected.

There is an opinion that the Pleistocene glaciations were one of the most important reasons for the formation of the Lena terraces and the restructuring of the Lena River valley. The center of glaciation was located in the Verkhoyansk Ridge. Glaciers descended from the mountains along the tributaries of the Lena River could reach its main channel, deflect it, and maybe stop the outflow of a stream. The question of the number, age and boundaries of the distribution of glaciers is debatable. According to V.V. Kolpakov, the Lower Lena valley is a complex of several isolated paleovalleys of different ages (Ajakit-Kelimyar, Motorchuna-Ajakit, Sobopol-Siktyach, Linde-Khoruongka segments) (Kolpakov, 1966). Its formation and disappearance was due to the fact, that glaciers shifted the Lena River to the west. He distinguishes 4 stages of glaciation. Three of them occurred in the Late Pleistocene. During the warm epochs that followed them, the 2nd and 1st terraces were formed.

N.V. Kind distinguished 6 stages of glaciation in the region, the last of which had an age of 16–15 thousand years (Kind, 1975). Recent studies indicate the existence of 5 stages of glaciation. They are based on remote sensing and IR-OSL dating of intermoraine deposits in the valleys of the Dyanyshka and Tumara rivers. The age of the most ancient stage is 135–141 ka, and the youngest is over 50 ka (Stauch, Lehmkuhl, 2010). These studies proved that the glaciers had not reach the modern channel of the Lena River since the end of the Middle Pleistocene. However, all known segments of the paleovalleys of the Lena River, the youngest of which is the Sobopol-Siktyach segment, formed by the end of the Middle Pleistocene (Alekseev, Drouchits, 2004).

## 4. CONCLUSION

The deposits composing the low floodplain have been formed over the past thousand years. The age of the high floodplain deposits is at least 3700 years. The first terrace in the central part of the Lena River Delta has the same age. The first terrace in the area of the mouth of the Dyanyshka River was formed in the first half of the Holocene, and the second terrace was formed by the end of the Late Pleistocene – the beginning of the Holocene.

During the Holocene, the Laptev Sea level repeatedly fluctuated up to a height of 7–8 m above the present level. This is the reason for the accumulation of the high floodplain deposits and thick strata of specific ingressive organic and mineral deposits in the Lena River Delta. Alluvium of the first terrace accumulated 6000–7000 BP for the same reason. The sea level during this period was higher than today. Therefore, the change in the basis of erosion is the main factor of the Lower Lena valley evolution in the Holocene. The relationship between the formation of the first terrace and the glaciation stages in the western foreland of the Verkhoyansk Ridge is not obvious, as noted earlier.

Higher terraces are usually located at a distance from the Lena main channel. Some outcrops of high terraces contain Late Pleistocene deposits. However, according to earlier ideas, they had a Middle Pleistocene age, and the stages of their accumulation were synchronized with the epochs of glaciations. Despite the existing contradictions, glaciations in the region played a key in the formation of highest and older terraces, but additional studies are required to identify their age and relationship with the accumulation of alluvium in the Lower Lena valley.

# HOLOCENE AND LATE NEOPLEISTOCENE PALEORECONSTRUCTIONS FOR THE LOWER LENA RIVER VALLEY: NEW DATA, CONTRADICTIONS AND PROBLEMS

**S. A. Pravkin[a,#] and D. Yu. Bolshiyanov[a]**

[a]*Arctic and Antarctic Research Institute, Saint Petersburg, Russia*

[#]*E-mail: s.pravkin@aari.ru*

The Lena River with its tributaries is one of the largest river systems in the world. During three field seasons, 18 outcrops of alluvial deposits on terraces of different levels of the Lower Lena Valley from the mouth of the Aldan River to the “Lena Pipe” were studied. Terrace heights were determined using topographic maps, leveling and GPS survey. The outcrops were described in the field with sampling for radiocarbon dating and infrared stimulated luminescence (IR-OSL) method. A total of 26 radiocarbon and IR-OSL ages were obtained. The low floodplain was studied most in detail on the section from the mouth of the Aldan River to the mouth Vilyuy River, where it has a height of 5–6 to 8–9 m. The deposits of the high floodplain in the section between the mouths of the Aldan River and Viluyu River, in the area of the mouth of the Dyanyshka River and in the section between the villages of Siktyakh and Kyusyur were studied. It has a height of 6–10 to 15–16 m. The deposits of the 1st terrace (7–15 m) and 2nd terrace (20–23 m) most in detail in the area of the mouth of the Dyanyshka River were studied. In some areas (the lower reaches of Dyanyshka River, near the mouth of the Menkere River and the mouth of the Natara River), deposits of higher terraces were dated. Investigation and dating of the floodplain and first terraces in the valley of the Lower Lena River confirms that their formation was caused by sea level fluctuations in Holocene and at the end of Late Pleistocene as well as in the Lena River Delta. The results of IR-OSL dating alluvial deposits of 40–60 me terraces contradict the ideas about their age, formed in the 3rd quarter of the 20th century. Glaciations of Verkhoyansk Ridge could not influence to configuration of the Lena River valley as mountain glaciers had not rich the Lena River since the end of Middle Pleistocene.

*Keywords:* Lower Lena Valley, floodplain, terrace, Holocene, Late Neopleistocene, dating of deposits

## ACKNOWLEDGMENTS

This study was supported by Alfred Wegener Institute, Helmholtz Centre for Polar and Marine Research (Germany) and Melnikov Permafrost Institute (Russia).

## REFERENCES

Alekseev M.N. and Drouchits V.A. Quaternary fluvial sediments in the Russian Arctic and Subarctic: Late Cenozoic development of the Lena River system, northeastern Siberia. *Proceedings of the Geologists' Association*. 2004. Vol. 115. No. 4. P. 339–346. https://doi.org/10.1016/S0016-7878(04)80013-0

Alekseev M.N., Kuprina N.P., Medyantsev A.I., and Khoreva I.M. *Stratigrafia i korrelyatsiya neogenovykh i chetvertichnykh otlozhenii Severo-Vostochnoi chasti Sibirskoi platformy i ee vostochnogo skladchatogo obramlenia* (Stratigraphy and correlation of neogene and quaternary deposits of the Northeastern part of the Siberian Platform and its eastern folded frame). *Trudy GIN AN SSSR*. 1962. Vol. 66. 134 p. (in Russ.)

Arslanov Kh.A. *Radiouglerod: geokhimiya i geokhronologiya* (Radiocarbon: geochemistry and geochronology). Leningrad: LGU (Publ.), 1987. 300 p. (in Russ.)

Biskaborn B.K., Herzschuh U., Bolshiyanov D.Yu., Schwamborn G., and Diekmann B. Thermokarst Processes and Depositional Events in a Tundra Lake, Northeastern Siberia. *Permafrost and Periglacial Processes*. 2013. Vol. 24. No. 3. P. 160–174. https://doi.org/10.1002/ppp.1769

Biskaborn B.K., Subetto D.A., Savelieva L.A., Vakhrameeva P.S., Hansche A., Herzschuh U., Klemm J., Heinecke L., Pestryakova L.A., Meyer H., Kuhn G., and Diekmann B. Late Quaternary vegetation and lake system dynamics in northeastern Siberia: Implications for seasonal climate variability. *Quaternary Science Reviews*. 2016. Vol. 147. P. 406–421. https://doi.org/10.1016/j.quascirev.2015.08.014

Bolshiyanov D.Y., Makarov A.S., Schneider V., and Stoof G. *Proiskhozhdenie i razvitie del'ty reki Leny* (Origin and development of the Lena River Delta). Saint Petersburg: AARI (Publ.), 2013. 267 p. (in Russ.)

Bolshiyanov D., Makarov A., and Savelieva L. Lena River delta formation during the Holocene. *Biogeosciences*. 2015. Vol. 12. No. 2. P. 579–593. https://doi.org/10.5194/bg-12-579-2015, 2015

Kind N.V. Glaciations of the Verkhoyansk Mountains and their position in the absolute geochronological scale of the upper anthropogen of Siberia. *Paleogeografia i periglyatsial'nye yavleniya pleistotsena*. Moscow: Science (Publ.), 1975. P. 124–132 (in Russ.)

Kolpakov V.V. *Paleogeografiya chetvertichnogo perioda v nizhnem techenii r. Leny* (Quaternary palaeogeography of the lower course of the Lena River). *Izvestiya VUZov. Seriya "Geologiya i razvedka"*. 1966. No. 5. P. 41–48. (in Russ.)

Molodkov A. and Bitinas A. Sedimentary record and luminescence chronology of the late glacial and Holocene aeolian sediments in Lithuania. *Boreas*. 2006. Vol. 35. No. 2. P. 244–254. https://doi.org/10.1111/j.1502-3885.2006.tb01154.x

Ramsey B.C., Dee M., Lee S., Nakagawa T., and Staff R.A. Developments in the calibration and modeling of radiocarbon dates. *Radiocarbon*. 2010. Vol. 52. No. 3. P. 953–961. https://doi.org/10.1017/S0033822200046063

Reimer P.J., Bard E., Bayliss A., Beck J.W., Blackwell P.G., Bronk Ramsey C., Buck C.E., Cheng H., Edwards R.L., Friedrich M., Grootes P.M., Guilderson T.P., Haflidason H., Hajdas I., Hatte C., Heaton T.J., Hoffmann D.L., Hogg A.G., Hughen K.A., Kaiser K.F., Kromer B., Manning S.W., Niu M., Reimer R.W., Richards D.A., Scott E.M., Southon J.R., Staff R.A., Turney C.S.M., and van der Plicht J. IntCal13 and Marine13 radiocarbon age calibration curves 0–50,000 years cal BP. *Radiocarbon*. 2013. Vol. 55. No. 4. P. 1869–1887. https://doi.org/10.2458/azu_js_rc.55.16947

Siegert K., Stauch G., Lehmkuhl F., Sergeenko A.I., Dikmann B., Popp S., and Belolyubsky I.N. *Razvitie oledeneniya Verkhoyanskogo khrebta i ego predgorii v pleistotsene: rezul'taty novykh issledovanii* (Development of glaciation of the Verkhoyansk ridge and its foothills in the Pleistocene: results of new research). *Regional geology and metallogeny*. 2007. No. 30–31. P. 222–228. (in Russ.)

Stauch G. and Lehmkuhl F. Quaternary glaciations in the Verkhoyansk Mountains, Northeast Siberia. *Quaternary Research*. 2010. Vol. 74. No. 1. P. 145–155. https://doi.org/10.1016/j.yqres.2010.04.003

Zech W., Zech R., Zech M., Leiber K., Dippold M., Frechen M., Bussert R., and Andreev A. Obliquity forcing of Quaternary glaciation and environmental changes in NE Siberia. *Quaternary International*. 2011. Vol. 234. No. 1–2. P. 133–145. https://doi.org/10.1016/j.quaint.2010.04.016

Zhuravlev V.S. *K voprosu o geologii mezhdurech'ya Olen'ka i Leny* (On the question of geology of the Olenek and Lena interfluves). *Trudy GIN AN USSR*. 1960. No. 7. P. 86–100. (in Russ.)

**EDN:** TQKERJ
*ГЕОМОРФОЛОГИЯ, 2022, том 53, № 5, с. 144–153*

## ПРОБЛЕМЫ ФЛЮВИАЛЬНОЙ ГЕОМОРФОЛОГИИ

*УДК 51.435.122:551.89(571.54)*

# ПОЙМЕННЫЙ АЛЛЮВИЙ БАССЕЙНА р. СЕЛЕНГИ: СТРОЕНИЕ, ВОЗРАСТ, ЭТАПЫ ФОРМИРОВАНИЯ

**© 2022 г. Ю. В. Рыжов[1,2,3,*], В. А. Голубцов[1,3], М. В. Смирнов[1,2]**
[1]*Институт земной коры СО РАН, Иркутск, Россия*
[2]*Иркутский государственный университет, Иркутск, Россия*
[3]*Институт географии имени В.Б. Сочавы СО РАН, Иркутск, Россия*
**E-mail: ryv@crust.irk.ru*

Поступила в редакцию 16.06.2022 г.
После доработки 28.06.2022 г.
Принята к публикации 15.07.2022 г.

Представлены новые данные о строении и возрасте аллювия пойм рек в бассейне р. Селенги. Выполнены описания разрезов, получена информация о составе речных осадков, радиоуглеродном возрасте. В бассейне р. Селенги выделяются два уровня пойм: низкие высотой до 2 м и высокие высотой 2–4 (5) м. Выявляются большие различия в строении и составе аллювия поймы в зависимости от морфологии долин рек, расходов воды, структурно-тектонических условий бассейнов. Установлено, что формирование отложений низких пойм в бассейне р. Селенги началось в позднем голоцене. Возраст отложений высокой поймы рек в бассейне р. Селенги – ранний-поздний голоцен. Выделены хронологические этапы осадконакопления и почвообразования. Установлено событие резкой смены литологического состава отложений, высоких паводков (3.8–3.4 тыс. кал. л. н.), выявлены криогенные деформации в верхнеголоценовом аллювии.

*Ключевые слова:* низкая пойма, высокая пойма, аллювий, осадконакопление, почвообразование, голоцен, бассейн р. Селенги
**DOI:** 10.31857/S0435428122050145

## 1. INTRODUCTION

Rivers are a dominant feature of most landscapes; therefore fluvial sediments are widespread. Fluvial deposits are represented by a continuum of sediment types (Shantser, 1951; Lazarenko, 1964) that range from clay– to gravel–size particles, and include both mineragenic and organic deposits. Distinctive features of river sediments are good sorting, roundness, horizontal and oblique bedding depending on sedimentary environments. Fluvial sediments provide an important link between weathering and slope processes in source areas as well as sedimentation processes within depositional basins (Allen, 1965). In this regard, much attention is paid to the study of alluvium (Nikolaev, 1947; Lamakin, 1948; Lavrushin, 1966). There are numerous studies of forming conditions, structure and age of alluvium on the territory of Baikal region and Mongolia (Ravskii, 1972; Logachev et al., 1964; Bazarov, 1968; 1986; Tseitlin, 1979; Devyatkin, 1981; Endrikhinskii, 1982; Konstantinov, 1994; Mats et al., 2001; Karasev, 2002; Lehmkuhl et al., 2011). At the same time, much less investigations is devoted to the study of floodplain deposits and the timing of their accumulation in the Selenga river basin (Ravskii, 1972; Bazarov, 1968; 1986; Lehmkuhl et al., 2011). Given that floodplains are among the most dynamic landforms, this information may shed light on the response of river systems on the impacts of climate changes (Törnqvist et al., 2015; Malsy et al., 2017) and permafrost dynamics (Moore et al., 2009; Törnqvist et al., 2015) during the Holocene.

The aim of this study is to assess of the chronological framework of floodplain deposits accumulation in the Selenga river basin as a reflection of the dynamics of hydrological conditions during the Holocene.

## 2. OBJECTS AND METHODS

Selenga River is most important tributary of Lake Baikal, which contributes about 50 to 60% of its surface water influx. Moreover, the Selenga's 447 060 km$^2$ watershed covers 82% of the Lake Baikal basin (Nadmitov et al., 2014), which means that any environmental changes along the Selenga and its tributaries may ultimately impact Lake Baikal.

Floodplains are one of the most common landforms of river valleys in the Selenga basin. They have different height (0.5–5 m), structure and age of deposits. On small rivers, floodplain heights do not exceed 1–3 m, on large rivers they reach 4–5 m. There is


**Fig. 1.** Location of the study territory and investigated floodplain sections.
**Рис. 1.** Местоположение исследуемой территории и изученных разрезов пойм.

a low (rarely low–medium) floodplain up to 2 m high and a high 2–4(5) m floodplain (fig. 1). Both the consistency of the height marks of the floodplain along the river valleys and significant differences in different parts of the valley are noted. The width of floodplains varies from 1–10 m in mountainous areas on small rivers to several km in large river valleys and basins. The floodplains are often leaning against the first river terraces (5–7 m high).

The study territory is located in Selenga middle mountains and Mongolia (fig. 1).

A detailed morphogenetic and stratigraphic description of floodplain deposits as well as sampling for further laboratory studies were carried out during the fieldworks. The sections are located within the floodplains of different heights. To identify the chronology of the formation of deposits of low floodplains, the structure of the floodplain (1–2 m high) on the right bank of the Tarbagatayka River was studied near the village Burnashevo (fig. 1, tabl. 1). The Tarbagatayka River flows in the Kuitun intermountain depression. The landscape and climatic conditions of this territory are described in detail earlier (Ryzhov, Golubtsov, 2017; Ryzhov et al., 2021). In addition, sections of low floodplains up to 1.5 m high were studied in the foothills of the Khangai ridge (Mongolia) in the upper reaches of the Orkhon River (fig. 2, tabl. 1).

To reveal the structure and chronology of the formation of high floodplains, the floodplain deposits of the Itantsa and Il'ka rivers (Selenga middle mountains) were studied. In addition, a high floodplain was studied on the right bank of the Boroo-Gol River (left tributary of the Kharaa-Gol River, Mongolia). The rivers are characterized by different hydrological regimes and structural-tectonic conditions. The Itantsa and Il'ka rivers flow, respectively, in the Itantsa and Il'ka basins. Section of the high floodplain of the Boroo-Gol River (Shivert-Gol) is located in an intermountain depression.

Under laboratory conditions, soil and sediment samples were air-dried, crushed, and sieved through a 1 mm sieve. The total organic carbon content was determined by the method of wet combustion according to Tyurin. The determination of particle size distribution was carried out on the basis of an average sample in stagnant water using the pipette method. The age of soils and sediments was determined by the radiocarbon method with scintillation measurement of $^{14}C$ activity at St. Petersburg State University and at the Institute of Geology and Mineralogy of the Siberian Branch of the Russian Academy of Sciences by the carbon of humic acids. Radiocarbon dates were calibrated using the IntCal20 scale (Reimer et al., 2020).

## 3. RESULTS

### *3.1. Structure of sediments and chronology of sedimentation on low floodplains*

*3.1.1. Tarbagatayka floodplain.* Following horizons are distinguished (from top to bottom) in the section of the low floodplain (1–1.5 m) of the Tarbagatayka river (fig. 2):

– brown sandy loam silty enriched in organic matter with coals (0–16 cm);

– brown sandy loam and fine-grained sands with the inclusion of medium-coarse-grained sands (16–26 cm);

– alternation of dark brown sandy loam, fine-grained light brown sands with the inclusion of medi-

**Table 1.** Radiocarbon and calibrated age of floodplain sediments in the Selenga river basin
**Таблица 1.** Радиоуглеродный и календарный возраст пойменных отложений в бассейне р. Селенги

| Dated material | Depth, sm | Lab. number | $^{14}$C Age, years BP | Cal. years BP (±1σ) |
|---|---|---|---|---|
| Low floodplain (1–1.5 m) Tarbagatayka River, 51°27′11.5″ N, 107°22′07.3″ E, 582 m | | | | |
| Humic sandy loam, charcoal | 43–46 | LU-9339 | 2580 ± 230 | 2616 ± 267 |
| Humic sandy loam, charcoal | 54–56 | LU-9340 | 1890 ± 70 | 1798 ± 81 |
| Humic sandy loam | 60–63 | LU-9387 | 860 ± 130 | 757 ± 78 |
| Low floodplain (1.5 m) Orkhon River (Mongolia), 47°24′06.8″ N, 102°51′51.0″ E, 1468 m | | | | |
| Humic sandy loam | 13–17 | LU-9820 | 1380 ± 120 | 1288 ± 112 |
| Humic sandy loam | 59–63 | LU-9821 | 2030 ± 140 | 1985 ± 164 |
| Humic sandy loam | 88–94 | LU-9822 | 2130 ± 110 | 2085 ± 96 |
| High floodplain (1.5–2 m) Itantsa River, 52°10′30.1″ N, 107°31′49.8″ E, 500 m | | | | |
| Humic peaty loam | 115–120 | SOAN-9761 | 3120 ± 65 | 3319 ± 79 |
| High floodplain (2.5–3 m) Boroo-Gol River, 48°25′26.2″ N, 106°11′42.7″ E, 1050 m | | | | |
| Humic loam | 3–7 | LU-9814 | $\delta^{14}$C=1.57 ± 0.83% | 1954–1958 гг. |
| Humic loam | 14–17 | LU-9815 | 1640 ± 100 | 1507 ± 101 |
| Humic loam | 26–31 | LU-9816 | 1940 ± 120 | 1856 ± 143 |
| Humic loam | 114–120 | LU-9342 | 3340 ± 220 | 3615 ± 270 |
| Humic loam | 196–204 | LU-9817 | 4050 ± 110 | 4533 ± 118 |
| High floodplain (2.5–3 m) Il'ka River, 51°41′43.9″ N, 108°37′20.3″ E, 629 m | | | | |
| Humic sandy loam | 10–15 | SOAN-9855 | 1930 ± 120 | 1857 ± 145 |
| Humic sandy loam | 27–32 | SOAN-9856 | 2535 ± 105 | 2618 ± 133 |
| Humic sandy loam | 40–45 | SOAN-9857 | 3200 ± 150 | 3410 ± 182 |
| Humic sandy loam | 45–50 | SOAN-9858 | 3400 ± 300 | 3709 ± 375 |
| High floodplain (2.5–3 m) Il'ka River, 51°41′58.2″ N, 108°37′26.5″ E, 625 m | | | | |
| Humic sandy loam | 59–67 | SOAN-9859 | 275 ± 40 | 357 ± 71 |
| Humic sandy loam | 87–96 | SOAN-9860 | 800 ± 180 | 783 ± 138 |

um-grained sands and thin (1–3 cm) interlayers of humus dark brown to black sandy loam with coals (26–63 cm);

– fine-grained light brown sands with the inclusion of medium and coarse-grained sands and coals (63–93 cm);

– grayish-brown fine–grained sands with coal inclusions (93–103 cm).

Three radiocarbon ages were obtained from the 26–63 cm layer (tabl. 1). The youngest one refers to the lower Ah layer. An inversion of radiocarbon ages occurs up the section. We consider this layer of sediments to be the result of the accumulation of products of runoff and erosion of soils from the watershed. The Ah layer at depths of 60–63 cm is located on sandy alluvium and reflects, in our opinion, the real time of its formation. In accordance with the structure and the obtained radiocarbon age the following stages of the formation of the studied deposits are assumed:

– accumulation of gray and light brown sands with the inclusion of coals (63–103 cm) > 0.84 kyr BP;

– accumulation of fine and medium-grained alluvial sands and thin layers of sandy loam enriched in organic matter (26–63 cm) 0.84–0.34 kyr BP;

– accumulation of fine-grained sands and sandy loams with the inclusion of medium-grained sands (16–26 cm) 0.34–0.21 kyr BP;

– accumulation of sandy loams enriched in organic matter with coal inclusions (0–16 cm) <0.21 kyr BP. This stage of sedimentation is associated with modern soil formation and sediment inflow from slopes as a result of soil erosion during agricultural land use in the last 250 years.

*3.1.2. Orkhon floodplain.* In the structure of the low floodplain of the Orkhon river the following horizons are distinguished (fig. 2) (from top to bottom):

– brown humic sandy loam with small pebbles (0–12 cm);

– grayish-brown sandy loam with Fe redox features (12–33 cm);

– grayish light brown sands with inclusions of clastic inclusions (gruss) and gravel (33–39 cm);

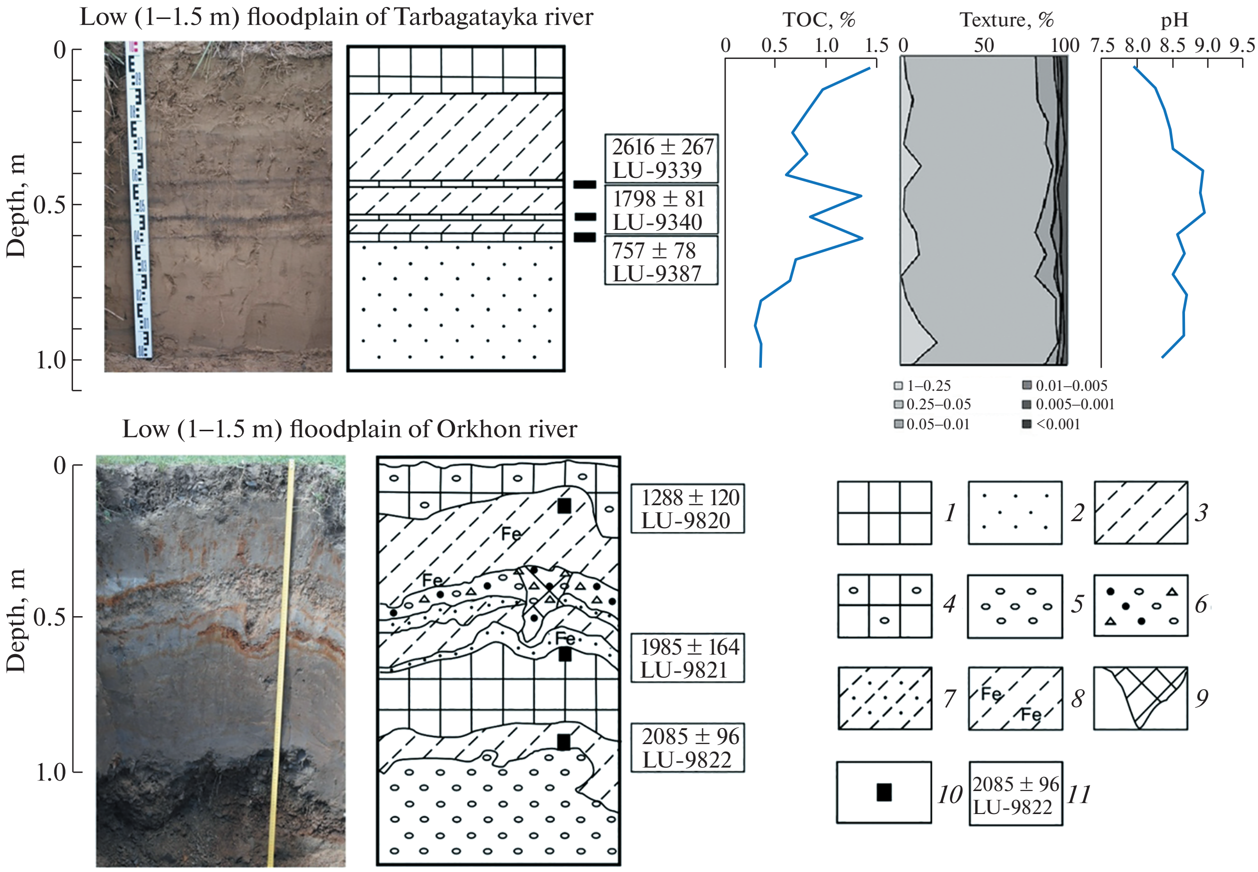


**Fig. 2.** Structure and calibrated age of studied low floodplains.

*1* – modern and buried soils; *2* – fine sands; *3* – sandy loams; *4* – soils with pebble inclusions; *5* – gravels and pebbles; *6* – sands with dress and gravels; *7* – sandy loam with sand; *8* – sandy loam with iron redox features; *9* – sands with pebbles and gravels; *10* – ground wedges; *11* – places for radiocarbon sampling; *12* – calibrated age and sample lab number.

**Рис. 2.** Строение и календарный возраст отложений низкой поймы (1–2 м) рек в бассейне р. Селенги.

*1* – современные и погребенные почвы; *2* – пески мелкозернистые; *3* – супеси; *4* – почвы с включением гальки; *5* – гравий с галькой; *6* – песок разнозернистый с включением дресвы и гравия; *7* – супеси с включением песка; *8* – супеси с пятнами, линзами и прослоями ожелезнения; *9* – пески разнозернистые с гравием и галькой; *10* – грунтовая жила; *11* – интервал отбора проб на $^{14}$C; *12* – календарный возраст и лабораторный номер образца.

– sandy loam gray whitish with sand inclusions (39–44 cm);

– whitish sandy loam with Fe redox features in the top of the layer (44–51 cm);

– fine-grained yellowish–brown sands with Fe redox features (51–58 cm);

– dark brown sandy loam enriched in organic matter and Fe redox features (58–81 cm);

– gray sandy loamy gleyed with Fe redox spots (81–94 cm);

– gravels and pebbles (94–130 cm).

The horizontal bedding of the layers is disturbed by cryogenic deformations. At 39–60 cm depths a ground wedge (tessellon) up to 14 cm wide on top is distinguished. It is composed mainly of sands with the small clastic inclusion (gruss) and gravel. The time of formation and filling of the wedge-shaped cryogenic structure is about 1.7–1.6 kyr BP. Layers at depths of 39–60 cm have a wavy bedding, indicating deformations during seasonal freezing and thawing of wet sandy loams and fine-grained sands, underlain by humic sandy loams.

The following stages of accumulation of deposits are distinguished:

– accumulation of channel alluvium (94–130 cm) >2.1 kyr BP;

– pedogenesis (58–81 cm) 2.1–1.95 kyr BP;

– accumulation of fine–grained sands (51–58 cm) 1.95–1.84 kyr BP;

– accumulation of gray whitish sandy loam (44–51 cm) 1.84–1.73 kyr BP;

– accumulation of gray whitish sandy loams with the inclusion of inequigranular sand (39–44 cm) 1.73–1.65 kyr BP;

– accumulation of sands with the small clastic inclusion (gruss) and gravel (33–39 cm) 1.65–1.55 kyr BP, indicating an increase in the water level of the river and high floods;

– accumulation of gray sandy loam with Fe redox features and enriched in organic matter (12–33 cm) 1.55–1.0 kyr BP;

– accumulation of humic sandy loam with pebble inclusions (0–12 cm) during the last 1 thousand years.

### *3.2. Structure of sediments and chronology of sedimentation on high floodplains*

*3.2.1. Itantsa floodplain.* In the section of a high floodplain (1.5–2 m) on the right bank of the Itantsa river floodplain (0–120 cm) and channel alluvium (120–150 cm) are distinguished (fig. 3).

Floodplain sediments are represented by the following horizons:

– dark brown sandy loam enriched in organic matter with small pebbles (0–10 cm);

– sandy loams with iron redox features (10–33 cm);

– fine and medium-grained sand with the gravel inclusions (33–46 cm);

– light peaty loams dark brown (46–75 cm);

– medium peaty loams with lenses of medium to fine-grained sands and iron redox features (75–120 cm);

– inequigranular sands with gravel and pebble inclusions (120–170 cm).

Radiocarbon dating 3120±65 (SOAN–9761) was obtained from the bottom of loams from a depth of 115–120 cm (tabl. 1). A cryogenic wedge up to 25 cm vide is located at 36–65 cm depths. The time of its formation and filling is about 0.8–0.5 kyr BP. The following stages of formation of floodplain deposits are distinguished:

– accumulation of channel alluvium (120–170 cm) >3.4 kyr BP;

– accumulation of peaty loams (46–120 cm) 3.4–1.3 kyr BP;

– accumulation of inequigranular sands with gravel inclusions (34–46 cm) 1.3–0.9 kyr BP;

– accumulation of brownish sandy loams (10–33 cm) 0.9–0.3 kyr BP;

– modern pedogenesis (<0.3 kyr BP).

*3.2.2. Boroo-Gol floodplain.* The following deposits and stages of their accumulation are distinguished from top to bottom (fig. 3):

– the upper part (0–31 cm) represented by the modern soil profile is composed of light brown sandy loam (1–3 cm), dark brown to black loams (3–7 cm), light silty brown loam (7–14 cm), light dark brown loam (14–31 cm). The formation of this part is divided into four stages: accumulation of humus light loams (14–31 cm) 1.9–1.3 kyr BP; accumulation of aeolian light brown silty loams (7–14 cm) 1.3–0.3 kyr BP; soil formation stage (3–7 cm) 300–40 yr BP; accumulation of silty aeolian sandy loam (1–3 cm) during the last 40 years.

– the second unit (31–74 cm) is represented by light loams and sandy loams of gray and dark gray color, uneven occurrence of layers of different lithological composition. The accumulation of deposits is confined to the time interval of 2.8–1.9 kyr BP;

– the third sediment unit (74–130 cm) is represented by dark gray humus loams that accumulated 3.8–2.8 kyr BP;

– below (130–175 cm) lie obliquely layered light loams with interlayers and lenses of brown sandy loam with sand inclusions. The color of deposits varies from brown, gray to dark gray. The thickness of the layer is not constant and varies from 30 to 45 cm with a slope downstream of the river. The accumulation of sediments based on the obtained radiocarbon dates took place 4.3–3.8 kyr BP;

– at depths of 175–204 cm (the fifth sediment member), light gray and dark gray loams occur with interlayers and lenses of gray and brown clayey and inequigranular sand, which accumulated 4.6–4.3 kyr BP;

– below (204–224 cm) there is an alternation of interlayers of gray and dark gray light loam and interlayers of grayish–brown sand with weathered clastic inclusions and a rare pebble inclusions. The accumulation of these deposits is confined to the interval of 4.8–4.6 kyr BP.

*3.2.3. Il’ka floodplain (Il’ka 1).* The sediment thickness of the Il’ka-1 section is about 1.5 m. The stages of sediment formation and pedogenesis have been identified. For section four radiocarbon dates were obtained at 10–50 cm depths in the range of 1.8–3.7 kyr BP (fig. 3, tabl. 1). Following horizons are distinguished in the section from top to bottom:

– dark brown to black humus peaty sandy loam (0–48 cm), accumulated during the last 3.4 kyr BP;

– alternation of fine to medium grained sands (48–80 cm), formed 3.4–4.2 kyr BP;

– coarse sands with small clastic inclusions (gruss), gravel and small pebbles (80–150 cm), representing the channel facies of alluvium and formed in the first half of the Holocene.

A ground wedge (tessellon) up to 40 cm wide with inclined and vertical occurrence of layers is located at 45–140 cm depths. The width of the wedge is 20–40 cm at 40–70 cm depths. It becomes thinner to 1–10 cm below. The wedge is covered with humus sandy loams younger than 3.4 kyr BP. At the same time, the wedge is filled by fine sands underlying the humus sandy loam the formation time of which is estimated at 3.8–3.4 kyr BP. The time of formation and filling of a ground wedge is about 3.8–3.6 kyr BP. Sands with small clastic inclusions and gravel occurred below in-

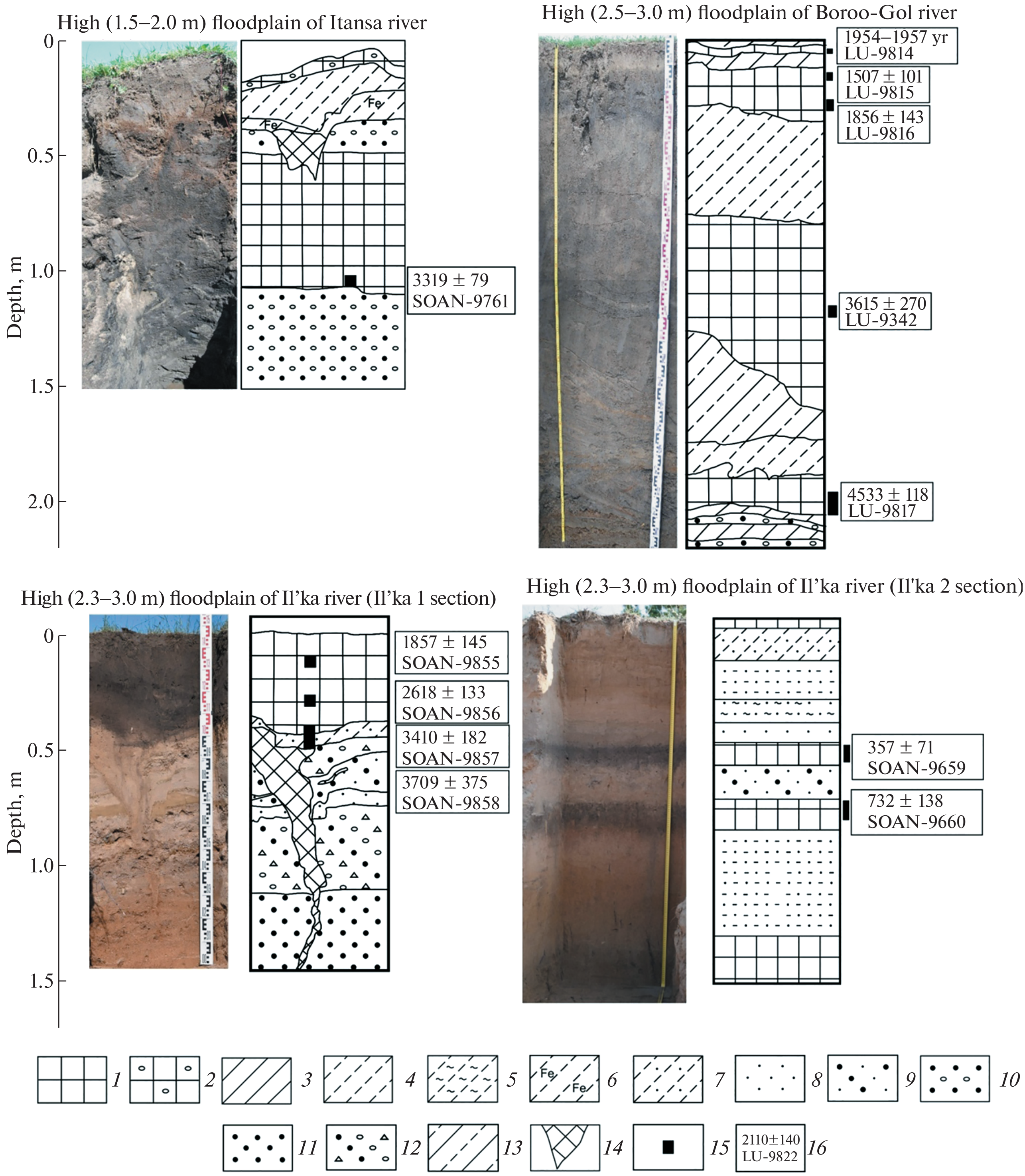


**Fig. 3.** Structure and calibrated age of high floodplain deposits of Selenga river basin.

*1* – modern and buried soils; *2* – soils with pebble inclusions; *3* – loam; *4* – sandy loam; *5* – loess-like sandy loam; *6* – sandy loam with iron redox features; *7* – sandy loam with sand inclusions; *8* – fine sand; *9* – coarse to medium sand; *10* – sand with gravel and pebbles; *11* – coarse sands with gravels and pebbles; *12* – coarse sand with small clastic inclusions, gravels and pebbles; *13* – loams with interlayers of sandy loams and sands; *14* – cryogenic wedges; *15* – sampling places for radiocarbon dating; *16* – age and sample lab number.

**Рис. 3.** Строение и календарный возраст отложений высокой поймы (2–3 м) рек в бассейне р. Селенги.

*1* – современные и погребенные почвы; *2* – почва с включением гальки; *3* – суглинок; *4* – супесь; *5* – супесь пылеватая карбонатная; *6* – супесь ожелезненная; *7* – супесь с мелкозернистым и тонкозернистым песком; *8* – песок мелкозернистый; *9* – песок разнозернистый; *10* – песок крупнозернистый; *11* – песок разнозернистый с включением гравия; *12* – песок разнозернистый с дресвой и гравием; *13* – гравий с галькой; *14* – грунтовая жила; *15* – интервал отбора проб на $^{14}C$; *16* – календарный возраст (кал. л. н.) и лабораторный номер образца.

dicates powerful floods. The time of their manifestation is about 4.2–3.8 kyr BP.

*3.2.4. Il'ka floodplain (Il'ka 2)*. The second section (Il'ka 2) with a thickness of 1.72 m was located 460 m north of the Il'ka 1 section on a high floodplain 2.5–3 m high with aeolian blowing sands (fig. 3, tabl. 1). Two radiocarbon dates were obtained for described section at depths of 59–67 and 87–96 cm in the time frames of 357–782 yr BP.

The following horizons are identified in the section:

– partially deflated Ah horizon of modern soil (0–4 cm), represented by dark brown sandy loam and formed over the past 70 years;

– gray-brown sandy loam (4–20 cm), formed as a result of aeolian activity 110–70 yr BP;

– fine-grained clayey, dark gray-brown, layered, alluvial sand (20–38 cm), formed 220–110 yr BP;

– fine-grained silty, dark brown sand with coal inclusions up to 3 mm, layered (38–49 cm), formed as result of aeolian activity 280–220 yr BP;

– fine-grained grayish-brown sand (49–58 cm), formed 330–280 yr BP;

– dark gray sandy loams enriched in organic matter with coal inclusions (58–69 cm), accumulated 450–330 yr BP;

– fine- and medium-grained yellowish-brown sand (69–86 cm), accumulated 700–450 yr BP;

– grayish-brown sandy loam with coal inclusions (86–100 cm), formed under conditions of lower flood heights and a stable subaerial surface 900–700 yr BP;

– fine-grained clayey, yellowish-light brown sands with humus streaks and coal along plant roots (100–156 cm), formed 1.7–0.9 kyr BP;

– fine-grained clayey sand gray to dark gray enriched in organic matter with coal inclusions along the plant roots (156–172 cm), accumulated 2.0–1.7 kyr BP.

## 4. DISCUSSION

On the one hand, the obtained data on the age and stages of accumulation of the floodplain deposits, generally confirm the previously obtained data on the time of formation of alluvium of the low (low and middle) and high floodplains (Ravskii; 1972; Bazarov, 1968; 1986). On the other hand, they specify the age and chronology of the stages of alluvium accumulation during the time of floods and soil formation when they decrease. The floodplains of large rivers are characterized by Holocene age (Endrikhinskii, 1982). Floodplain deposits of rivers of smaller orders accumulated mainly during the second half of the Holocene (Endrikhinskii, 1982). The alluvium of the high floodplain accumulated in the first half – the middle of the Holocene, while the low floodplain accumulated in the second half of the Holocene according to (Bazarov, 1986).

The stage of a sharp change in the lithological composition, high floods on rivers aged 3.8–3.4 have been identified in the floodplain deposits in Selenga river basin. For example, the bottom of the floodplain alluvium represented by peat has an age of 3.4 kyr BP on the Itantsa floodplain. There is unconformity boundary below determined by stage of erosion with interbedded sands and gravels, indicating strong floods and incision of the river. In the section of the high floodplain of the Boroo-Gol River oblique and wavy layered light loams with interlayers and lenses of sandy loam and sands aged 4.3–3.8 kyr BP occurs under humus light loams aged 3.8–2.8 kyr BP with sharp erosional boundary. Consequently, high floods and erosion were observed about 3.9–3.7 kyr BP. Gravel layers in the bottom sediments of Mongolian lakes with an age of about 3.6 kyr BP were revealed by V.P. Vipper et al. (Vipper et al., 1989). The authors attribute these deposits to the stage of heavy rains and the washing of gravel into lakes. Wet period 4.4–3.4 kyr BP identified according to the palynological and diatom analysis of peatlands in Northern Mongolia (Fukumoto et al., 2014). High Baikal stand was 3.7–3.6 kyr BP according to geoarchaeological data (Vorobieva, Goryunova, 2013). An anomalously high runoff into the Baikal lake (more than 250 $km^3$/year compared to average present-day values of 57 $km^3$/year) has been reconstructed 4.0–3.9(3.8) kyr BP (Goldberg et al., 2005).

Traces of high floods 3.8–3.4 kyr BP found in many river basins of Eastern Siberia. On the floodplain (6–8 m) of Muya river (near Ust'-Muya settlement) the floodplain facies of alluvium has a thickness of 1 m (layers 1–2). The exposed unit of the channel alluvium (layers 3–4) is 4.8 m (Kulchitskii et al., 1982). Layer 2, represented by siltstones with fine–grained sand lenses and inclusions of charcoal 0.75 m thick, is associated with large floods (Kulchitskii et al., 1982). A radiocarbon date of 3280 ± 35 years BP (SOAN–1599) was obtained from the top of layer 3 based on wood remains, which corresponds to 3514 ± 42 cal. years BP.

Traces of high floods in the interval of 4.4–3.4 kyr BP were found on the Ilya and Aga rivers in Transbaikalia (Bazarova et al., 2014). Phases of abnormally high river levels in the upper and middle reaches of the Yenisei river were identified (Yamskikh, 1993) about 4.0–3.5 and 3.3–2.7 thousand years ago (4.5–3.8 and 3.5–2.8 kyr BP). On the East European Plain palaeofluvial episodes of low (4.6–3.5 kyr BP) and high (3.5–1.9 kyr BP) fluvial activity were revealed (Panin, Matlakhova, 2015). Approximately ~3.9–3.8 kyr BP began increase in the frequency of high palaeofluvial activity events and decrease palaeofluvial events of low fluvial activity (Panin, Matlakhova, 2015).

## 5. CONCLUSIONS

1. Low and middle floodplains up to 2 m high and high floodplains (2–4(5) m high) are distinguished in the Selenga river basin. Floodplain deposits were formed in various dynamic conditions, have a horizontal, wavy, inclined bedding and are represented by sediments of channel, floodplain and oxbow facies of different thickness and grain size composition. Organogenic deposits (sandy loam and loam enriched in organic matter, peat bogs) accumulated on the floodplain with a decrease in river flood intensity.

2. The research results indicate that the low floodplain began to form in the Late Holocene. The channel alluvium of the low floodplains is older than 2.1 kyr, floodplain alluvium younger than this age. The soils are dated to less than 2.1 kyr BP.

3. A high floodplain is composed of Middle–Late Holocene alluvium and leans against the first river terrace. It is separated from the low floodplain by a ledge 0.5–2 m high. The formation time of the ledge is 3.8–3.5 kyr BP. The channel alluvium of the high floodplains is of Early Holocene age. The soils of the high floodplain began to form from the second half of the Holocene based on the radiocarbon dating.

4. A stage of a sharp change in the lithological composition of deposits, high floods (3.8–3.4 kyr BP) was established.

5. Cryogenic deformations in the floodplain deposits of Selenga river basin associated with climate cooling and local environmental conditions during Late Holocene.

# FLOODPLAIN ALLUVIUM IN THE SELENGA RIVER BASIN: STRUCTURE, AGE, FORMATION STAGES

**Yu. V. Ryzhov[a,b,c,#], V. A. Golubtsov[a,c], and M. V. Smirnov[a,b]**

[a]*Institute of the Earth's Crust SB RAS, Irkutsk, Russia*
[b]*Irkutsk State University, Irkutsk, Russia*
[c]*Sochava Institute of Geography SB RAS, Irkutsk, Russia*
[#]*E-mail: ryv@crust.irk.ru*

New data on the structure and age of alluvium of river floodplains in the Selenga river basin are presented. Based on the data of field and laboratory studies of floodplain sedimentary sections, data on the morphology, composition and radiocarbon age of river sediments were obtained. There are two main levels of floodplain in Selenga river basin: low (up to 2 m), high (2–4(5) m). The main differences in the structure and composition of floodplain alluvium are associated with the morphology of river valleys, differences in the dynamics of water discharge, structural and tectonic conditions of individual river basins. It was revealed that the formation of deposits of low floodplains in the Selenga river basin began in the late Holocene. The high floodplain sediments in the Selenga river basin are characterized by Early – Late Holocene age. The chronology of sedimentation stages and soil formation have been identified. The event of a sharp change in the lithological composition of deposits, high floods (3.8–3.4 kyr BP) was established, Cryogenic deformations in the Late Holocene alluvium have been revealed.

*Keyworlds:* low floodplain, high floodplain, alluvium, sedimentation, soil formation, Holocene, Selenga river basin

## ACKNOWLEDGMENTS

The study was carried out within the framework of the state assignments of the Institute of the Earth's Crust SB RAS (project No. 121042700218-2), V.B. Sochava Institute of Geography SB RAS (project No. AAAA-A21-121012190017-5, project No. AAAA-A21-121012190055-7), with partial financial support from the Grant of the Government of the Russian Federation, project No. 075-15-2021-631 "Baikal Siberia in the Stone Age: at the crossroads of the world".

## REFERENCES

Allen J.L. A review of the origin and characteristics of recent alluvial sediments. *Sedimentology*. 1965. Vol. 5. P. 91–191. https://doi.org/10.1111/j.1365-3091.1965.tb01561.x

Bazarov D.-D.B. *Chetvertichnye otlozheniya i osnovnye etapy razvitiya rel'efa Selenginskogo srednegor'ya* (Quaternary deposits and the main stages of the relief development of the Selenga middle mountains). Ulan-Ude: Buryat book (Publ.), 1968. 156 p. (in Russ.)

Bazarov D.B. *Kainozoi Pribaikal'ya i Zapadnogo Zabaikal'ya* (Cenozoic of the Baikal region and Western Transbaikalia). Novosibirsk: Nauka (Publ.), 1986. 184 p. (in Russ.)

Bazarova V.B., Lyashchevskaya M.S., and Orlova L.A. Paleoclimatic events of the Late Holocene in floodplain deposits of small rivers in Southeastern Transbaikalia. *Geography and Natural Resources*. 2014. Vol. 35.

P. 165–172.
https://doi.org/10.1134/S1875372814020085

Devyatkin E.V. *Kainozoi Vnutrennei Azii* (Cenozoic of Inner Asia). Moscow: Nauka (Publ.), 1981. 196 p. (in Russ.)

Endrikhinskii A.S. The sequence of the main geological events in the territory of Southern Siberia in the Late Pleistocene and Holocene. *Pozdnii pleistotsen i golotsen yuga Vostochnoi Sibiri*. Novosibirsk: Nauka (Publ.), 1982. 6–35 p. (in Russ.)

Fukumoto Y., Kashima K., and Ganzorig U. The Holocene environmental changes in boreal fen peatland of northern Mongolia reconstructed from diatom assemblages. *Quaternary International*. 2014. Vol. 348. P. 66–81. https://doi.org/10.1016/j.quaint.2011.10.014

Goldberg E.L., Grachev M.A., Chebykin E.P., Predorin I.A., Kalugin I.A., Khlystov O.M., and Zolotarev K. Scanning SRXF analysis and isotopes of uranium series from bottom sediments of Siberian lakes for high-resolution climate reconstruction. *Nuclear Instruments and Methods in Physics Research*. 2005. Vol. 543. No. 1. P. 250–254.
https://doi.org/10.1016/j.nima.2005.01.216

Karasev V.V. *Kainozoi Zabaikal'ya* (Cenozoic of Transbaikalia). Chita: FGUP Chitageols'emka (Publ.), 2002. 128 p. (in Russ.)

Konstantinov M.V. *Kamennyi vek vostochnogo regiona Baikal'skoi Azii* (Stone age of the eastern region of Baikal Asia). Ulan-Ude, Chita: Chitinskiш pedinstitut (Publ.), 1994. 180 p. (in Russ.)

Kulchitskii A.A., Firsov L.V., Panychev V.A., and Orlova L.A. The results of determining the absolute age (according to $^{14}C$) of the Holocene deposits of the high floodplain of the Muya river. *Pozdnii pleistotsen i golotsen yuga Vostochnoi Sibiri*. Novosibirsk: Nauka (Publ.), 1982. 165–166 p. (in Russ.)

Lamakin V.V. Dynamic phases of river valleys and alluvial deposits. *Zemlevedenie*. 1948. Vol. 2. No. 42. P. 154–187 (in Russ.)

Lavrushin Yu.A. Experience of comparative characteristics of the structure of alluvium in lowland rivers of different climatic zones. *Sovremennyi i chetvertichnyi continental'nyi litogenez*. Moscow: Nauka (Publ.), 1966. P. 162–175 (in Russ.)

Lazarenko A.A. *Litologiya alluviya ravnynnykh rek gumidnoi zony (na primere Dnepra, Desny i Oki)* (Lithology of alluvium in lowland rivers of the humid zone (on the example of the Dnieper, Desna and Oka)). Moscow: Nauka (Publ.), 1964. 236 p. (in Russ.)

Lehmkuhl F., Hilgers A., Fries S., Hülle D., Schlütz F., Shumilovskikh L., Felauer T., and Protze J. Holocene geomorphological processes and soil development as an indicator for environmental change around Karakorum, Upper Orkhon Valley (Central Mongolia). *Catena*. 2011. Vol. 87. P. 31–44.
https://doi.org/10.1016/j.catena.2011.05.005

Logachev N.A., Lomonosova T.K., and Klimanova V.M. *Kainozoiskie otlozheniya Irkutskogo amfiteatra* (Cenozoic deposits of the Irkutsk amphitheater). Moscow: Nauka (Publ.), 1964. 196 p. (in Russ.)

Malsy M., Flörke M., and Borchardt D. What drives the water quality changes in the Selenga basin: climate change or socio-economic development? *Regional Environmental Change*. 2017. Vol. 17. P. 1977–1989. https://doi.org/10.1007/s10113-016-1005-4

Mats V.D., Ufimtsev G.F., and Mandelbaum M.M. *Kainozoi Baikal'skoi riftovoi zony: stroenie i geologicheskaya istoriya* (Cenozoic of the Baikal rift zone: structure and geological history). Novosibirsk: Geo (Publ.), 2001. 249 p. (in Russ.)

Moore M.V., Hampton S.E., Izmest'eva L.R., Silow E.A., Peshkova E.V., and Pavlov B.K. Climate change and the world's "sacred sea" Lake Baikal, Siberia. *Bioscience*. 2009. Vol. 59 (5). P. 405–417.
https://doi.org/10.1525/bio.2009.59.5.8

Nadmitov B., Hong S., Kang S.I., Chu J.M., Gomboev B., Janchivdorj L., Lee C.H., and Khim J.S. Large-scale monitoring and assessment of metal contamination in surface water of the Selenga river basin (2007–2009). *Environmental Science and Pollution Research*. 2014. Vol. 22. No. 4. P. 2856–2867.
https://doi.org/10.1007/s11356-014-3564-6

Nikolaev N.I. About the structure of the floodplain and alluvial deposits. *Voprosy teoreticheskoi i prikladnoi geologii*. 1947. No. 2. P. 20–32 (in Russ.)

Panin A. and Matlakhova E. Fluvial chronology in the East European Plain over the last 20 ka and its palaeohydrological implications. *Catena*. 2015. Vol. 130. P. 46–61. https://doi.org/10.1016/j.catena.2014.08.016

Ravskii E.I. Osadkonakopla in the Antropogene). Moscow: Nauka (Publ.), 1972. 336 p. (in Russ.)

Reimer P.J, Austin W.E., Bard E., Bayliss A., Blackwell P.G., Bronk Ramsey C., Butzin M., Cheng H., Edwards R.L., Friedrich M., Grootes P.M., Guilderson T.P., Hajdas I., Heaton T.J., Hogg A.G., Hughen K.A., Kromer B., Manning S.W., Muscheler R., Palmer J.G., Pearson C., Van Der Plicht J., Reimer R.W., Richards D.A., Scott E.M., Southon J.R., Turney C.S., Wacker L., Adolphi F., Büntgen U., Capano M., Fahrni S.M., Friedrich R., Köhler P., Kudsk S., Miyake F., Olsen J., Reinig F., Sakamoto M., Sookdeo A., and Talamo S. The IntCal20 Northern Hemisphere radiocarbon age calibration curve (0–55 cal kBP). *Radiocarbon*. 2020. Vol. 62. P. 725–757.
https://doi.org/10.1017/RDC.2020.41

Ryzhov Yu.V. and Golubtsov V.A. Exogenous processes and soil formation within a small river basin of Western Transbaikalia in the second half of the Holocene. *Geography and Natural Resources*. 2017. Vol. 38. No. 3. P. 246–255.
https://doi.org/10.1134/S1875372817030052

Ryzhov Yu.V., Golubtsov V.A., and Opekunova M.Yu. The formation of the Tarbagataika river terraces (Western Transbaikalia) in the Late Glacial and the Holocene. *Geography and Natural Resources*. 2021. Vol. 42. No. 2. P. 164–171.
https://doi.org/10.1134/S1875372821020116

Shantser E.V. *Alluvii ravninnykh rek umerennogo poyasa i ego znachenie dlya poznaniya zakonomernostei stroeniya i formirovaniya alluvial'nykh svit* (Alluvium of lowland rivers of the temperate zone and its significance for understanding the regularities of the structure and forming of alluvial formations). Moscow: AN SSSR (Publ.), 1951. 275 p. (in Russ.)

Törnqvist R., Jarsjö J., Pietron J., Bring A., Rogberg P., Asokan S.M., and Destouni G. Evolution of the hydroclimate system in the Lake Baikal basin. *Journal of Hydrology*. 2015. Vol. 519. P. 1953–1962. https://doi.org/10.1016/j.jhydrol.2014.09.074

Tseitlin S.M. *Geologiya paleolita Severnoi Azii* (Geology of the Paleolithic of North Asia). Moscow: Nauka (Publ.), 1979. 288 p. (in Russ.)

Vipper P.B., Dorofeyuk N.N., Meteltseva E.P., and Sokolovskaya V.T. Landscape and climatic changes in Central Mongolia during the Holocene). *Paleoclimaty pozdnelednikov'ya i golotsena*. Moscow: Nauka (Publ.), 1989. 160–167 p. (in Russ.)

Vorobieva G.A. and Goryunova O.I. Paleolevels of Baikal in the second half of the Late Pleistocene and Holocene (according to geoarchaeological data)). *Izvestiya ISU Geoarchaeology. Ethnology. Anthropology.* 2013. Vol. 1. No. 2. P. 3–29 (in Russ.)

Yamskikh A.F. *Osadkonakoplenie i terassoobrazovanie v rechnykh dolinakh Yuzhnoi Sibiri* (Sedimentation and terrace formation in the river valleys of Southern Siberia). Krasnoyarsk: Krasnoyarsk state pedagogical institute (Publ.), 1993. 226 p. (in Russ.)

**EDN:** LOXSAZ
*ГЕОМОРФОЛОГИЯ, 2022, том 53, № 5, с. 154–161*

## ПРОБЛЕМЫ ФЛЮВИАЛЬНОЙ ГЕОМОРФОЛОГИИ

*УДК 551.4.024:631.42(470.321)*

# НЕКОТОРЫЕ ОСОБЕННОСТИ ПРИМЕНЕНИЯ РАДИОЦЕЗИЕВОГО МЕТОДА ИЗУЧЕНИЯ ПОТЕРЬ ПОЧВЫ ВСЛЕДСТВИЕ ЭРОЗИИ В ПЕРИГЛЯЦИАЛЬНОЙ ОБЛАСТИ БАССЕЙНА ВЕРХНЕЙ ОКИ

**© 2022 г. Л. Н. Трофимец[1,*], Е. А. Паниди[2], А. А. Лаврусевич[3]**

*[1]Орловский государственный университет имени И.С. Тургенева, Орел, Россия*
*[2]Санкт-Петербургский государственный университет, Санкт-Петербург, Россия*
*[3]Московский государственный строительный университет, Москва, Россия*
**E-mail: trofimetc_l_n@mail.ru*

Поступила в редакцию 14.06.2022 г.
После доработки 20.06.2022 г.
Принята к публикации 15.07.2022 г.

На примере экспериментального участка сельскохозяйственного поля в бассейне реки Сухая Орлица (бассейн верхней Оки в пределах Орловской области) рассматриваются особенности применения цезия-137 к оценке потерь почвы на распахиваемом склоне, расположенном в перигляциальной зоне Русской равнины. Обсуждается целесообразность учета полигонально-блочного строения водораздельной поверхности палеокриогенного происхождения при назначении опорного значения цезия-137. Удельная активность цезия-137 выступает в исследовании как индикатор в разной степени смытых почв. Приводятся величины коэффициентов вариации активности цезия-137, рассчитанных по всей совокупности точек пробоотбора вдоль двух трансект (114 и 91 224) на водораздельной поверхности склона южной экспозиции (86 точек). Коэффициенты вариации невелики (в пределах 0.12 для точек каждой из трансект). Обосновывается, что статистическая оценка вариабельности цезия-137 не должна быть основополагающей при установлении опорного значения цезия-137. Показано, что для опорной площадки следует выбирать те точки на блочных повышениях, почвенный профиль в которых имеет плужную подошву на глубине пахотного горизонта, глубже которой наблюдается резкое снижение активности цезия-137. Приводятся результаты сравнения удельной активности цезия-137, рассчитанной по трем точкам послойного пробоотбора, расположенным в пределах блочных повышений на водораздельной поверхности, со средней активностью, рассчитанной по 86 точкам в пределах трансект 114 и 91 224. Показано, что при принятии в качестве опорного значения средней активности цезия-137 по данным выборки из 86 точек значение интенсивности потерь почвы занижается в среднем на 7.3 т с 1 га в год. Сделан вывод, что удельную активность на опорной площадке необходимо рассчитывать по трем точкам послойного отбора проб почвы, расположенным в пределах блочных повышений, несмотря на невысокие значения вариабельности цезия-137 по выборке из 86 точек.

*Ключевые слова:* перигляциальная зона Русской равнины, бассейн верхней Оки, опорная площадка, удельная активность цезия-137, интенсивность потерь почвы вариабельность активности цезия-137, блочные повышения, послойный отбор проб почвы

**DOI:** 10.31857/S0435428122050170

## 1. INTRODUCTION

When applying the radiocaesium method to the assess soil losses in the areas where Chernobyl origin caesium is observed in the soil material, it is necessary to establish the background radioactivity value (specific activity or reserve of the caesium-137 at the reference plot, where minimal soil loss is observed due to erosion). Reference plot is selected at the watershed of the basin. It is generally assumed that the permissible value of the coefficient of variation for caesium-137 specific activity at the reference plot have not exceed 20% (0.2). This value of variability is considered acceptable for the lateral distribution of caesium-137 within the temperate latitudes belt of the Northern Hemisphere.

The variability of the caesium-137 specific activity values at the watershed within the reference plot depends on microrelief of the watershed. In the periglacial regions, the microrelief of watershed surfaces is composed of block elevations and interblock depressions. This structure of the surface is caused by presence of various types of relict cryogenic microrelief (Berdnikov, 1976; Velichko et al., 1987; Velichko et al., 1996; Alifanov et al., 2010). The relict microrelief appears cause of the structure of soil cover, and of the features of erosion processes (and, as a consequence, of the spatial differences in soil losses in result of soil runoff). Studies of the paleocryogenesis influence onto the soil formation processes developing actively in paleoecological soil science (according to Alifanov et al., 2010) allow in many cases to explain spatial differences of soil properties on micro scale. In particular, the influence of paleocryogenesis is detected at different levels of gray forest soil structures (Alifanov et al., 2010). This indicates the need to take into account the paleocryogenic microrelief landforms when studying the erosional transformation of topography surface using radiocaesium method, despite the apparent statistical uniformity of radioactive contamination of the soil material in the area of the reference plots. This conclusion is extremely important today, when precision agriculture is developed actively.

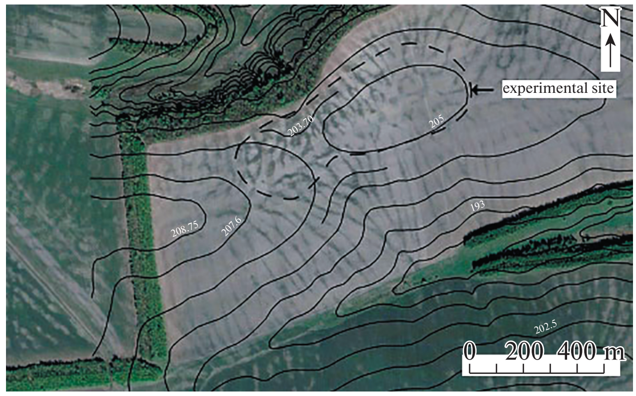


**Fig. 1.** An experimental area in the Sukhaya Orlitsa River basin; very high resolution satellite image courtesy of DigitalGlobe Foundation.

**Рис. 1.** Экспериментальный участок в бассейне реки Сухая Орлица на космическом снимке сверхвысокого разрешения.

## 2. MATERIALS AND METHODS

The study is based upon *in situ* data collected in 2017–2021 in the experimental area of an agricultural field located in the basin of Sukhaya Orlitsa River in the Oryol district of the Oryol region (fig. 1).

Local microrelief is composed of slope surface complicated with microravines. Elements of polygonal-block microrelief are presented in the watershed area (fig. 2). Block elevations of 15–30 m wide and interblock depressions of 2–15 m wide are presented in the experimental area (fig. 1). The study stage we are describing now is devoted to ensuring a decision on the expediency of paleocryogenic microrelief accounting when establishing a background value of caesium-137 radioactivity and assigning reference plots to do this (Markelov, 2004; Shamshurina et al., 2016; Trofimetz et al., 2020).

The specific activity of Chernobyl origin caesium-137 can act as a marker of the erosional soil runoff (Markelov, 2004; Panidi et al., 2016; Shamshurina et al., 2016; Trofimetz et al., 2019; Trofimetz et al., 2020) in the areas where global radioactive fallout was small (in the Orel region values are not exceed 10–15 Bq/kg). The radioactivity of the washed soil decreases (in comparison to the radioactivity of the soil material at the reference plot) due to mixing of the soil material in arable horizon with uncontaminated soil material delivered from deeper layers.

We conducted topography levelling alongside the transects located in watershed area (fig. 3, 4), simultaneous soil sampling (at every 2 m), and subsequent agrochemical and gamma-spectrometric analysis of collected samples. These allowed us both to assess the variability of caesium-137 in the watershed area, and to differentiate soil in the studied area in the meaning of washout degree. The soil-morphological method made it possible to determine whether the analyzed sampling plot refers to unwashed (or slightly washed) soil, or whether the soil is washed or washed/inwashed (fig. 5). The use of very high resolution satellite imagery (fig. 2–5) makes it possible to allocate sampling plots relative to microrelief elements of natural and anthropogenic origin. In the study, the anthropogenic microrelief forms are composed of plowing furrows located along the slope fall.

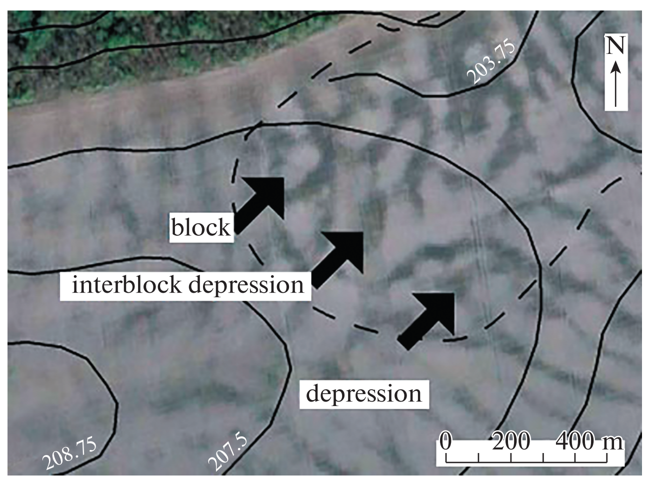


**Fig. 2.** Blocks and interblock depressions in the watershed area (for the slope of southern exposure); very high resolution satellite image courtesy of DigitalGlobe Foundation.

**Рис. 2.** Блоки и межблочные понижения на водораздельной поверхности склона южной экспозиции.

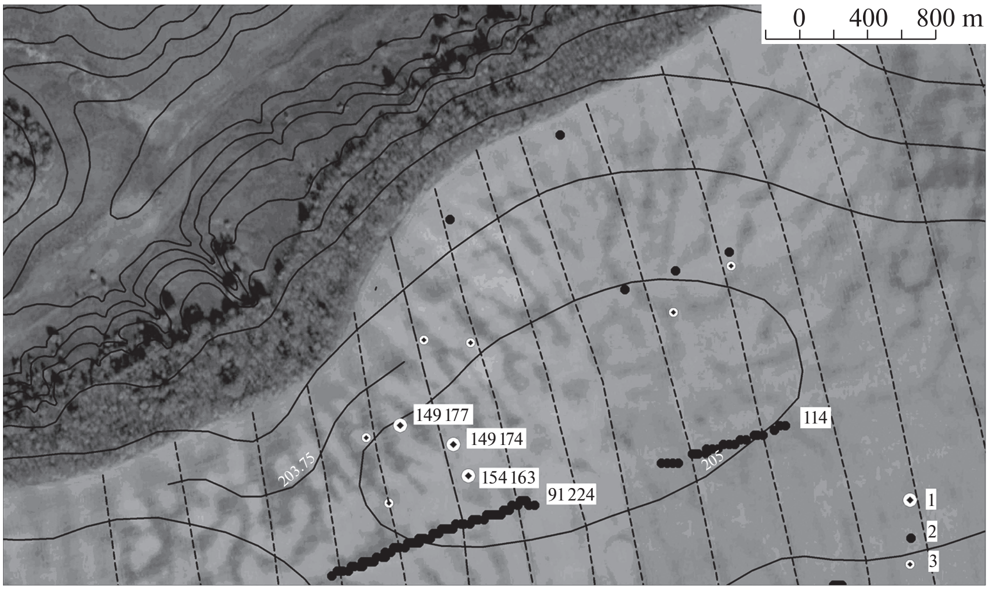


**Fig. 3.** Soil sampling transects at the watershed.

*1* – layer-by-layer soil sampling plots; *2* – transects #114 and #91 224; *3* – layer-by-layer soil sampling plots excluded from the analysis; dotted lines – plowing furrows; very high resolution satellite image courtesy of DigitalGlobe Foundation.

**Рис. 3.** Положение трансект с точками отбора проб в области водораздела.

*1* – точки опорной площадки; *2* – точки трансект 114 и 91 224; *3* – точки, исключенные из опорной группы; пунктирные линии – свально-развальные борозды.

## 3. RESULTS

Superimposing of the caesium-137 specificactivity data (for arable layer of 0–25 cm along transect #91 224 – fig. 3), of the levelling results (fig. 4), and the satellite imagery data allowed us to detect that the caesium-137 specificactivity depends on the sampling plot topographic position. Elevated areas (block elevations) correspond to higher values of caesium-137 (that indicates a low soil washout degree). Reduced radioactivity of caesium-137 is detected in the thalwegs of inter-block depressions, where soils of varying washout degree are presented.

Detected variability of the caesium-137 specific activity forced us to conduct a comparative analysis of the caesium-137 radioactivity reference value estimated using two different methods. The first method assumes reference value obtaining by averaging data of the set of 86 soil samples. It is applicable under the condition of a low value of the caesium-137 radioactivity coefficient of variation (for the entire samples set) (Owens, Walling, 1996; Markelov, 2004). The second method assumes obtaining of the average value of caesium-137 radioactivity at plots located within block elevations, where the in depth caesium-137 distribution corresponds to the features of unwashed (slightly washed) soils. The quantitative assessment of the soil radioactivity coefficient of variation was carried out both for each transect (#114 and #91 224) separately and for a combined sample set of 86 samples (fig. 3). The coefficient of variation did not exceed 0.12.

The analysis of the in depth caesium-137 and humus distribution (to detect the degree of soil plowing intensity) was carried out using the layer-by-layer (every 2 cm by depth) soil sampling data collected at nine sampling plots in the watershed area (light markers in fig. 3). After excluding of the sampling plots associated with local depressions (fig. 5), only three plots (#149 174, #149 177, #154 163) were analyzed. These sampling plots were used to estimate the reference value of caesium-137 radioactivity (fig. 3).

As the sampling was carried out in a number of years, the measurements were adjusted to basis year (2017) according to the radioactive decay formula (Imshennik, 2011). Since the variability of caesium-137 radioactivity in 86 soil samples is low, the average caesium-137 radioactivity was taken as a background value. This average value is estimated as 163.2 Bq/kg (44880 Bq/m$^2$) in sampling year, while adjusted in time value (referred to 2017) is 145.4 Bq/kg (39985 Bq/m$^2$). The average caesium-137 radioactivity estimated basing on three layer-by-layer soil samples collected in 2017 is 174.7 Bq/kg (48042.5 Bq/m$^2$).

Finally we concluded that the specific activity in the experimental area have to be estimated basing on layer-by-layer soil sampling at block elevations, despite the low variability of caesium-137 in a set of 86 soil samples (up to 0.12). Establishing the average caesium-137 radioactivity of 86 soil samples as a background value leads to underestimation of the soil runoff intensity by an 7.3 tons per 1 hectare per year in av-

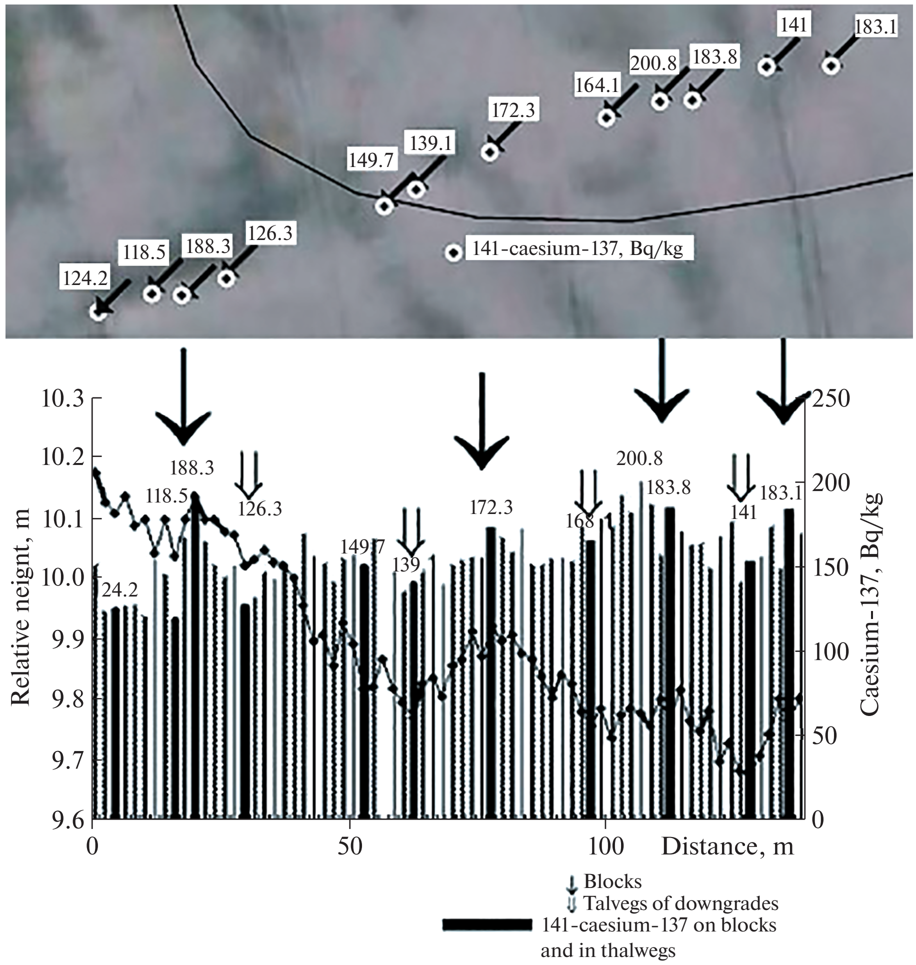


**Fig. 4.** A levelling profile combined with the radioactivity plot of caesium-137 (transect #91 224); and the transect location in a satellite image; very high resolution satellite image courtesy of DigitalGlobe Foundation.

**Рис. 4.** Нивелировочный профиль с наложенной на него активностью цезия-137 (трансекта 91 224) и космический снимок с положением трансекты.

erage. The control was carried out on an independent data composed of 200 soil samples.

## 4. DISCUSSION

Existing recommendations for caesium-137 radioactivity background value establishing when applying the radiocaesium method to the assess soil runoff require low caesium-137 content variability in analyzed soil samples. The study conducted by Markelov (Markelov, 2004) allowed to conclude that small variability of caesium-137 ensures the possibility of background value establishing using a set of four sampling plots.

As the watershed of the experimental area (fig. 2) is composed of block elevations (15–30 m wide) and interblock depressions (2–15 m wide), we have to estimate the magnitude of the caesium-137 coefficient of variation for sets of soil samples we use to establish background radioactivity value (samples collected at transects #114 and #91 224 – fig. 3, 4). The variability of caesium-137 radioactivity was analyzed for 86 samples of both transects. The sampling was carried out in 2012. Sampling plots were placed in block elevations (light areas in the satellite image), and in interblock depressions (dark areas in the satellite image) (fig. 3, 4), but this practically did not affect a coefficient of variation value.

It was estimated as 0.12 for transect #114, and as 0.11 for transect #91 224. This indicates that both datasets can be considered statistically homogeneous, and the value averaged for the two datasets can be taken as a background value of caesium-137 radioactivity.

However, combination of the caesium-137 radioactivity profile and the levelling profile along transect #91 224 (fig. 3, 4) show that increased values of caesium-137 radioactivity are associated with block elevations, and low values are associated with the thalwegs of interblock depressions. This feature indicates that the soil at block elevations is not washed or slightly

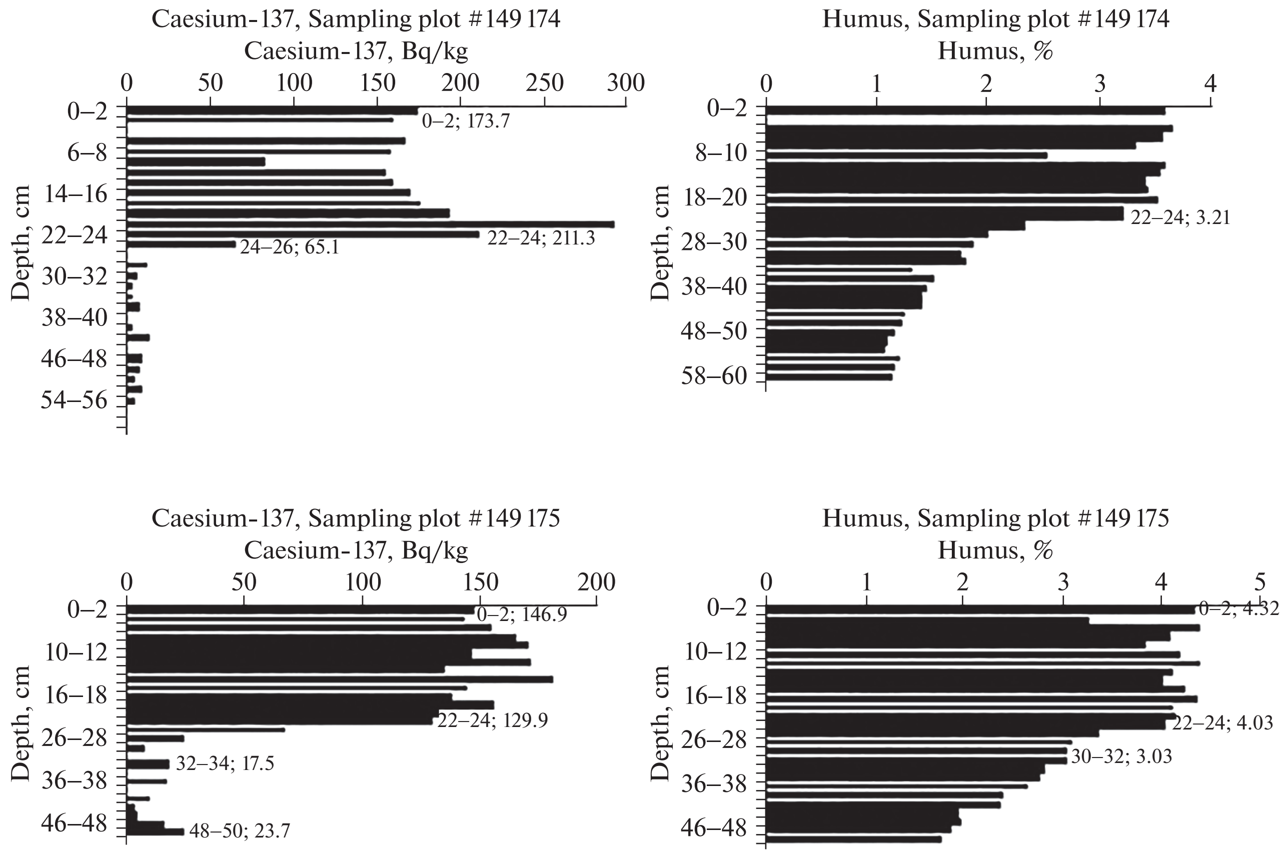


**Fig. 5.** In depth distribution of caesium-137 and humus; Sampling plot #149 174 is accepted when establishing background value (is located in block elevation); Sampling plot #149 175 is not accepted (is located in plowing furrow).

**Рис. 5.** Распределение цезия-137 и гумуса по глубине. Точка 149 174 принята к расчету опорного значения (приурочена к блочному повышению). Точка 149 175 “попала” в свально-развальную борозду.

washed, which is extremely important when establishing the background value of caesium-137 radioactivity. The background value is compared with the measured soil radioactivity at sample plots to detect the degree of soil wash. In the levelling profile in fig. 4 we can see that soil in interblock depressions (where reduced radioactivity is observed) can be attributed as washed soil of different degree.

These results would seem proofing the recommendation to assume the average value of soil radioactivity for the sample set collected within the separable transects as a background value of caesium-137 when using the radiocaesium method, since the variability of caesium-137 radioactivity values along transects #114 and #91 224 is low. So, for the slope of the southern exposure, the background caesium-137 radioactivity can be estimated equal to 163.2 Bq/kg (44 880 Bq/m$^2$) (average value for transect #91 224 is 155.9 Bq/kg (42 872.5 Bq/m$^2$), and average value for transect #114 is 170.6 Bq/kg (46 915 Bq/m$^2$). This value is adjusted additionally to basis year (that is 2017), according to a formula that takes into account the radioactive decay (Imshennik, 2011). Since the soil sampling along transects #114 and #91 224 was carried out in 2012, adjusted to 2017 caesium-137 radioactivity value is 145.4 Bq/kg (39 985 Bq/m$^2$).

As the radiocaesium method takes an important role in study of erosional soil losses, it is necessary to follow the recommendations of soil scientists regarding the consideration of microrelief when studying soil losses (Sibirtsev, 1951; Velichko et al., 1996; Velichko et al., 1987; Alifanov et al., 2010). Sibirtsev wrote: “There is nothing accidental in the distribution of soils, each of soil lies in its place, where it should lie, and occupies exactly the area that it should occupy according to natural laws or conditions of its origin ... The soil ... changes due to some reason certainly; the parent rock has changed, the relief has changed, the effect of atmospheric vapor has changed due to the relief, the accumulation of moisture has changed, .... the soil has changed also” (Sibirtsev, 1951). Thus, we neutralize the differences genetically inherent in these soils establishing the background radioactivity value as an average value of the soil specificactivity estimated using a heterogeneous series soil samples (collected either in depression areas or in block elevations).

However, this should be considered unacceptable in principle.

This feature forced us to study in depth distribution of caesium-137 in block elevations and in interblock depressions of the arable slope. Additionally, the analysis of humus content in soil material of block elevations and interblock depressions is involved. The analysis show that there is less humus content in the soil material of block elevations than in the interblock depressions (fig. 5). This can be explained by the intensive plowing of the soil of block elevations in conditions of insufficient application of organic fertilizers. The soil of block elevations is plowed deeper. The decrease in humus content varies from 15 to 50%. In our experimental area a decrease in the humus content in soil of block elevations and of interblock watersheds was found to be up to 20% and more. Thus, unwashed and slightly washed soils of micro-elevations are characterized by a reduced humus content.

Analysis of in depth distribution of the caesium-137 in the areas of block elevations and interblock depressions revealed characteristic features of the distribution (Trofimetz, 2020). In the area of block elevations (at sample plot #149174), a peak radioactivity value at the level of the plow sole (at a 25 cm depth) is presented, with a sharp decrease in the caesium-137 radioactivity of deeper than this level (fig. 5). The same pattern was described by Shamshurina et al. (Shamshurina et al., 2016). The humus content in the arable horizon of the block elevation (at sampling plot #149174) is less than 4% (fig. 5). Washed soil was found at sampling plot #149175. This sampling plot is located in plowing furrow (fig. 3, 5). Caesium-137 radioactivity exceeds 100 Bq/kg down to a 26 cm depth (in soil material of the block elevation caesium-137 value decreases to 20 Bq/kg or less under the arable horizon).

The humus content exceeds 4% down to a 32 cm depth (in the area of the block elevation, under the arable horizon, humus decreases to 3% or less) (fig. 5). Increased humus content can be explained by the result of rotting of crop residues at the depth deeper than 25 cm in the plowing furrows. Thus, the presence of a plow sole in the soil profile at the depth of the arable layer, a sharp decrease in caesium-137 and humus content deeper the plow sole, less than 4% humus content in the arable layer soil material can be considered as markers of unwashed or slightly washed soil. Soil profiles at sampling plots #154163, #149174, #149177 meet these conditions more or less. Remaining six sampling plots cannot be attributed to stable sites. Therefore, only these three sampling plots were recommended to be used when establishing background radioactivity value.

When taking into account the background value of the caesium-137 specific activity estimated using the data of sampling plots #154163, #149174, #149177, the radioactivity value of caesium-137 is estimated as 174.7 Bq/kg (48042.5 Bq/m$^2$). According to two transects (#114 and #91224), the average value of caesium-137 radioactivity is estimated as 163.2 Bq/kg (44880 Bq/m$^2$) (not adjusted to 2017) or as 145.4 Bq/kg (39985 Bq/m$^2$) (adjusted to 2017). The 174.7 Bq/kg (48042.5 Bq/m$^2$) value is greater than the 145.4 Bq/kg (39985 Bq/m$^2$) by 29.3 Bq/kg (8057.5 Бк/м$^2$) or 16.8%.

Affect of this difference onto the estimation of soil loss can be checked on the example of an independent sample set of 200 sampling plots located along the same slope of the southern exposure. When establishing the 145.4 Bq/kg (39985 Bq/m$^2$) as a background value, 50% of the 200 sampling plots are classified as unwashed soil (caesium-137 specific activity exceed the background value). The average value of soil loss for the remaining 50% of sampling plots (classified as washed) is estimated as 8.3 ton per ha per year (the variability of washing varies from 0.1 ton per ha per year to 24.3 ton per ha per year).

When establishing the 174.7 Bq/kg as a caesium-137 radioactivity background value, only 7 sampling plots of 200 (3.5%) are classified as unwashed soil (the radioactivity of the soil material is not less than the 174.7 Bq/kg) (48042.5 Bq/m$^2$). Remaining sampling plots are classified as soil of varying washing degree. Average value of the soil loss intensity is 15.5 ton per ha per year. The variability of the soil loss intensity (according to 174.7 Bq/kg (48042.5 Bq/m$^2$) background value) ranged from 0.1 ton per ha per year to 34.5 ton per ha per year.

Since very high resolution satellite images reflect that the micro-depressions area occupies more than 50% of whole studied area, we have to conclude that the 174.7 Bq/kg (48042.5 Bq/m$^2$) background radioactivity value more objectively reflects dynamic processes in the plowed area located in the periglacial region of the Russian Plain within the Upper Oka basin.

## 5. CONCLUSION

As a result of our study, we found that the microrelief of the watershed surfaces in the periglacial zone of Orel region is dotted with block elevations and interblock depressions. Despite the low variability of caesium-137 in the soil material of the watershed area (no more than 12%), the difference in the structure of soil profiles in block elevations and interblock depressions is proved experimentally. The soil profile in the areas of block elevations corresponds to unwashed or slightly unwashed soil profile. This indicates that the sampling plots for background radioactivity detection have to be assigned in the area of block elevations.

The radioactivity (inventories) of caesium-137 measured in the arable horizon of block elevations have to be accepted as a background value. Estimation of soil loss shows that at 96.5% of the sampling plots washed soil is detected, when establishing caesium-137 radioactivity as a background value using three sampling plots associated with block elevations. At the same time, the soil runoff value varies from 0.1 to 34.5 ton per ha per year.

Only at 50% of the sampling plots washed soil of varying degree is detected, when establishing caesium-137 radioactivity background value as the average value of radioactivity at 86 sampling plots located within two transects crossing the watershed surface.

These conclusions are obtained basing on the results of using independent control sample set composed of 200 sampling plots located along the entire slope of the southern exposure in different microrelief landforms.

We conclude that establishing a caesium-137 radioactivity background value using measurements conducted for block elevations, we can account variability of soil loss due to the impact of the microrelief of paleocryogenic origin more correctly. Since the principles of precision farming require a point-based approach to assess erosional soil loss, the conclusion have to be recognized as meeting modern requirements for soil loss estimation in plowed slope areas dotted with paleocryogenic origin microrelief landforms.

# SOME FEATURES OF THE RADIOCAESIUM METHOD APPLIED TO STUDY OF SOIL LOSSES DUE TO EROSION ON THE PERIGLACIAL AREA OF THE UPPER OKA BASIN

**L. N. Trofimetz[a,#], E. A. Panidi[b], and A. A. Lavrusevich[c]**

[a]*Orel State University, Orel, Russia*

[b]*Saint Petersburg State University, Saint Petersburg, Russia*

[c]*Moscow State University of Civil Engineering, Moscow, Russia*

[#]*E-mail: trofimetc_l_n@mail.ru*

In our study, we consider features the application of caesium-137 to the assess soil losses on an arable slope located in the periglacial zone of the Russian Plain. The study is conducted on the example of an experimental area (an agricultural field in the basin of the Sukhaya Orlitsa River, upper Oka basin within the Oryol region). We discuss the expediency of the polygonal-block structures (located at the paleocryogenic origin watershed surface) accounting when establishing a background value of caesium-137. The specific activity of caesium-137 acts as an indicator of washout degree of soils. We assessed the values of the coefficients of variation for caesium-137 radioactivity using set of soil samples collected along two transects (#114 and #91224) on the watershed surface (86 samples). The coefficients of variation are small (up to 0.12). We prove that the statistical evaluation of the caesium-137 variability have not be a basis when establishing background value of caesium-137 radioactivity. Our study shows that it is necessary to estimate the background value at block elevations where the soil profile has a plow sole at the depth of the arable horizon (caesium-137 radioactivity sharp decrease is observed directly below arable horizon). We compare also the results of caesium-137 specific activity estimations (made at three locations at block elevations of watershed surface, where layer-by-layer soil sampling was conducted) and the average radioactivity estimated at 86 locations (on transects #114 and #91224). We show that the average caesium-137 radioactivity (estimated at 86 locations) being taken as a background radioactivity value leads to underestimation of the soil loss intensity is by ~7.3 tons per 1 hectare per year. We conclude that the specific activity in the experimental area should be estimated basing on layer-by-layer soil samples collected at block elevations (despite the low variability caesium-137 radioactivity values in a set of 86 sample).

*Keywords:* periglacial zone of the Russian Plain, upper Oka basin, reference area, specific activity of caesium-137, intensity of soil losses, variability of caesium-137 activity, block elevations, layered soil sampling

## REFERENCES

Alifanov V.M., Gugalinskaya L.A., and Ovchinnikov A.Yu. *Paleokriogenez i raznoobrazie pochv tsentra Vostochno-Evropeiskoi ravniny* (Paleocryogenesis and soil diversity of the center of East European Plainy). Moscow: GEOS (Publ.), 2010. 160 p. (in Russ.)

Berdnikov V.V. *Paleokriogennyi mikrorel'ef tsentra Russkoi ravniny* (Paleocryogenic microrelief of the center of Russian Plain). Moscow: Nauka (Publ.), 1976. 126 p. (in Russ.)

Imshennik E.V. *Kartograficheskoe prognozirovanie zagryazneniya* $^{137}$*Cs naibolee postradavshikh v rezul'tate avarii na CHAES regionov Rossii* (Cartographic forecasting of $^{137}$Cs pollution in the regions of Russia most affected by the Chernobyl accident). *PhD tthesis*. Moscow: IGKE (Publ.), 2011. 30 p. (in Russ.)

Markelov M.V. *Sovremennye erozionno-akkumulyativnye protsessy v verkhnikh zven'yakh gidrograficheskoi seti lesnoi i lesostepnoi zon* (Modern erosion-accumulative processes in the upper parts of the hydrographic network of forest and forest-steppe zones). *PhD tthesis*.

Moscow: Moscow State University (Publ.), 2004. 26 p. (in Russ.)

Owens P.N. and Walling D.E. Spatial Variability of Caesium—137 Inventories at Reference Sites an Example from Two Contrasting Sites in Englsnd and Zimbabwe. *Applied Radiation and Isotopes*. 1996. Vol. 47. No. 7. P. 699—707. https://doi.org/10.1016/0969-8043(96)00015-2

Panidi E., Trofimetz L., and Sokolova J. Application of phyto-indication and radiocesium indicative methods for microrelief mapping. *IOP Conference Series: Earth and Environmental Science*. 2016. Vol. 34. No. 116. 012024. https://doi.org/10.1088/1755-1315/34/1/012024

Shamshurina E.N., Golosov V.N., and Ivanov M.M. Spatio-temporal reconstruction of the Chernobyl origin $^{137}$Cs on-the-soil-cover deposit field in the upper parts of the Lokna River basin. *Radiatsionnaya biologiya. Radioekologiya*. 2016. No. (4). P. 414—425. (in Russ.) https://doi.org/7868/S0869803116040123

Sibirtsev N.M. *Izbrannye sochineniya. Tom 1.* (Selected writings. Vol. 1). Moscow: Sel'skokhozyaistvennaya literatura (Publ.), 1951. 472 p. (in Russ.)

Trofimetz L.N., Panidi E.A., Chaadaeva N.N., Sankova E.A., Ivaneha T.L., and Petelko A.I. Estimation of the quantity of soil loss in the thalwegs of the streams formed by heavy rainfalls in the breakup furrows at arable slopes: Application of satellite imagery, GIS and radiocesium method. *InterCarto, InterGIS*. 2019. Vol. 25. No. 2. P. 217—231. (in Russ.) https://doi.org/10.35595/2414-9179-2019-2-25-217-231

Trofimetz L.N., Panidi E.A., Chaadaeva N.N., Sankova E.A., Ivaneha T.L., Tyapkina A.P., Petelko A.I., Alexandrova A.P., and Ladnova G.G. Determig the reference value of Cesium-137 specific activity on arable slopes in the periglacial area of the Upper Oka basin: application of satellite images, GIS and soil agrochemical indicators. *InterCarto, InterGIS*. 2020. Vol. 26. No. 3. P. 170—183. (in Russ.) https://doi.org/10.35595/2414-9179-2020-3-26-170-183

Velichko A.A., Morozova T.D., Berdnikov V.V., Nechaev V.P., and Tsatskin A.I. Paleogeographic preconditions for differentiation of soil cover and development of erosion processes. *Soil science*. 1987. No. 10. P. 102—112. (in Russ.)

Velichko A.A., Morozova T.D., Nechaev V.B., and Porozhnyakova O.M. *Paleokriogenez, pochvennyi pokrov i zemledelie* (Paleocryogenesis, soil cover and agriculture). Moscow: Nauka (Publ.), 1996. 150 p. (in Russ.)

**EDN:** FXDLFX
*ГЕОМОРФОЛОГИЯ, 2022, том 53, № 5, с. 162–172*

## ПРОБЛЕМЫ ФЛЮВИАЛЬНОЙ ГЕОМОРФОЛОГИИ

*УДК 551.435.1:551.89(9470.316)*

# СТРОЕНИЕ И ИСТОРИЯ ФОРМИРОВАНИЯ ДОЛИН ПРОРЫВА ВЕРХНЕЙ ВОЛГИ

**© 2022 г. А. О. Уткина[1,*], А. В. Панин[1]**
[1]*Институт географии РАН, Москва, Россия*
**E-mail: utkina@igras.ru*

Поступила в редакцию 14.06.2022 г.
После доработки 29.06.2022 г.
Принята к публикации 15.07.2022 г.

Несмотря на длительную историю изучения, история формирования долины верхней Волги представляет предмет дискуссий. Согласно наиболее распространенной в литературе модели, в максимум последнего оледенения в бассейне верхней Волги возникла система приледниковых озер, и долина Волги образовалась лишь 14–15 тыс. л. н. после спуска этих озер в результате образования участков прорыва у нынешних городов Тутаева и Плеса. Чтобы проверить эту гипотезу, мы попытались определить механизм формирования и возраст долин прорыва, используя метод люминесцентного датирования. Кроме того, для оценки одного из возможных механизмов образования приледниковых озер мы использовали модель гляциоизостатических деформаций. В долине прорыва у г. Плёс нами была обнаружена речная терраса, датированная позднемосковско-микулинским временем, что доказывает, что долина намного старше предполагаемого валдайского возраста. В долине не было обнаружено никаких признаков озерных отложений, а моделирование не показало такого влияния гляциоизостатических деформаций на бассейн, которое могло бы привести к образованию приледниковых озер. В связи с этим можно предположить, что валдайских приледниковых озер в долине не существовало. По-видимому, предыдущими исследователями за озерные отложения принимались широко развитые на склонах и дне долины делювиальные суглинки и эоловые алевриты, которые, по данным нашего датирования, действительно относятся к эпохе последнего оледенения. По данным моделирования, в последнюю ледниковую эпоху на изучаемый участок приходится формирование компенсационного приледникового вала. Его высоты было недостаточно для подпруживания Волги, но уменьшение уклона долины должно было вызвать направленную аккумуляцию в реке, что подтверждается наличием низкой речной террасы соответствующего возраста. В позднеледниковье разрушение вала вызвало врезание реки.

*Ключевые слова:* валдайское оледенение, приледниковые озера, гляциоизостазия, компенсационный приледниковый вал, люминесцентное датирование
**DOI:** 10.31857/S0435428122050182

## 1. INTRODUCTION

With a length of 3.530 km and the drainage basin area of 1.361 million km$^2$ (Tockner et al., 2009) the Volga is the largest river in Europe. Today the river is almost entirely regulated as it flows through Central Russia and into the Caspian Sea. The Volga has been a focus of geographic, geomorphologic and paleogeographic research for several decades, and many attempts to reconstruct its history have been made (Sidorchuk et al., 2009). Nevertheless, there is still much to uncover about how and when it was formed. Particularly this concerns the upstream part of the basin, as its evolution, though much studied, remains uncertain. The Volga River is traditionally divided into three unequal parts based on the major differences in its geological and geomorphological structure (Obedientova, 1977), and its upstream part is referred to as the Upper Volga (fig. 1). When compared to other parts of the valley, the amount of conducted research on the Upper Volga is significantly lesser.

One of the key issues of the paleogeography of the Upper Volga is the formation of incision valleys since this process is associated with the river network restructuring. These incision valleys are narrow sections of the Upper Volga valley characterised by a deeply cut channel, high banks, and the absence of river terraces. Their formation is assumed to involve a rapidly occurred cutting through the local watershed. Since such valley sections usually indicate that the valley itself is relatively young, the researchers (Schukina, 1933; Mirchink, 1935; Kvasov, 1979) conclude that it joined the rest of the river system only recently, supposedly, in late Pleistocene.

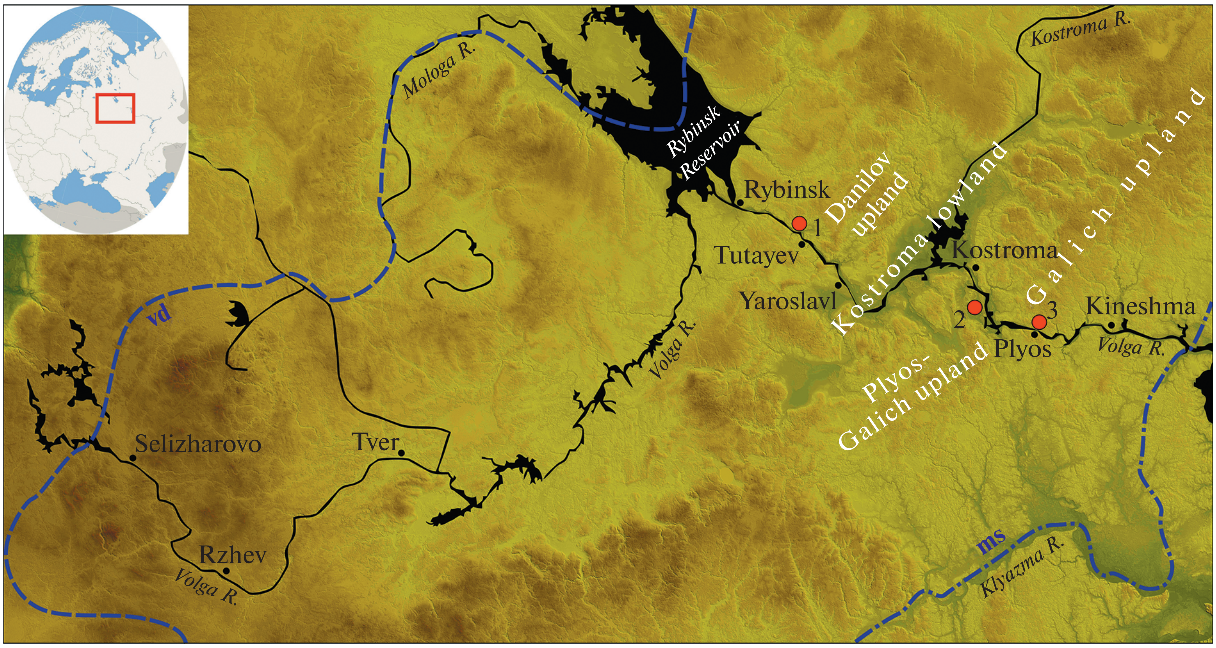


**Fig. 1.** Elevation map of the research area: digital elevation model (DEM) SRTM. Ice sheet extents are shown as blue dashed lines (vd – MIS 2 ice sheet extent (Astakhov et al., 2016), ms – MIS 6 ice sheet extent (Moskvitin, 1967)); red dots mark study sites (1 – Otmishchevo site, 2 – Pogorelka site, 3 – Plyos site).

**Рис. 1.** Схема района исследования. Основа – цифровая модель рельефа (ЦМР) SRTM. Границы оледенений показаны синими пунктирными линиями (vd – валдайское оледенение (MIS 2) (Astakhov et al., 2016), ms – московское (MIS 6) (Москвитин, 1967)); красными точками отмечены ключевые участки (1 – Отмищево, 2 – Погорелка, 3 – Плес).

Over the years, it had been established that the formation of the Upper Volga River must had been influenced by Pleistocene glaciations of the Northern Russian Plain. It is widely known that they played a major role in shaping the modern geomorphologic structure of the region (Kalm, 2012). Most researchers argue that the formation of the Upper Volga River occurred at the last stages of the Last Glaciation (called Valdai glaciation on the Russian plain) (Schukina, 1933; Kvasov, 1979). Since its basin was largely affected by the last glaciation event, the Upper Volga supposedly could have been one of the regions where proglacial lakes emerged during the Late Valdai (Bolshakova, 1963; Schik, Pisareva, 1998; Astakhov et al., 2016). This concept was first introduced by Kvasov (1979). According to his model, a major part of Upper Volga territory was covered by a large lake system that formed during the last glacial maximum (LGM, approx. 21 ka). The river itself was to appear only after this lake system had stopped existing. Presumably, it happened due to formation of an incision valley near the town of Plyos (fig. 1) about 14.5 ka (Kvasov, 1979). Kvasov does not go into detail on Tutaev incision valley's mechanism of formation but concludes that it was formed when the waters of the proglacial lake cut through the Danilov upland around 15 ka.

This concept of the Upper Volga River's emergence, through widely accepted, has not been thoroughly checked and lacks proper stratigraphical evidence. There are no direct determinations of the age of these events, as well as of the time of river valley adjustment. Many questions concerning the paleogeography of ice-dammed lakes are far from being resolved. Areas of flooding, elevation of the lake levels in relation to the thresholds of runoff, location, and chronology of overflow events, restructuring of valley systems – these issues have still been addressed mainly on the morphological basis (Mangerud et al., 2004). Virtually no geologically confirmed facts have still been published, i.e., reliably proved occurrence of deposits of the corresponding genesis and their age.

There is also one important aspect of the history of Pleistocene periglacial areas that could not had been considered by Kvasov in late 1970s. The formation of proglacial lakes in the Upper Volga basin could have been heavily influenced by glacial isostatic adjustment (GIA). One of the most important effects of GIA impact on the landscape development was the formation of large lithosphere uplifts located in the periglacial zones called glacial forebulges. Previous study of large rivers valleys in Europe, as well as the relief of the bottom of the North Sea and the English Channel, carried out by E.N. Bylinsky (1990), made it possible to outline the location of Late Valdai glacial forebulge around the Scandinavian ice sheet. According to Bylinsky's model (Bylinski, 1990), the glacial forebulge of the last glaciation crossed the Upper Volga basin in close vicinity of the Plyos incision valley. One of the possible mechanisms for the proglacial lakes' formation could involve slight inclination of the basin towards the glacier. This way, the part of the basin located within the glacial forebulge would be hypsometrically higher than its source. Such an incline of the basin surface would allow the waters to be dammed from both north (by the glacier) and south (by the forebulge). It is possible to determine the reliability of this mechanism by employing the GIA model (Spada, Melini, 2019).

This paper aims to demonstrate the results of recent studies that could provide a geochronological insight into the history of the Upper Volga. Our studies are focused mainly on the incision valleys, as their emergence might be the key event in the Upper Volga valley's history. The main goal of the study was to determine the age of the Plyos and Tutayev incision valleys and the mechanism of their formation. Also, since their emergence is possibly connected with the formation of the Upper Volga proglacial lakes, we used a GIA model (Spada, Melini, 2019) to assess one of the ways of their possible formation. As this study concerns questions of possible existence of proglacial lakes on the Northern Russian Plain, it can provide new knowledge about them. It is widely known that outbursts and overflows of the large proglacial lakes through watersheds exerted impact over geomorphological landscapes and caused the paleogeographic events of regional and possibly global rank (Svendsen et al., 2004).

## 2. MATERIALS AND METHODS

During fieldwork 9 excavations were made in the key areas (7 boreholes made by mechanical drilling, and 2 sections). Mechanical drilling was conducted using the Mount 80 drilling rig. Based on the sedimentological description we made assumptions of the possible genesis of the sediments.

We employed Optically Stimulated Luminescence (OSL) as the main dating method. It is widely used for dating glaciofluvial (Thrasher et al., 2009) and fluvial (Wallinga, 2002) sediments and has proven to be able to provide reliable results for low-gradient river systems in central Russia (Panin et al., 2017), and in particular in the Volga system (Kurbanov et al., 2020). All samples were collected in opaque plastic tubes secured with foil on both ends. To collect the samples during mechanical drilling a sampler designed specifically for this purpose was used. The potentially light-exposed ends of the sample were used for dose rate measurements. A total of 25 samples was collected. Preliminary sample preparation was performed in Moscow, MSU, under orange LED lights (Sohbati et al., 2017), following the procedure described by (Kurbanov et al., 2020) and (Murray et al., 2021). All measurements were performed at the Nordic Laboratory for Luminescence Dating at Risø, Denmark, using multi-grain aliquots. Samples were measured in a Risø TL/OSL reader, model TLDA20, equipped with a calibrated beta source (dose rate 0.057–0.220 Gy/s) (Hansen et al., 2015, 2018). For quartz, the single aliquot regenerative dose protocol was applied to 10 mm diameter multi-grain (180–250 mm) quartz aliquots to estimate the equivalent dose (Murray, Wintle, 2000, 2003), with blue (470 ± 30 nm) light stimulation, and 260°C preheating for 10 s. Multi-grain (180–250 mm) feldspar aliquots (2 mm diameter) were measured using a post IR-IR protocol, with a preheat temperature of 250°C for 1 min, and stimulation with IR (870 nm) for 100 s while the aliquot was held at 50°C ($IR_{50}$), followed by a further 100 s with the sample held at 290°C ($pIRIR_{290}$) (Thomsen et al., 2008; Buylaert et al., 2012). Large multi-grain aliquots were employed as it was important to identify well-bleached samples; the average dose is then the most appropriate dose estimate, and for a given number of measurements, this is most precisely measured using large aliquots.

The samples were analysed for natural radionuclide concentrations using high-resolution gamma spectrometry (Murray et al., 1987). These concentrations were converted into dose rates using conversion factors listed by (Olley et al., 1996); a cosmic ray contribution was calculated according to (Prescott, Hutton, 1994), assuming the modern burial depth has applied throughout the lifetime of the site. Laboratory saturated water contents were measured.

Dating sediments of glaciofluvial and fluvial origin is often associated with an incomplete bleaching of grains in the transport process (Alexanderson, Murray, 2012). Using both quartz and feldspar signals, we expected to investigate the degree of bleaching of the quartz by comparing quartz OSL ages with feldspar IR and pIRIR ages (Murray et al., 2012).

GIA modelling was also employed to investigate possible GIA influence on the Upper Volga during the Late Pleistocene. We used the open-source program SELEN (version 4.0) (Spada, Melini, 2019) that simulates the glacial isostatic adjustment (GIA) process in response to the melting of the Late Pleistocene ice sheets. SELEN solves the gravitationally and topographically self-consistent sea level equation for a spherically symmetric Earth with linear viscoelastic rheology, while considering the migration of the shorelines and the rotational feedback on sea level. SELEN thus allows to model GIA in any given part of the world and study a broad range of its geophysical effects. To simulate the GIA effect, SELEN uses data on the spatio-temporal distribution of glacier loads extracted from the ICE-6G model (Argus et al., 2014; Peltier et al., 2015), as well as information about modern topography based on ETOPO1. Following the user guide distributed along with the source code (Spada, Melini, 2019) we ran the program in its standard configuration. Using the resulting data on the reconstruction of topography we were able to study the changes in topography under the GIA influence for three time

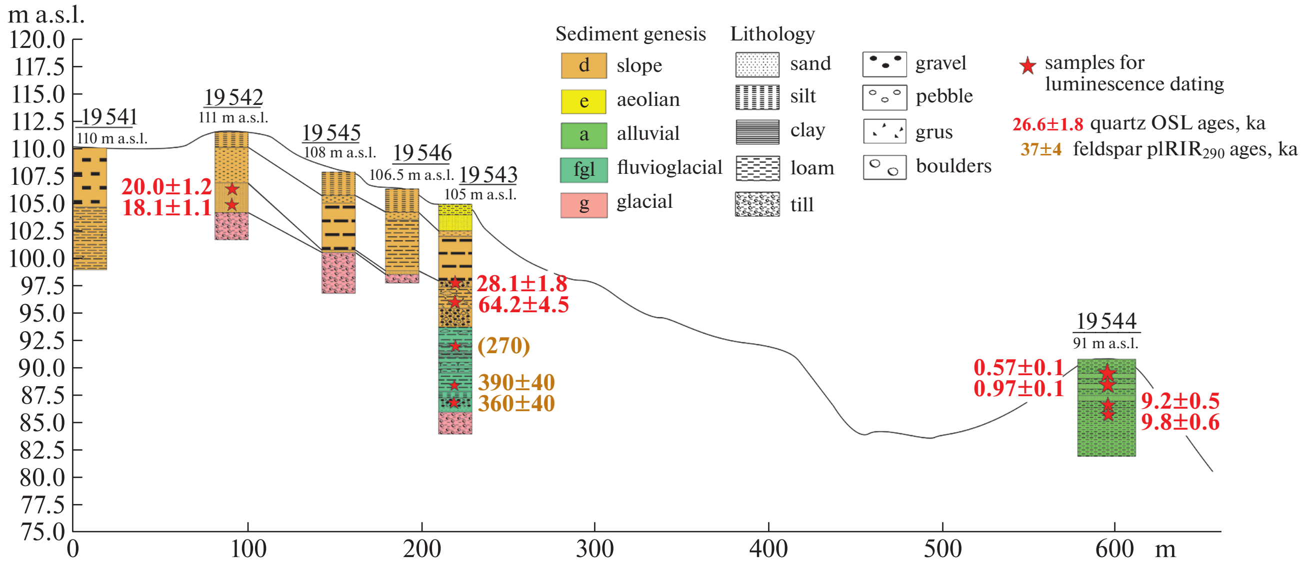


**Fig. 2.** Schematic profile through the Volga's left riverbank at Otmishchevo site (fig. 1, site 1).
**Рис. 2.** Схематический профиль через левый берег Волги на участке Отмищево (рис. 1, ключевой участок 1).

periods (21 ka (LGM), 17.5 ka, 15 ka). Kvasov (1979) chose these exact time stamps to reconstruct the Upper Volga proglacial lakes. Using the GIS software (ArcMap 10.5) DEMs of the "paleo-topography" for the mentioned time periods were created which allowed us to directly determine the changes in topography caused by the GIA effect. For a visual demonstration of these changes in the Upper Volga basin, river profiles were constructed for each of the time slices and for the modern river and then compared. More detailed explanation of our modelling strategy can be found in our recent paper (Utkina, 2020).

## 3. RESULTS

Both incision valleys are in the Upper Volga valley section extending from Rybinsk reservoir to Plyos (fig. 1). In the Rybinsk-Yaroslavl region the river flows in a narrow valley while crossing the Danilov upland. The terrain is relatively hilly alternating in places with flat areas, typically 150 to 200 m above sea level (a.s.l.). The valley width varies from 1.5 to 2 km, and the channel width from 700 to 900 m, with the narrowest part located near Tutayev (Tutayev incision valley). Downstream from Yaroslavl the valley expands up to 20 km while flowing through the Kostroma lowland, and then narrows again to cut through the Plyos-Galich upland, forming the Plyos incision valley. Here, about 150 km downstream from Tutayev, the valley is only 600–700 m wide, with 40–60 m high steep slopes (around 20°) lining the channel. According to previous studies (Schukina, 1933; Bolshakova, 1963; Obedientova, 1977; Kvasov, 1979), there are no alluvial sediments found in the incision valleys, however some were discovered a few kilometres upstream from them.

In this study we aimed to check if this pre-established view on the Upper Volga valley structure is true or not.

The resulting OSL equivalent doses, dose rates and ages are shown in tabl. 1 together with feldspar to quartz ratios. The general luminescence characteristics for the samples from the Upper Volga are reported in our previous paper (Utkina et al., 2022).

*3.1. Tutayev incision valley.* To examine the valley structure close to Tutayev incision valley, we studied a site near Otmishchevo village (located 4 km upstream from Tutayev (fig. 1, site 1)), where previous researchers identified three Volga terraces (Arslanov et al., 1972). We drilled 5 boreholes and studied one section in the proposed terrace levels, comprising the resulting data into a profile (fig. 2). The first borehole (19541) is in a depression on a gently sloping surface, previously interpreted as the third Volga River terrace. Up to a depth of 4.5 m and below the core is comprised of reddish-brown loam with sporadic grus. From 3.5 m, it becomes brick-red with large fragments of ground metamorphic rocks. Above 2.2 m it is overlain by a medium silt loam. Overall sequence displays slope wash deposits, and no sediments of alluvial origin are found.

The second borehole was placed closer to the edge of the same surface (19542, fig. 2). At 3.0–4.5 m and below, there is a heavy brick-red loam with rocks (till). Below 2.5 m it is covered by fine sand with layers of 2–3 cm thick loam. Fine-grained sand with a thin horizontal layering follows from 1.9 m. The upper 0.6 m reveal a light red-brown silty loam. 2 samples were taken for OSL dating: at 2.0–2.5, and at 2.5–3.0 m. The sediments date back to Late Valdai (18–20 ka, MIS 2). The age was determined with high reliability

**Table 1.** Quartz and feldspar doses, resulting ages and feldspar/quartz age ratios
**Таблица 1.** Результаты люминесцентного датирования: дозы, итоговые возраста и их соотношения по кварцу и полевому шпату

| Sample code | Depth. cm | Equivalent dose, Gy | | | Age, ka | | | Quartz dose rate (Gy/ka)[a] | $IR_{50}$/Q | $pIRIR_{290}$/Q | B[b] |
|---|---|---|---|---|---|---|---|---|---|---|---|
| | | Quartz OSL | $IR_{50}$ | $pIRIR_{290}$ | Quartz OSL | $IR_{50}$ | $pIRIR_{290}$ | | | | |
| 19542–1 | 225 | 35 ± 1 | 37 ± 1 | 50 ± 2 | 20 ± 1 | 14 ± 1 | 20 ± 1 | 1.76 ± 0.1 | 0.7 ± 0.1 | 1.0 ± 0.1 | ✓ |
| 19542–2 | 275 | 35 ± 1 | 37 ± 1 | 51 ± 2 | 18 ± 1 | 14 ± 1 | 19 ± 1 | 1.94 ± 0.1 | 0.8 ± 0.1 | 1.0 ± 0.1 | ✓ |
| 19543–1 | 295 | 50 ± 2 | 66 ± 4 | 117 ± 13 | 28 ± 2 | 26 ± 2 | 46 ± 6 | 1.78 ± 0.08 | 0.9 ± 0.1 | 1.64 ± 0.2 | ✓ |
| 19543–2 | 405 | 116 ± 5 | 189 ± 23 | 259 ± 40 | 64 ± 5 | 73 ± 9 | 100 ± 16 | 1.81 ± 0.09 | 1.14 ± 0.3 | 1.57 ± 0.4 | |
| 19543–3 | 525 | >200 | 389 ± 9 | 783 ± 66 | >90 | (130)[c] | (270) | 2.18 ± 0.10 | | | |
| 19543–4 | 670 | >200 | 576 ± 44 | 809 ± 77 | >160 | 280 ± 20 | 390 ± 40 | 1.29 ± 0.06 | | | |
| 19543–5 | 750 | >200 | 508 ± 30 | 701 ± 59 | >170 | 260 ± 20 | 360 ± 40 | 1.15 ± 0.06 | | | |
| 19544–1 | 85 | 1.1 ± 1 | 19 ± 1 | 65 ± 1 | 0.57 ± 0.1 | 8 ± 1 | 26 ± 2 | 1.73 ± 0.08 | 13 ± 2 | 43 ± 5.7 | |
| 19544–2 | 90 | 1.7 ± 1 | 20 ± 1 | 63 ± 1 | 0.97 ± 0.1 | 8 ± 1 | 26 ± 1 | 1.68 ± 0.08 | 8 ± 1 | 25 ± 3.4 | |
| 19544–3 | 180 | 21 ± 1 | 25 ± 1 | 57 ± 1 | 9.2 ± 0.5 | 8 ± 1 | 18 ± 1 | 2.33 ± 0.11 | 0.9 ± 0.1 | 2.0 ± 0.2 | |
| 19544–4 | 210 | 19 ± 1 | 24 ± 1 | 55 ± 1 | 9.8 ± 0.6 | 9 ± 1 | 20 ± 1 | 1.99 ± 0.10 | 0.9 ± 0.1 | 2.1 ± 0.2 | |
| 19535–1 | 150 | >200 | 463 ± 14 | 835 ± 158 | >260 | 300 ± 10 | 540 ± 110 | 0.78 ± 0.03 | | | |
| 19535–2 | 250 | >200 | 522 ± 36 | 976 ± 128 | >280 | 350 ± 30 | 660 ± 90 | 0.71 ± 0.03 | | | |
| 19535–3 | 350 | >200 | 444 ± 17 | 740 ± 35 | >230 | 270 ± 20 | 440 ± 30 | 0.89 ± 0.04 | | | |
| 19535–4 | 395 | >200 | 464 ± 22 | 899 ± 186 | >240 | 290 ± 20 | 560 ± 120 | 0.83 ± 0.04 | | | |
| 19534–3 | 690 | 18 ± 1 | 24 ± 1 | 35 ± 2 | 14 ± 1 | 10 ± 1 | 14 ± 1 | 1.69 ± 0.09 | 0.9 ± 0.1 | 1.3 ± 0.1 | ✓ |
| 19534–4 | 150 | 36 ± 1 | 35 ± 1 | 54 ± 1 | 16 ± 1 | 10 ± 1 | 16 ± 1 | 2.55 ± 0.13 | 0.7 ± 0.1 | 1.2 ± 0.1 | ✓ |
| 19534–5 | 380 | 36 ± 1 | 32 ± 1 | 50 ± 1 | 14 ± 1 | 11 ± 1 | 17 ± 1 | 2.20 ± 0.11 | 0.7 ± 0.1 | 1.0 ± 0.1 | ✓ |
| 19534–6 | 450 | 33 ± 1 | 33 ± 1 | 53 ± 1 | 11 ± 1 | 11 ± 1 | 17 ± 1 | 2.33 ± 0.12 | 0.8 ± 0.1 | 1.2 ± 0.1 | ✓ |
| 010–5 | 80 | 111 ± 4 | 154 ± 17 | 255 ± 20 | 119 ± 10 | 83 ± 10 | 136 ± 14 | 0.93 ± 0.04 | 0.69 ± 0.1 | 1.15 ± 0.1 | ✓ |
| 010–6 | 130 | 116 ± 5 | 163 ± 21 | 238 ± 15 | 108 ± 8 | 81 ± 12 | 118 ± 10 | 1.07 ± 0.04 | 0.75 ± 0.1 | 1.09 ± 0.1 | ✓ |
| 010–1 | 470 | 62 ± 7 | 207 ± 20 | 453 ± 57 | 59.5 ± 8 | 100 ± 11 | 230 ± 32 | 1.04 ± 0.05 | 1.71 ± 0.3 | 3.85 ± 0.67 | |
| 010–2 | 730 | 167 ± 23 | 265 ± 25 | 376 ± 29 | 153 ± 24 | 131 ± 14 | 186 ± 17 | 1.09 ± 0.04 | 0.85 ± 0.2 | 1.21 ± 0.2 | ✓ |
| 010–3 | 870 | 126 ± 6 | 137 ± 16 | 285 ± 7 | 124 ± 9 | 70.5 ± 9 | 146 ± 7.7 | 1.01 ± 0.04 | 0.57 ± 0.1 | 1.17 ± 0.1 | ✓ |
| 010–4 | 890 | 155 ± 5 | 244 ± 17 | 362 ± 26 | 120 ± 7 | 109 ± 9 | 162 ± 14 | 1.30 ± 0.05 | 0.92 ± 0.1 | 1.36 ± 0.1 | ✓ |

[a]One can derive the total feldspar dose rate by adding 0.94 to quartz dose rates.
[b]This column shows bleaching confidence. Ticked samples are confidently well-bleached.
[c]The uncertainties on ages indicated by parentheses are poorly known.
[a]Скорость накопления дозы для полевого шпата может быть получена при прибавлении коэффициента 0.94 к скорости накопления дозы для кварца.
[b]Данный столбец показывает степень засветки. Отмеченные галочкой образцы с большой вероятностью хорошо засвечены.
[c]Ошибка для возрастов, обозначенных скобками, плохо известна.

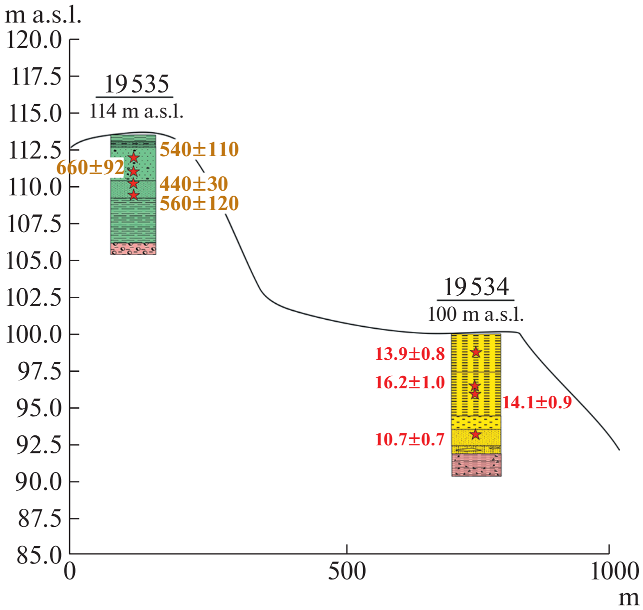


**Fig. 3.** Schematic profile through the Volga's right riverbank at Pogorelka site (fig. 1, site 2). See legend in fig. 2.

**Рис. 3.** Схематический профиль через правый берег Волги на участке Погорелка (рис. 1, ключевой участок 2). Легенду см. рис. 2.

since the quartz and feldspar ratios are 1.01–1.04 ($pIRIR_{290}/Q$) and 0.7–0.8 ($IR_{50}/Q$) (tabl. 1). The described sediment composition allows us to determine their slope genesis. Two additional boreholes were made here to trace the top of a till layer (19545 and 19546, fig. 2). The depth of the top changed from 3 to 7.7 m. The upper part of both revealed sequences is seemingly similar to the borehole 19542.

The next borehole (19543) is located down the slope, near the edge of a lower terrace level (105 m a.s.l.). The sequence starts with a till layer at the bottom. The next 6.8 m are comprised of a loamy sequence, probably water lain, with several coarser layers (at 7, 4, and 3 m deep). Samples for OSL dating were taken from depths of 7.0–7.5 m (clayey sand with debris), 6.6–6.9 m (sandy loam), 5.0–5.5 m (silty loam). This type of sediment cannot be directly attributed to one distinct deposition process, but given the abundance of fine-grained material, it was probably deposited in relatively calm water conditions with coarser layers corresponding to periods of faster water flow. The upper part of the section (1 m) is comprised of fine, probably aeolian, sands. Based on the ages, this section has two distinct parts: the upper 4 m appears to be from the last glacial period, and below that the sediments are much older, around 200–300 ka.

Down the slope the first floodplain terrace of the Volga River was discovered. The terrace ledge is sharp and clear at the confluence of the Dubenka River with the Volga. The ledge is steep, the height is about 8 m (91 m a.s.l.) above the Volga summer water level. A terrace section (19544) revealed reddish-brown layered sandy loam with fine-grained sand and sporadic pebbles continuing up to 1.8 m deep. Above 1.80 m, multiple layers (1 to 100 mm thick) of fine-grained sands alternating with sandy loam were observed. Below 1.5 m, the layers are thinner, 1–5 mm thick, with the increased number of loamy interlayers. Visible horizontal layering is characteristic for the entire sequence. Samples for OSL were collected at 0.75–0.80, 0.80–0.85, 1.80–1.85, 2.20–2.25 m. The resulting ages date back to the Holocene: the upper ones are around 1 ka, and the lower ones – around 10 ka. The quartz and feldspar ratios indicate the average reliability of the date (tabl. 1).

*3.2. Plyos incision valley.* Field studies in Plyos incision valley were conducted both inside the valley and 30 km upstream from it, where previous studies had described the terraces as particularly well defined (Bolshakova, 1963). The latter site (Pogorelka) is located ~100 km downstream from Tutayev (fig. 1, site 2). Bolshakova (1963) identified two terraces in this part of the Volga valley, with altitudes 110 m a.s.l. (a conjugate terrace of Volga and Kostroma Lake) and 100 m a.s.l. Our chosen site revealed what appeared to be 3 terraces at 90, 100 and 112 m a.s.l. We studied the sediment composition of the upper (oldest) terrace (19535, 112 m a.s.l.) and the middle terrace (19534, 100 m a.s.l.) (fig. 3). The oldest supposed terrace is composed of a 7.5 m-thick sandy and loamy sequence resting on loamy till layer with boulders. The sediment layer covering the till is made of fine loamy and silty layers, further up it is replaced by 1m of fine sand (sampled for OSL at 3.8 and 3.5 m deep) with visible horizontal layering. The next 2 m are represented by coarser sand with rare gravel and pebbles (sampled for OSL at 2.5 and 1.5 m). Finally, this layer is followed by 0.5 m of medium-grained sand and silt alternation and then by 0.5 m-thick sequence made up of loam. OSL dating revealed that these sediments are again much older than Late Valdai, around 400 ka and even up to 660 ka.

The second proposed terrace (19534, fig. 3) revealed a loamy till layer at a depth of 8 m, and further up it is replaced by fine-grained clayey sand. At 7.5 m, there is a silty loamy layer, and at 5.5 m – a silty layer with a clear horizontal layering. In the upper 2.6 m, the core is represented by silt with a clayey interlayer at 2.2–2.6 m. OSL samples were taken at 1.3–1.8 m (silt), 3.6–4.1 m (silt), 4.2–4.7 m (silt), 7–7.2 m (fine sand). The ages mainly correspond to the Late Valdai (13–16 ka), with the upper early Holocene one (10.7 ka). The sedimentological characteristics indicate that these sediments are of aeolian origin.

The last site is in the Plyos incision valley itself. Although it has been suggested that both Upper Volga incision valleys do not contain terraces (Kvasov, 1979), we identified at least one apparent terrace in the Plyos incision valley (fig. 4). It is a sand body leaning towards the left side of the valley, across from the town of Plyos, where a section naturally created by a slope-wash processes was studied. It contains a 15-m thick sequence of alternating coarse, medium, and fine sands with pebbles and gravel displaying horizontal and cross lamination. We can confidently identify these deposits as alluvial sediments of the Volga River. We took 6 samples from this section for dating: two from in the upper, two from the middle, and two from the lower part of the sand body. OSL dating revealed these to be late MIS 6 – MIS 5 sediments. Ages are not entirely stratigraphically consistent, but such scatter is considered typical for quartz. All quartz ages are in the range 108–153 ka, and consistent with a single deposition period, except for one outlier – the sample with a quartz age of 59 ka. Since it is totally inconsistent with all the other ages, it is thought to be wrong and is not considered further.

*3.3. GIA modeling.* The reconstructions of GIA influence on the Upper Volga basin prove that the axis of the glacial forebulge affected the Rybinsk-Plyos part of the river. The axis for all time slices lies between Kostroma and Plyos. The width and height of the forebulge, the length and height of the “slope” to the glacier change over time. For 21 ka, the maximum relative elevation of the forebulge is 17 m, and the maximum lowering near the Volga River source is –77 m. However, we must note that during this time, the source was covered by the glacier (Astakhov et al., 2016). For 17.5 ka, the maximum elevation of the forebulge is 12 m, and the maximum lowering near the source is –85 m. For 15 ka, the maximum elevation of the forebulge is 9 m, and the maximum lowering near the source is –65 m. GIA modelling also allowed us to study the possible changes in the Volga’s profile throughout the last deglaciation that were caused by the glacial influence. The comparison of the modelled profiles with the modern one (fig. 5) shows no sufficiently strong GIA influence to skew the river profile completely towards the glacier – it mostly retains its shape. Still, GIA had a certain effect on the Upper Volga basin. Some skewing can be seen in the upmost reaches of the river, but it does not affect our key region. We can also see that during the LGM and deglaciation the profile was slightly elevated in the area close to the forebulge axis (Kostroma-Plyos, fig. 1). According to our reconstructions, the height of the glacial forebulge gradually decreased throughout the deglaciation, and the riverbed followed these changes.

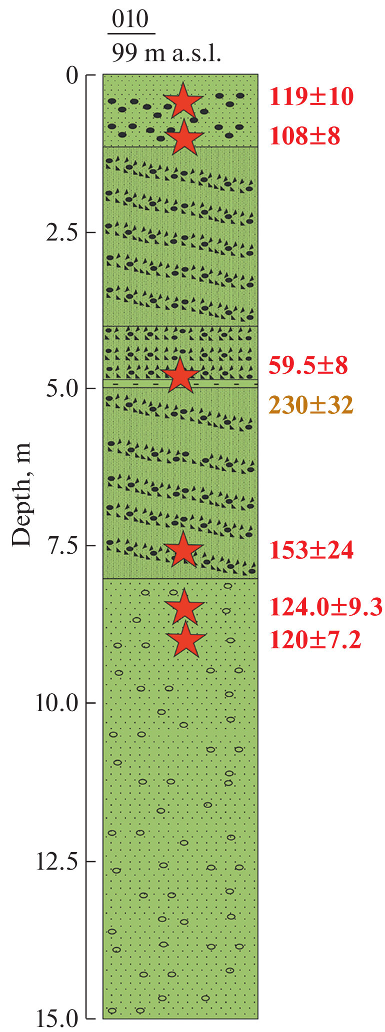


**Fig. 4.** Schematic section made on the left side of the Plyos incision valley. See legend in fig. 2.

**Рис. 4.** Схематическое отображение разреза, заложенного на левом берегу долины прорыва у г. Плёс. Легенду см. рис. 2.

## 4. DISCUSSION

The most widely accepted Upper Volga evolution model (Kvasov, 1979) proposes that the Upper Volga River valley was formed after the MIS 2 proglacial lakes drained to the south. Both Upper Volga incision valleys formed during the lake drainage, but it was the formation of Plyos incision valley specifically that gave way to the south drainage and the river valley emergence. Following this model, we expected the landforms in the incision valleys to date back mostly to MIS 2 or shortly thereafter. Moreover, according to previous studies, there was supposed to be no alluvial sediments and river terraces in the incision valleys itself. Nevertheless, our field studies allowed us to locate these in the Plyos incision valley. The sand body we discovered there is confidently identified as an alluvial sediment and dates back to the late MIS 6 – MIS 5 time. Thus, we can refute the previously stated statement about the absence of terraces in the Plyos incision valley, and, in addition, determine the time when the valley should have already existed. If it is filled with the late MIS 6 – MIS 5 sediments, we can safely assume that the valley was formed long before MIS 2.

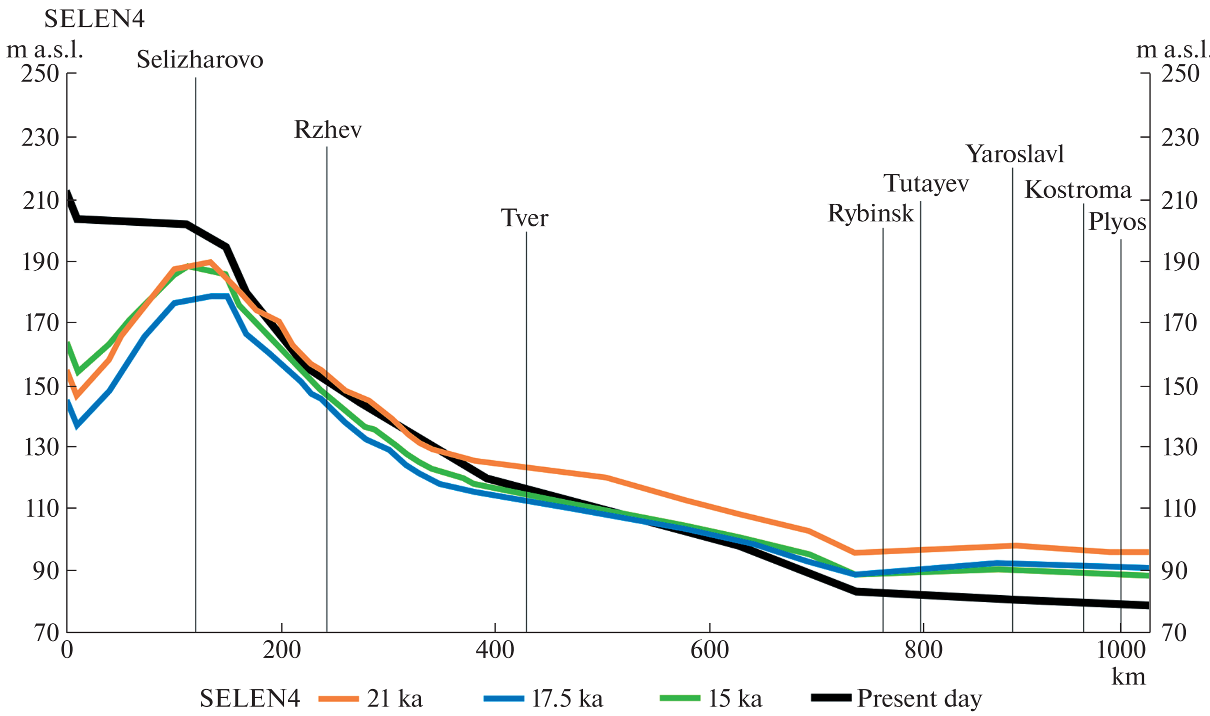


**Fig. 5.** Comparison of the present-day Upper Volga River profile with the ones built for 21, 17.5 and 15 ka using GIA modelling (Spada, Melini, 2019; Utkina, 2020).

**Рис. 5.** Продольные профили верхней Волги, построенные на временные срезы 21, 17.5 и 15 тыс. л. н. по палео-ЦМР, реконструированным с помощью программы SELEN4, моделирующей палеотопографию с учетом гляциоизостатических деформаций (Spada, Melini, 2019; Utkina, 2020).

During the study of the Tutayev incision valley, the first terrace of the Volga River with a height of 8 m above the summer water level (91 m a.s.l.) was discovered. According to the OSL dating results, the terrace formation continued throughout the Holocene (from approx. 10 ka to approx. 1 ka). Other boreholes further up the slope did not reveal confidently identified alluvial or lacustrine deposits. The upper part of the valley slope is covered by slope deposits, and in the middle part a layer of presumably fluvioglacial deposits (dating back to 200–300 ka) was discovered overlying the till. 30 km upstream from Plyos a similar sediment was found being even older than the one near Tutayev (400–500 ka). Other recent studies of the Upper Volga valley sediments showed similar results in some other places in the valley (Utkina et al., 2022). For now, we are uncertain of the correct interpretation of these data, and further studies are required to resolve this issue. Another borehole from the same site allowed us to determine the Late Valdai–early Holocene aeolian sedimentation in the valley.

Following the GIA modelling results, we can assume that the proglacial lakes formation under the GIA influence can be ruled out for the Rybinsk-Plyos section of the Volga, since we can see no sufficiently strong GIA influence to skew the river profile completely towards the glacier. Moreover, we did not find actual proof of late Pleistocene lake deposits in the Upper Volga valley. Slight skew in the upper reaches near the Volga source might mean that the proglacial lakes existed there during Late Valdai, but there is no evidence for it happening to the Rybinsk-Plyos part of the river. However, the GIA effect appears to have influenced this part in some other way – the gradual decrease of the glacial forebulge throughout the deglaciation caused notable change in elevation of the Volga riverbed. This process should have caused an increase in the slope of the riverbed and, in turn, its postglacial cutting episode.

Thus, according to the data we have obtained on the geological and geomorphological structure of the incision valleys, their formation should have occurred in the Late Moscow (Late MIS 6) time, which is most convincingly evidenced by the Plyos incision valley terrace. Excluding the possibility of proglacial lakes emergence in the Upper Volga basin, the most likely mechanism for the incision valleys formation is the meltwater erosion caused by the meltwater flows of the Moscow (MIS 6) glaciation, when the glacier border was last the closest to the key area. If so, the Upper Volga valley was formed and became part of the larger Volga River system at late MIS 6. The GIA effect of the MIS 2 glacier was manifested through the forebulge evolution during the last deglaciation. The gradual decrease in the forebulge height caused the cutting episode which is confirmed by the Holocene terrace.

## 5. CONCLUSION

New data on the structure of the incision valleys and the possible GIA influence on the development of the Upper Volga valley in the Late Pleistocene allows us to clarify some available information about the Upper Volga Valley and its evolution. According to the most popular model of the Upper Volga emergence, its valley did not exist yet in MIS 2 and its basin was occupied by a proglacial lake system dammed by the MIS 2 glacier. The valley was formed around 14.5 ka, when the Plyos incision valley emerged, and the lake system was drained to the south, although same parts of the modern valley, like the Tutayev incision valley, were formed even prior to this event. Since other researchers also connected the formation of the incision valleys to the formation of the entire Upper Volga valley, we chose them as key regions in this study. Other than that, we considered possible GIA influence on the basin which might have served as one of the possible reasons for the proglacial lakes' existence: the MIS 2 glacial forebulge cutting across the Rybinsk-Plyos river part could have skewed the topography of the basin towards the glacier, thus damming the waterflow between itself and the ice sheet.

It was found that most likely both incision valleys were formed in the MIS 6 (Late Moscow time) during the formation of a glacial meltwater runoff system connected to the retreat of the MIS 6 glacier. The late MIS 6 – MIS 5 terrace found in the Plyos incision valley serves as strong evidence of the valley existence during that time. No MIS 2 limnic or alluvial sediments were found in the valley, and the GIA modelling did not show any proof of possible lake formation due to the skew towards the glacier. During late MIS 2, the Upper Volga could have experienced a cutting episode caused by a gradual riverbed slope decrease, which occurred because of the glacial forebulge surface lowering as the ice sheet retreated. The accumulation began in the valley in the early Holocene and resulted in the formation of a terrace. This Holocene terrace was located in the Tutaev incision valley. Thus, the general configuration of the Upper Volga valley and its basin was established in the late MIS 6, when the incision valleys were also formed.

# UPPER VOLGA'S INCISION VALLEYS: GEOMORPHOLOGICAL ASPECTS AND DEVELOPMENT HISTORY

**A. O. Utkina[a,#] and A. V. Panin[a]**

*[a] Institute of Geography Russian Academy of Sciences, Moscow, Russia*

*[#] E-mail: utkina@igras.ru*

The evolution of the upstream part of the Volga River, the Upper Volga, is still uncertain. According to the most popular model, the river emerged after the MIS 2 proglacial lakes, supposedly formed in its basin, were drained 14.5 ka after the Plyos and Tutayev incision valleys formation. To test this hypothesis, we aimed to determine the mechanism of formation and age of the incision valleys using luminescence dating. Also, we used a GIA model to assess one of the possible ways of proglacial lakes formation. We found that the terrace located in the Plyos incision valley dates back to late MIS 6 – MIS 5, proving that the valley is much older than the proposed MIS 2 age. Since no evidence of limnic sediments were found in the valley and the modelling did not show a significant GIA influence on the basin that could lead to the proglacial lake formation, we can assume that the valley was not occupied by lake water in MIS 2. Apparently, previous researchers mistook various loams and silts, widely developed on the slopes and in the bottom of the valley, for MIS 2 lake sediments. According to our dating data, these sediments do date back to MIS 2, but are rather of slope and aeolian origin. Following our GIA modelling results, during MIS 2 the Upper Volga valley was affected by a glacial forebulge formation. Its height was not enough to dam up the Volga, but the forebulge relaxation process caused the valley slope to gradually decrease. Due to that accumulation followed, confirmed by the presence of a river terrace of an appropriate age. During late MIS 2, disappearance of the forebulge led the river to incise.

*Keywords:* Valdaian (Weichselian) glaciation, proglacial lakes, glacioisostasy, glacial forebulge, luminescence dating

## ACKNOWLEDGEMENTS

This study contributes to the Russian Science Foundation Project No. 22-17-00259. Data processing was performed with the use of the facilities of the Institute of Geography RAS, taskforce FMGE-2019-0005 (AAAA-A19-119021990091-4). We would like to extend our gratitude to A.S. Murray and R.N. Kurbanov for their help with the luminescence data interpretation and to other staff members of the Nordic Laboratory for Luminescence Dating for their help during dating.

## REFERENCES


Alexanderson H. and Murray A.S. Problems and potential of OSL dating Weichselian and Holocene sediments in Sweden. *Quaternary Science Reviews*. 2012. Vol. 44. P. 37–50. https://doi.org/10.1016/j.quascirev.2009.09.020

Argus D.F., Peltier W.R., Drummond R., and Moore A.W. The Antarctica component of postglacial rebound model ICE-6G_C (VM5a) based upon GPS positioning, exposure age dating of ice thicknesses, and relative sea level histories. *Geophysical Journal International*. 2014. Vol. 198. No. 1. P. 537–563. https://doi.org/10.1093/gji/ggu140

Arslanov H.A., Gromova L.I., Polevaya N.I., and Rudnev Yu.P. Data of the radiocarbon laboratory of the All-Union Scientific Research Geological Institute VSEGEI. *BKICHP*. 1972. Vol. 38. P. 50–72. (in Russ.)

Astakhov V., Shkatova V., Zastrozhnov A., and Chuyko M. Glaciomorphological Map of the Russian Federation. *Quaternary International*. 2016. Vol. 420. P. 4–14. https://doi.org/10.1016/j.quaint.2015.09.024

Bolshakova P.A. Geological structure and hydrogeological conditions of the territory of the sheet O-37-XXIV: Raslovskaya GGP report on the complex geological and hydrogeological survey conducted in 1960–63. Moscow: Russian Geologic Survey, 1963 (unpublished data). (in Russ.)

Buylaert J.P., Jain M., Murray A.S., Thomsen K.J., Thiel C., and Sohbati R. Arobust feldspar luminescence dating method for Middle and Late Pleistocene sediments. *Boreas*. 2012. Vol. 41. P. 435–451. https://doi.org/10.1111/j.1502-3885.2012.00248.x

Bylinsky E.N. Glacial isostatic uplifts of the lithosphere and their possible impact on the location of oil and gas deposits in the north of Europe. *Geomorfologiya*. 1990. No. 4. P. 3–13. (in Russ.)

Hansen V., Murray A., Buylaert J.-P., Yeo E.-Y., and Thomsen K. A new irradiated quartz for beta source calibration. *Radiation Measurements*. 2015. Vol. 81. P. 123–127. https://doi.org/10.1016/j.radmeas.2015.02.017

Hansen V., Murray A., Thomsen K., Jain M., Autzen M., and Buylaert J.-P. Towards the origins of overdispersion in beta source calibration. *Radiation Measurements*. 2018. Vol. 120. P. 157–162. https://doi.org/10.1016/j.radmeas.2018.05.014

Kalm V. Ice-flow pattern and extent of the last Scandinavian Ice Sheet southeast of the Baltic Sea. *Quaternary Science Reviews*. 2012. Vol. 44. P. 51–59. https://doi.org/10.1016/j.quascirev.2010.01.019

Kurbanov R., Murray A., Thompson W., Svistunov M., Taratunina N., and Yanina T. First reliable chronology for the early khvalynian Caspian Sea transgression in the Lower Volga River valley. *Boreas*. 2020. Vol. 50. No. 1. P. 134–146. https://doi.org/10.1111/bor.12478. ISSN 0300-9483

Kvasov D.D. The Late Quaternary history of large lakes and inland seas of Eastern Europe. Helsinki: Suomalainen tiedeakad, 1979. 71 p.

Mangerud J., Jakobsson M., Alexanderson H., Astakhov V., Clarke G.K.C., Henriksen M., Hjort C., Krinner G., Lunkka J.-P., Möller P., Murray A., Nikolskaya O., Saarnisto M., and Svendsen J.I. Ice-dammed lakes and rerouting of the drainage of northern Eurasia during the Last Glaciation. *Quaternary Science Reviews*. 2004. Vol. 23 (11–13). P. 1313–1332. https://doi.org/10.1016/j.quascirev.2003.12.009

Mirchink G.F. Quaternary history of the Volga River valley above the Mologa. *Trudy komissii po izucheniu chetvertichnogo perioda AN USSR*. 1935. Vol. 4. P. 5–37. (in Russ.)

Moskvitin A.I. Pleistocene stratigraphy in the European part of the USSR. *Trudy GIN AN SSSR*. 1967. Vol. 156. 236 p. (in Russ.)

Murray A.S. and Wintle A.G. Luminescence dating of quartz using an improved single-aliquot regenerative-dose protocol. *Radiation Measurements*. 2000. Vol. 32 (1). P. 57–73. https://doi.org/10.1016/S1350-4487(99)00253-X

Murray A.S., and Wintle A.G.. The single aliquot regenerative dose protocol: potential for improvements in reliability. *Radiation Measurements*. 2003. Vol. 37 (4–5). P. 377–381. https://doi.org/10.1016/S1350-4487(03)00053-2

Murray A.S., Arnold L.J., Buylaert J.-P., Guérin G., Qin J., Singhvi A.K., Smedley R., and Thomsen K.J. Optically stimulated luminescence dating using quartz. *Nature Review Methods Primers*. 2021. No. 1. 31 p. https://doi.org/10.1038/s43586-021-00068-5

Murray A.S., Marten R., Johnston A., and Martin P. Analysis for naturally occurring radionuclides at environmental concentrations by gamma spectrometry. *Journal of Radioanalytical and Nuclear Chemistry*. 1987. Vol. 115. P. 263–288. https://doi.org/10.1007/BF02037443

Murray A.S., Thomsen K.J., Masuda N., Buylaert J.-P., and Jain M. Identifying well-bleached quartz using the different bleaching rates of quartz and feldspar luminescence signals. *Radiation Measurements*. 2012. Vol. 47 (9). P. 688–695. https://doi.org/10.1016/j.radmeas.2012.05.006

Obedientova G.V. *Erozionnye tsikly i formirovanie doliny Volgi* (Erosion Cycles and Formation of the Volga River Valley). Moscow: Nauka (Publ.), 1977. 240 p. (in Russ.)

Olley J., Murray A., and Roberts R. The effects of disequilibria in uranium and thorium decay chains on burial dose rates in fluvial sediments. *Quaternary Science Reviews*. 1996. Vol. 15 (7). P. 751–760. https://doi.org/10.1016/0277-3791(96)00026-1

Panin A., Adamiec G., Buylaert J.P., Matlakhova E., Moska P., and Novenko E. Two late pleistocene climate-driven incision/aggradation rhythms in the Middle Dnieper River basin, west-central Russian plain. *Quarternary Science Reviews*. 2017. Vol. 166. P. 266–288. https://doi.org/10.1016/j.quascirev.2016.12.002

Peltier W.R., Argus D.F., and Drummond R. Space geodesy constrains ice-age terminal deglaciation: The global ICE-6G_C (VM5a) model. *Journal of Geophysical Research: Solid Earth*. 2015. Vol. 120 (1). P. 450–487. https://doi.org/10.1002/2014JB011176

Prescott J.R. and Hutton J.T. Cosmic ray contributions to dose rates for luminescence and ESR dating: large depths and long-term time variations. *Radiation Measurements.* 1994. Vol. 23 (2–3). P. 497–500. https://doi.org/10.1016/1350-4487(94)90086-8

Schik S. and Pisareva V. Main patterns of the Pleistocene lakes' spreading on the Russian plain. Chronostratigraphic divisions of the Pleistocene History of the Pleistocene lakes. Saint Petersburg: Nauka (Publ.), 1998. P. 8–23. (in Russ.)

Schukina E. The Upper Volga's terraces and its relation to glacial sediments of Gorkovsko-Ivanovskiy krai. *Byulleten' Moskovskogo obshchestva ispytatelei prirody. Otdel geologicheskii.* 1993. Vol. 11. No. 3. P. 195–224. (in Russ.)

Sidorchuk A., Panin A., and Borisova O. Morphology of river channels and surface runoff in the Volga River basin (East European Plain) during the Late Glacial period. *Geomorphology*. 2009. Vol. 113 (3–4). P. 137–157. https://doi.org/10.1016/j.geomorph.2009.03.007

Sohbati R., Murray A., Lindvold L., Buylaert J.-P., and Jain M. Optimization of laboratory illumination in optical dating. *Quaternary Geochronology.* 2017. Vol. 39. P. 105–111. https://doi.org/10.1016/j.quageo.2017.02.010

Spada G. and Melini D. SELEN4 (SELEN version 4.0): a Fortran program for solving the gravitationally and topographically self-consistent sea-level equation in glacial isostatic adjustment modeling. *Geoscientific Model Dev*. 2019. Vol. 12. P. 5055–75.

Svendsen J.I., Alexanderson H., Astakhov V.I., Demidov I., Dowdeswell J.A., Funder S., Gataullin V., Henriksen M., Hjort C., Houmark-Nielsen M., Hubberten H.W., Ingólfsson O., Jakobsson M., Kjær K.H., Larsen E., Lokrantz H., Lunkka J.P., Lyså A., Mangerud J., Matiouchkov A., Murray A., Möller P., Niessen F., Nikolskaya O., Polyak L., Saarnisto M., Siegert C., Siegert M.J., Spielhagen R.F., and Stein R. Late Quaternary ice sheet history of northern Eurasia. *Quaternary Science Reviews.* 2004. Vol. 23 (11–13). P. 1229–1271. https://doi.org/10.1016/j.quascirev.2003.12.008

Thomsen K.J., Murray A.S., Jai M., and Bøtter-Jensen L. Laboratory fading rates of various luminescence signals from feldspar-rich sediment extracts. *Radiation Measurements.* 2008. Vol. 43 (9–10). P. 1474–1486. https://doi.org/10.1016/j.radmeas.2008.06.002

Thrasher I.M., Mauz B., Chiverrell R.C., and Lang A. Luminescence dating of glaciofluvial deposits: a review. *Earth-Science Reviews.* 2009. Vol. 97 (1–4). P. 133–146. https://doi.org/10.1016/j.earscirev.2009.09.001

Tockner K., Uehlinger U., and Robinson C.T. Rivers of Europe. London: Academic Press (Publ.), 2009. 942 p.

Utkina A.O. Modelling the glacial isostatic adjustment using SELEN. *Natural and technical sciences.* 2020. No. 8. P. 110–115. (in Russ.)

Utkina A.O., Panin A.V., Kurbanov R.N., and Murray A.S. Unexpectedly old luminescence ages as an indicator of the origin of the upper Volga River valley sediments. *Quaternary Geochronology.* 2022. Vol. 73. 101381. https://doi.org/10.1016/j.quageo.2022.101381

Wallinga J. Optically stimulated luminescence dating of fluvial deposits: a review. *Boreas*. 2002. Vol. 31 (4). P. 303–322. https://doi.org/10.1111/j.1502-3885.2002.tb01076.x

**EDN:** NJWWTS
*ГЕОМОРФОЛОГИЯ, 2022, том 53, № 5, с. 173–176*

# СОДЕРЖАНИЕ
## Том 53, Номер 1–5, 2022

**DOI:** 10.31857/S0435428122050194

| | | |
|---|---|---|
| **Романенко Ф.А., Харченко С.В.** К истории геоморфологического картографирования Арктики | 1 | 3–25 |
| **ЭКОЛОГИЧЕСКАЯ И ПРИКЛАДНАЯ ГЕОМОРФОЛОГИЯ** | | |
| **Тютюнник Ю.Г.** Морфогенез в посттехногенных промышленных ландшафтах | 2 | 3–12 |
| **МЕТОДИКА НАУЧНЫХ ИССЛЕДОВАНИЙ** | | |
| **Дудакова Д.С., Юдин С.Н.** Цифровая модель подводных ландшафтов Ладожского озера как источник интегрированной информации о состоянии дна | 2 | 13–26 |
| **Лебедева Е.В., Балдина Е.А., Медведев А.А.** Склоновые процессы в долине р. Гейзерной (Камчатка): результаты дешифрирования разновременных космических снимков высокого пространственного разрешения | 4 | 3–16 |
| **Трубкин И.П., Немировская И.А.** Модельные расчеты динамики наносов в Печорском море | 4 | 17–24 |
| **Украинцев В.Ю.** Следы мощного речного стока в долинах рек бассейна Волги в поздневалдайскую эпоху | 1 | 26–34 |
| **Энтин А.Л., Михайлюкова П.Г., Кедич А.И., Харченко С.В.** Современный опыт использования радиолокационной интерферометрии для регистрации изменений высотных отметок поверхности суши | 2 | 27–42 |
| **НАУЧНЫЕ СООБЩЕНИЯ** | | |
| **Баранов Д.В.** Геоморфология долины Верхней Волги: история изучения и состояние проблемы (ст. 2. Верхневолжская низина) | 1 | 35–48 |
| **Беркович К.М., Злотина Л.В.** Релаксация русла в нижнем бьефе Новосибирской плотины | 2 | 43–50 |
| **Бричёва С.С., Гоников Т.В., Панин А.В., Деев Е.В., Матасов В.М., Дорошенков М.М., Энтин А.Л., Лобачева Д.М.** О происхождении грядового рельефа Курайской котловины (Юго-Восточный Алтай) в свете морфометрических и георадарных исследований | 4 | 25–41 |
| **Голубцов В.А., Опекунова М.Ю.** Строение и хронология формирования пойменных отложений рек бассейна р. Белая (Верхнее Приангарье) | 4 | 42–55 |
| **Григорьев И.И., Рысин И.И.** Многолетняя динамика линейного, площадного и объемного прироста оврагов на территории Удмуртии | 4 | 56–74 |
| **Каргаполова И.Н., Крыленко И.В.** Русловые процессы на полугорной реке (р. Белая, Западный Кавказ) (ст. 1. Горизонтальные деформации русла и сток воды как их основной фактор) | 1 | 49–64 |
| **Карпухина Н.В., Маккавеев А.Н., Захаров А.Л., Константинов Е.А., Курбанов Р.Н., Бричёва С.С., Сычев Н.В., Баранов Д.В.** Озерно-ледниковая терраса в Изборско-Мальской долине: строение, возраст и механизм формирования | 1 | 65–80 |
| **Ковалев С.Н.** Карта оценки воздействия эрозионно-русловых систем на инфраструктуру населенных пунктов | 4 | 75–85 |
| **Коркин С.Е., Исыпов В.А.** Анализ горизонтальных русловых деформаций средней Оби на основе стационарных наблюдений | 4 | 86–98 |
| **Куракова А.А., Чалов Р.С.** Морфодинамика русла нижнего Иртыша | 4 | 99–109 |

| | | |
|---|---|---|
| **Лебедева Е.В., Жарков Р.В.** Аккумулятивные формы рельефа в долинах с газогидротермальными проявлениями (на примере водотоков ряда вулканических массивов Курило-Камчатского региона) | 1 | 81–101 |
| **Осинцева Н.В., Шмидт И.В., Горбунова Т.А., Лауэр Т., Шнайдер Б., Тинапп Х., Штойбле Х.** Субаэральные отложения черноозерской гривы (долина р. Иртыш): гранулометрический состав, генезис, динамика осадконакопления | 2 | 51–60 |
| **Рыбальченко С.В.** Отличие склоновых селей от оползней-потоков | 2 | 61–71 |
| **Тубалов А.А.** Оценка эрозионной опасности сельскохозяйственных земель правобережья р. Хопер (в пределах Волгоградской области) | 2 | 110–124 |
| **Чалов Р.С., Куракова А.А., Камышев А.А., Михайлова Н.М.** Раздвоенные русла больших и крупнейших рек: условия формирования, рассредоточение стока и морфодинамика рукавов | 2 | 72–88 |
| **ДИСКУССИИ** | | |
| **Грачев А.М., Голосов В.Н.** Роль глобального горообразования и денудации в кайнозойском похолодании климата | 2 | 89–103 |
| **Зыков Д.С., Полещук А.В., Колодяжный С.Ю.** Морфоструктура Рыбинского узла среднерусской зоны дислокаций как отражение новейшей внутриплатформенной геодинамики | 2 | 104–112 |
| **ИСТОРИЯ НАУКИ** | | |
| **Асоян Д.С.** Юрий Александрович Мещеряков – основоположник спутниковой географии | 1 | 102–111 |
| **Иогансон Л.И.** Вклад А.А. Никонова в развитие отечественных наук о Земле | 2 | 113–115 |
| **Чичагов В.П.** 100-летний юбилей выдающегося российского ученого Юрия Александровича Мещерякова | 1 | 112–120 |
| **ПОТЕРИ НАУКИ** | | |
| **Янина Т.А.** Памяти Александра Адамовича Свиточа | 2 | 116–118 |
| **СПЕЦИАЛЬНЫЙ ВЫПУСК ПУТИ ЭВОЛЮЦИОННОЙ ГЕОГРАФИИ 2. ЧАСТЬ 1. ПАЛЕОГЕОГРАФИЯ ЧЕТВЕРТИЧНОГО ПЕРИОДА** | | |
| **Новенко Е.Ю.** От редколлегии (на англ. яз.) | 3 | 5–6 |
| **РЕКОНСТРУКЦИИ НА ОСНОВЕ ПАЛЕОБИОЛОГИЧЕСКИХ МЕТОДОВ** | | |
| **Кузьмина С.А., Сычёва С.А., Ершова Е.Г., Зюганова И.С., Захаров А.Л., Горбатов Е.С., Колесников С.Ф., Панин П.Г.** Иванцевский разрез погребенных средне-поздненеоплейстоценовых озерно-болотных отложений на окраине г. Дмитров Московской области (на англ. яз.) | 3 | 7–18 |
| **Борисова О.К., Нарышкина Н.Н., Константинов Е.А., Панин А.В.** Ландшафтно-климатические изменения в пребореале на северо-западе Европейской части России (на англ. яз.) | 3 | 19–28 |
| **Сапелко Т.В., Кузнецов Д.Д., Лудикова А.В., Колпаков Е.М., Шумкин В.Я.** История озера Канозеро в позднеледниковье и голоцене на юге Кольского полуострова (северо-запад России) (на англ. яз.) | 3 | 29–38 |
| **Тимирева С.Н., Филимонова Л.В., Зюганова И.С., Кононов Ю.М., Романенко Ф.А.** Изменения окружающей среды Терского берега Белого моря (Кольский полуостров) в голоцене по данным комплексного изучения болота Кузоменский мох (на англ. яз.) | 3 | 39–50 |
| **Новенко Е.Ю., Мазей Н.Г., Куприянов Д.А., Шатунов А.Е., Андреев Р.А., Макарова Е.А., Бородина К.А., Руденко О.В., Прокушкин А.С., Волкова Е.М.** Изменения растительности Приенисейской Сибири в последние 4700 лет: новые палеоэкологические данные из района Игарки (Красноярский край) (на англ. яз.) | 3 | 51–60 |
| **Безрукова Е.В., Кулагина Н.В., Решетова С.А., Щетников А.А., Крайнов М.А., Филинов И.А.** Природная среда Окинского плато (горы Восточного Саяна) в позднем ледниковье и голоцене: пример палинологической летописи из отложений озера Хикушка (на англ. яз.) | 3 | 61–73 |

**Мацковский В.В., Кузнецова В.В., Семеняк Н.С., Турчинская С.М., Зазовская Э.П., Энговатова А.В., Лазарев А.С., Жданова Е.Ю., Долгова Е.А., Соломина О.Н.** Дендроклиматический потенциал стабильных изотопов углерода в целлюлозе годичных колец *Pinus sylvestris* L. в Ярославской и Костромской областях (на англ. яз.) 3 74–82

## СЕДИМЕНТОЛОГИЯ, ПАЛЕОГЕОКРИОЛОГИЯ, ПАЛЕОГИДРОЛОГИЯ

**Садоков Д.О., Сапелко Т.В., Меллес М., Федоров Г.Б.** Динамика осадконакопления в озере Белом (Вологодская область, северо-запад России) с позднеледниковья до среднего голоцена (на англ. яз.) 3 83–95

**Мусаэлян Р.Э., Лебедева М.П., Ростовцева Ю.В., Варламов Е.Б.** Литолого-минералогическая характеристика нижнехвалынских шоколадных глин Нижней Волги (на примере разрезов Райгород и Средняя Ахтуба) (на англ. яз.) 3 96–106

**Константинов Е.А., Мазнева Е.А., Сычев Н.В., Захаров А.Л., Филиппова К.Г.** Изменчивость строения и состава верхнечетвертичных лёссов Предкавказья (юг европейской части России) (на англ. яз.) 3 107–116

**Алексеева В.А., Ларин С.И., Ларина Н.С.** Морфоскопия кварцевых зерен из отложений гривных толщ Тобол-Ишимского междуречья (на англ. яз.) 3 117–127

**Рябуха А.Г., Поляков Д.Г., Стрелецкая И.Д., Ковда И.В.** Морфология и современное функционирование меловых полигонов Общего Сырта, Юго-восток Восточно-Европейской равнины (на англ. яз.) 3 128–133

**Шашерина Л.В., Стефутин С.А., Зозуля С.С., Карпова Ю.О.** Геоморфологические условия формирования раннесредневековых поселений в Днепро-Двинском регионе, Северо-Запад Европейской России (на англ. яз.) 3 134–145

**Георгиади А.Г., Милюкова И.П.** Речной сток Волги в теплые климатические эпохи геологического прошлого, в период инструментальных наблюдений и сценарного будущего (на англ. яз.) 3 146–152

## СПЕЦИАЛЬНЫЙ ВЫПУСК ПУТИ ЭВОЛЮЦИОННОЙ ГЕОГРАФИИ 2. ЧАСТЬ 2. ПРОБЛЕМЫ ПАЛЕОПОЧВОВЕДЕНИЯ, ГЕОАРХЕОЛОГИИ, ФЛЮВИАЛЬНОЙ ГЕОМОРФОЛОГИИ

**Новенко Е.Ю.** От редколлегии (на англ. яз.) 5 5–6

## ПРОБЛЕМЫ ПАЛЕОПОЧВОВЕДЕНИЯ И ГЕОАРХЕОЛОГИИ

**Бобровский М.В., Куприянов Д.А., Смирнов А.Л., Ханина Л.Г., Добровольская М.В.** Динамика древесной растительности и антропогенная активность по данным анализа древесных углей из городищ раннего железного века и раннего средневековья на Верхней Волге (на англ. яз.) 5 7–24

**Коркка М.А., Романис Т.В., Савельева Л.А., Седов С.Н., Очередной А.К.** Детальная палеоэкологическая летопись валдайского криохрона (МИС 4–2) из почвенно-осадочной серии среднепалеолитического памятника Хотылёво I (на англ. яз.) 5 25–31

**Курбанова Ф.Г., Пузанова Т.А., Асеева Е.Н., Куст П.Г., Руденко О.В.** Реконструкция палеоландшафтов средних веков на основе изучения погребенных почв Гочевского археологического комплекса (Курская область) (на англ. яз.) 5 32– 47

**Лебедева М.П., Плотникова О.О., Чурилин Н.А., Романис Т.В., Шишков В.А.** Влияние состава и свойств хвалынских отложений на эволюцию почв Волго-Уральского междуречья (по результатам минералогических и микроморфологических исследований) (на англ. яз.) 5 47–59

**Павлов П.Ю.** О времени появления человека современного вида на северо-востоке Восточно-Европейской равнины и на Урале (по данным изучения палеолитической стоянки Заозерье) (на англ. яз.) 5 60–68

**Седов С.Н., Синицын А.А., Бессуднов А.А., Лев С.Ю., Бессуднов А.Н., Сычёва С.А., Романис Т.В., Шейнкман В.С., Коркка М.А.** Отражение вековых и тысячелетних изменений природной среды в палеопочвах верхнепалеолитических стоянок Восточно-Европейской равнины в МИС 3 и МИС 2 (на англ. яз.) 5 69–77

| | | |
|---|---|---|
| **Сычёва С.А., Бессуднов А.А., Бессуднов А.Н., Тимирева С.Н., Кононов Ю.М., Симакова А.Н., Захарова Е.Ю., Филиппова К.Г.** Локальная стратиграфия и палеоэкология стоянки поздней поры верхнего палеолита Дивногорье 1 в бассейне среднего Дона (на англ. яз.) | 5 | 78–88 |
| **Хмелева М.В., Панин П.Г., Чепалыга А.Л., Карпухина Н.В., Найдина О.Д., Бухонов А.В.** Строение и условия формирования палеопочв раннего плейстоцена в лёссово-почвенной серии разреза Алчак-Седловина (Республика Крым) (на англ. яз.) | 5 | 89–102 |
| **Чендев Ю.Г., Пузанова Т.А., Курбанова Ф.Г.** Палеочерноземы времени развития срубной культуры и тренды позднеголоценовой эволюции почв лесостепи Восточно-Европейской равнины (на англ. яз.) | 5 | 103–115 |

**ПРОБЛЕМЫ ФЛЮВИАЛЬНОЙ ГЕОМОРФОЛОГИИ**

| | | |
|---|---|---|
| **Лебедева Е.В.** Влияние газогидротермальной деятельности на формирование рельефа речных долин геотермальных зон (на англ. яз.) | 5 | 116–126 |
| **Матлахова Е.Ю., Украинцев В.Ю.** Строение поймы реки Мокши как ключ к позднеплейстоценовой истории развития долины (на англ. яз.) | 5 | 127–133 |
| **Правкин С.А., Большиянов Д.Ю.** Палеореконструкция долины Нижней Лены в голоцене и позднем неоплейстоцене: новые данные, противоречия и проблемы (на англ. яз.) | 5 | 134–143 |
| **Рыжов Ю.В., Голубцов В.А., Смирнов М.В.** Пойменный аллювий бассейна р. Селенги: строение, возраст, этапы формирования (на англ. яз.) | 5 | 144–153 |
| **Трофимец Л.Н., Паниди Е.А., Лаврусевич А.А.** Некоторые особенности применения радиоцезиевого метода изучения потерь почвы вследствие эрозии в перигляциальной области бассейна Верхней Оки (на англ. яз.) | 5 | 154–162 |
| **Уткина А.О., Панин А.В.** Строение и история формирования долин прорыва Верхней Волги (на англ. яз.) | 5 | 163–172 |